AIIM

Association for Information and Image Management

1100 Wayne Avenue, Suite 1100
Silver Spring, Maryland 20910
301/587-8202

Centimeter

Inches

MANUFACTURED TO AIIM STANDARDS
BY APPLIED IMAGE, INC.

1 of 4

ORNL-6714
Dist. Category UC-420

FUSION ENERGY DIVISION PROGRESS REPORT

Period from January 1, 1990, to December 31, 1991

J. Sheffield
C. C. Baker
M. J. Saltmarsh

Fusion Energy Division Staff

Date Published: March 1994

Prepared for the
Office of Fusion Energy
Budget Activity No. 25 19 00 00 0

Prepared by the
OAK RIDGE NATIONAL LABORATORY
Oak Ridge, Tennessee 37831-6285
managed by
MARTIN MARIETTA ENERGY SYSTEMS, INC.
for the
U.S. DEPARTMENT OF ENERGY
under contract DE-AC05-84OR21400

Report previously issued in this series are as follows:

ORNL-2693	Period Ending January 31, 1959
ORNL-2802	Period Ending July 31, 1959
ORNL-2926	Period Ending January 31, 1960
ORNL-3011	Period Ending July 31, 1960
ORNL-3104	Period Ending January 31, 1961
ORNL-3239	Period Ending October 31, 1961
ORNL-3315	Period Ending April 30, 1962
ORNL-3392	Period Ending October 31, 1962
ORNL-3472	Period Ending April 30, 1963
ORNL-3564	Period Ending October 31, 1963
ORNL-3652	Period Ending April 30, 1964
ORNL-3760	Period Ending October 31, 1964
ORNL-3836	Period Ending April 30, 1965
ORNL-3908	Period Ending October 31, 1965
ORNL-3989	Period Ending April 30, 1966
ORNL-4063	Period Ending October 31, 1966
ORNL-4150	Period Ending April 30, 1967
ORNL-4238	Period Ending October 31, 1967
ORNL-4401	Period Ending December 31, 1968
ORNL-4545	Period Ending December 31, 1969
ORNL-4688	Period Ending December 31, 1970
ORNL-4793	Period Ending December 31, 1971
ORNL-4896	Period Ending December 31, 1972
ORNL-4982	Period Ending December 31, 1973
ORNL-5053	Period Ending December 31, 1974
ORNL-5154	Period Ending December 31, 1975
ORNL-5275	Period Ending December 31, 1976
ORNL-5405	Period Ending December 31, 1977
ORNL-5549	Period Ending December 31, 1978
ORNL-5645	Period Ending December 31, 1979
ORNL-5674	Period Ending December 31, 1980
ORNL-5843	Period Ending December 31, 1981
ORNL-5919	Period Ending December 31, 1982
ORNL-6015	Period Ending December 31, 1983
ORNL-6111	Period Ending December 31, 1984
ORNL-6234	Period Ending December 31, 1985
ORNL-6332	Period Ending December 31, 1986
ORNL-6452	Period Ending December 31, 1987
ORNL-6528	Period Ending December 31, 1988
ORNL-6624	Period Ending December 31, 1989

CONTENTS

SUMMARY

The Fusion Program of the Oak Ridge National Laboratory (ORNL), a major part of the national fusion program, encompasses nearly all areas of magnetic fusion research. The program is directed toward the development of fusion as an economical and environmentally attractive energy source for the future.

The program involves staff from ORNL, Martin Marietta Energy Systems, Inc., private industry, the academic community, and other fusion laboratories, in the United States and abroad. Achievements resulting from this collaboration are documented in this report, which is issued as the progress report of the ORNL Fusion Energy Division; it also contains information from components for the Fusion Program that are external to the division (about 15% of the program effort).

The areas addressed by the Fusion Program include the following:

- experimental and theoretical research on magnetic confinement concepts,
- engineering and physics of existing and planned devices, including remote handling,
- development and testing of diagnostic tools and techniques in support of experiments,
- assembly and distribution to the fusion community of databases on atomic physics and radiation effects,
- development and testing of technologies for heating and fueling fusion plasmas,
- development and testing of superconducting magnets for containing fusion plasmas,
- development and testing of materials for fusion devices, and
- exploration of opportunities to apply the unique skills, technology, and techniques developed in the course of this work to other areas (about 15% of the Division's activities).

Highlights from program activities during 1990 and 1991 follow.

Toroidal Confinement Activities

The focus of the work in the toroidal confinement area changed dramatically during this reporting period because of a change in program emphasis by the Department of Energy from some support of research on alternate confinement concepts to strict concentration on tokamak research. There had been two major elements to the experimental confinement program in the Fusion Energy Division: the Advanced Toroidal Facility (ATF), the world's largest stellarator, and the Edge Physics and Particle Control (EPPC) program on various tokamaks. At the start of 1990, ATF was supported to contribute to fundamental toroidal confinement understanding of relevance to both tokamaks and stellarators and the EPPC program was being carried out through collaborations on tokamaks in Germany (TEXTOR at Jülich), France (Tore Supra at Cadarache), and the United States (DIII-D at San Diego). By the end of 1991, ATF had been shut down, the EPPC program on DIII-D and Tore Supra had been expanded, and new collaborative research efforts had been started on the Princeton Beta Experiment (PBX-M) and Tokamak Fusion Test Reactor (TFTR) tokamaks at Princeton Plasma Physics Laboratory.

A major focus for studies in ATF during the reporting period was energy confinement scaling and the identification of the mechanisms responsible for anomalous transport.

Microwave scattering measurements of electron density fluctuations in the core of low-collisionality plasmas with electron cyclotron heating show features that might be evidence of trapped-electron instabilities. Modification of the energy and particle confinement times was studied by introducing magnetic islands and modifying the electric field in the plasma.

On May 30, 1991, ATF operations were halted by an electrical arc-over at a helical field (HF) coil joint. Damage was limited to two HF coil segments. Temporary repairs were made, and operations resumed on September 25, 1991, with the toroidal field limited to 1 T because of the lack of water cooling. Pulse length and repetition rate were also restricted. Despite these limitations, the operating period that followed yielded several significant accomplishments, including data acquisition for numerous plasma configurations with the 2-mm scattering diagnostic developed and applied in collaboration with Russian scientists; a proof-of-principle test of the alpha particle diagnostic developed by the ORNL Physics Division, which produced positive results; discharge durations of 20.2 s, a new record for ATF, with second harmonic heating at 35 GHz, in a collaboration with Japan; and extensions of dimensionless scaling experiments. ATF was shut down on November 30, 1991, and work to fully repair the damaged coil joints was begun.

The EPPC program focused on pressure scaling studies in the divertor baffle of DIII-D, particle balance and control studies during long-pulse operation in Tore Supra, helium transport and exhaust studies in TEXTOR and DIII-D, and edge fluctuation and biasing studies in ATF.

Toroidal confinement activities also include some research on advanced fusion concepts. Reactor studies focused on developing the tools needed for a realistic assessment of the cost of electricity expected for a stellarator reactor. Initial results indicate that torsatron reactors are competitive with conventional tokamak reactors if the same assumptions are used for both.

Atomic Physics and Plasma Diagnostics Development

Activities in the atomic physics and plasma diagnostics development program are divided among atomic collisions research, atomic data compilation and evaluation, and advanced plasma diagnostics development.

The atomic collisions research program focuses on inelastic processes that are critical in determining the energy balance and impurity transport in high-temperature plasmas, and for plasma diagnostic measurements. Central to the experimental effort is an electron cyclotron resonance (ECR) multicharged ion source, which provides ions for colliding-beams experiments. A new collaborative electron-ion merged-beams experiment to measure cross sections for electron-impact excitation of multiply charged ions by electron energy-loss spectroscopy constitutes a major part of the current experimental effort. Merged beams have also been used to study charge-exchange collisions of multiply charged plasma impurity ions with hydrogen (deuterium) atoms at the lower kinetic energies relevant to the edge plasma.

Data compilation and evaluation are carried out by the Controlled Fusion Atomic Data Center (CFADC). The CFADC actively participates in the International Atomic and Molecular Data Center Network sponsored by the International Atomic Energy Agency. Through this network, the CFADC has a major role in the development and implementation of the ALADDIN system for the computer storage, retrieval, and exchange of recommended atomic data.

The plasma diagnostics program concentrates on the development of advanced diagnostics for magnetic fusion experiments. The current emphasis is on the application of pulsed infrared lasers to the diagnostics of alpha particles produced from the fusion of deuterium and tritium. The pulsed-laser Thomson scattering diagnostic for alpha particles was successfully tested on ATF, and a novel multichannel interferometer provided accurate measurements of the plasma electron density profile evolution during plasma discharges. To address the issue of optical beam refraction in higher density plasmas, a feasibility study was carried out for a two-color infrared interferometer/polarimeter system for the International Thermonuclear Experimental Reactor (ITER).

Fusion Theory and Computing

The fusion theory and computing effort is characterized by close interaction with experimental programs. During this reporting period, the balance between the development of new or advanced methods and theoretical models and the application of existing theories tipped fairly strongly toward the application side.

ORNL theorists contributed strongly to ITER, to the Burning Plasma Experiment (BPX) project, and to experimental and technological successes at the Joint European Torus (JET), TFTR, DIII-D, TEXTOR, and Tore Supra. The ORNL experimental program on ATF remained a primary focus for our stellarator analyses.

New insights into turbulence and transport in toroidal systems led to the analysis of plasma core and edge transport, the associated development of radial electric fields, and the diagnosis of controlling physics through detailed comparisons with ATF and experiments on the Texas Experimental Tokamak (TEXT).

The Numerical Tokamak Project is a major new thrust for the U.S. theory program. ORNL theorists and computational physicists have been strong contributors to the development of a proposal; in addition, ORNL contributed new methods for inclusion of essential kinetic phenomena, as well as substantial experience in the development of efficient means for using the latest hardware technologies such as massively parallel computers.

Better insight into the physics governing the transition from L-mode to H-mode in tokamaks remains a high priority in the fusion program, and ORNL contributions are an essential ingredient in the search for a fully validated model.

In the analysis of rf heating and current drive, the fundamental full-wave simulation model was significantly improved. Another important contribution to rf theory has been insight leading to the development of a method for estimating the current associated with rf processes.

Understanding the behavior of the ATF stellarator is a key part of the program, with substantial progress made in comparing results of theoretical calculations with data. An example has been the analysis of bootstrap current measurements and detailed comparison of the results with neoclassical models as the magnetic configuration is modified by changing the currents in the external coils. During 1990–91, it became clear that energy confinement in stellarators and in tokamaks follows broadly the same scaling with parameters, while key details differ.

The ATF data acquisition system and the software for initial analysis, database formation, and subsequent analysis of the data were refined and made more efficient. Several

workstation computers were added to improve visualization of scientific data and provide effective analysis at the middle scales.

Plasma Technology

The Plasma Technology Section is engaged in the development and application of plasma fueling systems and rf technology.

The research activities of the Plasma Fueling Group supported both the U.S. magnetic fusion program and international fusion research. Work continued in pneumatic and centrifugal pellet injector development, for present and near-term applications, and advanced development for more demanding applications anticipated for ITER and the next generation of fusion devices. One highlight was the development of a tritium pellet injector for deuterium-tritium operations on TFTR; this injector incorporates the two-stage light gas gun that has been a focus of the advanced development efforts.

In the rf technology program, new materials and fabrication techniques for the Faraday shield tubes of antennas operating in the ion cyclotron range of frequencies (ICRF) were developed and tested, and the effects of Faraday shield geometry and material on ICRF antennas were calculated and compared to measurements. Based on tests of a folded waveguide (FWG) antenna in the Radio Frequency Test Facility plasma, the design of an FWG antenna for the Frascati Tokamak Upgrade in Italy was initiated. A fast-wave current drive (FWCD) antenna array was operated on DIII-D to provide a proof-of-principle test of this technique. Collaborations continued on Tore Supra and TFTR, both of which are equipped with ORNL antennas. A new initiative to design a microwave reflectometer system for edge density profile measurements on TFTR began in 1991. An asymmetric double-loop antenna was operated on ATF, and the electron cyclotron heating system on ATF was upgraded to allow experiments with high plasma beta at lower magnetic fields for long pulses. A collaboration to design a power coupler for the new A_2 antennas on JET was begun. This effort entails extensive modeling of the complicated A_2 antenna geometry.

Advanced Systems Program

The Advanced Systems Program serves as the focal point for design studies for future fusion experiments. The Fusion Engineering Design Center (FEDC) is the major engineering resource for the program. During 1990 and 1991, program activities included ITER; BPX; a Steady-State Advanced Tokamak (SSAT) with resistive, demountable coils, designated SSAT-D; the Advanced Reactor Innovation and Evaluation Study (ARIES); a small, steady-state tokamak (triple-S tokamak, or TST) for integrated divertor testing; and support for systems code development and application.

The three-year Conceptual Design Activities (CDA) phase of the ITER program, an international program for cooperation on the design of a fusion test reactor, was completed in December 1990. The CDA established a reactor configuration as the basis for the Engineering Design Activities (EDA), scheduled to start in late FY 1992. The CDA also established a five-year R&D plan for the major reactor systems to be conducted in conjunction with the design activities during the EDA. ORNL was a major participant in the ITER physics, engineering design, and R&D activities at the national and international levels.

The BPX project, led by Princeton Plasma Physics Laboratory (PPPL), was directed toward developing a lower cost successor to the Compact Ignition Tokamak (CIT). ORNL served as a major partner in the project, with design and R&D responsibility for remote maintenance, vacuum system and thermal shield design, rf heating, and pellet injection. FEDC staff also carried out calculations of plasma shape control and plasma disruptions in collaboration with PPPL. The BPX project was cancelled in September 1991, and a new initiative, called the Tokamak Physics Experiment (TPX), was started.

The TPX mission, which draws on the work done in support of the SSAT, is to demonstrate integrated steady-state operating modes characterized by a noninductively driven plasma current, a high power density, an actively cooled and actively pumped divertor, and disruption-free operation. In addition, this device would provide a database on physics regimes that could be extrapolated to a more attractive fusion reactor than that projected by the present database. The facility should cost about $400 million and make maximum use of TFTR assets in the TFTR facility at PPPL. The design concept for a device with resistive, demountable coils, identified as SSAT-D, was developed in a design study initiated in fall 1991. FEDC staff developed both a configuration with a major radius R_0 = 2.25 m and an alternative configuration with R_0 = 1.5 m. Other designs with superconducting and copper coils were studied, and a superconducting tokamak was chosen for TPX.

As part of the ARIES program, a D-^{3}He-fueled tokamak reactor, ARIES-III, was designed. Key features include a standard aspect ratio, high poloidal beta, and dominant bootstrap currents (approximately equal to the plasma current). Potential advantages include high beta, which contributes to reducing the size and magnetic field of a fusion reactor, and modest current drive requirements, which reduce the recirculating power needed to maintain the plasma current in steady state.

The design study for the TST addressed the need for development of divertors and the associated plasma power and particle handling. These systems will be required for ITER and for all large, steady-state tokamaks that are driven with high auxiliary power. The TST, which could fulfil this R&D need in the near term, relies only on the physics and technology data of existing small to medium-size tokamaks and uses the facilities and equipment available at a typical fusion research institution such as ORNL.

In the systems code area, final development of the TETRA (Tokamak Engineering Test Reactor Analysis) code was completed, and the code was applied to the ITER CDA concept. In an effort led by Lawrence Livermore National Laboratory, a new code, called the Supercode, was created and applied to the conceptualization of the SSAT.

Fusion Materials Research

The Fusion Materials Program focuses on the development of reactor structural materials, first wall and high-heat-flux materials, and ceramics for electrical applications.

In the structural materials program, the primary emphasis is on the qualification of austenitic stainless steels for ITER and the development of low-activation ferritic steels, vanadium alloys, structural ceramics, and ceramic composites (e.g., SiC/SiC). In the seventh year of a collaborative program with the Japan Atomic Energy Research Institute, investigation of the effects of fusion reactor radiation damage levels on the engineering properties of these austenitic steels continued. Experimental irradiation of these alloys in the High Flux

Isotope Reactor (HFIR) provides data and understanding of radiation response at the temperatures and damage levels that are required for the ITER EDA.

Development of low- or reduced-activation materials is critical to achieving fusion's potential as a safe and environmentally attractive energy source. The development activities are focused on the most critical or limiting property of martensitic steels—the radiation-induced shift in ductile-to-brittle transition temperature (DBTT) and reduction of fracture toughness. Research is being conducted on vanadium alloys to determine their chemical compatibility with proposed fusion coolants and the effects of irradiation on their fracture toughness. From the viewpoint of induced activation, SiC is the ultimate fusion structural material. Monolithic SiC is not considered because of its fracture properties; thus, we are exploring the potential of SiC/SiC composites as fusion structural materials.

The effects of irradiation on the dielectric properties of ceramic insulators are of critical importance in the successful design and operation of numerous systems in a fusion reactor (e.g., rf heating, plasma diagnostics). Initial experimental work (initiated in 1991) has been directed at in situ measurements of the loss tangent during ionizing and ionizing-plus-displacive irradiation. Results show an increase in loss tangent of nearly two orders of magnitude at a displacement rate of 1×10^{-7} dpa/s. A change of this magnitude will affect materials selection and design of rf heating systems for ITER.

Graphite and carbon-carbon research activities are part of the plasma-interactive and high-heat-flux materials programs. Graphite and carbon-carbon composite materials are selected for these applications because their low Z number minimizes radiative heat losses from the plasma. However, their application requires graphite and carbon-carbon composites with extremely good thermal shock, erosion, and neutron damage resistance. Optimum thermal shock resistance is assumed to be offered by appropriately designed carbon-carbon composites (i.e., selected fibers, matrices, and architectures). Current work is directed toward the optimization of these materials for resistance to neutron damage.

Neutron Transport

The Neutron Transport program includes the work of the Radiation Shielding Information Center (RSIC) and cross-section evaluation and processing.

RSIC staff members serve as technical consultants to the fusion energy research community, as well as a variety of other research communities, on all matters relating to neutron transport. The evaluation and processing program is directed at producing accurate cross-section data for materials that are of specific interest to fusion reactor designers.

Nonfusion Applications

The ORNL Fusion Energy Division actively seeks opportunities to apply technology developed in the fusion program to other areas. Program initiation and development efforts will focus on areas in which the technology to be advanced is related to fusion, in that the majority of advances expected to result from the work will directly benefit future fusion system designs although the initial application may not be directly fusion-related.

The fusion technology development areas include plasma heating, plasma fueling, and magnetics and superconductivity. Technology applications are concentrated in four main

technical fields: energy, U.S. DOE facility environmental restoration and waste management, defense, and technology transfer to U.S. industry.

1

TOROIDAL CONFINEMENT ACTIVITIES

J. L. Dunlap, Toroidal Confinement Section Head

S. C. Aceto[1]
D. L. Akers[2]
E. Anabitarte[3]
F. S. B. Anderson[4]
G. C. Barber[5]
L. R. Baylor[6]
G. L. Bell[7]
J. D. Bell[8]
R. D. Benson[6]
T. S. Bigelow[5]
C. E. Bush
B. A. Carreras[9]
K. Carter[10]
L. A. Charlton[7]
T. L. Clark[12]
R. J. Colchin
M. J. Cole[6]
K. A. Connor[1]
M. J. Crouse[11]
N. Dominguez[9]
R. A. Dory[9]
G. R. Dyer
A. C. England
D. T. Fehling[9]
P. W. Fisher[13]
J. W. Forseman[6]
R. H. Fowler[8]
R. F. Gandy[7]
C. A. Giles[8]
D. C. Giles[8]
J. M. Gossett[12]
R. H. Goulding[5]
S. E. Grebenshchikov[14]
D. E. Greenwood[8]
C. L. Hahs[6]
G. R. Hanson[15]
J. H. Harris
G. R. Haste[5]
C. L. Hedrick[9]
M. A. Henderson[7]
G. H. Henkel
C. Hidalgo[3]
D. L. Hillis
S. Hiroe
S. P. Hirshman[9]
J. T. Hogan[9]
W. A. Houlberg[9]
H. C. Howe[9]
D. P. Hutchinson[16]
R. C. Isler
T. C. Jernigan
H. Ji[17]
L. M. Johnson[18]
R. L. Johnson[6]
G. H. Jones[6]
R. W. Jones[2]
H. Kaneko[17]
K. L. Kannan[8]
G. T. King[11]
C. C. Klepper
K. C. Klos[15]
L. M. Kovrizhnykh[14]
M. Kwon[15]
R. A. Langley
V. D. Latham[19]
E. A. Lazarus
J. N. Leboeuf[9]
D. K. Lee[8]
J. Lee[11]
U. P. Lickliter[6]
K. M. Likin[14]
J. W. Lue[20]
V. E. Lynch[8]
J. F. Lyon
C. H. Ma[16]
R. Maingi[21]
W. S. Mayfield[6]
T. J. McManamy[6]
M. M. Menon
P. K. Mioduszewski
S. Morita[1]
S. Morimoto[17]
R. N. Morris[8]
O. Motojima[17]
M. Murakami
G. H. Neilson
B. E. Nelson[6]
R. H. Nelson[6]
D. R. Overbey[9]
L. W. Owen[8]
S. L. Painter[11]
V. K. Paré[22]
T. C. Patrick[9]
J. L. Ping[6]
A. L. Qualls[11]
D. A. Rasmussen
T. F. Rayburn
T. M. Rayburn[11]
W. J. Redmond
T. L. Rhodes[10]
Ch. P. Ritz[10]
P. S. Rogers[11]
J. A. Rome[9]
M. J. Saltmarsh[23]
K. A. Sarksyan[14]
M. Sato[17]
C. R. Schaich
S. W. Schwenterly[20]
K. C. Shaing[9]
R. C. Shanlever[6]
M. G. Shats[14]
P. L. Shaw[15]
J. Sheffield[24]
T. D. Shepard[5]
J. E. Simpkins
P. N. Stevens[11]
K. D. St. Onge[6]
S. Sudo[25]
Y. Takeiri[17]
V. I. Tereshin[26]
C. E. Thomas[15]
J. S. Tolliver[8]
T. Uckan
W. I. van Rij[8]
M. R. Wade[15]
J. A. White[6]
J. B. Wilgen
C. T. Wilson[6]
W. R. Wing
R. J. Wood[6]
A. J. Wootton[10]
R. B. Wysor[6]
H. Yamada[17]
J. L. Yarber
J. J. Zielinski[1]

1. Rensselaer Polytechnic Institute, Troy, New York.
2. Section secretary.
3. Centro de Investigaciones Energeticas, Medioambientales, y Tecnologicas (CIEMAT), Madrid Spain.
4. University of Wisconsin, Madison.
5. Plasma Technology Section.
6. Engineering Division, Martin Marietta Energy Systems, Inc.
7. Auburn University, Auburn, Alabama.
8. Computing and Telecommunications Division, Martin Marietta Energy Systems, Inc.
9. Plasma Theory Section.
10. Fusion Research Center, University of Texas, Austin.
11. University of Tennessee, Knoxville.
12. Tennessee Technological University, Cookeville.
13. Chemical Technology Division.
14. General Physics Institute, Moscow, Russia.
15. Georgia Institute of Technology, Atlanta.
16. Physics Division.
17. National Institute of Fusion Science, Nagoya, Japan.
18. Management Services Group.
19. Maintenance Division, Y-12 Plant.
20. Magnetics and Superconductivity Section.
21. North Carolina State University, Raleigh.
22. Associate Division Director, Fusion Energy Division.
23. Division Director, Fusion Energy Division.
24. Plasma Physics Laboratory, Kyoto University, Uji, Japan.
25. Kharkov Institute of Physics and Technology, Kharkov, U.S.S.R.

1. TOROIDAL CONFINEMENT ACTIVITIES

Summary of Activities

The focus of the work in the toroidal confinement area changed dramatically during this reporting period because of a change in program emphasis by the Department of Energy from some support of research on alternate confinement concepts to strict concentration on tokamak research. There had been two major elements to the experimental confinement program in the Fusion Energy Division: the Advanced Toroidal Facility (ATF), the world's largest stellarator, and the Edge Physics and Particle Control (EPPC) program on various tokamaks. At the start of 1990, ATF was supported to contribute to fundamental toroidal confinement understanding of relevance to both tokamaks and stellarators, and the EPPC program was being carried out through collaborations on tokamaks in Germany (TEXTOR at Jülich), France (Tore Supra at Cadarache), and the United States (DIII-D at San Diego). At the end of 1991, ATF had been shut down, the EPPC program on DIII-D and Tore Supra had been expanded, and new collaborative research efforts had been started on the Princeton Beta Experiment (PBX-M) and Tokamak Fusion Test Reactor (TFTR) tokamaks at Princeton Plasma Physics Laboratory.

A major focus for studies in ATF has been energy confinement scaling and the identification of the mechanisms responsible for anomalous transport. Starting from gyro-Bohm scaling, the additional dependence of confinement on the dimensionless parameters collisionality ν_* and β has been investigated by modulating each of these parameters separately, revealing the additional favorable dependence, $\tau_E \propto \tau_{gB}\nu_*^{-0.18}\beta^{+0.3}$. Microwave scattering measurements of electron density fluctuations in the core of low-collisionality plasmas with electron cyclotron heating in ATF show features that might be evidence of trapped-electron instabilities. Modification of the energy and particle confinement times was studied by introducing magnetic islands and modifying the electric field in the plasma.

The EPPC program has focused on pressure scaling studies in the divertor baffle of DIII-D, particle balance and control studies in long-pulse operation in Tore Supra, helium transport and exhaust studies in TEXTOR and DIII-D, and edge fluctuation and biasing studies in ATF.

Reactor studies have focused on developing the tools needed for a realistic assessment of the cost of electricity expected for a stellarator reactor. Initial results indicate that torsatron reactors are competitive with conventional tokamak reactors if the same assumptions are used for both.

1.1 THE ATF PROGRAM

1.1.1 Overview

J. F. Lyon

Operation of the Advanced Toroidal Facility (ATF) was constrained by reduced funding during this report period, so most of the results were obtained in plasmas with only 0.2–0.4 MW of electron cyclotron heating (ECH). Most of the work focused on energy confinement scaling and the identification of the mechanisms responsible for anomalous transport. These studies included microwave scattering measurements of density fluctuations, dynamic variations of the magnetic configuration using modulation of dimensionless parameters, controlled introduction of magnetic islands, and biasing of movable limiters to affect the electric field in the plasma.

1.1.2 ATF Operations

T. C. Jernigan

During the two-year period covered by this report, ATF concentrated on operation over its entire operating envelope. Over 11,000 of ATF's total of 20,119 shots were accomplished during this period. Even with this emphasis on operation, a number of significant improvements were added to the device. These included extended-pulse operation (up to 20 s), feedback control of the line-averaged density, addition of a third gyrotron socket with a 200-kW, 35-GHz tube and magnet, installation and initial operation of one of the two 1-MW ion cyclotron range of frequencies (ICRF) transmitters, and installation of a microwave scattering experiment provided by the General Physics Institute in Moscow. These accomplishments were achieved despite significant funding reductions.

As a result of the reductions, maintenance was deferred except for essential items. The primary casualty was our neutral beam heating capability. By the end of operation in November 1991, only one neutral beam was operable, and only for short pulses (<0.1 s). During most of this reporting period, ATF was operated with only 0.2–0.4 MW of ECH at 53 GHz.

A significant failure in the helical field (HF) coil system occurred during this period. On May 30, 1991, an electrical arc occurred in one of the coil joints of the HF coil system, causing severe damage to two of the HF coil segments. Following an extended investigation of this incident, resumption of operation with a temporary repair was approved. ATF resumed operation on September 12, 1991. Operation was limited to 1 T with a repetition rate of about one shot every 10 min. A series of experiments on microwave scattering and ICRF heating was successfully completed, and ATF was shut down for a permanent repair on November 16, 1991. With the low level of funding available, the permanent repair to the HF coil will not be complete until mid-1993.

The maximum plasma parameters obtained (not simultaneously) during this period were central ion temperature $T_i(0) \approx$ 1 keV, central electron temperature $T_e(0) \approx$ 1.5 keV, line-averaged electron density $\bar{n}_e \approx 1.5 \times 10^{20}$ m^{-3}, energy confinement time $\tau_E \approx 30$ ms, and volume-average beta $\langle b \rangle \approx 1.7\%$. Sets of simultaneous plasma parameters for four operating regimes are shown in Table 1.1. The first three columns in Table 1.1 are results obtained using moderate levels of neutral beam injection (NBI). As noted, most of the operation during this period was obtained with 0.2–0.4 MW of 53.2-GHz ECH. Typical electron density and temperature profiles for ECH discharges are shown in Fig. 1.1. With ECH alone and helium (rather than the usual deuterium or

Table 1.1. ATF parameters for four different operating regimes

	Regime			
	High stored energy	High β	Low ν*	Long ECH pulse
B_0, T	1.9	0.45	1.9	0.95
$\bar{n}_e$, 10^{19} m^{-3}	11	4.3	0.53	0.5
P, MW	0.96	0.98	0.79	0.25
τ_E, ms	26	6.1	6.4	5.0
T_{e0}, keV	0.4	0.3	1.0	1.0
T_{i0}, keV	0.4	0.3	1.0	0.2
⟨β⟩, %	0.4	1.7	0.1	0.15
Duration, s	0.25	0.2	0.15	20

hydrogen) as the working gas, quasi-stationary discharges lasting for 20 s have been obtained with second harmonic ECH at $B_0 = 0.95$ T. There is no temporal increase of impurity radiation, as measured by either spectroscopy or a bolometer array [on loan from the Princeton Beta Experiment (PBX) group]. Such long-pulse operation allowed examination of the plasma response to different control parameters on a single-shot basis (without uncertainties caused by shot irreproducibility). Figure 1.2 shows results of dynamic configuration scans conducted during two 20-s ECH discharges. During one discharge, the vertical elongation (in the $\phi = 0°$ toroidal plane) was changed from 1.9 to 2.8; during the other, the elongation was changed from 1.9 to 1.3. The plasma current (bootstrap current) increases with increasing horizontal elongation and decreases with increasing vertical elongation, resulting in reversal of the current.

1.1.3 Confinement Studies

M. Murakami, R. A. Dory, T. S. Bigelow, B. A. Carreras, J. B. Wilgen, S. C. Aceto, L. R. Baylor, G. R. Dyer, A. C. England, J. H. Harris, H. C. Howe, D. P. Hutchinson,

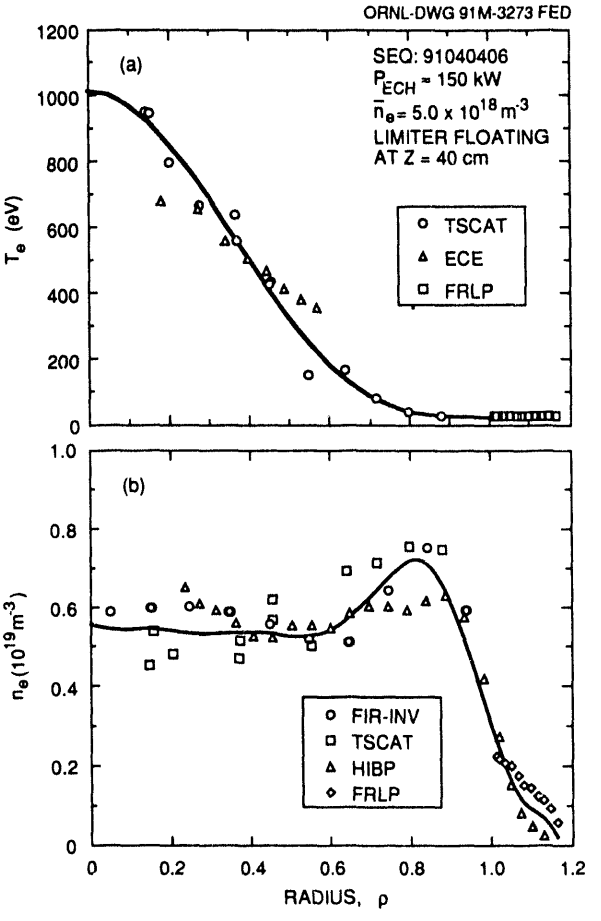

Fig. 1.1. Typical electron temperature and density profiles in ECH plasmas. (a) Temperature measured by Thomson scattering (TSCAT), electron cyclotron emission (ECE), and the fast reciprocating Langmuir probe (FRLP). (b) Densities measured by inversion of far-infrared interferometer (FIR-INV) signals, the heavy-ion beam probe (HIBP), TSCAT, and the FRLP.

R. C. Isler, T. C. Jernigan, H. Ji, C. H. Ma, S. Morimoto, O. Motojima, D. A. Rasmussen, M. Sato, W. R. Wing, H. Yamada, and J. J. Zielinski

Local transport analyses including measured electric fields indicate that electron energy transport in the confinement region (e.g., at the normalized radius $\rho \approx 2/3$) of ECH plasmas is substantially anomalous, while transport in the core region (e.g., $\rho \approx 1/3$) is close to the neoclassical predictions. Furthermore, electron heat diffusivity in the

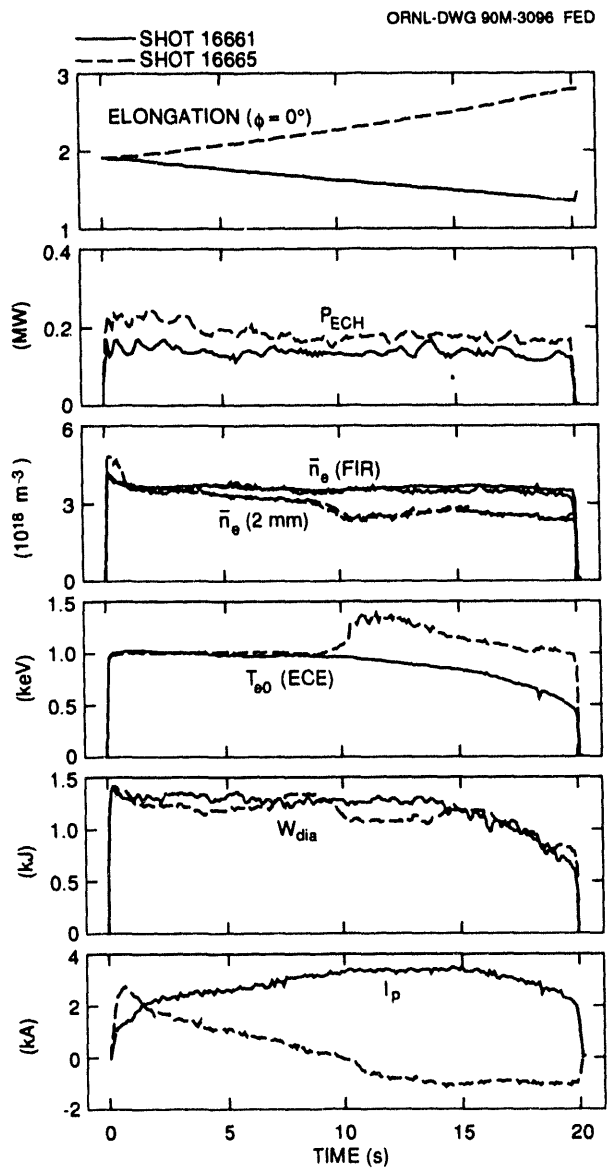

Fig. 1.2. Time histories of plasma parameters in two 20-s ECH discharges in which the configuration (elongation) was dynamically changed: vertical elongation in the $\phi = 0°$ toroidal plane; ECH power; line-averaged electron densities from the far-infrared (FIR) and 2-mm interferometers; central electron temperature from electron cyclotron emission (ECE) measurement; stored energy from diamagnetic measurement; and plasma current.

confinement region behaves in a manner expected from the global energy confinement. Since the latter can be measured more accurately than the former, studying the behavior of the global energy confinement time sheds light on anomalous transport mechanisms in the confinement region.

The product of the energy confinement time and the gyrofrequency Ω can be expressed in terms of a number of dimensionless variables,[1,2] in particular, the relative gyroradius $\rho_* = \rho_s/\bar{a}$, collisionality ν_*, plasma beta β, rotational transform ι, profile shapes of the plasma and heating power, etc. We focus on the dependence of the first three variables in the power law representation: $\tau_E\Omega \propto \rho_*^{\alpha_\rho}\, \nu_*^{\alpha_\nu}\, \beta^{\alpha_\beta}$. The ρ_* dependence reflects the turbulence scale length, ranging between long-wavelength and short-wavelength instabilities, which correspond to Bohm-like ($\alpha_\rho = -2$) and gyro-Bohm-like ($\alpha_\rho = -3$) scaling, respectively. The ν_* and beta dependences can help to elucidate the source of the turbulence by comparison with theoretical scaling.[2,3] Regression analysis of the ATF global database including both NBI and ECH data yields the exponents $\alpha_\rho = -2.8$, $\alpha_\nu = -0.41$, and $\alpha_\beta = +0.51$. This result is consistent with the conclusions of studies[4] that gyro-Bohm scaling is more closely followed than Bohm scaling. However, the determination of the ν_* and beta exponents tends to be less certain because of the problem of collinearity of the control variables and also the variation of other parameters (e.g., heating power profile shape).

To alleviate these problems, we conducted two specific ECH experiments. First, the magnetic field dependence in the global scaling was studied with second harmonic ECH (to produce similar power deposition profiles) using two different gyrotrons (53 GHz and 35 GHz for $B_0 = 0.96$ T and 0.64 T, respectively). Regression analysis of the results again shows $\alpha_\rho \approx -3.1$, indicating that the leading term is indeed gyro-Bohm-like. The second experiment was aimed at establishing the additional dependences to the gyro-Bohm scaling,[3,5] $\tau_E = \tau_{gB}\, \nu_*^{\alpha}\, \beta^{\gamma}$.

This involved modulation of one dimensionless variable (ν_* or beta) while keeping the other constant, which was accomplished by simultaneously modulating ECH power and electron density (with gas feedback) such that $\tilde{n}/n = (-2/3)\tilde{P}/P$ for ν_* modulation and $\tilde{n}/n = (4/9)\tilde{P}/P$ for beta modulation, both based on the gyro-Bohm scaling. Figure 1.3 shows the time evolution of global and local plasma parameters in the ν_* scan. Fourier analysis at the modulation frequency (12.5 Hz) shows that a modulation amplitude of 50% in ν_* (at $\rho \approx 2/3$) with a negligible beta modulation (3%) resulted in a modulation of 8% in the normalized confinement time, implying that $\alpha \approx -1/6$. Regression analysis on both the ν_* and beta scans yields $\alpha = -0.18$ and $\gamma = +0.36$ for the modification to the gyro-Bohm scaling. Application of the exact formula to the NBI and ECH data significantly improves the fit over that with the simple gyro-Bohm scaling, as shown in Fig. 1.4. The additional favorable beta and ν_* dependences indicate excellent prospects for improving confinement by increasing the heating power (implying higher beta and higher temperature) in ATF.

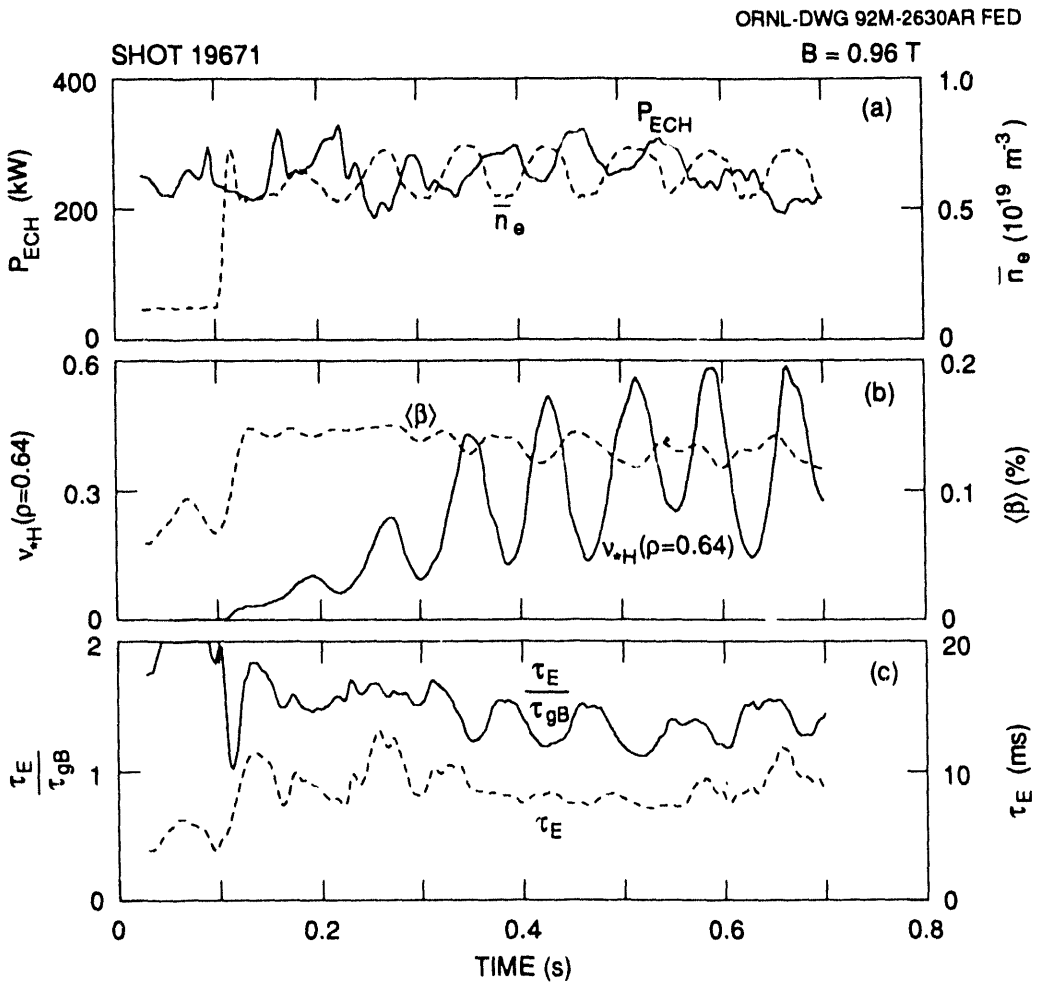

Fig. 1.3. Plasma parameters as a function of time for ν_* modulation with constant ⟨β⟩: (a) ECH power and line-averaged electron density, (b) local collisionality at $\rho = 0.64$ and volume-averaged beta, (c) energy confinement time and the confinement time normalized to gyro-Bohm scaling.

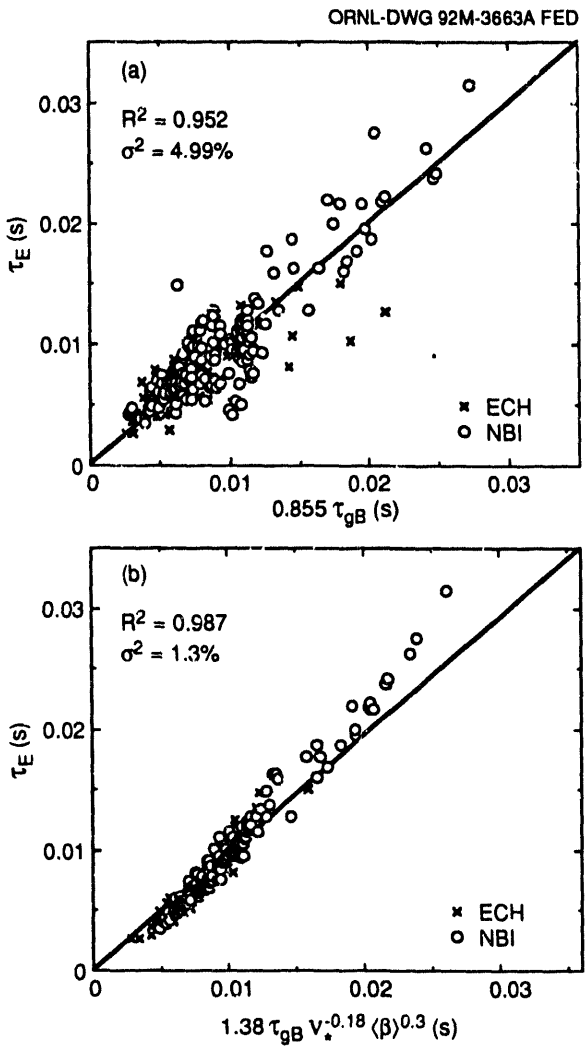

Fig. 1.4. ATF energy confinement time compared with (a) gyro-Bohm scaling and (b) modified gyro-Bohm scaling with the additional ν_* and β dependence.

In comparison with theoretical scalings,[3] dissipative trapped-electron mode (DTEM) models (developed for tokamaks) give an opposite dependence on ν_* (α = +0.4), implying that the DTEM may not govern the global confinement. However, the DTEM could play other roles (e.g., core confinement or constraining electron density profiles). A simple resistive magnetohydrodynamic (MHD) turbulence model shows that the ν_* dependence is close to the data (α = –0.4), but the beta dependence is opposite to that from the experiment. However, a more favorable trend of confinement with increasing beta may result from the modification of the curvature term by the beta self-stabilization.

The set of three vertical field coils on ATF allows variation in a controlled fashion of (1) the rotational transform, (2) the magnetic shear, (3) the magnetic field line curvature (as characterized by the radius of the magnetic well region), and (4) the confinement of trapped particles. Figure 1.5(a) shows the effect of sinusoidally modulating the radius of the magnetic well region [and, unavoidably (for low beta), the shear] while the confined trapped-particle fraction is held fixed. As the size of the magnetic well region expands, the plasma stored energy as measured by the diamagnetic loop [Fig. 1.5(b)] increases, and the confinement improves. Figure 1.5(c) shows the time variation of the electron temperature inferred from electron cyclotron emission (ECE) and also the plasma current, which is largely bootstrap current. The measured variation in the bootstrap current is consistent with neoclassical predictions for the magnetic configuration variation that is applied.[6]

The improvement of confinement with expansion of the magnetic well region is consistent with the interpretation that resistive interchange activity is dominating the confinement region, since interchange modes are stabilized by a magnetic well. Density fluctuation measurements showed radial behavior of $\tilde{n}/n$ consistent with theoretical predictions of resistive interchange modes. The shear also decreases as the magnetic well region expands, but the shear is most effective in stabilizing ideal interchange modes, whereas the magnetic well is effective in stabilizing resistive interchange modes. Difficulties in separating the effects of magnetic shear and well/hill can be mitigated by magnetic well broadening in higher-beta plasmas. Earlier experiments with centrally peaked pressure profiles (due

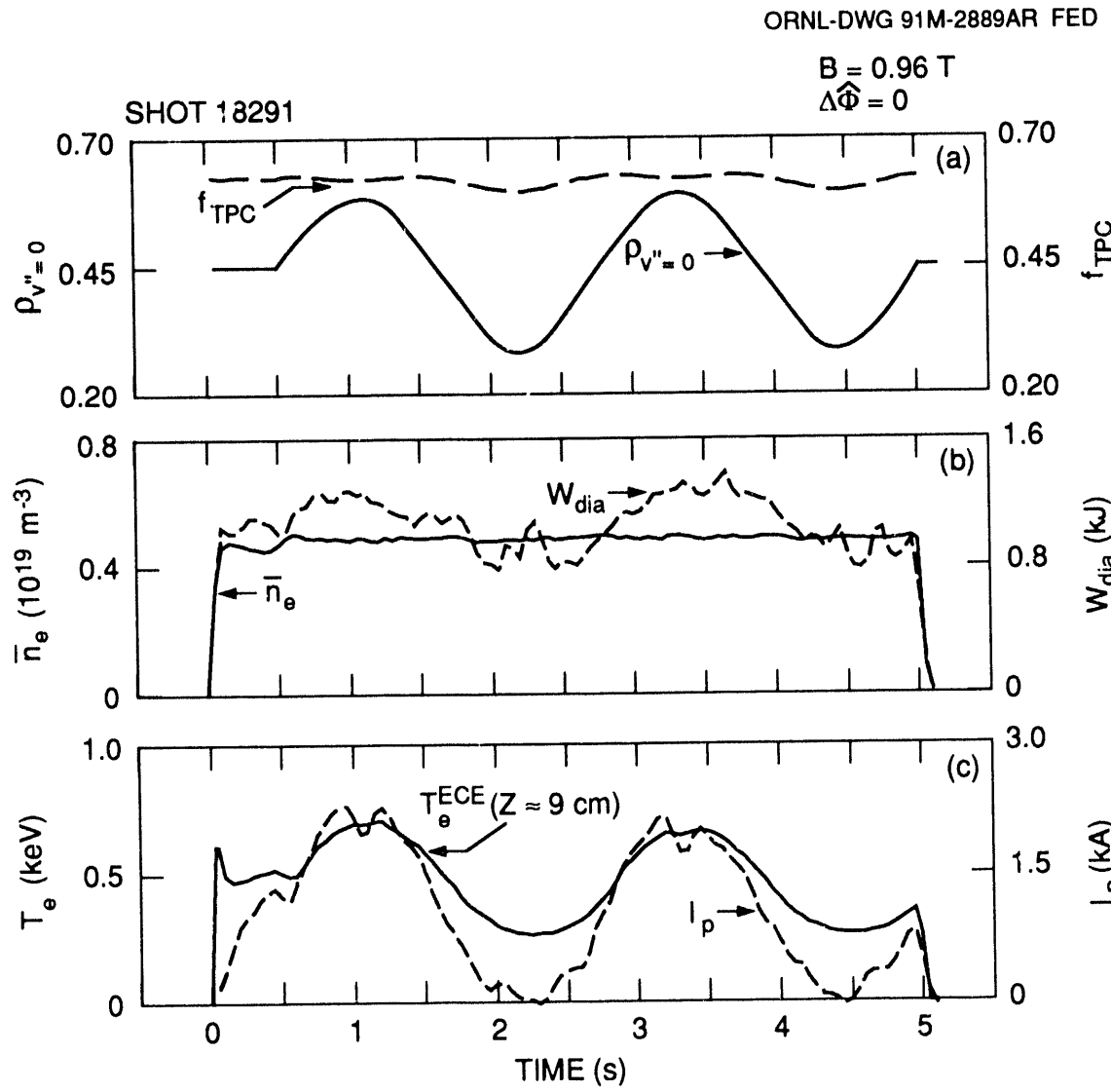

Fig. 1.5. Plasma parameters as a function of time for periodic modulation of the radius of the magnetic well region: (a) radius of the magnetic well region and the confined trapped-particle fraction, (b) line-averaged electron density and plasma stored energy, and (c) electron temperature and plasma current. The confined trapped-particle fraction f_{TPC} is held constant.

to field errors) showed suppression of interchange modes at relatively low beta ($\beta_0 \leq$ 1.5%), consistent with the theoretically predicted broadening of the magnetic well region with increasing beta, the so-called "beta self-stabilization" effect.[7] This is a plausible explanation for the favorable beta dependence observed in the confinement scaling studies, including the experiments involving the modulation of dimensionless parameters.

The confinement is far less sensitive to the fraction of confined trapped particles than to the magnetic well radius, indicating that if the DTEM is responsible for the observed internal fluctuations, they have little effect on transport. This result, together with the fact that the plasma relaxes to a state where the internal density gradients are small, suggests that the DTEM may control the density profiles by forcing the plasma to marginal stability.

Studies of electric field effects on confinement have been initiated with measurements of potentials using a heavy-ion beam probe and with limiter biasing experiments. Biasing the limiters negative with respect to the wall does not introduce significant perturbations of the plasma; positive biasing raises the particle confinement time by almost a factor of two, but with no appreciable increase in stored energy. The heavy-ion beam probe shows that the effect of this biasing leaves the general shape of the plasma potential unchanged but moves the velocity shear layer in the electron flow inward from $\rho \approx 1.1$ to the last closed flux surface (LCFS) at $\rho \approx 1.0$. The improvement in particle confinement is consistent with the idea that sheared flow reduces the radial transport and that moving the shear layer to the edge of the confined plasma creates a transport barrier at the edge.

Particle confinement, energy confinement, potential profiles, and fluctuation levels have also been investigated as a function of the size of magnetic islands that are deliberately introduced by means of error field coils. The largest structure is the $q = 2$ island, which has a maximum width of 7 to 10 cm. The particle confinement decreases by a factor of two as the islands grow, but if the electron density is maintained at a constant level by gas puffing, the energy confinement falls by only 20%. Even though the islands are spread over a large volume, the energy transport appears to depend more strongly on other factors. This may indicate that resistive interchange instabilities simply dominate other processes producing anomalous transport. The deliberate introduction of magnetic field errors steepens pressure profiles, validating the technique for accessing the second stability regime that was demonstrated in early ATF experiments.

1.1.4 Fluctuation Studies of ECH Plasmas

J. H. Harris, J. B. Wilgen, J. D. Bell, M. Murakami, B. A. Carreras, S. Aceto, L. R. Baylor, T. S. Bigelow, R. J. Colchin, J. L. Dunlap, N. Dominguez, G. R. Dyer, A. C. England, G. R. Hanson, R. C. Isler, T. C. Jernigan, L. M. Kovrizhnykh, J. N. Leboeuf, D. K. Lee, K. M. Likin, J. F. Lyon, C. H. Ma, D. A. Rasmussen, K. A. Sarksyan, M. Sato, M. C. Shats, C. E. Thomas, and J. Zielinski

An important element of the ATF program during this reporting period was the study of turbulent fluctuations in long-pulse (1- to 30-s), low-collisionality ECH discharges [$B_0 = 0.94$ T, $\bar{n}_e \approx (4\text{–}7) \times 10^{12}$ cm^{-3}, $T_e(0) \approx 1$ keV]. These plasmas are macroscopically quiet but exhibit anomalous outward transport (gyro-Bohm-like scaling) very much like that seen in tokamaks, suggesting that the underlying transport mechanisms in the two types of toroidal plasmas are similar.[8] The flexible magnetic configuration of ATF makes it possible to change (even within a single shot) properties—rotational transform, magnetic well, shear, trapped-particle confinement—that are expected to influence turbulence and transport.

An array of fluctuation diagnostics has been developed and installed on ATF through long-term collaborations with other institutions. These diagnostics include a heavy-ion beam probe, a microwave reflectometer, a fast reciprocating Langmuir probe and, most recently, a 2-mm microwave scattering diagnostic. Together, these diagnostics make it possible to measure fluctuation amplitudes and other characteristics from the core of the plasma to the edge. During this operating period, fluctuation

data from the various diagnostics have been combined to yield a picture of the turbulence as a function of normalized radius ρ, which can be compared with some theoretical concepts (see Fig. 1.6).

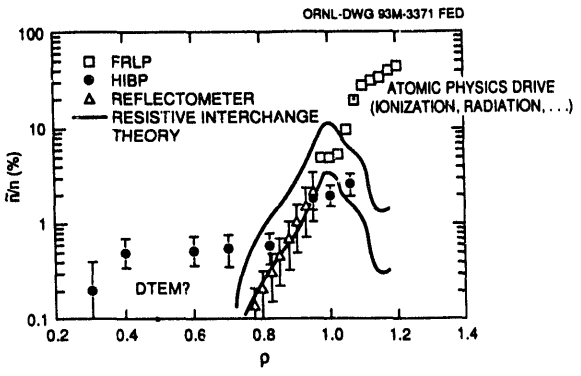

Fig. 1.6. Radial profile of normalized density fluctuations in an ECH plasma.

The edge plasma fluctuations show characteristics similar to those seen in tokamaks, provided that the radial position is normalized to the radius of the velocity shear layer.[9] This supports the hypothesis that drive mechanisms that do not depend on the plasma current (e.g., radiation, ionization, charge exchange) are responsible for the observed edge turbulence. Experiments with limiter biasing support earlier findings regarding the characteristics of the velocity shear layer and its role in edge turbulence.

In the gradient region, $0.7 \leq \rho \leq 0.9$, the fluctuations exhibit significant radial correlation lengths $L_c = 2$–5 cm and no radial propagation ($k_r \approx 0$). The measured fluctuation amplitudes $\tilde{n}/n$ are smaller than those predicted by simple mixing length estimates by a factor of 2–10, but are comparable to amplitudes predicted theoretically[10] for resistive interchange turbulence driven by the unfavorable average magnetic curvature in this region. Single-shot configuration variations that vary the magnetic curvature during a discharge indicate that this region governs the overall energy confinement in ATF: global confinement improves as the volume of the magnetic well region expands. This supports the conclusions of early high-beta experiments[7] on ATF that demonstrated transient access to the second stability regime for interchange instabilities.

In the plasma core, measurements using 2-mm microwave scattering[11] show features like those expected for DTEMs. Signals from scattering volumes on the small-major-radius side of the torus, where helically trapped particles are well confined, show features in the density fluctuation spectrum for $k_\theta \rho_s \sim 1$ that are absent in the fluctuation spectra measured on the large-major-radius side of the torus, where helically trapped particles are poorly confined (see Fig. 1.7). Plasma operation near the marginal stability condition for such instabilities could conceivably account for the persistence of flat and hollow density profiles in stellarator experiments (including ATF) with ECH alone.

1.1.5 Pellet Injection in ATF

A. L. Qualls, J. B. Wilgen, and P. N. Stevens

Pellet injection experiments in ECH plasmas in ATF focused on two main topics: (1) pellet ablation and particle deposition and (2) plasma thermal collapse and recovery induced by pellet injection.

The pellet fueling efficiency, defined as the ratio of the number of atoms in a pellet before it enters the plasma to the number of electrons added to the plasma, was estimated to be 73%. The rate of D_α emission from the pellet ablation was independent of the mass of the pellet, and the intensity of the emission coupled with the calculated position of the pellet in the plasma was not indicative of the measured particle deposition.

The injection of a properly sized pellet leads to a reproducible response in which the plasma stored energy collapses. As the

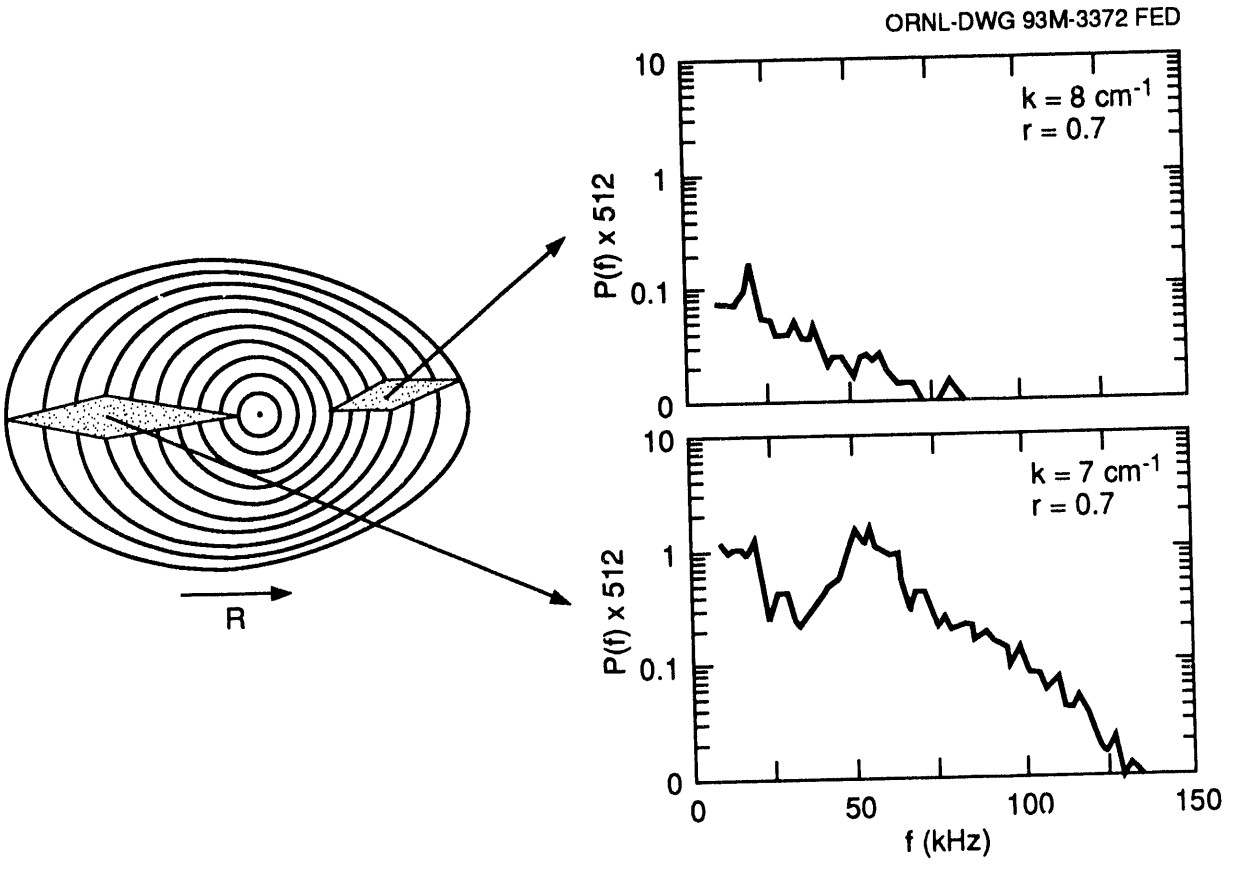

Fig. 1.7. Scattered 2-mm microwave signals from inboard and outboard scattering volumes in an ECH plasma.

plasma density recovers, it remains higher than the prepellet density and the central electron temperature increases. This is followed by a relaxation of the density to the prepellet value. The relaxation of the density to the prepellet value occurs in two stages. First the density profile broadens, and then the temperature profile broadens. The evolution of the pressure profile in the plasma is consistent with the hypothesis that the broadening of the density profile is due to unfavorable pressure gradients that occur in the plasma as the stored energy recovers. The actual loss of particles is due to the establishment of a new equilibrium between the particle confinement time and the amount of edge recycling that occurs as the temperature increases in the edge region of the plasma.

1.2 EDGE PHYSICS AND PARTICLE CONTROL PROGRAM

P. K. Mioduszewski (Program Manager), D. L. Hillis, J. T. Hogan, C. C. Klepper, R. Maingi, M. M. Menon, L. W. Owen, T. F. Rayburn, J. E. Simpkins, C. E. Thomas, T. Uckan, and M. R. Wade

The Edge Physics and Particle Control (EPPC) Program addresses issues related to the characterization of the plasma boundary, plasma interactions with the wall, and techniques for edge modification aimed at the improvement of plasma performance. This includes optimization of wall conditioning for particle and impurity control, as well as plasma edge properties, pump limiter and divertor operation for density control, confinement improvement, and helium ash

exhaust. Collaborations with DIII-D, Tore Supra, and TEXTOR offer opportunities to study these issues in both divertor and limiter machines. In addition, fundamental studies on edge transport mechanisms are carried out in ATF.

During the reporting period, activities were focused on pressure scaling studies in the divertor baffle of DIII-D, particle balance and control studies in long-pulse operation in Tore Supra, helium transport and exhaust studies in TEXTOR and DIII-D, and edge fluctuation and biasing studies in ATF.

1.2.1 The Collaborative DIII-D Advanced Divertor Program

1.2.1.1 Divertor baffle optimization and pressure scaling studies in DIII-D

C. C. Klepper, J. T. Hogan, R. Maingi, P. K. Mioduszewski, L. W. Owen, and J. E. Simpkins

During the design phase of the DIII-D divertor baffle, the DEGAS neutral transport code was used for optimizing the divertor baffle configuration with respect to maximum particle throughput and for estimating the energetic particle power load on the cryoloop.[12] A typical result of these studies is shown in Fig. 1.8, which illustrates the effect of changing the divertor throat opening on the exhaust throughput for two different pumping speeds.

During the first phase of the experimental program, the emphasis of the ORNL contribution was on scaling studies of the divertor pressure without pumping.[13] The first experiments were aimed at optimizing the divertor strike point location with respect to the maximum divertor pressure (see Fig. 1.9 and ref. 13 for details of the divertor baffle configuration). A typical pressure response during a strike point sweeping experiment is shown in Fig. 1.10. The pressure reaches a maximum as the strike point

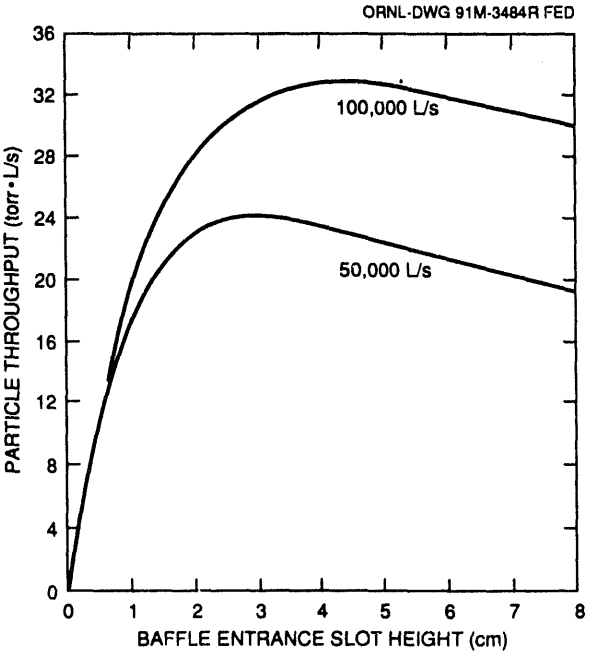

Fig. 1.8. Particle exhaust throughput as a function of the divertor throat opening for pumping speeds of 50,000 L/s and 100,000 L/s.

approaches the baffle, assumes a minimum when the strike point is on top of the baffle ring, and finally goes through a maximum again as the strike point is removed from the baffle. The achieved pressure maxima as functions of the strike point location are depicted in Fig. 1.11 for various values of the neutral beam power. The optimum separation increases with input power and reaches about 3 cm for 14 MW of neutral beam power. The scaling experiments showed that baffle pressures of up to 15 mtorr could be achieved.

Results from the neutral beam power scaling experiment, measuring the baffle pressure for a fixed strike point location, are shown in Fig. 1.12. A version of the B2 plasma edge code was applied to the analysis of the scaling experiments, in concert with DEGAS calculations. Estimates of expected pressures made during the conceptual design phase indicated $p \sim 1$ mtorr (without pumping); these estimates, however, were made before B2 modeling for the

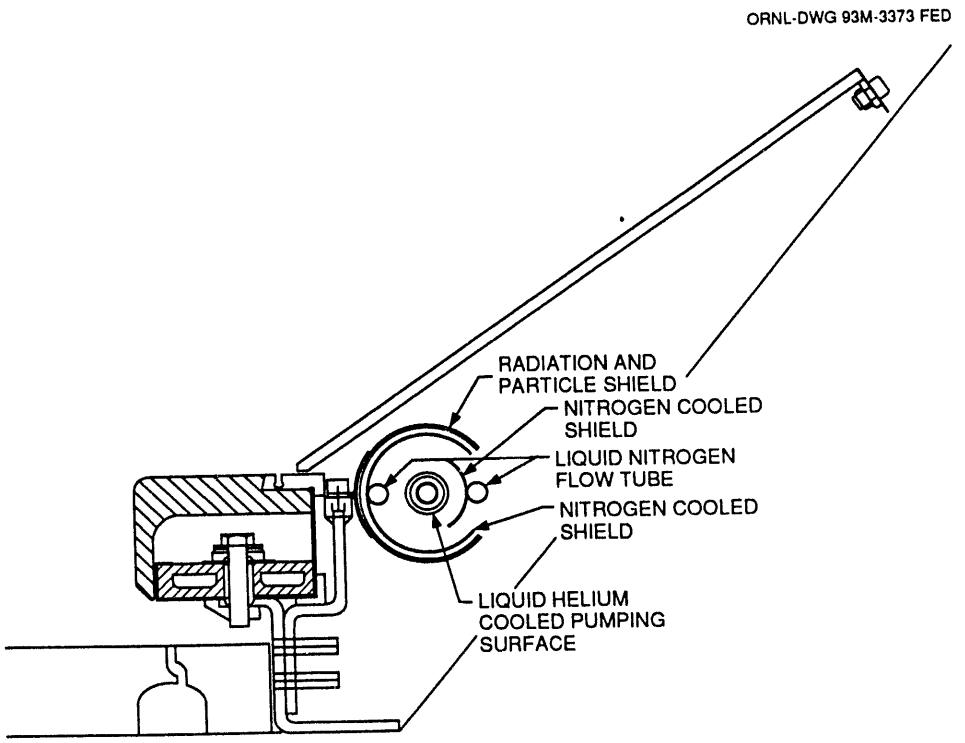

Fig. 1.9. Configuration of the cryopump inside the baffle chamber.

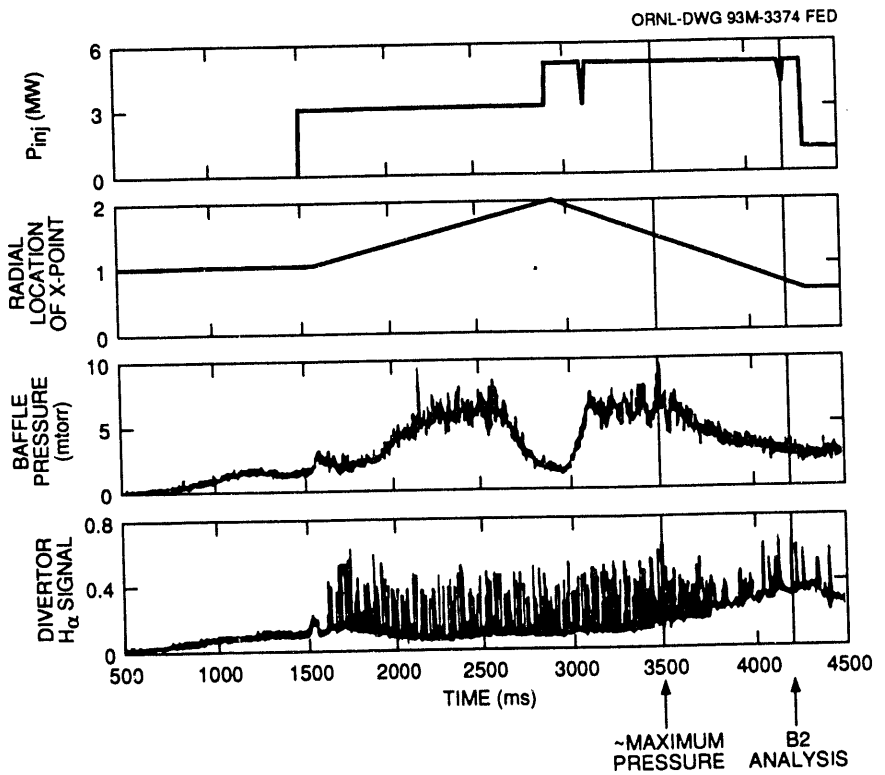

Fig. 1.10. Some typical traces of an X-point sweeping experiment (top to bottom): neutral beam power, position control signal for the radial position of the X-point, neutral pressure under the baffle, and divertor H_α signal.

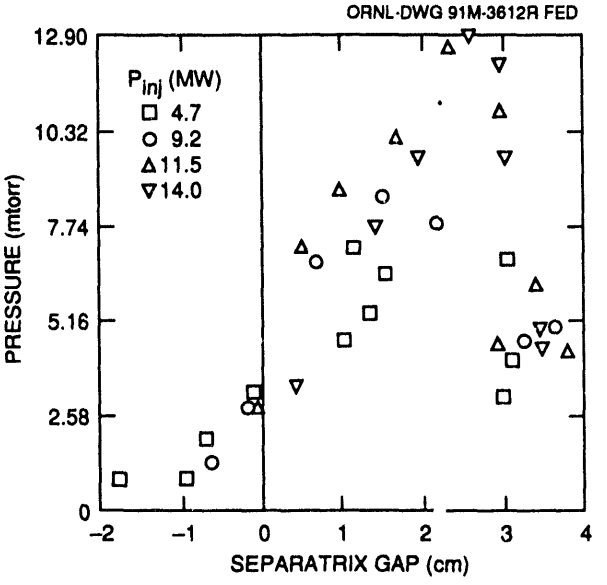

Fig. 1.11. Dependence of the neutral pressure on the gap distance between separatrix and baffle ring for various values of neutral beam injection power.

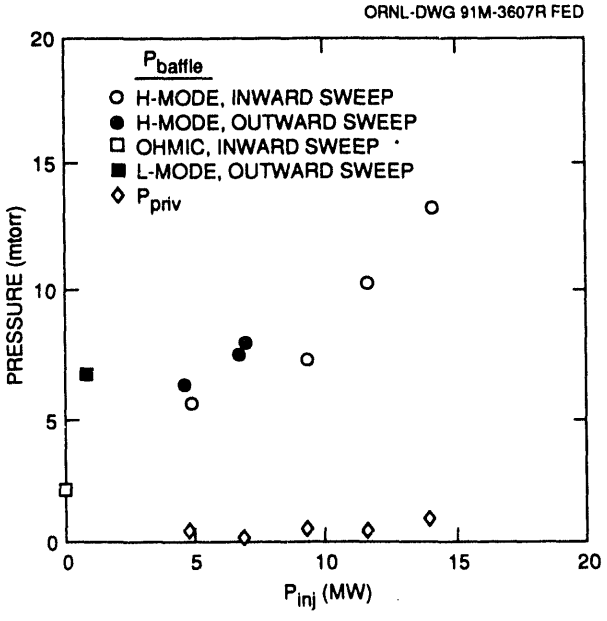

Fig. 1.12. Dependence of the baffle pressure on the neutral beam injection power. The pressure in the private flux region is also shown.

divertor pressure. The B2 calculations used heat flux measurements taken with an infrared television (IRTV) system and Thomson scattering data in the scrape-off layer (SOL) to calibrate the plasma transport model. The DEGAS results, which now use the B2 fluxes, indicate $p \sim 5$ mtorr for P_{NB} = 7 MW (experimentally $p = 7.5$ mtorr) and $p \sim 8$–14 mtorr for $P_{NB} = 14$ MW (experimentally 12 mtorr). The remaining discrepancy is very sensitive to details of the n_e and T_e distributions in the wings of the scrape-off layer, and efforts to obtain information about these profiles are under way.

DEGAS predictions of particle exhaust with the Advanced Divertor Program (ADP) cryopump indicate that approximately 50% of the neutrals entering the baffle are pumped. The neutral flux itself, however, depends sensitively on the divertor plasma response to active pumping. The effects of baffle pumping on the divertor plasma are being investigated with the B2 code and with an internal recycling model on the DEGAS code. Once these effects are known or predicted, better estimates of the particle throughput can be made with self-consistent plasma/neutral transport calculations.

Diagnostics of the divertor area have been improved by installing a capacitance manometer to measure absolute pressures under the baffle as well as in the private flux region. The manometer has provided independent pressure measurements and increased the confidence in the earlier measurements from the ASDEX-type gages. The capacitance manometer was also used during the gaseous divertor experiments to confirm the very high pressures in the private flux region, indicated by the saturation of the ASDEX-type gages. A combination of the ORNL divertor spectrometer with the fast optical multichannel analyzer (OMA) provided by General Atomics was successfully used to monitor carbon impurities (C III) in the X-point region.

These studies were performed in collaboration with the DIII-D Group of General Atomics, San Diego, California.

1.2.1.2 D' vertor pumping

M. M. Menon, L. W. Owen, and P. K. Mioduszewski

A particle exhaust scheme using a cryocondensation pump in the ADP configuration of the DIII-D tokamak is being designed. In this configuration, the pump is located inside a baffle chamber within the tokamak, designed to receive particles reflected off the divertor region. A liquid helium (LHe) loop with forced convection flow of two-phase helium is selected as the cryocondensation surface. The details of optimization of the pumping configuration and the heat loading contributions as a result of operating close to the tokamak plasma are described in ref. 14. A cross-sectional view of the cryopump in the baffle chamber is shown in Fig. 1.9. The LHe-cooled tube has an outer diameter of 2.5 cm and a toroidal length of about 11 m. The estimated pumping speed in the configuration shown in Fig. 1.9 is about 50,000 L/s.

In the original design, the pump is electrically isolated from the tokamak vacuum vessel and forms a loop that is discontinuous in the middle. In this configuration, recent estimates of the voltages developed on the pump during plasma disruptions yield values up to 500 V. By grounding the midpoint of the pumping loop, the effective voltage could be reduced to half this value. Nevertheless, the voltages induced are uncomfortably close to Paschen's minimum (about 300 V for deuterium). With the possible presence of a tenuous plasma in the baffle chamber, there is a concern that a Paschen-type breakdown could result along the magnetic field lines connecting the pump and its grounded surroundings. Such a breakdown could produce large currents flowing through portions of the pump; these currents, when crossed with the toroidal field, would generate large forces on the pump. On the other hand, a toroidally continuous closed-loop configuration of the pump would result in large resistive losses to the helium from voltages and currents induced during plasma current ramps. A closed loop would also place large forces on the pump during plasma disruptions. A detailed structural analysis is under way to see if a continuous version can be made rugged enough to withstand the disruption forces.

Apart from mechanical considerations, a toroidally continuous cryopump design would entail larger heat loadings on the pump, and this could elevate the temperature of the pumping surface. Calculations were carried out to determine the effect of surface temperature on the pumping speed. The results, for a plane parallel geometry, are shown in Fig. 1.13. The pumping speed for deuterium begins to drop significantly when the surface temperature exceeds 6 K. Similar calculations for hydrogen show deterioration in the pumping speed when the temperature exceeds 4.6 K. Experiments are under way on a cryogenic test loop to determine the surface temperatures under different pulsed load conditions.

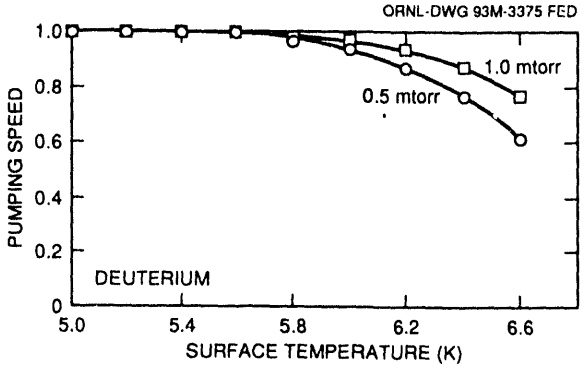

Fig. 1.13. Pumping speed for deuterium as a function of the temperature of the cryopump surface for pressures of 0.5 and 1 mTor .

This work was performed in collaboration with the DIII-D Group of General Atomics, San Diego, California.

1.2.1.3 Helium transport studies in DIII-D

D. L. Hillis, M. R. Wade, J. T. Hogan, C. C. Klepper, and P. K. Mioduszewski

To explore the helium transport in a divertor H-mode plasma, similar to that proposed for the International Thermonuclear Experimental Reactor (ITER), a collaborative program between ORNL and General Atomics was initiated in 1991 to measure helium transport and scaling on DIII-D during plasma conditions that include L-mode, H-mode, VH-mode, and H-mode with edge-localized mode (ELM) events.

To simulate the presence of helium ash in DIII-D, a 25-ms helium puff is injected into a DIII-D plasma, resulting in a helium concentration of ≈5%. The time dependence of the He^{2+} density profiles is measured with the charge-exchange recombination (CER) spectroscopy system on DIII-D. As presently configured, the CER system provides a total of 31 chords that view across two neutral beam lines and thereby can provide up to 31-point radial He^{2+} density profiles. Absolute calibration of the sensitivity of each chord has been accomplished using standard calibration lamps, supplemented with techniques involving (1) injection of the neutral beam into a gas-filled torus and (2) NBI into a pure helium plasma.

The DIII-D plasma for these experiments had a major radius R = 1.67 m, a plasma current I_p = 1.6 MA, a toroidal magnetic field of 2.1 T, and boronized walls. The magnetic configuration was a double-null divertor discharge. The D^0 beams were injected between 1.8 s and 3.8 s after discharge initiation, with a short (25-ms) helium puff injected at t = 2.3 s. Figure 1.14 contains individual time slices of the helium spatial profile from an L-mode shot at times just before (t = 2.28 s), just after (t = 2.36 s), and well after (t = 2.70 s) the helium gas puff at 2.3 s. The solid lines of Fig. 1.14 are spline

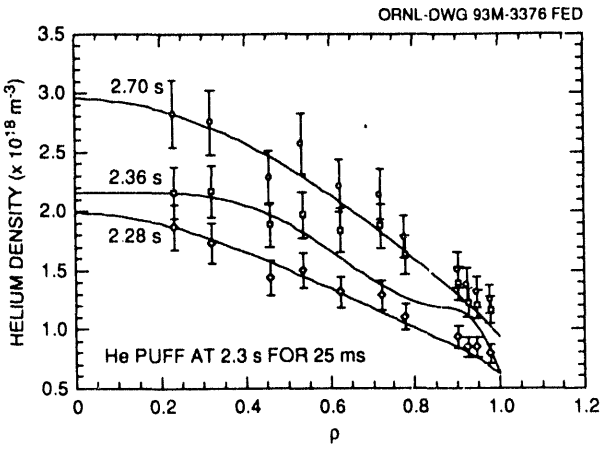

Fig. 1.14. Helium density profiles as measured by CER on DIII-D vs the normalized radius ρ at t = 2.28 s, just before the gas puff; t = 2.36 s, just after the gas puff; and t = 2.70 s, well after the gas puff. A 25-ms helium gas puff was injected at t = 2.3 s. Points are helium density profiles measured by CER; solid lines are spline fits to the Thomson scattering measurements of the electron density. The electron density profiles have been normalized to the helium density data at r = 0.23 to compare the shapes of the profiles.

fits to the Thomson scattering measurements of the electron density profile, which have been normalized to the CER helium density measurements at r = 0.23, such that the shapes of the helium density and electron density profiles can be compared. Clearly, the electron density and helium density profiles have similar shapes for the "steady-state" profiles at 2.28 s and 2.70 s. Some departure of the helium density data is noted during the period just after the gas puff at t = 2.36 s. However, this difference may be influenced by the fact that the Thomson measurement is an instantaneous measurement, while the CER measurement is integrated over 10 ms. The value ρ = 0 indicates the magnetic axis of the discharge, and ρ = 1.0 indicates the separatrix.

The influence of ELMs on the helium density profile was studied in an H-mode discharge with giant ELMs, shown in Fig. 1.15. The helium density profiles are displayed in Fig. 1.15 for the period of time

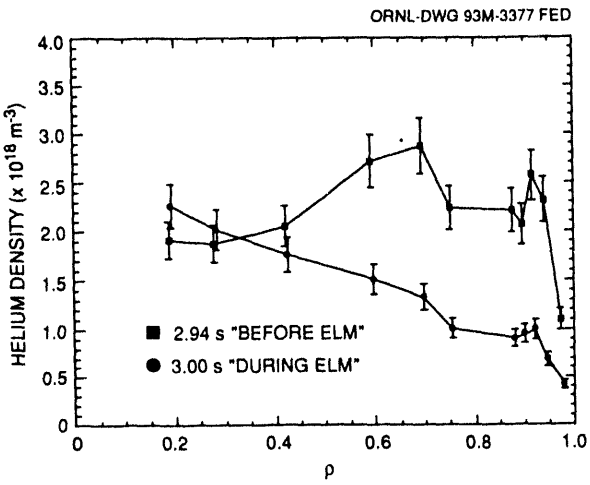

Fig. 1.15. Helium density profile, as measured by CER, vs ρ just before and during a giant ELM occurring at 3.0 s in an H-mode discharge.

just before (t = 2.94 s) and during a giant ELM at 3.0 s. From this preliminary investigation of the influence of ELMs on helium transport in DIII-D, the helium density profile suggests that helium is lost from the edge plasma for radii $r > 0.5$, while the profile is not affected for $r < 0.5$. The signal from a helium photodiode that views the DIII-D divertor region also indicates that when helium is purged from the core plasma edge, the He^+ line emission from the divertor increases abruptly, suggesting an increase in the divertor helium content. If helium pumping were provided in the baffle region, this helium could be removed. Further investigations are under way to investigate in greater detail the helium transport during ELMing H-mode plasmas on DIII-D.

Our current DIII-D experiments indicate that ELMs modify the helium radial profiles and that this effect can be used to improve helium pumping in a divertor tokamak. As part of the ADP on DIII-D, a cryopump will be installed in late 1992. In principle, the cryopump could be conditioned with an argon frost layer to provide helium pumping. This will permit measurements of both τ^*_{He} and τ_{He}, similar to those done previously during the TEXTOR experiments with active helium pumping. Future experiments on DIII-D should help to determine the pumping efficiencies required in a divertor configuration to meet the requirement that $\tau^*_{He}/\tau_E < 7–15$ (see Sect. 1.2.2).

This work was performed in collaboration with W. P. West, K. H. Burrell, C. M. Greenfield, P. Gohil, R. J. Groebner, J. Kim, and R. P. Seraydarian of General Atomics, San Diego, California, and D. Finkenthal of the Department of Nuclear Engineering, University of California, Berkeley, California.

1.2.2 Helium Transport and Exhaust Studies in TEXTOR

D. L. Hillis, J. T. Hogan, C. C. Klepper, and P. K. Mioduszewski

Estimates show that helium ash in a fusion reactor must be removed at a rate corresponding to $\tau^*_{He}/\tau_E < 7–15$ to maintain continuous reactor operation.[15] The results of helium transport and removal experiments in L-mode discharges in TEXTOR have been reported previously.[16,17] Here, we report on a series of helium experiments on TEXTOR in an enhanced confinement regime produced by an edge polarization electrode.[18] The results are compared with those found in L-mode discharges. We simulate the presence of recycled helium ash in a tokamak plasma by puffing concentrations of 3–5% He into the TEXTOR plasma just before or during NBI. The experiments are restricted to relatively low levels of neutral beam power (<200 kW) by the heat transfer limitations of the electrode. The transport of the helium into the plasma core and its subsequent pump-out using the Advanced Limiter Test–II (ALT-II) system are followed with spectroscopic techniques.

In the plasma core, the helium density is measured by charge-exchange excitation (CXE) spectroscopy in combination with

NBI. CXE spectroscopy is used to obtain the local He^{2+} density in the plasma core at two locations along the minor radius (r = –4 and 25 cm). The TEXTOR plasma for these experiments had a major radius R = 175 cm, a plasma current I_p = 190 kA, a toroidal magnetic field of 2.25 T, and boronized walls. To provide active CXE measurements, a 115-kW H^0 beam was injected between 0.8 s and 2.8 s after discharge initiation, with a short (10-ms) helium puff injected at t = 1.0 s, causing a rise in the average electron density. Typically, the central electron temperature $T_e(0) \approx 1.0$ keV.

In Fig. 1.16 the He^{2+} density vs time is shown at two radial locations within the plasma core (r = –4 and 25 cm) with full pumping of ALT-II and with [Fig. 1.16(a)] and without [Fig. 1.16(b)] a +900-V bias applied to the polarization electrode. For the discharges shown in Fig. 1.16(b), the polarization bias is applied between 0.8 s and 2.8 s with a 10-ms helium puff at 1.0 s. For the case without pumping (not shown), the He^{2+} density remains constant after the initial rise, indicating full recycling of the helium (recycling coefficient $R_{He} \approx 1.0$). For the L-mode discharges with full ALT-II pumping reported in ref. 16, the He^{2+} density drops rapidly and ≈90% of the helium puffed into the discharge is exhausted within ≈1.0 s. The helium density in an L-mode

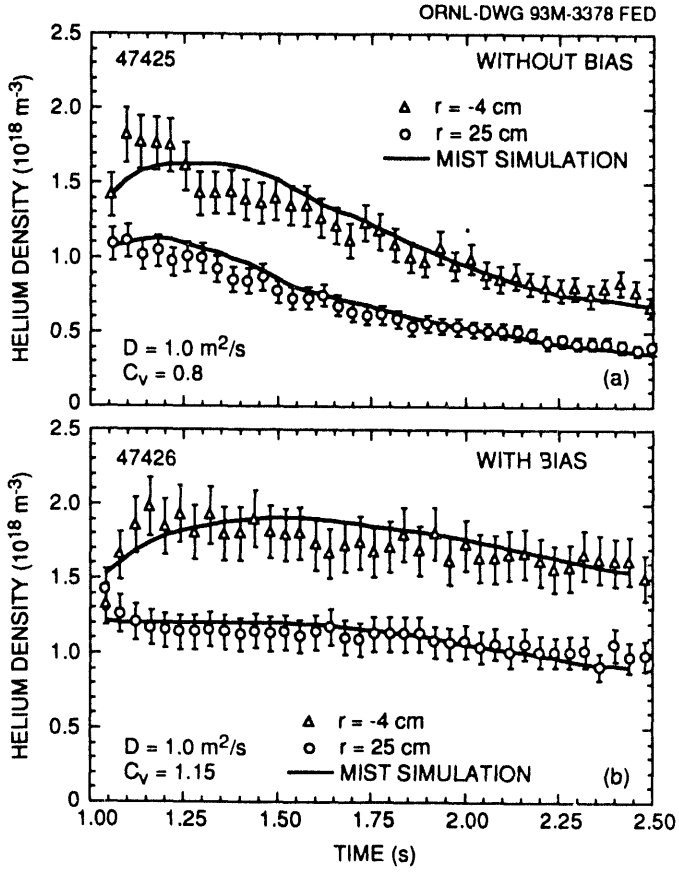

Fig. 1.16. (a) Helium density measured via CXE spectroscopy on TEXTOR vs time for two radial locations (r = –4 and +25 cm) for shot 47425 after a short helium puff at 0.6 s with full ALT-II pumping and without bias applied to the polarization electrode. (b) Helium density under the same conditions, but with a +900-V bias voltage applied to the polarization electrode. Data points: He^{2+} data, solid lines: MIST transport calculations with R_{He} = 0.92, D_A = 1.0 m^2/s, C_v = 0.8 for shot 47425 and C_v = 1.15 for shot 47426.

discharge similar to that reported in ref. 16 with full ALT-II pumping is also shown in Fig. 1.16(a).

When +900 V is applied to the polarization electrode ($t \approx 0.8$–2.8 s), a clear transition to an enhanced confinement regime is achieved. This regime (H-mode-like behavior) is evidenced by a strong increase in $\bar{n}_e$ and a sharp decrease in the D_α signal, both of which indicate an increase in the deuterium particle confinement time. In Fig. 1.16(b), the He^{2+} density measured in the plasma core by CXE is shown for this enhanced confinement condition, where ELMs were not present. Clearly, the He^{2+} density in Fig. 1.16(b) remains almost unchanged throughout the plasma discharge during both NBI and the biasing phase of the polarization electrode, even though full ALT-II pumping is applied. This is consistent with the observation that little helium is being conducted into the pumping duct. The data of Fig. 1.16(b) can be used to determine the helium particle confinement time, τ^*_{He}, from the decay of the helium density. For the L-mode case of Fig. 1.16(a), there was no electrode biasing and $\tau^*_{He} \approx 1.2$ s. In the enhanced confinement case of Fig. 1.16(b), with polarization bias applied, $\tau^*_{He} \approx 3.2$ s. The energy confinement time for both of these discharges is $\tau_E \approx 0.045$ s. The data in Fig. 1.16 have been modeled with the Multiple Impurity Species Transport (MIST) code[19] to determine the anomalous diffusivity D_A and the pinch coefficient C_v. The transport coefficients needed to match the helium evolution were $D_A \approx 1.0$ m^2/s and $C_v \approx 0.8$ for the L-mode discharge [Fig. 1.16(a)] and are similar to those found in earlier transport experiments.[20] For the enhanced confinement mode, $D_A \approx 1.0$ m^2/s is again found to match the profiles, while C_v must be increased to 1.15 if $R_{He} = 0.92$ as was found for the earlier L-mode measurements.

In summary, these helium transport experiments, in conjunction with the ALT-II pumping system, have provided a first estimate of fundamental helium transport processes under conditions where both recycling and the confinement mode are varied. The experimental data have shown that helium exhaust and transport mechanisms may be significantly different in the two confinement modes. When helium is puffed into the L-mode-type discharges, it quickly appears in the plasma core and is transported to the plasma boundary, where it is removed within about 1 s by the ALT-II pump limiter. For the enhanced confinement plasmas, on the other hand, the He^{2+} is maintained within the plasma core for longer periods of time (2–3 times τ^*_{He} in L-mode). For these plasmas the helium pressures in the pumping duct were found to decrease by a factor of two to four compared with similar L-mode conditions. However, with the appearance of large ELM-like fluctuations, the helium pressure in the duct did increase. Transport modeling has shown that, when the diffusivity is kept fixed, the inward pinch coefficient C_v, which characterizes the peaking of the helium density profile relative to the n_e profile, increases under enhanced confinement conditions. More detailed knowledge of the helium radial profile as a function of time during the helium influx and pump-out phase is needed to determine C_v and D_A uniquely. From these data for the ALT-II configuration, the polarization-induced enhanced confinement regime increases τ^*_{He}/τ_E to about 70, as compared to the L-mode value of 9–20. These measurements suggest that helium removal may be more difficult in the enhanced confinement regimes of future burning plasmas than in L-mode plasmas. However, neither the control of the particle confinement via ELMs nor the control of the sawtooth frequency was tested in these experiments. The CXE

spectroscopy system on TEXTOR is currently being upgraded to provide up to 15-point radial helium profiles.

These studies have been performed in collaboration with K. H. Dippel, H. Euringer, K. H. Finken, A. Pospieszczyk, D. Reiter, D. Rusbüldt, and G. Wolf of the Institut für Plasmaphysik, Association Euratom-KFA, Forschungszentrum Jülich, Jülich, Germany; W. Y. Baek, A. M. Messiaen, R. van Nieuwenhove, G. van Oost, and R. R. Weynants of the Laboratoire de Physique des Plasmas/ Laboratorium voor Plasmafysica, Association "Euratom-État Belge"/Associatie "Euratom–Belgische Staat," Ecole Royale Militaire/Koninkijke Militaire School, Brussels, Belgium; K. Akaishi and A. Miyahara of the National Institute for Fusion Science, Nagoya, Japan; and J. Boedo, R. W. Conn, R. Doerner, and D. S. Gray of the Institute of Plasma and Fusion Research, University of California, Los Angeles, California.

1.2.3 Particle Control Experiments in Tore Supra

J. T. Hogan, C. C. Klepper, P. K. Mioduszewski, L. W. Owen, T. Uckan, and J. E. Simpkins

Experiments on Tore Supra have shown that the particle balance is strongly affected by the wall reservoir. The carbon inner wall can absorb or release particles depending on whether the plasma is in contact with it and on the wall cleaning procedure applied before plasma operation. The plasma particle content is determined by the wall content and by the interaction of the plasma with the wall. This process could be a limitation to the control of density and/or isotopic ratio in long-pulse stationary discharges.

In spite of a rather high exhaust efficiency ($\approx 5 \times 10^{20}$ s^{-1}), the outboard pump limiter could only slightly modify the equilibrium density in the plasma core. An example of a series of four discharges, two discharges without pumping followed by two with pumping, is depicted in Fig. 1.17.

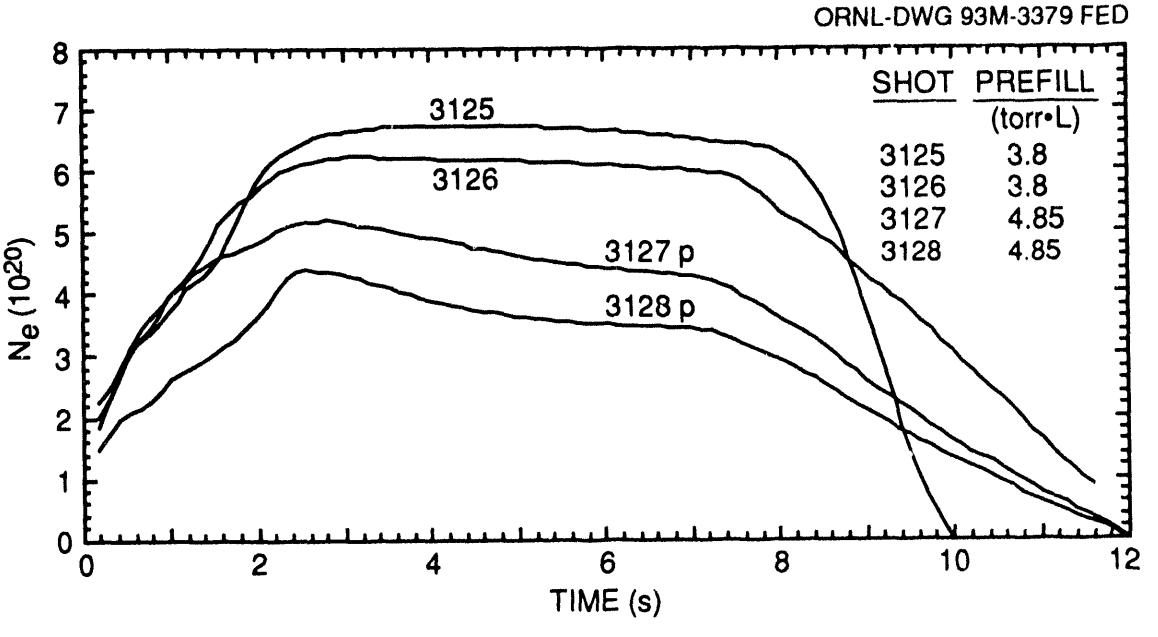

Fig. 1.17. Line-averaged densities as a function of time for pump limiter shot sequence: shots 3125 and 3126 without pumping; shots 3127p, 3128p with pumping.

The time scale for core density changes was estimated to be in the range of 20–40 s. This result is consistent with the previous observation because the wall particle content can be estimated in the range of $\approx 10^{23}$ particles, much larger than the plasma particle content ($\approx 5 \times 10^{20}$). In other words, before the plasma core density can be significantly changed, the active particle exhaust due to the pump limiter must change the equilibrium for the circulation of particles between the wall and the plasma. This can be achieved in two ways: either the particle content in the wall can be reduced significantly and then its "inertia" can be lowered (sufficiently long-pulse operation, e.g., >1 min, is required), or particle circulation processes around the limiter (ion convection, low-energy neutral or charge-exchange neutral transport, impurity effects, etc.) are adequately controlled. In the latter case, conceptual modeling work is required and could lead to advanced concepts of the first wall. A significant amount of work has been accomplished in modeling these experiments.

1.2.3.1 Effects of the ionizing scrape-off layer

In contrast to many previous experiments, it is assumed that ionization in the SOL is an important effect in Tore Supra. Two main phenomena contribute to this effect: (1) the dominant fraction of the fueling flux recycles from the graphite (carbonized) wall as molecules at the wall temperature, and (2) the electron temperature in the SOL is in the range (>20 eV) in which direct ionization of the recycling particles dominates Franck-Condon processes. The H^+ source rate for thermal molecular particles launched at the wall, as calculated with DEGAS in a typical Tore Supra SOL, is shown in Fig. 1.18. In this case, 66% of the particles are ionized in the SOL.

Under these conditions, the following procedure has been applied for the SOL modeling: to create the plasma density and temperature profiles in the SOL, Stangeby's analytical formula for the ionizing SOL is iterated with the DEGAS code until stable profiles emerge.[20] The values for $n_e(a)$ and

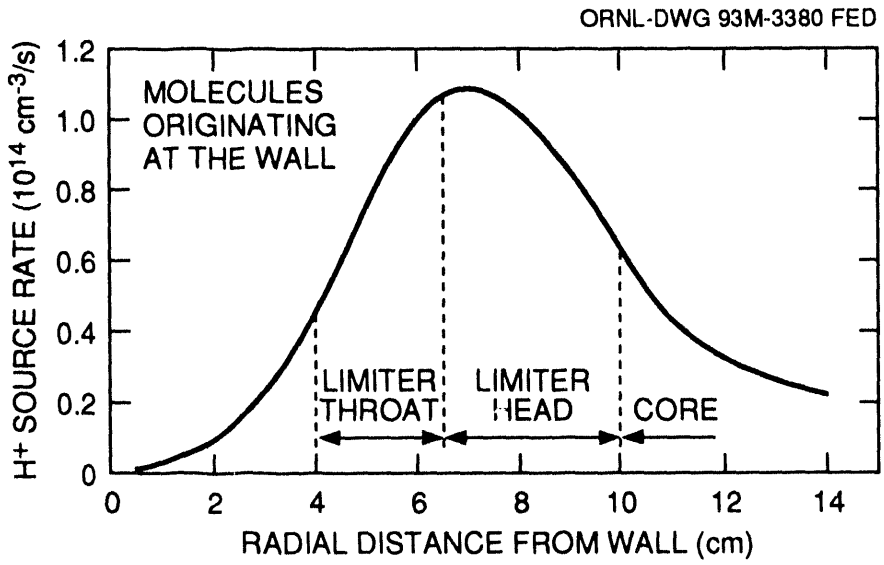

Fig. 1.18. H^+ source rate in the plasma edge of Tore Supra for thermal molecules launched at the wall.

$T_e(a)$ are taken from Thomson scattering profiles, and the average flux amplification (i.e., the ratio of the parallel ion flux in the SOL to the radial ion flux at the last closed flux surface) resulting from the DEGAS calculation is approximately two. These plasma profiles are then used in the DEGAS code to calculate the ion source profiles for neutral fluxes emerging from the wall as well as from the pump limiter head.

Because of the flux amplification in the SOL, the ion flux incident on the limiter is about twice as high as N/τ_p. Hence, approximately half of this flux is ionized and maintains the particle balance in the core, while the other half induces a charge-exchange flux to the limiter and walls around the limiter. This charge-exchange flux causes a recycling flux emerging from the wall, which is to a large extent ionized in the SOL. At this point, we distinguish two cases: (1) the pump limiter is not pumping and some of the particles ionized in the SOL will go back to the wall, or (2) the pump limiter is pumping and a fraction of the ionized particles can be exhausted through the pump limiter throat. The overall effect is that the pump limiter depletes the wall population such that wall fueling efficiency is reduced in subsequent discharges.

It appears that particle exhaust with the pump limiter controls the wall population, and the plasma density is controlled only through the different wall fueling efficiency with time constants of tens of seconds.

1.2.3.2 Modeling of core-wall particle dynamics in Tore Supra

To understand the core-wall dynamics in Tore Supra, a model for this process has been constructed. The model uses measurements of SOL fluxes from the Langmuir probes in the limiter throat, the Thomson scattering measurements of the evolution of $n_e(r,t)$ and $T_e(r,t)$, and the measured pump pressures. These data are combined with one-dimensional (1-D) radial transport modeling to obtain the evolution of $T_i(r,t)$ and the resulting charge-exchange efflux that is consistent with the data. By constructing a balance for the ions and neutrals, an estimate is made of the cold wall emission required by these balances. In parallel, a 1-D evolution code (WDIFFUSE) has been constructed for a C:H layer, to obtain an estimate of the cold wall emission that can be expected given the influxes to the wall and its state of saturation. When the required and predicted wall fluxes match, then there is a satisfactory particle balance.

A dedicated series of Tore Supra discharges (3125–3140) has been modeled with this code system. These discharges displayed the characteristic features of the ionizing SOL, and the pumped flux was dominated by the wall pumping. The analysis shows that the cold wall emission required by particle balance is found only with recycling coefficients > 1, and that (in the WDIFFUSE code) some heating of the C:H layer in the neighborhood of the outboard pump limiter must be assumed ($\Delta T_{wall} \approx$ 100 K). The level of charge-exchange power estimated from the model (150–300 kW) appears sufficient to justify such an increase; at the same time, local "hot spots" or particle-induced desorption may be the actual cause rather than a uniform rise in temperature. The affected area indicated by three-dimensional Monte Carlo modeling is approximately 4 m^2. These results suggest that additional dedicated experiments are desirable to improve the models; in these experiments, the particle balance should be studied separately for conditions with and without pumping and with and without gas puffing.

This work has been performed in collaboration with M. Chatelier, T. Loarer, and B. Pegourié of Tore Supra, Cadarache, France.

1.2.4 Plasma Edge Studies in ATF

1.2.4.1 Characteristics of edge plasma turbulence on ATF

T. Uckan, J. D. Bell, J. H. Harris, J. L. Dunlap, and J .B. Wilgen

Measurements of electrostatic turbulence at the edge of the ATF torsatron are used to study the effect of this phenomenon on the particle transport in this current-free magnetic configuration. Spatial profiles of the plasma electron density n_e, temperature T_e, and fluctuations in density ($\tilde{n}_e$) and in the plasma floating potential ($\tilde{\phi}_f$) are measured at the edge in ECH plasmas using a fast reciprocating Langmuir probe (FRLP) array. At the LCFS, $r/a \approx 1$, $T_e \approx 20$–40 eV, and $n_e \approx 10^{12}$ cm^{-3} for a line-averaged electron density $\bar{n}_e = (3$–$6) \times 10^{12}$ cm^{-3}. The relative fluctuation levels decrease as the FRLP is moved into the core plasma. For $T_e > 20$ eV, $\tilde{n}_e/n_e \approx 5\%$, and $e\tilde{\phi}_f/T_e \approx 2\tilde{n}_e/n_e$ at $r/a = 0.95$. The measured fluctuation spectra are broadband (40–300 kHz) with $\bar{k}\rho_s \approx (0.05$–$0.1)$, where $\bar{k}$ is the average wave number of the fluctuations and ρ_s is the ion Larmor radius at the sound speed. Near the LCFS, the density fluctuations can be approximated by $\tilde{n}_e/n_e \approx 0.4/\bar{k}L_n$, where L_n is the gradient scale length of n_e. The propagation direction of the fluctuations reverses to the electron diamagnetic direction at $r/a < 1$.

A velocity shear layer is observed in the ATF edge; this is also the case in the Texas Experimental Tokamak (TEXT). Figure 1.19(a) shows the spatial profile of the mean phase velocity of the fluctuations, $v_{ph} = 2\Sigma_{\omega>0}\, v_{ph}(\omega)$ with $v_{ph}(\omega) = \Sigma_k(\omega/k)S(k,\omega)/\Sigma_k S(k,\omega)$. The location of the shear layer approximately coincides with the peak of the plasma potential [Fig. 1.19(b)]. There the radial electric field $E_r = -d\phi_p/dr$ (where the plasma potential is $\phi_p \approx \phi_f + 2.5T_e$) changes its sign, and the density and electron temperature gradients are nearly zero. Thus $v_{ph} \approx v_{de} \approx 0$, where $v_{de} = (T_e/eB)(1/L_n + 1/L_T) - E_r/B$ is the electron drift velocity. At $r/a \approx 1.025$, where v_{ph} has its maximum, the estimated electric field is $E_r \approx -12$ V/cm, the electron temperature profile is flat with $T_e \approx 30$ eV, and $L_n \approx 4$ cm. The electron drift velocity is then $v_{de} \approx 2.1 \times 10^3$ m/s, which is comparable to the phase velocity of the fluctuations. Well inside the LCFS, where $E_r \approx 0$, it is estimated that $v_{de} \approx v_{ph} \approx 10^3$ m/s. These observations indicate that the phase velocity of the fluctuations and the electron drift velocity are comparable. The particle flux estimated from the fluctuations is consistent with fluxes obtained from the particle balance using the H_α spectroscopic measurements.

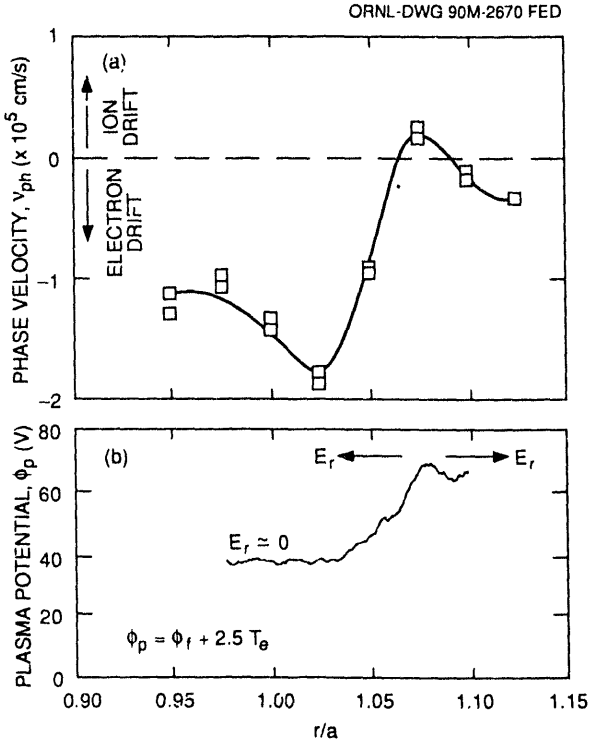

Fig. 1.19. (a) Spatial profile of the mean phase velocity v_{ph} of the fluctuations. Beyond the shear layer, the wave propagation is in the ion diamagnetic direction. (b) Spatial profile of the estimated edge plasma potential ϕ_p. The shear layer location nearly coincides with the peak of the plasma potential where the radial electric field $E_r = -d\phi_p/dr$ changes its sign.

Many of the features seen in the ATF edge fluctuations resemble those of ohmically heated plasmas in TEXT.

This work was performed in collaboration with Ch. P. Ritz, T. L. Rhodes, and A. J. Wootton of the University of Texas at Austin and C. Hidalgo of the Asociacion Euratom/CIEMAT, Madrid, Spain.

1.2.4.2 Biased limiter experiments on ATF

T. Uckan, S. C. Aceto, L. R. Baylor, J. D. Bell, T. S. Bigelow, A. C. England, J. H. Harris, R. C. Isler, T. C. Jernigan, J. F. Lyon, C. H. Ma, P. K. Mioduszewski, M. Murakami, D. A. Rasmussen, J. B. Wilgen, and J. J. Zielinski

Biasing experiments on tokamaks have been successful in improving the global confinement parameters (to H-mode-like values) by setting up a radial electric field at the plasma edge. These experiments have been extended to ATF for further study and characterization of the effects of the electric field on plasma confinement. Positive limiter biasing produces a significant increase in the particle confinement with no improvement in the energy confinement. Experiments have been carried out in 1-T plasmas with up to 400 kW of ECH. Two rail limiters, one at the top and one at the bottom of the device, are biased at positive and negative potentials with respect to the vacuum vessel. The limiters are inserted slightly inside the internal separatrix, $\rho = r/a \approx 1$, where the safety factor q is unity, compared to $q \sim 3$ at the plasma center. Here, the limiters are considered to be electrodes for biasing because they cover only ~15% of the LCFS owing to their small physical size and the low q value at the LCFS.

The limiters do not affect the plasma potential profile when they are floating. The plasma cross section is almost elliptical at the location of the limiters. When the limiters are positively biased at up to 300 V, the plasma density increases sharply, by about a factor of 3, to the ECH cutoff density as shown in Fig. 1.20(a). At the same time, the H_α radiation drops, indicating that the particle confinement improves. When the plasma density is kept constant with a reduced gas feed, the H_α radiation is further reduced, Fig. 1.20(b), and there is almost no change in the stored energy in the plasma. Under these conditions, the density profile becomes peaked, the velocity shear layer moves radially inward, from $\rho \approx 1.1$ to $\rho \approx 1$, and the electric field becomes outward pointing outside the LCFS and more negative inside the LCFS. The edge fluctuation levels decrease significantly, and the resulting fluctuation-induced particle flux is reduced as well. One explanation for this process is decorrelation of the turbulence mechanism around the shear layer that results in suppression of fluctuation-induced transport.

In contrast, negative biasing yields some reduction of the density and stored energy at constant gas feed. Simultaneous measurements of the plasma potential profile indicate almost no significant change with negative biasing of the limiters. Biasing causes almost no increase in the iron impurity signal from the plasma center or in the oxygen signal from the edge.

1.2.4.3 Power and particle balance studies with an instrumented limiter on ATF

T. Uckan, P. K. Mioduszewski, T. S. Bigelow, J. C. Glowienka, S. Hiroe, M. Murakami, J. B. Wilgen, and W. R. Wing

Power and particle balance studies on ATF were carried out using a rail limiter system.[21] Both top and bottom limiters are made of graphite tile arrays, and these tiles

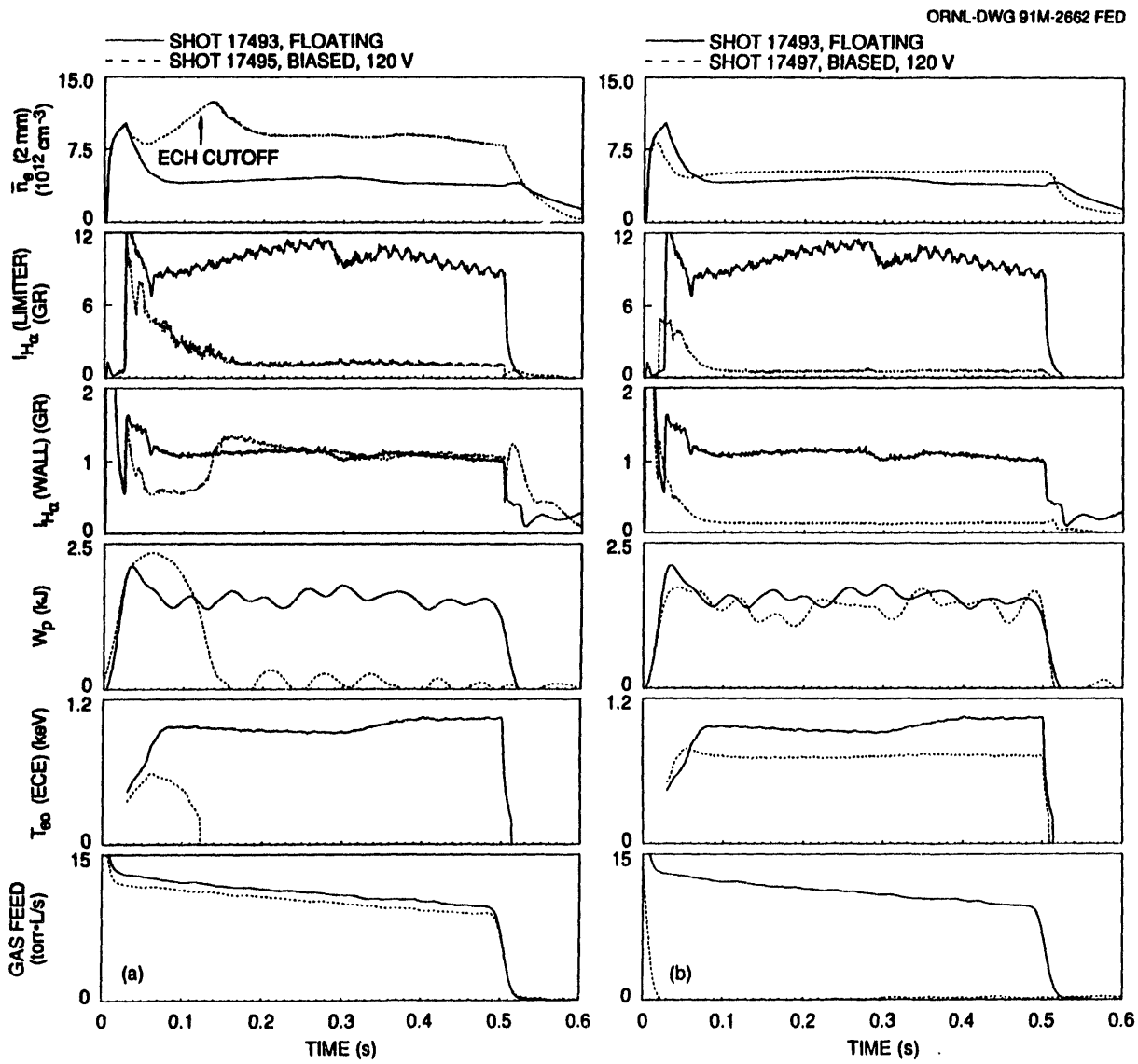

Fig. 1.20. Time evolution of plasma parameters ($\bar{n}_e$, $H\alpha$ signals, W_p, T_{e0}, and gas feed) for floating limiter (shot 17493) and positively biased (+120-V) limiter (shots 17495 and 17497), for (a) constant gas feed and (b) constant density.

are instrumented with thermocouples and Langmuir probes for calorimetric and particle flux measurements. The experimental results on the power accountability of ECH plasmas in ATF are as follows. The radiation loss estimated from the bolometric measurements is $P_{rad}/P_{input} \sim 30\%$, the limiter power loss is $P_{Lim}(total)/P_{input} \sim 12\%$, and the rest of the plasma heating power, about 58%, appears to be deposited at the vessel wall. The total limiter power coverage is about 16%. Measurements of the particle flux to the limiters and comparison with the total efflux indicate that the limiter particle flux coverage is about 18%. The fractions of power and particle flux to the limiters are relatively lower than in tokamaks because of the low edge safety factor at the natural

boundary of the ATF plasma where $q \sim 1$, rather than $q \sim 3$ as in a typical tokamak. Therefore, for limiters of the same size, these fractions are about a factor of q lower in ATF than in a comparable tokamak. The power flux distribution on the vessel wall is an important issue because long-pulse (30-s) operations are planned for ATF. Therefore, this issue will be investigated further, both with more experiments and with additional diagnostics.

1.2.4.4 Titanium gettering in ATF

J. E. Simpkins, R. C. Isler, T. F. Rayburn, and P. K. Mioduszewski

Titanium gettering has been successfully employed to overcome the deleterious effects of a leak rate of 2×10^{-4} torr•L/s in ATF. The leak/outgassing rates of the most abundant gaseous impurities (except methane, which is not gettered by titanium) have been observed to be as low as 10^{-9} torr•L/s after gettering. Spectroscopic analysis of the radiated power during discharges has determined that, before gettering, between 50 and 75% of the input power was radiated; after gettering, this fraction was reduced to between 15 and 20% (ref. 22).

As an example, Fig. 1.21 shows the behavior of water vapor before, during, and after plasma discharges with and without gettering. In the gettered case, the residual pressure is about an order of magnitude lower and remains constant, while the ungettered case shows the desorption of gas from the walls of the vessel. The pumping capacity of the gettered surface is large enough to exhibit some residual pumping of oxygen-bearing molecules as well as nitrogen, the most abundant gaseous impurity, as much as 24 h after the getter film has been deposited. In addition to impurity control, the titanium layer also provides an effective method for density control by reducing wall recycling. Figure 1.22 shows a constant-density sequence consisting of 25 shots with no intermediate gettering.

The combination of impurity and density control has enlarged the operating space of ATF considerably. Before gettering, achievable electron densities were in the range of several times 10^{18} m^{-3}, while after extensive gettering it was possible to operate with densities of up to 10^{20} m^{-3}.

1.3 STELLARATOR REACTOR STUDIES

J. F. Lyon

Stellarators have significant operational advantages over tokamaks as ignited steady-state reactors because stellarators have no dangerous disruptions, no need for continuous current drive and power recirculated to the plasma, less severe constraints on the plasma parameters and profiles, and access from the inboard side for easier maintenance. The torsatron type of stellarator configuration can have helical divertors outside the windings to reduce the power density on the divertor plates and, at the expense of a

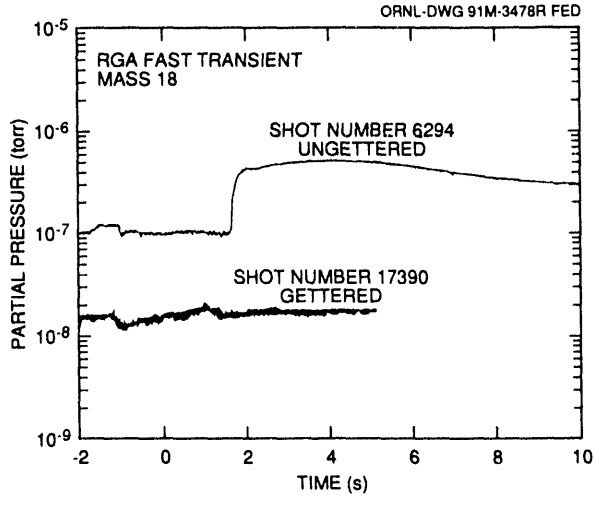

Fig. 1.21. Behavior of water vapor before, during, and after gettered and ungettered plasma discharges.

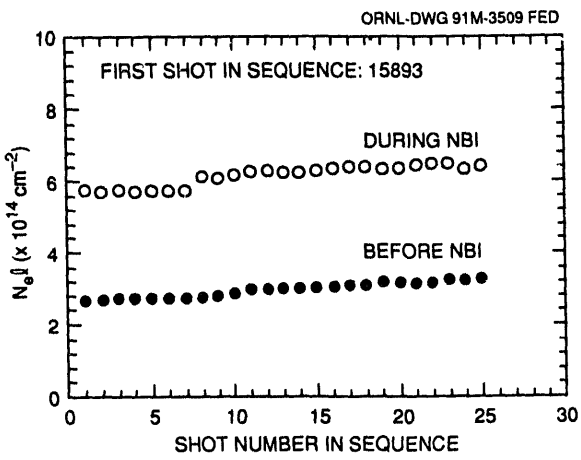

Fig. 1.22. Constant-density shot sequence with no intermediate gettering.

reduction in alpha particle heating, a near-perpendicular loss region to eliminate helium ash accumulation. Our study shows that torsatron reactors could also have a lower cost of electricity (COE) than conventional tokamak reactors.

1.3.1 Reactor Optimization Approach and Assumptions

We have applied the costing and component assumptions used in the recent extensive ARIES-I tokamak reactor studies[23,24] to optimization of stellarator reactors. This approach allows a more accurate relative comparison of stellarators and tokamaks as reactors. The models for the detailed reactor engineering and reactor performance constraints, however, are specialized for the example of a particular torsatron reactor. We recalculated the ARIES-I costs using the parameters for a May 1992 version of ARIES-I to benchmark our calculations and to provide a more detailed comparison with our torsatron reactor calculations. The values obtained for "our" ARIES-I, which we designate ARIES-I*, are very close (a few tenths of a percent) to the ARIES-I values.

The thicknesses, compositions, average mass densities, and unit costs for the first wall/blanket/reflector assembly and the neutron shielding are the same as those for ARIES-I. However, the thickness of the blanket directly under the helical windings on the inboard side of the torus is different. The maximum allowable current density j_{max} in the helical winding is calculated using the same relation as in the ARIES-I studies. The maximum magnetic field on the superconductor, B_{max}, is calculated from an expression that gives an excellent fit to results obtained using a finite element code with accurate helical winding trajectories. Although a continuous helical winding was used in most of the examples in this study for simplicity, these coil configurations can be modularized. The other engineering and materials assumptions are the same as those for ARIES-I.

The reference stellarator configuration chosen was a Compact Torsatron[25] with six toroidal field periods (CT6). Its relatively open coil geometry allows access between the helical windings for blanket removal and maintenance without disassembly of the reactor core. The thermal particles and alpha particles exit from the plasma in a thin helical strip between the helical windings. Because the minimum value possible for the major radius R_0 is proportional to the distance d between the plasma edge and the center of the coil winding pack, minimizing d (in particular, the radial depth of the winding pack and the blanket thickness under the inboard half of the helical winding) is important in reducing the cost of torsatron reactors.

A global energy confinement time τ_E is used to calculate the conduction power. We choose the dimensionally correct Lackner-Gottardi scaling, which fits both tokamak and stellarator data, with a confinement improvement factor H' similar to the H-mode confinement improvement factor for tokamaks. The density and temperature profiles are the same as those assumed in the

ARIES-I studies. Because the relatively large helical ripple in torsatrons, combined with symmetry-breaking toroidal effects, can lead to a near-perpendicular loss region for energetic particles, we assume that all helically and toroidally trapped alpha particles are lost and calculate the additional energy lost by pitch-angle scattering into the loss region during the slowing-down process. This loss reduces the effective alpha particle heating by up to ≈40%, but it also prevents accumulation of helium ash in the plasma and the attendant dilution of the fuel ions.

A confinement improvement factor $H' = 2.5$ was chosen as representing a reasonable target for stellarator confinement improvement; similar or better confinement improvement factors have been obtained in tokamaks. ARIES-I* also requires $H' = 2.5$. A thickness $b_i = 0$ was chosen for the blanket under the inboard half of the helical winding because it covers only a small fraction of the area available for the tritium breeding blanket; the decrease in the global tritium breeding ratio can be compensated for by increasing the local tritium breeding ratio. The transverse elongation k of the helical winding was chosen to be 3.

1.3.2 Comparison of the Reference CT6 Case with ARIES-I*

The main device and plasma parameters for the CT6 reference case are compared with those for ARIES-I* in Table 1.2. The CT6 reference case has a slightly smaller major radius, a field on axis 56% of that in ARIES-I*, and beta 2.5 times higher. The density-averaged temperature $\langle T \rangle$ is only one-third that in ARIES-I* and the volume-average density $\langle n \rangle$ is correspondingly higher. The mass utilization efficiency for CT6 is 2.1 times that of ARIES-I*, which results in a 22% lower unit direct cost and an 18% lower COE for the CT6 reactor. As in the ARIES reactor studies, the costs assume "learning curve" credits of ≈50% associated with a "tenth-of-a-kind" reactor and the level of safety assurance (LSA) factors appropriate to low-activation materials.

There are two main reasons for the lower costs for CT6: the absence of current drive and the smaller magnet mass. Because no power is needed for current drive in CT6, the recirculating power fraction is only 9% (vs 19% for ARIES-I*) and the cost of the supplemental heating system (needed only for plasma startup) is much lower. The helical winding mass is much less than the coil mass in ARIES-I* because the CT6 coil perimeter is smaller (the winding is closer to the plasma) and the cross section is much

Table 1.2. Main plasma and device parameters for CT6 torsatron and ARIES-I* tokamak reactors

	CT6	ARIES-I*
Net electric output, MW(e)	1000	1000
Major radius R_0, m	6.57	6.75
Average plasma radius a_p, m	1.74	1.95
Plasma volume, m^3	394	489
Toroidal field on axis, T	6.0	10.6
Maximum field on coils B_{max}, T	16.0	9.9
Electron density $\langle n \rangle$, 10^{20} m^{-3}	3.2	1.4
Plasma temperature $\langle T \rangle$, keV	6.8	20.0
Central ion temperature T_0, keV	13.0	39.0
Volume-average toroidal beta, %	4.7	1.9
Neutron wall loading, MW/m^2	2.8	2.7
Mass utilization efficiency, kW(e)/tonne	211	99.3
Unit direct cost, \$/kW(e)[a]	1819	2318
Cost of electricity, mill/kW(e)h[a]	67.0	81.4

[a] In constant 1990 dollars.

smaller (less total ampere-turns and higher average current density because of the lower magnetic field).

1.3.3 Dependence on Assumptions

The COE vs the confinement improvement factor H' is shown in Fig. 1.23 for two different values of b_i. Adding a 0.335-m-thick blanket, half the thickness used in ARIES-I but thicker than the beryllium-rich blankets used in earlier reactor studies, increases the COE to a level that is closer to the ARIES-I* value. The COE is less than that for ARIES-I* for $H' > 1.75$ ($b_i = 0$) and $H' > 2.3$ ($b_i = 0.335$ m). Improved energy confinement is reflected most strongly in a factor of 4 increase in $\langle\beta\rangle$, from 1.5% to 6%,

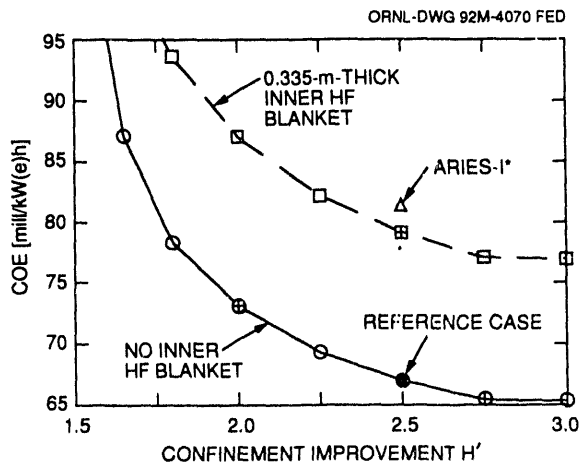

Fig. 1.23. Dependence of the cost of electricity on the confinement improvement factor H' for two different inboard blanket thicknesses.

and a factor of 2.3 decrease in the plasma volume, as H' increases from 1.65 to 3. The factor of ≈2 confinement improvement needed for an attractive reactor is similar to the L-to-H confinement improvement factor in tokamaks.

The nominal coil parameters (j_{max}, k, and B_{max}) chosen for the base reference case were varied to test the sensitivity of the COE to those assumptions. Decreasing j_{max} by a factor of 2 only increased the COE by 4.6%. Decreasing k to 1 (a square coil cross section) led to a larger change (15%) in the COE. Lower values of B_{max} are possible at somewhat higher COE. A case with B_{max} = 12 T, 60% of that for ARIES-I*, and a COE of 72.8 mill/kW(e)h may be more attractive from an engineering viewpoint than the reference CT6 case with higher B_{max} (16 T) and lower COE [67 mill/kW(e)h].

The nominal physics parameters chosen for the base reference case were also varied to test the sensitivity of the COE to those assumptions. Several of these variations [e.g., more peaked density and temperature profiles, higher wall reflectivity (90%), less oxygen impurity content (0.5%), and no alpha particle losses] lowered the COE, but none reduced the COE by more than 3.3%. Broader density and temperature profiles and higher oxygen impurity content (1.5%) increased the COE, but not by more than 6.4%. Better reactor economics were obtained for larger power plants: increasing P_E to 1.5 GW(e) and 2 GW(e) reduced the COE by 18% and 25%, respectively.

1.3.4 Comments

Although this study indicates that torsatron reactors could be competitive with tokamak reactors for a range of assumptions, improvements in the study are needed. The CT6 reference case is not an optimum stellarator configuration for a reactor; it has continuous helical coils that were obtained by maximizing the average radius of the last closed magnetic surface (minimizing the distance between the plasma edge and the coil center), subject to constraints that maximize the beta limit. In a reactor, the plasma-coil distance needs to be maximized for a modular coil configuration with a moderate beta value. More realistic calculations of the blanket and shielding requirements also need

to be done, and more refined 1-D stellarator transport models that include self-consistent calculations of the radial profiles of the ion and electron temperatures and densities and the ambipolar radial electric field should be used.

REFERENCES

1. B. B. Kadomtsev, *Sov. J. Plasma Phys.* **1**, 295 (1975).

2. J. W. Connor and J. B. Taylor, *Nucl. Fusion* **17**, 1047 (1977); J. W. Connor, *Plasma Phys. Controlled Fusion* **30**, 619 (1988).

3. J. P. Christiansen, J. G. Cordey, and K. Thomsen, *Nucl. Fusion* **30**, 1183 (1990). [Note the wrong sign of the exponent of resistive fluid turbulence in Table II (should read +1, not -1)].

4. R. A. Dory et al., "Energy Confinement Scaling in the ATF Stellarator," *Comments Plasma Phys. Controlled Fusion* **14**, 237 (1991).

5. F. W. Perkins, PPPL-2708, Princeton Plasma Physics Laboratory, Princeton, New Jersey, 1990.

6. M. Murakami et al., "Bootstrap-Current Experiments in a Toroidal Plasma-Confinement Device," *Phys. Rev. Lett.* **66**, 707 (1991).

7. J. H. Harris et al., "Second Stability in the ATF Torsatron," *Phys. Rev. Lett.* **63**, 1249–52 (1989).

8. M. Murakami et al., "Recent Results from the ATF Torsatron," *Phys. Fluids B* **3**, 2261 (1991).

9. C. P. Ritz et al., "Comparative Studies of Edge Turbulence in the TEXT Tokamak and the ATF Stellarator," p. 589 in *Plasma Physics and Controlled Nuclear Fusion Research 1990*, Vol. 2, IAEA, Vienna, 1991.

10. B. A. Carreras and P. H. Diamond, "Thermal Diffusivity Induced by Resistive Pressure-Gradient-Driven Turbulence," *Phys. Fluids B* **1**, 1011 (1989).

11. G. M. Batanov et al., *Fiz. Plazmy* **15**, 527 (1989), in Russian.

12. P. K. Mioduszewski, L. W. Owen, M. M. Menon, and J. T. Hogan, "Particle Exhaust Modeling for the Collaborative DIII-D Advanced Divertor Program," *J. Nucl. Mater.* **176 & 177**, 733 (1990).

13. C. C. Klepper et al., *Divertor Neutral Pressure Enhancement with Baffle in DIII-D*, GA-A20774, General Atomics, San Diego, California, November 1991.

14. M. M. Menon et al., "Particle Exhaust Scheme Using an In-Vessel Cryocondensation Pump in the Advanced Divertor Configuration of the DIII-D Tokamak," *Fusion Technol.* **22**, 356 (1992).

15. D. Reiter, G. H. Wolf, and H. Kever, *Nucl. Fusion* **30**, 2141 (1990).

16. D. L. Hillis et al., "Helium Removal Experiments and H_α Studies on ALT-II in TEXTOR," pp. 23–24 in *Fusion Energy Division Annual Progress Report for the Period Ending December 31, 1989*, ORNL-6624, Martin Marietta Energy Systems, Inc., Oak Ridge National Laboratory, Oak Ridge, Tennessee, July 1991.

17. D. L. Hillis et al., "Helium Removal and Transport Studies with the ALT-II Pump Limiter in TEXTOR," *Phys. Rev. Lett.* **65**, 2382 (1990).

18. R. R. Weynants et al., *Europhys. Conf. Abstr.* **15C**, Pt. 1, 287 (1990).

19. R. A. Hulse, *Nucl. Technol./Fusion* **3**, 259 (1983).

20. L. W. Owen et al., "Effects of Ionizing Scrape-Off Layers on Local Recycling in Tore Supra Pump Limiter Experiments," *J. Nucl. Mater.* **196–198**, 1125 (1992).

21. T. Uckan et al., "Power and Particle Balance Studies Using an Instrumented Limiter System on ATF," *Plasma Phys. Controlled Fusion* **33**, 703 (1991).

22. R. C. Isler et al., "Radiative Losses and Improvement of Plasma Parameters Following Gettering in the Advanced Toroidal Facility," *Nucl. Fusion* **31**, 245 (1991).

23. F. Najmabadi, R. W. Conn, and the ARIES Team, "The ARIES-I Tokamak Reactor Study," *Fusion Technol.* **19**, 783 (1991).

24. R. L. Miller, R.A. Krakowski, and the ARIES Team, "Options and Optimizations for Tokamak Reactors: ARIES," *Fusion Technol.* **19**, 802 (1991).

25. J. F. Lyon et al., "Compact Torsatron Reactors," *Fusion Technol.* **15**, 1401 (1989).

2

ATOMIC PHYSICS AND PLASMA DIAGNOSTICS DEVELOPMENT

R. A. Phaneuf,[1] Program Manager

N. R. Badnell[2]
M. E. Bannister[1]
E. W. Bell[3]
C. A. Bennett[4]
C. Bottcher[1]
G. H. Dunn[3]
H. B. Gilbody[5]
D. C. Gregory[1]
D. C. Griffin[6]
X. Guo[3]
J. W. Hale[1]
C. C. Havener[1]
D. P. Hutchinson[1]
M. I. Kirkpatrick[1]
C. H. Ma[1]
E. W. McDaniel[7]
F. W. Meyer[1]
T. J. Morgan[8]
S. H. Overbury[9]
F. M. Ownby[1,10]
M. S. Pindzola[11]
R. K. Richards[1]
D. R. Schultz[12]
A. C. H. Smith[13]
E. W. Thomas[7]
J. S. Thompson[3]
D. M. Zehner[14]
P. A. Zeijlmans van Emmichoven[15]

1. Physics Division.
2. Auburn University, Auburn, Alabama.
3. Joint Institute for Laboratory Astrophysics, Boulder, Colorado.
4. University of North Carolina, Asheville.
5. Consultant, Queen's University, Belfast, Northern Ireland.
6. Research subcontractor, Rollins College, Winter Park, Florida.
7. Consultant, Georgia Institute of Technology, Atlanta.
8. Consultant, Wesleyan University, Middletown, Connecticut.
9. Chemistry Division.
10. Program secretary.
11. Consultant, Auburn University, Auburn, Alabama.
12. ORAU Fusion Energy Postdoctoral Research Program Fellow.
13. University College of London, London, United Kingdom.
14. Solid State Division.
15. The University of Tennessee, Knoxville.

2. ATOMIC PHYSICS AND PLASMA DIAGNOSTICS DEVELOPMENT

Summary of Activities

Research on atomic physics and plasma diagnostics development is part of the ORNL Fusion Program and is carried out within the ORNL Physics Division. The principal activities of this program are threefold: atomic collisions research, atomic data compilation and evaluation, and advanced plasma diagnostics development.

The atomic collisions research program focuses on inelastic processes that are critical in determining the energy balance and impurity transport in high-temperature plasmas, and for plasma diagnostic measurements. The objective is to obtain a better fundamental understanding of collision processes involving highly ionized impurity atoms at the kinetic energies characteristic of magnetic fusion plasmas and to determine cross sections for these processes. Close coordination of experimental and theoretical programs guides the selection of key experiments and provides both benchmarks and challenges for theory.

Central to the experimental effort is an electron cyclotron resonance (ECR) multicharged ion source, which provides ions for colliding-beams experiments. A crossed-beams approach is applied to the measurement of cross sections for electron-impact ionization of highly ionized ions in initial charge states as high as +16. A new collaborative electron-ion merged-beams experiment to measure cross sections for electron-impact excitation of multiply charged ions by electron energy-loss spectroscopy constitutes a major part of the current experimental effort. Merged beams have also been used to study charge-exchange collisions of multiply charged plasma impurity ions with hydrogen (deuterium) atoms at the lower kinetic energies relevant to the edge plasma. Ejected-electron spectroscopy has been applied as a diagnostic tool to study the interaction of multiply charged ions with solid surfaces.

The theoretical effort has focused on the development of close-coupling methods for treating electron-impact excitation of highly charged ions, in support of the merged- and crossed-beams experiments and of the fusion program in general. These calculations require development and implementation of sophisticated computer codes and depend heavily on the advanced computing capabilities of the National Energy Research Supercomputer Center.

The Controlled Fusion Atomic Data Center (CFADC) is operated by the atomic physics group, with the assistance of a network of expert consultants. The CFADC searches the current literature and maintains an up-to-date bibliography of fusion-related atomic and molecular processes that is available for on-line searching. This facilitates the primary mission of the CFADC: the compilation, evaluation, and recommendation of relevant atomic collision data to the fusion research community. The CFADC actively participates in the International Atomic and Molecular Data Center Network sponsored by the International

Atomic Energy Agency and cooperates with other data centers in Europe and Japan. Through this network, the CFADC has a major role in the development and implementation of the ALADDIN system for the computer storage, retrieval, and exchange of recommended atomic data.

The plasma diagnostics program concentrates on the development of advanced diagnostics for existing and future magnetic fusion experiments, using optical and laser technology. The current emphasis is on the application of pulsed infrared lasers to the diagnostics of alpha particles produced from the fusion of deuterium and tritium. A prototype diagnostic system based on small-angle Thomson scattering of a pulsed CO_2 laser beam was developed and installed on the Advanced Toroidal Facility (ATF), and a proof-of-principle test was successfully completed. This test consisted of absolute measurements of a scattered signal at an angle of less than 1° from the plasma electrons. A novel multichannel interferometer operating at a wavelength of either 214 or 119 μm was also developed and successfully operated on ATF. The relatively large number of channels was realized by use of a single reflective cylindrical beam expander, a technique that significantly reduces the number of optical elements required for a conventional system. The interferometer was operated routinely on ATF to provide accurate measurements of the plasma electron density profile evolution during plasma discharges. To address the issue of optical beam refraction in higher density plasmas, a feasibility study was carried out for a two-color infrared interferometer/polarimeter system for the International Thermonuclear Experimental Reactor.

2.1 EXPERIMENTAL ATOMIC COLLISIONS

2.1.1 Merged-Beams Experiment for Electron-Impact Excitation of Ions

M. E. Bannister, E. W. Bell, G. H. Dunn, D. C. Gregory, X. Guo, R. A. Phaneuf, A. C. H. Smith, and J. S. Thompson

Researchers from ORNL and the Joint Institute for Laboratory Astrophysics (JILA) are engaged in a collaborative experiment at the ORNL Electron Cyclotron Resonance (ECR) Multicharged Ion Research Facility. The objective of this collaboration is absolute cross-section measurements of electron-impact excitation of multicharged ions. The technique, developed at JILA, involves merging beams of electrons and multiply charged ions in a uniform axial magnetic field and detecting electron-impact excitation events via electron energy-loss spectroscopy. The beams are merged and demerged using trochoidal ($\mathbf{E} \times \mathbf{B}$) analyzers. The magnetic field ensures complete collection of inelastically scattered electrons, which are directed onto a position-sensitive detector.

The first cross-section measurements for a multiply charged ion with this technique were reported recently[1] for 3s-3p excitation of Si^{3+}:

$$e + Si^{3+}(3s\ ^2S_{1/2}) \rightarrow e + Si^{3+}(3p\ ^2P_{1/2,3/2}) \qquad -8.88\ \text{eV} .$$

This system was chosen because cross-section calculations for Na-like ions are

expected to be of high reliability, and thus a comparison of experiment and theory serves to test the validity of both. The absolute experimental cross-section measurements are compared in Fig. 2.1 to benchmark seven-state close-coupling calculations by Badnell, Pindzola, and Griffin.[2] Since the cross section for electron-impact excitation of an ion is finite at threshold, and usually reaches its largest value there, an abrupt jump from zero is expected at 8.88 eV. The theoretical cross section in Fig. 2.1 has been convoluted with a Gaussian electron-energy distribution of 0.2 eV (FWHM) to simulate the energy resolution of the experiment. In fact, there are actually two fine-structure components in the 3s-3p excitation ($^2P_{1/2}$, $^2P_{3/2}$), and thus two expected steps in the cross section, which are separated by 0.06 eV. Although the experimental energy resolution is insufficient to resolve these two steps, it may be slightly better than 0.2 eV. This is an order-of-magnitude improvement over our previous multicharged ion excitation measurements based either on detection of photon emission or on signatures in ion-

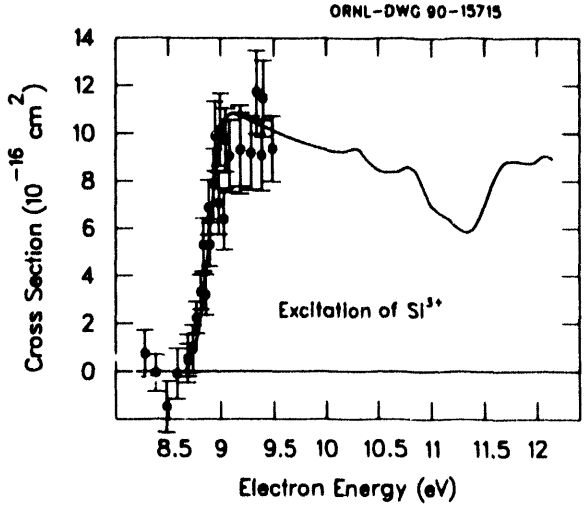

Fig. 2.1. Comparison of absolute cross-section measurements with seven-state close-coupling calculation of Badnell et al. for 3s-3p excitation of Na-like Si^{3+} by electron impact.

ization cross sections due to inner-shell excitation-autoionization.

Trajectory modeling of the primary electron beam, and of both elastically and inelastically scattered electrons, indicates that the merged-beams electron-energy-loss apparatus is, in principle, capable of covering the entire energy range shown in Fig. 2.1. This could not be realized in these initial measurements because of high background levels encountered as the relative energy was increased above the excitation threshold. It is believed that this elevated background was caused by components in the primary electron beam with increased transverse energy, whose trajectories either impacted the position-sensitive detector directly or interacted with nearby surfaces. Such effects become increasingly severe as the relative energy is increased above the threshold, since the difference in energy between the primary and scattered electron beams decreases, and thus their spatial separation in the demerger is reduced.

Improvements were made to the electron gun and merger, based on more detailed computer trajectory modeling calculations. However, a systematic series of measurements of electron-impact excitation of O^{5+}, Ar^{6+}, and Ar^{7+} failed to yield data of sufficient reliability. The problem was traced to a small fraction ($<10^{-5}$) of the primary electron beam that interacts with apertures and other surfaces, producing spurious space-charge modulated signals that preclude accurate scattering measurements. On the basis of these measurements and systematic tests, more extensive modifications to the apparatus were initiated. The solenoid was rewound because of internal shorts of two windings to the core. The electron gun, electron collector, and ion analyzer were redesigned on the basis of the trajectory modeling calculations. An order was placed for a new position-sensitive detector capable of higher count rates. Measurements with

the improved apparatus have yielded preliminary data for 3s-3p excitation of Na-like Ar^{7+}.

These improvements are expected to increase the sensitivity and extend the energy range of the energy-loss technique further above the excitation threshold, where strong resonance effects are predicted to occur for many ions. The structure in the theoretical cross section shown in Fig. 2.1 is due to such resonances, whose resolution will provide stringent tests of excitation theory. The first measurements on Si^{3+} establish the proof of principle of the merged-beams electron-energy-loss technique for excitation of multiply charged ions, and the threshold measurement demonstrates that the experimental resolution should be sufficient to uncover such resonance structures. The energy range accessible to the technique is, in principle, constrained only by the decreasing dispersion of elastically and inelastically scattered electrons as the energy is raised above the inelastic threshold. Future experiments will focus on fusion-relevant ion species and will be selected in order to provide the most sensitive tests of theory.

2.1.2 Electron-Impact Ionization of Si^{q+} Ions

J. S. Thompson, D. C. Gregory, P. A. Zeijlmans van Emmichoven, X. Guo, and E. W. Bell

Accurate cross sections for electron-impact ionization of multicharged impurity ions are critical to accurate modeling of the ionization balance in magnetic fusion plasmas. Such cross sections are often dominated by indirect ionization mechanisms involving excitation of inner-shell electrons. The ionization cross section will be enhanced by such mechanisms if the core-excited states thus formed decay by autoionization. In some cases this enhancement can be more than an order of magnitude.[3]

As part of a Research Program on Atomic Data for Medium- and High-Z Impurities in Fusion Plasmas, coordinated by the International Atomic Energy Agency (IAEA), a series of cross-section measurements was initiated for electron-impact ionization of multicharged Si^{q+} ions. The measurements were performed as part of the ongoing ORNL-JILA collaboration using the electron-ion crossed-beams apparatus and beams from the ORNL ECR multicharged ion source. Absolute cross-section measurements have been completed for initial charge states q = 4, 5, 6, and 7, and measurements for q = 1, 2, 3, and 8 are planned.

A typical result for electron-impact ionization of Si^{6+} is shown in Fig. 2.2, along with the prediction of the widely applied Lotz semiempirical formula.[4] The measurements are seen to exceed the Lotz prediction by about 25% but to exhibit no distinct features due to indirect ionization. An atomic structure calculation indicates that such indirect contributions for this case must

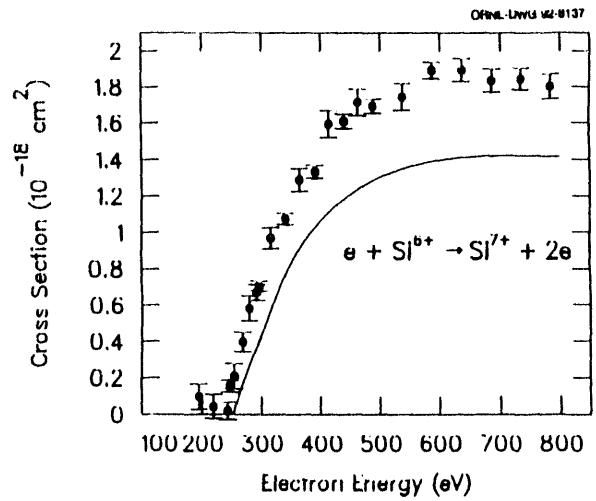

Fig. 2.2. Measured cross sections for electron-impact ionization of Si^{6+}, compared to the prediction of the Lotz semiempirical formula (curve).

involve the excitation of a 1s electron and thus become possible only at energies above ≈800 eV. This is therefore a good case for testing the reliability of the Lotz formula for direct ionization, which is seen to underestimate the cross section by 25%. The comparison is similar for Si^{4+}, Si^{5+}, and Si^{7+}, whose ionization cross sections also display no features due to indirect mechanisms but exceed the Lotz predictions.

2.1.3 Multicharged Ion-Surface Interactions

F. W. Meyer, C. C. Havener, S. H. Overbury, D. M. Zehner, and P. A. Zeijlmans van Emmichoven

Our focus has been on trying to understand the remarkably rapid neutralization[5] of the projectile that occurs when slow multicharged ions interact with metal surfaces. The experimentally inferred neutralization rate is too fast by orders of magnitude to be explained within the framework of the frequently invoked Arifov model.[6] In this model, the primary neutralization mechanism is above-surface, multiple-resonant, electron capture of metal valence electrons into autoionizing projectile Rydberg levels, which deexcite through a time-consuming, complex autoionization cascade.

We have found that this discrepancy can be resolved by considering the additional neutralization channels that open after projectile penetration of the metal surface. To this end, we have studied projectile KLL-Auger transitions for 60-keV N^{6+} ions incident on gold and copper single crystals in the range of angles from 0.2° to 20°. We find the energy spectrum of the observed projectile K-Auger emission to be characterized by two resolvable components[7,8] with strikingly different dependences on perpendicular ion velocity, as illustrated for the case of a gold target in Fig. 2.3 (similar results have also been obtained with copper). A "fast" component, limited by the rate of K-Auger decay in the essentially neutralized projectile, dominates [see Fig. 2.3(a)] and is ascribed to "subsurface" emission. We have been able to model this component using a Monte Carlo simulation[8,9] of the detailed projectile trajectories and close binary encounters with target atoms inside the bulk *after* surface penetration. Results of the subsurface simulation are shown in Fig. 2.4 as the hatched region labeled "Monte Carlo simulation." The simulation assumes a projectile L-shell filling rate of 2×10^{14} s^{-1} and a KLL-Auger decay rate of 1×10^{14} s^{-1}.

At very small angles of incidence, a much weaker "slow" component appears [see Fig. 2.3(b)]. This component has a time dependence characteristic of the neutralization-deexcitation cascade (see hatched region in Fig. 2.4 labeled "cascade calculation") that occurs above the surface *before* surface penetration.[10] Our measurements for the copper target, which extend to even more grazing incidence angles, indicate a premature saturation of the intensity of this component, in agreement with more detailed calculations.[11] These calculations, which include the effects of image potential acceleration on the above-surface projectile trajectory, suggest that this effect imposes an upper limit on the above-surface interaction time that cannot be exceeded, irrespective of how grazing the asymptotic incidence angle is made.

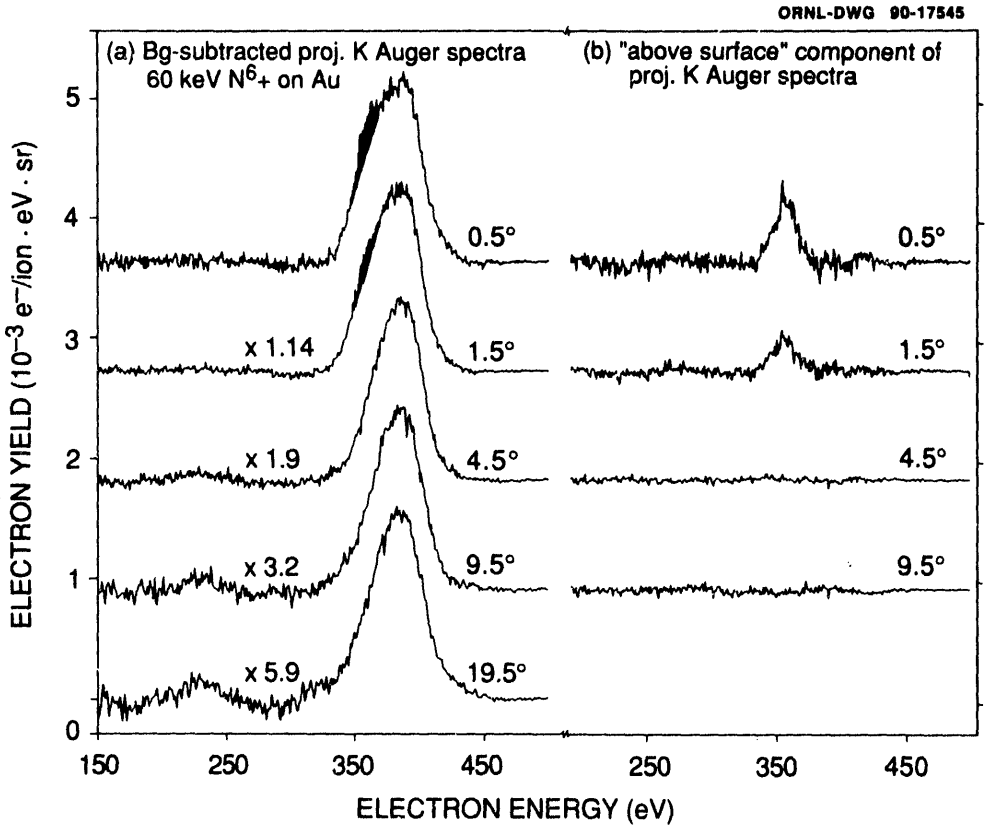

Fig. 2.3. (a) Background-subtracted projectile K-Auger spectra for 60-keV N^{6+} ions incident on gold at various angles of incidence, observed normal to the incident beam direction and scaled to the peak intensity of the 0.5° spectrum. (b) Unscaled above-surface components of the KLL-Auger electron spectra.

2.1.4 Very Low Energy Collisions of Multiply Charged Ions in Merged Beams

C. C. Havener, F. W. Meyer, and R. A. Phaneuf

It is now possible with the merged-beams technique to measure, with a single apparatus, total electron capture cross sections for multicharged ions in collisions with hydrogen or deuterium over an energy range covering four orders of magnitude: 0.1 eV/amu to over 1000 eV/amu. This corresponds to a collision energy almost an order of magnitude lower than has previously been reported (e.g., as in ref. 12). Comparison of experiment with theory over such a wide energy range provides a stringent test of our understanding of such processes, which are fundamental to modeling of both laboratory and astrophysical plasmas. For example, electron translation effects and rotational coupling mechanisms, while important at keV/amu energies, are of decreasing importance below 10 eV/amu. As collision energies decrease below 1 eV/amu, the ion-induced dipole attraction between ion and neutral becomes strong enough to significantly affect the reactant trajectories. These trajectory effects can lead to enhancements in the cross section that increase with decreasing energy.

During the last year the merged-beams apparatus has been used to extend previous measurements for O^{3+} + H (D) and O^{5+} + H (D) below 1 eV/amu. This was possible

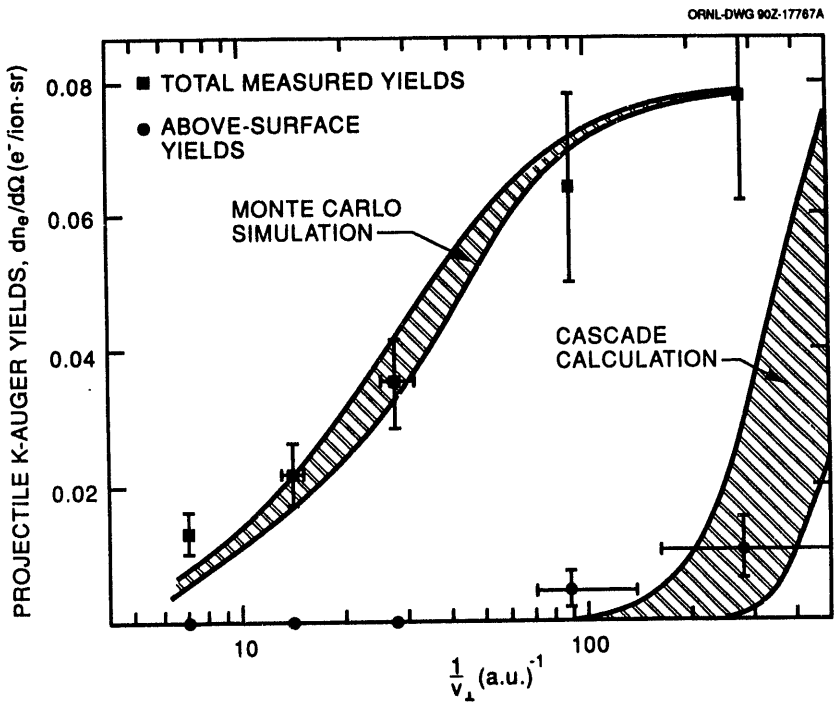

Fig. 2.4. Differential electron yields for projectile K-Auger emission normal to the incident beam direction as a function of inverse perpendicular projectile velocity. Squares: total measured yields; circles: experimentally deduced above-surface components; hatched regions: simulation results (see text).

owing to recent improvements in the sensitivity and angular collection of the apparatus, along with an improvement in the purity of the hydrogen beam. The new measurements[13] for the O^{3+} + H (D) system, presented in Fig. 2.5, join smoothly with our previous measurements[14] above 1 eV/amu and for energies below 1 eV/amu were able to verify the predicted sharp rise in the cross section due to capture to the 3p state. As can be seen in the figure, there remains a discrepancy between the measurements and theory throughout the whole energy range. The calculations may overestimate the contribution due to capture to the 3p state. However, note that a finite fraction (~16%) of the B-like O^{3+} ion beam is in the $(1s^22s2p^2)^4P$ metastable state, which may contribute, at least in part, to this discrepancy.

In Fig. 2.6, new merged-beam measurements[13] for O^{5+} + H (D) are presented along with previous measurements and theoretical calculations. Unlike the O^{3+} case, the present measurements for O^{5+} show as much as a 30% deviation from previous merged-beams results[12] in some energy regions. It has been observed experimentally that for collision energies less than about 50 eV/amu, the collision-energy-dependent beam-beam signal due to the estimated 0.1% of the hydrogen beam that was in excited states can account for a significant fraction of the measured signal and therefore resulted in artificially high cross-section values around 50 eV/amu. The previous measurements also show a distinct minimum in the cross section between 1 and 10 eV/amu. Recent differential cross-section calculations[15] show that this minimum was due to insufficient angular collection of the H^+ (D^+) products. The angular collection of the present apparatus is sufficient to guarantee no significant loss of signal. Indeed, as seen

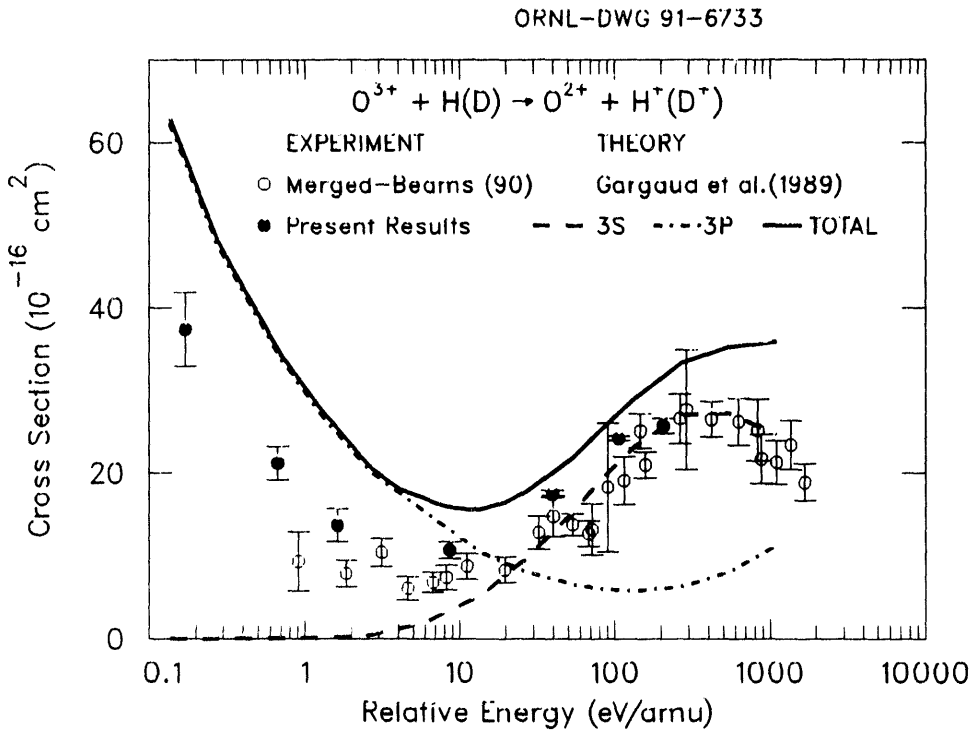

Fig. 2.5. Comparison of merged-beams data for O^{3+} + H (D) with theoretical calculations (Gargaud et al., 1989) for capture to the 3s and 3p states.

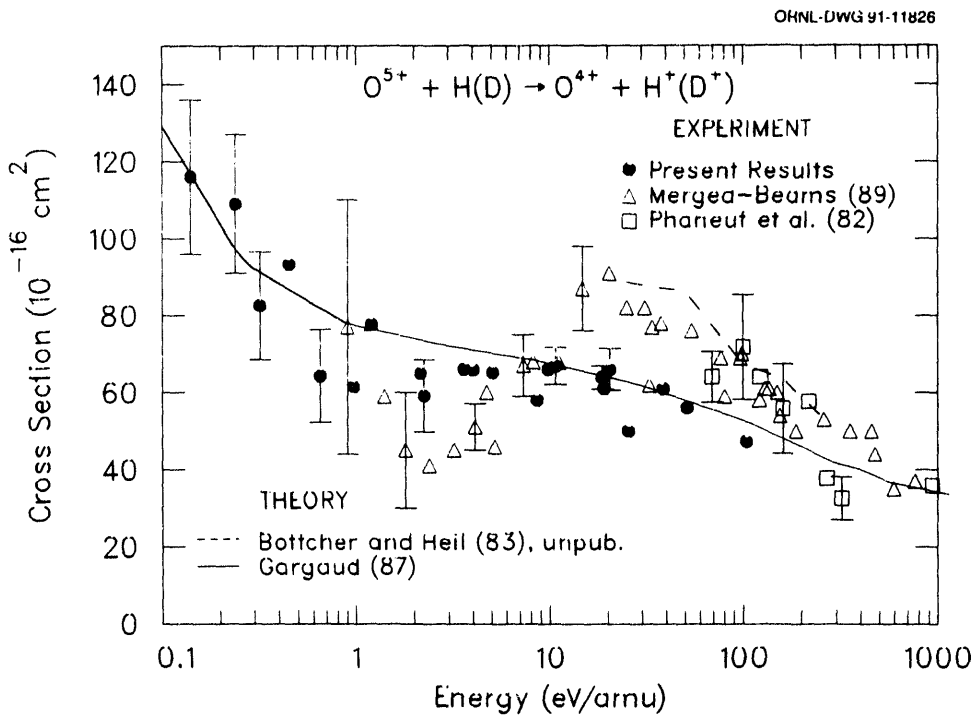

Fig. 2.6. Comparison of merged-beams data for O^{5+} + H (D) with other measurements and theoretical calculations. Measurements at the lower energies were performed with D.

in Fig. 2.6, the present O^{5+} measurements agree well with the calculations of Gargaud.

The sharp increase in the cross section for O^{5+} + D below 1 eV/amu is attributed to a trajectory-enhanced capture into the 4p state. Landau-Zener calculations indicate that approximately 30% of the cross section around 0.1 eV/amu is due to these trajectory enhancements. With the completion of the upgrade to the ECR ion source facility described in Sect. 2.1.5, measurements below 1 eV/amu will be attempted with hydrogen, which, according to the Landau-Zener estimate, should show an additional 20% trajectory enhancement. Observation of this isotope effect would be a direct measure of such trajectory effects in low-energy multicharged ion-atom collisions.

2.1.5 ECR Multicharged Ion Facility Upgrade

F. W. Meyer, C. C. Havener, J. W. Hale, and R. A. Phaneuf

A capital equipment project was initiated during FY 1991 to upgrade the ORNL ECR Multicharged Ion Research Facility. The ion charge state and beam intensity capabilities of the facility will be improved by significantly increasing both the axial and the radial confining magnetic field gradients and by incorporating the capability for raising the microwave operating frequency of the source from 10.6 GHz to 14.5 GHz. At the locally hosted 10th International ECR Ion Source Workshop,[16] held November 1–2, 1990, in Knoxville, both modifications were shown to result in sizable improvements in source performance. Included in the upgrade are computerized monitors and controls for the facility, as well as network-linked data acquisition systems for the various on-line experiments. The target date for completion of this project is December 1992.

2.2 THEORETICAL ATOMIC COLLISIONS: ELECTRON-ION COLLISION THEORY

D. C. Griffin, M. S. Pindzola, N. R. Badnell, and C. Bottcher

The program in electron-ion collision theory continues to focus on collision processes of critical importance to energy balance, impurity transport, and diagnostic measurements in laboratory plasmas. Theoretical and computational methods have been developed that allow for the generation of data of direct fusion interest. This research has also provided a more complete understanding of the various complex collisional processes that are important in laboratory plasmas. Finally, these theoretical efforts have been conducted in close collaboration with the electron-ion experiments at ORNL and elsewhere in order to help select key experiments, aid in the interpretation of experimental results, and test the accuracy of various theoretical methods.

During the past year, all the atomic structure and scattering programs currently being employed within this activity have been converted to run under the UNICOS operating system at the National Energy Research Supercomputer Center at Lawrence Livermore National Laboratory. Especially with some of the older programs, extensive changes and significant testing of the converted codes were required.

Because of the plasma edge problem, and with design work on the International Thermonuclear Experimental Reactor (ITER) now proceeding, emphasis with respect to the impurity ions has shifted from highly ionized species to more complex ions in lower stages of ionization. In such ions, the atomic structure is more complex, configuration-interaction within the target states is more pronounced, and continuum

coupling effects are more important. The close-coupling approximation is the most accurate way to include the effects of quantum mechanical interference between various continuum channels and between resonance states and the background continua. However, because of the complexity of the bound-state configurations in such ions, the required close-coupling expansion can become quite large. This is especially true of doubly excited states.

For example, we recently completed 21-state and 26-state R-matrix close-coupling calculations of the $3p^63d \rightarrow 3p^53d^2$ excitation on Ti^{3+} (ref. 17). The three highest terms of the $3p^53d^2$ configuration are autoionizing, and they dominate the ionization cross section near threshold through the process of inner-shell excitation followed by autoionization. Both the 21-state and the 26-state calculations give results in excellent agreement with earlier measurements at ORNL[18] and are a significant improvement on the earlier distorted-wave[19] and the 10-state close-coupling calculations.[20] However, the additional singly excited states included in the 26-state calculation, in comparison to the 21-state calculation, caused a pronounced reduction in the size of the resonance structure associated with excitation to the 16 bound terms of the $3p^53d^2$. It is very difficult to include a sufficient number of singly excited states to obtain convergence, and this poses a serious problem for calculations of excitation to doubly excited states in such ions.

The R-matrix method has proved to be the most efficient technique for solving the close-coupling equations. However, in complex ions, the amount of time required to obtain a solution can be quite large. For example, our recent 31-state calculation for excitation of the valence-shell electron in Zn^+ required over 50 hours of CRAY-2 time for 16 partial waves.[21] The fact that this is not a particularly complicated case, compared to many of the ions of current interest, provides some indication of the magnitude of the computational problem in complex ions. To find solutions to this problem we are considering two possibilities. First, in collaboration with Keith Barrington and Phil Burke at Queen's University in Belfast, we are beginning to explore how existing R-matrix codes might be modified to take advantage of the power of new massively parallel machines such as the 128-node Intel Hypercube at ORNL and the 500-node Intel Paragon to be installed. Second, we wish to investigate whether the independent-processes approximation using distorted waves, which we have used effectively in highly ionized species, might be modified to include interference between the resonance structure and the nonresonant background. Calculations done using this approximation are much faster than those performed using the close-coupling approximation, and, with these modifications, they might be sufficiently accurate to provide reliable cross sections and rate coefficients in complex ions in lower stages of ionization.

We have recently performed calculations of the differential excitation cross section in Na-like Ar^{7+} in support of merged-beams electron-energy-loss measurements being performed at ORNL. The differential cross section of the $3s \rightarrow 3p$ excitation in this ion, for energies close to threshold, indicates that most of the electrons will be scattered at angles greater than 60°. This may explain the difficulties associated with this technique in performing measurements of the cross section of energies of more than a few electron volts above threshold. Preliminary differential cross-section calculations for the Mg-like ion Ar^{6+} reveal the same sort of backscattering for dipole-allowed transitions; however, they also indicate much more forward scattering in the case of spin-changing transitions. Additional work is needed on such differential cross sections to

aid with the selection and interpretation of current experiments and to provide better understanding of the physical reasons for such pronounced backscattering peaks.

There is a great deal of current interest in searching for cases where interference between direct radiative recombination and dielectronic recombination, as well as interference between individual dielectronic capture resonances, might be important. We have been involved in a study to better understand why the independent-processes approximation, which does not include any of these effects, continues to accurately predict the results obtained from the current generation of high-resolution electron-ion recombination experiments. We have examined the results of a number of recent calculations in which various levels of approximations have been employed to incorporate these interference effects. In addition, we have performed a series of model calculations based on perturbation theory to study the effects of overlapping resonances on dielectronic recombination cross sections.

Our general conclusions from this study are that effects of interference between radiative recombination and dielectronic recombination should be less than 1% for ions in lower stages of ionization and no more than 3% for extremely ionized heavy systems. Furthermore, we expect that the effect of overlapping resonances on dielectronic recombination should be quite small in ions with relatively simple atomic structure. Effects on the shapes of the individual resonances should be very difficult to detect in current experiments, and integrated cross sections should be affected by less than 10%. However, for complex ions in lower stages of ionization, the resonances associated with large numbers of fine-structure levels can be quite close together, and the effects of interference could be more pronounced. Therefore, future research on electron-impact recombination should focus on more complex ions in relatively low stages of ionization, where the atomic structure is difficult to calculate and interference effects might be more pronounced. In addition, much more effort is needed to investigate plasma density effects on recombination rate coefficients.

2.3 CONTROLLED FUSION ATOMIC DATA CENTER

H. B. Gilbody, D. C. Gregory, C. C. Havener, M. I. Kirkpatrick, E. W. McDaniel, F. W. Meyer, T. J. Morgan, R. A. Phaneuf, M. S. Pindzola, D. R. Schultz, and E. W. Thomas

The Controlled Fusion Atomic Data Center (CFADC) collects, reviews, evaluates, and recommends numerical atomic collision data that are relevant to controlled thermonuclear fusion research. The CFADC operates with the equivalent of 1.3 full-time staff members and a number of expert consultants under contract. Members of the experimental atomic physics for fusion group also contribute a small fraction of their time to literature searches and categorization of relevant publications. The major activities of the CFADC are

- The maintenance of an on-line computer bibliographic database of fusion-related publications on atomic collision processes, and periodic distribution of updates to other data centers.
- The preparation and publication of compilations of recommended atomic collision data for fusion applications.
- The deduction of scaling laws and parametrizations of atomic collision data to facilitate application in fusion research.
- The establishment and dissemination of a computer database of recommended collision cross sections and rate coefficients.

- The review of the existing atomic collision database with respect to current applications in fusion research and identification of data needs.
- The handling of individual requests for data or literature searches on specific processes.

The CFADC participates in the IAEA's Atomic and Molecular Data Center Network in Vienna and has cooperative agreements with a number of other data centers. Bibliographic updates are sent semiannually on computer diskettes to the IAEA and to Japanese data centers at Nagoya and the Japan Atomic Energy Research Institute (JAERI). This forms the basis for the semiannual IAEA *International Bulletin on Atomic and Molecular Data for Fusion.* Specific activities of the past year and plans for the next year are summarized below.

2.3.1 Bibliographic Database

The on-line bibliographic database has been kept up to date and now contains 24,150 categorized and indexed references from 120 journals, covering the period from 1978 to the present; 1050 new references were added during 1991. Literature searches are performed monthly by four ORNL staff members and by five expert consultants under contract to the CFADC. A version of the CFADC personal-computer-based on-line search and retrieval system has been installed at Justus Liebig University in Giessen, Germany, where updates of the dBase III+™ database files are sent periodically. The CFADC answers specific requests for data and bibliographic searches at a rate of two per week.

2.3.2 Data Compilation and Evaluation

In collaboration with R. K. Janev of the IAEA and H. Tawara of the National Institute for Fusion Studies in Japan, data were collected and evaluated for state-selective electron capture in collisions of C^{q+} and O^{q+} ions with H, H_2, and He. Cross sections were recommended for 87 reaction channels for C^{6+} + H and O^{8+} + H collisions, and a preliminary ALADDIN database was created based on spline fits to the data. A manuscript containing graphical representations of the data was submitted to *Atomic Data and Nuclear Data Tables* for publication. Analytical fits will be made to the recommended cross sections by T. Shirai of JAERI, and an ALADDIN database will be created for distribution. The recommended database will be expanded to include the other reactants as more data become available.

2.3.3 Atomic Database for Beryllium and Boron Ions

The database for collisions of beryllium and boron ions with H, H_2, and He was reviewed and evaluated as part of an IAEA Consultants' meeting, and a Working Group Report was prepared by the CFADC. This will be published in an Atomic and Molecular Data Supplement to *Nuclear Fusion.*

2.3.4 ALADDIN Database

The CFADC has continued to distribute the ALADDIN database program and ORNL "Redbook" data files via diskette and electronic mail. A user-accessible ALADDIN database will be created on a local IBM-6000 RISC workstation.

2.3.5 Data Parametrization

In collaboration with T. Shirai of JAERI, analytical expressions have been fitted to the cross sections for 21 reactions from the "Redbook" compilation on collisions of H, H_2, He, and Li atoms and ions

(ORNL-6086). These expressions permit the recommended data to be more reliably extrapolated to higher or lower collision energies.

2.3.6 CAMOS Survey of AMO Experimentalists in the United States

A survey of experimental atomic, molecular, and optical (AMO) scientists in the United States was carried out by the Committee on Atomic, Molecular, and Optical Sciences (CAMOS) of the National Research Council. The data from this survey were analyzed by the CFADC, and a summary report was presented to CAMOS in December 1991. The CFADC will coordinate data input and analysis for a new CAMOS questionnaire on Future Opportunities in Atomic, Molecular and Optical Sciences.

2.4 ADVANCED PLASMA DIAGNOSTICS DEVELOPMENT

2.4.1 Proof-of-Principle Test of an Alpha Particle Diagnostic

R. K. Richards, D. P. Hutchinson, C. A. Bennett, and C. H. Ma

An alpha particle diagnostic designed for the measurement of fusion-product alpha particles has been tested on the Advanced Toroidal Facility (ATF), a nonburning plasma device. The diagnostic is based on CO_2 laser Thomson scattering and heterodyne detection. The plasma parameters in a machine such as ITER require detection of scattered laser radiation at small angles (around 1°) for the measurement of alpha particles.[22] Because these conditions pose the problem of detection of small signals (typically 10^{-9} W) in the presence of a large source (>10^6 W) while maintaining optical alignment over long distances (several tens of meters), a proof-of-principle test was conducted under these conditions. With no high-energy alpha particle source available, the test consisted of a measurement of an electron resonance.[23] The source laser was a 4-MW, 1-μs pulsed CO_2 laser with unstable resonator optics. It was pumped with a 250-mW continuous-wave (cw) CO_2 laser. The cw laser set the wavelength, pulse length, polarization, and alignment for the pulsed source.

The heterodyne receiver was aligned to view scattering at 0.86° from the pulsed source and was set at 63.23 GHz from the pulsed laser frequency by a local oscillator tuned to a CO_2 sequence band line. Alignment of the receiver was maintained by continuously viewing a warm blackbody source set next to the source laser at 0.86°.

Results from this test are given in Fig. 2.7. The plasma density was scanned by varying the plasma conditions or the time during the discharge that data were taken. The resonance feature occurs at an electron density near 4×10^{13} cm^{-3} and matches the theoretical prediction over the variation of electron temperatures (300–500 eV) during this test. The scattering amplitude was determined by a measurement of the signal from the blackbody source, which gave the receiver quantum efficiency.

Results from the proof-of-principle test may be summarized as follows:

1. Small signal levels can be measured at small scattering angles in the presence of a large source laser—conditions essential for measurements on a burning plasma.
2. Alignment over tens of meters during a plasma experiment can be maintained, allowing remote siting of source and receiver.

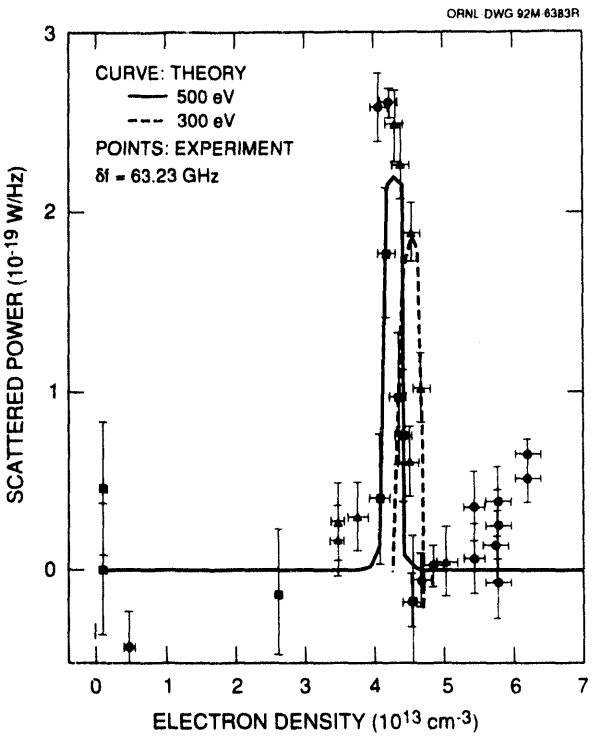

Fig. 2.7. Results from the proof-of-principle scattering test of the alpha particle diagnostic on ATF compared to theory, showing the electron resonance shifted by 63.23 GHz from the source laser frequency.

3. Signal levels can be quantified for plasma measurements by an in situ calibration source.
4. The diagnostic proved nonperturbing to the plasma.
5. Only a small access port is required for the scattering and alignment systems.

2.4.2 FIR Density Profile Measurement on ATF

C. H. Ma, L. R. Baylor,* D. P. Hutchinson, M. Murakami,* and J. B. Wilgen*

The multichord far-infrared (FIR) interferometer system on ATF is described in ref. 24. During 1990 and 1991, significant improvements were made in both the hardware and the data analysis codes. The system has been routinely employed to study density evolution in plasma discharges with both electron cyclotron heating (ECH) and neutral beam injection (NBI), fueled by both gas fueling and pellet injection. The standard deviation of the output of the system for a constant phase shift is less than 5×10^{-2} fringe. Since one fringe corresponds to a line-averaged electron density of 1.3×10^{13} cm^{-3}, density variations as small as 6.5×10^{11} cm^{-3} can be measured. The time resolution of the system, set by the frequency of the beat signal, is typically 5 μs. Figure 2.8 shows the time-resolved traces of the line-integrated electron density of an ATF plasma discharge for the proof-of-principle test of the alpha particle diagnostic described in Sect. 2.4.1. This discharge is initiated with ECH, followed by NBI. The density rises rapidly during the NBI pulse.

A chordal inversion code has been developed and used to reconstruct the spatial distribution of electron density in ATF.[25] The measured chordal data are inverted to a local electron density profile by a technique extended from an asymmetric inversion method developed for tokamak plasmas.[26] The basic principle of the method is to divide the flux surface geometry into shells that are assumed to have a constant particle density. The measured chordal data are interpolated to provide data for chords that pass through the center of each shell at the horizontal midplane. The path length of the interpolated chords through the shells is calculated, and the local density within the shell is determined by starting at the outermost shell and working toward the innermost shell. This is done independently for the chords on the inside and outside of the magnetic axis, which allows for an asymmetric profile. The flux surface geometry is expressed in a Fourier spectral form and is determined from the three-dimensional equilibrium code VMEC.[27] The inversion code has been employed routinely to provide density profile information for ATF plasma

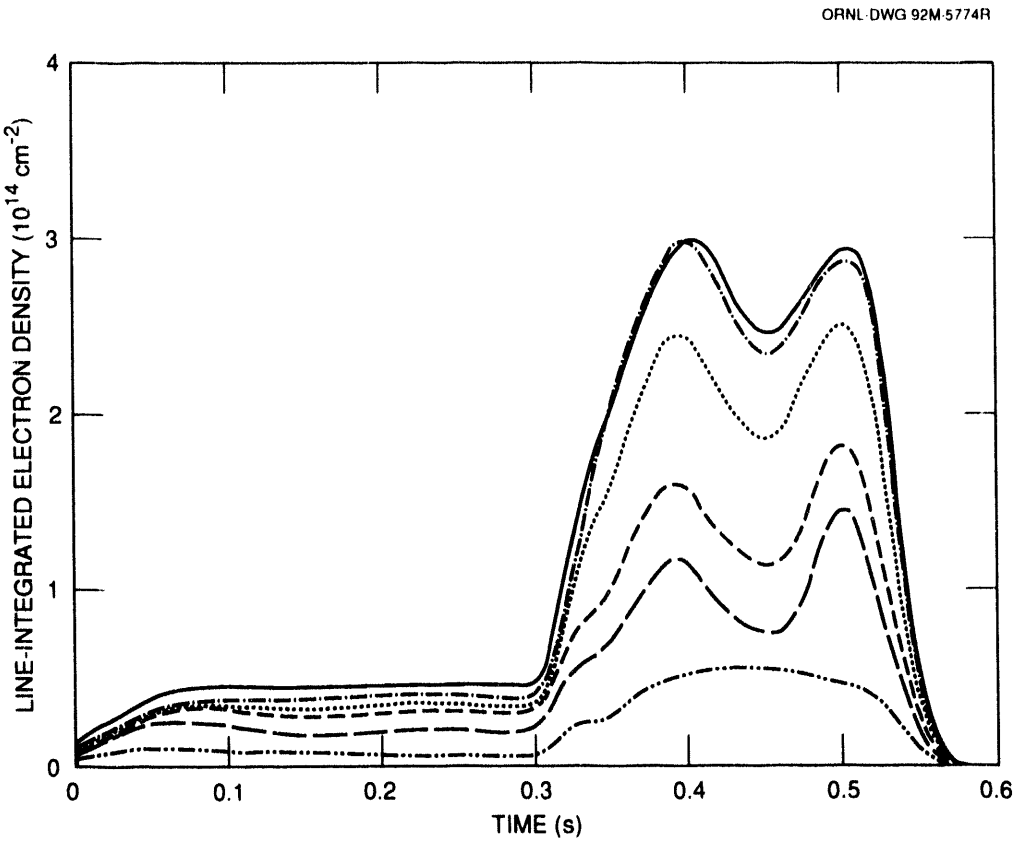

Fig. 2.8. Time variations of the line-integrated electron density, measured by the multichord FIR interferometer system on ATF for a proof-of-principle test of an alpha particle diagnostic based on CO_2 laser small-angle Thomson scattering.

studies. The inverted density profile from the discharge discussed in Fig. 2.8 is shown in Fig. 2.9. The density profile during the ECH-only portion of the discharge is generally hollow, which is similar to results from other stellarator experiments. With NBI, the profile becomes slightly peaked.

Cross-correlation of density profile measurements among the FIR interferometer, Thomson scattering, the heavy-ion beam probe, and the fast reciprocating Langmuir probe has been achieved. Density profiles measured by these diagnostics are generally in good agreement and are hollow or flat under most experimental conditions with ECH plasmas.

---

*Fusion Energy Division.

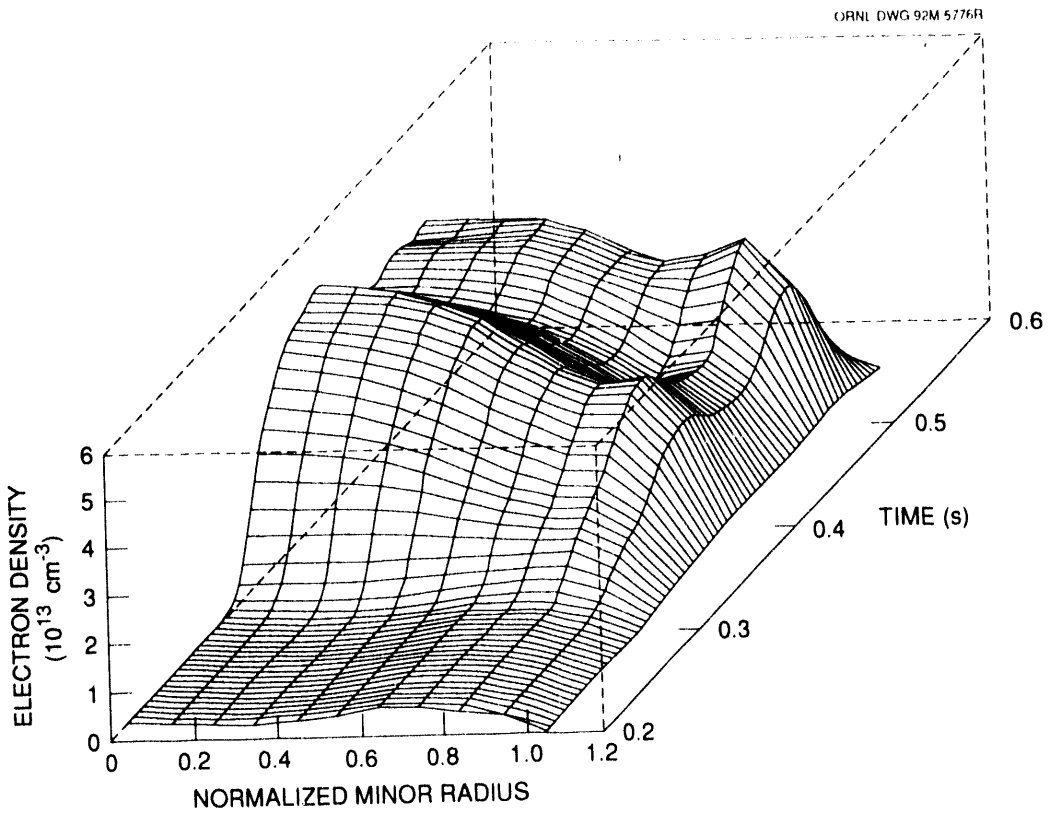

Fig. 2.9. Inverted density profile from the discharge discussed in Fig. 2.8. The density profile became slightly peaked as a result of NBI.

REFERENCES

1. E. K. Wåhlin et al., *Phys. Rev. Lett.* **66**, 157 (1991).

2. N. R. Badnell, M. S. Pindzola, and D. C. Griffin, *Phys. Rev. A* **43**, 2250 (1991).

3. R. A. Phaneuf, "Experiments on Electron-Impact Excitation and Ionization of Ions," pp. 117–56 in *Atomic Processes in Electron-Ion and Ion-Ion Collisions*, ed. F. Brouillard, Plenum, New York, 1986 (NATO ASI Series B: Physics, Vol. 145).

4. W. Lotz, *Z. Phys.* **206**, 205 (1968); **216**, 241 (1968); **220**, 466 (1969).

5. H. J. Andrä, *Nucl. Instrum. Methods Phys. Res.* **B43**, 306 (1989).

6. U. A. Arifov et al., *Sov. Phys.–Tech. Phys.* **18**, 118 (1973).

7. F. W. Meyer et al., "Evidence for Above-Surface and Subsurface Neutralization during Interactions of Highly Charged Ions with a Metal Target," *Phys. Rev. Lett.* **67**, 723 (1991).

8. F. W. Meyer et al., "Electron Emission during Interactions of Multicharged N and Ar Ions with Au(110) and Cu(001) Surfaces," *Phys. Rev. A* **44**, 7214–28 (1991).

9. S. H. Overbury, F. W. Meyer, and M. T. Robinson, "Computer Simulations of Relaxation Processes in Scattering of Multicharged Ions from Metal Surfaces," presented at the 14th International Conference on Atomic Collisions in Solids, Salford, United Kingdom, July 28–August 2, 1991 (proceedings to be published in *Nucl. Instrum. Methods Phys. Res.* **B**).

10. P. A. Zeijlmans van Emmichoven, C. C. Havener, and F. W. Meyer, *Phys. Rev. A* **43**, 1405 (1991).

11. J. Burgdörfer, P. Lerner, and F. W. Meyer, "Above-Surface Neutralization of Multicharged Ions: The Classical Overbarrier Model," *Phys. Rev. A* **44**, 5674–85 (1991).

12. C. C. Havener et al., "Merged-Beams Measurements of Electron-Capture Cross Sections for O^{5+} + H at Electron-Volt Energies," *Phys. Rev. A* **39**, 1725 (1989).

13. C. C. Havener, F. W. Meyer, and R. A. Phaneuf, "Electron Capture in Very Low Energy

Collisions of Multicharged Ions with H and D in Merged Beams," presented at the XVII International Conference on the Physics of Electronic and Atomic Collision, Brisbane, Australia, July 10–14, 1991 (proceedings to be published).

14. C. C. Havener et al., *Nucl. Instrum. Methods Phys. Res.* **B56/57**, 95 (1991).

15. L. R. Andersson, M. Gargaud, and R. McCarroll, *J. Phys. B* **24**, 2073 (1991).

16. *Proceedings of the 10th International Workshop on ECR Ion Sources*, ed. F. W. Meyer and M. I. Kirkpatrick, CONF-9011136, Martin Marietta Energy Systems, Inc., Oak Ridge National Laboratory, January 1991.

17. D. C. Griffin, M. S. Pindzola, and N. R. Badnell, *J. Phys. B* **24**, L261 (1991).

18. R. A. Falk et al., *Phys. Rev. Lett.* **47**, 494 (1981).

19. C. Bottcher, D. C. Griffin, and M. S. Pindzola, *J. Phys. B* **16**, L65 (1983).

20. P. G. Burke, W. C. Fon, and A. E. Kingston, *J. Phys. B* **17**, L733 (1984).

21. M. S. Pindzola, D. C. Griffin, and N. R. Badnell, *Phys. Rev. A* **44**, 5628 (1991).

22. R. K. Richards et al., "CO_2 Laser Thomson Scattering Diagnostic for Fusion Product Alpha Particle Measurement," *Rev. Sci. Instrum.* **59**, 1556–8 (1988).

23. J. Sheffield, *Plasma Scattering of Electromagnetic Radiation*, Academic Press, New York, 1975, pp. 137–43.

24. C. H. Ma, D. P. Hutchinson, and K. L. Vander Sluis, "A Difluoromethane Laser Interferometer System on ATF," *Rev. Sci. Instrum.* **61**, 2891 (1990).

25. L. P. Baylor, C. H. Ma, and S. Hiroe, *Inversion of Chordal Data from the ATF Torsatron*, ORNL/TM-11758, Martin Marietta Energy Systems, Inc., Oak Ridge National Laboratory, February 1991.

26. H. K. Park, *Plasma Phys. Controlled Fusion* **31**, 2035 (1989).

27. S. P. Hirshman, W. I. Van Rij, and P. Merkel, *Comput. Phys. Commun.* **43**, 143 (1986).

3

FUSION THEORY AND COMPUTING

R. A. Dory

S. E. Attenberger[1]
D. B. Batchelor
B. A. Carreras
M. D. Carter
L. A. Charlton[1]
P. J. Christenson[2]
P. H. Diamond[3]
N. Dominguez
D. T. Fehling
R. H. Fowler[1]
L. Garcia[4]
C. E. Gibson
C. A. Giles[1]
D. C. Giles[1]
R. C. Goldfinger[1]
D. E. Greenwood
R. D. Hazeltine[5]
C. L. Hedrick
S. P. Hirshman
J. T. Hogan
J. A. Holmes[1]
W. A. Houlberg
E. F. Jaeger
K. L. Kannan[1]
J. N. Leboeuf
D. K. Lee[1]
V. E. Lynch[1]
J. F. Lyon[6]
D. R. Overbey
L. W. Owen[1]
T. C. Patrick
J. A. Rome
K. C. Shaing
K. L. Sidikman[7]
D. A. Spong
N. A. Uckan
W. I. van Rij[1]

1. Computing and Telecommunications Division, Martin Marietta Energy Systems, Inc.
2. Graduate student, the University of Michigan, Ann Arbor.
3. University of California at San Diego, La Jolla.
4. Universidad Complutense, Facultad de Ciencias Fisicas, Madrid, Spain.
5. The University of Texas, Austin.
6. Toroidal Confinement Section.
7. Oak Ridge Associated Universities, Oak Ridge, Tennessee.

3. FUSION THEORY AND COMPUTING

Summary of Activities

During this reporting period, the balance between the development of new or advanced methods and theoretical models and the application of existing theories tipped fairly strongly toward the application side. This reflects manifold opportunities to confront existing models with data (and vice versa) and to make useful applications of mature techniques. It also reflects changed funding patterns. The ability of the U.S. fusion program to carry on fundamental theory work has decreased because of flat to slightly decreasing budgets for several years, accompanied by a substantial rise in costs—resulting largely from mandated changes in the way that laboratories do business. Moreover, the U.S. and international fusion programs have undergone substantial changes.

ORNL theorists contributed strongly to the International Thermonuclear Experimental Reactor (ITER), to the Burning Plasma Experiment (BPX) project, and to experimental and technological successes at the Joint European Torus (JET), the Tokamak Fusion Test Reactor (TFTR), DIII-D, TEXTOR, and Tore Supra. The ORNL Advanced Toroidal Facility (ATF) experimental program remained a primary focus for our stellarator analyses; substantial activities in this area also contributed to the definition of new devices in Japan, the former Soviet Union, Australia, and Spain.

New insights into turbulence and transport in toroidal systems led to the analysis of plasma core and edge transport, the associated development of radial electric fields, and the diagnosis of controlling physics through detailed comparisons with ATF and experiments on the Texas Experimental Tokamak (TEXT).

The Numerical Tokamak Project is a major new thrust for the U.S. theory program. ORNL theorists and computational physicists have been strong contributors to the development of a proposal in the national Grand Challenge Computational Initiative. In addition to helping to define overall directions of the proposal, ORNL contributed new methods (such as gyrofluid models with an efficient Landau closure scheme) for inclusion of essential kinetic phenomena, as well as substantial experience in the development of efficient means for using the latest hardware technologies such as massively parallel computers.

Better insight into the physics governing the transition from L-mode to H-mode in tokamaks remains a high priority in the fusion program, and ORNL contributions are an essential ingredient in the search for a fully validated model. However, final validation, with agreement by all concerned parties, remains in the future.

In the analysis of rf heating and current drive, a large and successful effort was made to improve the fundamental full-wave simulation model, which does not rely on the geometrical optics approximation of ray tracing models. With the new spectral approach, it is possible to

give good representation to the important effect of upshift of the $k_{\|}$ spectrum. Another important contribution to rf theory has been insight leading to the development of a method for estimating the current associated with rf processes. Applications of these and related rf models to the design of antennas and launch structures were made for specific experiments such as ITER, BPX, DIII-D, Tore Supra, and the Toroidal Physics Experiment (TPX) project.

Understanding the behavior of the ATF stellarator is a key part of our activity, with substantial progress made in comparing results of theoretical calculations with data. An example has been the measurement and analysis of bootstrap current and its detailed comparison with neoclassical models as the magnetic configuration is modified by changing external coils.

During 1990–91, it became clear that energy confinement in stellarators and in tokamaks follows broadly the same scaling with parameters, while key details differ. One of these details is that ATF has not yet been able to attain the improved H-mode confinement that results in tokamaks when sufficient auxiliary heating power is available. A second detail is that ATF energy confinement closely follows the dependence expected from processes caused by (gyro-reduced Bohm) turbulence on small spatial scales, while tokamaks apparently suffer from (Bohm) turbulence at larger radial scales. As a result, stellarator confinement extrapolated by using the ATF scaling with plasma density and magnetic field is rather more favorable.

The ATF data acquisition system and the software for initial analysis, database formation, and subsequent analysis of the data were refined and made more efficient. This made possible the rapid assessment of results and modification of the experimental program to capitalize on the understanding. Several workstation computers were added to improve visualization of scientific data and provide effective analysis at the middle scales, where massive computers of the CRAY class are not required.

3.1 EQUILIBRIUM AND STABILITY

3.1.1 Overview

The magnetohydrodynamic (MHD) equilibrium and stability studies are directed toward understanding and improvement of the global confinement properties of tokamaks and stellarators. Equilibrium and stability theory is applied to complement configuration optimization studies and for interpretation of experimental results. Because of changes in the priorities of the U.S. fusion program, work on MHD equilibrium and stability of stellarators has decreased. Most of the ORNL research in this area was through collaborations with other institutions.

In collaboration with the Kharkov Institute of Physics and Technology, we have investigated the effect of finite beta on stellarator confinement in the l/n regime. The quadrupole magnetic field was used to improve the confinement in this regime for the vacuum magnetic field. However, the finite-beta shift of the magnetic axis reduces the transport optimization done for the vacuum magnetic fields. The stability properties of Uragan-2M have been investigated in detail, and new ways of improving its performance have been found. A new model for representing the Uragan-2M vacuum magnetic field led to more optimistic stability results. With the Mercier criterion, it is possible to develop scenarios for access to the second stability regime. Joint papers have been presented and published.[1–3]

Studies continued to explore the role of the flexibility of the TJ-II flexible heliac in broadening its operational space. The role of ballooning modes for this configuration was investigated. External magnetic field control of the ballooning instabilities has not been as effective as that of the interchange instabilities. This work was done in collaboration with the Centro de Investigaciones Energéticas, Medioambientales, y Tecnológicas (CIEMAT), Madrid, Spain.[4–7]

Research on MHD equilibrium and stability of the Large Helical Device (LHD) stellarator has continued in collaboration with Kyoto University.[8]

In the Advanced Toroidal Facility (ATF), the effects and control of the bootstrap current have been investigated. In collaboration with the experimental group, we have analyzed long-pulse ATF discharges to investigate the properties of the bootstrap current. This series of experiments, in which the magnetic configuration was varied during the course of a discharge, has shown results similar to those of the sequence of short-pulse, fixed-configuration experiments done last year. It has led to the demonstration of the capability for external control of the bootstrap current. These results agree with previous theoretical predictions and with detailed analysis using the measured temperature and density profiles.[9–12]

Profile analyses and fluctuation measurements for the experiments in which ATF's magnetic configuration was varied have led to an assessment of the needs and the potential for drift trapped-electron mode (DTEM) studies. This assessment concluded that the DTEM regime is accessible. However, the density profiles are such that the most dangerous DTEMs are stable. Pellet injection was used to modify the experimental profiles, and the stability properties of the profiles after pellet injection were investigated. Comparisons of fluctuations measured inside and outside the magnetic axis were predicted to be an important discriminating criterion because of the difference in the trapped-particle populations in the two regions.

Regarding tokamak stability, we have continued to survey the stability properties of shaped tokamaks to provide a database for scaling studies for the design of the International Thermonuclear Experimental

Reactor (ITER). We have included the evaluation of the resistive and alpha particle stability properties for ITER equilibria in the ideal MHD database. Using the three-dimensional (3-D) codes developed to study alpha particle instabilities, we have collaborated with the ITER team to investigate possible beam-driven instabilities.

3.1.2 Highlights

3.1.2.1 Stellarator MHD studies

Collaborative design studies for the Uragan-2M device, nearing completion at the Kharkov Institute of Physics and Technology, are described in refs. 2 and 13. Uragan-2M will have a redesigned and rebuilt magnetic configuration that was designed by the Kharkov group and other Russian Federation groups, working with theorists at ORNL (as part of a U.S.–Russian Federation exchange) and at the Max Planck Institute for Plasma Physics, Garching bei München, Federal Republic of Germany. Among the ORNL-developed theoretical tools applied in the design were a magnetic field line code, the VMEC 3-D equilibrium code, the DKES 3-D transport coefficient code, and the NDM 3-D Mercier stability code.

For stellarator devices, a wide range of available magnetic field configurations permits experiments to be optimized jointly for stability and confinement based on collisional processes or for flexibility to change the combination. In the new Uragan-2M design, the two helical windings are split and separately energizable, and there are four separate sets of vertical field windings, giving a large range of magnetic conditions. Of special interest are modes of operation with stability limits ranging from 1.2% to 6%, obtained by controlling the degree of magnetic well or hill. The rebuilt device is expected to be finished in late 1991, but optimization studies for a new vacuum vessel are still in progress.

3.1.2.2 Bootstrap current control

Increasing the bootstrap current I_B is a potentially important optimization for obtaining sufficient current in a large, long-pulse tokamak. Conversely, reducing or controlling I_B is useful for obtaining the best performance in a device such as the ATF torsatron. In either case, understanding how well I_B follows predictions is essential to exploiting or avoiding its effects. Measurements in ATF have provided strong confirmation that I_B behaves as $f_t/f_c \cdot \nabla p \cdot G_b \cdot \mathbf{B}^{-1}$, where f_t/f_c is the ratio of the fractions of trapped and circulating particles, ∇p is the pressure gradient, G_b is a geometrical factor, and $\mathbf{B}$ is the magnetic field, confirming the predictions of detailed theoretical expressions. The calculation has been extended from the highly collisional regime into the transitional "plateau" regime and has incorporated detailed prescriptions of the plasma shape. The work applies analytical kinetic theory, validation for complex geometries by use of the DKES model, and evaluation of specific geometrical factors using 3-D equilibrium analysis and experimentally observed plasma profiles. Use of the ability in ATF to modify G_b by changing the $\mathbf{B}$ spectrum via shaping-field currents was essential to demonstration of detailed correlation between measured and predicted I_B. The close correlation between the data and collisional (neoclassical) theory also supports the conclusion by Shaing and colleagues that turbulence effects should not be large in I_B, although they dominate energy transport.

3.2 THE NUMERICAL TOKAMAK

3.2.1 Overview

In the last two years, the Numerical Tokamak Project has emerged as one of the most interesting initiatives of the U.S. fusion program. The ORNL group has been an integral part of the project since its beginnings. A national consortium, with members from the fusion modeling, simulation, and computing communities, collaborates closely with the supporting high-performance computer facilities in the development of computational models with the long-term goal of simulating a large tokamak on massively parallel computers. This project is a Grand Challenge in computation.

The ORNL fusion theory group is contributing to this project in several areas:

1. Development of gyrofluid models that incorporate Landau closure. The new formulation of fluid closure with the N-pole approximation for the Z-function, which allows the incorporation of Landau damping in the fluid equations, has been applied to several dynamical models.[14] Linear stability calculations incorporating the Landau damping with 2- to 5-pole approximations give results very close to the full kinetic theory. For several of the problems considered, the 2-pole approximation is probably accurate enough for the nonlinear studies. Finite ion Larmor radius effects have been incorporated in the model through the use of a Padé approximant to the modified Bessel function.[15]

As an application of this approach, a toroidal geometry fluid code has been implemented, tested, and applied to study alpha particle instabilities. We have shown the linear destabilization of gap modes by alpha particles and compared these results with analytical results from Van Dam et al. for toroidal Alfvén eigenmodes (TAE modes).[16] The effect of continuous damping on the TAE modes has been studied in detail. Comparisons have been made with the analytical models of Rosenbluth et al. The agreement is good and shows the capability of the code. Electron and ion Landau damping effects are being included. This code allows us to initiate nonlinear studies of alpha particle instabilities.

2. Development of algorithms on massively parallel computers. Numerical algorithms for fluid equations on parallel computers have been under development and testing for the last six years. The main emphasis has been on the use of the different Intel hypercubes at ORNL.[17] During last year, work on the iPSC/860 machine has continued; the efficiency of the code on this machine has been on increased by a factor of three.[18,19] We have also performed the first test of the Delta machine in collaboration with the Jet Propulsion Laboratory (JPL), and we are developing convolution software for the CM-2 machine, to be tested in FY 1993, and have started tests of the Butterfly machine in collaboration with the National Energy Research Supercomputer Center (NERSC).

3. Development of the hybrid fluid–particle code. This opens a third alternative approach to solving multiple-species nonlinear plasma physics problems. The main application of the hybrid fluid–particle approach has been to alpha particle stability. In this approach, the background plasma is treated as a fluid while the alphas are treated as particles. This approach complements the gyrofluid approach. Initial dynamical studies for two-dimensional (2-D) geometry have been performed in collaboration with the Massachusetts Institute of Technology (MIT). The code is being extended to 3-D geometry.[20]

3.2.2 Highlights

3.2.2.1 Gyrofluid models with Landau closure

We have defined a method for adding Landau damping, in a good approximation, to nonlinear fluid equations for a variety of instability models. This has importance because omitting linear Landau damping causes modes to extend over far too broad a radial region in many cases. The work reformulates and extends a result by Hammett and Perkins for ion temperature gradient driven drift waves. We focus initially on resistive-g modes because of their fundamental importance and because they can be treated with a relatively small number of nonlinear fluid equations. Linear analysis of local and radially resolved eigenfunctions (in both fluid and kinetic treatments) shows good agreement—which can be improved further by increasing the complexity of the closure conditions. These conditions correspond to N-pole approximations to the plasma dispersion function. For the resistive-g modes, a 2-pole approximation gives answers that are in remarkably good agreement with full kinetic results; for example, the growth rates are correct to within 1% in a scan of the curvature parameter using radially resolved analysis. This should provide a useful tool for comparison of tokamak and ATF results and later for nonlinear treatments of other modes.

3.2.2.2 An application of the gyrofluid approach: Alpha particle instabilities

Low-mode-number (fluidlike) instabilities can be kinetically destabilized by alpha particles on passing orbits through inverse Landau damping. This occurs when the phase velocity of gap modes (waves in gaps between the stable shear-Alfvén continua) is roughly equal to the mean alpha parallel velocity. The modes could be unstable in ignited devices such as ITER; they are dangerous because of their large radial extent. A fluidlike model has been developed; it uses a simplified treatment of kinetic effects but gives agreement with analysis for growth rates and frequencies. The fluid approach makes nonlinear calculations possible, including mode coupling and profile modification effects.

The model uses a pressure moment of the alpha gyrokinetic equation coupled to an Ohm's law and vorticity equation for the main plasma. It is solved by an adaptation of the ORNL toroidal initial value code FAR, giving (1) isolation of the fastest-growing mode, (2) systematic convergence tests, (3) flexibility to alter the evolution equations to test new physics, and (4) the possibility of examining higher-n (toroidal mode) gap waves. The model has been tested against linear theory and will be run in nonlinear regimes to evaluate saturation mechanisms and levels for assessing the relevance of gap mode instabilities to ignited devices.

Since the Alfvén wave continuous spectrum is associated with singular eigenfunctions, there has been a long-standing question about the ability of numerical codes to deal with instabilities that couple to the continuous spectrum. An important example is the case of the TAE modes, which are destabilized by energetic particle populations. These modes couple to the continuum. As shown by Rosenbluth,[21] this coupling is critical for the determination of the threshold of the TAE modes. Careful numerical calculations, based on a gyrofluid model with Landau closure, show excellent agreement with the analytical results of Rosenbluth et al. for the effect of continuum damping on TAE modes. These results show that the numerical calculations are reliable in reproducing the effects of coupling to the continuum spectrum.

3.2.2.3 Algorithms for massively parallel computers

One approach to improving the real-time efficiency of plasma turbulence calculations is to use a parallel algorithm. Four years ago, we first tested such an algorithm on the 64-node Intel iPSC hypercube. The basic algorithm was modified to allocate a radial region to each processor. In this way, convolutions at a fixed radius were performed in parallel, and interprocessor communication was needed only at the boundary values for each radial region. The effective memory configuration was a ring. It was shown that 16 nodes gave a speedup of a factor of 4 to 5; however, while it was possible to perform sample calculations, no production computations were practical. Two years ago, our work shifted to the new Intel iPSC/860 (RX) Hypercube (128 processors, 8 megabytes per processor), which offers clear possibilities as a production machine. Before any optimization of the code was done, results showed that the speed was 30% better for the RX machine using 32 processors than for a single-processor CRAY II (300 modes and 129 radial grid points). Direct allocation of all arrays in the KITE code to the nodes (processors) of the iPSC/860 (RX) Hypercube has allowed the full use of all 128 nodes. Using this configuration and recent improvements in the compiler, we have a factor of 5 speedup over a single-processor CRAY II. The JPL Intel iPSC/860 (64 processors, 16 megabytes per processor) complements results from the ORNL Hypercube by having more memory per processor. With the collaboration of the JPL group, it has been possible to complete the code optimization studies; that is, to find the optimal number of processors for a problem of a given size. From these results, we can estimate the main characteristics of the next-generation hypercubes needed for plasma turbulence calculations.

Also in collaboration with JPL, the first runs of this code on the Touchstone Delta machine (512 processors, 8 megabytes per processor) have been made. A 25% speedup has been found for the same number of processors (128) as the iPSC/860. This is because of the faster communication processes in the Delta machine. Comparison with a single CRAY II processor for the largest memory job on the Delta machine (385 modes, 1025 radial grid points) shows, a speedup factor of 16.

3.2.2.4 Nonlinear hybrid fluid–particle model of fast ion–Alfvén wave interactions

The kinetic Alfvén wave is important because it can be driven unstable both directly by the alpha particles and indirectly by TAE mode frequencies exciting a continuum resonance. In a hybrid particle–fluid code, the bulk plasma is fluidlike and the energetic alphas are treated as guiding center particles. We consider the nonlinear evolution of kinetic Alfvén wave turbulence and anomalous alpha particle transport in simplified geometry. Extensive computational studies have been carried out, showing that the electrostatic and magnetic Alfvén fluctuations $\tilde{\phi}$ and $\tilde{\psi}$ are highly correlated in the absence of magnetic shear. Such correlated fluctuations lead to cancellation or inhibition of the nonlinear fluid (wave-wave) interactions. The saturation of turbulence occurs because of the steepening of the velocity gradient of the resonant alphas, thereby enhancing wave damping (Landau damping). Preliminary indications are that the correlation between $\tilde{\phi}$ and $\tilde{\psi}$ is reduced when magnetic shear is included, thus allowing wave-wave coupling effects to enter in regions with strong shear.

3.3 TURBULENCE

3.3.1 Overview

The plasma turbulence research effort at ORNL is characterized by the parallel use of analytical and numerical fluid models to study the behavior of magnetically confined plasmas. Calculations are also made of nonlinearly evolved fluctuation levels and their consequences for particle and heat transport. Research is carried out on two strongly interconnected levels. First, fundamental physics research is performed, generally in a simplified geometry, to unveil the basic mechanisms that underlie plasma behavior. This work establishes a sound basis for further theoretical development. Theoretical results are then applied to specific devices, providing basic physics understanding and tools for configuration optimization and for plasma modeling. In these studies, the combination of analytical and computational work has led to several significant new results.[22,23]

A model for drift wave turbulence that is simple enough to be amenable to analytical treatment and to high-resolution numerical studies has been developed. This model allows the incorporation of the radial electric field. High-resolution nonlinear calculations have shown that the mixing length approach does not give the right saturation level for these instabilities. Spatial intermittencies associated with the location of low-order rational surfaces dramatically change the dynamics of the turbulence and cause the enhancement of the turbulence level. The effect of the shear in the radial electric field, which is strong in the linear regime, is absent in the nonlinear regime. However, the effect of curvature (E'') in the electric field is to reduce the level of saturation.[24,25]

For resistive pressure-gradient-driven turbulence, we have shown that fluctuations can be the cause of the sheared electric field at the plasma edge. On the other hand, the instabilities couple to the Kelvin-Helmholtz (K-H) drive, which in general is stabilizing in the linear regime. Again, the shear electric field is ineffectual in the nonlinear regime. Curvature in the flow (V'') is important.[26–29]

From these studies, a new picture of the transition from L-mode to H-mode (L-H transition) is emerging. The radial structure of the flows (radial electric field) is essential. A parabolic dependence in x ($V'' \neq 0$) is essential for suppression of the turbulence. This, in turn, can be generated through the diamagnetic term in the turbulence or by a seed flow. These results are supported by the results of flow measurements in the edge of DIII-D.

The collaboration between the ATF and Texas Experimental Tokamak (TEXT) groups for analysis and modeling of edge fluctuation data from machines has continued with a consideration of ionization effects. Dissipative drift waves can be linearly destabilized by ionization sources. The main pending problem is to model these sources. Measurements are under way in TEXT to identify these terms. Nonlinear calculations have been done to understand the saturation mechanism for ionization-driven turbulence.[30–32]

3.3.2 Highlights

3.3.2.1 Drift wave turbulence

A simplified, single-equation model of drift wave turbulence has been developed to permit both analytic and numerical calculation of the effects of velocity shear. Nonlinear analytic calculations predicted that these effects should lead to a reduction in the turbulent saturation level. Numerical calculations did produce the predicted linear effects. However, calculations that reached nonlinear saturation did not show a reduction in the fluctuation level. Recently, it has

been found that nonlinear, single-helicity effects greatly alter the nonlinear dynamics. Since all the modes are centered at a single surface, their spatial variation is reinforced by mode coupling rather than averaged out, as it is in a case with many neighboring surfaces. Nonlinear analytic calculations show that the effect of this spatial variation is to create a potential well, which confines the eigenfunction. The energy of the drift wave no longer propagates away, subject to linear magnetic shear damping. Since the damping effect of velocity shear operates through the magnetic shear damping, this effect is reduced. For cases in which all modes are linearly stable because of velocity shear, initialization below the threshold for nonlinear effects results in decay of the energy. For cases initialized above the threshold, the energy settles down and then begins to grow, indicating the suppression of the linear magnetic shear damping by the nonlinear effects followed by the reassertion of the linear drive. Multiple-helicity calculations have shown that the single-helicity effects occur only near low-order rational surfaces. Suppression of the turbulence in the saturated state should occur at other locations.

3.3.2.2 Edge turbulence

Single-particle orbit analysis is one of the basic building blocks for understanding fusion plasmas. We have developed a simple multiple-time-scale theory for orbits in fluctuating edge electric fields of the type observed in TEXT and modeled at ORNL. This theory, in terms of approximate constants of the motion, has been used to show that edge fluctuations have little effect on direct convective losses from the plasma interior. The lowest-order nonlinear corrections to the unperturbed orbits suggest a simple modification of neoclassical ion diffusive transport in regions of modest fluctuation levels. For regions of very strong fluctuations, the theory shows that ions tend to follow the fluctuating equipotentials. Because this new development allows the exploitation of the duality of fluid and particle descriptions, it is expected to lead to a better understanding of fluctuations and dc electric fields.

3.3.2.3 Radial electric field effects on turbulence

There is increasing evidence that the radial electric field is important in controlling the edge turbulence and plays a critical role in the L-H transition. Up to now, most theoretical analysis has been concentrated on the effect of the radial electric field on the resistivity-gradient-driven turbulence, which can model some of the features of the edge turbulence for ohmically heated tokamaks. Recently, extensive numerical studies have been done for the resistive pressure-gradient-driven turbulence, which can reproduce some of the characteristics of edge plasmas in devices with neutral beam injection. In this case, the shear flow in the plasma couples the resistive interchange instability to the K-H instability. The latter is strongly stabilized by shear for realistic values of edge plasma flows. This contributes to the reduction of the edge turbulence by shearing. When the edge radial electric field is constant and such that $e\phi_E/T_e = \pm 1$, there is no effect on the turbulence. For a sheared electric field, there is a clear reduction of the fluctuation levels. The fluctuations themselves nonlinearly generate a dc electric field that contributes to their own stabilization. This suggests that both stability and transport considerations govern the radial edge electric field formation.

3.4 TRANSPORT AND CONFINEMENT MODELING

3.4.1 Plasma Viscosity, Anisotropy, and Poloidal Rotation

An expression found for the plasma viscosity in the long mean-free-path regime extends the regime of validity of the collisional fluid equations and can be used to study low-frequency instabilities in the collisionless regime. The expressions for the pressure anisotropy and viscous stress are valid for arbitrary toroidal magnetic configurations.

Ion orbit losses play an important role in tokamak plasma edge physics. It has been demonstrated that the ion orbit loss rate is related to the plasma viscosity by considering the conservation property of the Coulomb collision operator. Because of this relationship, the ion orbit loss rate represents a loss of poloidal momentum and can induce strong poloidal rotation. The region over which the ion orbit loss is important is of the order of the squeezed ion orbit width, which has no poloidal or toroidal magnetic field dependence. This lack of magnetic field dependence has been observed in DIII-D experiments, in which the region of strong poloidal rotation was found to be independent of toroidal field and plasma current.

Poloidal asymmetries in plasma density and potential are predicted to arise from high poloidal rotation velocities (poloidal Mach number M_p) and the inclusion of compressibility effects. Earlier work on weak shocks has been extended to the strong shock regime, where $M_p \sim 1$. As M_p approaches unity, the plasma density should first drop on the inside of the torus where the poloidal flow is compressed and rotate poloidally as M_p increases, indicating that the physics of shock may play a role in the L-H transition. Furthermore, the poloidal asymmetries found in the theory suggest a possible connection with Marfe phenomena.

3.4.2 Ignitor Physics Assessment

A preliminary assessment of the physics of the Ignitor device was carried out for use in discussions of possible collaboration between the United States and Italy on this project. The WHIST transport code was modified to include growing-plasma scenarios—an important consideration in current profile evolution when the total pulse length is no more than a few current skin times. The work confirmed earlier calculations performed with the TSC transport code, with minor differences resulting from the use of a fixed-boundary MHD equilibrium model in WHIST and a free-boundary model in TSC and from the inclusion of particle fueling and transport effects in WHIST. Among the physics issues needing further assessment are verification of the confinement model and boundary physics (limiter plasma).

3.5 RF HEATING

In our rf heating work, we develop and test theories of plasma wave generation, propagation, and absorption, as well as plasma response to the waves, in all fusion-relevant frequency regimes. These theories, as well as results from other institutions, are incorporated into analytical and numerical predictive models. These models are then applied to validate the theory; to interpret experimental results from tokamaks, stellarators, and other devices; to develop means for enhancing the effectiveness of plasma heating and current drive; and to evaluate and optimize designs of future experiments and technologies. Of course, the objective of rf heating or current drive is ultimately to modify the plasma distribution

function in a specific way. Therefore, the theoretical efforts are closely coupled to kinetic theory, to transport theory, and to stability. The modeling efforts are closely allied with experimental, engineering, and technology studies. This is accomplished through interpretation of current experimental and theoretical results, followed by application to the design and optimization of advanced devices and heating techniques.

The role of rf power in fusion continues to expand as this technique is considered for heating to ignition, stabilization of sawteeth and other instabilities, optimization of confinement by central heating, and noninductive current drive. It should be a key element on the proposed Tokamak Physics Experiment (TPX) and is a prime alternative for ITER. Critical rf activities include analysis and design for TPX and other new initiatives, for high-power ion cyclotron range of frequencies (ICRF) heating experiments on the Tokamak Fusion Test Reactor (TFTR) and the Joint European Torus (JET), and for current drive experiments on JET and DIII-D. Understanding high-power experiments—especially, interpreting the effects of rf power on confinement—requires increasingly accurate prediction of deposition profiles. The major rewrite of the ORION 2-D full-wave code into the poloidal mode expansion code PICES (Poloidal Ion Cyclotron Expansion Solution), carried out during this reporting period, marks a considerable advance in the accuracy with which we can predict power deposition and current drive profiles.

Application of these codes to antenna analysis and design for existing machines as well as for performance projections for advanced tokamaks such as the Burning Plasma Experiment (BPX), TPX, and ITER has increased considerably. The emphasis in the area of code application has been in evaluation of fast-wave current drive (FWCD) scenarios for DIII-D and ITER and in the analysis of rf antenna fields and loading characteristics for BPX and TFTR. The 2-D recessed antenna modeling code RANT was improved considerably and was the basis for design of the BPX antenna system. Work on rf effects at the plasma edge has continued. Our work on rf-driven sheaths has been extended to two dimensions to study the characteristics of finite-length probes, which are of significance for plasma diagnostics.

3.5.1 Full-Wave Modeling of ICRF Plasmas

Almost a year was spent in development of a new ICRF full-wave code, PICES, which represents ICRF wave fields as a superposition of poloidal modes in general tokamak geometry. The motivation for this work was to include variation and upshift in the $k_{\|}$ spectrum produced by FWCD antenna arrays. When fast waves propagate inward from the edge of a tokamak toward the plasma center, the $k_{\|}$ spectrum produced by the antenna is not maintained but is shifted and deformed because of the presence of the finite poloidal magnetic field. This $k_{\|}$ shift causes a variation in the parallel phase speed of the wave and can therefore have a strong effect on electron damping and current drive efficiency. We now include this effect by representing the wave fields as a superposition of poloidal modes, thereby reducing $k_{\|}$ to an algebraic operator.

In full-wave calculations that use finite differencing in the poloidal dimension, such as ORION, $k_{\|}$ appears as a differential operator $\left(\vec{B} \bullet V\right)$ in the argument of the plasma dispersion function. Since this would lead to a differential system of infinite order, such codes of necessity assume $k_{\|} \sim k_j =$ const, where k_j is the toroidal wave number. Thus, it is not possible to correctly include effects of the poloidal magnetic field on $k_{\|}$, and these codes tend to underestimate

electron damping rates and overestimate current drive efficiency. The problem can be alleviated by expressing the electric field as a superposition of poloidal modes, in which case $k_{||}$ is purely algebraic. PICES uses poloidal and toroidal mode expansions to solve the wave equation in general flux coordinates. The calculation includes a full (nonperturbative) solution for $k_{||}$ and uses a reduced-order form of the conductivity tensor to eliminate numerical problems associated with resolution of the very short wavelength ion Bernstein wave.

The code calculates three components of the ICRF wave electric field (E_y, E_h, E_b) and the power absorbed per unit length,

$$\dot{W} = \frac{1}{2}\,\mathrm{Re}\left(\vec{E}^{*} \cdot \vec{J}_p\right) ,$$

by solving in two spatial dimensions (r, J). A poloidal mode expansion in J allows the variation in $k_{||}$ to be included rigorously, while the r dimension is treated by finite differences. Variations in the toroidal dimension (z) are calculated by summing toroidal harmonics weighted by a particular antenna spectrum. Toroidal harmonics are uncoupled because of axisymmetry in tokamak geometry and can thus be calculated individually. Poloidal modes, on the other hand, are tightly coupled by the toroidal ($1/R$) dependence of $\vec{B}$ and must therefore be calculated simultaneously. This is accomplished by direct matrix inversion of the finite difference equations for all poloidal modes simultaneously. For this, PICES uses the MA32 package for solving sparse, unsymmetric systems using a modification of the frontal scheme of Hood.

3.5.2 Modeling of FWCD for ITER and DIII-D

The need for some type of noninductive current drive in reactor-scale tokamaks has been recognized for some time. Studies of lower hybrid (LH) current drive have yielded successful results in tokamaks such as Alcator and JET. In reactor-grade plasmas, however, high density and temperature may limit the accessibility of LH waves to just the outer layers of the plasma. Fast ICRF waves, on the other hand, easily penetrate to the center of such high-density plasmas. With sufficient directivity in the launched wave spectrum, currents can be driven by combined damping of the fast waves on electrons through Landau damping (ELD) and transit-time magnetic pumping (TTMP). Experiments to demonstrate and study FWCD in present-day tokamaks such as DIII-D have only recently begun, but theoretical predictions look promising.

Numerical calculations of FWCD efficiency have generally been of two types: either ray tracing or global wave calculations. Ray tracing results show that the projection of the wave number $k_{||}$ along the magnetic field can vary greatly over a ray trajectory, particularly when the launch point is above or below the equatorial plane. This variation is caused both by the $1/R$ gradient in the magnetic field and by the presence of the poloidal magnetic field in a tokamak. As the wave penetrates toward the center of the plasma, $k_{||}$ increases, causing a decrease in the parallel phase speed ($\omega = v_{phase}/v_{th} = \omega/k_{||}v_{th}$) and a corresponding decrease in the current drive efficiency γ. However, the assumptions of geometrical optics, namely short wavelength and strong single-pass absorption, are not generally applicable in FWCD scenarios. Eigenmode structure, which is ignored in ray tracing, can play an important role in determining electric field strength and Landau damping rates. In such cases, a full-wave or global solution for the wave fields is desirable.

Although the expansion in poloidal modes used in PICES allows for much more accurate calculation of electron heating on a flux surface, it is still difficult to separate

this power deposition according to resonant parallel velocity and poloidal position on a flux surface and therefore to calculate driven current. We have developed a method to make this separation and have obtained a current drive model that includes toroidal effects such as trapped particles. PICES is the first poloidal mode expansion code to have such a current drive model.

Figure 3.1 shows contours of electron power absorption in ITER, $\dot{W}e(p,\vartheta)$ for k_j = –0.8333 or n = –5. When the variation in $k_{||}$ is artificially removed by setting $k_{||} = k_j$ = const in Fig. 3.1 (b), v_{phase} is constant and power absorption is peaked on axis. But when the effect of the poloidal field on $k_{||}$ is included, as in Fig. 3.1(a), the waves slow down rapidly as they propagate inward (v_{phase} decreases), and the result is more wave damping in the outer regions of the plasma, where current drive efficiency is poor because of particle trapping. A useful figure of merit here is the normalized current drive efficiency $\gamma = \bar{n}_e R_0 I / P_{rf}$, which is the ratio of driven current to power absorbed. In Fig. 3.1(a), $\gamma = 0.166 \times 10^{20}$ A/W•m^2, and in Fig. 3.1(b), $\gamma = 0.285 \times 10^{20}$ A/W•m^2.

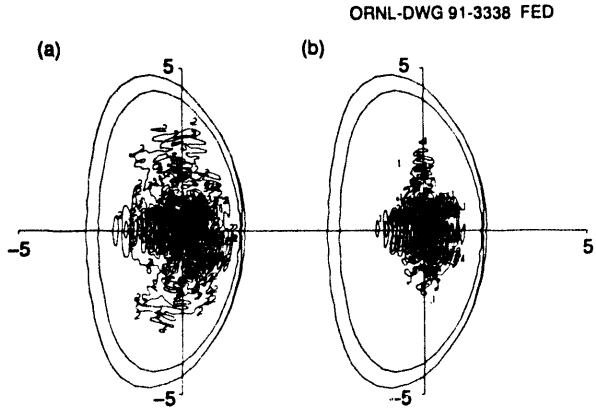

Fig. 3.1. Electron power deposition in ITER at 17 MHz (a) including $k_{||}$ variations and (b) with $k_{||} = k_j$ = const.

3.5.3 Electromotive Excitation of a Plasma Sheath

The heating of the electrons in a plasma by rf fields results in an electron distribution function that can be highly non-Maxwellian. The response of these heated electrons can lead to a substantially larger total potential drop than that obtained by arbitrarily choosing a single temperature parameter to describe the electron distribution in a traditional Boltzmann approximation. The floating potential of a plasma that is excited by electromotively driven rf plasma currents parallel to a strong static magnetic field has been calculated using a Fermi acceleration heating model and linear estimates for the rf fields with plasma. When this non-Maxwellian distribution function is used for estimates of the static potential, the results show that the total potential drop is proportional to the rf oscillation energy and the square root of the ion-to-electron mass ratio. Numerical solutions to Poisson's equation for non-Boltzmann electrons and analytic estimates of parasitic rf power absorption and edge profile modification using a Bohm diffusion model have been obtained. Estimates for a purely electrostatic heating operator were also made for comparison with the electromagnetic result.

The electrostatic potential of a plasma in contact with a grounded conductor will adjust to maintain a nearly charge-neutral state within the plasma. This potential drops rapidly inside a sheath region with a scale of the order of the Debye length, so that the loss of very mobile electrons will be retarded. The much less mobile ions are accelerated out of the interior plasma region by a presheath potential drop so as to enhance the ion loss rate. The manner in which these effects occur depends on the

physics of the plasma source, the distribution of electrons, the plasma species mix, and numerous other variables. We are concerned with the effects of changing the electron distribution function by externally exciting the electrons with a periodically time-varying (rf) driver. Specifically, we consider weakly collisional plasmas in which the electron distribution function is not well described by a Maxwellian distribution function.

For an rf driver, we assume the existence of a small parallel rf electric field inside the plasma whose curl arises from an externally applied rf magnetic field. The consideration of such electromotive effects is specifically of interest for studying the plasma response to rf fields near ICRF antennas for fusion applications. These effects can be considered in addition to the usual, extensively studied problem of the sheath response to electrostatic rf fields. The problems that we consider assume that a strong static magnetic field B exists such that the quasilinear electron plasma response along a field line is the dominant effect. Boundary and nearby structures that carry large rf currents are then considered to provide the near-field electromotive excitation of electrons when they encounter a static plasma sheath at the intersection point of the field line and a boundary structure. The ion losses are along field lines; however, the possibility of ion gyro-orbit losses to nearby structures also exists and can increase the ion loss rate.

Some analytic results obtained for order-of-magnitude comparisons with experiments are reported here. Consider an rf antenna that produces an rf magnetic field of roughly 20 G with the main current tilted at an angle of 15° from a direction that is perpendicular to the static magnetic field. In this case, the driving rf magnetic field has a component perpendicular to the static magnetic field of roughly 5 G, yielding a parallel electromotive electric field amplitude in the skin depth region of roughly 500 V/m at 30 MHz for a plasma edge density of roughly $10^{12}\,cm^{-3}$. If the antenna configuration allows this driving field to extend to the antenna bumper limiter region, the predicted electron response for these parameters yields an estimate for the static potential in the skin depth region on the order of 120 V for a pure deuterium plasma. The rf scrape-off layer (SOL) scale length is then roughly 4 mm for a connection length L of 0.5 m and a 2-T static magnetic field. The rf power that is parasitically absorbed in the skin depth region is estimated to be ≈2 kW for an antenna that is roughly 1 m long. If the rf power from the antenna is doubled for this example, the parallel electromotive field increases by a factor of $\sqrt{2}$, yielding a doubling of the electrostatic potential and average electron energy in the skin depth region. This power increase leads to a roughly 20% increase in the rf SOL scale length, indicating a flattening of the edge density profile for increasing power with the Bohm diffusion model. The parasitic power absorbed in the skin depth region increases to nearly 7 kW.

3.5.4 Characteristics of a Cylindrical Langmuir Probe of Finite Length

The current collected by a finite-length cylindrical probe is calculated numerically from a self-consistent solution to the Poisson-Vlasov system of equations. A Boltzmann distribution is assumed for the electrons, and results are compared to the standard "orbital-motion-limited" theory. When the probe is very long compared to the sheath thickness and the ratio of probe radius to electron Debye length $R_p/l_{De} \lesssim 1$, the collected current agrees with the orbital-motion theory for cylindrical probes; when the probe is very short compared to the sheath thickness and $R_p/l_{De} \lesssim 1$, the collected current agrees with the orbital

motion theory for spherical probes. When the probe length is comparable to the sheath thickness, there is a critical potential above which the probe behaves as a sphere and below which it behaves as a cylinder. Ion charge density, space potential, and ion particle orbits in the sheath plasma surrounding the probe tip can be displayed graphically.

We have shown that end effects in a finite-length cylindrical probe can be treated accurately by a numerical solution to the Poisson-Vlasov system of equations. The numerical technique, which has its origins in ion beam optics studies for fusion research, assumes a Boltzmann distribution for electrons and solves the ion Vlasov equation indirectly by calculating individual ion trajectories. The effects of ion and electron space charge around the probe tip are automatically included. Solutions have been benchmarked against known analytical results in the limit that $R_p/l_{De} \lesssim 1$ (see Fig. 3.2). Accuracy in these cases appears to be limited only by the statistics of the finite set of ion orbits used. For a finite-length cylindrical probe, our results show that errors due to the finite length can be a factor of two or more for probe dimensions that are frequently used. These errors are most evident at high potentials, where the linear dependence on the potential ϕ_p for the sphere dominates the square-root dependence for the cylinder, and also at high densities, where the variation of the spherical result with R_p/l_{De} dominates that of the cylinder. Accurate analysis must take these effects into account. The heuristic treatment of Tarrh, which assumes a linear combination of currents collected by an infinite cylinder and a hemispherical tip, gives a rough approximation to the end effects that we calculate.

Higher accuracy in these calculations requires a greater number of ion orbits. In this work, the ion orbits have been

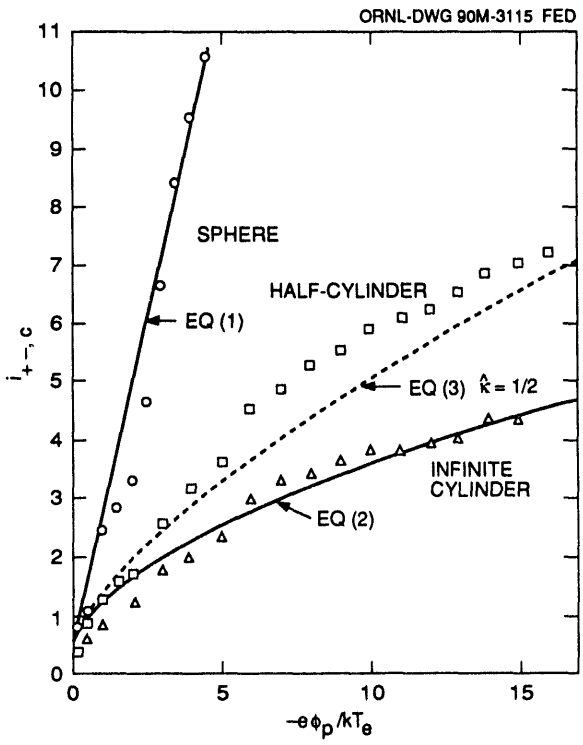

Fig. 3.2. Ion current $i_{+,c}$ vs probe potential from numerical solution (points) and analytic models (lines) for $n_e = 7.77 \times 10^{16}$ m^{-3}, $R_p/l_{De} = 0.5$, and $T_i/T_e = 0.2$.

calculated sequentially, and for this reason they are the most time-consuming part of the calculation. With the advent of modern parallel processing computers, it may be possible to calculate hundreds of orbits simultaneously rather than sequentially. If feasible, such a scheme could reduce the required computing resources, significantly increasing the usefulness of the methods described.

3.6 COMPUTING AND OPERATIONS

Computing in the Fusion Energy Division (FED) can be roughly divided into four categories: the User Service Center (USC), experimental data acquisition, workstations, and support of personal computers (PCs). The present climate of restricted funding has placed a considerable

premium on developing methods that require minimum staffing levels while providing support in all areas.

The USC operates with only partial operator coverage. A second 8-mm (helical-scan) tape device has been recently added. This device has two drives and attaches to the HSC (and is therefore accessible to all members of the VAXcluster). With the original single-drive 8-mm unit we are now able to do all incremental backups—both weekly and daily—without operator intervention. In addition to reducing operator requirements, the 8-mm drives allow us to do incremental backups seven days a week. The recently acquired ion deposition printer has proven to be a success as far as printing speed and reducing the amount of paper handling required, especially in the output bins. However, it does not handle graphics output successfully, and a replacement for the Versatec printer/plotters is still required for large graphics jobs. Another industry standard that has recently been added to the FED systems is the X-windows® graphical interface. For devices and terminals that support X-windows this provides a standard, user-friendly windowing environment for use with FED systems.

In the workstation area, the division now has three IBM PowerStation 6000s, two DECstation 3100s, a Silicon Graphics Personal IRIS, and a Hewlett Packard Model 425. These workstations are networked with the USC and therefore with the rest of the Energy Sciences Network (ESNET) via TCP/IP protocols. Workstations are used for data analysis, modeling, design, data visualization, and X-windows applications. Extensive use is made of network capabilities such as X and NFS between the workstations and the USC VAX computers.

The most interesting development in the PC area was the connecting of all the AppleTalk zones to the Ethernet backbone. This has made it possible for users to print on any printer in the division, use the Public Folder utility for sharing information, connect to the USC with AlisaShare, and have access to the Internet.

3.6.1 Programming and Software

The FED VAXcluster has become a part of the international collection of networks known as the Internet using industry standard TCP/IP protocols. A site license for the necessary software for this was purchased by Energy Systems from TGV, Inc. This has provided a more direct path for remote host and file and mail transfers, largely supplanting the ESNET, which in turn replaced the Magnetic Fusion Energy Network (MFENET). In addition to remote host and file transfers, TCP/IP allows "task-to-task" communications between the FED VAXes and other computers worldwide. This capability was instrumental in the testing and implementation of software to provide direct access to Tore Supra data from FED VAXes both in Oak Ridge and at Tore Supra.

3.6.2 Data Acquisition

The computing group supports data acquisition, storage, and retrieval in several areas. When ATF is operating, the data acquisition processes are controlled by software running on the USC computers. Experimental data are immediately collected from USC computers, and data from other networked computers are made available. Physicists and operators use a variety of machines to review and analyze the experimental data before the next shot so that ATF operating parameters may be adjusted. The data are maintained on a bank

of magnetic disks as space permits. As the information ages and is needed less often, it is compressed and eventually relocated to an online optical jukebox. If the data are needed for further analysis, they can be recalled to a recall magnetic disk for direct access. Shadowing of the disks and a regimented backup strategy with off-site storage ensure data preservation.

Numerous programs using the USC machines, networked computers, and workstations were developed to provide the control, monitoring, analysis, and support required by projects such as ATF. An X-windows-based system was developed to provide the responsible physicist for the experiment with immediate data comparison capabilities.

Development continued in the area of optical multichannel analyzer (OMA) data acquisition, with systems installed on ATF and DIII-D. Future use will include final installation at TEXTOR and Tore Supra, with the incorporation of a 3-D array OMA.

Support for plasma technology programs has continued with data acquisition for pellet injectors; a new initiative in this area has been the development of the control and operation programmable logic controller (PLC) for the tritium pellet injector for TFTR (see Sect. 4.1.1.2 of this report).

REFERENCES

1. B. A. Carreras et al., "Plasma Stability, Equilibrium, and Transport in Uragan-2M Torsatron," p. 149 in *18th EPS Conference on Controlled Fusion and Plasma Physics, Berlin, 3–7 June 1991: Contributed Papers, Part II*, European Physical Society, Petit-Lancy, Switzerland, 1991 [*Europhys. Conf. Abstr.* **15C**, Pt. II, 149 (1991)].

2. N. Dominguez et al., *Equilibrium, Mercier Stability, and Transport Properties of the Uragan-2M and the ATF Torsatron*, ORNL/TM-11701, Martin Marietta Energy Systems, Inc., Oak Ridge National Laboratory, 1991.

3. C. D. Beidler et al., "Physics Studies for Uragan-2M," pp. 519–24 in *Stellarators: Proceedings of the 8th IAEA Technical Committee Meeting, Kharkov, U.S.S.R., 27–31 May 1991*, International Atomic Energy Agency, Vienna, 1991.

4. A. Varias et al., "Ideal Mercier Stability for the TJ-II Flexible Heliac," *Nucl. Fusion* **30**, 2597 (1990).

5. C. Alejaldre et al., "Self-Stabilization of Ideal Modes in a Heliac," p. 497 in *17th EPS Conference on Controlled Fusion and Plasma Heating, Amsterdam, 25–29 June 1990: Contributed Papers, Part II*, European Physical Society, Petit-Lancy, Switzerland, 1990 [*Europhys. Conf. Abstr.* **14B**, Pt. II, 497 (1990)].

6. A. Lopez Fraguas et al., "Equilibrium and Stability of High ι TJ-II Configurations," p. 509 in *17th EPS Conference on Controlled Fusion and Plasma Heating, Amsterdam, 25–29 June 1990: Contributed Papers, Part II*, European Physical Society, Petit-Lancy, Switzerland, 1990 [*Europhys. Conf. Abstr.* **14B**, Pt. II, 509 (1990)].

7. A. Varias et al., "Effect of the Aspect Ratio on the Stability Limits of TJ-II-Like Stellarators," p. 125 in *18th EPS Conference on Controlled Fusion and Plasma Physics, Berlin, 3–7 June 1991: Contributed Papers, Part II*, European Physical Society, Petit-Lancy, Switzerland, 1991 [*Europhys. Conf. Abstr.* **15C**, Pt. II, 125 (1991)].

8. Y. Nakamura et al., "Equilibrium, Stability, and Deeply Trapped Particle Orbit Calculations for $l = 2$ Torsatron-Heliotron Configurations," *Fusion Technol.* **19**, 217 (1991).

9. M. Murakami et al., "Energy Confinement and Bootstrap Current Studies in the Advanced Toroidal Facility," p. 455 in *Plasma Physics and Controlled Nuclear Fusion Research: Proceedings of the 13th IAEA International Conference, Washington, 1990*, Vol. 2, International Atomic Energy Agency, Vienna, 1991.

10. M. Murakami et al., "Bootstrap Current Studies in the Advanced Toroidal Facility," p. 443 in *17th EPS Conference on Controlled Fusion and Plasma Heating, Amsterdam, 25–29 June 1990: Contributed Papers, Part II*, European Physical Society, Petit-Lancy, Switzerland, 1990 [*Europhys. Conf. Abstr.* **14B**, Pt. II, 443 (1990)].

11. J. H. Harris et al., "Configuration Control, Fluctuations, and Transport in Low-Collisionality Plasmas in the ATF Torsatron," p. 169 in *18th EPS Conference on Controlled Fusion and Plasma Physics, Berlin, 3–7 June 1991: Contributed Papers, Part* II, European Physical Society, Petit-Lancy, Switzerland, 1991 [*Europhys. Conf. Abstr.* **15C**, Pt. II, 169 (1991)].

12. M. Murakami et al., "Bootstrap Current Studies at the Advanced Toroidal Facility," *Phys. Rev. Lett.* **66**, 707 (1991).

13. C. Beidler et al., "Physics Studies for URAGAN-2M," p. 663 in *Plasma Physics and Controlled Nuclear Fusion Research: Proceedings of the 13th IAEA International Conference, Washington, 1990*, Vol. 2, International Atomic Energy Agency, Vienna, 1991.

14. C. L. Hedrick, "Landau Fluid Equations for Finite Beta Three Species Alfvén Waves," presented at the Sherwood International Fusion Theory Conference, Seattle, Washington, April 22–24, 1991.

15. P. J. Christianson et al., "A Fluid-Kinetic Model with FLR Corrections to Study Hot Particle Destabilized Shear Alfvén Eigenmodes," *Bull. Am. Phys. Soc.* **36**, 2395 (1991).

16. D. A. Spong et al., "Destabilization of the Toroidicity-Induced Shear Alfvén Eigenmode by Alpha Populations Using Fluid Moment Descriptions," presented at the Sherwood International Fusion Theory Conference, Seattle, Washington, April 22–24, 1991; D. A. Spong et al., "Alpha Destabilization of the TAE Mode Using a Reduced Gyrofluid Model with Landau Closure," *Phys. Scr.* **45**, 159–62 (1992).

17. V. E. Lynch et al., "Parallel Computing at ORNL," p. 8 in *Proceedings of the Workshop on Massively Parallel Computing in Magnetic Fusion Energy, Williamsburg, VA, April 26–27, 1990*, UCRL-JC-104774, Lawrence Livermore National Laboratory, Livermore, California, 1990.

18. B. A. Carreras et al., "Plasma Turbulence Calculations on Supercomputers," *Int. J. Supercomput. Appl.* **4**, 97 (1990).

19. V. E. Lynch et al., "Plasma Turbulence Calculations on the Intel iPSC/860 (RX) Hypercube," *Int. J. Comput. Sys. Eng.* **2**, 299 (1991).

20. Y. Gang, D. J. Sigmar, and J. N. Leboeuf, "Saturation of Energetic Particle Driven Alfvén Wave Instability through Velocity Space Diffusion," *Phys. Lett. A* **161**, 517–22 (1992).

21. M. N. Rosenbluth, "Asymptotic Theory of Toroidal Alfvén Eigenmodes in Ignited Tokamaks," *Bull. Am. Phys. Soc.* **36**, 2401 (1991); M. N. Rosenbluth et al., "Mode Structure and Continuum Damping of High-*n* Toroidal Alfvén Eigenmodes," *Phys. Fluids B* **4**, 2189 (1992).

22. B. A. Carreras, "Fluid Approach to Plasma Turbulence: Resistive and Pressure Gradient-Driven Turbulence," *Fiz. Plasmy* **16**, 1245 (1990) [*Sov. J. Plasma Phys.* **16**, 722 (1991)].

23. A. J. Wootton et al., "Fluctuations and Anomalous Transport in Tokamaks," *Phys. Fluids B* **2**, 2879 (1990).

24. P. H. Diamond et al., "Developments in the Theory of Trapped-Particle Pressure Gradient-Driven Turbulence in Tokamaks and Stellarators," p. 9 in *Plasma Physics and Controlled Nuclear Fusion Research: Proceedings of the 13th IAEA International Conference, Washington, 1990,* Vol. 2, International Atomic Energy Agency, Vienna, 1991.

25. B. A. Carreras et al., "Theory of Shear Flow Effects on Long-Wavelength Drift Wave Turbulence," *Phys. Fluids B,* submitted for publication (1992) [available from the author as Oak Ridge National Laboratory preprint ORNL/P-91/51278 (1991)].

26. B. A. Carreras, V. E. Lynch, and L. Garcia, "Sheared Electric Field Effects on the Resistive Pressure-Gradient-Driven Turbulence," in *Proceedings of the 2nd International Toki Conference on Plasma Physics and Controlled Nuclear Fusion: Nonlinear Phenomena in Fusion Plasmas—Theory and Computer Simulation,* NIFS-PROC-6, National Institute for Fusion Science, Nagoya, Japan, April 1991.

27. H. Biglari et al., "Influence of Sheared Poloidal Rotation on Edge Turbulence Dynamics and Access to Enhanced Confinement Regimes," p. 191 in *Plasma Physics and Controlled Nuclear Fusion Research: Proceedings of the 13th IAEA International Conference, Washington, 1990,* Vol. 2, International Atomic Energy Agency, Vienna, 1991.

28. B. A. Carreras, V. E. Lynch, and L. Garcia, "Electron Diamagnetic Effects on the Resistive Pressure-Gradient-Driven Turbulence and Poloidal Flow Generation," *Phys. Fluids B* **3**, 1438 (1991).

29. L. Garcia, B. A. Carreras, and V. E. Lynch, "Electric Field Effects on the Resistive Pressure-Gradient-Driven Turbulence," p. 13 in *18th EPS Conference on Controlled Fusion and Plasma Physics, Berlin, 3–7 June 1991: Contributed Papers, Part IV,* European Physical Society, Petit-Lancy, Switzerland, 1991 [*Europhys. Conf. Abstr.* **15C**, Pt. IV, 13 (1991)].

30. C. Hidalgo et al., "Edge Fluctuation Studies in ATF," p. 1353 in *17th EPS Conference on Controlled Fusion and Plasma Physics, Amsterdam, 25–29 June, 1990: Contributed Papers, Part III,* European Physical Society, Petit-Lancy, Switzerland, 1991 [*Europhys. Conf. Abstr.* **14B**, Pt. III, 1353 (1990)].

31. Ch. P. Ritz et al., "Comparative Studies of Edge Turbulence in the TEXT Tokamak and the ATF Stellarator," p. 589 in *Plasma Physics and Controlled Nuclear Fusion Research: Proceedings of the 13th IAEA International Conference, Washington,* 1990, Vol. 2, International Atomic Energy Agency, Vienna, 1991.

32. J. N. Leboeuf et al., "TEXT Edge Turbulence Modeling," *Phys. Fluids B* **3**, 2291 (1991).

4

PLASMA TECHNOLOGY

H. H. Haselton, Section Head

B. E. Argo
S. E. Attenberger[1]
F. W. Baity
G. C. Barber
L. R. Baylor[2]
T. S. Bigelow
L. A. Charlton[1]
M. J. Cole[2]
I. Collazo[3]
S. K. Combs
J. F. Cox
A. Fadnek
D. T. Fehling[4]
P. W. Fisher[5]
S. C. Forrester
C. A. Foster
C. R. Foust
W. L. Gardner
R. C. Goldfinger[1]
M. J. Gouge
R. H. Goulding
G. R. Hanson[3]
G. R. Haste
P. P. Helton
D. J. Hoffman
W. A. Houlberg[4]
R. C. Isler[6]
H. D. Kimrey
M. Kwon[3]
R. L. Livesey
S. L. Milora
A. L. Qualls[7]
D. A. Rasmussen[6]
P. F. Rice
P. M. Ryan
C. R. Schaich[6]
D. E. Schechter
L. K. Shaver
T. D. Shepard
D. O. Sparks
W. L. Stirling
D. W. Swain
D. J. Taylor
C. E. Thomas[3]
C. C. Tsai
M. R. Wade
J. H. Whealton
G. A. White
J. A. White[8]
T. L. White
J. B. Wilgen[6]
J. J. Yugo[9]

1. Computing and Telecommunications Division, Martin Marietta Energy Systems, Inc.
2. Engineering Division, Martin Marietta Energy Systems, Inc.
3. Georgia Institute of Technology, Atlanta.
4. Plasma Theory Section.
5. Chemical Technology Division.
6. Toroidal Confinement Section.
7. The University of Tennessee, Knoxville.
8. Management Services Group.
9. Fusion Engineering Design Center and TRW, Inc., Redondo Beach, Calif.

4. PLASMA TECHNOLOGY

Summary of Activities

The Plasma Technology Section of the Fusion Energy Division is engaged in the development and application of technologies that support fusion research. Work in the areas of plasma fueling and rf technology is described in this section. Research on plasma technologies for the International Thermonuclear Experimental Reactor (ITER) and for the Burning Plasma Experiment, performed in collaboration with the Fusion Engineering Design Center, is described in Sect. 5 of this report. Spin-offs from fusion technology with applications beyond fusion research are described in Sect. 8.

The Plasma Fueling Group participated in a broad range of research activities in support of both the U.S. magnetic fusion program and international fusion research. Work continued in the general areas of pneumatic and centrifugal pellet injector development, to support present and near-term applications, and advanced development, in support of more demanding applications anticipated for ITER and the next generation of fusion devices. One highlight was the development of a tritium pellet injector to be used during deuterium-tritium operations on the Tokamak Fusion Test Reactor (TFTR); this injector incorporates the two-stage light gas gun that has been a focus of the advanced development efforts.

The rf technology program encompassed basic development, a variety of projects, and a strong modeling effort. New materials and fabrication techniques for the Faraday shield tubes of antennas operating in the ion cyclotron range of frequencies (ICRF) were developed and tested, and the effects of Faraday shield geometry and material on ICRF antennas were calculated and compared to measurements. Tests of a folded waveguide (FWG) antenna in the Radio Frequency Test Facility plasma indicated that this concept is sufficiently developed for application to a tokamak, and the design of an FWG antenna for the Frascati Tokamak Upgrade was initiated. A fast-wave current drive (FWCD) antenna array was operated on DIII-D to provide a proof-of-principle test of this technique. Collaborations continued on Tore Supra and TFTR, both of which are equipped with ORNL antennas. A new initiative to design a microwave reflectometer system for edge density profile measurements on TFTR began in 1991. An asymmetric double loop antenna was operated on the Advanced Toroidal Facility (ATF), and the electron cyclotron heating system on ATF was upgraded to allow experiments with high plasma beta at lower magnetic fields for long pulses. A collaboration to design a power coupler for the new A_2 antennas on the Joint European Torus was begun. This effort entails extensive modeling of the complicated A_2 antenna geometry.

4.1 PLASMA FUELING PROGRAM

The Plasma Fueling Group in the ORNL Fusion Energy Division is engaged in pneumatic and centrifuge injector development, supporting present and near-term applications, and advanced development, in support of the greater demands expected in the future. ORNL has recently reestablished a program of centrifugal pellet injector development in support of the collaboration on pellet fueling on the Tore Supra facility in Cadarache, France, and as part of a broader development effort to meet the long-pulse fueling needs of the International Thermonuclear Experimental Reactor (ITER). This activity will include an extension of the performance of the Tore Supra injector to longer pulse durations (from the present 100-pellet capability to approximately 400 pellets) and further refinement of the storage wheel/in situ redeposition technique for pellet formation to quasi-steady-state operation.

In the area of pneumatic injector development, ORNL's efforts have focused on development of the two-stage light gas gun concept for repetitive operation. In the first known test of a repetitive two-stage light gas gun, low-density, 4-mm-diam plastic pellets were accelerated to 3 km/s at a rate of 1 Hz in a facility that incorporates a small two-stage gun and automatic loading mechanism. As a consequence of this work, ORNL has embarked on a collaborative program with ENEA-Frascati to modify the ORNL repeating pneumatic injector facility to incorporate a two-stage light gas gun developed at Frascati in order to demonstrate repetitive operation with deuterium pellets in the 3-mm size range.

As a follow-on to the successful operation of the tritium proof-of-principle (TPOP) experiment in 1989, ORNL designed and fabricated a four-shot pneumatic tritium pellet injector (TPI) for the Tokamak Fusion Test Reactor (TFTR). The new TPI features three single-stage light gas guns designed for speeds up to 1.5 km/s in tritium and a two-stage light gas gun to give one of the four barrels a projected performance capability of up to 3 km/s. The injector operation is based on the pipe gun concept for production of pellets in a minimum inventory configuration that is particularly attractive for tritium operations.

The proof-of-principle electron-beam (e-beam) rocket accelerator, which was completed in 1989, has undergone extensive testing to determine the parametric dependence of the propellant burn velocity and the resulting pellet acceleration. Analysis of the data indicates that the performance in relation to the electron-beam parameters scales in accordance with a model that is derived from the neutral gas shielding theory for the interaction of a hydrogenic pellet in a magnetized plasma. Incremental pellet velocities in the range of 500 m/s have been achieved in a 0.4-m-long acceleration column.

ORNL staff members participated in pellet fueling experiments on a number of plasma confinement devices in the United States and abroad, including the ORNL Advanced Toroidal Facility (ATF), TFTR, and the Tore Supra and Joint European Torus (JET) devices. Participation in the latter two programs was carried out as part of major international collaborations between the U.S. Department of Energy (DOE) and the European Atomic Energy Commission (Euratom). On JET, the experimental program emphasized the fueling of high-performance discharges. The so-called pellet-enhanced performance (PEP) mode, which was discovered in 1989 in limiter plasmas with high-power central heating, was extended to H-mode discharges, producing both an increase in core confinement associated with the PEP mode and an increase in global confinement

associated with the H-mode. The Tore Supra program concentrated on exploring long-pulse pellet fueling scenarios in combination with lower hybrid current drive (LHCD) operation. A technique was developed to extend pellet penetration in such discharges by interrupting the lower hybrid power pulse for short periods of time in order to affect slowing down of energetic (nonthermal) electrons that were found to be responsible for anomalously high pellet ablation in previous experiments.

4.1.1 Pellet Injector Development

4.1.1.1 Electron-beam rocket pellet injector

C. A. Foster, C. C. Tsai, and D. E. Schechter

The general objective of the e-beam rocket pellet accelerator project is to develop technologies for producing ultrahigh-velocity pellets of deuterium (D_2) and/or tritium (T_2) for fueling fusion reactors such as ITER.[1–4] The original conceptual accelerator was proposed to use a magnetically compressed electron beam to evaporate a hydrogen propellant "ice stick" and to heat the exhaust gas, and subsequently to accomplish rocket-like acceleration of D_2 and/or T_2 pellet payload. The actual performance of an e-beam rocket pellet accelerator depends strongly on the beam transmission efficiency, the burn velocity, and the exhaust velocity. For constant beam conditions, the beam transmission efficiency, the burn velocity, and the exhaust velocity will affect each other and, thus, the final pellet speed. To study the effects of these factors on the pellet acceleration, we have operated the e-beam pellet accelerator, collected data on accelerated pellets, and performed data analyses during the last two years.

Following the first demonstration of e-beam rocket pellet acceleration in 1989, the accelerator (Fig. 4.1) was upgraded with several improvements. A triode electron gun with controllable beam energy and current has been developed. With a negatively biased grid, the electron gun can form a constant-current beam during the pellet acceleration for various beam energies. Two Rogowski-coil current sensors have been fabricated, assembled, and calibrated. Each current sensor consists of three coils installed between guide rails either at the entrance end or at the exit end of the pellet acceleration column. The current sensors can measure the actual beam current passing by and estimate the beam current incident on the accelerated pellet. With the proper arrangement of the solenoid magnets, the beam current for accelerating the pellet has been raised about one order of magnitude to a level of 1 A. The pellet maker has been upgraded with the capability of forming either bare pellets or pellets encased in sabots. To produce pellets of consistent size and strength, we make pellets automatically by employing a computer-controlled gas feed system, which uses a programmable logic controller (PLC) to control pneumatic valves in the gas feeding and evacuation system.

The pellet maker is a pipe-gun-type freezing cell. For normal operation, the gas feed system is purged with dry, pure hydrogen (or deuterium as needed for experiments), and then the liquid helium is fed into the freezing cell. When the freezing cell is cooled to 5 K, the pellet maker is ready for making cryogenic pellets. When the start button on the PLC control panel is pushed, the PLC initiates the following sequence: the pneumatic valves feed a preset amount of gas into the reservoir; then a controlled gas flow into the freezing cell is initiated. After a cylindrical pellet (4 mm in diameter and up to 12 mm long) is made, the freezing cell is evacuated. When the pellet is pushed out by a mechanical piston, a fraction of the pellet is converted into high-pressure gas,

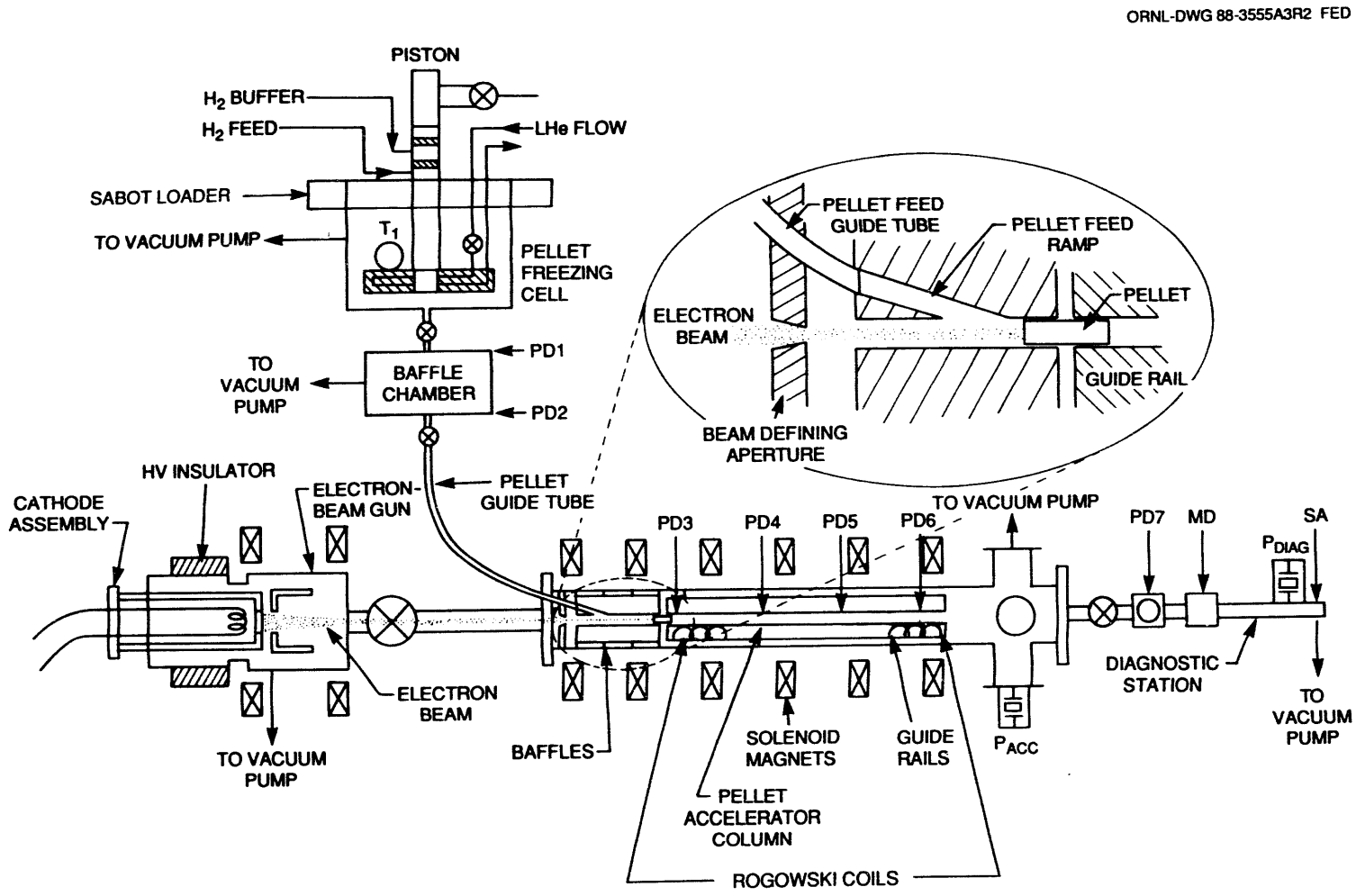

Fig. 4.1. Sketch of the e-beam rocket pellet accelerator, which consists of a pipe-gun-type pellet maker, an electron gun, and a pellet accelerator with guide rails and electromagnet. From the known distances between the light detectors, PD1 to PD7, a microwave mass detector (MD), and a shock accelerometer (SA), the pellet speed can be estimated by the time-of-flight method. A video camera, located at PD7, records the image of the accelerated pellet. The mass of accelerated pellets can be measured by a Baratron gage (P_{DIAG}). With Rogowski coil sensors installed at the entrance and exit of the guide rails, the actual beam current on pellets during acceleration can be estimated.

which provides the initial kinetic energy of the pellet. Through the baffle chamber, the guide tube, and the feed ramp, the pellet is loaded into the guide rails of the pellet accelerator. Typical initial pellet speeds are 50 to 100 m/s. In a similar way, we can make a composite shell/hydrogen pellet automatically after loading a shell into the freezing cell. To accomplish this, the pellet maker was modified with a shell-loading mechanism. Shell materials such as carbon foam, carbon composite, and Teflon have been used in our studies.

The pellet is accelerated in the 0.6-m-long graphite guide rails by a magnetically compressed e-beam, one-twelfth of the cathode size. The solenoid magnet installed on the accelerator tube guides and confines the beam electrons along the guide rails. The speeds of accelerated pellets are measured by using the time-of-flight method with light gates and a shock transducer installed along the pellet trajectory.[3,4] A shadowgraph of each accelerated pellet is taken by a video camera system. Finally, the accelerated pellet reaches the diagnostic chamber with its gas trapped there. The measured gas trapped in the diagnostic chamber is used to estimate the size of the accelerated pellet. In the last two years, experimental data have been collected for thousands of accelerated intact pellets of hydrogen. The e-beams used for pellet acceleration are variable, with beam energy up to 16 keV, current up to ~1 A, and pulse length up to 5 ms. A typical speed increment of 300 to 500 m/s is observed (Fig. 4.2), which increases with the beam power. The highest speed for an intact hydrogen pellet is 575 m/s; this pellet was accelerated by an electron beam of 10 keV, 0.8 A for 1 ms.

Data from the accelerated bare hydrogen pellets have been analyzed. For pellets to be accelerated by low-current (<0.1-A) electron beams, the measured burn velocity increases roughly with the square of the beam voltage, as the theoretical model predicts.[4] We have attempted to analyze the exhaust velocity of the ablated gas as a function of beam power. At low beam currents or powers, the thermal evaporation energy of the pellets is also included in the analysis. We note that the calculated and measured exhaust velocities would be consistent if the beam transmission efficiency and the directional factor of the heated exhaust gas were factored into calculation. If the acceleration efficiency can be maintained for higher beam powers, pellets could be accelerated to speeds near 1000 m/s by 14-keV, 1-A beams with a duration of 1.3 ms (ref. 4). Thus, higher pellet velocities and higher exhaust

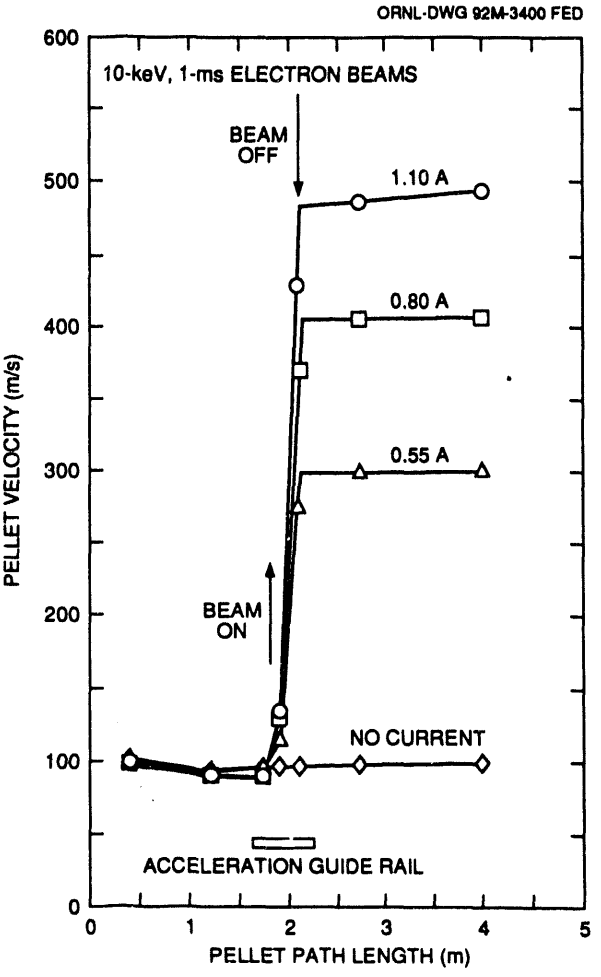

Fig. 4.2. Velocity of bare hydrogen pellets accelerated at various beam currents.

velocities may be achievable by using higher beam currents and longer acceleration lengths.

From our present understanding on the scaling of this technique. it appears that a performance level competitive with other state-of-the-art acceleration techniques (1 to 5 km/s) is possible by

1. using a sabot to enhance acceleration and maintain the pellet integrity under intense beam acceleration, and
2. extending the acceleration path length to a few meters (compared with the present 0.4-m accelerator).

Preparations for the first task are complete, and it will be carried out soon. If the exhaust velocity increases according to the theoretical prediction, we will pursue the second task in the next fiscal year. We view this as a necessary scaling effort for extrapolating the performance of this concept and developing a pellet injector with a long acceleration length (~ 20 m) to fulfill the ITER high-velocity (>10-km/s) objective.

4.1.1.2 Tritium pellet injector

M. J. Gouge, P. W. Fisher, S. K. Combs, C. R. Foust, S. L. Milora, L. R. Baylor, D. T. Fehling, M. J. Cole, A. L. Qualls, and J. B. Wilgen

The TPI is a cryogenic pellet injector to be used before and during the deuterium-tritium (D-T) phase of operations on TFTR. The injector is shown in perspective in Fig. 4.3; it has replaced the eight-shot deuterium pellet injector (DPI) at TFTR Bay T (see ref. 5). The DPI formed pellets by a cryogenic extrusion process; the TPI forms its four cylindrical pellets by the in situ condensation process. Two of these pellets have diameters of 3.4 mm (guns 1 and 2); the other two, diameters of 4.0 mm (guns 3 and 4). The nominal pellet aspect ratio is 1.25, but pellets can be formed with aspect ratios in the range from 1.0 to ≥1.5. One of the 4.0-mm guns (gun 4) is equipped with a two-stage light gas gun driver. while the other three operate with a conventional single-stage light gas gun using fast-acting electromagnetic propellant valves developed at ORNL. In the configuration described here, the single-stage guns are capable of producing velocities approaching 1.7 to 1.8 km/s in deuterium and 1.5 km/s in tritium.[6]

Use of the TPI during the D-T phase of TFTR operations will permit access to both a regime suitable for initial alpha particle physics studies and a regime suitable for studies of particle and energy confinement in high-density D-T plasmas with $n_e(0) = (1–5) \times 10^{20}$ m^{-3}. It will provide the capability for extending the supershot regime to densities suitable for high-Q operation and provide access to both the peaked-density-profile, pellet-fueled PEP regime and a regime of sustained high-density operation using multiple tritium pellets and heating in the ion cyclotron range of frequencies (ICRF). The project is divided into two phases. Phase I activities allow the deuterium fueling capability to be used during 1992 operations, while the Phase II activities incorporate systems required for tritium operation (secondary containment and a D-T fuel manifold) and include an extended period of testing at the TFTR site, ending with the formation and acceleration of tritium pellets in 1993.

The TPI consists of several systems, shown in Figs. 4.3–4.5. The injector has a gaseous-helium-cooled cryostat that provides cooling for cryogenic pellet formation. The injector is located within the guard vacuum system, and its design is based on the so-called "pipe-gun" concept, in which hydrogenic (H, D, T) pellets are formed by direct condensation in the gun

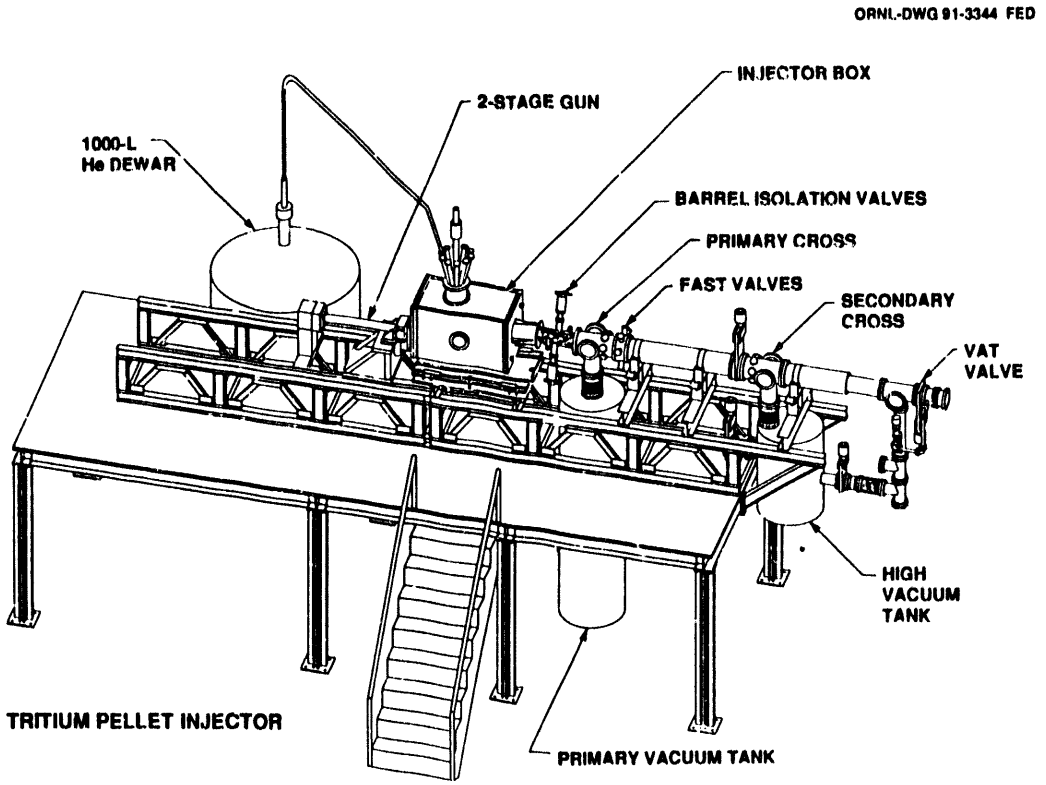

Fig. 4.3. Perspective view of the TPI installation on the TFTR.

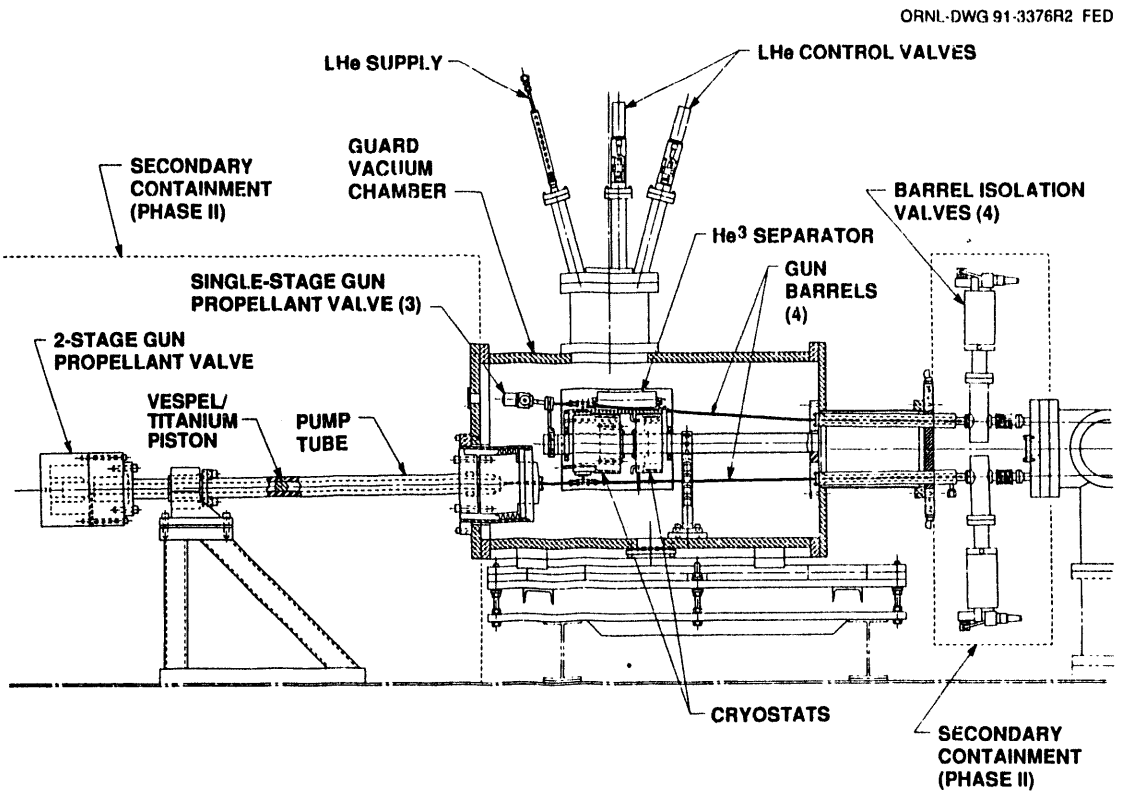

Fig. 4.4. The TPI injector and two-stage light gas gun assembly.

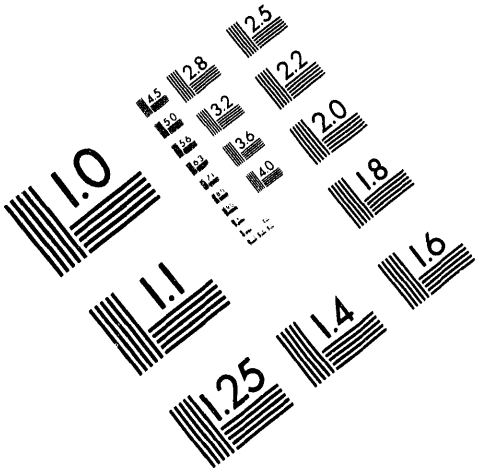

Association for Information and Image Management
1100 Wayne Avenue, Suite 1100
Silver Spring, Maryland 20910
301/587-8202

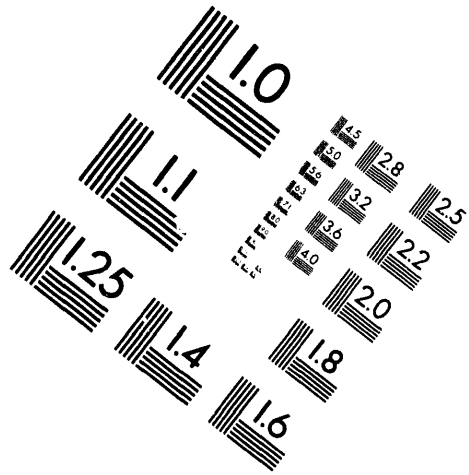

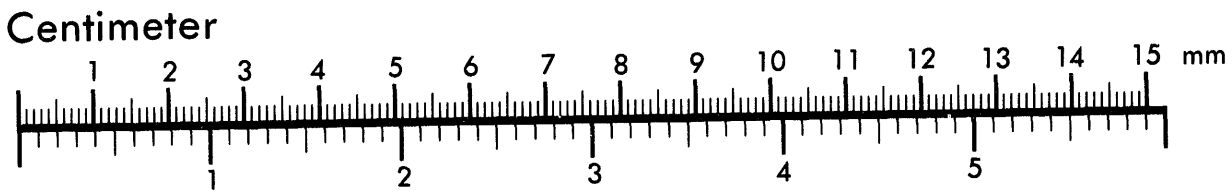

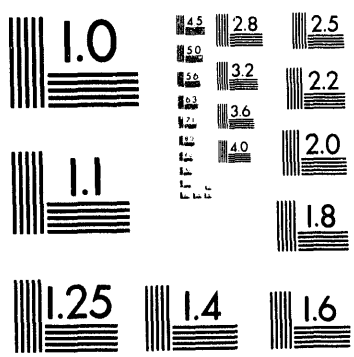

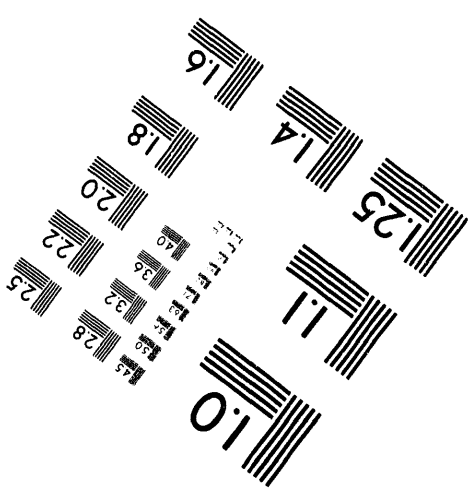

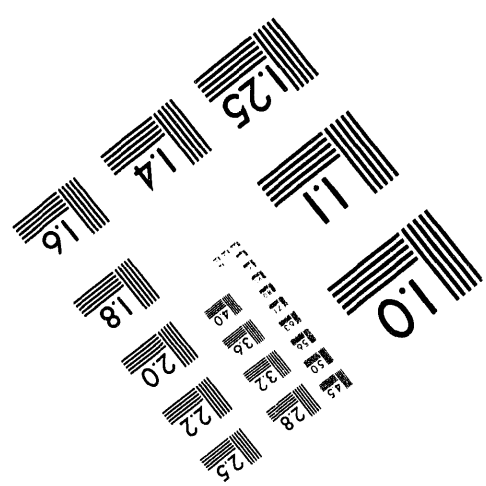

2 of 4

Fig. 4.5. Photograph of TPI during assembly.

barrel, a segment of which is held below the hydrogen triple-point temperature by contact with an oxygen-free, high-conductivity (OFHC) copper block cooled by gaseous helium.[7] This design is ideal for tritium service because there are no moving parts inside the gun and because little excess tritium is required in the pellet production process. The injector uses four independent 1-m-long gun barrel assemblies mounted around the perimeter of two OFHC copper cryostats; the rear cryostat provides conduction cooling for the four barrel pellet freezing zones, and the front cryostat provides conduction cooling for the four barrel collars. The cryostats shown in Fig. 4.4 are based on designs used for pipe-gun injectors built for ATF and the Princeton Beta Experiment (PBX).[7,8] Three of the barrel assemblies are coupled to an ORNL-designed fast propellant valve (single-stage driver). This valve develops full pressure within 300 ms and has operated with a supply pressure of up to 138 bar (2000 psi) using upgraded power supplies. The remaining barrel assembly is connected to the two-stage driver.

The two-stage driver system shown in Figs. 4.4 and 4.5 provides the high-pressure, high-temperature drive gas required to accelerate pellets to ≈2.5 to 3 km/s. It is based on development of two-stage light gas guns at ORNL[9] and in Europe.[10] In the two-stage driver, moderate-pressure (20- to 50-bar) helium propellant gas initially in a 0.64-L first-stage reservoir accelerates a 25- to 50-g titanium piston to velocities in the range of 100 to 150 m/s in a thick-walled pump tube. The accelerating piston compresses (nearly adiabatically) low-pressure, room-temperature hydrogen propellant gas initially at about 1 bar. This hydrogen gas becomes the driving gas for the cryogenic pellet. At the high pressure reached following near-adiabatic compression, the mechanical strength of the hydrogenic pellet becomes a design constraint and determines the maximum muzzle velocity, which is estimated to be of order 2.5–3 km/s.

The TPI will be controlled by a PLC (Allen Bradley PLC 5/40) located in the TFTR mezzanine beneath the injector. The operator will control the injector through a touch panel color mimic screen provided with the PLC (one primary unit in the control room and a second unit in the mezzanine for checkout) or with a color mimic display/terminal interfaced to the existing pellet injector MicroVAX, which will have a communications link to the PLC. To the operator, the PLC will appear as a finite-state engine in which the injector will be in one of several defined states or modes. In each of these states, the PLC will perform a series of operations (a procedure to enable the injector to go to the next state). The operator controls the system by setting the state to which the PLC is to go. All setpoints for temperatures and pressures within the injector are set automatically within the procedures by the PLC but can be modified by changing the preset values in the PLC, either through the touch panel via a pop-up keypad or through the MicroVAX interface. Firing of the propellant valves and timing of hydrogen propellant prefill and pump tube vacuum exhaust for the two-stage light gas gun are controlled by the TFTR fire sequencer, which is programmable through the MicroVAX. In addition to the automated operation of the TPI, the injector can be operated manually by controlling individual valves and changing individual setpoints.

The TPI has two light gate stations separated by 1.41 m to provide timing signals for pellet speed measurement. The pellet interrupts a continuous light beam to provide the timing pulse. This system also provides a pellet-speed-dependent trigger pulse for the two 3-ns pulsed nitrogen dye lasers in the pellet photography system. A

fiber-optic beam splitter enables a single laser to photograph pellets in two separate barrels within the constraints of the 20-Hz laser repetition rate. The photography system for the ORNL testing period used both a CID camera (guns 2 and 3) and a charge-coupled device (CCD) camera (guns 1 and 4). The system for the TFTR D-T operations will use only CID cameras designed to function at integrated doses estimated for the D-T phase. Windows used for pellet speed measurement and photography were kept at minimum size and tested at 2.5 atm to provide a reliable tritium barrier for the D-T phase. A microwave cavity system was also implemented for TPI. It operates at a nominal resonant frequency of 4.21 GHz and provides a relative measure of pellet mass. It was initially calibrated at ORNL by measuring the fast pressure rise due to a pellet striking a target plate in a known volume tank. A photograph of a 3.4- by 4.3-mm pellet at a speed of ~1.4 km/s and the corresponding microwave cavity signal are shown in Fig. 4.6.

The TPI was initially tested at ORNL over a three-week period. This testing emphasized initial operation of the three single-stage light gas guns (guns 1, 2, and 3) and the two-stage driver (gun 4) and integration of gun mechanical systems into

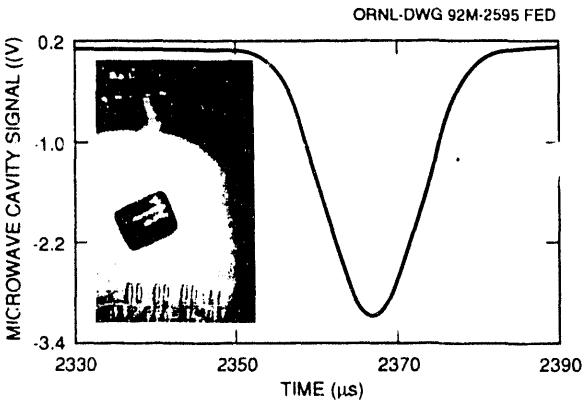

Fig. 4.6. Microwave cavity signal and photograph of a 3.4- × 4.3-mm pellet at 1.4 km/s.

the PLC-based control system. One major goal was to verify that the helium gas cooling circuit had a sufficiently low pressure drop at operating temperatures to allow operation at TFTR with a closed cryogenic helium system developed for the TFTR neutral beam injectors. It was found that the gun copper cooling cryostat could be maintained at the 9 to 12 K range needed for deuterium pellet fabrication with a dewar pressure of 3 to 4 psi. Cold helium gas at 5 to 6 K was used for gun cooling; this gas was generated by immersion of a 50-Ω electrical heater into a 500-L liquid helium dewar. Steady-state heater currents of 0.3 to 0.4 A indicated a liquid helium consumption of 8 to 12 L/h, meeting a TPI design goal.

Testing of the three single-stage light gas guns verified the ability to make 3.4-mm and 4-mm deuterium pellets at aspect ratios of 1, 1.25, and 1.5. Each single-stage light gas gun was tested at various hydrogen propellant supply pressures in the range from 69 to 138 bar. In particular, it was verified that the upgraded propellant power supplies could open the electromagnetic propellant valves at the design pressure of 138 bar. Figure 4.7 shows a scan of pellet speed as a function of breech propellant gas pressure for gun 1. Also shown are predicted values from interior ballistics theory.[11]

Initial testing of the two-stage light gas gun was conducted to quantify operating valve response and gas dynamics time scales. The results of these initial timing runs were used to program the fire sequencer and PLC to provide consistent performance from the two-stage light gas gun. Pellet speeds in this initial phase ranged from 1.5 to 2.2 km/s and were limited by a leak in the pump tube high-pressure head metal O-ring seal, which developed as high pressures (up to 1100 bar) were attained during the shot. This small, transient leak limited the pellet speed performance and caused occasional lockup of the titanium piston in the pump

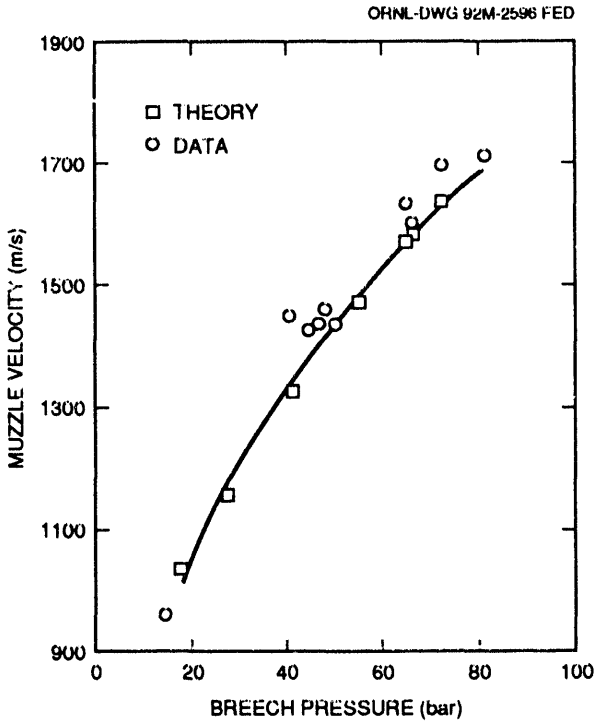

Fig. 4.7. Pellet speed vs breech pressure for gun 1.

tube. A new seal configuration is being developed at ORNL and will be retrofitted on the TPI at TFTR.

4.1.1.3 Two-stage light gas gun

S. K. Combs, C. R. Foust, D. T. Fehling, M. J. Gouge

Some preliminary results from a repetitive two-stage light gas gun were reported in the last progress report.[12] In general, applications of the two-stage light gas gun have been limited to only single shots, with a finite time (at least minutes) needed for recovery and preparation for the next shot. The new device overcomes problems associated with repetitive operation, including rapidly evacuating the propellant gases, reloading the gun breech with a new projectile, returning the piston to its initial position, and refilling the first- and second-stage gas volumes to the appropriate pressure levels. In addition, some components are subjected to and must survive severe operating conditions, which include rapid cycling to high pressures and temperatures (up to thousands of bars and thousands of kelvins) and significant mechanical shocks. Small plastic projectiles (4-mm nominal size) and helium gas have been used in the prototype device, which was equipped with a 1-m-long pump tube and a 1-m-long gun barrel, to demonstrate repetitive operation (up to 1 Hz) at relatively high pellet velocities (up to 3000 m/s). The highest experimental velocity is twice that available from conventional repeating single-stage pneumatic injectors. The pellet test repetition rate of 1 Hz is relevant for fueling applications on future large fusion research devices.

A 4-mm-diam pellet has been used in the ORNL experimental studies, since this size is applicable to large present-day tokamak fueling experiments. For instance, pellet fueling systems on both JET[13] and TFTR[5] are now equipped with this pellet size. Projections indicate that nominal pellet diameters of 6 to 10 mm will be required to fuel reactor-grade plasmas (a pellet diameter of ≈8 mm is the baseline design parameter for the high-speed injection system for the proposed ITER experiment[14]). Previous papers[9,15,16] describe initial results of ORNL experiments using two-stage light gas guns. With 35-mg plastic projectiles (4 mm in diam), speeds of up to 4500 m/s have been recorded in single-shot tests. Also, by using the "pipe-gun" technique[17] for freezing hydrogen isotopes in situ in the gun barrel (at temperatures of ≈10 K) in combination with a two-stage light gas gun, single deuterium pellets (nominal diameter of 4 mm) have been accelerated to velocities of up to 2850 m/s. To aid in understanding the physical phenomenon, two computer codes[18,19] that model the gas dynamics of the two-stage gun processes have been used

in designing the equipment and in evaluating the experimental data.

A schematic of the repetitive two-stage light gas gun and key subsystems is shown in Fig. 4.8, and physical parameters of the gun and operating test ranges are listed in Table 4.1. The actual layout of most key components is shown in Fig. 4.9. The device comprises several components (and features) that must interact precisely to accomplish repetitive operation. The repetitive device consists of some standard components for two-stage light gas guns: a first-stage reservoir for high-pressure gas (2.2-L internal volume), a pump tube (27.0 mm ID and 1.0 m long), and a gun barrel (4.0 mm ID and 1.1 m long). The typical piston was ≈40 mm long (with a 45° taper on the front) and weighed 25–30 g; it was constructed of polyimide with 15% graphite filler by weight (supplied as Vespel® by E. I. du Pont de Nemours & Co., Inc.). Typically, a piston survived for up to hundreds of shots without excessive wear/damage or significant effects on gun performance. Various plastic pellets (nylon, polypropylene, polycarbonate, acetal, etc.) with a 4-mm diameter were used in this study, including two geometric forms (right circular cylinders and spheres). Special components developed for repetitive operation include a fast valve, mechanisms for automatic pellet loading, and a pneumatic clamping device for sealing the pump tube/gun barrel interface. Necessary techniques for rapid filling and evacuation of gases and control of pressure levels were also developed. A schematic diagram of the control/data acquisition system is shown in

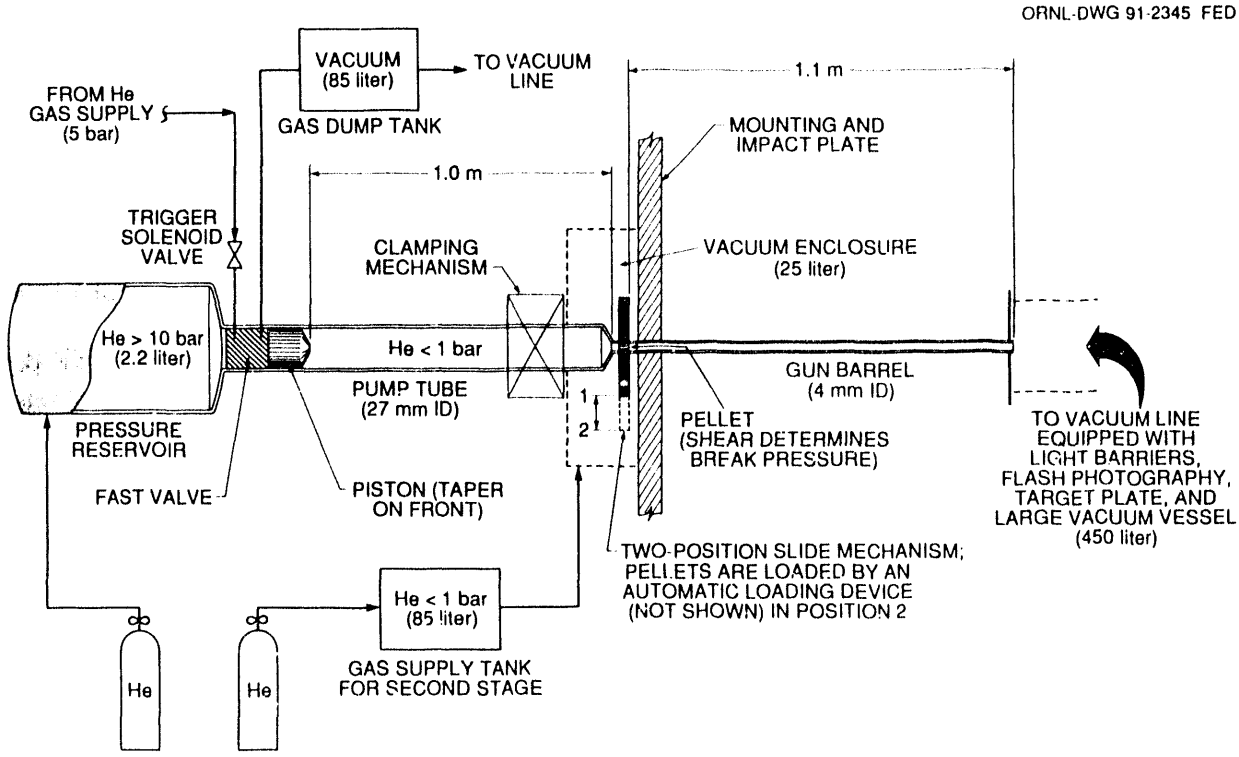

Fig. 4.8. Schematic of ORNL repetitive two-stage light gas gun.

Table 4.1. Parameters for repetitive two-state light gas gun

First stage	
Material	304 stainless steel
Volume, cm^3	2250
Length, m	≈0.42
Inside diameter, mm	≈82
Gas	Helium
Initial pressure, bar	>10 (typically 50–100)
Activation mechanism	Fast valve
Second stage[a]	
Pump tube material	4130 carbon steel
Volume, cm^3	585
Length, m	1.02
Inside diameter, mm	27.0
Wall thickness, mm	5.6
Gas	Helium
Initial pressure, bar	<1 (typically 0.8)
Piston	
Material	Plastic
Geometry	Solid cylinder with tapered front
Diameter, mm	27.0
Mass, g	25–30
Gun barrel	
Material	4130 carbon steel
Length, m	1.14
Inside diameter, mm	4.0
Wall thickness, mm	2.8
Pellet	
Material	Plastic
Geometry	Solid cylinders, spheres
Diameter, mm	4
Mass, mg	29–55

[a]Includes small section (4.0 mm ID, ≈38 mm long) between end of pump tube and base of projectile.

Fig. 4.10. The key components and features are described briefly below. The device is described thoroughly in ref. 20.

The operating sequence consists of the following cycle (see Fig. 4.8). (1) A pellet is automatically loaded into the slide bar when it moves to position 2 (initially the valve output is connected to the vacuum system and the clamp is disengaged). (2) After the slide bar returns to position 1, the pneumatic clamp is engaged and held. (3) While clamped, the fast valve is triggered. This switches the valve output from vacuum to high pressure to drive the piston and shoot the pellet; the controller-type fast valve then automatically switches back from pressure to vacuum and dumps the remaining gas to the vacuum system after a finite time, which is adjustable. (4) The clamp is released; this automatically starts the refill of the pump tube with gas from the volume surrounding the pump tube/gun barrel interfaces (this volume is relatively large and regulated at a constant pressure); and the gas flow (and

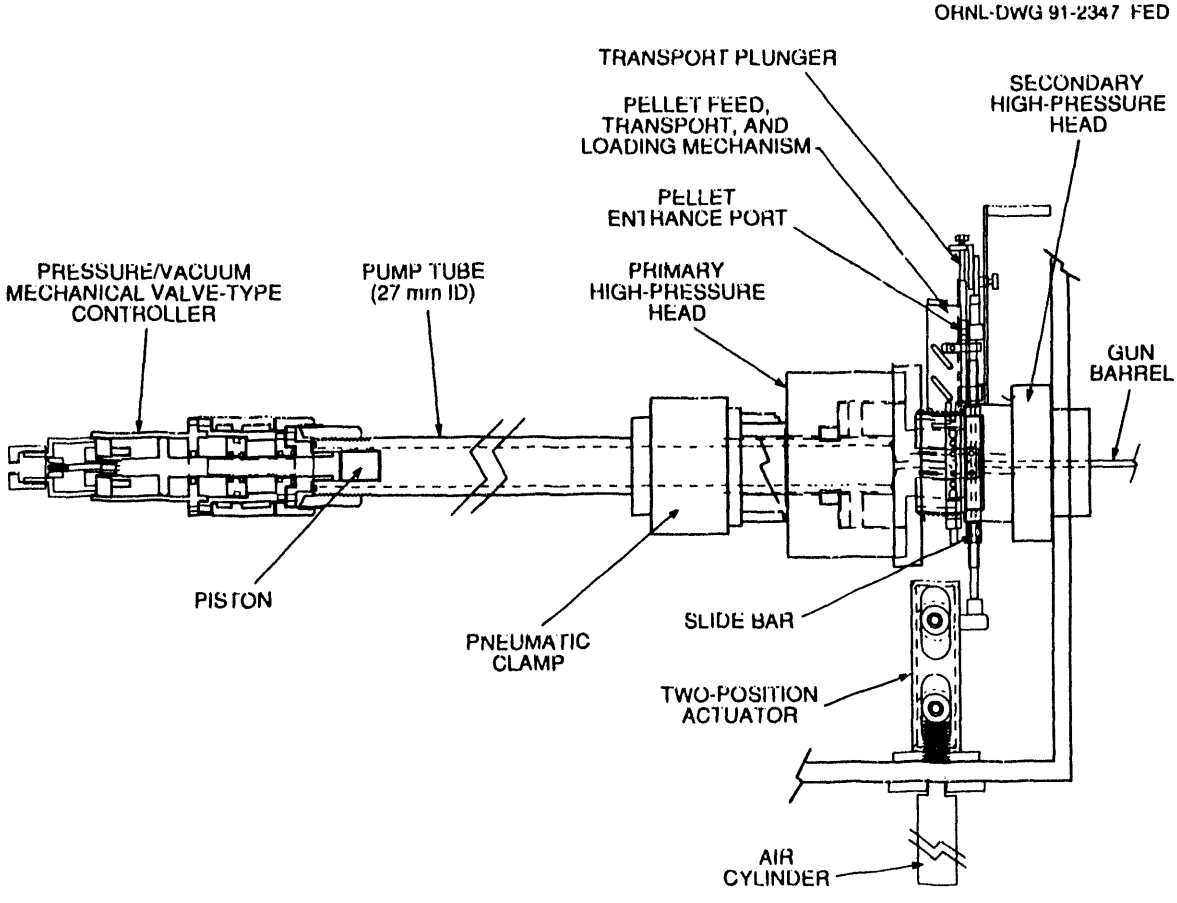

Fig. 4.9. Assembly drawing of ORNL repetitive two-stage light gas gun.

pressure) also ensures that the piston returns to its home position (where it seals against an O-ring). The cycle is then repeated.

In laboratory tests with this device exhausting into a 450-L vacuum vessel, the gun was operated using helium gas in both stages and plastic pellets of 4-mm nominal diameter. To demonstrate repetitive operation of the two-stage light gas gun, experiments were carried out in which pellets were fired consecutively at frequencies of up to 1 Hz. Experimental data for two ten-pellet test sequences (1056 and 1109) are summarized in Table 4.2. Examples of the transient data recorded by the CAMAC digitizers for an individual pellet (fifth pellet of test sequence 1109) are shown in Figs. 4.11 and 4.12. All times are relative to the start of the initial fire pulse

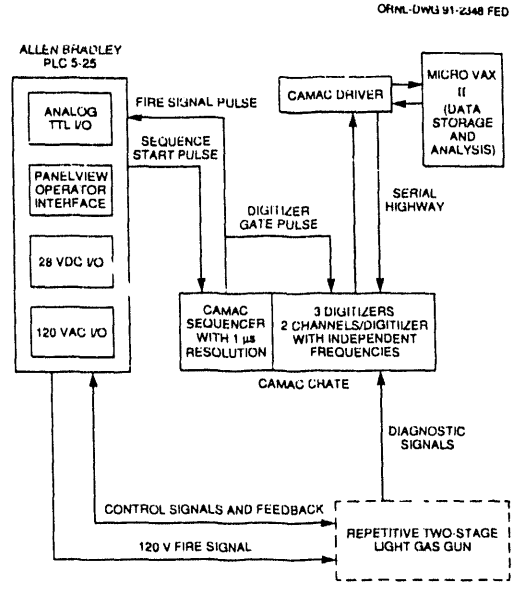

Fig. 4.10. Schematic diagram of control/data acquisition system.

Table 4.2. Experimental data for two ten-pellet test sequences with repetitive two-stage light gas gun operating at 1 Hz

Pellet number	Transient timing data[a] (s): Gun muzzle light gate	Transient timing data[a] (s): Target plate accelerometer	Flight time[b] (ms)	Pellet velocity (m/s)
Test sequence 1056				
First-stage pressure: 62 bar		Piston mass: 25 g	Pellet material: acetal	
Second-stage pressure: 0.8 bar		Pellet mass: 0.055 g	Pellet shape: solid cylinders	
Pellet size: 4.0 mm diam × 3.5 mm long				
1	0.071106	0.071811	705	2130
2	1.0737659	1.0745409	775	1935
3	2.0740361	2.074781	745	2015
4	3.074631	3.075371	740	2030
5	4.075336	4.0760708	735	2040
6	5.0758257	5.076561	735	2040
7	6.076481	6.077211	730	2055
8	7.0688057	7.069541	735	2040
9	8.077776	8.078511	735	2040
10	9.070187	9.070921	734	2045
				Avg = 2040
Test sequence 1109				
First-stage pressure: 100 bar		Piston mass: 30 g	Pellet material: polypropylene	
Second-stage pressure: 0.8 bar		Pellet mass: 0.029 g	Pellet shape: solid spheres	
Pellet size: 4.0 mm diam				
1	0.051846	0.052321	475	3160
2	1.0476309	1.0481009	470	3190
3	2.0481758	2.048681	505	2970
4	3.0510309	3.0515509	520	2885
5	4.048901	4.0494113	510	2940
6	5.049611	5.0501113	500	3000
7	6.0423713	6.042881	520	2885
8	7.0497513	7.050221	470	3190
9	8.050951	8.05148	529	2835
10	9.051056	9.051620	564	2660
				Avg = 2970

[a]Taken as time of abrupt change in instrument signals as determined by software code that analyzes raw transient data.

[b]Separation distance of 1.5 m between muzzle light gate and target plate.

from the PLC, which serves as the zero time reference.

In Fig. 4.11, the top trace is the pressure at the upstream end of the pump tube (values shown were obtained by multiplying the voltage signal from the pressure transducer by its calibration constant). The pressure, which is initially subatmospheric (0.8 bar absolute), suddenly increases to ≈45 bar as the transducer is exposed to the first-stage gas upon the piston transit; the piston actually oscillates in the pump tube after the pellet is shot, as indicated by the cyclic nature of the signal. The decay of the

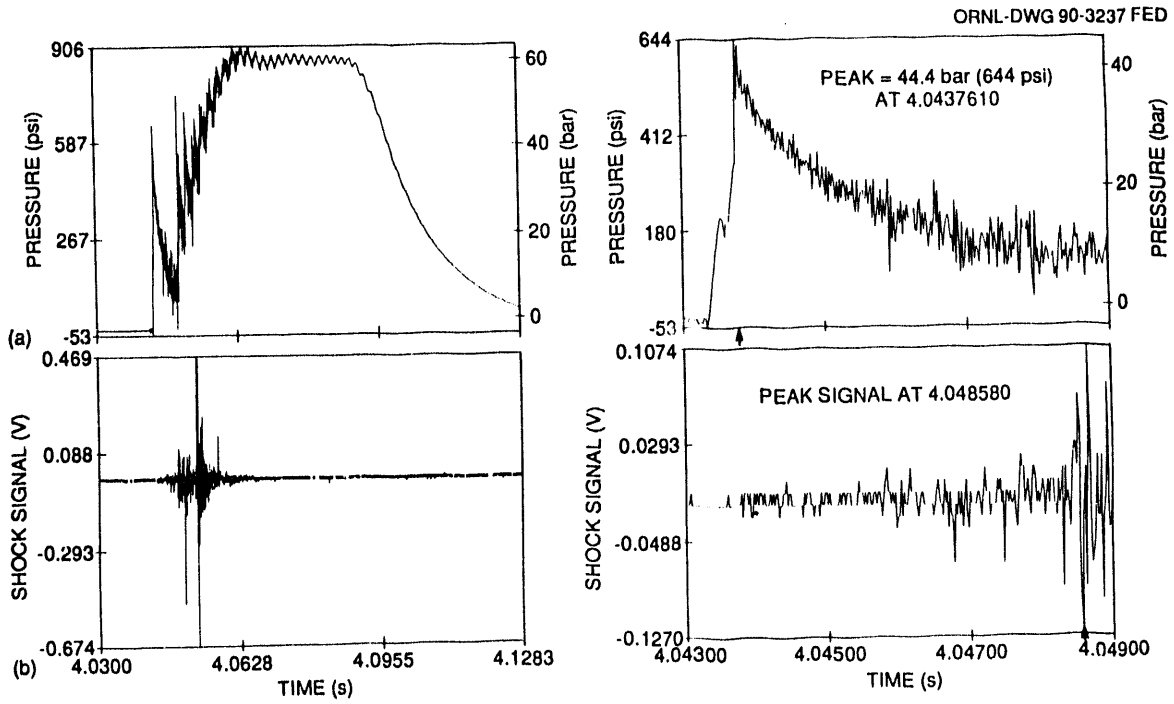

Fig. 4.11. Experimental data for fifth pellet of test sequence 1109: (a) pressure in upstream end of pump tube and (b) output signal from shock accelerometer located at downstream end of pump tube (data sampling rate of 50 kHz).

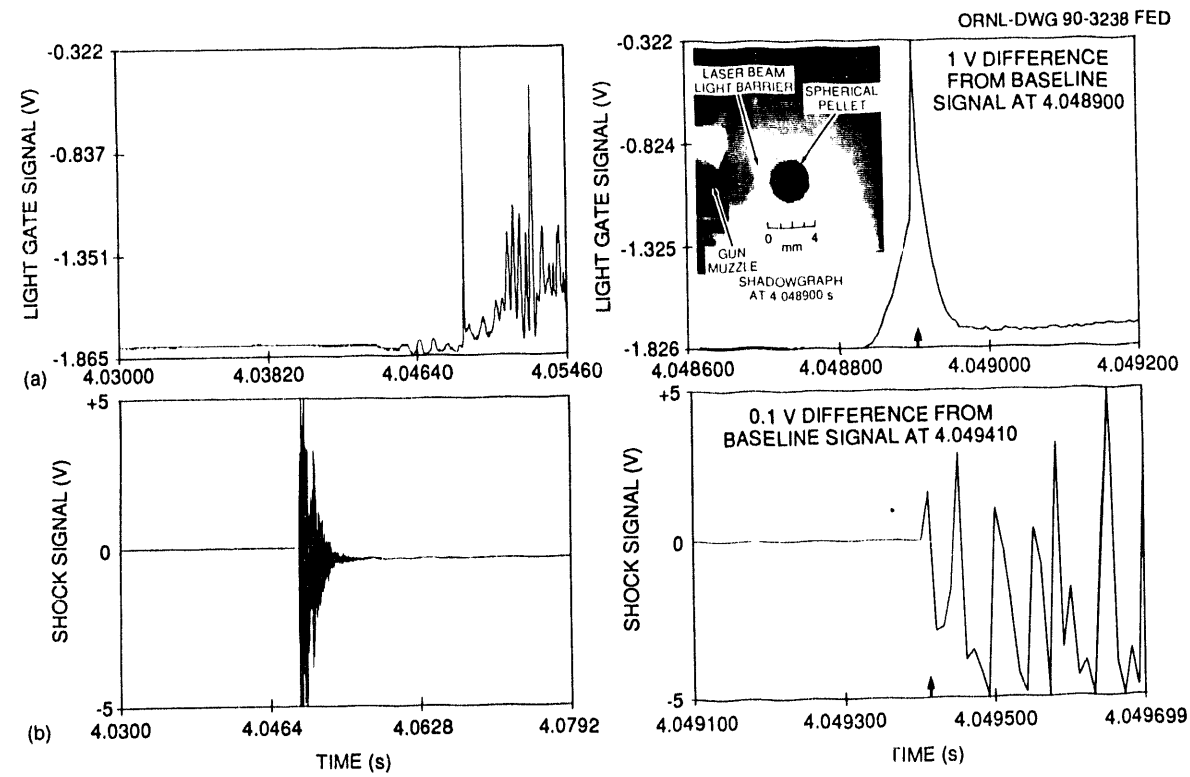

Fig. 4.12. Experimental data for fifth pellet of test sequence 1109: (a) output of diode that monitors light intensity at gun muzzle light barrier and (b) output signal from shock accelerometer located on target plate (data sampling rates of 200 kHz and 100 kHz, respectively).

pressure toward the end of the data trace corresponds to the switching of the fast valve output back to the vacuum mode and the dumping of the remaining gas from the pump tube. The bottom trace in Fig. 4.11 is the output of the shock accelerometer mounted at the downstream end of the pump tube. Although there is some uncertainty, the data provided by these transducers can be used to estimate the flight time for the piston to travel the ≈1-m length during the initial compression. As shown in the expanded traces on the right-hand side of Fig. 4.11, the time for the piston to travel from the transducer (peak pressure at 4.0438 s) to the end of the pump tube (shock signal peak at 4.0486 s) is estimated as 4.8 ms.

Accurate pellet velocities were determined using timing data from instruments located in the pellet injection line downstream of the gun barrel as shown in Fig. 4.12. A ≈10-ns flash from a nitrogen dye laser was used to freeze the in-flight pellet in a shadowgraph, which was monitored and stored by a standard video camera and recorder; the shadowgraph for the test shot is shown in the inset of Fig. 4.12(a). Only test sequences with photographs for all pellets are reported in this study, and this guarantees that the correct times for these events were selected.

Table 4.2 summarizes the experimental data for the two ten-pellet test sequences (1056 and 1109). The key differences in input parameters for the data sets were the type and mass of the pellets and the first-stage pressure. In test sequence 1056, solid 4-mm-diam, 3.5-mm-long cylinders of acetal plastic were used for the pellets, and the first-stage pressure was regulated at 62 bar. For this test, the average pellet velocity is 2040 m/s with all pellets falling within 5% of the average; examining only the last eight pellet speeds indicates a maximum variation of only 30 m/s (or 1.5%) from the average. For the higher-performance test sequence 1109, solid 4-mm-diam spheres of polypropylene were used for the pellets, and the first-stage pressure was maintained at 100 bar. For this ten-shot sequence, the average pellet velocity is 2970 m/s with all pellets falling within about 10% of the average.

In Fig. 4.13, we show data for all ten pellets of test sequence 1109 by plotting the data over the entire time window of data acquisition (data were actually collected for only a small time window for each pellet, as shown in Figs. 4.11 and 4.12, with the time interval between pellets void in Fig. 4.13). Thousands of pellets have been fired in this study, including hundreds of multiple-pellet sequences. The data presented here are typical, with test sequence 1056 representative of modest operating parameters and test sequence 1109 exemplifying the highest performance parameters observed to date for repetitive operation. No more than ten pellets were fired in standard test sequences; the number was limited by the capability of the original data acquisition system. Also, some gun components were exposed to high-temperature gases during operation, and active cooling may be required for test durations much longer than ≈10 s. However, ten-pellet sequences were sufficient to demonstrate the feasibility of repetitive two-stage gun operation.

In addition to the repetitive work, the larger two-stage gun (pump tube ID of 41.3 mm) was equipped with a rifled 6-mm-diam gun barrel, and velocities of up to 5.1 km/s were achieved with 140-mg plastic pellets. This system provides a test bed for evaluating pellet/sabot arrangements. The larger gun bore gives more versatility in the sabot geometry design; for example, a 6-mm-OD, 4-mm-ID shell is a reasonable size for sabots encasing nominal 4-mm-diam hydrogen pellets. Rifled barrels will be used to test the "spin-separation" technique. This involves launching sabot packages from

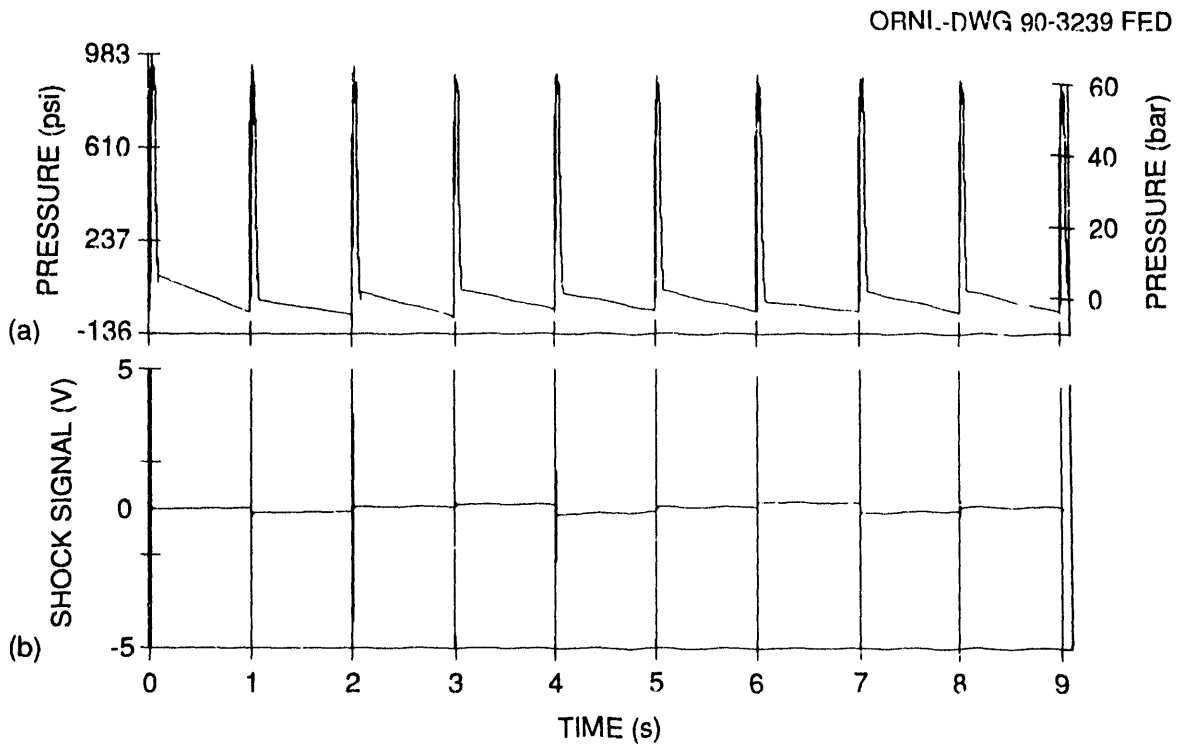

Fig. 4.13. Experimental data for test sequence 1109: (a) pressure from transducer located in upstream end of pump tube and (b) output signal from shock accelerometer located on target plate (data sampling rates of 50 kHz and 100 kHz, respectively).

rifled tubes that spin them at high angular velocities. The sabot elements then travel away from the nominal launcher trajectory at prescribed angles because of centrifugal effec' hile the projectile payload travels alon, the original trajectory since its center of rotation and center of gravity are concentric with the trajectory.

In CY 1991, a significant effort in support of the two-stage driver for the TPI, described in Sect. 4.1.1.2, was carried out. The support work included the construction of a test stand for two-stage component development. A large-orifice fast valve closely coupled to a 0.64-L volume was developed and used to propel the piston in the pump tube. The pump tube was sealed at the downstream end where the pressure was measured. With this experimental arrangement, the piston essentially experiences the same parameters as those for actual two-stage gun operation with projectiles. Different piston designs were evaluated, and pistons constructed of titanium alloys were cycled for thousands of shots with the corresponding wear recorded. Along with thorough testing of all prototype components, operating sequences were developed for the two-stage driver. These results are described briefly in ref. 21. In general, the information obtained from experiments on the test stand has been incorporated in the final design of the TPI two-stage driver, and this should improve the initial reliability of the equipment in pellet fueling experiments on TFTR.

The next step in developing a functional high-speed repetitive hydrogen pellet injector is to combine the acceleration technology described here with the cryogenic

extruder technology for supplying hydrogen ice previously developed at ORNL (see, e.g., ref. 16). The key elements of the present design can, however, be readily integrated into a pellet injection system, with or without sabot-handling capability. Other key development issues for applying this technique to plasma fueling include piston design, incorporation of active cooling for long-pulse operation, and sabot configurations including separation techniques. Even though a single standard plastic piston appears adequate for up to hundreds or thousands of shots, longer lifetimes (at least tens of thousands of shots) are needed in a practical plasma fueling system. Active cooling of some of the gun components will probably be required to limit the exposure of bulk materials to elevated temperature during long-pulse operation. Reliable techniques to continuously supply sabots to the gun and to accomplish the stripping action near the gun muzzle are yet to be demonstrated.

In general, the designs of all components need to be reexamined with respect to materials and operating lifetime. In summary, even though considerable progress has been made, a significant development effort is still required before a practical plasma fueling system based on the two-stage light gas gun can demonstrate reliability approaching that attained by present pellet injection systems (see, e.g., ref. 22).

4.1.2 Pellet Injector Applications

4.1.2.1 JET pellet injector

L. R. Baylor, S. L. Milora, W. A. Houlberg, S. E. Attenberger, and L. A. Charlton

PEP H-mode experiments

The primary focus of pellet experiments in the JET 1990 and 1991 campaigns was the coupling of the PEP mode with the H-mode. Previous experiments with 4-mm pellet injection in H-mode discharges yielded a fusion product of 5×10^{20} m^{-3}•keV•s. This performance was enhanced by injection of the pellet and formation of the H-mode plasma early in the discharge before a $q = 1$ surface formed and sawteeth appeared. A fusion product of 7×10^{20} m^{-3}•keV•s was produced in plasmas having nearly the same electron and ion temperatures of 10 keV. The thermonuclear neutron rate of these deuterium discharges was approximately 10^{16} s^{-1}. The central electron and ion thermal conductivities in these PEP H-mode discharges are reduced by a factor of two to three with respect to the usual anomalous values and may be related to negative shear in the core, which may be brought about by a substantial bootstrap current.

Further PEP H-mode studies were made in 1991 with 6-mm pellets. Central densities of 2.2×10^{20} m^{-3} were achieved in 4-MA discharges; these were significantly higher than the density achieved with the 4-mm pellets, as shown in Fig. 4.14, where the density profiles measured by light detection and ranging (LIDAR) Thomson scattering 20 ms after 4-mm and 6-mm pellet injection are overlaid. As much as 11 MW of neutral beam injection (NBI) and 10 MW of ICRF heating (ICRH) were applied following 6-mm pellet injection and resulted in central electron temperatures of 5 keV. The power density available on JET was determined to be insufficient to heat the dense plasma following 6-mm pellet injection to values as high as that achieved with 4-mm pellet injection.

The PEP mode has been found to be terminated by an abrupt loss of central pressure often associated with magnetohydrodynamic (MHD) phenomena. This termination appears to be the result of an instability with a fast time scale that is triggered when the safety factor drops below 1.5. The ideal infernal mode has been studied in relation to

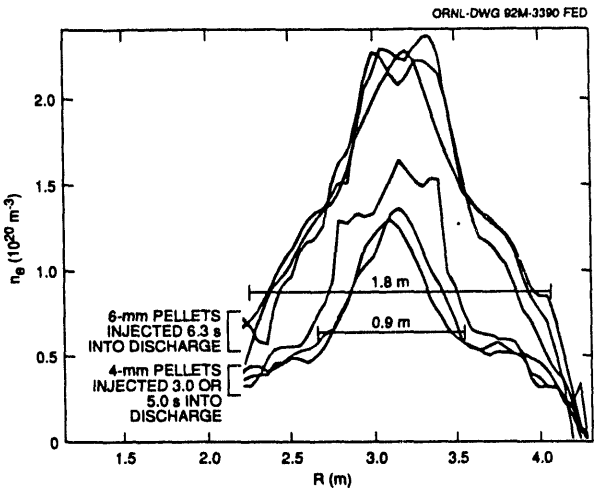

Fig. 4.14. Density profiles measured 20 ms after pellet injection by LIDAR Thomson scattering.

these discharges and is thought to be a candidate for the instability.[23]

Particle transport analysis

The particle transport analysis of pellet-fueled discharges begun in 1988 was summarized in 1990.[24] It was found that the effective particle diffusivity in pellet-fueled discharges was a strong function of the density profile peaking factor $n_e(0)/\langle n_e \rangle$. The effective particle diffusivity from a number of discharges is shown as a function of density peaking factor in Fig. 4.15. The effective particle diffusivity in the core region is as low as 0.04 m^2/s in discharges with highly peaked density profiles. The dependence of the effective particle diffusivity on density profile peakedness correlates well with the effective thermal diffusivity from power balance calculations. Both pellet-fueled and non-pellet-fueled sawtooth-free discharges were satisfactorily modeled without any anomalous convective (inward pinch) term.

Further analysis of the particle transport in pellet-fueled plasmas was performed in 1991. The PTRANS code developed earlier at JET was modified to allow modeling of the density profile evolution with the nonlinear transport model used successfully by R. Hulse to model a TFTR pellet-fueled discharge. The same model and variations were applied to a variety of JET pellet-fueled discharges in Ohmic, L-mode, and H-mode conditions and resulted in poor agreement with the measured density profile evolution.

Pellet penetration experiments

The pellet penetration analysis begun in 1989 was completed in 1991.[25] The conclusion of this work is that the scaling of pellet penetration depth with plasma and pellet parameters agrees with predictions of the neutral gas shielding (NGS) ablation model; however, the penetration depth is

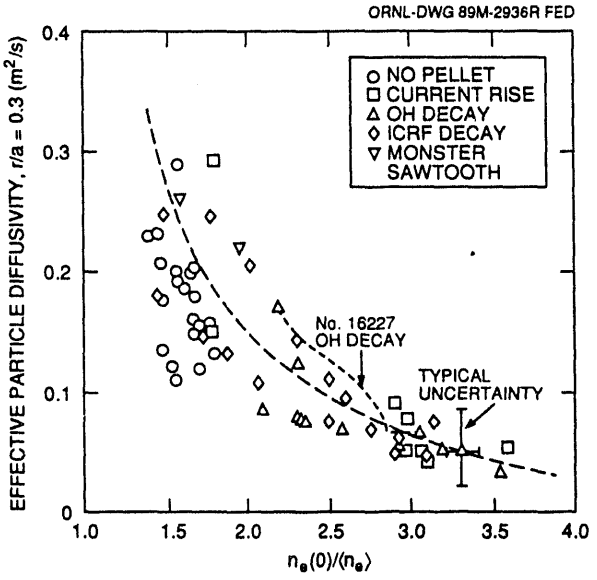

Fig. 4.15. Effective particle (electron) diffusivity at $r/a = 0.3$ as a function of density profile peakedness. The particle diffusivity is derived from a particle balance calculation assuming no anomalous inward particle convection. Values are averaged over 400 ms during a discharge, and each point represents a different discharge. The time history of Ohmic discharge 16227 is shown on the same plot.

nearly twice that predicted by local ablation calculations. Additional shielding mechanisms need to be incorporated in the model to explain the discrepancy.

Pellet deposition analysis

A study of pellet deposition in JET pellet injection experiments was begun in 1990. The goal of the study was to examine the measured density profile shortly after pellet injection and infer the pellet ablation rate required to produce the resulting density profiles. Measurements of the density profile on JET were made with the LIDAR Thomson scattering diagnostic within 4 ms of injecting a pellet. These profiles were analyzed to determine the effective ablation rate required to produce the resulting density profile. An example of this analysis is shown in Fig. 4.16, which shows the effective ablation rate for three identical Ohmic discharges after 4-mm pellet injection and the calculated ablation rate using the NGS model with the neutral shielding enhanced by a factor of 15 over the standard NGS model. We find a strong discrepancy between the model and the data

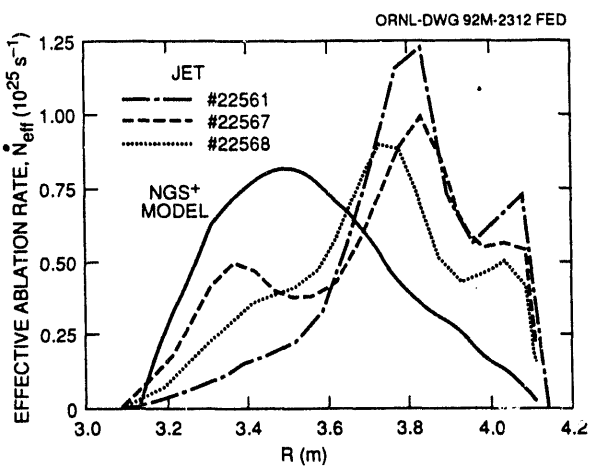

Fig. 4.16. The effective ablation rates calculated for 4-mm pellets injected into identical Ohmic discharges and the ablation rate calculated from the NGS model with enhanced shielding.

and have thus far been unable to diagnose any fast response of the plasma that might mask the effective ablation rate.

4.1.2.2 Tore Supra pellet injector

C. A. Foster

A centrifuge-type pellet fueling system, shown in Fig. 4.17, has been in operation on Tore Supra since the fall of 1989. Tore Supra is a long-pulse superconducting tokamak experiment located at Cadarache, France, administered by the French for Euratom. This injector was developed at ORNL to provide a quasi-continuous pellet source for plasma discharges lasting up to 30 s. Deuterium ice is formed by freezing gas on a rotating copper disk, which is cooled to 4.3 K by liquid helium. Pellets are then cut from the rim of the ice and injected into a high-speed rotating track in which they are accelerated to 800 m/s and injected into the tokamak through a guide tube. Up to 100 pellets can be injected at a time at a rate of up to 10 Hz. By adjusting the cutting knife, the mass of the pellets can be varied from 3 to 10 torr•L per pellet (equivalent gas content).

The experimental program is continuing with the goal of producing long-pulse, pellet-fueled discharges with continuous pellet fueling and plasma exhaust using the ergodic divertor and pump limiters on Tore Supra. Figure 4.18 shows data from a 10-s discharge[26] that was fueled by 23 pellets with Ohmic plasma conditions and used the preconditioned graphite walls to pump the plasma exhaust. Experiments with auxiliary heating were started in 1991. Figure 4.19 shows data from an experiment combining pellet fueling with lower hybrid heating (LHH).[27] Normally, LHH produces non-thermal electrons in the edge of the plasma that prematurely ablate pellets, causing poor fueling efficiency. In the experiment shown,

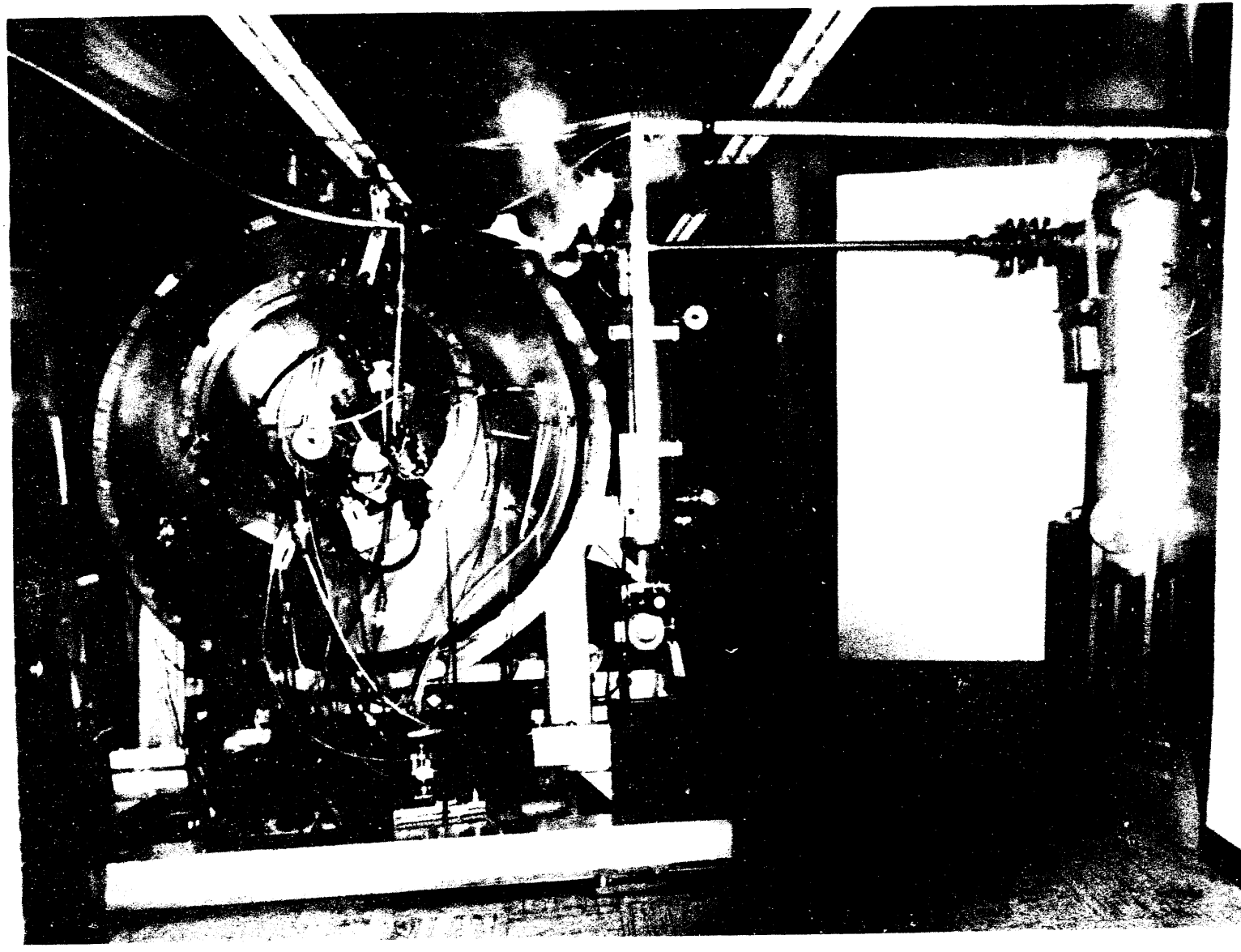

Fig. 4.17. ORNL centrifuge pellet injection system in operation a ORNL prior to shipment to Tore Supra.

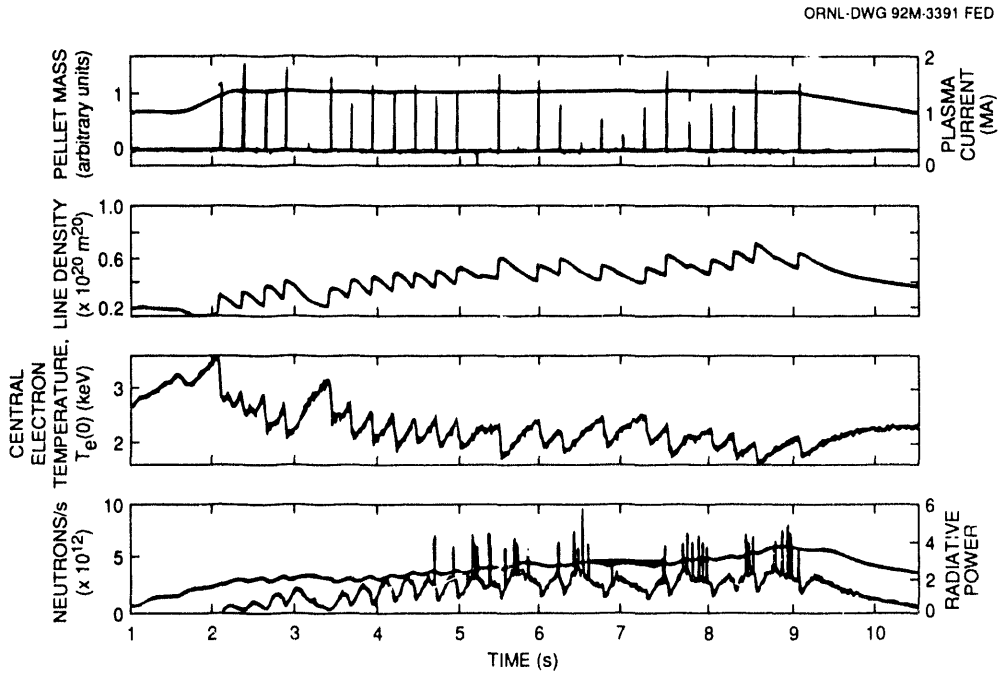

Fig. 4.18. Long-pulse Ohmic discharge fueled by multiple pellet injection.

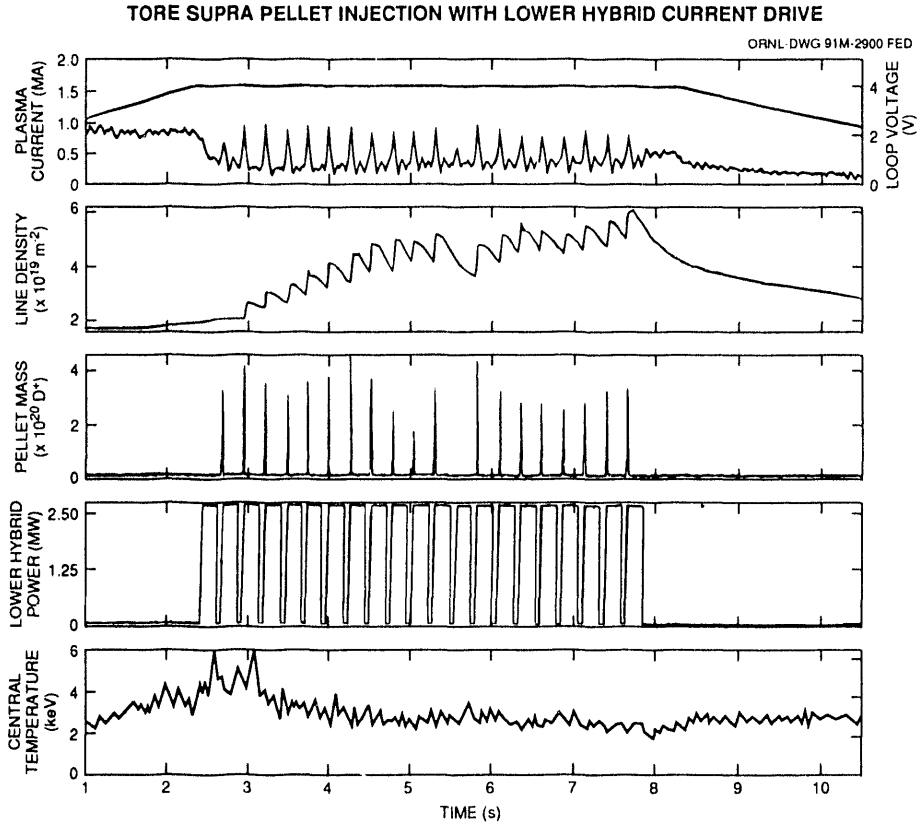

Fig. 4.19. Lower hybrid current drive discharge with multiple pellet injection.

normal pellet penetration was achieved by temporarily turning off the LHH power just prior to each pellet. The experimental program will continue with the addition of both rf and neutral beam heating along with a full set of pump limiters.

4.2 RF TECHNOLOGY

The rf technology area comprises basic development, applications, and modeling. In the basic development area, work continued on the development of fast-wave current drive (FWCD), the folded waveguide (FWG), and Faraday shields. The four-strap FWCD phased array launcher was completed and installed on the DIII-D tokamak at General Atomics in San Diego. After the inital operation phase was completed, the antenna was returned to ORNL for upgrades to the Faraday shield and antenna box and then reinstalled on DIII-D.

The 80-MHz folded waveguide (FWG) was tested in the Radio Frequency Test Facility (RFTF) plasma. The maximum power achieved was 730 kW. Higher powers should be available in a device with higher plasma loading. A 433-MHz FWG was constructed for low-power testing. A collaboration with the Frascati Tokamak Upgrade (FTU) team in Frascati, Italy, was begun; this effort includes the design, fabrication, and installation of two 500-kW, 433-MHz FWG antennas.

New materials and fabrication techniques for Faraday shield tubes were developed and tested. The effects of Faraday shield geometry and material on the antenna were calculated, and the results were compared to measurements. The calculations can predict the effect of different shields on magnetic shielding, antenna inductance, phase velocity of the launched waves, and rf power dissipation in the shield itself. In addition, the effects of slotting the antenna side walls and septa have been modeled and measured experimentally.

Applications of rf technology included work on ATF at ORNL, continuing collaborations on the Tore Supra tokamak and on TFTR, and a new effort on JET. A single-strap antenna was modified and reinstalled on ATF, where it operated at power levels up to 900 kW. The two-strap antenna for Tore Supra was installed and operated at power levels up to 2 MW.

In the collaboration on TFTR, a combined total of 6 MW of ICRH power has been injected into TFTR using the Bay M and modified Bay L antennas. A new initiative on TFTR is a microwave reflectometer, designed at ORNL, which will initially be installed in a toroidal sector removed from the antennas. After its initial operation, it will be installed inside one of the two additional TFTR antennas. The reflectometer will allow measurement of the edge density profile and of the effects of rf power on the profile.

A collaboration was begun to design a power coupler for the new A_2 antennas for JET. This work involved extensive modeling of the complicated A_2 antenna geometry to predict the mutual coupling between antenna elements. The power coupler will be designed to optimize power flow from the individual transmitters to the antenna straps over a broad frequency range for arbitrary values of antenna phasing.

Design work on heating schemes and antennas for the proposed Burning Plasma Experiment (BPX) was performed in collaboration with the Fusion Engineering Design Center during the period. This effort will be redirected to support the Toroidal Physics Experiment (TPX) proposal.

4.2.1 Basic Development

R. H. Goulding, F. W. Baity, W. L. Gardner,
G. R. Haste, D. J. Hoffman,
D. A. Rasmussen, P. M. Ryan,
and D. W. Swain

4.2.1.1 Fast wave current drive

DIII-D

The successful operation of the DIII-D FWCD antenna array, as described in Sect. 4.2.2.2, is due in part to the development of a new tuning algorithm. The algorithm is used to adjust five tuning elements so as to obtain equal current magnitudes on each of the four antenna elements with the desired phasing and a match to the transmitter impedance. Voltage and impedance measurements obtained during a particular shot are used to improve settings for the following shot. Figure 4.20 is a graph of the phases of the voltages measured using probes on three of the feed lines relative to that of the first feed line as a function of time during a shot. The target for the phase difference between neighboring lines for this shot was 90°, and as the figure shows, the actual phase obtained was very close to this target value. This result represents the first time in which a phased antenna array operating in the ICRF has been driven by a single power source. The fact that all array elements are driven by a single source requires that control of phasing and balancing of currents occur at high power.

Progress has also been made in the modeling of the self-consistent behavior of the system composed of the feed circuit, antenna array, and plasma during phased operation. Measurements in air of the rf magnetic fields generated by a mock-up of the antenna array (Fig. 4.21) have been used as input to the ORION code in order to predict changes in antenna loading caused by changes in phasing and the relative magnitudes of array element currents.[28] In this way the performance of the system under varying plasma conditions and the effects of modifications of antenna geometry can be predicted.

JET

A power compensation system has been developed to allow full-power operation of the JET ICRF heating system in a FWCD mode in which neighboring antenna elements are arbitrarily phased with respect to one another. The system has been designed to operate in conjunction with the four-element A_2 antenna arrays that will be installed in 1993.[29] Phased operation is difficult because power is transferred

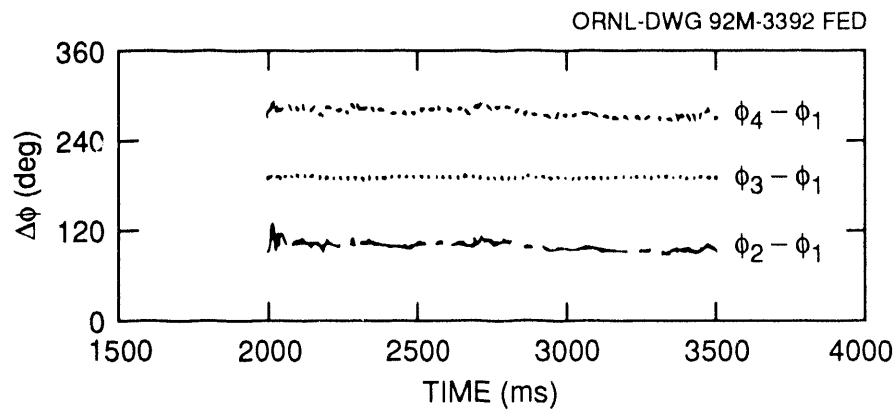

Fig. 4.20. Phases of voltages measured in the feed lines during operation of the DIII-D FWCD antenna array. The target values were $\phi_2 - \phi_1 = 90°$, $\phi_3 - \phi_1 = 180°$, and $\phi_4 - \phi_1 = 270°$.

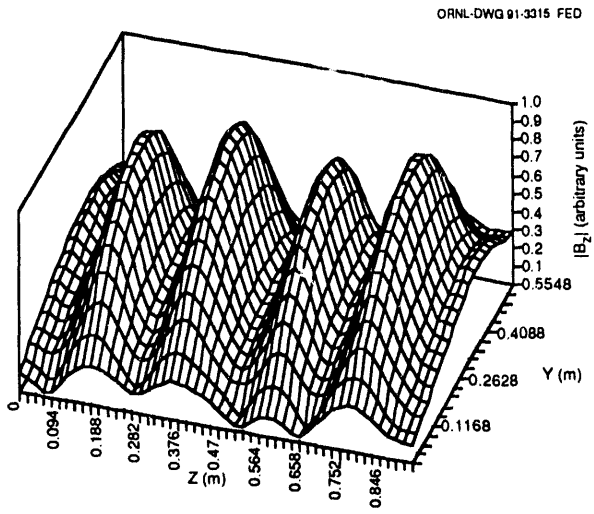

Fig. 4.21. Toroidal rf magnetic field amplitude measured 5 cm in front of the Faraday shield. Here Y is the poloidal direction, with the bottom of the antenna box at $Y = 0$, and Z is the toroidal direction.

between antenna elements due primarily to their mutual inductance, with the magnitude of the power transfer proportional to the sine of the relative phase angle. If the input power to each element is equal, then there can be a large imbalance in the radiated powers due to this transfer. This imbalance reduces the power handling capability of the system, as well as producing a degraded wave spectrum. JET has previously operated the A_1 ICRF antennas in a phased mode by using unbalanced input powers to compensate for the transfer, but this method reduces the total available power by as much as half.[30]

The JET A_2 antenna elements will each be driven by a separate transmitter, in contrast to the DIII-D case in which a single power source drives all elements. Thus, it is possible to control the amplitudes and phases of currents on the elements automatically using feedback. To take advantage of these capabilities, the power compensation problem for JET had to be solved in a completely different way than that used for DIII-D. A system has been devised, based on a proposal by G. Bosia of JET, to use a four-port quarter-wave coupler to transfer power equal in magnitude and opposite in direction to that transferred at the antennas. The magnitude and direction of the power transfer are controlled using capacitors (Fig. 4.22), which can be adjusted by automatic feedback control to obtain equal radiated powers with equal input powers. We have developed coupled transmission line models of the antenna array, quarter-wave coupler, and feed lines in order to predict the performance of this system. The model predicts that available power can be increased by nearly 50% for a relative antenna phasing of ±90° (Fig. 4.23). Installation of a prototype version of this system on JET is planned for early 1993, with FWCD experiments expected to commence the following year.

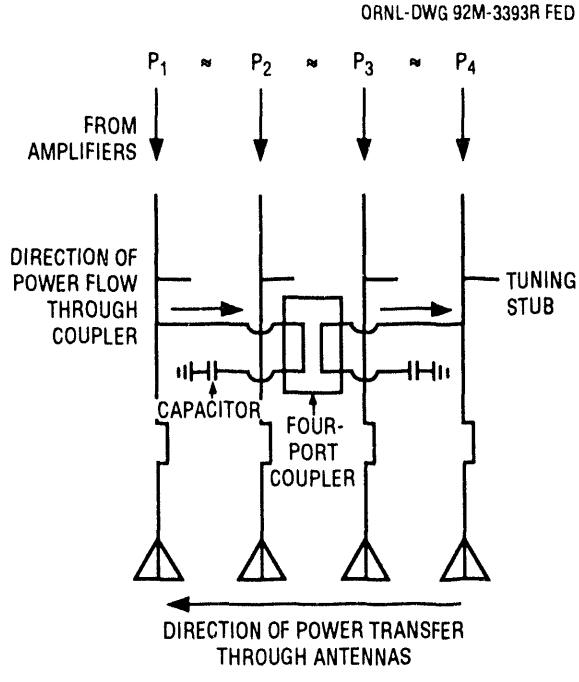

Fig. 4.22. Power compensation system for the JET A_2 antennas.

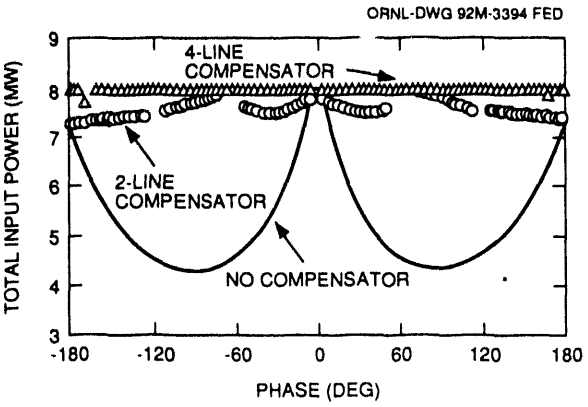

Fig. 4.23. Input power vs phase with and without power compensators assuming equal current magnitudes at the array element grounds.

4.2.1.2 Folded waveguide

The 80-MHz prototype FWG has now been operated at power levels above 700 kW in the presence of plasma. The very large increase in power handling capability has been achieved as the result of both design changes and advances in conditioning methods. A movable shorting plate located at the back end of the waveguide was replaced by a fixed plate to eliminate problems with finger stock in this high-current region. Arcing at high power was sharply reduced by eliminating gaps between the waveguide vanes and the polarizing plate bolted to the front of the waveguide and by improving connections between the feed coaxial outer conductor and the waveguide.

In addition, a new surface conditioning technique was employed following vacuum openings. It consists of a bakeout at 150°C for 8 h or longer, followed by application of rf at power levels ≤ 2 kW to produce a multipactor discharge, which is run continuously until improved surface conditions cause it to terminate spontaneously. A final improvement was the addition of a water-cooled stainless steel face plate mounted over the polarizing plate.

After these improvements were made, it became possible to operate the FWG prototype at input power levels of 550 kW in vacuum and 736 kW with plasma, corresponding to a maximum internal electric field in the waveguide of 20 kV/cm. When a loop antenna was operated at approximately the same plasma density ($n_e \sim 10^{17}$ m^{-3}), the maximum achievable power level was between 100 and 135 kW. Thus, the FWG performed approximately seven times better than the loop in power handling. Note that the power density of 400 W/cm^2 is extremely high, given the sparse plasma load.These power handling results indicate that the FWG concept has been sufficiently developed for application on a tokamak.

Figure 4.24 shows the FWG that is being designed for use on the FT-U tokamak. The

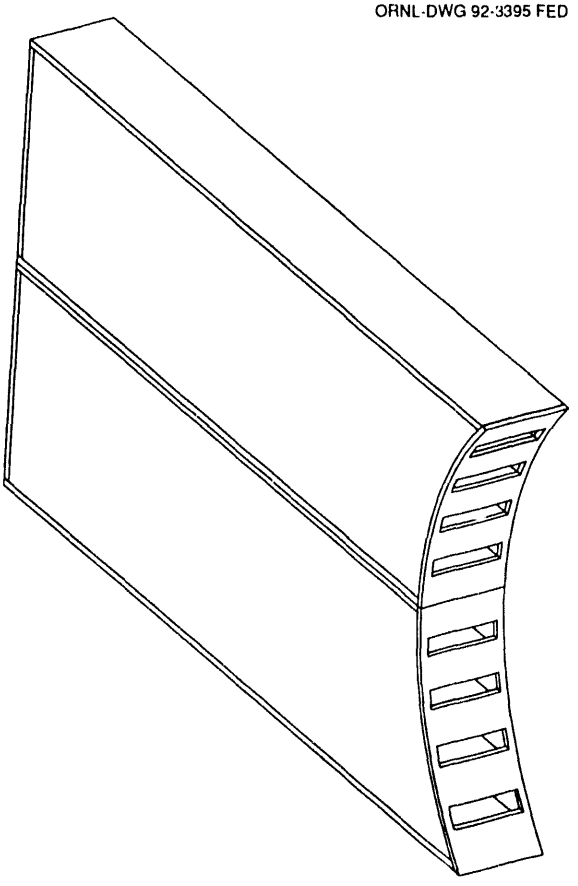

Fig. 4.24. The folded waveguide antenna for FT-U.

concept is also being considered for application on PBX and JT-60 and could be a prime candidate for ITER.

4.2.1.3 Faraday shield studies

Uncooled bent-rod Faraday shield

A prototype bent-rod Faraday shield has been built for the single-strap development antenna in order to test the performance of the concept during long-pulse operation with no active cooling. The shield is a single-tier open design in which the rf losses are minimized by a large spacing between elements. The shield elements are readily interchangeable so that a wide variety of protective coatings can be tested. A principal advantage of the bent-rod design is that it should have much lower thermal stresses than a straight-rod design.

Very good results have been obtained in long-pulse experiments performed in vacuum on RFTF. The shield was run with copper-plated, TiCN-coated stainless steel rods for pulse lengths up to 20 s and a transmitter power level of 40 kW at an operating frequency of 42 MHz. An infrared camera was used to monitor temperatures, which reached a maximum of 290°C at the end of a series of 17 pulses. The maximum temperature rise during a pulse was 50°C. The heating appeared to be very localized, with high temperatures limited to several tubes near the shield center and occurring only in the region of the 90° bends. There was no observable damage to the shield rods when they were inspected after the test. A second test was performed using Inconel rods covered with brazed graphite (POCO AXF-5Q) tiles. In this case, average transmitter power levels of 55 kW were attained for 25-s pulses, and power levels of up to 39 kW were attained for 38-s pulses. The maximum temperature observed in this case was 397°C, with the temperature rise distributed more broadly over the shield than it was for the TiCN-coated shield. The power deposited in the shield in this case is the same as that which would occur if the antenna were operating at a power level of ~1 MW in the presence of a 4-Ω resistive plasma load.

Short-pulse (100-ms) tests of the shield have also been performed in low-density ($n_e \leq 10^{17}$ m^{-3}) plasmas, in which maximum antenna voltages of 40 kV peak and maximum currents of >1 kA rms have been attained.

Mechanically attached tiles

Mechanically attached tiles have an advantage for use on uncooled Faraday shield elements in that there is little thermal contact between them and the underlying support rod. This acts to reduce the peak temperature reached by the support rod, since much of the heat generated in the tiles is radiated to other surrounding surfaces rather than conducted into the rod. In previous tests, tiles attached to a stainless steel tube by metal pins were successfully tested in the High Heat Flux Test Facility (HHFTF).[31] In subsequent rf compatibility tests, two tubes covered by brazed graphite tiles in the original development antenna Faraday shield were replaced by solid rods covered by tiles attached with pins. The modified shield was tested in RFTF using the development antenna with strap currents up to 900 A and pulse lengths to 2 s. Tile surface temperatures up to 900°C were achieved without any arcing observed in the vicinity of the tiles, indicating that this method of tile attachment is compatible with the presence of high rf fields.

4.2.2 RF Projects

4.2.2.1 Tore Supra

G. R. Haste, F. W. Baity, and T. D. Shepard

Three ICRF antennas are installed on Tore Supra. All three antennas use the same basic design, which was developed at ORNL, but there are differences in their final configurations that were deliberately introduced to test various design concepts. One of these antennas was built at ORNL, and the other two were built in France. Each one has two independent current straps and is installed in its own port on Tore Supra.

When first operated, all three antennas had Faraday shields with double layers of cooling tubes. The inner half of the inner layer of tubes (that facing the plasma) had semicylindrical carbon tiles brazed to the tube surface. Protection along the sides was provided by "bumper" limiters. On the two French antennas, the bumper limiters have a single cooling passage and flat, planar surfaces to which graphite tiles have been brazed. The ORNL bumper limiters have three cooling passages and curved carbon tiles.

Initially, all three antennas used integral feedthroughs in which the ceramic insulation was brazed to the metallic parts. All of the antennas have proved vulnerable to problems with the coaxial vacuum feedthroughs, and the French design has been changed to use O-ring seals, thus avoiding the troublesome vacuum braze procedure. As a side benefit, it has proved possible to change the feedthroughs without removing the antennas from the port. With the brazed design, the antenna must be removed to replace the feedthrough.

During spring 1991, while operating with the two-layer Faraday shield, one of the two French antennas achieved a power level of 3.2 MW at 57 MHz for a 3-s pulse. During fall 1991, the Faraday shields in both French antennas were replaced with a new design that incorporates a single layer of cooling tubes, coated with B_4C on the surface facing the plasma. In addition, a new central septum with water cooling replaced the original septum between the two antenna halves. These changes resulted in a higher Q; that is, the rf losses in the Faraday shield structure were significantly reduced. Detailed comparison of the properties of the antennas and of their interactions with the plasma are planned for 1992.

4.2.2.2 DIII-D

F. W. Baity, R. H. Goulding, and P. M. Ryan

Noninductive current drive appears to be required for a tokamak fusion reactor. Among existing fusion experiments, the DIII-D device at General Atomics offers the best opportunity for testing FWCD, which is one of the most promising candidates for noninductive current drive. The ORNL rf technology group designed and constructed an FWCD antenna array for a proof-of-principle ICRF current drive demonstration on DIII-D.

The DIII-D array is designed to operate at 2 MW for a 2-s pulse every 10 min and to cover the frequency range from 30 to 60 MHz. The antenna array is mounted in a 50- by 100-cm recess in the DIII-D vacuum vessel wall covering the 285° and 300° ports. Key features of the antenna array include a highly directed wave number spectrum and external control of the relative phasing between adjacent radiating elements. Algorithms for tuning and matching the array were developed with the aid of a full-scale antenna mock-up.

A magnetic loop probe was used to make two-dimensional (2-D) measurements of the magnetic field patterns in front of the antenna array before it was shipped to

DIII-D. The array was installed on DIII-D by ORNL personnel, with assistance from General Atomics staff, in June 1990, and operations began in September 1990. Minority heating experiments at 32 MHz were conducted first to qualify the hardware and test the tuning algorithms. Typical plasma conditions were a toroidal field of 2.15 T, a plasma current of 1 MA a line-averaged density of $(2–4) \times 10^{13}$ cm^{-3}, and less than 2% hydrogen. Up to 1.5 MW of power was applied, and almost all experiments were conducted with π phasing between adjacent loops.

Next, the direct absorption of fast waves at 60 MHz was verified in low-density plasmas at 1 T with the antenna array phased symmetrically. A threshold of about 1 keV in the electron temperature was required for significant absorption of the rf waves. Strong single-pass absorption of the rf is desired for FWCD, since the directionality of the waves may be compromised by multiple passes through the plasma. The absorption increases with increasing electron temperature, so current drive is expected to be most efficient during high-power ECH. However, the high cost of operating the DIII-D ECH system limited its availability to one DIII-D run period during the phased experiments that followed the symmetric phasing runs.

After these experiments, the first attempts were made to drive current with fast waves from antenna elements phased at 90°. In shots both with and without ECH, the tokamak loop voltage dropped, with the reductions exceeding those expected on the basis of increased electron temperature and the bootstrap effect, thus indicating probable current drive. The rf power in these experiments was generally limited to ≤1 MW because of voltage limitations in the transmission line system, and electron temperatures were less than optimum owing to inoperative waveguides in part of the ECH system. Consequently, the magnitude of the FWCD was small, on the order of 100 kA, in most cases. In addition, the FWCD was observed to be positive regardless of the direction of the launched rf wave spectrum, contrary to theoretical predictions.

The double-tier, Ti(C,N)-coated Faraday shield was removed during the fall vacuum opening of DIII-D, and the antenna housings were modified to increase the mutual coupling between antenna elements so as to increase the directionality of the launched wave spectrum. The antenna array was reinstalled in DIII-D without a Faraday shield in order to study the effect of the shield on plasma loading and impurity levels during high-power rf operation. These experiments are expected to continue for a few months, after which a new single-tier, B_4C-coated Faraday shield, with rods tilted at 12° to match the pitch of the toroidal magnetic field lines at the antenna radius, will be installed. The B_4C coating is expected to help reduce impurity generation during current drive experiments at 90° phasing.

4.2.2.3 TFTR

ICRF collaboration

D. J. Hoffman, F. W. Baity, W. L. Gardner, R. H. Goulding, D. A. Rasmussen, T. S. Bigelow, I. Collazo, G. R. Hanson, J. B. Wilgen, R. C. Goldfinger, J. R. Wilson,* J. C. Hosea,* J. H. Rogers,* G. Schilling,* J. Stevens,* and C. K. Phillips*

The TFTR rf program conducted experiments in a variety of plasma conditions, including plasmas with rf heating and with Ohmic heating, pellet fueling, and NBI. Total power launched from the two TFTR antennas exceeded 6 MW. Previous ICRF experiments on TFTR used two rf antennas of different design.[32,33] The loading characteristics of these two antennas were quite different. In order to determine whether the design features or local plasma/antenna geometry effects were responsible for the difference in loading characteristics, the design of the Bay L antenna was modified during 1990 to make it similar to the Bay M antenna. The changes included modifications to the Faraday shield geometry and the protective tile geometry and slotting of the antenna side walls and septum. Some significant differences between the two antennas remain. The toroidal separation between the two straps in each antenna is different, which produces different $k_{\|}$ spectra. Also, one of the antennas is closer to the plasma than the other, which may result in different plasma density profiles at the antenna faces.

Initial experiments indicate that the design differences may have been responsible for the previously observed differences in antenna loading, although the edge density profile (and, implicitly, the coupling) has changed since the early runs. This is due in part to the installation, around the TFTR vacuum vessel, of additional "rf" plasma limiters. The modified Bay L antenna achieved a power of 3.5 MW with an antenna voltage of 50 kV (the typical operating voltage of the previous runs). In experiments in which the density was ramped during the rf portion of the discharge, the loading was maximized at different densities for the two antennas. Two more antennas of similar design are scheduled to be installed on TFTR, which should lead to a total antenna power of 12 MW.

Physics issues investigated during the reporting period are

1. central heating of ions and electrons,
2. sawtooth stabilization,
3. enhancement of neutron production when pellet injection and rf operation were combined,
4. impurity injection from the antennas (typically low), and
5. modification of the edge conditions by the rf power.

Microwave density profile reflectometer

T. S. Bigelow, G. R. Hanson, J. B. Wilgen, and I. Collazo

The design of a microwave reflectometer for edge density profile measurements on TFTR was undertaken in 1991, with conceptual design completed by the end of the year. The reflectometer will eventually be used to facilitate the coupling of ICRF power to the plasma; it will also provide edge density profile and fluctuation data that are not readily available from the existing diagnostics.

The reflectometer launches a swept-frequency (90- to 115-GHz) test wave into the plasma edge. This wave reflects off the

*Princeton Plasma Physics Laboratory, Princeton, New Jersey.

extraordinary-mode cutoff layer and returns to the launcher. Measurement of phase shift vs frequency of the reflected wave can be inverted to reconstruct the density profile. A new dual-frequency, differential-phase configuration that has been developed reduces the effect of density fluctuations and eliminates problems with the long path length from the generator to the plasma. The diagnostic will initially be installed away from the antennas so that it can share the existing TFTR fluctuation reflectometer waveguide system. Plans are to later build a waveguide system to connect to a launcher mounted inside one of the two new ICRF antennas.

4.2.2.4 ATF

Ion cyclotron heating experiments with an asymmetric resonant double loop antenna

D. A. Rasmussen, R. H. Goulding, T. D. Shepard, D. J. Hoffman, F. W. Baity, R. C. Isler, C. E. Thomas, M. R. Wade, and M. Kwon

ICRF waves were used in heating experiments on the ATF plasma. A single-strap tunable asymmetric resonant double loop antenna with carbon limiters was used at power densities up to 13.6 MW/m^2 (900 kW). Hydrogen minority heating experiments at 14.4 MHz were performed for various central density levels from 5×10^{12} cm^{-3} to 2×10^{13} cm^{-3} in deuterium plasmas formed initially with both second harmonic ECH and NBI. Because of the low level of plasma coupling, no significant ICRH was observed in the low-density ECH target plasma.

Two distinct operating modes with both NBI and ICRH were observed. In the first, the combination of relatively low beam input power (≈600 kW) and inadequate machine conditioning resulted in discharges that suffered a collapse of the stored energy when beam heating was initiated. Thus, the plasmas had a central electron temperature of 50–100 eV when the ICRH was applied. This "target" plasma would remain in a collapsed stored energy state throughout the discharge unless ICRH was applied. When more than 200 kW of ICRH was applied, the plasma edge would heat, and as a consequence more efficient coupling of NBI power would result in a global plasma "reheat."

With further conditioning of the beams and vacuum vessel (via titanium gettering), a limited number of discharges was obtained in the second mode, with "noncollapsing" target plasmas. The addition of ICRH appears to result in a modest increase in heating for these discharges for the initial portion of the rf pulse, but it also seems to accelerate the collapse of the stored energy. This earlier collapse is probably the result of impurities (increased titanium radiation is measured) entering the plasma after being sputtered from the vessel walls because of the rf heating of the edge plasma. Because of the limitations on ATF operating time, the antennas could not be adequately conditioned for high-power operation. It is expected, on the basis of results from other devices, that significant heating will occur once the impurity level is reduced by conditioning the antenna and vacuum vessel with high-power rf.

ECH systems

T. S. Bigelow, C. R. Schaich, J. B. Wilgen, J. A. White, T. L. White, M. Sato,* and S. Kubo*

Significant progress was made with the ECH system on the ATF stellarator in 1990 and 1991. Accomplishments include

*National Institute for Fusion Science, Nagoya, Japan.

(1) making a second 200-kW gyrotron system fully operational, (2) upgrading the high-voltage dc power supply to significantly higher power capability, (3) installing a 35-GHz, 200 kW gyrotron system, (4) carrying out detailed measurements and analysis of the launcher performance, and (5) measuring plasma absorption and leakage on ATF. Operation of two gyrotrons at pulse lengths up to 20 s has become routine.

The launcher configuration developed for ATF is shown in Fig. 4.25. This launcher converts the unpolarized TE_{01} input wave from the gyrotron into a polarized beam. The plane of polarization can be rotated arbitrarily by rotating a corrugated-surface twist reflector. The beam is focused slightly to produce a narrow pattern at the plasma edge. Laboratory measurements of the launcher beam were made; a contour plot of the measured pattern is shown in Fig. 4.26. Numerical analysis of the beam pattern indicates that the –20-dB beam efficiency is ~80%, which includes side-lobe and cross-polarized power loss. First-pass absorption of the beam was measured under a variety of conditions, and general agreement with theory is obtained when polarization rotation effects caused by magnetic field shear are included in the model.

The upgrade to the ECH high-voltage dc power supply was completed in preparation for installation of a 106-GHz, high-power gyrotron system to be installed on ATF in collaboration with the Heliotron-E project in Japan. New transformers and rectifiers, obtained from the Mirror Fusion Test Facility (MFTF) project at Lawrence Livermore National Laboratory (LLNL), were installed on ATF as shown in Fig. 4.27. The power supply capability is now –90 kV at 90 A for 30-s pulses and 50 A cw. The upgrade was completed in three months, and the performance of the new system is excellent.

A 35-GHz, 200-kW gyrotron system was also added to ATF to allow experiments with high plasma beta at lower magnetic fields with very long pulse operation and edge heating. A new gyrotron socket was constructed, and a portion of a waveguide transmission system was installed. The gyrotron was obtained from the MFTF project at LLNL. Operation of the tube has been quite successful, although coil problems on ATF limited pulse lengths to 21 s. Researchers from the National Institute for Fusion Science in Japan provided assistance

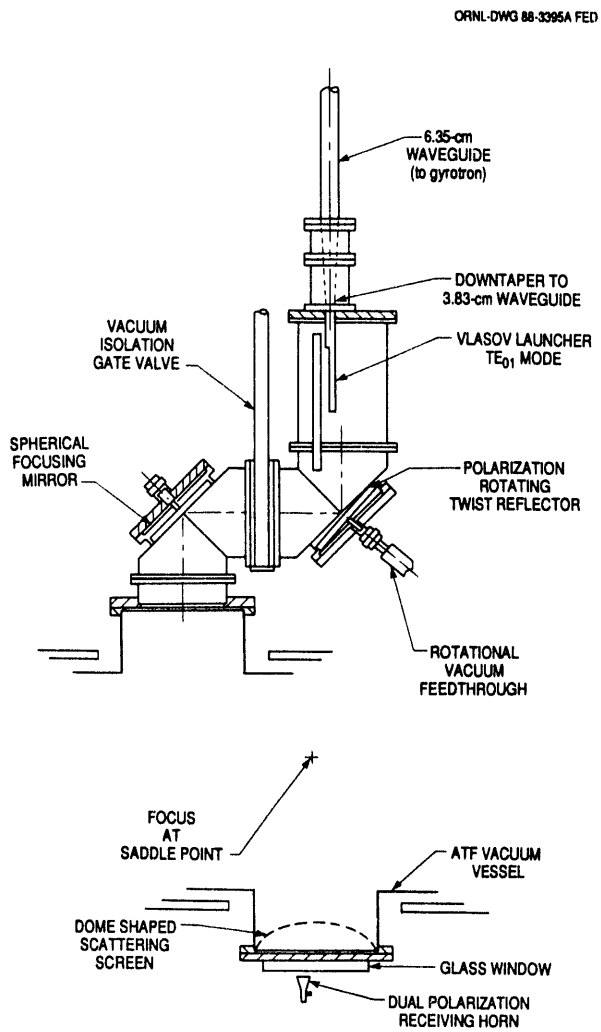

Fig. 4.25 The ATF ECH launcher.

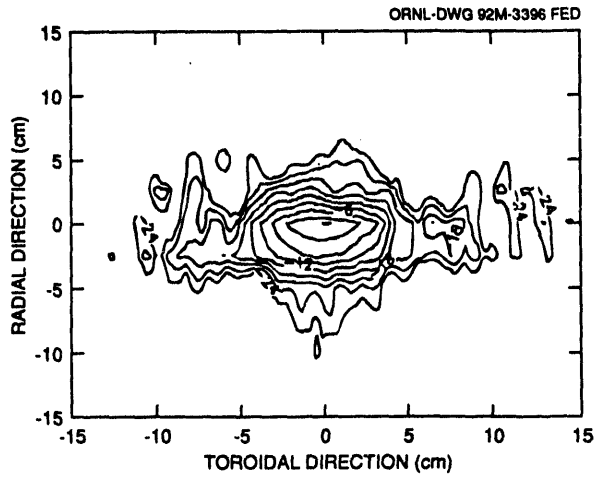

Fig. 4.26. Contour plot of the ATF launcher pattern. Contours indicate –3-dB steps.

in construction of some of the waveguide components and participated in the 35-GHz heating experiments.

4.2.3 RF Modeling

ICRF antennas, Faraday shields, and FWCD launchers for a variety of devices were designed and/or analyzed during the reporting period. Much of this work was done in collaboration with the Plasma Theory Section. Some of the new computational techniques developed during this period are described.

4.2.3.1 Faraday shield loading

A method was developed to calculate the rf power dissipation arising from the eddy currents induced in the Faraday shield of an ICRF antenna.[34] The analyses are performed with magnetostatic codes[35] in two and three dimensions, with all metallic surfaces represented by perfect conductors. Once the current distributions are determined, the

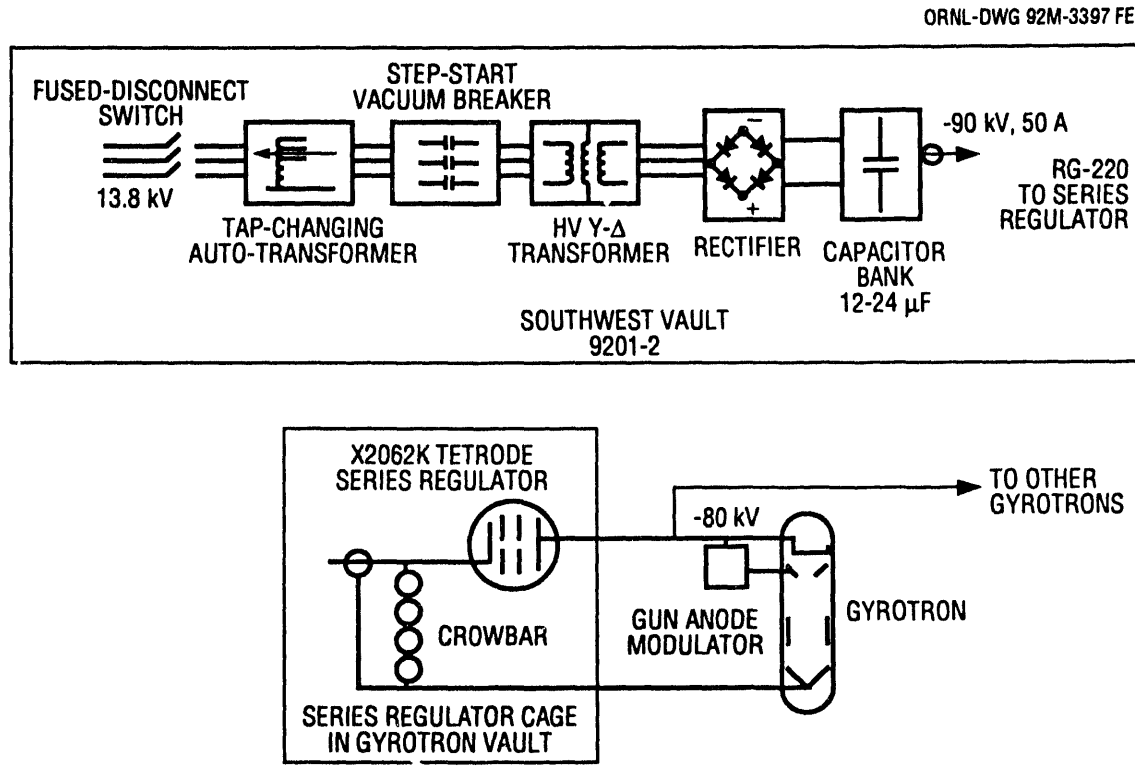

Fig. 4.27. ECH system power supply configuration.

power distributions are calculated by employing a nonzero surface resistance that is a function of the operating frequency and of the conductivity and distribution of the shield materials. The total power dissipated in the shield can be expressed in terms of the strap current as a loss resistance that is in series with the plasma loading resistance. Figure 4.28 compares the calculated and measured loss resistances at 55 MHz for a single-tier Faraday shield consisting of 0.375-in. copper tubes with 0.0625-in. graphite tiles brazed to the front surface. This figure demonstrates the role of the shield geometry in determining the rf losses; the losses increase as the gap between tubes (optical transparency) decreases. The dependences on shield material (electrical resistivity) and operating frequency can be seen in Table 4.3, which compares calculated and measured loss resistances for a fixed shield geometry.

Table 4.3. Comparison of loading measurements and calculations on the ORNL development antenna for different shield materials

Material and resistivity	Loading (mΩ) Calculated	Measured
Copper, 1.673 μΩ•cm		
At 29 MHz	4.44	4.137
At 57 MHz	5.79	5.746
At 81 MHz	6.51	6.227
Stainless steel, 69 μΩ•cm		
At 29 MHz	26.0	25.35
At 57 MHz	33.9	35.21
At 81 MHz	38.2	38.16
Solid graphite, 1340 μΩ•cm		
At 29 MHz	113.9	83.28
At 57 MHz	148.4	136.2
At 81 MHz	167.0	166.3
Half graphite, 1340 μΩ•cm		
At 29 MHz	56.7	43.03
At 57 MHz	74.1	71.96
At 81 MHz	83.5	95.95

4.2.3.2 Septum slotting

Providing slots in the side walls of ICRF antennas is a method of allowing expansion of the current strap's magnetic field distribution, thus downshifting the peaks in the toroidal wave spectrum and increasing the plasma loading. Placing slots in the septa that separate straps in multiple-strap arrays also changes the wave spectrum by redistributing the return currents, at the expense of increasing the interstrap coupling. The effectiveness of such slots is determined by their transparency to magnetic flux, which is a function of slot shape, area, position, thickness, and poloidal periodicity. A method was developed to determine the fields of a slotted side wall/septum antenna over one poloidal field period using the three-dimensional (3-D) magnetostatic code.[36] The mutual inductance, or interstrap coupling, can be calculated from these 3-D fields and used to define an "effective" solid septum that gives the same mutual inductance; this equivalent solid septum can then be used in 2-D codes. Figure 4.29 compares the measurements of the B_z component in front of the antenna with the results of 2-D and 3-D calculations (the 2-D calculation uses a solid septum adjusted to give the same mutual coupling between straps).

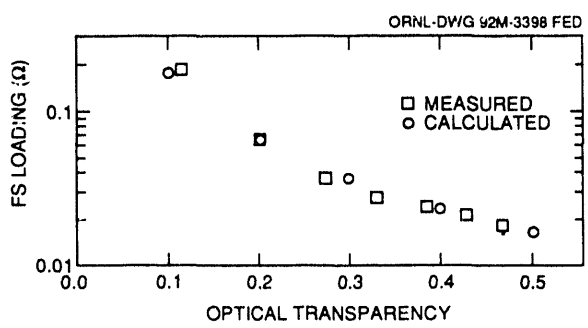

Fig. 4.28. Calculated and measured loading for a single-tier Faraday shield (0.375-in. copper tubes with 180°, 0.0625-in. graphite tiles).

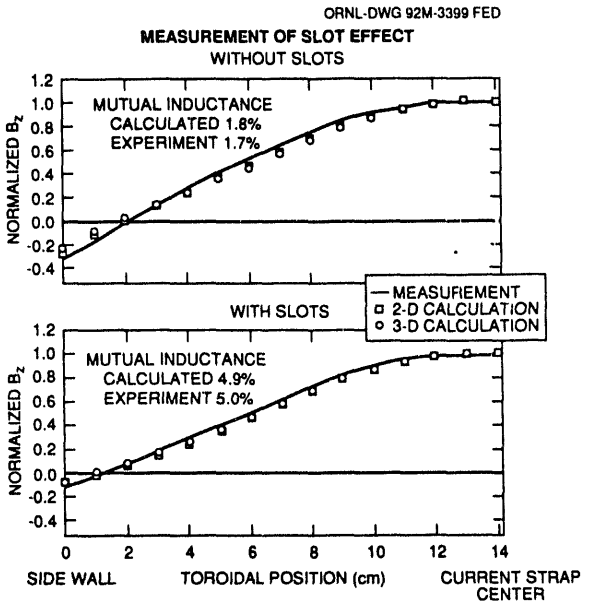

Fig. 4.29. Measured and calculated toroidal magnetic field B_z for an antenna (a) with slots and (b) without slots.

4.2.3.3 Arbitrarily coupled, lossy transmission line antenna model

A transmission line model was developed for modeling the complicated, highly coupled geometry of the JET A_2 antenna array. The scattering matrix, port impedances, and poloidal current distributions on the N straps of the antenna come from the solutions to a set of coupled transmission line equations:

$$\frac{\partial^2 I_i}{\partial x_i^2} = -j\omega C_i'(j\omega L_i' + R_i')I_i(x_i) - \sum_{m=1}^{N} j\omega C_m'(j\omega M_{im}')I_m(x_m) \times \exp\left(-j\frac{\omega}{c}d_{im}\right) + \sum_{m=1}^{N} j\omega K_{im}'(j\omega L_m' + R_m')s_{im}I_m(x_m) \times \exp\left(-j\frac{\omega}{c}d_{im}\right),$$

where I_i is the current in strap i; C_i' is the capacitance to ground per unit length of strap i; L_i' is the self-inductance per unit length of strap i; R_i' is the resistance per unit length of strap i (plasma loading); M_{im}' is the mutual inductance (positive or negative) per unit length between current position on strap i and the appropriate position on strap m (note: m can equal i, indicating self-coupling to another position on the same strap); K_{im}' is the mutual capacitance per unit length between current position on strap i and the appropriate position on strap m; x_i is the present position along strap i, referenced to the ground point of i; x_m is the appropriate position along strap m, referenced to the ground point of i, to which current at x_i couples; d_{im} is the distance from strap i to strap m (phase lag effect); and s_{im} is the direction of x_m compared to x_i (if $s_{im} = +1$, then x_m increases with increasing x_i; if $s_{im} = -1$, then x_m decreases with increasing x_i).

The input conditions specify the magnitude and phase of the current at the ground point of one of the pair of parallel straps. The magnitude (and, if necessary, the phase) of the current at the ground point of the other strap is adjusted so that the voltages (magnitude and phase) match at the mutual feed point (i.e., the input port). Typically, the magnitudes of the ground point currents of all the upper straps are held fixed, while those of the lower straps are allowed to adjust themselves; this convention is arbitrary. The input inductance and capacitance matrices are calculated with the 2-D and 3-D magnetostatic codes. This model is being tested and refined by comparison with detailed measurements carried out with a JET A_2 mock-up antenna.

REFERENCES

1. C. A. Foster et al., "Electron-Beam Rocket Pellet Accelerator," presented at the International Pellet Fueling Workshop, La Jolla, California, October 30–November 3, 1985.

2. C. A. Foster et al., "The ORNL/Tore Supra Pellet Injector and The E-Beam Rocket Pellet Accelerator," p. 275 in *Pellet Injection and Toroidal Confinement: Proceedings of the IAEA Technical Committee Meeting, Gut Ising, Germany, October 24–26, 1988*, IAEA-TECDOC-534, International Atomic Energy Agency, Vienna, 1989.

3. C. C. Tsai, C. A. Foster, and D. E. Schechter, "Characteristics of Electron-Beam-Rocket Pellet Accelerator," pp. 1230–35 in *Proceedings of the IEEE 13th Symposium on Fusion Engineering, Knoxville, 1989*, Vol. 2, Institute of Electrical and Electronics Engineers, New York, 1990.

4. C. C. Tsai et al., "Characteristics of an Electron-Beam-Rocket Pellet Accelerator," pp. 724–8 in *Proceedings of the 14th IEEE/NPSS Symposium on Fusion Engineering, Monterey, 1991*, Vol. 2, Institute of Electrical and Electronics Engineers, New York, 1991.

5. S. K. Combs et al., "Eight-Shot Pneumatic Pellet Injection System for the Tokamak Fusion Test Reactor," *Rev. Sci. Instrum.* **58**, 1195 (1987).

6. P. W. Fisher, D. T. Fehling, M. J. Gouge, and S. L. Milora, "Tritium Proof-of-Principle Pellet Injector Results," p. 1236 in *Proceedings of the 13th Symposium on Fusion Engineering, Knoxville, TN, October 2–6, 1989*, Vol. 2, Institute of Electrical and Electronics Engineers, New York, 1990.

7. D. D. Schuresko et al., "Simplified Eight-Shot Pneumatic Pellet Injector for Plasma Fueling Applications on the Princeton Beta Experiment and on the Advanced Toroidal Facility," *J. Vac. Sci. Technol. A* **7**, 949 (1989).

8. A. L. Qualls et al., "Eight-Shot Pneumatic Pellet Injector for the Advanced Toroidal Facility," p. 1244 in *Proceedings of the 13th Symposium on Fusion Engineering, Knoxville, TN, October 2–6, 1989*, Vol. 2, Institute of Electrical and Electronics Engineers, New York, 1990.

9. S. K. Combs, C. R. Foust, M. J. Gouge, and S. L. Milora, "Acceleration of Small, Light Projectiles (including Hydrogen Isotopes) to High Speeds using a Two-Stage Light Gas Gun," *J. Vac. Sci. Technol. A* **8**, 1814 (1990).

10. A. Reggiori et al., "Solid Deuterium Pellet Injection with a Two-Stage Pneumatic Gun," *J. Vac. Sci. Technol. A* **7**, 959 (1989).

11. A. E. Seigel, *The Theory of High Speed Guns*, AGARDograph-91, NATO-AGARD Fluid Dynamics Panel, May 1965.

12. S. K. Combs, "Two-stage light gas gun," pp. 98–103 in *Fusion Energy Division Annual Progress Report for Period Ending December 31, 1989*, ORNL-6624, Martin Marietta Energy Systems, Inc., Oak Ridge National Laboratory, July 1991.

13. S. K. Combs et al., "A Three-Barrel Repeating Pneumatic Pellet Injector for Plasma Fueling of the Joint European Torus," *J. Vac. Sci. Technol. A* **6** (3), 1901 (1988).

14. M. J. Gouge et al., "ITER Pellet Fueling System: Conceptual Design and Description," presented at the International Thermonuclear Experimental Reactor Fuel Cycle Meeting, Garching, Germany, February 1990 (on file as ITER Document IL-FC3.2-0-12 with the ITER Conceptual Design Activity, Garching, Federal Republic of Germany).

15. S. K. Combs et al., "Development of a Two-Stage Light Gas Gun to Accelerate Hydorgen Pellets to High Speeds for Plasma Fueling Applications," *J. Vac. Sci. Technol. A* **7** (3), 963 (1989).

16. M. J. Gouge et al., "Pellet Injector Development at ORNL," p. 675 in *Fusion Technology 1990: Proceedings of the 16th Symposium on Fusion Technology, London, 1990*, Vol. 1, ed. B. E. Keen, M. Huguet, and R. Hemsworth, North-Holland, Amsterdam, 1991.

17. S. K. Combs, S. L. Milora, and C. R. Foust, "Simple Pipe Gun for Hydrogen Pellet Injection," *Rev. Sci. Instrum.* **57** (10), 2636 (1986).

18. M. J. Gouge et al., "Design Considerations for Single-Stage and Two-Stage Pneumatic Pellet Injectors," *Rev. Sci. Instrum.* **60**, 570 (1989).

19. S. L. Milora, S. K. Combs, M. J. Gouge, and R. W. Kincaid, *QUICKGUN: An Algorithm for Estimating the Performance of Two-Stage Light Gas Guns*, ORNL/TM-11561, Martin Marietta Energy Systems, Inc., Oak Ridge National Laboratory, September 1990.

20. S. K. Combs et al., "Repetitive Two-Stage Light Gas Gun for High-Speed Pellet Injection," *Rev. Sci. Instrum.* **62**, 1978 (1991).

21. S. L. Milora et al., "Design of a Tritium Pellet Injector for TFTR," pp. 716–20 in *Proceedings of the IEEE/NPSS 14th Symposium on Fusion Engineering, Monterey, 1991*, Vol. 2, Institute of Electrical and Electronics Engineers, New York, 1991.

22. S. K. Combs et al., "Performance of a Pneumatic Hydrogen-Pellet Injection System on the Joint European Torus," *Rev. Sci. Instrum.* **60** (8), 2697 (1989).

23. L. A. Charlton et al., "Theoretical Analysis of the Role of the Infernal Mode in the Stability of Peaked Pressure Profiles in Pellet Fuelled JET Discharges," *Nucl. Fusion* **31**, 1835 (1991).

24. L. R. Baylor et al., "Particle Transport in Pellet Fuelled JET Plasmas," *Nucl. Fusion* **31**, 1249 (1991).

25. W. A. Houlberg et al., "Pellet Penetration Experiments on JET," submitted to *Nucl. Fusion* (1992).

26. A. Grosman et al., "Plasma Edge Control in TORE SUPRA," *Plasma Phys. Controlled Fusion* **32**, 1011–27 (1990).

27. A. Grosman et al., "Density Control in TORE SUPRA with Ergodic Divertor and Multi-Pellet Injection," pp. 317–20 in *18th EPS Conference on Controlled Fusion and Plasma Physics, Berlin, 3–7 June 1991: Contributed Papers, Part 1*, European Physical Society, Petit-Lancy, Switzerland, 1991 [*Europhys. Conf. Abstr.* **15C**, Pt. 1, 317–20 (1991)].

28. R. H. Goulding et al., "Design and Performance of Fast Wave Current Drive Systems in the ICRF," p. 287 in *Radio Frequency Power in Plasmas: Proceedings of the 9th Topical Conference, Charleston, South Carolina, August 19–21, 1991*, ed. D. B. Batchelor, American Institute of Physics, New York, 1992 [*AIP Conf. Proc.* **244**, 287 (1992)].

29. R. Lobel et al., "ICRF Antennae for the JET Pumped Divertor Configuration," p. 1104 in *Fusion Technology 1990: Proceedings of the 16th Symposium on Fusion Technology, London, 1990*, Vol. 2, ed. B. E. Keen, M. Huguet, and R. Hemsworth, North-Holland, Amsterdam, 1991.

30. T. Wade et al., "High Power (22 MW) ICRH at JET and Developments for Next Step Devices," pp. 902–7 in *Proceedings of the IEEE/NPSS 14th Symposium on Fusion Engineering, Monterey, 1991*, Vol. 2, Institute of Electrical and Electronics Engineers, New York, 1991.

31. T. D. Shepard, F. W. Baity, and D. J. Hoffman, "Faraday shield studies," pp. 108–10 in *Fusion Energy Division Annual Progress Report for Period Ending December 31, 1989*, ORNL-6624, Martin Marietta Energy Systems, Inc., Oak Ridge National Laboratory, July 1991.

32. D. J. Hoffman et al., "The Design of High-Power ICRF Antennas for TFTR and Tore Supra," p. 302 in *Applications of Radio-Frequency Power to Plasmas*, ed. S. Bernabei and R. W. Motley, American Institute of Physics, New York, 1987 [*AIP Conf. Proc.* **159**, 302 (1987)].

33. J. R. Wilson et al., "TFTR ICRF Antenna Design," pp. 294–7 in *Applications of Radio-Frequency Power to Plasmas*, ed. S. Bernabei and R. W. Motley, American Institute of Physics, New York, 1987 [*AIP Conf. Proc.* **159**, 294–7 (1987)].

34. P. M. Ryan et al., "Calculation of RF Power Dissipation in Faraday Shield Elements," p. 310 in *Radio Frequency Power in Plasmas: Proceedings of the 9th Topical Conference, Charleston, South Carolina, August 19–21, 1991*, ed. D. B. Batchelor, American Institute of Physics, New York, 1992 [*AIP Conf. Proc.* **244**, 310 (1992)].

35. P. M. Ryan et al., "Determination of ICRF Antenna Fields in the Vicinity of a 3-D Faraday Shield Structure," *Fusion Eng. Des.* **12**, 37 (1990).

36. P. M. Ryan et al., "The Effect of Realistic Antenna Geometry on Plasma Loading Predictions," p. 309 in *18th EPS Conference on Controlled Fusion and Plasma Physics, Berlin, 3–7 June 1991: Contributed Papers, Part 3*, European Physical Society, Petit-Lancy, Switzerland, 1991 [*Europhys. Conf. Abstr.* **15C**, Pt. 3, 309 (1991)].

5

ADVANCED SYSTEMS PROGRAM

T. E. Shannon[1]

C. C. Baker
T. W. Burgess[2]
D. L. Conner[1]
F. C. Davis[1]
E. G. Elliott[3]
B. R. Everman[1]
C. A. Flanagan[1]
P. J. Fogarty[1]
J. D. Galambos[4]
P. L. Goranson[1]
M. J. Gouge[5]
J. N. Herndon[6]
T. J. Herrick[1]
J. T. Hogan[7]
M. J. Hollis[1]
W. A. Houlberg[7]
H. W. Jernigan
G. H. Jones[1]
D. C. Lousteau
T. J. McManamy[1]
J. F. Monday[1]
G. H. Neilson
B. E. Nelson[1]
Y-K. M. Peng
B. W. Riemer[1]
R. O. Sayer[4]
D. J. Strickler[4]
D. W. Swain
N. A. Uckan
D. E. Williamson[1]
J. J. Yugo[4]

1. Engineering Division, Martin Marietta Energy Systems, Inc.
2. Robotics and Process Systems Division.
3. Section secretary.
4. Computing and Telecommunications Division, Martin Marietta Energy Systems, Inc.
5. Plasma Technology Section.
6. Robotics and Process Systems Division.
7. Plasma Theory Section.

5. ADVANCED SYSTEMS PROGRAM

Summary of Activities

The Advanced Systems Program serves as the focal point for design studies for future fusion experiments. The Fusion Engineering Design Center is the major engineering resource for the program. During 1990 and 1991, activities in the Advanced Systems Program included the International Thermonuclear Experimental Reactor (ITER); the Burning Plasma Experiment (BPX); a Steady-State Advanced Tokamak (SSAT) with resistive, demountable coils, designated SSAT-D; the Advanced Reactor Innovation and Evaluation Study (ARIES); a small, steady-state tokamak (triple-S tokamak, or TST) for integrated divertor testing; and support for systems code development and application.

The three-year Conceptual Design Activity (CDA) phase of the ITER program, an international program for cooperation on the design of a fusion test reactor, was completed in December 1990. The CDA established a reactor configuration as the basis for the next project phase, the Engineering Design Activity (EDA), scheduled to start in late FY 1992. The CDA also established a five-year research and development (R&D) plan for the major reactor systems to be conducted in conjunction with the design activities during the EDA. ORNL was a major participant in the ITER physics, engineering design, and R&D activities at the national and international levels.

The BPX project, led by Princeton Plasma Physics Laboratory (PPPL), was directed toward developing a lower cost successor to the Compact Ignition Tokamak (CIT). ORNL served as a major partner in the project, with design and R&D responsibility for remote maintenance, vacuum system and thermal shield design, rf heating, and pellet injection. Design Center staff also carried out calculations of plasma shape control and plasma disruptions in collaboration with PPPL. The BPX project was cancelled in September 1991.

The mission of the SSAT is to demonstrate integrated steady-state operating modes characterized by a noninductively driven plasma current, a high power density, an actively cooled and actively pumped divertor, and disruption-free operation. In addition, this device would provide a database on physics regimes that could be extrapolated to a more attractive fusion reactor than that projected by the present database. The design concept for an SSAT with resistive, demountable coils, identified as SSAT-D, was developed in a design study initiated in fall 1991 to determine whether the SSAT mission could be accomplished in a facility with a moderate capital cost (near $400 million) sited in the present Tokamak Fusion Test Reactor (TFTR) facility at PPPL and making maximum use of available TFTR assets. Design Center staff developed both a configuration with a major radius $R_0 = 2.25$ m and an alternative configuration with $R_0 = 1.5$ m.

As part of the ARIES program, a D-^{3}He-fueled tokamak reactor, ARIES-III, was designed. Key features of this reactor include a standard aspect ratio, high poloidal beta, and dominant bootstrap currents (approximately equal to the plasma current). Potential advantages include high beta, which contributes to reducing the size and magnetic field of a fusion reactor, and modest current drive requirements, which reduce the recirculating power needed to maintain the plasma current in steady state.

The design study for the TST addressed the need for development of divertors and the associated plasma power and particle handling. These systems will be required for ITER and for all large, steady-state tokamaks that are driven with high auxiliary power. The TST, which could fulfil this R&D need in the near term, relies only on the physics and technology data of existing small to medium-size tokamaks and uses the facilities and equipment available at a typical fusion research institution such as ORNL.

In the systems code area, final development of the TETRA (Tokamak Engineering Test Reactor Analysis) code was completed, and the code was applied to the ITER CDA concept. In an effort led by Lawrence Livermore National Laboratory, a new code, called the Supercode, was created. The Supercode was applied to the conceptualization of the SSAT.

5.1 ITER

N. A. Uckan, D. C. Lousteau, C. C. Baker, D. L. Conner, F. C. Davis, B. R. Everman, C. A. Flanagan, P. J. Fogarty, J. D. Galambos, P. L. Goranson, M. J. Gouge, J. N. Herndon, T. J. Herrick, J. T. Hogan, M. J. Hollis, W. A. Houlberg, G. H. Jones, B. E. Nelson, B. W. Riemer, R. O. Sayer, D. W. Swain, D. E. Williamson, and J. J. Yugo

The International Thermonuclear Experimental Reactor (ITER) program was prompted by international agreements in 1986 for cooperation on the design of a fusion test reactor. The three-year joint Conceptual Design Activity (CDA) carried out by the United States, the European Community, Japan, and the former Soviet Union was successfully completed in December 1990. The CDA established a reactor configuration, agreed on by the four parties, as the basis for the next project phase, the Engineering Design Activity (EDA), scheduled to start in late FY 1992. The CDA also established a five-year research and development (R&D) plan for the major reactor systems to be conducted in conjunction with the design activities during the EDA.

In the period between the completion of the CDA and the start of the EDA, work was performed by the U.S. Home Team in order to provide continuity to the project by (1) answering technical questions identified either by the international team during the CDA or during reviews of the CDA conducted within the United States and (2) assessing modifications to the CDA design resulting from systems optimization studies conducted within the United States. In the latter category, a high-aspect-ratio design (HARD) option was identified and characterized.

ORNL was a major participant in the ITER physics, engineering design, and R&D activities at the national and international levels. In physics, ORNL was active in the areas of confinement, operational limits,

alpha particle physics, fueling, rf heating and current drive, disruptions, and physics R&D. ORNL led the U.S. design efforts in remote handling, containment structures, electromagnetic analysis, configuration integration, and fueling. In addition, ORNL was responsible for specific components of the rf heating system, the blankets, and the divertors and for performing systems-level trade studies. At the international level, ORNL supplied full- and part-time participants to the four-party joint working team at Garching, Germany, in facility design, reliability/availability analysis, and cost estimating in addition to the physics and engineering areas previously listed. In addition to ITER-specific R&D in fueling, materials, and ion cyclotron range of frequencies (ICRF) heating discussed in Sect. 4 of this report, plans were drawn for new R&D programs at ORNL in remote handling and containment structures in response to direct project needs identified during the CDA.

5.1.1 Physics Studies

N. A. Uckan, J. T. Hogan, W. A. Houlberg, R. O. Sayer, and D. W. Swain

5.1.1.1 Confinement and plasma performance

Confinement capability

We have examined the confinement capability of the ITER CDA design for a number of operational scenarios. The reference ITER CDA physics baseline scenario (I_p = 22 MA) allows ignited burn under H-mode conditions [τ_E(H-mode) ~ 2 × $\tau_E^{ITER89\text{-}P}$(L-mode)]. At the higher plasma currents (I_p = 25–28 MA) at which ITER can operate for limited pulse durations, there is an increased ignition margin if low-q operation proves acceptable. A reduction of about a factor of 2 in helium ash concentration (from the baseline value of 10% to 5%) in the reference ITER CDA scenario has about the same impact on ignition capability as increasing the plasma current by about 15% (from the baseline value of 22 MA to ≥25 MA). It might be possible to further optimize the ignition capability of ITER if some of the limits on operational boundaries can be relaxed by tailoring plasma profiles.

1 ½-D transport studies

We have used the time-dependent, one-and-one-half-dimensional (1 ½-D) WHIST transport code to examine two reference operational scenarios for the ITER CDA design: an ignition scenario (22 MA, τ_E ~ 2 × $\tau_E^{ITER89\text{-}P}$ with 30 MW of ICRF heating) and a long-pulse scenario (15.4 MA, τ_E ~ 1.2 × $\tau_E^{ITER89\text{-}P}$ with 75 MW of neutral beam heating for current drive). Plasma profiles were evaluated self-consistently from the source profiles and radially dependent transport properties. Among the time-dependent issues addressed were the time scales for startup and shutdown as determined by current profile relaxation rates (skin times), fueling and particle pumping rates, and auxiliary heating and current drive sources. Operational constraints were monitored throughout the simulations: β (toroidal and poloidal), l_i, line-average electron density n_e, $n_e(a)$, etc. In general, the simulations confirmed the consistency of the reference ignition and long-pulse scenarios as initially determined from global models. It was observed that simultaneously keeping the density below empirical limits and precipitating a thermal quench so that the current in the center of the plasma can resistively decay may not be easy with only particle pumping and toroidal current control. Longer ramp-down times and impurity pellet injection may be needed.

Physics R&D assessment

We have analyzed the ranges of confinement-relevant (dimensional and dimensionless) plasma parameters for the major tokamaks—including the Joint European Torus (JET), JT-60U, the Tokamak Fusion Test Reactor (TFTR), and DIII-D—that are expected to contribute to the ITER physics R&D in the 1990s to characterize confinement and plasma performance in ITER-like designs. We found that the largest tokamaks (JET, JT-60U) should be able to demonstrate H-mode operation [with edge-localized modes (ELMs), as in ITER] with $n\tau_E T_i$ values within an order of magnitude of those required in ITER and should have relevant dimensionless plasma parameters (ρ/a, $\nu*$, etc.) within a factor of 2 of those in ITER. Extrapolations from dimensionally similar discharges in DIII-D and JET show high-Q/ignition operation in ITER-like plasmas at plasma currents (~16 MA) well below the nominal (22-MA) design value. Another critical issue for achieving ignition-level plasma performance is the anomalous alpha particle effects, mainly the toroidal Alfvén eigenmode (TAE mode). The deuterium-tritium (D-T) experiments in TFTR and JET (and simulations using fast beam ions) should realize alpha particle (fast-ion) parameters roughly similar, in relation to TAE mode thresholds, to those projected for ITER.

Alpha particle studies

We have examined the TAE instabilities for the beam current drive scenario of the ITER CDA technology phase. The TAE/FL initial value code was applied for ITER parameters and profiles obtained from ITER transport simulations. Unstable regimes were found, and sensitivities to the fast ion density profile shape, density, and toroidal mode number were examined.

5.1.1.2 Physics basis and guidelines

ORNL was responsible for preparing and compiling the ITER physics design guidelines during the ITER CDA.[1] The U.S. studies during the period 1990–91 have indicated that there may be significant benefits in moving the ITER CDA design point from the low-aspect-ratio, high-current baseline (A = 2.79, I = 22 MA) to a high-aspect-ratio machine at A ~ 4, I ~ 15 MA, especially in terms of steady-state technology testing performance. To assess the physics and technology testing capability of design options at higher aspect ratios, several changes were proposed to the original ITER guidelines to reflect the latest (although limited) developments in physics understanding at higher aspect ratios. These changes were compiled and published in ref. 2. The critical issues for design options with higher aspect ratios include the uncertainty in the scaling of confinement with aspect ratio, the variation of vertical stability with elongation and aspect ratio, plasma shaping requirements, the ability to control and maintain plasma current and q profiles for magneto-hydrodynamic (MHD) stability (and volt-second consumption), access for current drive, and restrictions on field ripple and divertor plate incident angles.

5.1.1.3 Operational limits

MHD stability considerations at high aspect ratio

We have carried out global MHD stability calculations using the PEST code as part of the U.S. ITER Team's HARD study. Approximately 15,000 cases were evaluated for both global and local (ballooning) modes. In addition to the aspect ratio

variations ($2.78 < A < 5$), a range of plasma shapes ($1.5 < \kappa < 2$, $0 < \delta < 0.6$) was examined, and the safety factor was varied: $1.05 < q(0) < 1.85$ and $1.85 < q_\psi(95\%) < 4.55$. For global aspect ratio scaling, these results show no significant increase or decrease in the maximum Troyon parameter (g^{max}) within the level of variation imposed by profile differences: the scaling of g^{max} is found to be independent of A if optimal profiles are considered at each aspect ratio. There is some reduction in g^{max} as A increases for $q_\psi < 3.2$, but g^{max} is still ~2.5 for $A = 5$ at low q, and $g^{max} \sim 3$–3.5 is obtained for $3.2 < q_\psi < 4.5$. Specific results for the HARD configuration ($A = 4$, $\kappa = 2$, $\delta = 0.4$, $q_\psi = 3.1, 4$) show that the required g can be obtained with values of $l_i(3) \approx 0.65$–0.85 in both the ignition and steady-state phases.

Density limit

We have constructed a database of results from the B2 edge transport code in order to extract scaling relations for divertor parameters and edge density limit. Approximately 1500 database entries have been made for a range of separatrix boundary conditions and scrape-off layer (SOL) geometries. Divertor results have been compared with scaling relations derived from the Next European Torus (NET)/ITER Team's Harrison-Kukushkin-Hotston global model and the NET Team's results of a similar B2 database for the ITER CDA parameters. These results were also used for a preliminary comparison of density limit scaling with the Borrass model.

5.1.1.4 Plasma disruption modeling

We have used the Tokamak Simulation Code[3] (TSC) to model ITER CDA physics phase disruptive episodes to predict the evolution of plasma motion, current decay, and forces. Vertically moving, disrupting plasmas with and without a surrounding halo have been modeled. Before thermal quench, the plasma drifted vertically as much as 1.0 m off midplane. Initial plasma parameters were $I_p = 22$ MA, $\beta = 5.6\%$, $\beta_{pol} = 0.47$, $R_0 = 6.01$ m, $a = 2.06$ m, and $\kappa_{95} = 1.81$. In the TSC model, a low-density, low-temperature "halo" region is located outside the main plasma. In this region, force-free currents may flow along open field lines, intersect conductors, flow along minimum impedance paths, and return to the halo plasma. For the halo simulation the temperature was 2.0 eV, and the halo extent corresponded to 40% of the initial poloidal flux.

The plasma halo retards plasma vertical motion and current decay. The maximum vertical velocity was 400 m/s, compared with 700–1700 m/s for no-halo simulations. Dramatic changes in the time evolution and spatial distribution of in-vessel component loads are produced by large poloidal currents flowing between the plasma halo and first wall conductors. The extreme net vessel vertical force reverses sign and becomes much smaller in magnitude for the halo case, in part because of slowing of vertical plasma motion by the halo and in part because of large poloidal currents in the bottom of the vessel. Because continuous poloidal current paths connect in-vessel components, more severe load distributions are found for the halo case. Although poloidal segmentation would mitigate the inductive transfer of poloidal current from the plasma to in-vessel structures, conductive poloidal transfer would still produce sizable forces. Further investigation is needed to determine optimum configurations of connecting elements to minimize such effects.

5.1.1.5 Reports of work

Members of the ITER physics team from each ITER partner completed the collection,

summarization, and distribution of reports of work done from October 1990 through November 1991. These contributions were collected by the ITER Home Teams as part of the Home Team activities between the end of the ITER CDA and the beginning of the ITER EDA. In the United States, the reports were collected at ORNL, and ORNL has been responsible for coordinating the summarization process and for distributing the summary and R&D reports. During this reporting period, most of the experiments in the United States and Europe, as well as some from the Commonwealth of Independent States, submitted reports. No reports were obtained from JET or from Japan.

5.1.2 Engineering Design

D. C. Lousteau, B. E. Nelson, F. C. Davis, P. L. Goranson, D. L. Conner, D. E. Williamson, M. J. Hollis, T. J. Herrick, J. N. Herndon, B. W. Riemer, J. J. Yugo, J. D. Galambos, R. O. Sayer, P. J. Fogarty, G. H. Jones, and B. R. Everman

5.1.2.1 Systems analysis

Systems analysis for ITER consisted primarily of defining operational scenarios and of carrying out scoping studies for alternative devices. The nominal CDA operational scenarios for technology testing were defined through systems analysis, which balanced the current drive, divertor heat load, confinement, and beta issues. The divertor heat load issue proved to be especially difficult for technology testing. Two primary modes of technology testing were identified: hybrid operation, which uses a combination of inductive and noninductive current drive, and steady-state operation, which uses only noninductive current drive. Higher plasma density and wall loads can be attained with hybrid operation than with steady-state operation, and an acceptable divertor heat load can be maintained.

Overall device parametric studies showed that, in comparison with the CDA, the HARD has more favorable technology testing capabilities and a similar ignition probability (with the ITER-89 Power scaling). This result prompted the U.S. team to investigate the details of the HARD (see Sect 5.1.2.7). Other trade studies involved scoping the European (NET) proposed changes to the CDA.

5.1.2.2 Plasma disruption and electromagnetic effects

ITER is a tokamak with a major radius of 6 m, requiring a plasma current of 22 MA. It employs a dual vacuum region formed by a toroidal vacuum vessel contained within a cylindrical outer tank. The interior vessel must not only contain the gases required for plasma operation but also mechanically support reactor components located in its interior. Instabilities can lead to plasma disruptions and an accompanying rapid loss of plasma current. When this occurs, eddy currents are induced in surfaces close to the plasma. In combination with the existing magnetic fields, the currents produce large forces. A significant effort at ORNL has been directed toward accurately characterizing these loads and incorporating them into the design process for the individual components and their mounting system.

TSC has been used to model the interaction of the plasma motion and current decay with the conducting surfaces, in a self-consistent manner, to yield the time evolution of plasma parameters and poloidal flux. EddyCuFF, a code developed for use on fusion projects, is used to calculate the resulting eddy currents and forces in the reactor components. A finite element code is then used to analyze the resulting stresses and evaluate the reaction loads at the

required interfaces. TSC can also be used to study the sensitivity of the forces to the current decay time and to various initial conditions to determine the disruption scenario that produces the most severe loads.

Figure 5.1 shows how these codes are used to determine and analyze these effects in a typical in-vessel blanket/shield module. The plasma motion induces three-dimensional (3-D) field effects in the module [see Fig. 5.1(a)]; these effects result in the eddy current patterns shown in Fig. 5.1(b) and the load pattern in Fig. 5.1(c). Finite element stress analysis programs are then applied to determine the resulting stress and deflections in the modules, which are shown in Fig. 5.1(d).

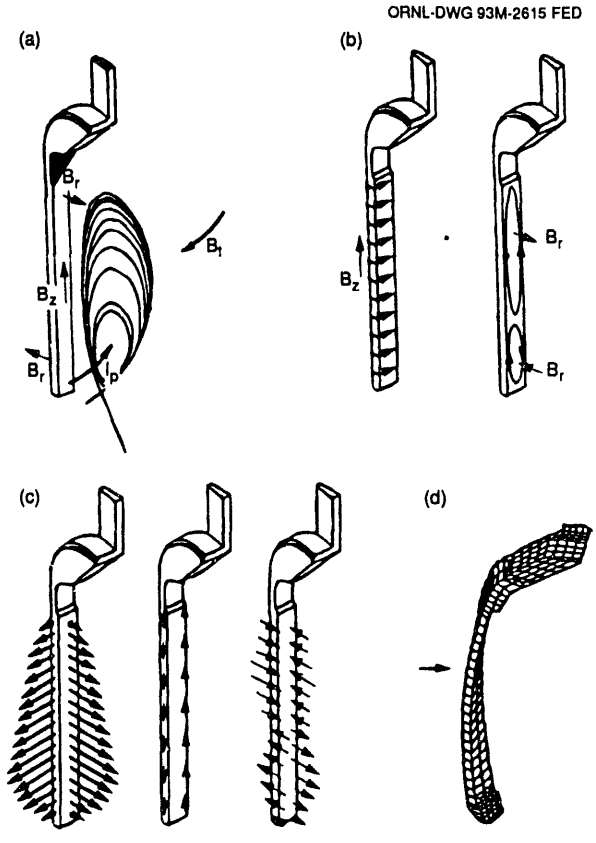

Fig. 5.1. Plasma disruption effects on in-vessel blanket/shield modules. (a) Blanket/shield module and plasma. (b) Currents induced in modules by plasma motion. (c) Force components resulting from induced currents. (d) Deflection and stress contours.

5.1.2.3 Pellet fueling system

ITER will use an advanced, high-velocity pellet injection system to achieve and maintain ignited plasmas. Three pellet injectors are proposed. For ramp-up to ignition, a highly reliable, moderate-velocity single-stage pneumatic injector (1–1.5 km/s) and a high-velocity two-stage pneumatic injector (1.5–5 km/s), using frozen hydrogenic pellets encased in sabots, will be used. For the steady-state burn phase, a continuous, single-stage pneumatic injector (or, alternatively, a centrifuge pellet injector) is proposed. This injector will provide a flexible fueling source beyond the edge region to aid in decoupling the edge region (constrained by divertor requirements) from the high-temperature burning plasma.

All three pellet injectors are designed for operation with a variable ratio of tritium and deuterium feed gases. Table 5.1 lists the parameters of the two moderate-velocity single-stage light gas gun injectors and the high-velocity two-stage light gas gun injector.

The largest pellet (7.4 mm in diameter) results in a 15% perturbation to an ITER plasma at an average ion density of 1.2×10^{20} m^{-3}. Thus, during the density ramp-up, the smaller (5-mm-diam) pellets will be first injected into ITER at a constantly increasing repetition rate. As the plasma density becomes high enough, a transition will be made to the larger 7.4-mm-diam pellets with velocities in the range from 1 to 5 km/s at a lower repetition rate. The larger pellets will penetrate farther into the plasma and provide more control on the evolving density profile as the plasma temperature increases. The moderate-velocity injector will be used for continuous fueling well beyond the edge region during the extended burn phase.

Table 5.1. Pellet injector parameters

	Moderate-velocity injectors	High-velocity injector
Pellet speed, km/s	1–1.5	1.5–5.0
Barrel diameter, mm	5.6, 8.3[a]	9.0[b]
Pellet type[c]	H, D, T, D-T	H, D, T, D-T
Pellet species	Nominal 50-50 D-T, variable to 20-80 D-T, 80-20 D-T, pure D, pure T	Nominal 50-50 D-T, variable to 20-80 D-T, 80-20 D-T, pure D, pure T
Repetition rate, Hz	0–5	0–2
Total number of pellets		
During ramp-up	30	30
During burn phase	Continuous	Continuous (goal)
Availability,[d] %	96	94
Reliability,[e] %	99	95

[a]Barrel diameter accounts for radial growth to compensate for erosion loss in barrel; two pellet sizes obtained through two separate light gas gun assemblies in common enclosure.
[b]Barrel diameter accounts for 2.0-mm radial growth for sabot; variable pellet size obtained through sabot design (wall thickness).
[c]H: hydrogen, D: deuterium, T: tritium.
[d]Achieved through pellet injector and support component redundancy.
[e]Achieved through sound design, prototyping, and missed pellet compensation system.

The moderate-velocity pellet injector design is similar to the JET pneumatic pellet injector and consists of two single-stage light gas guns in a common vacuum enclosure. (As noted, a centrifuge injector could be used instead to provide continuous plasma fueling just beyond the separatrix.) The high-velocity pellet injector is based on the two-stage light gas gun concept, in which a piston is pneumatically accelerated in a high-pressure pump tube and provides adiabatic compression of a second stage of propellant gas between the piston and the pellet/sabot. The resulting high pressures (up to 6000 bar) and, more importantly, high temperatures (4000–8000 K) can accelerate the pellet/sabot payload to muzzle velocities in the 4- to 5-km/s range. For the pellet/sabot combinations used for ITER, the accelerated mass is usually less than 0.5 g, and the mass per unit area is less than 0.75 g/cm^2. This permits consideration of repetitive operation, because the pump tube conditions are moderate enough to allow multiple shots with a single piston. The sabots are separated from the hydrogenic pellets in the injection line to the torus and allowed to hit a ruggedly designed target plate. Two-stage light gas gun pellet injectors are under development at ORNL (see Sect. 4) and in Europe.

A plan view of the pellet injector installation is shown in Fig. 5.2. Table 5.2 lists the major components indicated by numbers in the figure. The two-stage high-velocity injector is located approximately 12 m from the flange on the ITER vacuum vessel port. The moderate-velocity injectors (single-stage light gas gun and centrifuge pellet injectors) are on either side of the two-stage pneumatic injector; the centerlines of the three injection systems converge in the midplane at the ITER major radius of 6.0 m.

A differentially pumped vacuum injection line uses tritium-compatible vacuum pumps and limits hydrogen propellant gas to the ITER vessel to significantly less than 0.1 mbar•L/s. The pellet injectors are isolated from the torus by a series of three separately pumped vacuum chambers

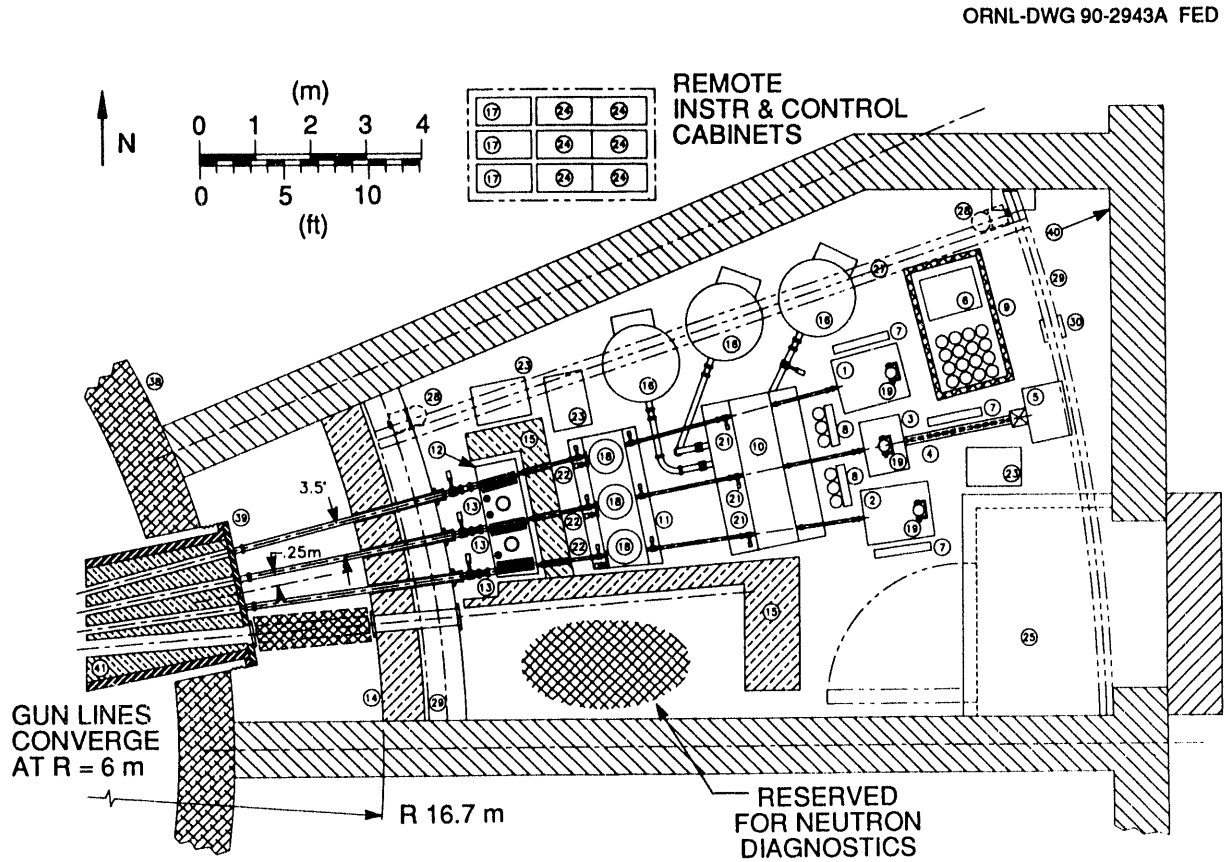

Fig. 5.2. ITER pellet injection cell. (Table 5.2 provides a key to numbered components.)

Table 5.2. Components of the ITER pellet injectors
Numbers refer to Fig. 5.2

1. Moderate-velocity injector	22. Rotatable targets
2. Moderate-velocity injector	23. Backing pumps
3. High-velocity injector (HVI)	24. Instrumentation cabinets
4. HVI pump tube	25. Airlock
5. HVI propellant reservoir	26. Crane, 10-ton capacity
6. HVI propellant compressor	27. Crane beam
7. Propellant gas manifolds	28. Crane beam gearmotors
8. Fuel gas manifolds	29. Crane rails
9. High-pressure cage	30. Crane rail columns
10. Low-vacuum chamber	31. Manipulator turret
11. Mid-vacuum chamber	32. Telescoping boom
12. High-vacuum chamber	33. Manipulator and camera
13. Torus isolation valves, breaks, bellows	34. Dual replaceable end effectors
14. Structural shielding wall	35. Manipulator bridge
15. Modular shielding	36. Manipulator bridge gearmotors
16. Normetex 1300-m^3/h scroll pumps	37. Manipulator bridge rails
17. Normetex control cabinets	38. ITER cryostat
18. Turbopumps, 5000 L/s	39. ITER vacuum vessel, port 14
19. Turbopumps, 500 L/s	40. Metal room liner
20. Rotatable shielding drums and motors	41. In-port shielding
21. Flow-limiting fast valves	42. Centrifuge pellet injector

(volumes of 2–4 m^3) connected by conductance-limiting pellet guide tubes and flow-limiting fast-acting valves. The pellet injector bay is shielded by the structural shielding wall, by a rotating eccentrically bored shielding drum in each injection line (to limit line-of-sight exposure of the injectors), and by modular shielding around the high-vacuum isolation chamber. The bay also serves as a redundant containment boundary and is sealed by bellows at the shielding wall and by an airlock at the entrance. The walls, floor, and ceiling of the bay have a metal liner that acts as a tritium boundary.

Equipment in the pellet injector bay is serviced by a 10-ton crane and a bridge-mounted articulated manipulator supported on curved rails. Instruments and control equipment for the pneumatic injectors and the vacuum components are located outside the pellet injection bay. The high-pressure propellant gas compressor and storage system is located in the pellet injection bay because of the possibility of low-level tritium contamination (1% maximum) and is surrounded by an interior wall acting as a missile shield in case of a high-pressure gas rupture. The ITER vessel port is shared with neutron and gamma diagnostic systems (a neutron spectrometer on one side of the pellet injection bay and an assembly of neutron and gamma cameras between the pellet injection bay and the port 16 flange). Since all injectors will have tritium or D-T mixtures in the gas fuel supply, three layers of containment will be provided throughout the pellet injection system.

The primary level of containment will be the pellet injector itself. It will have tritium-compatible materials throughout, including feed lines to the hydrogenic extruders, the extruders, the pellet-forming mechanism, the breech/barrel assembly, the pellet injection line, and the interface to ITER. The second level of containment is the tritium isolation boundary defined by the pellet injection bay metal liner inside the reactor building and double-walled piping for all penetrations of this boundary. The third level of containment is the ITER reactor building itself.

In principle, activation of injector components can be low due to the small diameter (a few centimeters) of the guide tubes used for pellet transport in the vacuum injection line. With shielding around the guide tubes, use of a shielded isolation valve when the injector is idle, a rotating synchronized neutron shield plug for the continuous injector, and perhaps a slight curvature of the guide tubes to eliminate a direct line of sight to the vacuum vessel, the neutron flux to injector components may be reduced to tolerable levels for limited hands-on maintenance. A design goal is to maintain the capability of hands-on maintenance for all components beyond the modular shielding wall (item 15, Fig. 5.2).

System reliability and availability goals are believed to be achievable through improvements to existing designs and the use of redundancy in the two moderate-velocity pellet injectors, each with two different pellet sizes. There is also redundancy in the pellet injection line vacuum components and the control system.

5.1.2.4 RF systems and design

The ORNL theory, rf development, and engineering groups have been working for the last year and a half on the design of a current drive system for ITER that uses ICRF waves to drive a steady-state current. For ITER, fast-wave current drive (FWCD) has been calculated to be competitive with using neutral beams as current drive sources. Although the efficiency of FWCD is lower, the absence of a high-energy beam beta component allows a comparable amount of current to be driven for equal injection powers.

In conjunction with other ITER collaborators, the rf team has designed an FWCD system that will operate from 15 to 60 MHz. This system can be operated at ~17 MHz to deliver all of the rf power to the electrons for current drive, or it can be tuned to ion resonance frequencies for direct ion heating to ignition. The FWCD system will use an array of up to 42 contiguous antennas that will fit in and between the ITER main horizontal ports, as shown in Figs. 5.3 and 5.4. Each antenna is driven by a separate rf transmission and matching line, which is connected to a 3-MW rf power system. Up to 100 MW of rf power can be delivered to the plasma using this system.

Improvements in antenna technology to allow higher power per antenna (with correspondingly fewer antennas) will result in a more compact system that would take less blanket space. A conceptual design is being developed for a high-power antenna that can be remotely maintained with Faraday shields that can withstand the steady-state radiation environment of ITER. The rf development group also is working with the ITER team to clarify the interfaces between the antenna and transmission line system and the rest of the tokamak, most notably the blanket/shield assembly, and the routing of the transmission lines in the torus room.

ORNL is also working on a collaborative FWCD program on the DIII-D tokamak at General Atomics. An FWCD proof-of-principle experiment, using a four-element antenna array designed and built by ORNL, should provide initial experimental results by fall 1992.

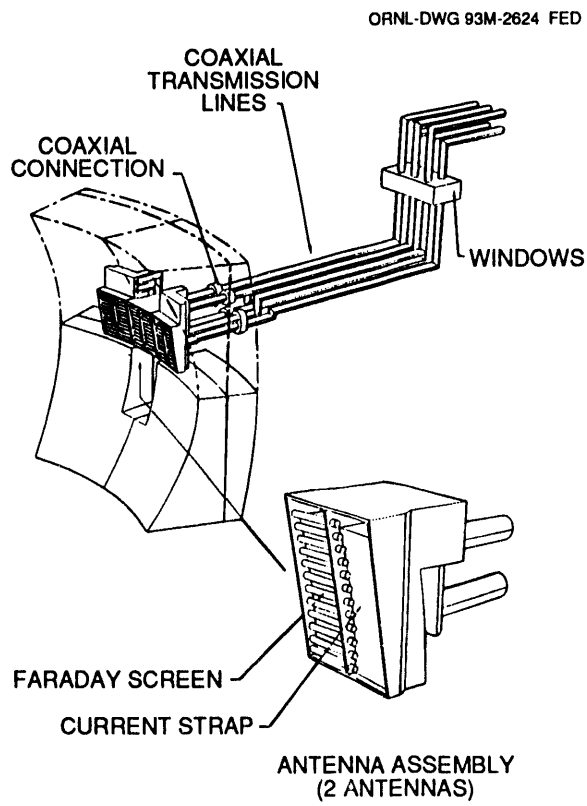

Fig. 5.3. The reference ICRF system for ITER. (a) Portion of the antenna array in the blanket modules. (b) Details of antenna construction.

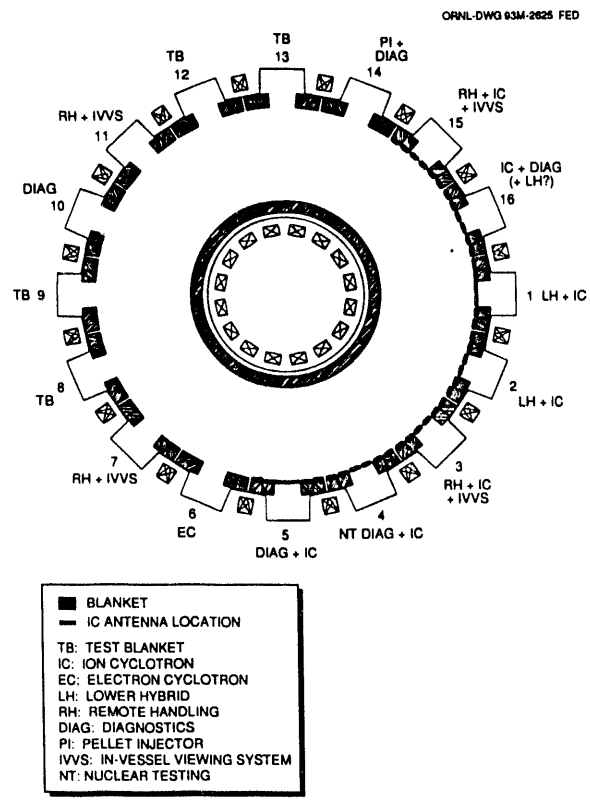

Fig. 5.4. Plan view of ITER, showing possible port allocation that includes the full fast wave current drive system.

5.1.2.5 Containment structure

ORNL led the design effort on the double-wall vacuum vessel concept. This concept includes toroidally curved sections, vertical port sections, radial port sections, and stiffening beams as shown in Fig. 5.5. The toroidal sections have a total thickness of 25 cm, with 1.5-cm-thick face sheets separated by rib stiffeners and box section cooling channels, as shown in Fig. 5.6. The face sheets and box sections are sized to give the required toroidal resistance of 20 μΩ. The ribs are sized to accept the bolts that connect the semipermanent shield segments to the vessel. The box sections are sized for lateral stability to in-plane bending loads. The vertical and radial port ducts have total thicknesses of 10 cm and 20 cm, respectively, with 2-cm face sheets and a system of rib stiffeners and box section cooling channels similar to that used in the torus sections. The strength of the vessel has been checked with a finite element analysis for the pressure, thermal, and electromagnetic loads for a vertical plasma disruption. The peak stress occurs at the intersection of the upper and lower vertical ports with the inboard side of the torus and is within design allowables.

Figure 5.5 also shows the concept for assembly of the vacuum vessel modules for insertion into the reactor. Two opposite-hand 1/32 vessel modules are welded together around a toroidal field (TF) coil to form 16 assemblies that can be installed vertically into the reactor. This approach improves the original design concept by reducing (by half) the number of poloidal welds that must be made in situ, allowing for the preassembly of the cooling manifolds, and, most importantly, removing the field welds from areas where radiation damage is high and thus allowing for weld repair during most of the useful life of the reactor.

5.1.2.6 Assembly and maintenance

The arrangement of the components in the top vertical port is critical to establishing a feasible concept for the remote assembly of the blanket/shield modules within the vacuum vessel. Figure 5.7 shows the arrangement of the 48 pipes required to supply breeding and cooling services to the divertor and blanket/shield modules in the vacuum topology developed for maintenance considerations. The arrangement

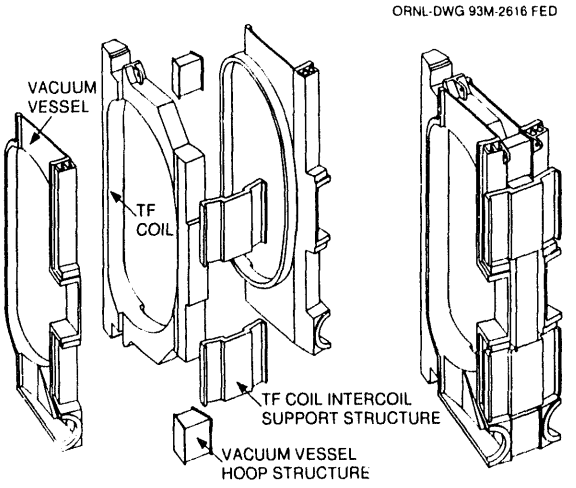

Fig. 5.5. ITER vacuum vessel assembly.

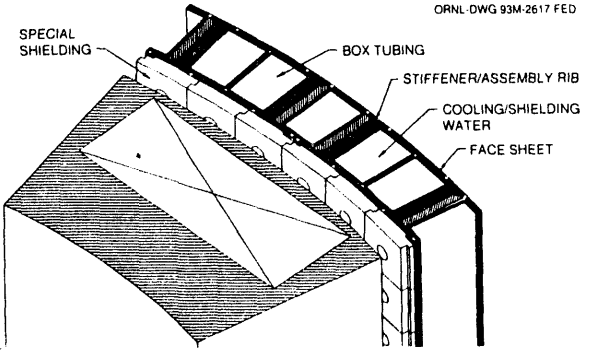

Fig. 5.6. Cross section of ITER vacuum vessel.

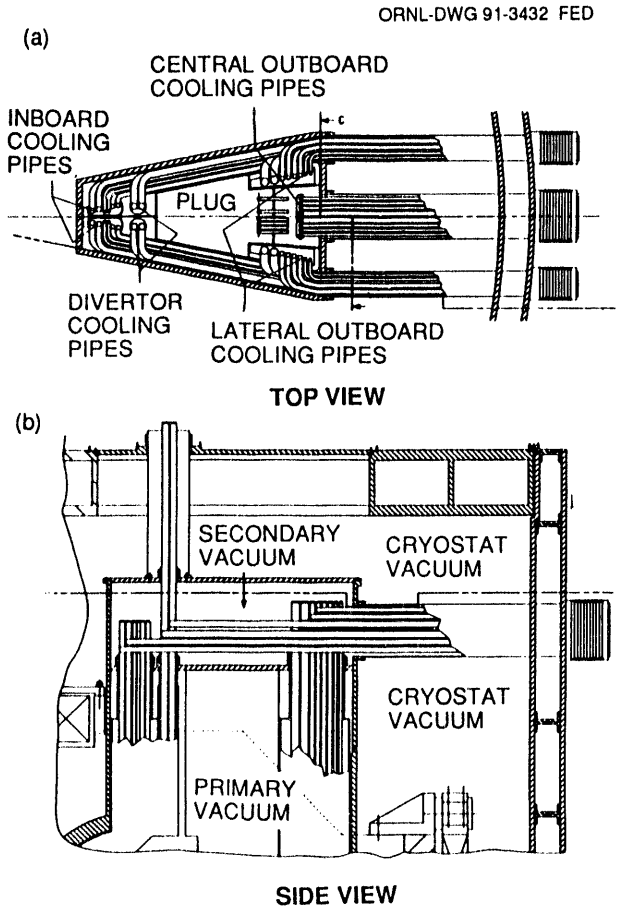

Fig. 5.7. Top port arrangement for ITER. (a) Top view. (b) Side view.

shown provides direct access for internal cutting/welding of divertor pipes from outside the external cryostat. Thus, it allows replacement of divertors without disturbing either of the two principal vacuum zones. The headers for the blanket/shield module service pipes are located in a separate zone, isolated from both the plasma and the cryostat vacuum, that isolates potential leaks and allows maintenance operations with the primary vacuum sealed. Remote pipe-joining techniques must be used to allow the selective assembly/disassembly of the piping required for individual module replacement. The modules will be handled with an overhead crane and special lifting fixtures using contamination control techniques.

Structural restraint of the blanket/shield module, one of the most difficult mechanical design problems in ITER, involves interactive efforts between electromagnetics, containment structure, and remote handling and was studied extensively at ORNL. The magnitude and distribution of the electromagnetic forces resulting from the plasma disruptions require that the in-vessel blanket/shield modules be tied to each other rather than to the vacuum vessel to avoid large local forces that would cause the vessel to fail. Approximately 200 of the connectors shown in Fig. 5.8 are placed between the adjacent faces of the blanket/shield modules in each of the 16 machine sectors to provide the toroidally continuous load path that eliminates the need for radially tying each module to the vacuum vessel. In order to be structurally integral to the blanket/shield modules, the connectors must be located 30 cm from the first wall. Remote handling design generated a concept for welding and cutting of these connectors with equipment carried on long-reach positioners. Prototypical welding equipment was designed and procured, leading to a demonstration of the ability to make the required weld between connectors placed 30 cm deep in a 2-cm-wide gap.

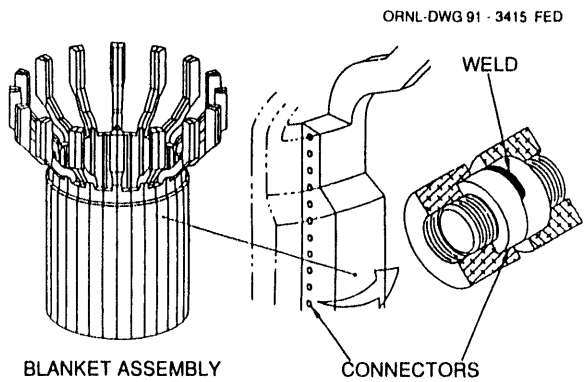

Fig. 5.8. Blanket/shield module connectors.

5.1.2.7 HARD

The HARD concept was developed by the U.S. ITER team as an alternative to the low-aspect-ratio design developed during the CDA. Systems code analysis conducted jointly at Lawrence Livermore National Laboratory (LLNL) and ORNL identified a set of machine parameters that provided the same ignition performance as the CDA, in a device of comparable size and cost but with enhanced potential for technology testing. An engineering design was then compiled in sufficient detail to allow comparison with the CDA design. The HARD option employs the same physics and technology database as the CDA design in a device that has a major radius of 6.33 m, an aspect ratio of 4, and 15 MA of plasma current.

Configuration integration

Since the intent of the HARD study was to preserve the CDA design concepts to the maximum extent possible, the resulting configuration closely resembles that of the CDA device. HARD has 16 TF coils, the same general poloidal field (PF) coil arrangement (including a central solenoid), a double vacuum vessel, and blanket/shield modules and divertors located within the inner vacuum vessel. The increased major plasma radius of 6.33 m results in a radius of 14.25 m at the outer surface of the cryostat vessel, a 0.55-m increase from CDA. Figure 5.9 is a comparison of the HARD and CDA designs.

The clear bore of the central solenoid is increased by 1 m. The increase in outboard shielding available in HARD also can be seen in this section. This increase results from filling the space between the first wall and the outboard leg of the TF coil with shielding and the primary vacuum vessel. The total shield thickness so obtained is larger than that required for nuclear shielding, and the vacuum vessel could be reconfigured to leave more radial clearance between the vessel and the outer TF coil leg or to leave clearance between the shield and vacuum vessel.

The comparative sections between the TF coils (i.e., through the vacuum vessel ports) show a 1.1-m reduction in the midplane horizontal port height for HARD. This reduction, which is one of the most significant differences in the two configurations, is a result of the decreased spacing of the outboard PF coils, corresponding to a reduced vertical distance to the X-point in HARD. The size of the vacuum pumping duct (the outboard lower port) was not changed from the CDA design. The duct opening remains at 0.775 m and tapers to a 2-m-diam duct. Even though the height of the port has been decreased, HARD retains three beam lines per port by modifying the vertical stacking arrangement.

Vacuum vessel design

In general, the HARD configuration produces only minor effects on the containment structures. Advantages include better distribution of resistance and lower loads and stresses for the vacuum vessel. Disadvantages include higher electromagnetic loads on the outboard blankets, less margin in the stability parameter, and a possible requirement to put passive loops on the inboard blankets. No significant change in cost is expected.

The CDA reference design uses a vacuum vessel concept based on heavy steel sections bolted together across electrically insulated joints. An alternative concept is based on a continuously welded, double-wall sandwich structure that achieves the required toroidal resistance without electrical breaks. Based on analyses to date, both design concepts (thick-wall and thin-wall) meet the functional requirements and are structurally feasible.

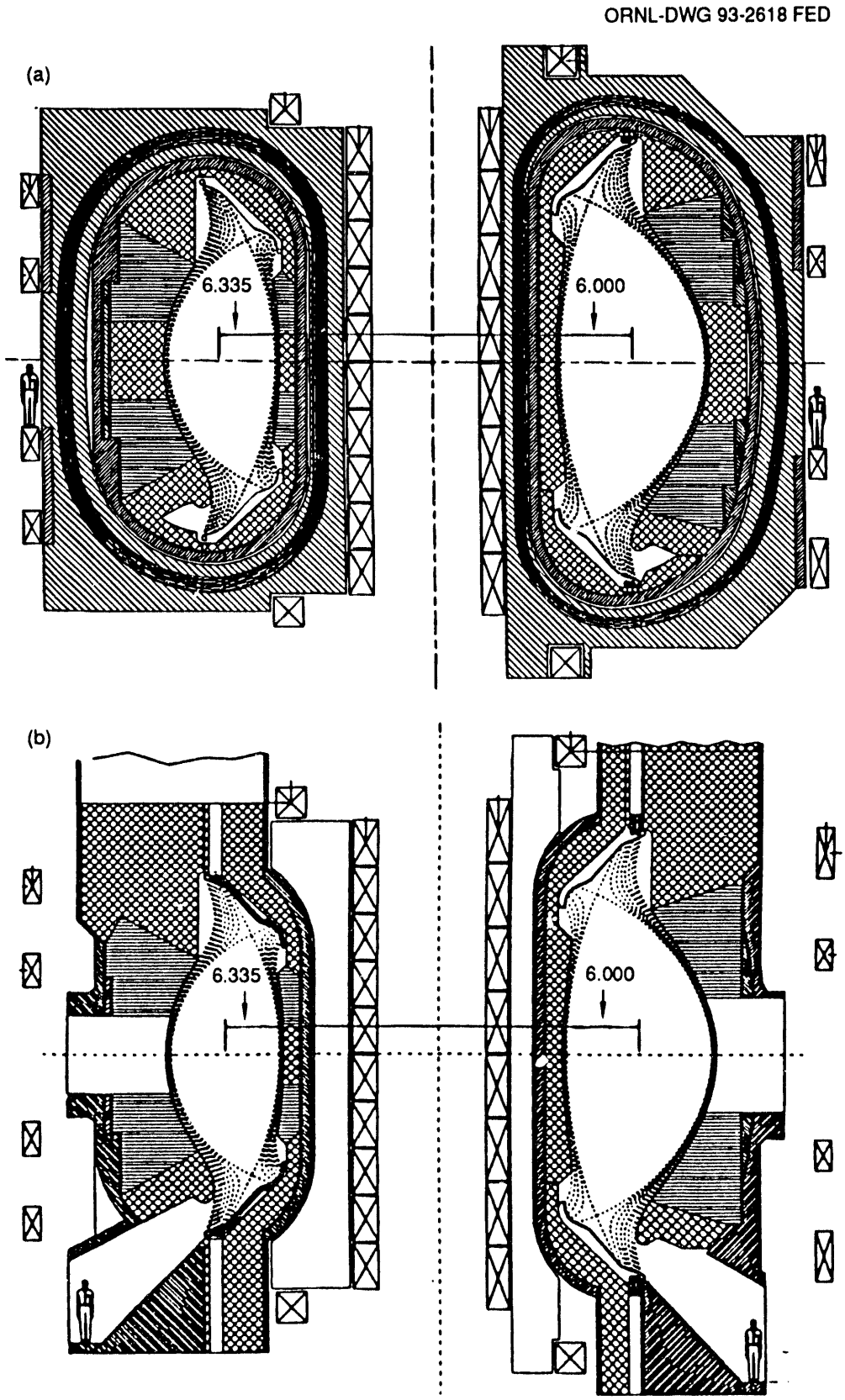

Fig. 5.9. The HARD concept (left) and the ITER CDA concept (right). (a) Section through TF coils. (b) Section between TF coils.

Either vacuum vessel concept can be used with the HARD parameters. The higher aspect ratio increases the circumference of the inboard portion of the vessel, and this increase allows an increase in the toroidal dimension of the segment containing the resistive elements (in the bore of the TF coil). A wider resistive element would distribute the resistance over a larger area and reduce some of the load and stress concentrations that result from the localized resistance of the CDA design. A secondary effect is that the sides of this segment would be parallel, resulting in a less complicated shape to fabricate.

The HARD version of the thin-wall vacuum vessel has a slight advantage over the vessel based on the CDA parameters. This advantage stems from the fact that the HARD vessel, which has the same wall thickness, has a higher toroidal resistance. This higher toroidal resistance provides the option of increasing the skin thickness of the sandwich structure to reduce stresses or of increasing the thickness of the copper conductor used for the vacuum vessel portion of the passive stability loops. Increasing the copper thickness pushes the effective current center of the sandwich vacuum vessel closer to the plasma and increases the efficiency of the loops.

Electromagnetics

Design of the vacuum vessel and internal blanket/shield modules is strongly influenced by the magnitude of electromagnetic loads due to plasma disruption. The HARD option for ITER affects many important load parameters, such as the size and position of components, response characteristics, and the magnitude of driving fields. Calculations with the finite element code EddyCuFF have been performed to quantify these effects and compare them to the reference design.

Calculations were performed for an axisymmetric vacuum vessel of uniform thickness with a 100-ms time constant, similar to previous ITER analysis models. A single-filament plasma centered at $R = 6.33$ m and $Z = -1.0$ m, with an exponential current decay of various durations, was assumed. Blanket/shield calculations employ a linear 1-MA/ms current decay and exponential vertical motion given by $A = Z_0 e^{Tt}$, where $Z_0 = -5$ cm and $T = 30$ s^{-1}. These conditions are from the ITER benchmark analysis that generated the reference design loads.

Induced current in the toroidally continuous vacuum vessel varies from 5.9 MA for a 0.2-MA/ms plasma disruption to 13.1 MA for a 3-MA/ms decay. When plotted as a percentage of initial plasma current, this variation follows closely the results for the reference design and suggests that small calculational differences in geometry, plasma current distribution, and PF coil currents have only a small effect on total current, compared to the effect of L/R time for the structure.

Poloidal variation in toroidal current does change somewhat because of differences in mutual inductance between the plasma and the vessel. For a given initial current, the inboard toroidal current density is increased by 23% in HARD, which means that eddy current heating would be 84% of that in the reference design instead of 68%, the ratio of plasma currents. This analysis neglects the presence of integral passive stability plates that would move the current distribution to the outboard.

The variation of net radial and vertical loads with decay time is shown in Figs. 5.10 and 5.11. For a 1-MA/ms current quench, radial loads are reduced by the ratio of plasma currents, from –45 MN/rad (20 MN per 1/16 sector) to –22 MN/rad (12 MN). The maximum vertical force is reduced from 8 MN/rad (3 MN) to 4.6 MN/rad (2 MN).

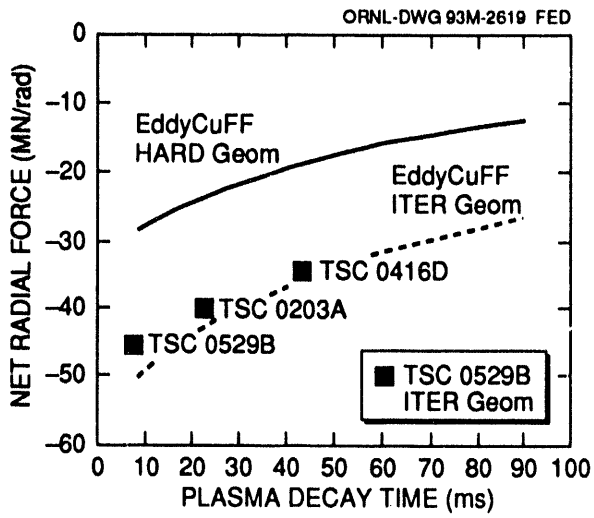

Fig. 5.10. Effect of plasma decay time on net radial force.

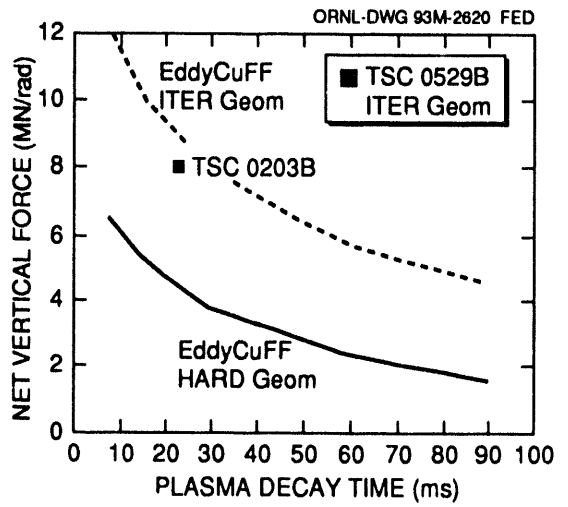

Fig. 5.11. Effect of plasma decay time on net vertical force.

Induced current in the HARD inboard blanket/shield module is influenced by differences in size, position, and magnetic field. A decrease in poloidal field at the center of the inboard module is offset by an increase in radial position and flux area per segment. The result is an increase in driving voltage and a 50% increase in circulating current, even though the loop resistance is higher. The toroidal field at the module center is increased from 8.5 T to 10.0 T, and the end result is a doubling of the forces acting on a quarter of the geometry. Net radial and vertical loads on a module are changed slightly.

The outboard module for the HARD option has a 50% higher driving voltage to induce circulating currents but a higher loop resistance, so that induced currents are unchanged from the reference design. The toroidal field at the center of a module is increased from 3.5 to 5 T, which suggests that a 40% increase in radial and vertical loads on a quarter-module is possible. Vertical loads may also be increased by the interaction of the toroidal field with longer radial current paths around the box. Detailed calculations with EddyCuFF have not been completed.

In summary, calculations have shown that the reduced plasma current in the HARD option has a beneficial effect on disruption loads for the vacuum vessel. Higher current in the inboard blanket/shield modules and higher toroidal field double the local forces. Outboard blanket forces are locally higher than those in the reference design.

Assembly and maintenance

The assembly and maintenance evaluation studied the effects of the HARD concept on the baseline assembly/maintenance concepts and equipment for some major components and critical maintenance operations of these components. The evaluation concentrated on the areas that were emphasized during the CDA design: the top vertical port design and maintenance operations and the segmentation and in-vessel removal schemes for divertors and blanket/shield modules. The weights of the CDA design and the HARD components are compared in

Table 5.3. The design and maintenance concepts for the top port were recently established for the CDA design and were discussed and compared to those for HARD.

Table 5.3. Component weights for CDA design and HARD

Component	Weight (metric ton)	
	CDA	HARD
Central solenoid	720	986
Cryostat top	700	800
Divertor	1.15	1.75
Inboard blanket/shield module	40	36
Lower inboard plug	20	20.5
Side outboard blanket/shield module and upper plug	80	76
Upper central outboard blanket/shield module	64	67
Lower central outboard blanket/shield module	35	37

In general, HARD requires an increase in the main crane capacity of more than 1000 tons. HARD facilitates the performance of remote maintenance tasks on the inboard blanket/shield module piping in the upper port, shown in Fig. 5.12. Removal of the divertor blanket/shield modules is physically possible for both the CDA design and HARD. However, HARD requires more removal steps with an increased degree of difficulty.

5.2 BPX

The Burning Plasma Experiment (BPX) project was aimed at developing a lower cost successor to the Compact Ignition Tokamak (CIT) design. The project, led by Princeton Plasma Physics Laboratory (PPPL), was cancelled in September 1991. ORNL served as a major partner in the project, with design and R&D responsibility for remote maintenance, vacuum system and thermal shielding, rf heating, and pellet injection. Work performed for the BPX project is reported here.

5.2.1 Ex-Vessel Remote Maintenance

F. C. Davis

BPX will operate initially in a non-activating hydrogen phase for approximately one year. This will permit hands-on repair of equipment that fails during shakedown runs and demonstration of remote maintenance operations. This phase will be followed by deuterium-deuterium (D-D) operations, during which limited access to the cell may still be possible. However, once D-T fuel is introduced, personnel access to the test cell that houses the machine will be prohibited, and repair and replacement of machine components must be accomplished by remotely operated equipment. Virtually all the machine components must be designed for remote replacement and handling. Once removed, the components will be transported to a hot cell where they will be repaired or packaged for disposal.

ORNL has prime responsibility for the development of the ex-vessel remote handling systems concepts, the hot cell equipment concepts, and the interface with the designers of equipment to be remotely maintained for BPX.

5.2.1.1 Remote maintenance systems

The basic remote handling systems concept for BPX includes five manipulator-transporter systems and two remotely operated overhead crane systems. These systems, supplemented by remotely operable tooling, provide the basic capability to correct failures or to make modifications within the BPX tokamak and its auxiliary systems and diagnostics in the center cell.

ORNL-DWG 93M-2621 FED

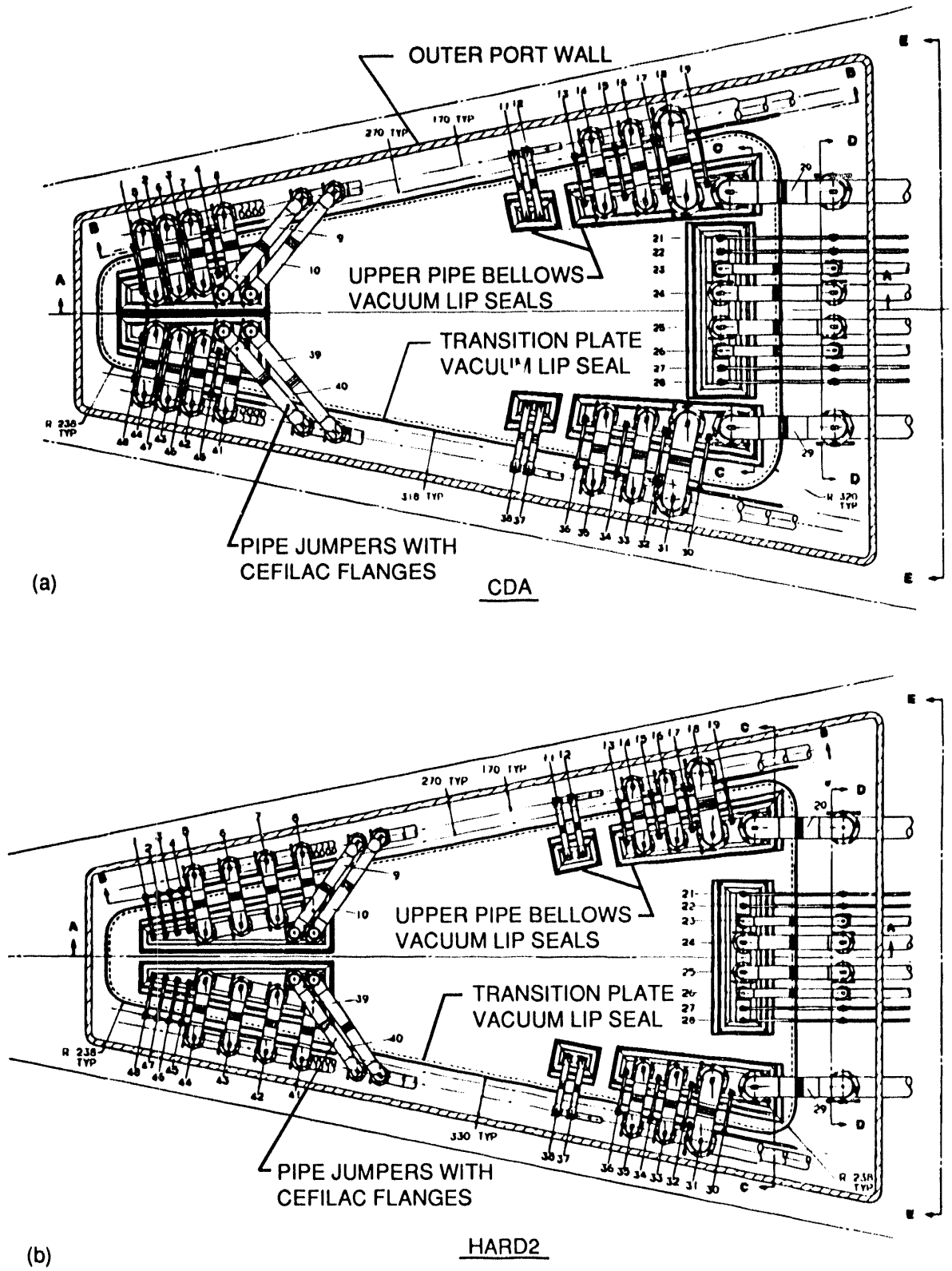

Fig 5.12. Plan views of pipe jumper layout for top port of (a) the ITER CDA concept and (b) the HARD2 concept.

Each manipulator-transporter system maintains a specific area on the machine. The overhead system, which consists of an overhead bridge-trolley with a vertically telescoping boom that supports a teleoperated manipulator package located in the high bay area, is responsible for maintaining the top and sides of the machine. A "cherry picker" articulated boom with a teleoperated manipulator package supplements the overhead system, particularly for the lower areas of the machine.

Components inside the vacuum vessel will be maintained by a manipulator system mounted on the end of an articulated boom similar to the booms designed for JET and TFTR.

Maintenance tasks under the machine will be performed by an articulated boom similar in configuration to the boom used to perform the maintenance tasks in the vessel, supplemented by a small floor-mounted vehicle equipped with a manipulator package. The boom will provide the weight handling capability, while the floor-mounted system will provide sensitivity and dexterity.

5.2.1.2 Coil replacement

The BPX project staff deemed it prudent to investigate how the program would be affected if the capability to recover from any coil failure were required, since TFTR, JET, and Tore Supra all experienced coil failures.

A detailed replacement sequence was developed for what was judged to be the worst-case scenario, failure of a TF coil. Replacement schedules and costs were generated for each step in the sequence for both hands-on and remote replacement scenarios. The replacement sequence provided a consistent and thorough basis for generating the replacement time estimates, identifying tools and fixtures, itemizing costs, and ensuring that no aspect of the replacement task was overlooked. The estimated time to remotely replace a TF coil was about two years, approximately three times longer than hands-on replacement.

Three-dimensional computer modeling, using the Interactive Graphics Robot Instruction Program (IGRIP), was used to generate a real-time graphic simulation. With this simulation, a model was developed for work spaces around the machine and the kinematics of the manipulators, cranes, transporters, etc. This model proved to be a very valuable design tool. From this work, a videotape was prepared and used as a means to present the sequence of operations.

As a result of this study, the BPX Requirements Document was modified to include a full remote maintenance design requirement to ensure recovery capabilities from all potential failures, including TF and PF coil failures. This required various design modifications of the BPX machine. In many cases, the design concepts developed would have been adopted even if the remote replacement requirement had not been invoked. The ability to remotely maintain requires simplicity, which normally enhances performance, reliability, and maintainability.

5.2.1.3 Remote maintenance development plans

The adopted BPX remote maintenance requirement exceeds the demonstrated capability on any fusion facility in the world. A task was undertaken to determine the development program necessary to increase the remote maintenance technology base to address the BPX needs. Most of the available remote technology has evolved from the nuclear fission industry over the past 40 years. The JET project has expanded and improved this technology base for fusion applications, but the BPX requirements present many new and unique remote maintenance tasks, many of which are more

difficult than those previously attempted. Design solutions from previous programs will be applied to BPX where possible, but considerable additional development is needed owing to the unique and comprehensive remote maintenance requirements. The key technical areas requiring development include manipulation, transport, component designs for maintenance, and remote tooling. This development must occur early enough to support the BPX design activities.

An important element of the development program is the design and qualification of the standard remote maintenance features that are incorporated into the component modules. Examples are mechanical fasteners, electrical and pipe couplings, vacuum joints, and feedthroughs. As designs are qualified, they will be cataloged in a BPX Remote Maintenance Design Manual for reference and use by the component design groups. Qualification will largely be achieved on mock-up facilities at ORNL. Later, a full-scale mock-up of a sector of the BPX machine will be installed with representative remote handling systems in a dedicated test facility at the project site. Mock-up tests in this stage of the program will focus on remote maintenance tests of individual systems and demonstration of maintenance procedures. The facility will continue to function throughout the life of the project for operator training, remote maintenance rehearsals, and special development efforts. Remote maintenance validation tests on the actual machine during assembly will provide the final demonstration of this technology.

This remote maintenance program will produce the systems and equipment necessary to ensure continued operation of BPX and should provide a major step toward the requirements for future fusion machines.

5.2.2 Vacuum System and Thermal Shield

5.2.2.1 Vacuum pumping system

B. E. Nelson

BPX will require an ultrahigh-vacuum pumping system to evacuate the plasma chamber from atmospheric pressure to low pressure and to maintain the required vacuum levels during bakeout, discharge cleaning, and pulsed burn operation. The base partial pressure requirements are 1.34×10^{-6} Pa (1×10^{-7} torr) for fuel gases and 1.34×10^{-8} Pa (1×10^{-9} torr) for other constituents. These pressure requirements are very stringent for a system of this size and surface area. In addition, the presence of tritium in the pumped stream prevents the use of lubricants or organic seal materials anywhere in the system.

In FY 1991, the BPX vacuum pumping system design was modified to accommodate the increased volume (150 m^3) and surface area (>400 m^2) of the torus. The modified system includes two radial pumping ducts instead of one, with each duct connected to eight magnetic bearing turbomolecular pumps (TMPs), providing a total net pumping speed of slightly over 7000 L/s. The connecting ductwork is routed through concrete shielding with three 90° bends to prevent neutron activation of the pumping system. The TMPs are backed by a common roughing system consisting of two pairs of scroll pumps in series. The base pressure requirements can be met with this system only if the total impurity gas load is kept below 10^{-6} torr•L/s. This requires extremely rigorous cleaning and baking procedures to maintain a low outgassing rate and very careful manufacturing and assembly procedures to minimize the leak rate into the torus.

A second major change was the requirement for He:O glow discharge cleaning at relatively high pressure. The pumping system must provide 15,000 L/s over a pressure range of 1×10^{-3} to 2×10^{-2} torr to clear the 150-m^3 torus volume every 10 s. This will require a system of compound turbomolecular/drag pumps backed by Roots blowers with gas-purged bearings. The large uncertainty (factor of about 10) in the performance of the compound pumps is being addressed through an R&D effort to obtain several pumps on loan and measure their pumping speed over the appropriate pressure range.

An ongoing part of the BPX vacuum pumping system design effort was the verification of the series scroll pump performance parameters for pumping fuel gases (H_2, D_2, T_2). Experience in operating these pumps is necessary to ensure that they will perform reliably and according to the assumptions of the analysis. An R&D program was planned to procure representative pumps, install them in a test stand, and run performance characterization tests. Communication and collaboration with other laboratories and programs [including Kernforschungszentrum Karlsruhe (KfK) and JET] will continue to be beneficial.

5.2.2.2 Thermal shield

BPX will require a thermal shield to insulate the coil set, which is cooled with liquid nitrogen at 77 K before each operating pulse. To prevent water vapor from condensing on the coils, the shield is maintained at a slight positive pressure. A strict leak rate requirement of 1 L/s is imposed to prevent overloading the test cell exhaust "holdup line."

The original thermal shield design consisted of a double-wall, all-welded sandwich structure with thermal insulation between the walls. In FY 1991 the thermal shield design was modified in accordance with new requirements for remote maintenance (see Sect. 5.2.1). Access to any part of the device must now be possible with a minimum amount of interference from the thermal shield. A new modular approach to the thermal shield design was undertaken as part of the conceptual design effort. The new concept is based on a structural frame covered with double-wall insulated panels. The panels can be individually or collectively removed via remote maintenance techniques to provide access to device components. A critical feature of this design is the flexible "seal plug" that fills the space between adjacent insulating panels and furnishes the gas seal.

In parallel with the design effort on the thermal shield, an R&D program was planned to identify thermal insulation materials that will remain effective after exposure to the high neutron flux. Several candidate materials were identified through a literature search, and plans call for irradiation of these materials followed by testing for deterioration of their thermal and mechanical properties. A further R&D task is to investigate, develop, and test seal plug materials and concepts.

5.2.3 Ion Cyclotron Resonance Heating

D. W. Swain

The main activities for this reporting period were the documentation of the design for the ICRF heating (ICRH) system for BPX (ref. 4) and presentation of this design

at the Conceptual Design Review (CDR), a study of an alternative wall-mounted antenna, and improved calculations of disruption loads in the Faraday shield.

5.2.3.1 System design

A "hybrid" antenna design was presented at the CDR. The Faraday shield is mounted directly to the vacuum chamber wall covering the opening to a main horizontal port, with and the current straps and vacuum coaxial transmission lines are inserted through the horizontal port, mating with the Faraday shield.

The present design for the system consists of four current straps mounted in each port, with each current strap delivering 1.25 MW of rf power to the plasma, for a total of 5 MW per port. This design is shown in Fig. 5.13. For a plasma heating power of 20 MW, four ports are required. Table 5.4 lists the design parameters.

5.2.3.2 Wall-mounted antenna design study

We studied an alternative antenna design that consists of an array of current straps

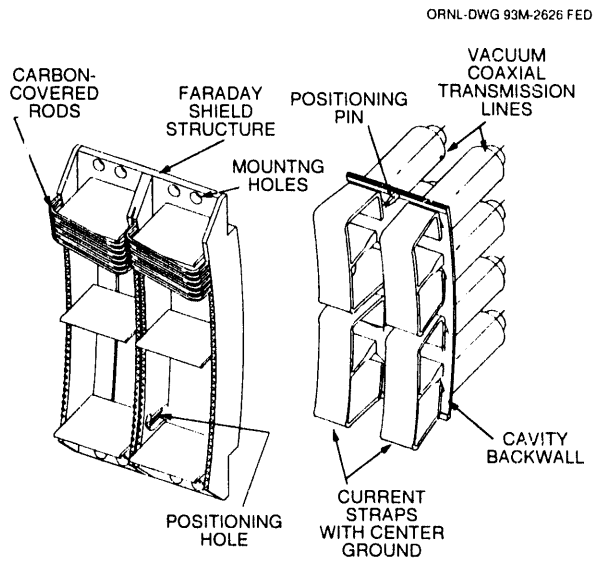

Fig. 5.13. ICRH antenna design for BPX.

Table 5.4. ICRH system parameters

Antennas	
Total power, MW	20 (minimum at 85 MHz)
Number	4 (1 per port)
Type	Hybrid (1 m × 0.6 m)
Number of current straps per antenna	4
Location	In front of ports
Cooling	Gas, edge cooling
Capability for radial motion capability	None
Faraday shield configuration	Double layer[a] (single layer option)
Material	Graphite on Inconel rod[a] (beryllium on Inconel option)
Angle, deg	≈15
Power units	
Number of transmitters	16
Power output of each transmitter, MW	2 (at 85 MHz)
VSWR at rated power	1.5
Tuning range of transmitters, MHz	50–100
System design	
Power per current strap, MW	1.25 (to plasma)
RF power flux (average), MW/m^2	8.5
Plasma load,[b] Ω/m	5 (at 85 MHz)
Maximum voltage in system, kV	50
Peak voltage at design load, kV	≈37
Pulse duration, s	15
Time between pulses, min	60

[a]Needs further study; subject to change.

[b]Calculated load ≈ 16 Ω/m.

mounted on the vacuum vessel wall. The advantage of this design is that the straps can be located in a continuous array, thus providing for the possibility of using the array to drive current in the plasma. In addition, the total number of current straps and the Faraday shield surface area can be increased if desired, thereby decreasing the

rf voltages in the system and the rf power flux through the Faraday shield.

The primary disadvantage of the wall-mounted design is the increased need for remote maintenance equipment for installation of the antennas. In the hybrid design, all rf connections are made outside the vacuum vessel, and the current straps and rf transmission lines are inserted as a unit through the ports. In the wall-mounted design, the current straps must be installed individually inside the vacuum vessel and then connected to rf transmission lines that extend through the ports. In both cases, the Faraday shield will be installed from inside the vacuum vessel.

The results of the study indicate that the wall-mounted antenna is feasible. The relative advantages and disadvantages of the two concepts make it difficult to say that either is obviously superior to the other. The answer varies depending on the weight that different criteria are given.

5.2.3.3 Improved disruption studies

Disruption calculations for the BPX antenna, carried out using the SPARK code, are documented in ref. 5, which summarizes the results obtained through September 1991. Analytical results were methodically compared with increasingly detailed models of the antenna structure. The aim of these comparisons was to ensure that the results from the 3-D SPARK runs were easily understandable relative to the underlying phenomena. Agreement (within about 17%) was obtained between analytic calculations and SPARK cases for a single Faraday shield tube. More detailed analyses done with SPARK indicate that stress would be a problem with the antenna design as it stood at the end of September. The primary difficulty with the design arises from the eddy currents that are induced in the resonant cavity box by a vertical disruption and that "spill over" into the Faraday shield rods nearest the top (or bottom). Because of this three-dimensional effect, which could not be calculated in the analytic models, the end rods carry about ten times the average current in the Faraday shield rods. This raises the stress level beyond that sustainable in a Faraday shield box of conventional design (i.e., metal with no insulators).

5.2.4 BPX Pellet Injection System

M. J. Gouge

The BPX pellet injection system supplies fuel to the plasma in the form of frozen hydrogenic (H_2, D_2, D-T, T_2) pellets. The pellet injection system will fuel the BPX device, both during the current ramp-up to plasma burn and during the current flattop. Some degree of density profile control will also be provided by the system. Density profiles are expected to be more peaked with pellet fueling than with gas injection alone. The expected pellet penetration in BPX is sufficient to significantly decouple core plasma fueling from the edge region, which is not possible with gas puffing alone. This allows higher fueling efficiencies and lower tritium inventories, since the high hydrogenic fluxes required in the edge for optimum divertor conditions can be met with deuterium gas puffing and the plasma can be predominantly fueled with D-T pellets with controllable isotopic concentration.
The pellets provide a local plasma density gradient in the ablation region, which may also allow a net outward flux of impurities (including helium ash) from the core plasma to the edge region. This is difficult to achieve with gas puffing alone. The pellet injection system can be used in a feedback mode to maintain a programmed average density or, potentially, fusion power. The system will have a vacuum subsystem to

provide vacuum for the injector housings and pumping of the deuterium propellant gas that accelerates the pellet through the gun barrel. The pellet injection system also will have pellet diagnostics to determine the pellet speed and size. Pellet injection system requirements are shown in Table 5.5.

Table 5.5. Pellet injection system requirements

Pellets	
Size,[a] atoms	$(1–5) \times 10^{21}$ ($\Delta n/n$ = 20–40%)
Velocity, km/s	1–5
Maximum fueling rate,[b] atom/s	8×10^{21}
Fuel per pulse,[c] atoms	7.5×10^{22}
Composition	H_2, D_2, D-T, or T_2
Propellant	
Flow rate to torus, mbar•L/s	<1.0 (D_2)
Gas load to fuel reprocessing system per tokamak pulse, bar•L	<30
System tritium inventory, g	<1.5
Reliability (with limited hands-on maintenance)	To be determined
Operational life, y	6

[a] As pellet enters plasma.
[b] Achieved with the largest pellet size.
[c] Achieved through a combination of pellet sizes/repetition rates during the tokamak pulse.

The range in the $\Delta n/n$ pellet plasma perturbation indicated in Table 5.5, as well as the expected range in plasma operating densities, requires some flexibility in the pellet size. This is attained by using three different barrel diameters (3.2, 4.1, and 5.2 mm) in the single-stage injectors. During the ramp-up phase, the plasma density will continuously increase, and the target plasma burn density will be different with different plasma temperatures and heating profiles. The largest pellet (5.2 mm in diameter) results in a 40% perturbation to a BPX at an average density of 2×10^{20} m^{-3}. Thus, during the density ramp-up, the smaller 3.4- and 4.1-mm-diam pellets can be injected into BPX at a constantly increasing repetition rate. As the plasma density becomes high enough, a transition can be made to the larger 5.2-mm-diam pellets or the high-velocity pellets from the two-stage injector at a lower repetition rate. The larger/faster pellets will penetrate farther into the plasma and provide more control on the evolving density profile as the plasma temperature increases. Penetration of a pellet into a hot plasma is a function of pellet initial size (proportional to $r_p^{5/9}$), and the largest possible pellet (given perturbation limits) should be used to provide the most leverage on plasma density profile peaking. Density profile peaking can increase the ignition margin even if plasma transport is unchanged because of the increased fusion rate with peaked profiles.

During the density ramp-up phase, fueling will probably begin with pure deuterium or deuterium-rich D-T pellets. This permits some reduction in the required tritium inventory per full-power D-T shot and allows for shot termination without introducing significant amounts of tritium into the torus if the computer-based plasma control system decides early in the shot sequence that evolving plasma and support system conditions are not met for a full-power D-T shot. Larger pellets with a higher percentage of tritium will be used in the flattop burn part of the shot sequence. Since each of the three single-stage repeating pneumatic injectors has dedicated hydrogenic ice extruders, up to three D-T ratios are available with the pellets for each tokamak shot, subject, of course, to total system tritium inventory limits. Triple containment of tritium is provided for equipment areas with significant inventories of tritium (>0.1 g).

The pellet injection system will consist of two pellet injectors located in the pellet injection cell in the north diagnostics area of the BPX facility. A plan view of the pellet injection cell is shown in Fig. 5.14. One injector is a highly reliable, moderate-velocity (1- to 1.5-km/s), single-stage pneumatic

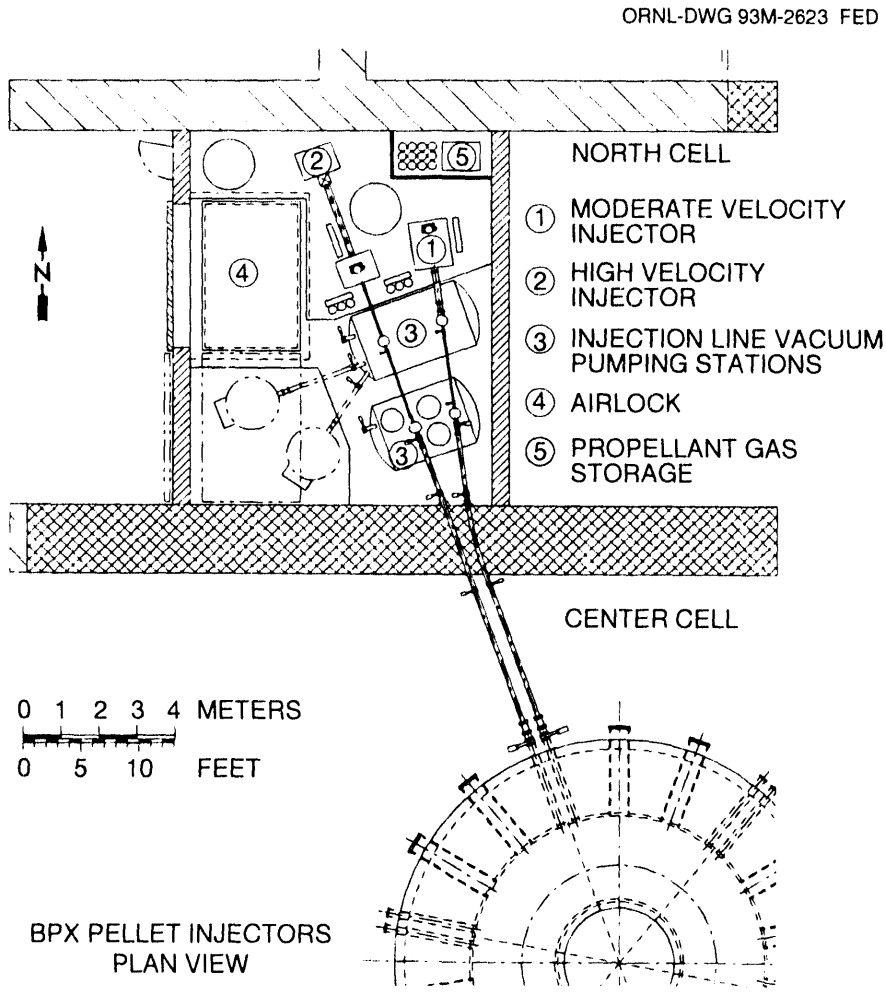

Fig. 5.14. Plan view of the BPX pellet injectors.

injector similar to the JET pneumatic pellet injector. It consists of three single-stage, repeating light gas guns in a common vacuum enclosure. The second injector is a high-velocity (1.5- to 5-km/s), two-stage pellet injector that accelerates frozen hydrogenic pellets encased in sabots. (The two-stage injector concept is described in Sect. 5.1.2.3.) Both pellet injectors are qualified for operation with tritiated feed gas and will use deuterium as the propellant gas to simplify the requirements for gas reprocessing. Two vacuum pumping stages are provided along the injection lines to pump away the propellant gas. The conductances of the injection line guide tubes limit the propellant gas flow rate into the torus to well below the maximum specified level of 1.0 mbar•L/s.

Since both injectors will have tritium or D-T mixtures in the gas fuel supply, three levels of containment will be provided throughout the pellet injection system. The primary level of containment will be the pellet injector itself, which will have tritium-compatible materials throughout. This includes feed lines to the hydrogenic extruders, the extruders, the pellet-forming mechanism, the breech/barrel assembly, the pellet injection line, and the interface to BPX. The second level of containment is the pellet injection cell itself inside the north cell, which will have an air lock for access

(alternatively, glove boxes around primary containment structures could be used for this second level of containment). All penetrations of this boundary that transport significant quantities of tritium (e.g., the pellet injection lines to the torus) will be double-walled piping. The third level of containment is the north and center cells themselves.

A design goal is to maintain the capability of hands-on maintenance for all components in the pellet injection cell. In principle, activation of injector components can be low because of the small diameter of the guide tubes used for pellet transport in the vacuum injection line. With wall shields and shielding around the guide tubes, use of a shielded isolation valve when the injector is idle, and perhaps a slight curvature of the guide tubes to eliminate a direct line of sight to the vacuum vessel, the total neutron flux to injector components in the north cell can be reduced to tolerable levels. On the basis of a multidimensional neutronics calculation, limited hands-on maintenance of injector components appears feasible. The Monte Carlo/discrete ordinates nucleonics analysis indicated that activation dose levels around the pellet injector 30 min after shutdown will be <1 mrem/h. This permits hands-on preventive maintenance and repair, which allows use of standard components on the injectors. Several components will require remote maintenance or replacement: (1) the pellet injection lines in the BPX center cell, including penetrations through shielding; and (2) the torus vacuum isolation valve and adjacent bellows and ceramic break in each injection line.

Components in the pellet injection cell will be designed for efficient disconnection and removal through the airlock to a hot cell in case they become contaminated or activated. Because the activation of injector components should be low, it should be possible to enter the pellet injection cell without protective clothing after purging the tritium lines.

5.2.5 Plasma Shape Control Calculations for BPX Divertor Sweep Optimization

D. J. Strickler and G. H. Neilson

The equilibrium code BEQ[6] is used to optimize the BPX divertor sweep. A sequence of double-null (DN) diverted equilibria with constant q during flattop and a prescribed path for the outer strike point (OSP) demonstrates the feasibility of the BPX divertor surface geometry and maximizes the sweep distance of the OSP subject to limits imposed on distances between X-point and strike points. Plasma profiles and linked flux are consistent with a fiducial discharge simulation using the TSC code.[3]

The control matrix MHD equilibrium code BEQ, with input generated by TSC, is used to compute solutions characterized by fixed plasma radii, current, field, volt-seconds, and profile parameters (β_p, $l_i/2$) at a given set of time points (4.5 s < t < 13.2 s). Values of the safety factor and the OSP position are also prescribed as functions of time Plasma current, field, and profile parameters are determined in a preliminary TSC simulation. The BEQ code computes the PF currents controlling the plasma shape and the poloidal flux distribution on the divertor plates for use in optimization of the divertor sweep scenario and for design of the divertor geometry.

For each prescribed OSP position on the divertor plate, the field line length between the X-point and the strike points is maximized by determining the plasma elongation κ such that q = 3.2 (the design value). The length of the OSP sweep is optimized by starting near the outboard edge of the divertor surface and sweeping the OSP inward until the distance from X-point to either

the inner strike point (ISP) or the OSP approaches its minimum value. Plasma elongation for this sequence of equilibria is initially $\kappa = 1.90$ (corresponding to $q = 4.3$) at $t = 4.5$ s, increases to $\kappa = 2.08$ ($q = 3.2$) at beginning of flattop (BOFT), and returns to $\kappa = 1.91$ ($q = 3.2$) at end of burn (EOB). Since the elongation is growing prior to BOFT, the ISP initially follows an outward trajectory before sweeping inward. During flattop (constant q), the path of the X-point is almost linear. The resulting sweep distance for the OSP is 39.3 cm during flattop (46.4 cm between $t = 4.5$ s and EOB). The ISP sweep during flattop is 30.5 cm, and the ISP is at its minimum distance from the divertor surface (10.0 cm) at EOB. The radial coordinate of the outer separatrix flux surface at points 0.5 m above the plasma midplane, a measure associated with antenna coupling, is $R = 3.346$ m at $t = 4.5$ s, $R = 3.357$ m at BOFT, and $R = 3.337$ m at EOB. This variation of 0.02 m during flattop is a further indication that the OSP sweep distance is maximum for the divertor geometry.

The divertor surface[7] used for this study (Figs. 5.15 and 5.16) is based on a sequence of equilibria with constant safety factor ($q = 3.2$) and was designed to significantly extend the sweep distance of the OSP over previous divertor designs.

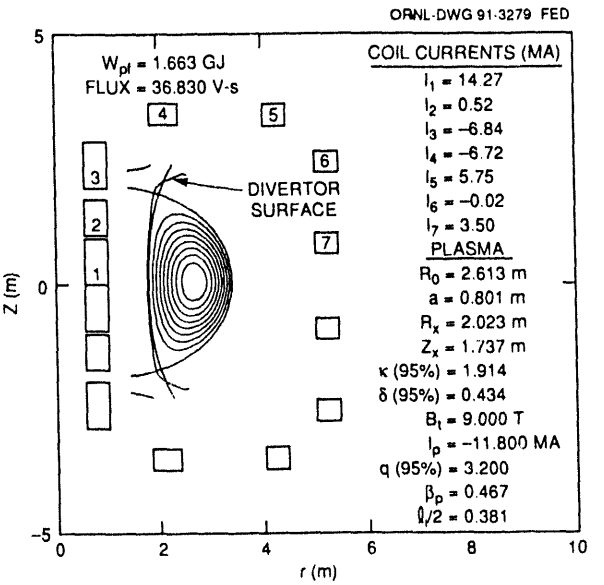

Fig. 5.15. The BPX PF coil system, limiter and divertor surface geometry, and an end-of-burn equilibrium.

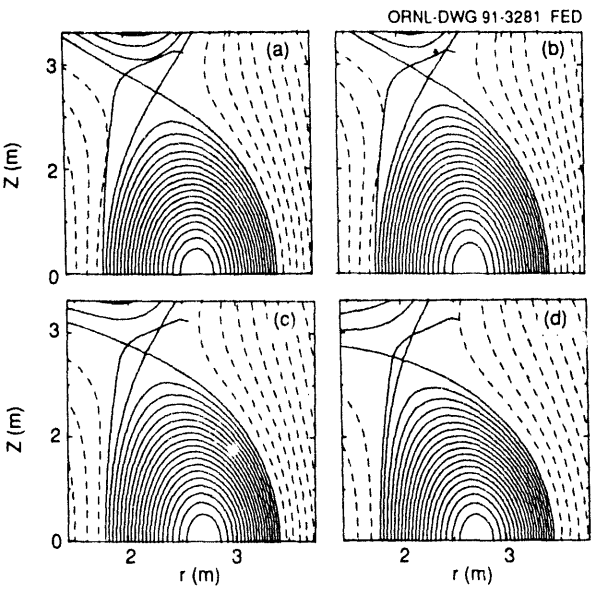

Fig. 5.16. Equilibrium solutions at (a) $t = 4.5$ s, (b) $t = 7.5$ s (BOFT), (c) $t = 11.74$ s, and (d) $t = 13.2$ s (EOB) show the sweep of the separatrix flux surface across the divertor target surface.

5.2.6 Plasma Disruption Calculations

R. O. Sayer, S. C. Jardin,* G. H. Neilson, and Y-K. M. Peng

Design of the BPX vacuum vessel is strongly driven by disruption-induced forces produced by plasma motion and current decay. Accurate predictions of the time behavior of disruptive effects are therefore needed.

The TSC code[3] has been used to simulate disruptions to predict the evolution of plasma motion, current decay, induced eddy

*Princeton Plasma Physics Laboratory Princeton, N.J.

currents, and forces for the BPX design with $R_0 = 2.59$ m. We studied the sensitivity of net vacuum vessel forces to dI_p/dt and to various initial conditions to determine the disruption scenarios that produce the most severe loads. Analysis of the evolution of currents, plasma motion, extreme forces, and force distributions led to the selection of candidate cases for the most severe loads. Several disruption cases (e.g., fast radial, fast vertical, slow vertical) were considered because various cases tend to drive the design of different parts of the vacuum vessel.

For load analysis of 3-D BPX conducting structures, the TSC plasma current history output was converted for the three-dimensional eddy current analysis code SPARK[8] to approximately 200 coils whose currents were programmed to vary with time so as to represent the disrupting plasma. SPARK computations with this detailed plasma driver and with finite element representations of the 3-D conducting structures yielded induced eddy currents and loads suitable for input to structural analysis codes.

We simulated vertically moving disrupting plasmas with a surrounding halo for a range of halo temperature T_{halo} and width W_{halo}. Initial conditions of $I_p = 11.8$ MA, $\beta = 2.1\%$, and $\beta_{pol} = 0.36$ were used for all simulations. Before thermal quench, the plasma was allowed to drift vertically until $q_{95} = 2.0$ ($Z_{mag} = -0.62$ m) or until $q_{95} = 1.5$ ($Z_{mag} = -0.84$ m).

The plasma halo retards plasma vertical motion and current decay. The maximum vertical velocity was reduced from 330 m/s with no halo to 150 m/s for $\langle T_{halo}\rangle_{quench} = 1.5$ eV and to 50 m/s for $\langle T_{halo}\rangle_{quench} = 4.5$ eV. The predicted peak vacuum vessel poloidal currents, up to $0.19I_p$, are in good agreement with measured values of $0.2I_p$ on DIII-D. The peak vacuum vessel inboard pressure of 3.5 MPa occurs for the fastest current decay (3.0 MA/ms), whereas peak pressure on the bottom of the vacuum vessel occurs for the slowest current decay (highest T_{halo}). Large localized forces arise from currents flowing between the plasma halo and and the vacuum vessel. For example, the maximum (compressive) vertical forces on the bottom of the vessel (near the decaying plasma) are up to three times larger when halo cuurents are include; however, the net vertical and radial vacuum vessel forces are relatively insensitive to the presence of the halo. For the vessel bottom, the extreme values of F_Z(halo) and pressure increase as $\langle T_{halo}\rangle_{quench}$ increases from 0.2 to 4.5 eV.

Simulations with different initial β_{pol} and Z_{mag} would be expected to alter the relative importance of the poloidal and toroidal current effects but not to change the overall forces significantly. Extreme vessel radial forces are not highly sensitive to dI_p/dt, but the extreme net vertical force is 25% larger for the slowest current decay than for the fastest current decay. Slower plasma current decay rates give more severe net vertical loads because the plasma current decay occurs when the plasma has moved farther off midplane.

Because the halo retards both plasma vertical motion and current quench rate, higher halo temperatures give larger extreme vacuum vessel halo currents and larger $\mathbf{J}_{pol} \times \mathbf{B}_{tor}$ forces in the vacuum vessel region where halo currents flow. For the cases considered, the slowest current quench rate, 0.3 MA/ms, corresponding to $\langle T_{halo}\rangle_{quench} = 4.5$ eV, gave the largest bottom wall pressure, 1.4 MPa. Higher halo temperature (i.e., a slower current quench rate) would give at most about 1.6 MPa for bottom wall pressure.

Detailed structural analysis indicates that stresses in the critical inboard wall region are within allowable limits for cases that have their maximum loads there. The sizing

of divertor and first wall tiles and their supports has been driven by disruption eddy and halo current loads. Engineering analysis for a disruption case with a maximum current decay rate and for one with maximum halo current shows that the tiles will be able to withstand disruptions.

5.3 STEADY-STATE ADVANCED TOKAMAK WITH RESISTIVE DEMOUNTABLE COILS

B. E. Nelson and D. W. Swain

The design concept for a steady-state advanced tokamak (SSAT) with resistive, demountable coils, identified as SSAT-D, was developed as one of three tokamak design studies initiated in fall 1991 to fulfill an SSAT mission. Such a device is needed to demonstrate integrated steady-state operating modes characterized by a noninductively driven plasma current, a high power density, an actively cooled and actively pumped divertor, and disruption-free operation. In addition, this device would provide a database on physics regimes that extrapolate to a more attractive fusion reactor than that projected by the present database. These regimes are characterized by a high bootstrap current fraction (to minimize auxiliary power requirements), enhanced confinement (relative to 2 × L-mode scaling), and high beta (relative to the Troyon limit). Detailed control of the plasma current profile is necessary for exploration of such regimes. For example, high-bootstrap configurations require an externally driven "seed" current near the axis for stability, and second-stable configurations require profile control to achieve a high value of the safety factor on axis (e.g., $q_0 = 2$).

A goal of the three design studies was to determine whether the SSAT mission could be accomplished in a facility with a moderate capital cost (near $400 million) sited in the present TFTR facility at PPPL and making maximum use of available TFTR assets. The other two design studies, for an SSAT with superconducting coils (SSAT-SC) and an SSAT with resistive wound coils (SSAT-R), were developed by other groups.

5.3.1 Requirements and Assumptions

The SSAT-D tokamak configuration was developed around the "compulsory" SSAT design parameters:

- major radius $R_0 = 2.25$ m,
- minor radius $a = 0.5$ m,
- elongation $\kappa_x = 2$,
- triangularity $\delta_{95} = 0.3$,
- toroidal field $B_0 = 3.35$ T,
- TF ripple $\lesssim 5\%$, and
- a single-null (SN) divertor with "open" or "closed" configuration.

Several key assumptions and constraints were included:

- steady-state, water-cooled copper TF and PF coils,
- total TF and PF dc power less than 200 MW, and
- access for four TFTR neutral beam injectors.

In addition, SSAT-D incorporates three specific features that were thought to make the machine easier to build, maintain, and/or modify:

- demountable TF coils,
- modular "cassette" divertors, and
- nuclear shielding between the vacuum vessel and the TF coils.

Demountable TF coils have several advantages. First, the PF coil set can be located inside the bore of the TF coils, which results in smaller, lower-power PF coils; lower out-of-plane forces on the TF coils; and easier modification or replacement of the PF coil set. Second, it is possible to

fabricate the vacuum vessel, fast coils, and passive stability structures as complete units that can be pretested before they are installed in the device. This allows more assembly and fabrication operations to proceed in parallel and can substantially shorten the overall construction schedule. Finally, it is—in principle—possible to replace a failed section of the TF coil without complete disassembly of the machine. On the other hand, demountable joints add complexity to the TF coil set and introduce additional areas for failures to occur.

Modular "cassette" divertors also have several advantages. First, since all the divertors are withdrawn as complete assemblies through radial access ports, repair or change-out of the divertors can be done quickly, without deployment of any robotic manipulators inside the vacuum vessel. Second, all the piping, instrumentation, and other service line penetrations are integral with the divertor assembly and can be tested and leak checked before they are installed on the machine. Third, special "focus" coils can be readily incorporated in the divertor module to provide a means for locally modifying the field contours for a better match to the divertor geometry. The disadvantage of divertor cassettes is that they require large openings between TF coils, which results in fewer, larger TF coils.

Nuclear shielding inside the TF coil bore minimizes the activation of the TF coil and external structure and maximizes the possibility of hands-on access to critical maintenance areas such as the TF coil joints and cooling connections. The PF coils and the shielding itself would still be activated, so ex-vessel remote maintenance equipment would be still be required for operations on these coils. Lead shielding attached to the plasma side of the neutron shield would help to limit the gamma dose inside the vacuum vessel.

5.3.2 Design Description

The basic configuration of the SSAT-D is shown in Fig. 5.17. This configuration, with R_0 = 2.25 m, meets all the design requirements, constraints, and assumptions for the "compulsory" design.

ORNL-DWG 93M-2627 FED

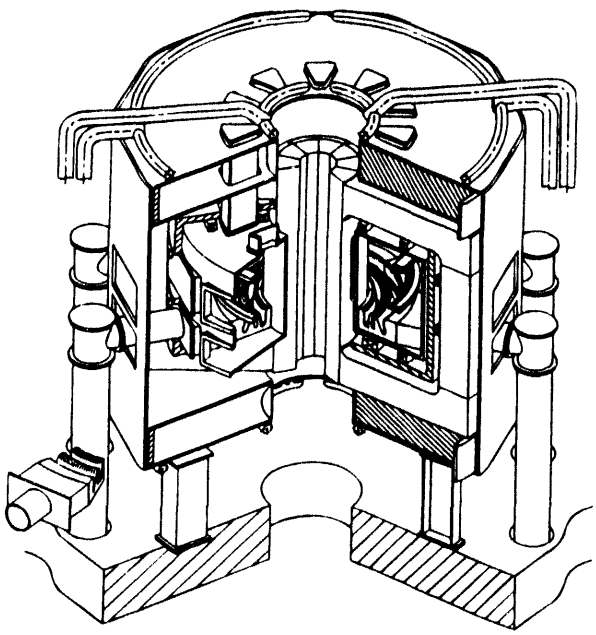

Fig. 5.17. SSAT-D configuration.

5.3.2.1 TF coils

The dominant feature of SSAT-D is the TF coil/structure combination. The device has ten rectangular, water-cooled copper TF coils with a demountable joint at each corner. This number of coils results in the smallest coils that meet both the ripple criteria and the access requirement for divertor cassettes. Table 5.6 illustrates the trade-off between the location of the outboard TF coil leg, total coil weight, and number of coils.

Table 5.6. TF coil size vs number of TF coils
Ripple = 0.5% ripple at 2.75 m, outboard current density = 600 A/cm^2

Number of coils	Radius to outer leg (m)	Total weight of coil set (metric tons)
8	6.18	970
10	5.45	898
12	5.49	913
16	5.96	953

The TF coil joint is a sliding design patterned after the joint used for the Alcator C-Mod TF coils. This design was thought to provide the best option for remote maintainability. Access to the vacuum vessel or PF coil set is provided by removing the top leg of each coil in a straight vertical motion. The inboard legs of all ten TF coils are preassembled into a single unit to resist the applied centering force and twisting moments. The upper, lower, and outboard TF coil legs are constrained by the upper and lower bridge structures and the outer structural cylinder. Each TF coil has 18 turns to limit the current per turn to 210 kA. This number was chosen as the highest reasonable current consistent with the existing TFTR power supply capability. Cooling is supplied to each turn near the sliding joints. The core requires a total of 720 connections, and the outer turns have a total of 1080 connections. Two circular headers are attached to the top and bottom TF bridge structures to supply the cooling water.

5.3.2.2 PF coils

The PF coils are arranged inside the bore of the TF coils and outside the vacuum vessel. The upper and lower PF coils are attached to cap structures suspended from the TF coil bridge structures. The outer PF coils are attached to columns and beams that form a cylindrical frame between the vacuum vessel and the TF coil. The solenoid coils are designed with sufficient clearance to be slipped over the TF coil core and are also suspended from the upper and lower cap structures. All the coils are multiple-turn, water-cooled copper except the internal fast coils, which are single-turn, water-cooled aluminum. These are suspended inside the vacuum vessel, directly outboard of a set of water-cooled passive stability plates.

5.3.2.3 Vacuum vessel

The vacuum vessel consists of a double-wall aluminum structure with carbon tiles attached directly to the inner surfaces. Midplane access for neutral beam injection (NBI) and diagnostics is provided by ten large ports, each 1 m high and 1.8 m wide. The outer wall of the vacuum vessel is placed as close to the outer PF coils as possible to provide the maximum tangential access for NBI. In this way no special port openings are required, only different port extensions. Divertor cassette access and vacuum pumping access are provided by ten radial ports, each 0.8 m high and 1.8 m wide, near the bottom of the vessel. As shown in Fig. 5.17, the radial withdrawal of the divertor cassette does not interfere with the TFTR neutral beam injectors. Vertical access is provided at the top by ten smaller ports, connected to 1.5-m-long extensions through the TF coil bridge structure. The flanges on the radial ports are designed to clear PF coils in the vertical direction such that the PF coils can be removed without cutting any port extensions. Similarly, the port flanges clear the TF coils assuming straight radial translations.

5.3.2.4 Divertor

The SSAT-D divertor is mounted in a cassette module that can be inserted or withdrawn with a simple radial motion through

access ports in the vacuum vessel. The module locks into a radial track at the bottom of the vacuum vessel that resists loads in the event of a plasma disruption. All cooling, diagnostic, and other service penetrations are integral with the connecting flange of the cassette and can be pretested and checked before installation. The cassette envelope accommodates both the "open" and "closed" divertor concepts with the addition of focus coils. The focus coils consist of discrete, picture-frame coils that are integral with the cassette and act to pull the inboard flux line down to reduce the vertical height of the divertor assembly. If the focus coils prove unworkable because of field errors or other problems, then the cassette withdrawal motion would have to be changed to an oblique angle to accommodate the taller divertor geometry.

5.3.2.5 Vacuum pumping

Vacuum pumping is provided by a combination of cryopumps and TMPs that are located in a well-shielded area below and outboard of the tokamak. As shown in Fig. 5.17, the pump ducts attach directly to the flange of the divertor. The first elbow is removed to gain access to withdraw the cassette. Preliminary calculations show that 20 cryopumps, each with a 10,000-L/s capacity, are required to provide the necessary 140,000 L/s of continuous pumping speed. The system would be capable of up to ≈1 h of operation before regeneration. In addition, five 2000-L/s TMPs would be provided for torus evacuation and discharge cleaning.

5.3.2.6 Nuclear shielding

Neutron shielding is provided between the vacuum vessel and the TF coils to reduce the neutron activation of the TF coils and support structure. The shielding is integral with the PF coil support assemblies and consists of containers filled with borated water and, if necessary, stainless steel balls. Additional lead shielding is provided on the vacuum vessel side of the shield to reduce the gamma level inside the vacuum vessel.

5.3.3 SSAT-D with R_0 = 1.5 m

Although the SSAT-D configuration with R_0 = 2.25 m meets all of the functional requirements, it is a very large, heavy, and expensive device and probably approaches the size limit for demountable TF coils. To determine the approximate scaling of cost with size, we investigated a second design point at R_0 = 1.5 m. As shown in Fig. 5.18, the configuration is basically the same for both the large and small machines. With the coil set sized for approximately the same power, the total TF coil weight for the small machine is reduced by a factor of three. The PF coil weight, structure, and power requirements are also reduced, even though the plasma current is increased. The parameters of the two configurations are compared in Table 5.7.

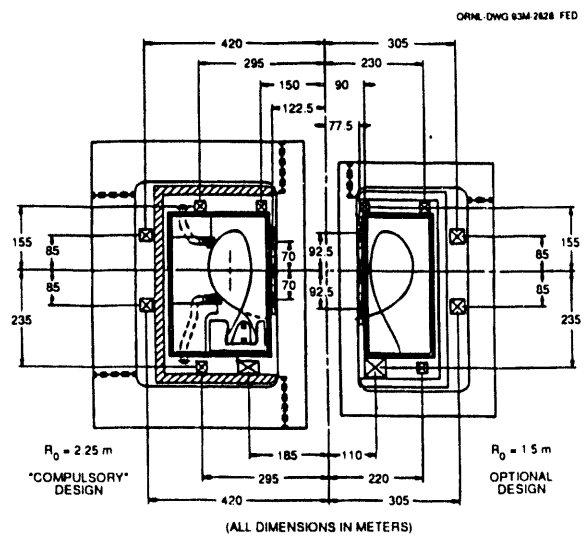

Fig. 5.18. Comparison of SSAT-D concept with "compulsory" design parameters (R_0 = 2.25 m) and optional design parameters (R_0 = 1.5 m).

Table 5.7. Comparison of parameters for SSAT-D configurations with R_0 = 2.25 m and 1.5 m

	Compulsory SSAT-D	Optional SSAT-D
Major radius R_0, m	2.25	1.5
Minor radius a, m	0.5	0.5
Elongation κ	2	2
Toroidal field B_0, T	3.35	3.35
Plasma current, MA	1.7	2.5
Number of TF coils	10	10
Number of turns per coil	18	12
Current per turn, kA	209	209
Power in TF coil set, MW	138	158
Power in PF coil set, MW	41	27
Total dc power, MW	179	185
Weight of TF coil set, metric tons	900	300
Weight of PF coil set, metric tons	82	71
Total weight, metric tons	1500	900

Some problems exist at the smaller size, however. The beam line access is somewhat marginal for the smaller machine, and the withdrawal path of the divertor cassette interferes slightly with the beam box. A possible solution is to reduce the number of TF coils from ten to eight to increase the size of the access port. In addition, the current density in the TF central core is relatively high for steady-state operation, and the space available for the sliding joint is very limited. If the joint is moved radially outward, the solenoid coils would have to be wound in place, which further complicates the design.

5.4 ARIES

Y-K. M. Peng

As part of the Advanced Reactor Innovation Evaluation Study (ARIES), a D-^{3}He-fueled tokamak reactor, ARIES-III, has been designed. Among the key features are a plasma with standard aspect ratio (~3), high β_p (~$1.3R_0/a$), and dominant bootstrap currents ($I_{bs} \sim I_p$). Theoretically, such plasmas have the advantage of high plasma beta while requiring only a modest amount of current drive. The high beta contributes to reducing the size and field of a magnetic fusion reactor; the modest current drive, to reducing the recirculating power needed to maintain the plasma current in steady state. However, the plasma pressure and current profiles must be "tailored" in detail to ensure second stability and to operate with a relatively high edge safety factor ($q_{95} \sim 7$) to allow high bootstrap currents. These constraints usually lead to some limitations to the plasma beta, as can be seen in the condition

$$\beta = F(\varepsilon,\kappa,\delta)\beta_p\varepsilon^2/q_{95}^2, \quad \varepsilon \equiv a/R_0 ,$$

where $F(\varepsilon,\kappa,\delta) \sim 20$ for plasmas with $\varepsilon \approx 0.3$ and vertically elongated, D-shape plasma cross sections.

The free-boundary divertor MHD equilibria and ballooning stability of such plasmas were examined during this study. A typical result is summarized in Table 5.8 and shown in Figs. 5.19 and 5.20. Divertor plasmas with high beta (~23%) and $\varepsilon\beta_p$ (~1.3) can be properly shaped with a proper

Table 5.8. Divertor MHD equilibrium parameters of ARIES-III-like plasmas

Major radius R_0, m	7.5
Minor radius a, m	2.5
Vertical elongation κ_{95}	1.8
Triangularity δ_{95}	0.7
Toroidal field B_{t0}, T	7.7
Plasma current I_p, MA	30
Edge safety factor q_{95}	7
Central safety factor q_0	2
Volume-average beta β, %	23
Normalized poloidal beta $\varepsilon\beta_p$	1.3

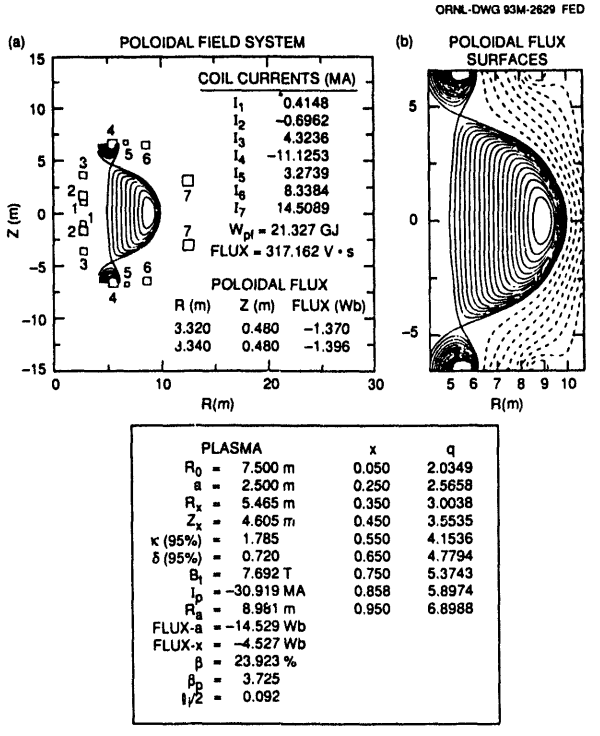

Fig. 5.19. Poloidal flux surfaces and PF coil locations for ARIES-III-like plasmas.

placement of the PF coils. The pressure and field gradient values vanish at the plasma edge defined by the divertor flux surface, ensuring that the plasma current also vanishes there. A region of second stability is calculated for the plasma between 60% and 80% of the poloidal flux, whereas in other regions the plasma is marginally stable in the first stability regime. While such a case serves as a good candidate for further second stability studies, the very steep gradient of J_ϕ is expected to induce MHD kink instabilities near the plasma edge.

5.5 STUDY OF TST FOR INTEGRATED DIVERTOR TESTING

Y. M. Peng, R. J. Colchin,* D. W. Swain,
B. E. Nelson, J. F. Monday,
J. G. Arterburn,† S. E. Attenberger,‡
D. B. Batchelor,** T. S. Bigelow,††
P. J. Fogarty, J. D. Galambos,
P. L. Goranson, C. L. Hedrick,**
J. T. Hogan, W. A. Houlberg, E. F. Jaeger,**
G. H. Jones, P. K. Mioduszewski,*
R. O. Sayer, D. A. Spong,**
W. L. Stirling,†† D. J. Strickler,
D. J. Taylor,† C. C. Tsai,†† J. A. White,‡‡
D. E. Williamson, and J. J. Yugo

The concept definition[9] of the ITER CDA identified the divertors and the associated plasma power and particle handling as an area in need of development. Similar needs exist for all large, steady-state tokamaks that are driven with high auxiliary power. New pumped divertors are being or have already been installed in JET[10] and DIII-D[11,12] to begin to address this issue for significant but limited plasma durations (10–100 s). We have carried out a study to define a small, steady-state tokamak (triple-S tokamak, or TST) that fulfills this R&D need in the near term. The TST relies only on the physics and technology data of existing small- to medium-size tokamaks and uses the facilities and equipment available at a typical fusion research institution such as ORNL.

*Toroidal Confinement Section.
†Engineering Division, Martin Marietta Energy Systems, Inc.
‡Computing and Telecommunications Division, Martin Marietta Energy Systems, Inc.
**Plasma Theory Section.
††Plasma Technology Section.
‡‡Management Services Section.

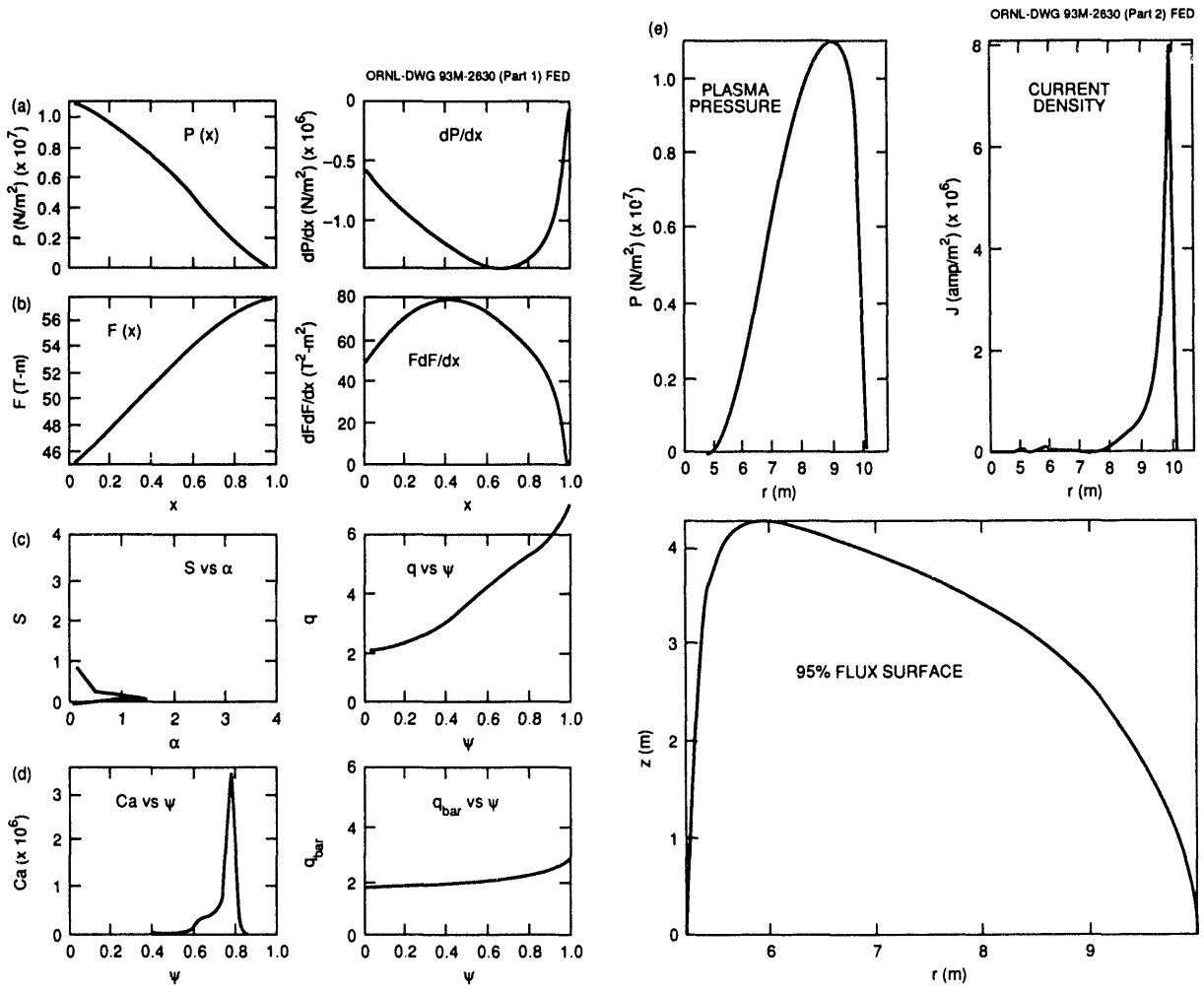

Fig. 5.20. Equilibrium profile functions: (a) pressure gradient $dP/d\psi$, (b) field gradient $F\,dF/d\psi$, (c) safety factor $q(\psi)$, (d) ballooning stability parameter C_a as a function of poloidal flux ψ, and (e) toroidal plasma current density profile on the midplane J_ϕ.

The results of this design study, described in refs. 13 and 14, show that small, steady-state tokamaks with standard aspect ratios can be built and operated with confidence to produce the plasma edge and divertor conditions of future large tokamaks. The TST, as an example, is estimated to have modest size (R_0 = 0.75 m), field (B_{t0} = 2.2 T), current (I_p = 0.5 MA), drive power (P_{aux} = 4.5 MW), and magnet power supply ($P_{tfc} \leq 40$ MW). The engineering design for the TST provides ample access for divertor and component replacement to permit a high duty cycle (~10%). This will permit the testing in TST of various divertor concepts[15] for possible use in future tokamaks. Much of the equipment and facilities required for TST should be available in fusion research laboratories throughout the world.

Recent results from the Small Tight-Aspect Ratio Tokamak[16] have provided added impetus to experiment with low R_0/a at the level of I_p ~ 0.5 MA. A TST-like device with R_0/a = 1.7 is estimated to cost less than the R_0/a = 2.5 option but entails added risk in plasma current drive operation.

Successful operation of a low-R_0/a TST will contribute to making possible a small, steady-state neutron tokamak of low R_0/a (with $R_0 \sim 1$ m) that produces a significant neutron wall load.[17] Such a neutron-producing tokamak may be a highly cost-effective approach to testing fusion nuclear technologies needed by a fusion demonstration power reactor. It may also serve as a minimum-cost option for the fusion pilot plant.[18]

5.6 SYSTEMS CODE DEVELOPMENT AND APPLICATION

Progress in the systems code area was highlighted by the final development of the TETRA (Tokamak Engineering Test Reactor Analysis) code and its application to the ITER CDA concept and, in an effort led by LLNL, the creation of the Supercode and its application to the conceptualization of the SSAT.

5.6.1 TETRA Code

The TETRA code was the primary systems analysis tool during the ITER CDA effort. This code uses a numerical nonlinear minimization approach to determine the key design parameters (variables such as R_0, a, I_p, B_{t0}, radial build, and vertical build) that minimize a figure of merit (e.g., total direct cost). It is also incorporated into a shell that eases code upgrade and the graphical presentation of the results. The TETRA code development and application were carried in collaboration with LLNL.

During this period, the TETRA code was expanded to include plasma and device operational variables simultaneously for both the physics and technology phases of ITER. This permitted the calculation of cost-effective designs for both the inductive-ignition operation and the steady-state driven burn operation. The need to achieve ignition as well as high neutron wall loads during the technology phase without overloading the divertor plates and the requirement for large current drive power led to the HARD concept for the ITER CDA.

As indicated in Table 5.9, HARD is characterized by significantly higher R_0/a (= 4) and B_{t0} (= 7 T) at about the same R_0, with significantly smaller I_p ($\approx$ 15 MA) and stored thermal and magnetic energies (0.35 GJ and 1.4 GJ, respectively). It is about 30% higher in inductive capability, leading to about four times the inductive burn pulse length of the CDA. It has a much higher neutron wall load for the technology phase (~1.1 MW/m^2) and bootstrap current fraction (~0.8) according to the same physics assumptions as the CDA. The engineering design assumptions are also maintained, including the stability and quench limits of the superconducting TF magnets at the maximum field location. The capital cost of HARD is estimated to be about 5% below that for the CDA.

Elevation views of the CDA and a version of HARD are depicted in Fig. 5.21. Because of the significantly reduced minor radius (~1.5 m), the total weight of HARD is expected to be significantly reduced as well.

5.6.2 Supercode

The Supercode is being developed under the leadership of LLNL with major contributions from ORNL. The purpose of this code is to fill the gap between the sophisticated multidimensional plasma transport simulation codes and the zero-dimensional tokamak systems codes (such at TETRA). The Supercode, when fully developed, will calculate the self-consistent 1½-D plasma evolution coupled to a more nearly realistic tokamak engineering modeling. It uses variational techniques and emphasizes simpler formulation to limit the CPU time

Table 5.9. Comparison of the ITER CDA and the HARD concept

	ITER-CDA	HARD
Characteristics		
Aspect ratio, R_0/a	2.79	4.0
Major radius, m	6.0	5.98
Minor radius, m	2.15	1.50
Plasma current, MA/q_ψ(95%)	22.0/3.0	14.8/3.0
Toroidal field on axis/at coil, T	4.85/11.1	7.01/13.3[a]
Thermal/inductive stored energies, GJ	0.580/2.24	0.346/1.35
Relative capital cost	1.00	0.95
Inductive, ignited performance		
Neutron wall loading, MW/m^2	1.0	1.0
Fusion power, MW	1080	784
Required Troyon beta coefficient, %	1.99	1.73
Required H-mode enhancement		
ITER power confinement scaling	2.0	2.0[f]
ITER H-mode confinement scaling	0.65 to ~0.87[b]	0.61 to ~0.81[b]
Volt-second capability, V•s	326	417
Volt-seconds available for burn, V•s	46.1	179
Burn pulse length, s	400	1660
Number of cycles for 1- to 3-MW•year/m^2 fluence	78,000–237,000	19,000–57,000
Technology phase performance[c]		
Steady-state operation under original beta and bootstrap models		
Maximum attainable wall load,[c] MW/m^2	0.42	1.10
Q	3.7	7.6
Bootstrap current fraction	0.33	0.46
Steady-state operation under improved beta and bootstrap models		
Maximum attainable wall load,[c] MW/m^2	0.65	2.84
Q	6.2	20
Bootstrap current fraction	0.54	0.82
Hybrid operation		
Pulse length at 1-MW/m^2 wall load,[c] s	~3,000	~9,000
Number of cycles for 1- to 3-MW•year/m^2 fluence	11,000–32,000	4,000–11,000

[a]At same coil design constraints as ITER (i.e., same stress, protection, and stability).

[b]Lowest value is for operation with no edge-localized modes (ELMs); higher value assumes a degradation of τ_E (i.e., an increase in required enhancement factor) to ~75% of the ELM-free value.

[c]Impurity-seeded operation with divertor, beta, and confinement constraints applied.

required for calculation of a large number of tokamak design points, such as that needed in systems analysis. It is also fully compatible with the latest workstations and not limited to the CRAY computers. Initial applications of the preliminary versions of the Supercode have been directed to SSAT and ITER EDA.

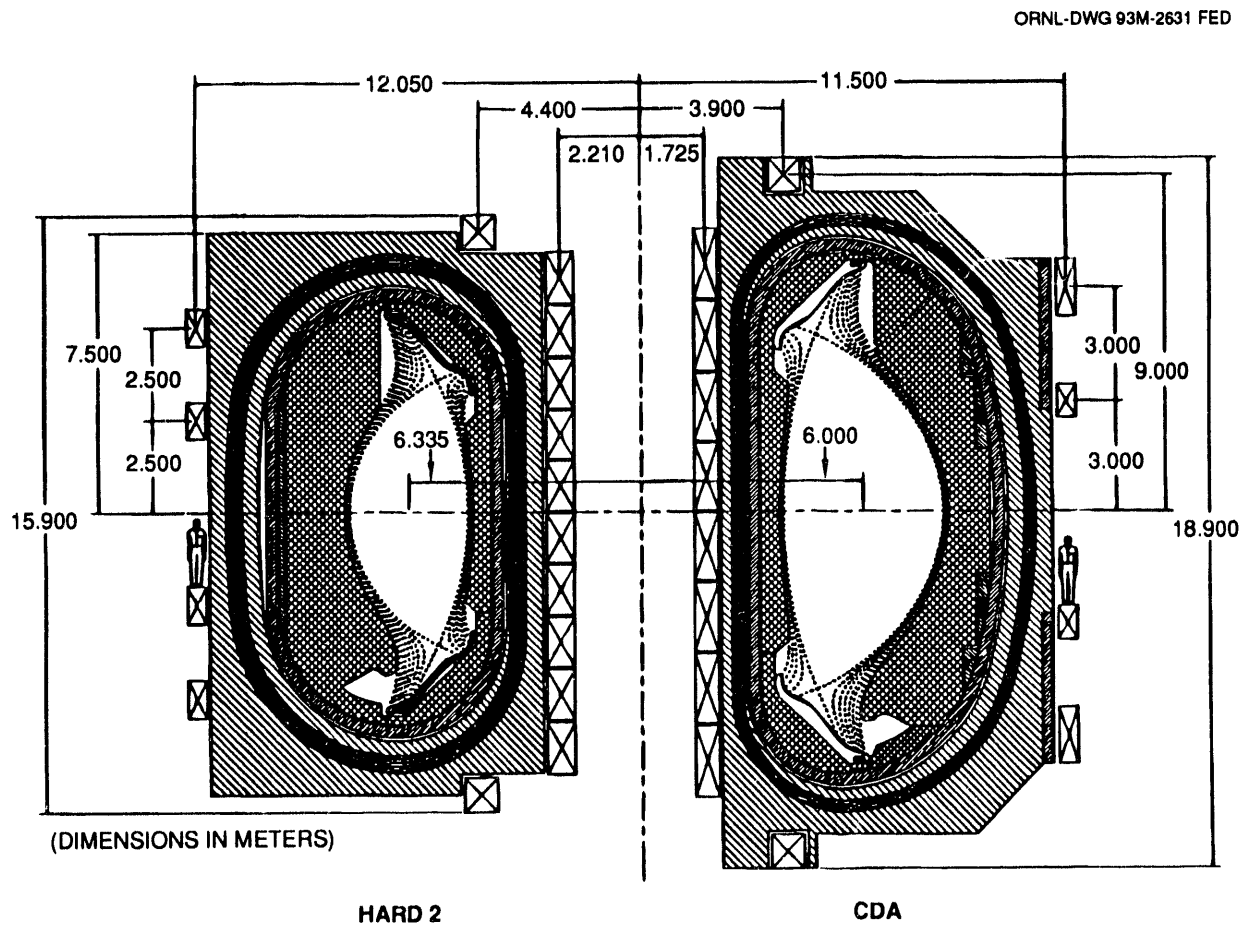

Fig. 5.21. Elevation view of HARD concept (left) and ITER CDA concept (right).

REFERENCES

1. *ITER Physics Design Guidelines*, ITER Documentation Series No. 10, International Atomic Energy Agency, Vienna, 1990.

2. N. A. Uckan, "ITER Physics Design Guidelines at High Aspect Ratio," in *Proceedings of the 17th Symposium on Fusion Engineering, San Diego, California, October 1–4, 1991*, IEEE, New York, 1992.

3. S. C. Jardin, N. Pomphrey, and J. Delucia, "Dynamic Modeling of Transport and Positional Control of Tokamaks," *J. Comput. Phys.* **66**, 481 (1986).

4. D. W. Swain et al., "The Ion Cyclotron Heating (ICH) System for BPX," in *Proceedings of the 17th Symposium on Fusion Engineering, San Diego, California, October 1–4, 1991*, IEEE, New York, 1992.

5. BPX memo L-92-0121-OR-01.

6. D. J. Strickler, Y-K. M. Peng, S. C. Jardin, and N. Pomphrey, "Dependence of CIT PF Coil Currents on Profile and Shape Parameters Using the Control Matrix," *Fusion Technol.* **19**, 1452 (1991).

7. J. R. Haines, Princeton Plasma Physics Laboratory, personal communication, 1991.

8. D. W. Weissenburger and U. R. Christensen, "A Network Mesh Method to Calculate Eddy Currents on Conducting Surfaces," *IEEE Trans. Magn.* **18**, 422 (1982); D. W. Weissenburger, *SPARK Version 1.1 User Manual*, PPPL-2494, Princeton Plasma Physics Laboratory, Princeton, New Jersey, 1988.

9. *ITER Concept Definition*, Vol. 2, ITER Documentation Series No. 10, International Atomic Energy Agency, Vienna, 1989, pp. 415–508.

10. P. H. Rebut, in *Fusion Technology 1990*, Vol. 1, North-Holland, Amsterdam, 1991, pp. 171–82.

11. M. A. Mahdavi et al., in *Plasma Physics and Controlled Nuclear Fusion Research 1990,* Vol. 1, IAEA, Vienna, 1991, pp. 335–43.

12. DIII-D Team, in *Plasma Physics and Controlled Nuclear Fusion Research 1990,* Vol. 1, IAEA, Vienna, 1991, pp. 69–91.

13. Y-K. M. Peng et al., "Small Steady-State Tokamak (TST) for Divertor Testing," in *Fusion Technology 1992,* ed. C. Ferro, M. Gasparotto, and H. Knoepfel, Elsevier, Amsterdam, in press.

14. Y-K. M. Peng et al., *The TST: A Small Steady-State Tokamak for Integrated Divertor Testing,* ORNL/TM-12216, Martin Marietta Energy Systems, Inc., Oak Ridge National Laboratory, 1993.

15. *ITER Concept Definition,* Vol. 2, ITER Documentation Series No. 10, International Atomic Energy Agency, Vienna, 1989, pp. 530–62.

16. A. Sykes et al., *Nucl. Fusion* **32**, 694–99 (1992); A. Sykes et al., "Behavior of Low-Aspect-Ratio Tokamak Plasmas," presented at the 1992 International Conference on Plasma Physics, Innsbruck, Austria, June 29–July 3, 1992.

17. Y-K. M. Peng, J. D. Galambos, and P. C. Shipe, "Small Tokamaks for Fusion Technology Testing," *Fusion Technol.* **21**, 1729–38 (1992).

18. S. O. Dean et al., "Pilot Plant: A Shortened Path to Fusion Power," presented at the 14th International Conference on Plasma Physics and Controlled Nuclear Fusion Research, Würzburg, Germany, September 30–October 7, 1992.

6

FUSION MATERIALS RESEARCH

E. E. Bloom[1]
Fusion Materials Program Manager

D. J. Alexander[1]
G. E. C. Bell[1]
T. D. Burchell[1]
L. T. Gibson[1]
G. M. Goodwin[1]
R. H. Goulding
M. L. Grossbeck[1]
E. A. Kenik[1]
R. L. Klueh[1]
A. W. Longest[2]
L. K. Mansur[1]
P. J. Maziasz[1]
J. E. Pawel[1]
R. L. Senn[2]
I. I. Siman-Tov[2]
R. E. Stoller[1]
K. R. Thoms[2]
P. F. Tortorelli[1]
R. Yamada[3]
S. J. Zinkle[1]

1. Metals and Ceramics Division.
2. Engineering Technology Division.
3. Japan Atomic Energy Research Institute, Ibaraki-ken, Japan.

6. FUSION MATERIALS RESEARCH

Summary of Activities

The Fusion Energy Materials Program has three major points of focus: (1) development of reactor structural materials, (2) development of first wall and high-heat-flux materials, and (3) development of ceramics for electrical applications. Within the Office of Fusion Energy, these efforts are supported by the neutron-interactive materials and the plasma-interactive materials programs. The ORNL effort supports U.S. participation in the International Thermonuclear Experimental Reactor (ITER) as well as the ultimate objective of making fusion an economically competitive, safe, and environmentally attractive energy source.

In the structural materials program, the primary emphasis is on the qualification of austenitic stainless steels for ITER and the development of low-activation ferritic steels, vanadium alloys, structural ceramics, and ceramic composites (e.g., SiC/SiC).

Austenitic steels are the leading candidate for structural applications in ITER because of their advanced state of development and commercial practice. In a collaborative program with the Japan Atomic Energy Research Institute, we are investigating the effects of fusion reactor radiation damage levels on the engineering properties of these alloys. Central to this effort is the irradiation of these alloys in the High Flux Isotope Reactor with tailoring of the neutron spectrum to produce damage levels [i.e., transmutation-produced helium and displacements per atom (dpa)] equivalent to those produced in a fusion reactor spectrum. These experiments are providing data and understanding of radiation response at temperatures and damage levels that are precisely those required for the ITER Engineering Design Activity (i.e., 60 to 400°C, up to 30 dpa).

Development of low- or reduced-activation materials is critical to achieving fusion's potential as a safe and environmentally attractive energy source. Development of low-activation ferritic steels requires that metallurgically important elements such as Ni, Mo, Nb, and N be removed or reduced to relatively low levels and that potential impurity elements be controlled to acceptable levels. To develop low-activation martensitic steels, tungsten is being used as a substitute for molybdenum, and niobium is replaced by tantalum and vanadium. The development activities are focused on the most critical or limiting property of this class of alloys—the radiation-induced shift in ductile-to-brittle transition temperature and reduction of fracture toughness. The vanadium alloys that are being considered for fusion have attractive activation characteristics, so compositional modification is not required to achieve this goal. The focus of our research on vanadium alloys is chemical compatibility with proposed fusion coolants and the effects of irradiation on fracture toughness. From the viewpoint of induced activation, SiC is the ultimate fusion structural material. Monolithic SiC is not considered because of its fracture properties, but SiC/SiC composites offer an

approach to improved fracture toughness. Our understanding of the performance of these materials in an irradiation environment is extremely limited. The focus of our present research is to explore the effects of irradiation on properties so as to provide a basis for accurately assessing the potential of SiC/SiC composites as fusion structural materials and to begin efforts to tailor these materials for the fusion environment.

The effects of irradiation on the dielectric properties of ceramic insulators are of critical importance in the successful design and operation of numerous systems in a fusion reactor (e.g., rf heating, plasma diagnostics). Our initial experimental work (initiated in 1991) has been directed at in situ measurements of the loss tangent during ionizing and ionizing-plus-displacive irradiation. Results to date show an increase in loss tangent of nearly two orders of magnitude at a displacement rate of 1×10^{-7} dpa/s. A change of this magnitude will affect materials selection and design of rf heating systems for ITER. Measurement of in situ properties will be expanded to investigate radiation-enhanced dielectric breakdown and the effects of irradiation on structural evolution and mechanical properties.

Graphite and carbon-carbon research activities are part of the plasma-interactive and high-heat-flux materials programs. Graphite and carbon-carbon composite materials are selected for these applications because their low Z number minimizes radiative heat losses from the plasma. However, their application requires graphite and carbon-carbon composites with extremely good thermal shock, erosion, and neutron damage resistance. Optimum thermal shock resistance is assumed to be offered by appropriately designed carbon-carbon composites (i.e., selected fibers, matrices, and architectures). Current work is directed toward the optimization of these materials for resistance to neutron damage.

6.1 STRUCTURAL MATERIALS

The multinational program to design and build the International Thermonuclear Experimental Reactor (ITER) is moving into the engineering design phase. Correspondingly, the Fusion Materials Program at ORNL is being refocused to address the following major tasks in the ITER R&D program in structural materials: austenitic stainless steels for the first wall and blanket (FWB) structure; structural materials for the divertor and blanket stabilizer; structural alloys for an advanced blanket module; and ceramic materials for diagnostic systems, insulators, feedthroughs, and windows.

An assessment was completed of the properties of a range of U.S. and Japanese steels irradiated to 7 displacements per atom (dpa) in an Oak Ridge Research Reactor (ORR) experiment spectrally tailored to reproduce the damage and helium generation rates characteristic of ITER. Further irradiation of this experiment to 20 dpa is continuing satisfactorily in the High Flux Isotope Reactor (HFIR) at temperatures of 60 and 330°C. Capsules for operation at 200 and 400°C will be inserted in HFIR mid-1992.

The results of the first phase of the spectrally tailored experiment raised several issues requiring further investigation.

Irradiation at 60 to 400°C produced large increases in yield stress and severe reductions in work-hardening capacity, which will have some impact on fracture toughness. Accordingly, three HFIR capsules were designed, constructed, and irradiated in HFIR target positions to a dose of 3.5 dpa. The capsules operate at 100 and 250°C and contain miniature compact tension specimens, sheet tensiles, and transmission electron microscopy (TEM) disks fabricated from U.S., Japanese, and European Community alloys.

A second important issue is radiation-assisted stress corrosion cracking in water. Preliminary electrochemical measurements on materials irradiated in the spectrally tailored experiments indicate that the ITER radiation environment will not induce susceptibility to cracking at temperatures below 330°C. Confirmation through in-cell SSRT in an autoclave is planned.

A third ITER FWB-related issue is that of repair welding once the machine has been activated. In a study conducted jointly with Auburn University, autogenous, single-pass, full-penetration welds were produced in type 316 stainless steel using a technique to introduce compressive stresses during welding. Helium was uniformly introduced into steels prior to welding using tritium doping and decay. Experimental results show that the grain-boundary helium bubble growth was effectively suppressed by the stress technique. Additionally, the bubble growth was altered such that the bubbles occurred predominantly on grain boundaries perpendicular to the weld, whereas previously they occurred principally on grain boundaries parallel to the weld direction. These results suggest that the proposed stress GTA welding technique may be used to eliminate the catastrophic cracking encountered during welding of helium-containing materials.

For advanced blanket modules, several ferritic-martensitic steels are being evaluated, and reduced-activation versions are being developed. Neutron irradiation experiments in HFIR, which simulated the simultaneous generation of helium and displacement damage characteristic of a fusion reactor first wall structure, showed that ferritic-martensitic steel structural alloys such as HT-9 and 9Cr–1MoVNb are highly resistant to both void swelling and grain-boundary embrittlement. Irradiations were carried out at 400 to 600°C to displacement doses (~80 dpa) that approach expected lifetime doses in fusion power reactors.

Neutron irradiation of HT-9 and 9Cr–1MoVNb at temperatures ≤ 400°C typically induces an increase in the ductile-to-brittle transition temperature (DBTT) of at least 100°C. These materials may then be susceptible to rapid cleavage crack propagation during certain low-temperature operating conditions. Alternative ferritic-martensitic steels have been developed with compositions tailored to reduce long-term radioactivity by three to four orders of magnitude. Initial results indicate that one of these new alloys based on 9Cr–2W,V,Ta has excellent resistance to radiation-induced loss of toughness. Neutron irradiation to ~7 dpa at 365°C resulted in an increase in DBTT of only 4°C. This is an encouraging indication that it should be possible to overcome the low-temperature radiation embrittlement problem in this class of alloys.

6.2 CERAMICS FOR ELECTRICAL APPLICATIONS: RADIATION DAMAGE STUDIES IN CERAMIC MATERIALS

Ceramic materials are specified for use in the fabrication of many components in current fusion reactor designs. Many of these applications rely on the high electrical

resistivity that these materials typically exhibit. The applications for insulating ceramics range from simple dc voltage standoffs to components in microwave heating systems that operate at high frequencies. Other potential applications depend on the structural stability of the ceramic material (e.g., swelling resistance). The well-known phenomenon of radiation-induced conductivity at dc or low-frequency ac conditions and the recently discovered phenomenon of radiation-induced electrical degradation give rise to concern about whether the candidate materials will retain their electrical properties when exposed to a radiation field that is typical of a deuterium-tritium (D-T) fusion reactor. Radiation-induced degradation of thermal conductivity could also lead to component failure due to high thermal stresses in components near the first wall.

A series of experiments has been completed to determine the influence of radiation on mechanical properties, microstructural evolution, and electrical properties of several candidate ceramic materials. The materials include sapphire, alumina, magnesium oxide, magnesium-aluminate spinel, aluminum nitride, silicon nitride, and silicon carbide. A theoretical analysis of the possible mechanisms whereby radiation could affect thermal conductivity has been used to plan additional experiments to investigate this parameter.

Mechanical properties have been measured on specimens of a silicon carbide composite material (CVD SiC/C/Nicalon) following neutron irradiation in HFIR to 1 and 3 dpa and irradiation with carbon ions to 30 dpa. Irradiation to 1 dpa in HFIR led to a 25% reduction in the composite strength and an increase in the toughness. However, a slight increase in strength and a large decrease in toughness were observed after 3 dpa. Two factors have been identified as responsible for this reversal in the properties. The matrix-composite interface initially opens because of densification of the Nicalon fibers, but subsequent swelling of the carbon interfacial layer closes this gap. Following high-dose carbon ion irradiation, the mechanical property changes are dominated by amorphization and swelling.

A significant influence of ionizing radiation on microstructural evolution has been observed following ion irradiation of alumina, magnesia, and spinel. These materials were irradiated using a range of charged particles: protons and helium, magnesium, aluminum, and argon ions. The irradiation temperature varied from 25 to 800°C. Dislocation loop formation was inhibited when the ratio of ionizing to displacive irradiation was above a material-dependent threshold value. For an irradiation temperature of 650°C, this value was ~1000 for alumina, 500–1000 for magnesia, and ~10 for spinel. These results indicate that irradiated ceramics may be more sensitive to the type and energy spectrum of the irradiating particle than are metals.

The dielectric properties of several ceramic materials have been measured in the presence of ionizing and displacive irradiation. The HFIR Gamma Irradiation Facility (GIF), which uses spent fuel elements from HFIR, was used to provide an intense source of ionizing irradiation for some of the measurements, and a pulsed fission reactor at the University of Illinois was used to provide an irradiation field that produced both ionization and atomic displacements. The dielectric measurements were made using a capacitively loaded resonant cavity, which is well suited to these measurements because the power dissipation in the ceramic relative to the balance of the experimental apparatus is maximized. These experiments used cavities that were sized to permit the measurement of the dielectric properties at 100 MHz, typical of ion cyclotron resonance heating systems. No effect of ionizing

radiation was observed in the HFIR GIF experiments at a damage rate of ~5 × 10^9 Gy/h, while a large increase in the dielectric loss was observed in the fission reactor irradiations. It is not possible to attribute all of the change observed in the fission reactor to the atomic displacements since the ionizing damage rate was up to 400 times higher than in the HFIR GIF. However, the ionizing and displacive damage rates in the fission reactor are within the range of those expected for ITER. Thus, the dielectric property changes observed in these experiments are directly relevant to ITER, and they highlight the need for a careful experimental program to verify the performance of candidate ceramic materials.

6.3 FIRST WALL AND HIGH-HEAT-FLUX MATERIALS

Research activities for fusion energy applications have been carried out in support of plasma-interactive or high-heat-flux materials needs. Graphite and carbon-carbon composite materials are selected for these applications because their low atomic number minimizes radiative heat losses from the plasma. Plasma-facing materials requirements include extremely good resistance to thermal shock, erosion, and neutron damage.

Carbon studies are focused in two major areas: experimental determination of the effects of neutron damage on candidate plasma-facing materials and the development of theoretical models for neutron-induced crystal structure damage in carbons. Postirradiation examination (PIE) of specimens from two HFIR irradiation experiments, HTFC I and II, was undertaken. These two capsules were irradiated at 600°C to peak damage levels of 1.6 and 4.7 dpa, respectively. The experiments contained a variety of carbon materials, including nuclear-grade graphite (H-451); one-, two-, and three-directional carbon-carbon composites; and a random-fiber carbon-carbon composite. Specimen PIE included dimensional, thermal conductivity, electrical resistivity, and strength (brittle-ring) measurements. These data were analyzed in terms of composite fiber type (precursor), architecture, and final heat-treatment temperature. Analysis of HTFC I data indicated that the most irradiation-stable carbon-carbon composite materials were three-directional materials manufactured from pitch precursor fibers that had been heat treated (graphitized) above 3000°C. These data were presented at the 20th Biennial Conference on Carbon in Santa Barbara, California, and a paper describing them has been submitted to the *Journal of Nuclear Materials*.

A computer model has been developed to simulate the behavior of self-interstitials with particular attention to clustering. Owing to the layer structure of graphite, atomistic simulations were performed using a large, parallelepipedic supercell containing two layers. Frenkel pairs were randomly produced. Vacancies were assumed immobile, whereas interstitials were given a certain mobility. Two point-defect sinks were considered: direct recombination of Frenkel pairs and interstitial clusters. The conditions under which interstitial clustering takes place were studied. It was found that when clustering occurs, the cluster size population gradually shifts toward large clusters. The implications of the present results for irradiation growth and irradiation-induced amorphization were discussed.

7

NEUTRON TRANSPORT

R. G. Alsmiller, Jr.[1]

J. M. Barnes[2]
C. Y. Fu[1]
D. M. Hetrick[1]
D. C. Larson[1]
R. A. Lillie[1]
J. B. Manneschmidt[1]
R. W. Roussin[1]
R. T. Santoro[1]
D. K. Trubey[1]
J. E. White[1]

1. Engineering Physics and Mathematics Division.
2. Computing and Telecommunications Division, Martin Marietta Energy Systems, Inc.

7. NEUTRON TRANSPORT

Summary of Activities

The neutron transport program includes two elements: the work of the Radiation Shielding Information Center (RSIC) and cross-section evaluation and processing.

Staff members of the RSIC serve as technical consultants to the fusion energy research community, as well as a variety of other research communities, on all matters relating to neutron transport. The evaluation and processing program is directed at producing accurate cross-section data for materials that are of specific interest to fusion reactor designers.

7.1 RADIATION SHIELDING INFORMATION CENTER

R. W. Roussin, D. K. Trubey, J. E. White, and J. B. Manneschmidt

The Radiation Shielding Information Center (RSIC) serves an international community by responding to inquiries about radiation transport problems. Staff members provide guidance by drawing on a technical database that includes a computerized literature file, a collection of complex computer programs, and a substantial body of nuclear data libraries pertinent to the solution of such problems.

Acquiring the needed computer-based technology base requires the collaboration of the neutronics community with RSIC staff members to collect, organize, process, evaluate, and package relevant technology developed in the community. This technology is disseminated to the community with a mechanism for feedback of experience through use, which results in an improved product. The resulting technology base provides an advancement of the state of the art.

A sample of recent technology products contributed as a result of this information cycle process shows the international character of the RSIC community. The Nuclear Energy Agency Data Bank, Saclay, France, contributed DLC-157/VITAMIN-J/COVA, a 175-neutron-group covariance data set based on Joint Evaluated File (JEF-1). The DLC-155/ACTIV-F/H neutron activation cross-section library for fusion reactor design was provided by the International Atomic Energy Agency's Nuclear Data Section. The Chinese Nuclear Data Center supplied the PSR-288/UNIFY-ECN cross-section nuclear model code.

From Japan came the University of Osaka's CCC-582/NITRAN radiation transport system using doubly differential cross sections, and an upgrade for the University of Tokyo's CCC-501/SUSD sensitivity and uncertainty analysis system. The DLC-150/VITAMIN-J/KERMA multigroup neutron kerma factors based on the European Fusion File were contributed by the ENEA, Bologna, Italy. The Paul Scherrer Institute, Würenlingen, Switzerland, supplied DLC-151/ MATXS175/42-JEF87 multigroup cross sections generated using NJOY with the JEF-1 file and also PSR-196/NJOY-UTIL-EIR programs to manipulate output files produced with NJOY.

The nuclear model code PSR-292/ EMPIRE for calculating cross sections was provided by the Institute of Nuclear Studies, Warsaw, Poland, and the neutron spectrum unfolding code PSR-295/SAIPS was contributed by the Latvian University, Riga, Latvia.

Major U.S. laboratories are also actively involved in neutronics developments that benefit the fusion community thanks to their availability from RSIC. Argonne National Laboratory developed and transmitted the PSR-305/KAOS-V neutron kerma factor processing system and generated and supplied the DLC-160/KAOSLIB multigroup neutron kerma factor data in the VITAMIN-E group structure. A unique one-dimensional discrete ordinates system for electron/photon transport, CCC- 544/CEPXS/ONELD, was contributed by Sandia National Laboratories and Los Alamos National Laboratories (LANL). LANL also supplied updates to the CCC-200/MCNP Monte Carlo radiation transport system and its cross-section library DLC-105/MCNPDAT, the cross-section processing system PSR-171/NJOY, and a package CCC-547/TWODANT-SYS, which includes the discrete ordinates codes TWODANT, TWOHEX, and ONEDANT. Lawrence Livermore National Laboratory (LLNL) updated the PSR-146/ALICE nuclear model code and provided a kerma factor library, DLC-142/KERMAL.

ORNL updated the CCC-336/ASFIT-VARI radiation transport code developed in India, contributed the nuclear model code PSR-298/TNG1 and the PSR-284/NUFACE interface code for calculating nuclear responses, and provided a new version of the three-dimensional discrete ordinates code CCC-543/TORT.

This selection represents a small portion of the total activity of the center. Information processing (including evaluation and packaging) is a daily function. In addition to a comprehensive literature database, RSIC-packaged products include 163 data packages (DLC), 602 neutronics and shielding code packages (CCC), and 315 data processing and other miscellaneous code packages (PSR).

7.2 DATA EVALUATION AND PROCESSING FOR FUSION NEUTRONIC DATA NEEDS

D. C. Larson, C. Y. Fu, D. M. Hetrick, and J. E. White

Evaluated and processed neutron cross-section data are produced to meet the needs of fusion reactor designers. Nuclear data needs for the magnetic fusion energy program are given in ref. 1 and include evaluated cross sections for copper, nickel, and chromium. Isotopic evaluations for chromium, copper, and nickel were accepted for ENDF/B-VI, which was released in 1990. Also accepted for ENDF/B-VI were isotopic evaluations for iron and lead and an evaluation for natural carbon. Several of the evaluations were selected by an international committee for inclusion in the Fusion Evaluated Nuclear Data Library (FENDL). This is the first version of ENDF in which

special attention has been paid to data of priority to fusion energy. All of this work has been jointly funded by the Offices of Fusion Energy, Basic Energy Sciences, and High Energy and Nuclear Physics in the U.S. Department of Energy and the Defense Nuclear Agency.

Evaluated cross sections must be processed into forms that can be used in radiation transport computer codes. The focus of this effort has been the development of VITAMIN-E,[2] a 174-neutron, 38-photon-group cross-section library. It can be used in conjunction with the AMPX-II system[3] to derive cross-section data suited to a particular application.

A continuing effort is under way to lead an international effort to develop a cross-section library in AMPX's format in 175-neutron, 42-photon-group structure (based on VITAMIN-E) from the ENDF/B-VI and other major evaluated libraries. A multigroup library in this group structure based on FENDL will be made available in the AMPX format. These libraries will be maintained on the National Energy Research Supercomputer Center at LLNL and will also be distributed by RSIC.

References

1. *Proceedings of the Fifth Coordination Meeting of Participants in the Office of Basic Energy Sciences Program to Meet High Priority Nuclear Data Needs of the Office of Fusion Energy, Argonne, Illinois, September 17–19, 1986*, Appendix D, DOE/ER/02490-4, Ohio State University, Columbus, 1986.

2. R. W. Roussin et al., *VITAMIN-E: A Coupled 174-Neutron, 38-Gamma-Ray Multigroup Cross-Section Library for Deriving Application-Dependent Working Libraries for Radiation Transport Calculations* [computer program], available from the Radiation Shielding Information Center, Engineering Physics and Mathematics Division, Oak Ridge National Laboratory, as DLC-113/VITAMIN-E.

3. N. M. Greene et al., *AMPX: A Modular Code System for Generating Coupled Multigroup Neutron Gamma Libraries from ENDF/B*, ORNL-3706, Union Carbide Corp. Nuclear Div., Oak Ridge National Laboratory, 1976.

8

NONFUSION APPLICATIONS

H. H. Haselton

Applications Development Manager

F. W. Baity
L. A. Berry
J. B. O. Caughman
L. Dresner
P. W. Fisher
C. A. Foster
W. L. Gardner
J. M. Googin[1]
D. J. Hoffman
D. A. Kirkman[2]
M. S. Lubell
J. W. Lue
J. N. Luton
R. J. Raridon[3]
S. W. Schwenterly
L. M. Thompson[1]
C. C. Tsai
J. H. Whealton
T. L. White

1. Development Division, Oak Ridge Y-12 Plant.
2. University of California, Irvine.
3. Computing and Telecommunications Division, Martin Marietta Energy Systems, Inc.

8. NONFUSION APPLICATIONS

Summary of Activities

The ORNL Fusion Energy Division actively seeks opportunities to apply technology developed in the fusion program to other areas. The concentration of program initiation and development efforts follows two guidelines: (1) the technology to be advanced is related to fusion in that the majority of advances expected to result from the work will directly benefit future fusion system designs and (2) the technology is expected to be applicable to fusion, although the initial application may not be directly fusion related.

The fusion technology areas on which development is based include plasma heating, plasma fueling, and magnetics and superconductivity. Technology applications are concentrated in four main technical fields: energy, U.S. Department of Energy facility environmental restoration and waste management, defense, and technology transfer to U.S. industry.

8.1 PLASMA HEATING TECHNOLOGY DEVELOPMENT

8.1.1 Microwave Processing of Radioactive Wastes

T. L. White

A proprietary microwave applicator developed for the Waste Handling and Packaging Plant (WHPP) project was modified to improve its power-handling capabilities and diagnostic access. The WHPP project was deferred pending U.S. Department of Energy (DOE) approval. The microwave technology developed for the WHPP waste form (sodium nitrate slurries) is being marketed for other wastes, such as ash and scrubber liquids from the Toxic Substances Control Act (TSCA) incinerator at the Oak Ridge K-25 Site. Interest in the microwave technology has been shown by staff at other DOE sites, including Los Alamos National Laboratory, Idaho National Engineering Laboratory, Savannah River Laboratory, and Hanford Engineering Development Laboratory.

Some initial testing was carried out on a concept to measure the average amount of water present in a drum of waste grout by means of a low-power, swept-frequency microwave cavity technique. Results were inconclusive because the 1-gal waste container chosen for the tests was too small to validate the technique. Further testing at the

55-gal scale will be required to demonstrate the concept.

A microwave heating process is being developed to remove radiologically contaminated surface layers from concrete. The microwave energy is directed at the concrete surface and heats the concrete and free water present in the concrete matrix. Continued heating produces mechanical stresses, induced by steam pressure, that cause the concrete to burst. The concrete particles from this steam explosion are small enough to be removed by a vacuum system, yet less than 1% of the debris is small enough to pose an airborne contamination hazard. The first phase of this program has demonstrated reliable removal of noncontaminated concrete surfaces at frequencies of 2.45 GHz and 10.6 GHz. Continuous concrete removal rates of 1.07 cm^3/s with 5.2 kW of 2.45-GHz power and 2.11 cm^3/s with 3.6 kW of 10.6-GHz power have been demonstrated. Figures of merit for microwave removal of concrete have been calculated to be 0.21 cm^3/s per kilowatt at 2.45 GHz and 0.59 cm^3/s per kilowatt at 10.6 GHz. The amount of concrete to be removed in a single pass can be controlled by choosing the frequency and power of the microwave system.

8.1.2 RF Sintering

F. W. Baity and D. J. Hoffman

Sintering of ceramic materials using microwave power can provide notable improvements in densification temperature, as discussed in ref. 1. However, these improvements are not seen in materials such as boron carbide. From first principles, one can determine that radio frequencies should induce higher fields than microwaves. We have built a test setup and densified ZTA, alumina, and boron carbide. Work is in progress to evaluate densification as a function of temperature and to determine the appropriate heating profile.

8.1.3 Plasma Processing

C. C. Tsai, J. M. Googin, H. H. Haselton, and L. M. Thompson

The ORNL plasma processing program began work on a novel technique for surface cleaning of finished workpieces, providing an alternative to conventional chemical cleaning techniques that should minimize the generation of secondary waste. This is a collaborative project with the Development Division of the Oak Ridge Y-12 Plant.

The surfaces of finished workpieces tend to be coated with thin layers of protective oxide that are contaminated with undesirable materials (grease, oils, cutting fluids, etc.) This contamination is usually removed by mechanical or chemical cleaning. Other potential methods are heating (e.g., electromagnetic, infrared, and ultraviolet), and plasma processing. The plasma-based methods that we are developing should provide uniform cleaning of workpiece surfaces without physical distortion, overheating, nonuniform heating, or hot spots.

Plasma generation based on microwave and rf techniques offers several approaches to surface cleaning, including plasma-assisted chemical etching, physical sputtering, and submicron-layer surface heating and evaporation. Ionized plasmas of argon, oxygen, or a mixture of these two gases with ion energies below 1000 eV have been successfully used for plasma etching in manufacturing electronics. We are working to develop and optimize these plasma etching techniques for surface cleaning of finished workpieces.

An existing microwave electron cyclotron resonance (ECR) multicusp plasma source[2,3] in the Plasma Source Laboratory

has been modified and prepared with a high-vacuum system, electrical supplies, and diagnostics. Figure 8.1 shows the test stand with the ECR plasma source, the vacuum chamber, and the vacuum system components. The laboratory has been equipped with control consoles, microwave and rf power supplies, and diagnostic equipment. The output of the microwave power supply is carried through waveguides and applied to the ECR plasma after the proper discharge conditions are established.

The vacuum system includes a turbomolecular pump with a pumping speed of about 400 L/s to maintain a base pressure of 1×10^{-6} torr in the vacuum chamber. The gas feed and vacuum system and the power supplies can control the gas pressure and plasma density in the source. During experiments, the ECR plasma source is operated by using the 2.45-GHz microwave power supply to create a plasma from the desired gas at pressures ranging from 0.1 to 10 mtorr. Two solenoid magnets control the plasma distribution over the sample holder. The rf biased supply controls the level of biasing to the sample holder and thus the energy of the incident ions.

The microwave plasma source has been operated with argon, oxygen, helium, and hydrogen. Plasmas created from different gases respond similarly to the effects of pressure, applied magnetic field, substrate biasing, and microwave power. Electrical

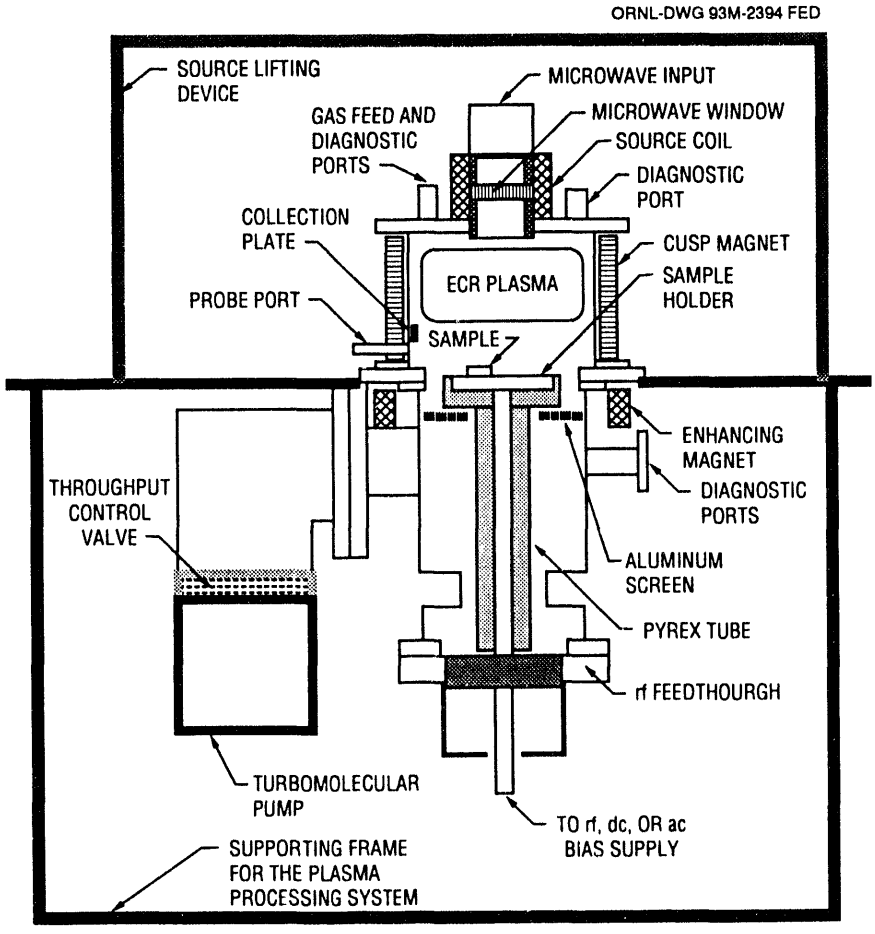

Fig. 8.1. ECR plasma cleaning experiment with biasing sample holder.

probe measurements, made at a plane 20 cm from the ECR zone in the microwave launcher, indicate that the plasma source has a density of 1×10^{11} cm^{-3} and a cold electron temperature of 2–5 eV. The plasma radial uniformity changes with the gas pressure, the biased potential of the sample holder, the input power, and the applied magnetic field. This plasma source can be used to create plasmas with hollow, flat, or peaked density profiles tailored to a particular geometry.

Data are collected for evaluating the progress of surface cleaning on test samples. A residual gas analyzer is used to monitor the offgas before and during discharges with and without test samples on the sample holder.

Small flat samples have been cleaned in oxygen and argon plasmas. Oxygen plasma processing has been used to demonstrate the removal of oil films of Shell Vitrea from sample surfaces. This has been confirmed by sample surface analysis conducted using x-ray photoelectron spectroscopy (XPS) analysis at Y-12.

8.1.4 Diamond Films

W. L. Gardner

Diamond film growth is being investigated as a part of a program for fundamental studies of chemical vapor deposition (CVD) materials growth processes. The goal of this program is to develop the diagnostics and advanced deposition techniques necessary to establish a program for fundamental studies of film growth by CVD processes. The program is a collaboration of three ORNL divisions: Fusion Energy, Metals and Ceramics, and Analytical Chemistry. Diamond film growth was chosen for study because diamond is a material with broad technological applications, there is local expertise for film growth, simple growth reactors are possible, the spectroscopy of hydrocarbon species is well established (combustion), and no toxic gases are required. Various processing techniques, diagnostics, and materials characterization techniques are being developed for CVD growth. With these we will gain knowledge of molecular dynamics, important process variables, and the relationship of film microstructures to material properties required to model growth and optimize film properties. For its part in the collaboration the Fusion Energy Division is providing an rf-based discharge reactor. The particular discharge technique being used dissociates molecular species required for diamond formation. Growth rates competitive with typical filament- and microwave-based processes have been achieved. We expect to integrate this reactor concept with the existing diagnostics located in the Analytical Chemistry Division in the near future. Additional support for this effort has also been provided by the RF Technology Group of the Fusion Energy Division to develop diamond coatings for Faraday shields.

8.1.5 Optics Calculations for Electrostatic Ion Thrusters

J. H. Whealton

Ion beam modeling techniques are being used to advance the technology for space thrusters, which may be necessary for future space propulsion. An ion thruster consists of a large plasma chamber, in which a source plasma is created, with a number of extraction holes and acceleration channels. The plasma sheath formed when the ions leave the thruster strongly affects the trajectories of the positive ions and electrons in the downstream plasma.

In the modeling studies, two- and three-dimensional optical calculations, including

both source and exhaust plasmas, are performed. These calculations include both a self-consistent ion source extraction plasma sheath and an explicit computation of the primary ion optics, including sheath- and electrode-induced aberrations. A study has been carried out to determine the effects of beam space charge, accelerator geometry, and properties of the downstream plasma sheath on the position of the saddle point in the electrostatic potential near the extractor electrode. The height of the electron blocking potential barrier as a function of electrode thickness and secondary plasma processes has been determined. The results have been compared with those of earlier work for various perveances and secondary plasma potentials. The effects of accelerator electrode thickness and of space charge on blocking potential are being examined. Studies to evaluate the effect of the secondary plasma potential and space charge on secondary ions from the exhaust plasma are also in progress.

8.2 PLASMA FUELING TECHNOLOGY DEVELOPMENT

8.2.1 Argon Pellet Cleaning

C. A. Foster

A study of the use of high-velocity solidified gases for cleaning metals was begun in 1991. An existing centrifugal pellet accelerator in the Fusion Energy Division was modified to test the capability of solidified gases for cleaning material surfaces.

Any solidified gas can be used as a cleaning medium in this apparatus; argon is particularly useful because it is inert and will not react chemically with reactive metals. Continuous production of good-quality solidified argon pellets has been demonstrated. Samples of oxidized steel have been cleaned, demonstrating the feasibility of the technique. A prototype apparatus with significant throughput capability will be fabricated for use and tested.

8.2.2 CO_2 Pellets for Paint Stripping

P. W. Fisher

The argon pellet cleaning concept described in Sect. 8.2.1 has been extended to the use of CO_2 pellets for removal of paint from surfaces. A project is under way to develop a "cryoblaster" that provides pellets of frozen CO_2 for stripping paint from aluminum substrate. Initial results indicate that this process might be superior to the system presently used at Warner Robins Air Logistics Center to remove paint from aircraft.

8.3 MAGNETICS AND SUPERCONDUCTIVITY TECHNOLOGY DEVELOPMENT

8.3.1 Superconducting Motor Research and Development

S. W. Schwenterly

The first tests of a unique axial-gap superconducting motor, shown in Fig. 8.2, were carried out in September 1990 and November 1990 in the Superconducting Motor Research Facility (SMRF) at the Oak Ridge K-25 Site. The motor incorporates a four-pole superconducting stator that produces an axial dc magnetic field. This component was designed and fabricated by the Magnetics and Superconductivity (M&S) Section and by the Y-12 shops. The armature contains radial copper conductors that are energized via slip rings with three-phase ac power from a solid-state invertor. A light-emitting diode (LED) encoder on the shaft controls current switching to the armature coils. The armature, shaft, and ac drive

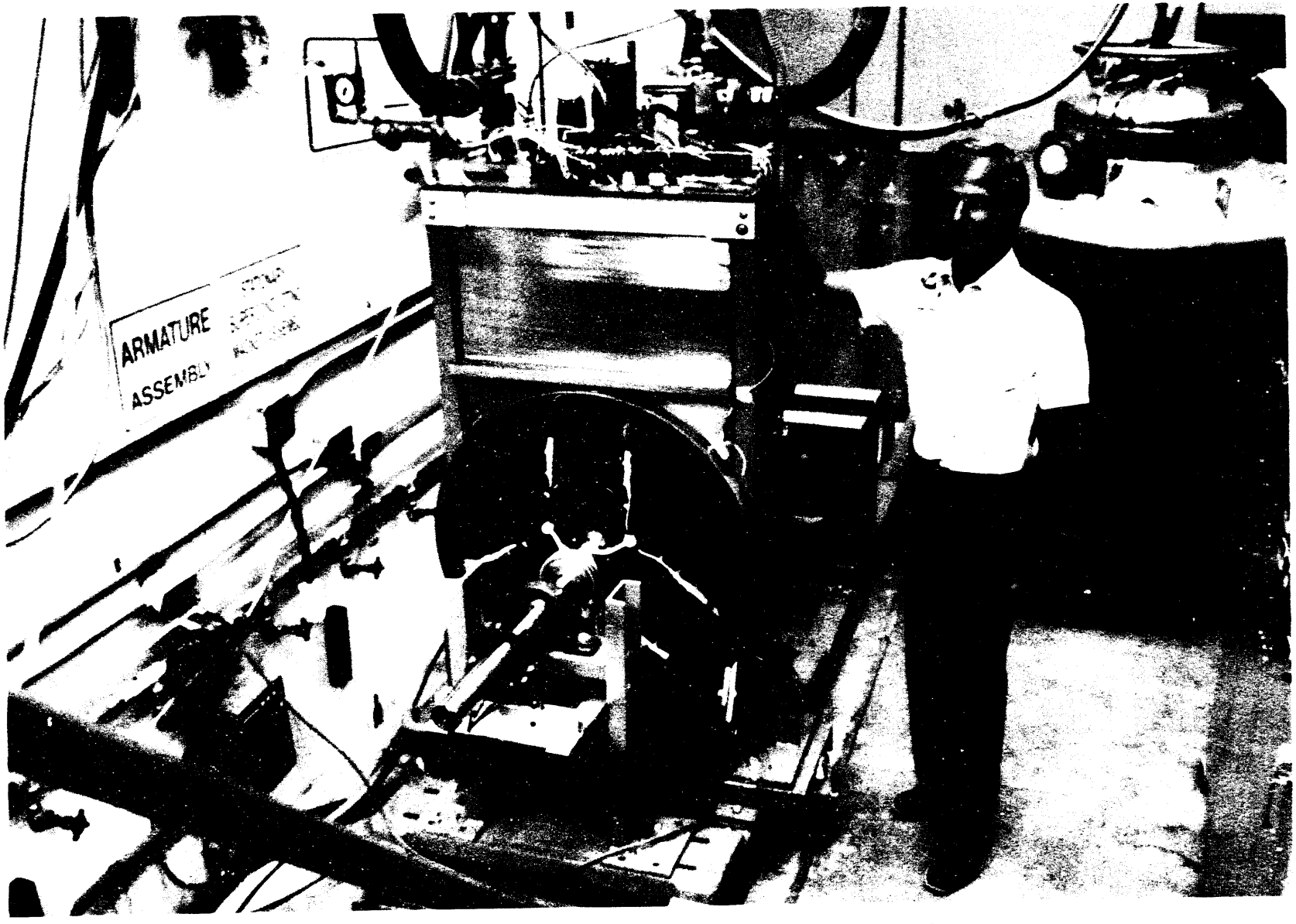

Fig. 8.2. The axial-gap superconducting motor installed in the SMRF.

package were designed and fabricated by personnel from the Applied Technology, Energy, Engineering Technology, and Instrumentation and Controls divisions and the University of Tennessee.

In the initial series of tests, the motor was limited to 600 rpm because there is no enclosure around the armature to contain fragments in case of mechanical failure. The design speed is 1800 rpm. During the first test run, the stator was cooled down and filled with liquid helium (LHe) in about 8 h and charged in steps to a current of 2200 A (79% of the critical current) with no difficulty. This produced a maximum axial field of 2 T, as measured by a Hall probe on the warm surface of the cryostat. The field could be reduced to zero in about 5 s without driving the magnets normal.

In locked-rotor tests, a maximum torque of 84 N•m (62 ft-lb) was produced. However, with the armature rotating, large electrical drag forces appeared and limited the no-load speed to 400 rpm. This was traced to ac eddy currents circulating in internal loops produced by the series-parallel connection of the armature coils. These loops were eliminated by disconnecting half of the coils, and another test run was made. The dissipation was practically eliminated, and the maximum allowable 600 rpm was reached easily with no load. When the motor was loaded by the dynamometer and the armature current was increased, large current spikes were produced by the solid-state switches. These tripped off the invertor and limited the power output to about 2 hp. It is expected that these spikes can be reduced by adding inductances between the invertor and the armature. The stator fields have not been affected by the ac field of the armature. The second test run was filmed for the Cooperative Research and Development Agreement (CRADA) videotape being produced by ORNL.

8.3.2 SSC Analysis

L. Dresner, M. S. Lubell, and J. W. Lue

Very large propagation velocities, ranging from 75 m/s to 225 m/s depending on the current, have been observed in the Superconducting Super Collider (SSC) 17-m dipoles. These velocities are much larger than those predicted by the classical conduction theory of normal zone propagation. A possible explanation for this rapid propagation is a hydrodynamic mechanism called thermal hydraulic quenchback (THQ), proposed by Luongo et al.[4] An approximate analytic theory of THQ was developed and used to analyze the propagation data from the SSC dipoles. It was concluded that THQ in the helium in the interstices of the cable can explain the large propagation velocities observed. Additional experiments were proposed to test the hydrodynamic explanation.

8.3.3 SSC Detector Design

J. N. Luton

Particle detectors whose bending magnets are toroidal arrays of individual coils are of interest for the SSC. In a cooperative program with Princeton Plasma Physics Laboratory, M&S Section staff members studied the feasibility of particle detectors with air-core superconducting toroidal magnets for high-resolution measurements of muon momenta. The results, described in ref. 5, were favorable.

As the detector requirements evolved, it became necessary to minimize interactions of the magnet winding and structure with the passing particles, and a further study was carried out to examine the feasibility of low-mass conductors (e.g., aluminum) for these detectors.[6] This study, sponsored in part by the State University of New York at Stony Brook, concentrated on cable-in-conduit

superconductors that use aluminum alloy for the conduit and pure aluminum for stabilization of the superconductor.

An unoptimized sample design that used a residual resistivity ratio of 1360 for aluminum and a current density of 3.5 kA/cm^2 over the uninsulated 32-kA conductor for a 4.5-T toroid with 1 GJ of stored energy (Fig. 8.3) resulted in a hot-spot temperature of 120 K with a maximum dump voltage of 3.6 kV and inductive transfer of 24% of the initial current into the shorted aluminum structure. The stability margin was 200 mJ per cubic centimeter of cable space. Limiting the quench pressure to 360 atm to give conservative stresses in the sheath and assuming that the entire flow path quenched immediately resulted in a distance of 1 km between helium taps if the flow friction factor is the same as that experienced in the coil produced by Westinghouse Electric Corporation for the Large Coil Task. This indicates that the 530-m conductor length of each of the 72 individual coil segments would be a single flow path. If some practical uncertainties can be resolved by producing and testing sample conductors, the use of a conductor with clad-aluminum stabilizer and extruded aluminum alloy sheath should be both feasible and economical.

8.3.4 Cryogenic Thermography

S. W. Schwenterly

The surface temperature of an object can be measured thermographically by applying a phosphor to a small area, illuminating this area with an ultraviolet (uv) laser pulse, and observing the decay times of various emission lines. Work in the Applied Technology Division (ATD) had shown a dependence of temperature on decay time in some materials; this dependence extended to liquid nitrogen temperature, 77 K.

In a collaborative program with ATD personnel, members of the M&S Section demonstrated that usable sensitivity could be obtained at LHe temperature, 4.2 K. As part

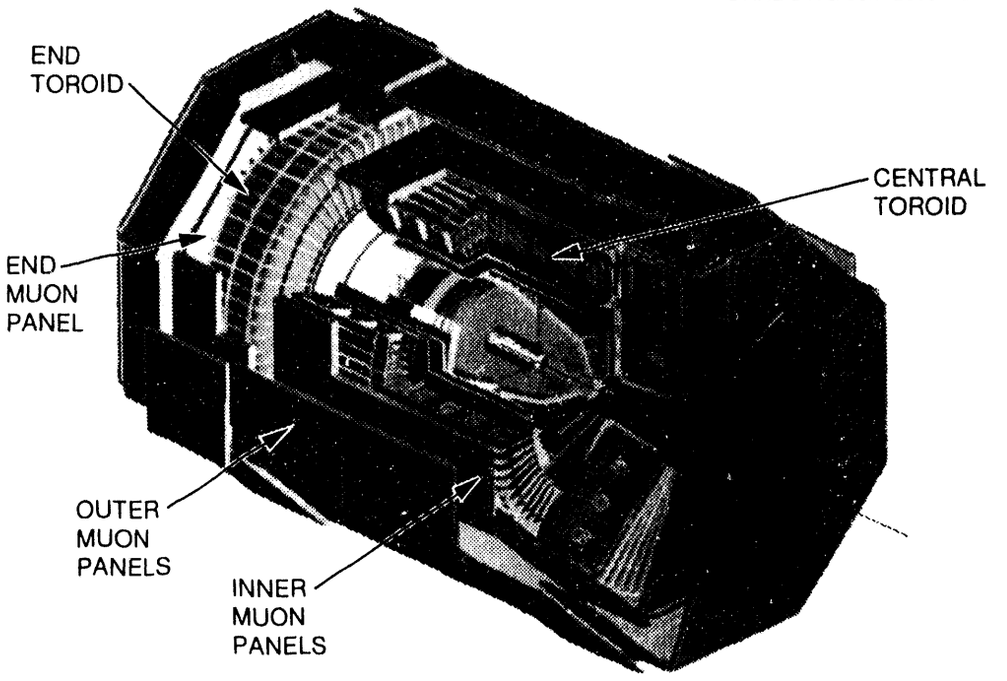

Fig. 8.3. SSC muon detector.

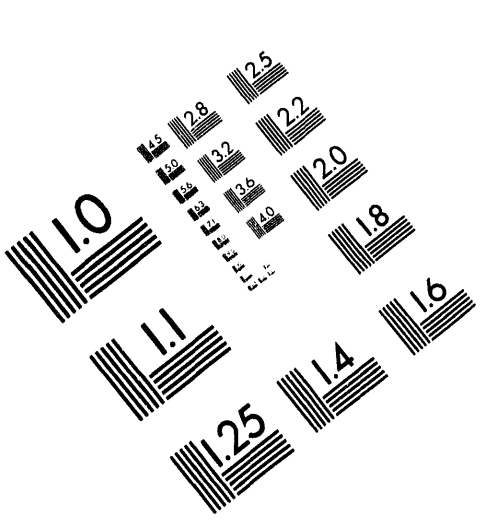

Association for Information and Image Management
1100 Wayne Avenue, Suite 1100
Silver Spring, Maryland 20910
301/587-8202

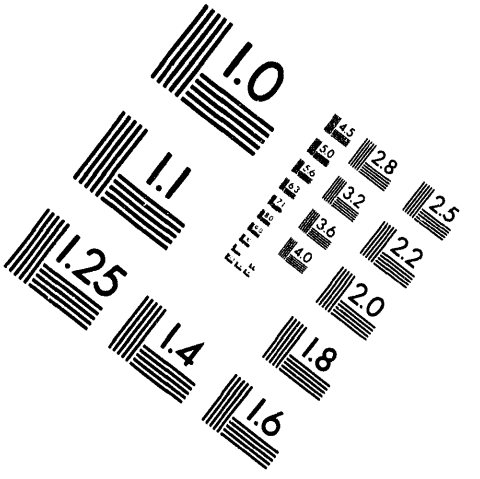

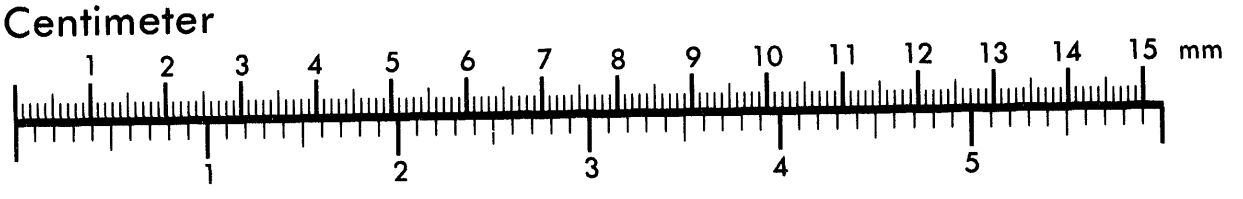

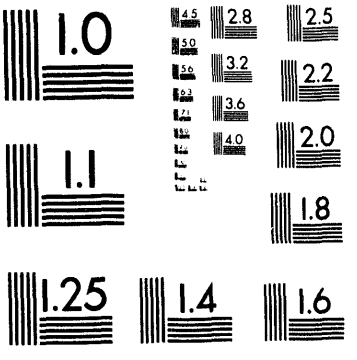

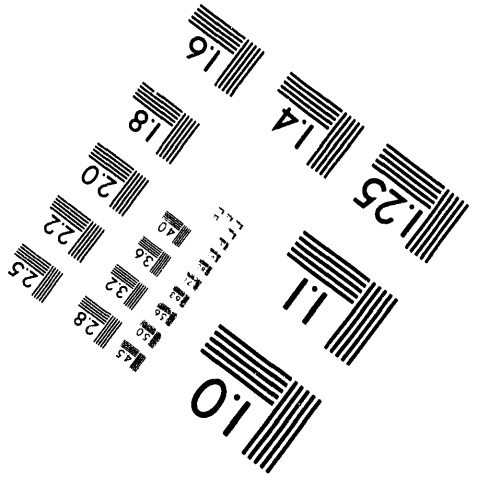

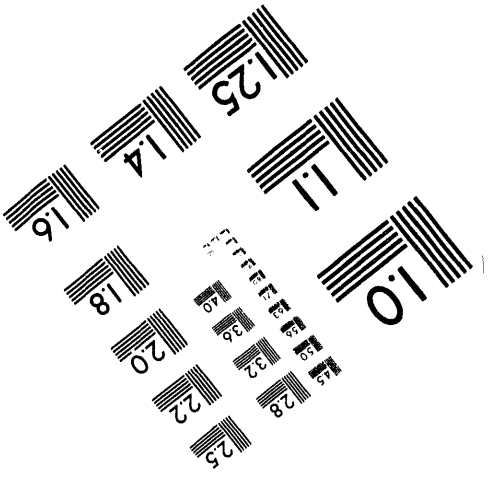

MANUFACTURED TO AIIM STANDARDS
BY APPLIED IMAGE, INC.

3 of 4

of a program to develop cryogenic thermography for NASA, a compact, variable-temperature cryostat that will fit into a standard LHe dewar was designed and fabricated.

The phosphor sample was pressed into a shallow, 6-cm-diam cup in a temperature-controlled copper block suspended above the LHe surface by a stainless steel tube. An optical fiber brought in the excitation light pulse from the uv laser, and a second optical fiber led the emitted light out to a monochromator and photomultiplier tube. Several different phosphors were surveyed to determine the decay time temperature dependences in their emission lines. In one of the better materials, manganese-doped magnesium fluorogerminate, the decay time of the 657-nm line increased from 4.7 ms to 5.5 ms as the temperature was lowered from 150 K to 10 K. The observed temperature depended linearly on the logarithm of the decay time.

Thermographic thermometry offers several advantages for applications in cryogenic equipment. Because there are no electrical leads to the phosphor, sensor heat loads can be minimized, and it is easy to make measurements on moving or rotating objects. Because the phosphor is in intimate contact with the surface and needs no electrical insulation, fast response is possible. The optical fibers are electrical insulators, so temperatures on conductors at high voltage can be measured easily and safely. Finally, the measurement may be insensitive to magnetic fields, although this remains to be determined. The sensitivity increases at higher temperatures, and the method should have many applications at near-ambient temperatures or on equipment using the new high-temperature ceramic superconductors.

8.3.5 Development of Lightweight, High-Performance Coils

J. W. Lue, L. Dresner, and M. S. Lubell

A cable-in-conduit force-cooled superconductor was chosen as the conductor form for developing lightweight, high-performance superconducting magnets. Two 127-mm-ID, 221-mm-OD test coils have been fabricated; one of these is shown in Fig. 8.4. The conductors have rectangular

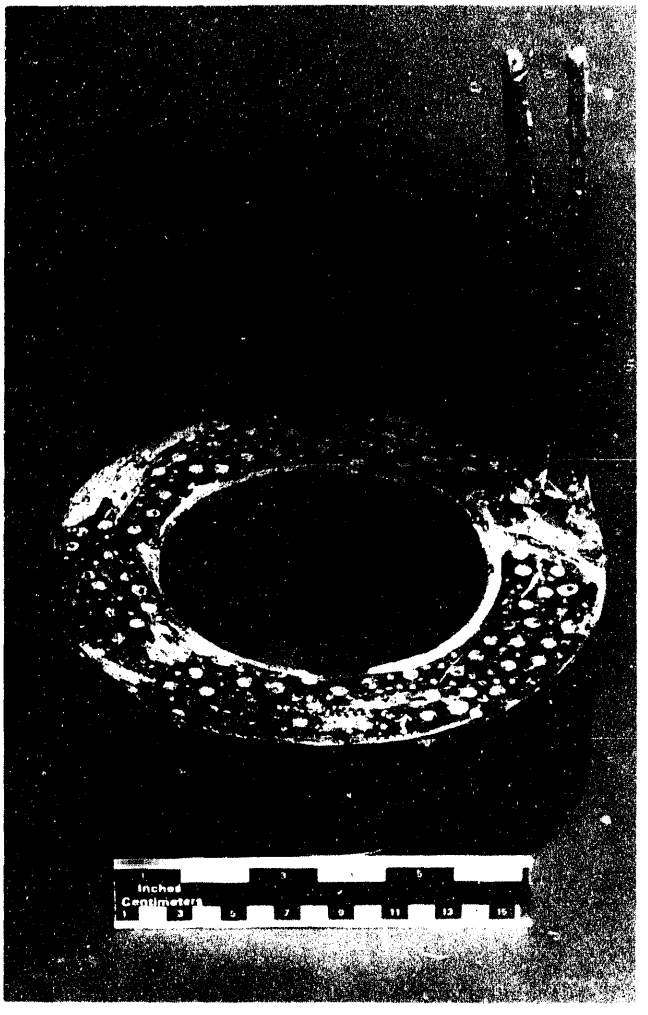

Fig. 8.4. Development magnet with cable-in-conduit force-cooled superconductor.

(7.2-mm by 5.8-mm) oxygen-free, high-conductivity (OFHC) copper conduit. One has a superconducting cable pattern of 6×5 around a copper core, and the other has a 9×6 pattern around a copper core. The void fractions inside the conduit are 26 to 28%, substantially lower than those used elsewhere. The conductor was wrapped with a carbon fiber stocking, and the winding was vacuum impregnated with epoxy to form a rigid structure. Thermal analysis indicates that these coils should be stable at a conductor current density of ≥ 10 kA/cm^2 at 8 T.

8.3.6 Support for Superconducting Magnetic Energy Storage

M. S. Lubell and L. Dresner

Experts from the M&S Section served on a review panel for a project to develop superconducting magnetic energy storage (SMES) with funding from the Defense Nuclear Agency and the Electric Power Research Institute. The project, which involved teams headed by Bechtel National, Inc., and Ebasco Services, Inc., called for the design, fabrication, and testing of a 20-MWh experimental test model to demonstrate the viability of large (2- to 5000-MWh) SMES systems. The phase I design effort was successfully completed at the end of FY 1991.

8.3.7 SSC Cryogenic Systems Development

S. W. Schwenterly

A project was begun in October 1990 to assist the SSC Laboratory in planning and designing the cryogenic systems for the Accelerator Main Ring and the Accelerator System String Test. Division staff participated in the preparation of equipment specifications and carried out technical surveillance of the progress of selected vendors in equipment design and fabrication.

8.3.8 Low-Mass Conductor Development

J. N. Luton

A project was carried out to produce a sample length of low-mass conductor by production means that would be applicable to long lengths of conductor. High-energy particle detectors with long interaction lengths, transportation magnets or other magnets that must be low in weight, and magnets for containing fusion plasmas are possible applications.

Multifilamentary NbTi in a copper matrix was selected as the superconductor, with a cladding of pure aluminum to serve as the stabilizer. These strands are cabled together in several stages, and the cable is wrapped with Kapton or stainless steel foil to hold the cable's shape and to prevent dirt or materials from the sheath (added later) from entering the interstices between strands. The sheath is added by a hot continuous process and, if necessary, turk's-headed to reach its final rectangular shape with the desired cable void fraction.

M&S staff members located and purchased existing aluminum-clad strands of superconductor that had been produced for another development program. The sample design was modified to fit the strand dimensions, and cabling was contracted to an outside firm. Although this firm had extensive experience with cabling superconducting strands, the aluminum cladding changed the workability of the strands, affecting the best

choice of twist pitch lengths, and the schedule and cable quality were affected

Another firm was engaged to apply a sheath to lengths of plain aluminum stranded cable with the same diameter as the superconducting cable. A high-quality seamless sheath around slightly compacted strands, with suitable interstices, was produced. The Kapton foil did not have enough elongation to remain intact, but the stainless steel foil produced good results.

Trials on the superconducting cable were not as successful because its greater irregularity and compactability led to sheaths of poor quality. No other suitable strands have been located, so further short-sample trials with a modified process will be carried out before the main sample length is processed.

8.3.9 Energy Storage Solenoid

L. Dresner

As part of the design of a 1-kWh, high-field SMES solenoid, a survey was conducted to determine magnet sizes and shapes that fulfilled prescribed requirements for total stored energy and maximum field at the conductor. On the basis of the survey results, the size and shape of the solenoid were chosen. A pool-boiling layer winding and a forced-flow winding were designed for illustrative purposes. This work is described in detail in ref. 7.

8.3.10 SMES Survey

L. Dresner

A survey of domestic research on SMES was conducted. Each entry contains

- the name, address, and telephone and facsimile numbers of the principal investigator and other staff members;
- funding for FY 1991, FY 1992, and FY 1993;
- brief descriptions of the program, technical progress to date, and expected future progress; and
- a note on other collaboration.

The survey was published by the ORNL High-Temperature Superconductivity Pilot Center.[8]

References

1. H. D. Kimrey et al., "Microwave Sintering," pp. 212–215 in *Fusion Energy Division Annual Progress Report: Period Ending December 31, 1989*, ORNL-6624, Martin Marietta Energy Systems, Inc., Oak Ridge National Laboratory, Oak Ridge, Tennessee, 1991.

2. C. C. Tsai et al., "Potential Applications of an Electron Cyclotron Resonance Multicusp Plasma Ion Source," *J. Vac. Sci. Technol. A* **8**, 2900 (1990).

3. C. C. Tsai, "Potential Applications of a New Microwave ECR Multicusp Plasma Ion Source," p. 1166 in *Application of Accelerators in Research and Industry* **90**, North-Holland, Amsterdam, 1991.

4. C. A. Luongo, R. J. Loyd, and C. L. Chang, "Current Diffusion Effects on the Performance of Large Monolithic Conductors," *IEEE Trans. Magn.* **25**, 1576–81 (1989).

5. J. N. Luton and P. Bonanos, *Toroidal Detector Scoping Study*, SSCL-N-697, Superconducting Super Collider Laboratory, Dallas, Texas, March 1990.

6. J. N. Luton, "The Feasibility of Low-Mass Conductors for Toroidal Superconducting Magnets for SSC Detectors," pp. 569–71 in *Proceedings of the Symposium on Detector Research and Development for the Superconducting Super Collider, October 15–18, 1990*, World Scientific Publishing Co., Singapore, 1991.

7. L. Dresner, *Design Considerations for a 1-kWh Energy Storage Magnet*, ORNL/HTSPC-2, Martin Marietta Energy Systems, Inc., Oak Ridge National Laboratory, Oak Ridge, Tennessee, January 1992.

8. L. Dresner, *Survey of Domestic Research on Superconducting Magnetic Energy Storage*, ORNL/HTSPC-1, Martin Marietta Energy Systems, Inc., Oak Ridge National Laboratory, Oak Ridge, Tennessee, September 1991.

9

MANAGEMENT SERVICES, ES&H ACTIVITIES, AND QUALITY ASSURANCE

Management Services

F. E. Gethers*

A. C. Atencio[1]
S. B. Armstrong
B. J. Beem[2]
S. A. Boatman[1]
J. L. Burke
M. G. Eckerd[1]
C. H. Johnson[1]
D. Y. Johnson[1]
L. M. Johnson[3]
I. A. Kunkel
R. A. Langley*
M. R. McBee[1]
J. C. Neeley[1]
M. B. Nestor
J. C. Parrott[1]
T. F. Rayburn
W. J. Redmond*
J. O. Richardson
E. M. Ruckart
D. G. Sharp[4]
B. J. Smith[1]
P. A. Sumner[1]
E. W. Whitfield[1]
S. J. Yates[2]

ES&H Activities

F. E. Gethers*

R. A. Langley,* Radiation Control Officer
D. A. Rasmussen,[5] Laser Safety Officer
W. J. Redmond,* Environmental Protection Officer

Quality Assurance

L. M. Jordan[6]

---

*Dual capacity.

1. Publications Division, Martin Marietta Energy Systems, Inc.
2. Group secretary.
3. Finance and Materials Division, Martin Marietta Energy Systems, Inc.
4. Graphics Division, Martin Marietta Energy Systems, Inc.
5. Toroidal Confinement Section.
6. Quality Department.

9. MANAGEMENT SERVICES, QUALITY ASSURANCE, AND ES&H ACTIVITIES

Summary of Activities

Broad technical and administrative support for the programmatic research and development activities of the Fusion Energy Division is provided by the Management Services Group and by the division's environmental, safety, and health (ES&H) and quality assurance (QA) programs.

The Management Services Group provides support in the following areas:

- General personnel administration, material and service procurement, subcontracting, and coordination of national and international agreements.
- Nonprogrammatic engineering services for support systems and equipment; identification, planning, and coordination of general plant project and facility improvements; coordination of maintenance and production shop work; labor relations; and telecommunications.
- Financial management.
- Library services and resources.
- Publications services.

Support is provided through effective communication with division programmatic staff and through the coordination of resources from disciplines outside the division.

The division's ES&H activities include a formal safety program, environmental protection services, and self-assessment activities. The safety resource team established in 1989 continued to identify and resolve safety-related issues. A database is in place to identify and track ES&H deficiencies, which are being corrected using a graded approach.

The QA activity in the division emphasizes the development and documentation of a QA program that conforms to national standards, the review and approval of engineering documents, supplier surveillance, identification and documentation of nonconforming items, audits, and QA assessments/plans.

9.1 MANAGEMENT SERVICES

9.1.1 General Administration Services

9.1.1.1 Personnel

In response to declining budgets, staff levels in the Fusion Energy Division (FED) dropped during the period, from 135 employees on December 31, 1989, to 130 employees on December 31, 1990, and then to 110 employees on December 31, 1991. The composition of the division's scientific and technical staff over the past five years is shown in Fig. 9.1.

The University and College Co-Op Program sponsored three students (one from the University of Tennessee, in electrical engineering, and two from the Georgia Institute of Technology, one in nuclear engineering and one in physics) in 1990 and four students (two from the University of Tennessee, one in electrical engineering and one in physics, and two from the Georgia Institute of Technology, one in nuclear engineering and one in physics) in 1991. University subcontracts brought 11 students to the division in 1990 and 12 in 1991; 11 technical students participated in university programs in 1990, with 9 in 1991. The division was host to 12 international scientific guests and 14 subcontractors in 1990 and to 9 international guests and 11 subcontractors in 1991.

Division personnel served on long-term assignments to other laboratories; in 1990, two staff members were assigned to the Joint European Torus (JET) in Abingdon, England, as part of the JET Joint Undertaking, and six were assigned to the Tore Supra tokamak at the Centre d'Etudes Nucléaires, Cadarache, France. In 1991, there were three division staff members at JET and two at Tore Supra. Long-term domestic assignments to General Atomics in San Diego, California, involved two staff members in 1990 and three in 1991. Three division employees were on relocation assignments for 1990 and 1991.

9.1.1.2 Procurement

During 1991, the division's procurement group processed 1025 requisitions, with a total value of about $1.2 million, and 380 shipping orders. This group actively monitors 200 to 300 open purchase orders.

An effort is under way to establish a shipping order database as a tool for tracking outstanding loaned equipment. This project was approximately 25% complete at the end of 1991.

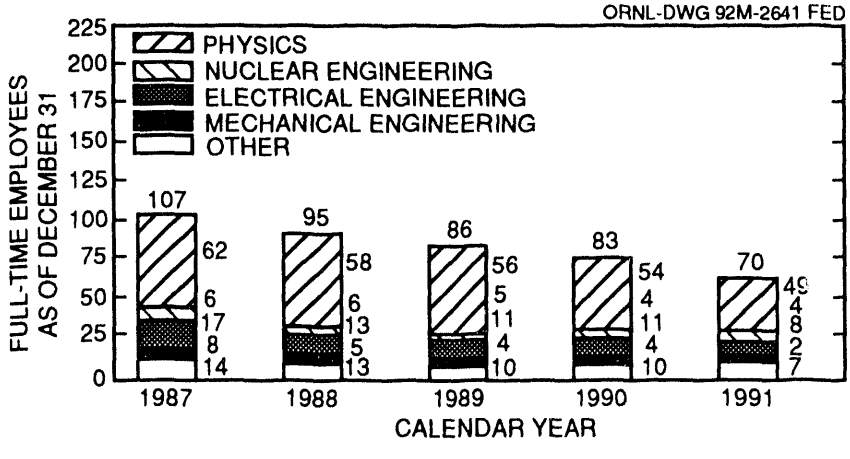

Fig. 9.1. Fusion Energy Division professional staff by discipline.

Industrial participation through subcontracts to the division approximated $0.4 million in 1991. Most of the subcontract cost ($0.3 million) was applicable to the ORNL Fusion Program.

9.1.1.3 International agreements and collaborations

The division participated in several personnel exchanges and collaborations during 1990 and 1991. The Management Services Group (MSG) played a key role in organizing these activities, with responsibility for coordinating administrative, legal, and protocol matters for outbound Fusion Program representatives and inbound international guests.

In this capacity, MSG staff members worked with the ORNL Office of Guest and User Interactions, the ORNL and Y-12 Plant security organizations, the Office of General Counsel and the Office of the Comptroller and Treasurer of Martin Marietta Energy Systems, and the Washington and Oak Ridge offices of DOE, as well as other service and support organizations. Responsibilities included ensuring adherence to general laboratory and company policies and to federal laws and procedures, monitoring the processing of paperwork to ensure timeliness and accuracy, obtaining the necessary approvals, and generally supporting the satisfactory implementation of exchanges, cooperative programs, and collaborations.

9.1.2 Engineering Services

The Engineering Services Group coordinates all engineering and maintenance work performed on general facility additions, modifications, and repairs in the division. Despite limited resources, work continued to improve the physical facilities during the reporting period. Engineering Services Group staff worked closely with the Engineering Division of Energy Systems, with division staff members, and with Y-12 Maintenance Division to implement needed improvements.

Major areas of effort during 1990 and 1991 included the completion of phases I and II of the General Plant Project (GPP) for restoration of 480-V electrical systems in Bldg. 9201-2. The 45-year-old transformers and switch gear of four 480-V power distribution substations were replaced. A proposal is in progress to replace one additional substation; this would complete the restoration of one of the building's four transformer vaults.

The division was one of the first organizations to participate in a plant-wide effort to correct National Pollutant Discharge Elimination System (NPDES) violations involving discharges into the East Fork of Poplar Creek. A number of building drains were connected to the sanitary sewer system instead of the storm drain system, which discharges into the creek. The Engineering Services Group worked closely with Environmental Management and Y-12 Maintenance Division personnel to correct this problem.

Operations performed by previous occupants of Bldg. 9201-2 had left low levels of fixed alpha and beta contamination in concrete floors in the building. Covering these areas with vinyl floor tile to prevent exposure to this contamination has considerably improved the appearance of these areas.

Emphasis on housekeeping and safety continued through the period. A high level of importance was placed on compliance with codes, standards, and procedures imposed for the protection of employees and the environment.

9.1.3 Financial Services

The Finance Office is a functional part of the MSG and provides financial manage-

ment support for administrative, engineering, and research personnel in areas including budget preparation, cost scheduling, and variance analysis. The office also provides meaningful and appropriate accounting and cost control. Interaction with division management is an essential part of administering the budget, accounting policies, and procedures. Figure 9.2 and Table 9.1 show the funding trends for the ORNL Fusion Program.

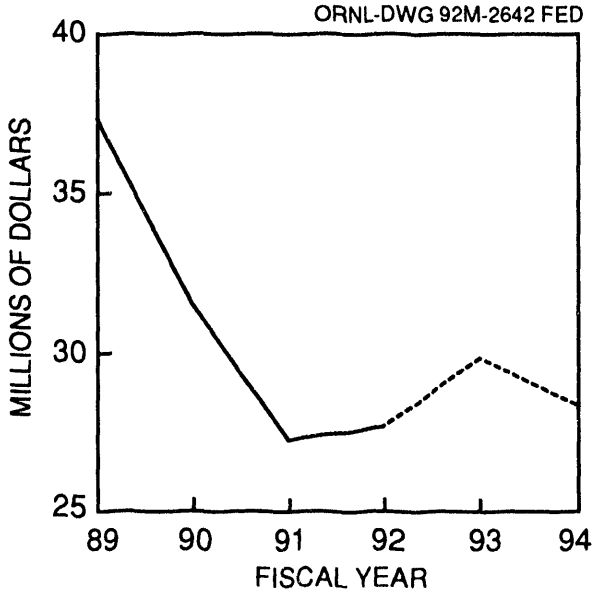

Fig. 9.2. Fusion Program expense funding (budget outlay).

9.1.4 Library Services

The Fusion Energy Library maintains a specialized collection in plasma physics and fusion technology and is a branch of the Information Services Division Library System that serves Energy Systems. Library staff members select materials for acquisition, provide reference assistance and online literature searching, circulate library materials, and retrieve information in support of research activities.

During 1990 and 1991, additional shelving units and microfiche cabinets were obtained to increase the storage capacity of the library annex, and an air conditioning unit was installed there. A third workstation was created with the acquisition of a Northgate 386 computer and a LaserJet printer. The library held an open house during National Library Week each year, featuring free online searching and demonstration of CD-ROM databases.

A usage survey of the library's journal subscriptions was conducted to determine which journal titles were seldom used and could be replaced by new subscriptions to journals of greater interest to library users.

9.1.5 Publications Services

Publications services are provided to FED by the Engineering Technology/Fusion Energy Division Publications Office (ET/FE DPO), which serves both FED and the ORNL Engineering Technology Division (ETD). The publications office provides technical editing and writing, composition, conventional and computer graphics, and reproduction services. It also serves as liaison with the Laboratory Records Department of the Energy Systems Information Services Division for clearance of all documents prepared by FED staff.

The range of services available reflects the capabilities provided by the diverse skills of the 18 staff members, a wide variety of computer hardware and software, and two new copiers. The ET/FE DPO is committed to providing high-quality, cost-effective publications support to its customers.

9.2 ES&H ACTIVITIES

The division has continued to direct significant efforts toward the improvement of its environmental, safety, and health

Table 9.1. Fusion Program expense funding (in thousands of dollars)—budget outlay

Activity	FY 1989 Actual cost	FY 1990 Actual cost	FY 1991 Actual cost	FY 1992 Funding as of April 1992	FY 1993 Budget submission	FY 1994 Budget submission
Applied plasma physics						
Toroidal theory	$2,465	$2,172	$2,152	$2,336	$2,464	$2,562
Atomic physics theory	126	305	95	146	110	115
Plasma experiments	17	280	321	525	700	729
Diagnostics	462	611	488	687	400	435
Atomic physics	649	703	641	807	760	801
National MFE computer network	353	167	401	300	312	324
Technical progrma support	0	0	102	29	0	0
	$4,072	$4,238	$4,200	$4,830	$4,746	$4,966
Confinement systems						
Doublet III	$922	$914	$1,106	$2,400	$2,500	$2,500
Confinement, other	2,487	2,575	1,966	3,330	3,480	3,619
PBX	0	0	0	1,800	1,730	953
Advanced toroidal research	14,769	11,436	7,605	1,100	0	0
ATF, other	409	0	0	0	0	0
TFTR physics program	0	0	0	1,345	1,395	1,451
TFTR tokamak operation	53	0	0	0	0	0
TFTR heating	228	96	82	150	150	156
Burning Plasma Experiment	2,315	2,643	2,272	1,730	2,859	1,952
	$21,183	$17,664	$13,031	$11,855	$12,114	$10,631
Development and technology						
Base technology	$0	$0	$0	$100	$125	$175
High-field magnets	471	24	10	0	0	0
Negative-ion neutral beams	123	0	0	0	0	0
ICR/LHR heating systems[a]	2,796	2,086	2,018	1,800	2,650	2,080
ECR heating systems[b]	140	133	49	0	0	0
Fueling systems	1,986	1,461	1,834	800	450	260
Nuclear analysis	157	85	65	60	120	130
Environmental analysis	58	38	40	40	40	45
Neutron source	0	0	0	75	250	465
Fusion materials	383	256	336	0	0	0
Neutron-interactive materials	3,296	3,109	3,129	1,900	2,100	2,200
ITER	2,384	2,237	2,329	5,735	7,059	7,202
Fusion systems studies	300	221	201	180	200	210
ORR	0	0	0	300	0	0
	$12,094	$9,650	$10,011	$10,990	$12,994	$12,767
Total ORNL funding	$37,349	$31,552	$27,242	$27,675	$29,854	$28,364

[a]ICR/LHR: ion cyclotron resonance/lower hybrid resonance.
[b]ECR: electron cyclotron resonance.

(ES&H) programs. As part of these efforts, FED and ETD have implemented mutual self-assessment teams. The primary objectives of these teams are to survey both divisions' facilities for safety hazards, document the findings, and recommend corrective action. By the end of 1991, the two divisions had completed six self-assessments, which have been extremely effective in today's climate.

In response to constant changes in environmental protection regulations and DOE Orders, the division continued to implement new compliance initiatives, in areas including the control of contamination in division facilities, hazardous waste, transformer inventories, mercury vapor, and surveys of noise levels and air and water quality. Efforts were directed toward reducing the environmental concerns in the facilities, verifying that policies and procedures were in place, and keeping employees well informed about the issues. The division's intent is to minimize hazardous waste, to control effluents in and out of the facilities, and to continue to protect and preserve the environment.

A total of 1455 ES&H deficiencies have been identified and entered in the FED Tracking and Trending Database. A graded approach is being used to address the 465 deficiencies that remain open.

The FED safety resource team established in 1989 continued to identify and resolve safety-related issues. This team is responsible for bimonthly inspections, documentation of safety and health problems, and recommendations to correct or prevent occurrences.

The division continued its promotion of safety awareness through its monthly safety meetings, facility assessments, bulletins, and basic two-way communication. The focus of the program, encouraging employees to maintain a safer attitude on and off the job, will continue to drive FED safety policies, rules, and regulations.

9.3 QUALITY ASSURANCE

In October 1990, the division's quality assurance (QA) staff level was reduced from one full-time QA specialist to a half-time QA specialist. This position is currently shared by two QA specialists.

The division's QA specialists reviewed engineering and procurement documents, including drawings and specifications defining technical requirements for items to be fabricated, to ensure that they contained the proper QA requirements. During the period, 9 nonconformance reports, 9 deviation reports, 3 quality investigation reports, and 15 occurrence reports were written to document problems, produce corrective actions, and disseminate information to other organizations.

APPENDICES

Appendix 1

PUBLICATIONS AND PRESENTATIONS

1990 BOOKS AND JOURNAL ARTICLES

S. C. Aceto, K. A. Connor, P. E. McLaren, J. J. Zielinski, J. G. Schatz, and G. H. Henkel, "Energy Analyzer for the ATF Heavy Ion Beam Probe," *Rev. Sci. Instrum.* **61** (10), 2958 (1990)

C. Alejaldre, A. Varias, A. L. Fraguas, B. Carreras, N. Dominguez, and V. E. Lynch, "Self-Stabilization of Ideal Modes in a Heliac," *Europhys. Conf. Abstr.* **14B**, 497 (1990)

E. Anabitarte, G. R. Hanson, J. D. Bell, J. L. Dunlap, J. H. Harris, C. Hidalgo, C. E. Thomas, T. Uckan, and J. B. Wilgen, "Density Fluctuation Measurements on ATF Using a Two-Frequency Reflectometer," *Europhys. Conf. Abstr.* **14B**, 1492–5 (1990)

F. S. B. Anderson, A. C. England, R. J. Colchin, J. H. Harris, D. L. Hillis, M. Murakami, G. H. Neilson, J. A. Rome, M. J. Saltmarsh, M. A. Henderson, and C. M. Simpson, "Electron Beam Mapping of the ATF Vacuum Magnetic Surfaces," pp. 389–91 in *Stellarator Physics: Proceedings of the 7th International Workshop*, IAEA-TECDOC-558, ed. J. F. Lyon, IAEA, Vienna, 1990

V. Arunasalam, N. L. Bretz, P. C. Efthimion, R. J. Goldston, B. Grek, D. W. Johnson, M. Murakami, K. M. McGuire, D. A. Rasmussen, F. J. Stauffer, and J. B. Wilgen, "Self-Consistency of the Principle of Profile Consistency Results for Sawtoothing Tokamak Discharges," *Nucl. Fusion* **30** (10), 2111 (1990)

S. E. Attenberger, B. Balet, D. J. Campbell, J. P. Christiansen, G. A. Cottrell, A. Edwards, T. T. C. Jones, P. Kupschus, P. J. Lomas, P. Nielsen, J. O'Rourke, D. Pasini, R. Prentice, G. Sadler, G. Schmidt, P. Stubberfield, A. Tataroni, F. Tibone, and H. Weisen, "Peaked Profiles in Low q High Current Discharges in JET," *Europhys. Conf. Abstr.* **14B**, 5 (1990)

S. E. Attenberger and W. A. Houlberg, "Transport Simulation of ITER Startup," pp. 99–101 in *Proceedings of the IEEE Thirteenth Symposium on Fusion Engineering*, Vol. 1, ed. M. S. Lubell, M. B. Nestor, and S. F. Vaughan, IEEE, New York, 1990

C. C. Baker, E. E. Bloom, M. J. Gouge, J. T. Hogan, R. C. Isler, D. L. Lousteau, N. A. Uckan, and D. W. Swain, "The Oak Ridge National Laboratory (ORNL)," *ITER Newsletter* **3** (5), 8–11 (1990)

J. D. Bell, J. H. Harris, J. L. Dunlap, V. K. Paré, M. Murakami, and H. Kaneko, "Fluctuation Studies in ATF," pp. 307–11 in *Stellarator Physics: Proceedings of the 7th International Workshop*, IAEA-TECDOC-558, ed. J. F. Lyon, IAEA, Vienna, 1990

J. M. Bialek, D. W. Weissenburger, M. Pelovitz, and R. O. Sayer, "Modeling the Forces Produced by Plasma Disruptions on the Compact Ignition Tokamak (CIT) Vacuum Vessel," pp. 132–35 in *Proceedings of the IEEE Thirteenth Symposium on Fusion Engineering*, Vol. 1, ed. M. S. Lubell, M. B. Nestor, and S. F. Vaughan, IEEE, New York, 1990

T. S. Bigelow, C. R. Schaich, and T. L. White, "Measurements of ECH Absorption on ATF Using a Polarization-Controlled Beam Launcher," pp. 243–46 in *Stellarator Physics: Proceedings of the 7th International Workshop*, IAEA-TECDOC-558, ed. J. F. Lyon, IAEA, Vienna, 1990

E. E. Bloom, "Status of Fusion Reactor Structural Materials Research and Development," *Nucl. Fusion* **30**, 1879–96 (1990)

A. H. Boozer, D. E. Baldwin, C. W. Horton, R. R. Dominguez, A. H. Glasser, J. A. Krommes, G. H. Neilson, K.-C. Shaing, W. L. Sadowski, and H. Weitzner, "Alternate Transport," *Phys. Fluids B* **2** (12), 2870–78 (1990)

K. H. Burrell, K. W. Gentle, N. C. Luhmann, Jr., E. S. Marmar, M. Murakami, K. F. Schoenberg, W. M. Tang, and M. C. Zarnstorff, "Status of Local Transport Measurements and Analysis in Toroidal Devices," *Phys. Fluids B* **2** (12), 2904–12 (1990)

C. E. Bush, R. J. Goldston, S. D. Scott, E. Fredrickson, K. McGuire, J. Schivell, G. Taylor, C. W. Barnes, M. G. Bell, R. L. Boivin, N. Bretz, R. V. Budny, A. Cavallo, P. C. Efthimion, B. Grek, R. Hawryluk, K. Hill, R. A. Hulse, A. Janos, D. W. Johnson, S. Kilpatrick, D. M. Manos, D. K. Mansfield, D. M. Meade, H. Park, A. T. Ramsey, B. Stratton, E. J. Synakowski, H. H. Towner, R. M. Wieland, M. C. Zarnstorff,

and S. J. Zweben, "Peaked Density Profiles, Circular-Limiter *H*-Modes on the TFTR Tokamak," *Phys. Rev. Lett.* **65**, 424 (1990)

C. E. Bush, J. Schivell, G. Taylor, N. Bretz, A. Cavallo, E. Fredrickson, A. Janos, D. K. Mansfield, K. McGuire, R. Nazikian, H. Park, A. T. Ramsey, B. Stratton, and E. J. Synakowski, "Application of TFTR Diagnostics to Study Limiter *H*-Modes," *Rev. Sci. Instrum.* **61**, 3532 (1990)

C. E. Bush, E. Fredrickson, N. Bretz, A. Cavallo, A. Janos, Y. Nagayama, H. Park, J. Schivell, G. Taylor, R. Nazikian, and A. T. Ramsey, "ELM Activity During Limiter *H*-Modes on TFTR," *J. Nucl. Mater.* **176 & 177**, 786 (1990)

B. A. Carreras, "Fluid Approach to Plasma Turbulence: Resistive Pressure-Gradient-Driven Turbulence," *Fiz. Plazmy* **16**, 1245–57 (1990) [*Sov. J. Plasma Phys.* **16**,722–29 (1990)]

B. A. Carreras, L. A. Charlton, N. Dominguez, J. B. Drake, L. Garcia, J. A. Holmes, J.-N. Leboeuf, D. K. Lee, and V. E. Lynch, "Plasma Turbulence Calculations on Supercomputers," *Int. J. Supercomput. Appl.* **4**, 97 (1990)

B. A. Carreras, N. Dominguez, J.-N. Leboeuf, V. E. Lynch, and P. H. Diamond, "Dissipative Trapped Electron Modes in $l = 2$ Torsatrons," pp. 329–32 in *Stellarator Physics: Proceedings of the 7th International Workshop*, IAEA-TECDOC-558, ed. J. F. Lyon, IAEA, Vienna, 1990

B. A. Carreras, V. E. Lynch, E. F. Jaeger, D. B. Batchelor, and J. S. Tolliver, "Full-Wave Calculations in Flux Coordinates for Toroidal Geometry," *J. Comput. Phys.* **88** (1), 183–204 (1990)

M. D. Carter, "Plasma Production Using Microwave and Radiofrequency Sources," pp. 275–79 in *Stellarator Physics: Proceedings of the 7th International Workshop*, IAEA-TECDOC-558, ed. J. F. Lyon, IAEA, Vienna, 1990

M. D. Carter, D. B. Batchelor, and E. F. Jaeger, "Electron Heating and Static Sheath Enhancement in Front of Energized RF Antennas," *Fusion. Eng. Des.* **12** (1 & 2), 105 (1990)

M. D. Carter, A. I. Lysojvan, V. Y. Moiseenko, N. I. Nazarov, O. M. Shvets, and K. N. Stepanov, "Plasma Production Using Radiofrequency Fields Near or Below the Ion Cyclotron Range of Frequencies," *Nucl. Fusion* **30** (4), 723–30 (1990)

J. R. Cary, J. D. Hanson, B. A. Carreras, and V. E. Lynch, "Simple Method for Calculating Island Widths," pp. 413–16 in *Stellarator Physics: Proceedings of the 7th International Workshop*, IAEA-TECDOC-558, ed. J. F. Lyon, IAEA, Vienna, 1990

J. B. O. Caughman II, D. N. Ruzic, and D. J. Hoffman, "Experimental Evidence of Increased Electron Temperature, Plasma Potential, and Ion Energy near an ICRF Antenna Faraday Shield," *Fusion Eng. Des.* **12** (1 & 2), 179 (1990)

J. B. O. Caughman II, D. N. Ruzic, D. J. Hoffman, R. A. Langley, and M. B. Lewis, "Ion Energy Measurements at the Surface of an ICRF Antenna Faraday Shield," *J. Vac. Sci. Technol. A* **8** (6), 4011–16 (1990)

L. A. Charlton and B. A. Carreras, "The Effect of Compressibility on Magnetohydrodynamic Instabilities in Toroidal Tokamak Geometry," *Phys. Fluids B* **2** (3), 539–46 (1990)

L. A. Charlton, B. A. Carreras, J.-N. Leboeuf, and V. E. Lynch, "Magnetic Fluctuations Due to Pressure Driven Instabilities in ATF," p. 313–16 in *Stellarator Physics: Proceedings of the 7th International Workshop*, IAEA-TECDOC-558, ed. J. F. Lyon, IAEA, Vienna, 1990

L. A. Charlton, B. A. Carreras, and V. E. Lynch, "Linear and Nonlinear Properties of Infernal Modes," *Phys. Fluids B* **2** (7), 1574–83 (1990)

L. A. Charlton, J. A. Holmes, V. E. Lynch, and B. A. Carreras, "Compressible Linear and Nonlinear Resistive MHD Calculations in Toroidal Geometry," *J. Comput. Phys.* **86** (2), 270–93 (1990)

R. J. Colchin, A. C. England, J. H. Harris, D. L. Hillis, T. C. Jernigan, M. Murakami, G. H. Neilson, J. A. Rome, M. J. Saltmarsh, F. S. B. Anderson, R. F. Gandy, J. D. Hanson, M. A. Henderson, D. K. Lee, V. E.

Lynch, and C. M. Simpson, "ATF Flux Surfaces and Related Plasma Effects," pp. 369–72 in *Stellarator Physics: Proceedings of the 7th International Workshop*, IAEA-TECDOC-558, ed. J. F. Lyon, IAEA, Vienna, 1990

R. J. Colchin, M. Murakami, E. Anabitarte, F. S. B. Anderson, G. L. Bell, J. D. Bell, T. S. Bigelow, E. C. Crume, J. L. Dunlap, G. R. Dyer, A. C. England, P. W. Fisher, W. A. Gabbard, J. C. Glowienka, R. H. Goulding, J. W. Halliwell, G. R. Hanson, J. Harris, G. R. Haste, C. Hidalgo-Vera, D. L. Hillis, S. Hiroe, L. D. Horton, H. C. Howe, D. P. Hutchinson, R. C. Isler, T. C. Jernigan, M. Kwon, R. A. Langley, D. K. Lee, J. F. Lyon, J. W. Lue, C. H. Ma, M. M. Menon, R. N. Morris, P. K. Mioduszewski, G. H. Neilson, A. L. Qualls, D. A. Rasmussen, P. S. Rogers, P. L. Shaw, T. D. Shepard, J. E. Simpkins, S. Sudo, C. E. Thomas, T. Uckan, M. R. Wade, J. B. Wilgen, W. R. Wing, H. Yamada, and J. J. Zielinski, "Overview of Results from the ATF Torsatron," *Phys. Fluids B* **2** (6, Pt. 2), 1347–52 (1990)

S. K. Combs, C. R. Foust, M. J. Gouge, and S. L. Milora, "Acceleration of Small, Light Projectiles (Including Hydrogen Isotopes) to High Speeds Using a Two-Stage Light-Gas Gun.," *J. Vac. Technol. A* **8**, 1814 (1990)

T. P. Crowley, S. C. Aceto, K. A. Connor, J. W. Heard, R. L. Hickok, J. W. Lewis, P. E. McLaren, A. Ouroua, J. G. Schatz, P. M. Schoch, J. Schwelberger, V. J. Simcic, and J. J. Zielinski, "Recent Advances in Heavy Ion Beam Probe Diagnostics," *Rev. Sci. Instrum.* **61**, 2989 (1990)

F. C. Davis and D. P. Kuban, "Remote Maintenance for Fusion: Requirements vs Technology Gap," pp. 251–53 in *Proceedings of the IEEE Thirteenth Symposium on Fusion Engineering*, Vol. 1, ed. M. S. Lubell, M. B. Nestor, and S. F. Vaughan, IEEE, New York, 1990

P. H. Diamond, J. F. Drake, H. Matsumoto, J. Sheffield, P. W. Terry, and A. J. Wootton, "Transport Task Force Workshop: Progress in Research on Plasma Edge Turbulence and Transport," *Comments Plasma Phys. Controlled Fusion* **13** (4), 327 (1990)

N. Dominguez, J.-N. Leboeuf, B. A. Carreras, and V. E. Lynch, "Ideal Low-n and Mercier Mode Stability Boundaries for $\ell = 2$ Torsatrons," pp. 225–29 in *Stellarator Physics: Proceedings of the 7th International Workshop*, IAEA-TECDOC-558, ed. J. F. Lyon, IAEA, Vienna, 1990

R. A. Dory, "Macros in a Spreadsheet," *Comput. Phys.* **4** (5), 558 (1990)

R. A. Dory, "Neural Networks," *Comput. Phys.* **4** (3), 324 (1990)

R. A. Dory, W. A. Houlberg, and S. E. Attenberger, "Energy Requirements for Neutral Beam Current Drive in a Large Tokamak," *Comments Plasma Phys. Controlled Fusion* **13** (1), 29 (1990)

L. Dresner, "Propagation of Normal Zones of Finite Size in Large, Composite Superconductors," p. 1084 in *11th International Conference on Magnet Technology (MT-11)*, Vol. 2, ed. T. Sekiguchi and S. Shimamoto, Elsevier, Tsukuba, Japan, 1990

G. R. Dyer and T. Uckan, "Amplifier for Use with Large-Area Photodiodes," *Rev. Sci. Instrum.* **61** (12), 3909–10 (1990)

J. R. Ferron, M. S. Chu, F. J. Helton, W. Howl, A. G. Kellman, L. L. Lao, E. A. Lazarus, J. K. Lee, T. H. Osborne, R. D. Stambaugh, E. J. Strait, T. S. Taylor, and A. D. Turnbull, "The Beta Limit in the DIII-D Tokamak," *Europhys. Conf. Abstr.* **14B**, 371 (1990)

J. R. Ferron, M. S. Chu, F. J. Helton, W. Howl, A. G. Kellman, L. L. Lao, E. A. Lazarus, J. K. Lee, T. H. Osborne, E. J. Strait, T. S. Taylor, and A. D. Turnbull, "High-Beta Discharges in the DIII-D Tokamak," *Phys. Fluids B* **2** (6), 1280–86 (1990)

R. H. Fowler, R. N. Morris, J. A. Rome, and K. Hanatani, "Neutral Beam Injection Benchmark Studies for Stellarators/Heliotrons," *Nucl. Fusion* **30** (6), 997 (1990)

A. L. Fraguas, A. Varias, C. Alejaldre, B. Carreras, N. Dominguez, and V. E. Lynch, "Equilibrium and Stability of High-q TJ-II Configurations," *Europhys. Conf. Abstr.* **14B**, 509 (1990)

J. D. Galambos and Y-K. M. Peng, "Scenarios for ITER Steady-State and Technology Testing Operation," pp. 243–46 in *Proceedings of the IEEE Thirteenth Symposium on Fusion Engineering*, Vol. 1, ed. M. S. Lubell, M. B. Nestor, and S. F. Vaughan, IEEE, New York, 1990

L. Garcia, B. A. Carreras, and N. Dominguez, "Averaged Equilibrium and Stability in Low-Aspect-Ratio Stellarators," pp. 289–94 in *Stellarator Physics: Proceedings of the 7th International Workshop*, IAEA-TECDOC-558, ed. J. F. Lyon, IAEA, Vienna, 1990

L. Garcia, B. A. Carreras, N. Dominguez, J.-N. Leboeuf, and V. E. Lynch, "Low-*n* Stability Calculations for Three-Dimensional Stellarator Configurations," *Phys. Fluids B* **2** (9), 2162–67 (1990)

J. L. Geary, J.-N. Leboeuf, and T. Tajima, "Computer Simulation of Alfvén Wave Heating," *Phys. Fluids B* **2** (4), 773–86 (1990)

Y. Gohar, H. Attaya, M. C. Billone, P. Finn, S. Majumdar, L. R. Turner, C. C. Baker, B. E. Nelson, and R. Raffray, "Solid Breeder Blanket Option for the ITER Conceptual Design," pp. 53–57 in *Proceedings of the IEEE Thirteenth Symposium on Fusion Engineering*, Vol. 1, ed. M. S. Lubell, M. B. Nestor, and S. F. Vaughan, IEEE, New York, 1990

R. C. Goldfinger and D. B. Batchelor, "An Analytical Model for Electron Cyclotron Heating Profiles," pp. 281–85 in *Stellarator Physics: Proceedings of the 7th International Workshop*, IAEA-TECDOC-558, ed. J. F. Lyon, IAEA, Vienna, 1990

R. J. Goldston, G. Bateman, M. G. Bell, R. Bickerton, E. A. Chaniotakis, D. R. Cohn, P. L. Colestock, D. N. Hill, W. A. Houlberg, S. C. Jardin, S. S. Medley, G. H. Neilson, W. A. Peebles, F. W. Perkins, N. Pomphrey, M. Porkolab, J. A. Schmidt, D. J. Sigmar, R. D. Stambaugh, D. P. Stotler, M. Ulrickson, R. E. Waltz, and K. G. Young, "A Physics Perspective on CIT," *Europhys. Conf. Abstr.* **14B**, 134–37 (199.)

S. M. Gorbatkin, L. A. Berry, and J. B. Roberto, "Behavior of Ar Plasmas Formed in a Mirror Field Electron Cyclotron Resonance Microwave Ion Source," *J. Vac. Sci. Technol. A* **8** (3), 2893 (1990)

M. J. Gouge, S. K. Combs, and S. L. Milora, "A Combined Microwave Cavity and Photographic Diagnostic for High-Speed Projectiles," *Rev. Sci. Instrum.* **61** (8), 2102–5 (1990)

M. J. Gouge and S. L. Milora, "Fusion Engineering (Technical Summary of the 13th Symposium, Knoxville, TN, USA, 2–6 October 1989)," *Nucl. Fusion* **30** (5), 957 (1990)

R. H. Goulding, F. W. Baity, D. B. Batchelor, S. C. Chiu, D. J. Hoffman, E. F. Jaeger, M. J. Mayberry, and P. M. Ryan, "Development of Fast-Wave ICRF Current Drive Systems at ORNL," *Europhys. Conf. Abstr.* **14B**, 1311 (1990)

R. H. Goulding, D. J. Hoffman, D. L. Conner, C. J. Hammonds, J. L. Ping, B. W. Riemer, P. M. Ryan, D. J. Taylor, R. B. Wysor, and J. J. Yugo, "The ORNL Fast-Wave ICRF Antenna for Alcator C-Mod," pp. 215–20 in *Proceedings of the IEEE Thirteenth Symposium on Fusion Engineering*, Vol. 1, ed. M. S. Lubell, M. B. Nestor, and S. F. Vaughan, IEEE, New York, 1990

D. L. Grekov, V. E. D'yakov, R. C. Goldf[illegible]ger, and D. B. Batchelor, "Ray Tracing Studies of Lower Hybrid Heating in an $l = 2$ Torsatron," *Nucl Fusion* **30** (10), 2039 (1990)

M. L. Grossbeck, K. Ehrlich, and C. Wassilew, "An Assessment of Tensile, Irradiation Creep, Creep Rupture, and Fatigue Behavior in Austenitic Stainless Steels with Emphasis on Spectral Effects," *J. Nucl. Mater.* **174**, 264–81 (1990)

J. W. Halliwell, G. R. Dyer, and J. E. Simpkins, "Design and Development of a Fast-Response Ionization Gauge Controller," pp. 178–80 in *Proceedings of the IEEE Thirteenth Symposium on Fusion Engineering*, Vol. 1, ed. M. S. Lubell, M. B. Nestor, and S. F. Vaughan, IEEE, New York, 1990

G. R. Hanson and C. E. Thomas, Jr., "Analysis of the Expected Resolution of the ECE Crossed-Sightline Magnetic Field Diagnostics," *Rev. Sci. Instrum.* **61**, 671–85 (1990)

G. R. Hanson, J. B. Wilgen, E. Anabitarte, J. D. Bell, J. H. Harris, J. L. Dunlap, and C. E. Thomas, "The ATF Two-Frequency Correlation Reflectometer," *Rev. Sci. Instrum.* **61** (10), 3049 (1990)

J. H. Harris, E. Anabitarte, G. L. Bell, J. D. Bell, T. S. Bigelow, B. A. Carreras, L. A. Charlton, R. J. Colchin, E. C. Crume, N. Dominguez, J. L. Dunlap, G. R. Dyer, A. C. England, R. F. Gandy, J. C. Glowienka, J. W. Halliwell, G. R. Hanson, C. Hidalgo-Vera, D. L. Hillis, S. Hiroe, L. D. Horton, H. C. Howe, R. C. Isler, T. C. Jernigan, H. Kaneko, J.-N. Leboeuf, D. K. Lee, V. E. Lynch, J. F. Lyon, M. M. Menon, R. N. Morris, M. Murakami, G. H. Neilson, V. K. Paré, D. A. Rasmussen, C. E. Thomas, T. Uckan, M. R. Wade, J. B. Wilgen, and W. R. Wing, "Second Stability in the ATF Torsatron—Experiment and Theory," *Phys. Fluids B* **2** (6, Pt. 2), 1353–58 (1990)

J. H. Harris, T. C. Jernigan, F. S. B. Anderson, R. D. Benson, R. J. Colchin, M. J. Cole, A. C. England, R. F. Gandy, J. C. Glowienka, M. A. Henderson, D. L. Hillis, R. L. Johnson, D. K. Lee, J. F. Lyon, G. H. Neilson, B. E. Nelson, J. A. Rome, M. J. Saltmarsh, C. W. Simpson, D. J. Taylor, P. B. Thompson, and J. C. Whitson, "Realization of the Advanced Toroidal Facility Torsatron Magnetic Field," *Fusion Technol.* **17** (1), 51 (1990)

J. H. Harris, M. Murakami, B. A. Carreras, J. D. Bell, G. L. Bell, T. S. Bigelow, L. A. Charlton, N. Dominguez, J. L. Dunlap, J. C. Glowienka, H. C. Howe, H. Kaneko, R. R. Kindsfather, J.-N. Leboeuf, V. E. Lynch, M. M. Menon, R. N. Morris, G. H. Neilson, V. K. Paré, N. F. Perepelkin, D. A. Rasmussen, J. B. Wilgen, and W. R. Wing, "Second Stability Studies in ATF," pp. 223–24 in *Stellarator Physics: Proceedings of the 7th International Workshop*, IAEA-TECDOC-558, ed. J. F. Lyon, IAEA, Vienna, 1990

C. L. Hedrick, C. O. Beasley, and W. I. Van Rij, "Optimization of Transport in Stellarators," pp. 93–96 in *Stellarator Physics: Proceedings of the 7th International Workshop*, IAEA-TECDOC-558, ed. J. F. Lyon, IAEA, Vienna, 1990

W. Hess, M. Druetta, T. Fall, D. Guilhem, C. C. Klepper, and M. Mattioli, "Fast Scanning Fiber-Multiplier Used for Plasma-Edge Visible Spectroscopy on Tore Supra," *Europhys. Conf. Abstr.* **14B**, 1580 (1990)

C. Hidalgo, T. Uckan, J. D. Bell, J. H. Harris, B. A. Carreras, J. L. Dunlap, G. R. Dyer, C. P. Ritz, K. Carter, T. L. Rhodes, and A. J. Wootton, "Edge Turbulence Studies in ATF," *Europhys. Conf. Abstr.* **14B**, 1353–56 (1990)

D. L. Hillis, K. H. Finken, J. T. Hogan, K. H. Dippel, R. A. Moyer, A. Pospieszczyk, D. Rusbüldt, K. Akaishi, R. W. Conn, H. Euringer, D. S. Gray, L. D. Horton, R. A. Hulse, R. C. Isler, C. C. Klepper, P. K. Mioduszewski, A. Miyahara, and G. H. Wolf, "Helium Removal and Transport Studies with the ALT-II Pump Limiter in TEXTOR," *Phys. Rev. Lett.* **65**, 2382 (1990)

S. Hiroe, R. R. Kindsfather, J. B. Wilgen, D. B. Batchelor, T. S. Bigelow, W. R. Wing, G. L. Bell, R. F. Gandy, and R. C. Goldinger, "Bolometric Measurements in ATF," pp. 167–71 in *Stellarator Physics: Proceedings of the 7th International Workshop*, IAEA-TECDOC-558, ed. J. F. Lyon, IAEA, Vienna, 1990.

S. P. Hirshman, R. N. Morris, C. L. Hedrick, J. F. Lyon, J. A. Rome, S. L. Painter, and W. I. van Rij, "Low-Aspect-Ratio Optimization Studies for ATF-II," pp. 493–99 in *Stellarator Physics: Proceedings of the 7th International Workshop*, IAEA-TECDOC-558, ed. J. F. Lyon, IAEA, Vienna, 1990

S. P. Hirshman, U. Schwenn, and J. Nührenberg, "Improved Radial Differencing for Three-Dimensional Magnetohydrodynamic Equilibrium Calculations," *J. Comput. Phys.* **87**, 396–407 (1990)

L. M. Hively and J. A. Rome, "TF Ripple Losses of Alphas Below the Critical Energy in ITER," *Nucl. Fusion* **30** (6), 1129–35 (1990)

L. M. Hively and D. J. Sigmar, "Bibliography of Fusion Product Physics in Tokamaks," *Fusion Technol.* **17** (2), 316 (1990)

D. J. Hoffman, F. W. Baity, R. H. Goulding, G. R. Haste, P. M. Ryan, D. J. Taylor, D. W. Swain, M. J. Mayberry, and J. J. Yugo, "The Technology of Fast-Wave Current Drive Antennas," pp. 267–71 in *Proceedings of the IEEE Thirteenth Symposium on Fusion Engineering*, Vol. 1, ed. M. S. Lubell, M. B. Nestor, and S. F. Vaughan, IEEE, New York, 1990

L. D. Horton, R. C. Isler, E. C. Crume, T. C. Jernigan, and S. Morita, "Impurity Transport in ATF and the Effect of Controlled Impurity Injection," *Europhys. Conf. Abstr.* **14B**, 447–50 (1990)

L. D. Horton, E. C. Crume, H. C. Howe, and R. C. Isler, "Impurity Studies and Transport in ATF," pp. 589–92 in *Stellarator Physics: Proceedings of the 7th International Workshop*, IAEA-TECDOC-558, ed. J. F. Lyon, IAEA, Vienna, 1990

W. A. Houlberg, D. W. Ross, G. Bateman, S. C. Cowley, P. C. Efthimion, W. W. Pfeiffer, G. D. Porter, D. E. Shumaker, L. E. Sugiyama, and J. C. Wiley, "Modeling Transport in Toroidal Plasmas: Status and Issues," *Phys. Fluids B* **2** (12), 2913–25 (1990)

H. C. Howe, L. D. Horton, E. C. Crume, J. H. Harris, R. C. Isler, M. M. Murakami, D. A. Rasmussen, J. B. Wilgen, and W. R. Wing, "Transport Modeling of ECH and Neutral-Beam-Heated Plasmas in the Advanced Toroidal Facility," pp. 79–82 in *Stellarator Physics: Proceedings of the 7th International Workshop*, IAEA-TECDOC-558, ed. J. F. Lyon, IAEA, Vienna, 1990.

H. Iguchi, M. Hosokawa, H. C. Howe, K. Ida, H. Idei, O. Kaneko, S. Kubo, K. Masai, K. Matsuoka, S. Morita, K. Nishimura, N. Noda, S. Okamura, T. Ozaki, A. Sagara, H. Sanuki, T. Shoji, S. Sobhanian, C. Takahashi, Y. Takeiri, Y. Takita, K. Tsuzuki, H. Yamada, T. Amano, and M. Fujiwara, "Transport Study on ECH- and NBI-Heated Plasmas in the Low-Aspect-Ratio Helical System CHS," *Europhys. Conf. Abstr.* **14B**, 451–54 (1990)

R. C. Isler, G. L. Bell, T. S. Bigelow, E. C. Crume, A. C. England, J. C. Glowienka, L. D. Horton, T. C. Jernigan, R. A. Langley, J. F. Lyon, P. K. Mioduszewski, S. Morita, M. Murakami, D. A. Rasmussen, J. E. Simpkins, J. B. Wilgen, and W. R. Wing, "Cleanup and Improvement of Operational Performance of ATF by Chromium and Titanium Gettering," *Europhys. Conf. Abstr.* **14B**, 455–58 (1990)

R. C. Isler, G. L. Bell, T. S. Bigelow, E. C. Crume, A. C. England, J. C. Glowienka, L. D. Horton, T. C. Jernigan, R. A. Langley, P. K. Mioduszewski, M. Murakami, D. A. Rasmussen, J. E. Simpkins, J. B. Wilgen, and W. R. Wing, "The Effects of Chromium and Titanium Gettering on the Operation of the Advanced Toroidal Facility," *J. Nucl. Mater.* **176 & 177**, 332–36 (1990)

E. F. Jaeger, D. B. Batchelor, M. D. Carter, and H. Weitzner, "Global ICRF Wave Propagation in Edge Plasma and Faraday Shield Regions," *Nucl. Fusion* **30** (3), 505 (1990)

T. T. C. Jones, P. J. Lomas, S. E. Attenberger, J. P. Christiansen, G. A. Cottrell, R. Gianelli, L. de Kock, P. Kupschus, A. McCracken, C. G. Lowry, P. Nielsen, D. Pasini, R. Prentice, G. Sadler, M. F. Stamp, D. D. R. Summers, M. von Hellerman, and H. Weisen, "Fusion Performance of JET Limiter Plasmas Using Be-Coated Graphite and Solid Be Surfaces," *Europhys. Conf. Abstr.* **14B**, 9 (1990)

S. M. Kaye, C. W. Barnes, M. G. Bell, J. C. DeBoo, M. Greenwald, K. Riedel, D. Sigmar, N. Uckan, and R. Waltz, "Status of Global Energy Confinement Studies," *Phys. Fluids B* **2** (12), 2926–40 (1990)

C. C. Klepper, P. Bonnel, J. L. Bruneau, M. Chatelier, C. Gil, C. Grisolia, G. R. Haste, L. D. Horton, T. Loarer, G. Martin, P. K. Mioduszewski, B. Pegourie, L. Rodriguez, T. Uckan, and J. G. Watkins, "Particle Exhaust Studies in Tore Supra with a Pump Limiter," *J. Nucl. Mater.* **176 & 177**, 798–802 (1990)

C. C. Klepper, J. E. Simpkins, D. L. Hillis, P. K. Mioduszewski, R. A. Moyer, D. Gray, K. H. Dippel, and A. Pospieczszyk, "Application of Modern Optical Fiber Technology to the Study of Plasmas of Closed Divertors and Pump Limiters in Reactor-Relevant Conditions," *Rev. Sci. Instrum.* **61** (10), 2943–45 (1990)

M. Kwon, C. E. Thomas, D. J. Hoffman, T. D. Shepard, and C. L. Rettig, "Measurement of the Effects of Faraday Shields on ICRH Antenna Coupling," *IEEE Trans. Plasma Sci.* **PS-18** (2), 184–89 (1990)

R. A. Langley, "Graphite as a Plasma-Facing Material in Fusion Experiments," p. 522 in *Proceedings of the IEEE Thirteenth Symposium on Fusion Engineering*, Vol. 1, ed. M. S. Lubell, M. B. Nestor, and S. F. Vaughan, IEEE, New York, 1990

R. A. Langley, "Review of Wall Conditioning and Wall Materials for Fusion Research Devices," *MRS Bull.* **15**, 42 (1990)

R. A. Langley, T. L. Clark, ' C. Glowienka, R. H. Goulding, P. K. Mioduszewski, D. A. Rasmussen, T. F. Rayburn, C. R. Schaich, T. D. Shepard, J. E. Simpkins, and J. L. Yarber, "Recent Results on Cleaning and Conditioning the ATF Vacuum System," pp. 19–29 in *Surface Conditioning of Vacuum Systems: Los Angeles, CA 1989*, American Institute of Physics, New York, 1990

R. A. Langley, T. L. Clark, J. C. Glowienka, R. H. Goulding, P. K. Mioduszewski, D. A. Rasmussen, T. F. Rayburn, C. R. Schaich, T. D. Shepard, J. E. Simpkins, and J. L. Yarber, "Wall Conditioning in ATF," pp. 127–36 in *Stellarator Physics: Proceedings of the 7th International Workshop*, IAEA-TECDOC-558, ed. J. F. Lyon, IAEA, Vienna, 1990

R. A. Langley, D. L. Flamm, H. C. Hseuh, W. L. Hsu, and T. W. Rusch, eds., *Surface Conditioning of Vacuum Systems: Los Angeles, CA 1989*, American Institute of Physics, New York, 1990 [*American Vacuum Society Ser.* **8**; *AIP Conf. Proc.* **199**]

R. A. Langley, J. C. Glowienka, P. K. Mioduszewski, T. F. Rayburn, J. E. Simpkins, and J. L. Yarber, "Wall Conditioning and Leak Localization in ATF," *J. Vac. Sci. Technol.* **8**, 3058 (1990)

R. A. Langley and J. M. McDonald, "A Technique for Efficiently Cleaning and Conditioning Low- and Medium-Energy Accelerators," p. 106 in *Proceedings of the American Vacuum Society Topical Conference on Surface Conditioning of Vacuum Systems, Los Angeles, April 1989*, American Institute of Physics, New York, 1990

E. A. Lazarus, J. B. Lister, and G. H. Neilson, "Control of the Vertical Instability in Tokamaks," *Nucl. Fusion* **30** (1), 111 (1990)

E. A. Lazarus, A. D. Turnbull, A. G. Kellman, J. R. Ferron, F. J. Helton, L. L. Lao, J. A. Leuer, E. J. Strait, and T. S. Taylor, "Experiments at High Elongation in DIII-D," *Europhys. Conf. Abstr.* **14B**, 429 (1990)

D. K. Lee, "Application of Theta Functions for Numerical Evaluation of Complete Elliptic Integrals of the First and Second Kind," *Comput. Phys. Commun.* **60** (3), 319 (1990)

D. K. Lee, J. H. Harris, R. J. Colchin, A. C. England, G. S. Lee, V. E. Lynch, G. H. Neilson, M. J. Saltmarsh, F. S. B. Anderson, and J. D. Hanson, "Field Error Modeling Studies in the ATF," pp. 393–96 in *Stellarator Physics: Proceedings of the 7th International Workshop*, IAEA-TECDOC-558, ed. J. F. Lyon, IAEA, Vienna, 1990

D. K. Lee, J. H. Harris, and G. S. Lee, "Magnetic Island Widths due to Field Perturbations in Toroidal Stellarators," *Nucl. Fusion* **30** (10), 2177 (1990)

I. S. Lehrman, P. L. Colestock, and E. F. Jaeger, "Edge Modelling of ICRF Heated Plasmas on PLT," *Nucl. Fusion* **30** (8), 1399 (1990)

R. K. Linford, S. Luckhardt, J. F. Lyon, G. A. Navratil, and K. F. Schoenberg, "Transport Task Force Workshop: Basic Experiments Highlights," *Comments Plasma Phys. Controlled Fusion* **13** (4), 311 (1990)

J. B. Lister, E. A. Lazarus, A. G. Kellman, J. M. Moret, J. R. Ferron, F. J. Helton, L. L. Lao, J. A. Leuer, E. J. Strait, T. S. Taylor, and A. D. Turnbull, "Experimental Study of the Vertical Stability of High Decay Index Plasmas in the DIII-D Tokamak," *Nucl. Fusion* **30** (11), 2349 (1990)

D. C. Lousteau, B. E. Nelson, V. D. Lee, S. L. Thomson, J. M. Miller, and W. B. Lindquist, "The International Thermonuclear Experimental Reactor Configuration Evolution," pp. 247–50 in *Proceedings of the IEEE Thirteenth Symposium on Fusion Engineering*, Vol. 1, ed. M. S. Lubell, M. B. Nestor, and S. F. Vaughan, IEEE, New York, 1990.

J. W. Lue, L. Dresner, and M. S. Lubell, "High-Field, High-Current-Density, Stable Superconducting Magnets for Fusion Machines," p. 551–56 in *Stellarator Physics: Proceedings of the 7th International Workshop*, IAEA-TECDOC-558, ed. J. F. Lyon, IAEA, Vienna, 1990

V. E. Lynch, B. A. Carreras, N. Dominguez, and J.-N. Leboeuf, "Equilibrium and Ideal Stability Studies for ATF," pp. 333–36 in *Stellarator Physics: Proceedings of the 7th International Workshop*, IAEA-TECDOC-558, ed. J. F. Lyon, IAEA, Vienna, 1990

J. F. Lyon, "Near-Term Directions in the World Stellarator Program," *Fusion Technol.* **17** (1), 19 (1990)

J. F. Lyon, "Preface: Special Issue on Stellarators," *Fusion Technol.* **17** (1), 17–18 (1990)

J. F. Lyon, "Review of Recent Stellarator Results in the U.S.A., the U.S.S.R., and Japan," *Plasma Phys. Controlled Fusion* **32** (11), 1041–59 (1990)

J. F. Lyon, "Stellarators (Report on the 7th International Workshop—IAEA Technical Committee Meeting, Oak Ridge, TN, USA, 10–14 April 1989)," *Nucl. Fusion* **30** (1), 175 (1990)

J. F. Lyon, "Summary of Presentations," pp. 11–22 in *Stellarator Physics: Proceedings of the 7th International Workshop*, IAEA-TECDOC-558, ed. J. F. Lyon, IAEA, Vienna, 1990

J. F. Lyon, S. C. Aceto, F. S. B. Anderson, G. L. Bell, J. D. Bell, T. S. Bigelow, B. A. Carreras, M. D. Carter, R. J. Colchin, K. A. Connor, E. C. Crume, N. Dominguez, J. L. Dunlap, G. R. Dyer, A. C. England, R. H. Fowler, R. F. Gandy, J. C. Glowienka, R. C. Goldfinger, R. H. Goulding, J. W. Halliwell, J. D. Hanson, J. H. Harris, M. A. Henderson, D. L. Hillis, S. Hiroe, L. D. Horton, H. C. Howe, D. P. Hutchinson, R. C. Isler, T. C. Jernigan, H. Kaneko, R. R. Kindsfather, M. Kwon, R. A. Langley, D. K. Lee, J.-N. Leboeuf, V. E. Lynch, C. H. Ma, M. M. Menon, F. W. Meyer, P. K. Mioduszewski, T. Mizuuchi, R. N. Morris, O. Motojima, M. Murakami, G. H. Neilson, V. K. Paré, N. F. Perepelkin, D. A. Rasmussen, R. K. Richards, P. S. Rogers, J. A. Rome, M. J. Saltmarsh, F. Sano, P. L. Shaw, J. Sheffield, T. D. Shepard, J. E. Simpkins, C. M. Simpson, Y. Takeiri, C. E. Thomas, T. Uckan, K. L. Vander Sluis, G. S. Voronov, M. R. Wade, J. A. White, T. L. White, J. B. Wilgen, W. R. Wing, and J. J. Zielinski, "Overview of the ATF Program," pp. 33–44 in *Stellarator Physics: Proceedings of the 7th International Workshop*, IAEA-TECDOC-558, ed. J. F. Lyon, IAEA, Vienna, 1990

J. F. Lyon, G. L. Bell, J. D. Bell, R. D. Benson, T. S. Bigelow, K. K. Chipley, M. J. Cole, E. C. Crume, J. L. Dunlap, A. C. England, J. C. Glowienka, R. H. Goulding, J. H. Harris, D. L. Hillis, S. Hiroe, L. D. Horton, H. C. Howe, R. C. Isler, T. C. Jernigan, R. L. Johnson, R. A. Langley, M. M. Menon, P. K. Mioduszewski, R. N. Morris, M. Murakami, G. H. Neilson, B. E. Nelson, D. A. Rasmussen, J. A. Rome, M. J. Saltmarsh, P. B. Thompson, M. R. Wade, J. A. White, T. L. White, J. C. Whitson, J. B. Wilgen, and W. R. Wing, "Construction and Initial Operation of the Advanced Toroidal Facility," *Fusion Technol.* **17** (1), 33 (1990)

J. F. Lyon, B. A. Carreras, N. Dominguez, L. Dresner, C. L. Hedrick, S. P. Hirshman, M. S. Lubell, J. W. Lue, R. N. Morris, S. L. Painter, J. A. Rome, and W. I. van Rij, "Advanced Toroidal Facility II Studies," *Fusion Technol.* **17** (1), 188 (1990)

J. F. Lyon, G. Grieger, F. Rau, A. Iiyoshi, A. P. Navarro, L. M. Kovrizhnykh, O. S. Pavlichenko, and S. M. Hamberger, "Stellarators," *Nucl. Fusion* **30** (9), 1695–1715 (1990)

C. H. Ma, D. P. Hutchinson, Y. Fockedey, K. L. Vnader Sluis, and C. A. Bennett, "FIR Interferometer and Scattering Measurements on ATF," pp. 155–58 in *Stellarator Physics: Proceedings of the 7th International Workshop*, IAEA-TECDOC-558, ed. J. F. Lyon, IAEA, Vienna, 1990

C. H. Ma, D. P. Hutchinson, and K. L. Vander Sluis, "A Difluoromethane Laser Interferometer System on ATF," *Rev. Sci. Instrum.* **61** (10), 2891 (1990)

M. J. Mayberry, S. C. Chiu, R. I. Pinsker, R. Prater, D. J. Hoffman, F. W. Baity, P. M. Ryan, and Y. Uesugi, "Coupling of Fast Waves in the Ion Cyclotron Range of Frequencies to H-Mode Plasmas in DIII-D," *Nucl. Fusion* **30** (4), 579–97 (1990)

K. McGuire, V. Arunasalam, C. W. Barnes, M. G. Bell, M. Bitter, R. Boivin, N. L. Bretz, R. Budny, C. E. Bush, A. Cavallo, T. K. Chu, S. A. Cohen, P. Colestock, S. L. Davis, D. L. Dimock, H. F. Dylla, P. C. Efthimion, A. B. Ehrhardt, R. J. Fonck, E. Fredrickson, H. P. Furth, G. Gammel, R. J. Goldston, G. Greene, B. Grek, L. R. Grisham, G. Hammett, R. J. Hawryluk, H. W. Hendel, K. W. Hill, E. Hinnov, D. J. Hoffman, J. Hosea, R. B. Howell, H. Hsuan, R. A. Hulse, A. C. Janos, D. Jassby, F. Jobes,

D. W. Johnson, L. C. Johnson, R. Kaita, C. Kieras-Phillips, S. J. Kilpatrick, P. H. LaMarch, B. LeBlanc, D. M. Manos, D. K. Mansfield, E. Mazzucato, M. P. McCarthy, D. C. McCune, D. H. McNeill, D. M. Meade, S. S. Medley, D. R. Mikkelsen, D. Monticello, R. Motley, D. Mueller, J. A. Murphy, Y. Nagayama, D. R. Nazakian, E. B. Nieschmidt, D. K. Owens, H. Park, W. Park, S. Pitcher, A. T. Ramsey, M. H. Redi, A. L. Roquemore, P. H. Rutherford, G. Schilling, J. Schivell, G. L. Schmidt, S. D. Scott, J. C. Sinnis, J. Stevens, B. C. Stratton, W. Stodiek, E. J. Synakowski, W. M. Tang, G. Taylor, J. R. Timberlake, H. H. Towner, M. Ulrickson, S. von Goeler, R. Wieland, M. Williams, J. R. Wilson, K.-L. Wong, M. Yamada, S. Yoshikawa, K. M. Young, M. C. Zarnstorff, and S. J. Zweben, "High-Beta Operation and Magnetohydrodynamic Activity on the TFTR Tokamak," *Phys. Fluids B* **2** (6), 1287–90 (1990)

T. J. McManamy, J. E. Brasier, and P. Snook, "Insulation Interlaminar Shear Strength Testing with Compression and Irradiation," pp. 342–47 in *Proceedings of the IEEE Thirteenth Symposium on Fusion Engineering*, Vol. 1, ed. M. S. Lubell, M. B. Nestor, and S. F. Vaughan, IEEE, New York, 1990

J. Mervine, P. Sichta, R. Wilson, D. Giles, and G. Skelly, "The ICRF Computer Control and Monitoring System," pp. 455–58 in *Proceedings of the IEEE Thirteenth Symposium on Fusion Engineering*, Vol. 1, ed. M. S. Lubell, M. B. Nestor, and S. F. Vaughan, IEEE, New York, 1990.

D. R. Mikkelsen, M. G. Bell, M. Bitter, C. E. Bush, H. F. Dylla, B. Grek, L. R. Grisham, K. W. Hill, D. W. Johnson, A. T. Ramsey, J. F. Schivell, F. J. Stauffer, G. Tyalor, M. C. Zarnstorff, and TFTk Team, "Tokamak Global Confinement Data: TFTR," *Nucl. Fusion* **30** (9), 1972 (1990)

P. K. Mioduszewski, L. W. Owen, M. M. Menon, and J. T. Hogan, "Particle Exhaust Modeling for the Collaborative DIII-D Advanced Divertor Program," *J. Nucl. Mater.* **176 & 177**, 733–38 (1990)

P. K. Mioduszewski, T. Uckan, D. L. Hillis, J. A. Rome, R. H. Fowler, J. C. Glowienka, M. Murakami, and G. H. Neilson, "Edge Plasma and Divertor Studies in the ATF Torsatron," pp. 121–25 in *Stellarator Physics: Proceedings of the 7th International Workshop*, IAEA-TECDOC-558, ed. J. F. Lyon, IAEA, Vienna, 1990

R. N. Morris, C. L. Hedrick, S. P. Hirshman, J. F. Lyon, and J. A. Rome, "Numerical Methods for Stellarator Optimization," pp. 539–44 in *Stellarator Physics: Proceedings of the 7th International Workshop*, IAEA-TECDOC-558, ed. J. F. Lyon, IAEA, Vienna, 1990

R. A. Moyer, K. H. Finken, D. Reiter, C. C. Klepper, R. W. Conn, K. H. Dippel, D. Gray, D. L. Hillis, A. Pospieszczyk, G. H. Wolf, the TEXTOR Team, and the NI Team, "Influence of Plasma-Neutral Interactions on ALT-II Pump Limiter Performance During NI Heating of TEXTOR," *Europhys. Conf. Abstr.* **14B**, 1447 (1990)

M. Murakami, B. A. Carreras, G. L. Bell, T. S. Bigelow, G. R. Dyer, A. C. England, J. C. Glowienka, S. Hiroe, H. C. Howe, T. C. Jernigan, D. K. Lee, V. E. Lynch, S. Morita, D. A. Rasmussen, J. S. Tolliver, M. R. Wade, J. B. Wilgen, W. R. Wing, and the ATF Group,, "Bootstrap Current Studies in the Advanced Toroidal Facility," *Europhys. Conf. Abstr.* **14B**, 443–46 (1990)

Y. Nakamura, K. Ichiguchi, H. Sugama, M. Wakatani, H. Zushi, J. L. Johnson, G. Rewoldt, B. A. Carreras, N. Dominguez, J.-N. Leboeuf, J. A. Holmes, and V. E. Lynch, "Relation Between Mercier Criterion and Low-*n* Mode Stability," pp. 295–98 in *Stellarator Physics: Proceedings of the 7th International Workshop*, IAEA-TECDOC-558, ed. J. F. Lyon, IAEA, Vienna, 1990

Y. Nakamura, K. Ichiguchi, M. Wakatani, B. A. Carreras, N. Dominguez, J.-N. Leboeuf, V. E. Lynch, J. L. Johnson, and G. Rewoldt, "Beta Limit Study of $\ell = 2$ Heliotron/Torsatron and a new Low-*n* Mode Stability Analysis," in *Theory of Fusion Plasmas: ISPP-6 Piero Caldirola*, Societa Italia Fisica/Editrice Compositore, Bologna, Italy, 1990

G. H. Neilson, S. C. Aceto, E. Anabitarte, F. S. B. Anderson, G. L. Bell, J. D. Bell, R. D. Benson, T. S. Bigelow, B. A. Carreras, T. L. Clark, R. J. Colchin, E. C. Crume, W. R. DeVan, J. L. Dunlap, G. R. Dyer, A. C. England, J. C. Glowienka, J. W. Halliwell, G. R. Hanson, J. H. Harris, C. L. Hedrick, C. Hidalgo, D. L. Hillis, S. Hiroe, L. D. Horton, H. C. Howe, R. C. Isler, T. C. Jernigan, R. A. Langley, D. K. Lee,

J. W. Lue, J. F. Lyon, C. H. Ma, P. K. Mioduszewski, R. N. Morris, M. Murakami, D. A. Rasmussen, C. P. Ritz, P. S. Rogers, S. W. Schwenterly, P. L. Shaw, T. D. Shepard, J. E. Simpkins, C. E. Thomas, T. Uckan, M. R. Wade, J. A. White, J. B. Wilgen, C. T. Wilson, W. R. Wing, H. Yamada, and J. J. Zielinski, "Studies of Plasma Performance and Transport in the Advanced Toroidal Facility (ATF)," pp. 7–12 in *Proceedings of the IEEE Thirteenth Symposium on Fusion Engineering*, Vol. 1, ed. M. S. Lubell, M. B. Nestor, and S. F. Vaughan, IEEE, New York, 1990

A. Nicolai, Y-K. M. Peng, and J. T. Hogan, "Implementation of Scaling Laws in the 1-1/2-D Transport Code and Applications to the Ignition Spherical Torus," *Europhys. Conf. Abstr.* **14B**, 825 (1990)

J. M. Noterdaeme and D. B. Batchelor, eds., *Proceedings of the IAEA Technical Committee Meeting on ICRH/ Edge Physics, Garching, October 2–5, 1989*, North-Holland, Amsterdam, 1990 [*Fusion Eng. Des.* **12** (1 & 2), 1–286 (1990)]

D. Overskei, R. R. Parker, and J. Sheffield, "High Beta and/or High Field Tokamaks and Stellarators," *J. Fusion Energy* **8**, 43 (1990)

L. W. Owen, T. Uckan, P. K. Mioduszewski, and A. Pospieszczyk, "H_α Measurements and Modeling of Plasma Confinement in TEXTOR with the ALT-II Pump Limiter," *J. Nucl. Mater.* **176 & 177**, 803–809 (1990)

S. L. Painter and J. F. Lyon, "Alpha-Particle Losses in Compact Torsatron Reactors," pp. 557–66 in *Stellarator Physics: Proceedings of the 7th International Workshop*, IAEA-TECDOC-558, ed. J. F. Lyon, IAEA, Vienna, 1990

S. L. Painter and J. F. Lyon, "Transport Studies of Compact Torsatron Reactors," pp. 102–6 in *Proceedings of the IEEE Thirteenth Symposium on Fusion Engineering*, Vol. 1, ed. M. S. Lubell, M. B. Nestor, and S. F. Vaughan, IEEE, New York, 1990

S. L. Painter and J. F. Lyon, "Transport Survey Calculations Using the Spectral Collocation Method," pp. 567–75 in *Stellarator Physics: Proceedings of the 7th International Workshop*, IAEA-TECDOC-558, ed. J. F. Lyon, IAEA, Vienna, 1990

D. A. Rasmussen, A. C. England, M. Murakami, H. C. Howe, T. C. Clark, R. R. Kindsfather, T. M. Rayburn, P. S. Roger, K. A. Stewart, G. L. Bell, P. L. Shaw, and C. E. Thomas, "Recent Electron Temperature and Density Results from the ATF Thomson Scattering System," pp. 159–65 in *Stellarator Physics: Proceedings of the 7th International Workshop*, IAEA-TECDOC-558, ed. J. F. Lyon, IAEA, Vienna, 1990

R. L. Reid and Y-K. M. Peng, "Potential Minimum Cost of Electricity of Superconducting Coil Tokamak Power Reactors," pp. 258–63 in *Proceedings of the IEEE Thirteenth Symposium on Fusion Engineering*, Vol. 1, ed. M. S. Lubell, M. B. Nestor, and S. F. Vaughan, IEEE, New York, 1990

A. Rodriguez Yunta, W. I. van Rij, and S. P. Hirshman, "Bootstrap Currents in Heliac TJ-II Configurations," *Europhys. Conf. Abstr.* **14B**, 505 (1990)

J. A. Rome, R. N. Morris, S. P. Hirshman, R. H. Fowler, and P. Merkel, "Coil Configurations for Low Aspect Ratio Stellarators," pp. 545–49 in *Stellarator Physics: Proceedings of the 7th International Workshop*, IAEA-TECDOC-558, ed. J. F. Lyon, IAEA, Vienna, 1990

P. M. Ryan, K. E. Rothe, J. H. Whealton, and T. D. Shepard, "Determination of ICRF Antenna Fields in the Vicinity of a 3-D Faraday Shield Structure," *Fusion Eng. Des.* **12** (1 & 2), 37 (1990)

G. Sadler, J. M. Adams, S. E. Attenberger, B. Balet, J. G. Cordey, O. N. Jarvis, T. T. C. Jones, P. Kupschus, B. Laundy, P. J. Lomas, M. J. Loughlin, F. B. Marcus, M. Olsson, P. Stubberfield, D. F. H. Start, A. Tanga, P. R. Thomas, B. Tubbing, and P. van Belle, "D-D Neutron Production from JET Plasmas," *Europhys. Conf. Abstr.* **14B**, 1 (1990)

F. Sano, Y. Takeiri, K. Hanatani, H. Zushi, M. Sato, S. Sudo, T. Mutoh, K. Kondo, H. Kaneko, T. Mizuuchi, H. Okada, S. Morimoto, K. Itoh, S. Besshou, M. Nakasuga, Y. Nakamura, N. Noda, K. Akaishi, O. Motojima, M. Wakatani, T. Obiki, A. Iiyoshi, M. Murakami, and H. C. Howe, "Parametric Scaling Studies of the Energy Confinement Time for Neutral Beam Heated Heliotron E Plasmas," *Nucl. Fusion* **30** (1), 81 (1990)

S. D. Scott, V. Arunasalam, C. W. Barnes, M. G. Bell, M. Bitter, R. Boivin, N. L. Bretz, R. Budny, C. E. Bush, A. Cavallo, T. K. Chu, S. A. Cohen, P. Colestock, S. L. Davis, D. L. Dimock, H. F. Dylla, P. C. Efthimion, A. B. Ehrhardt, R. J. Fonck, E. Fredrickson, H. P. Furth, R. J. Goldston, G. Greene, B. Grek, L. R. Grisham, G. Hammett, R. J. Hawryluk, H. W. Hendel, K. W. Hill, E. Hinnov, D. J. Hoffman, J. Hosea, R. B. Howell, H. Hsuan, R. A. Hulse, K. P. Jaehnig, A. C. Janos, D. Jassby, F. Jobes, D. W. Johnson, L. C. Johnson, R. Kaita, C. Kieras-Phillips, S. J. Kilpatrick, P. H. LaMarche, B. LeBlanc, R. Little, D. M. Manos, D. K. Mansfield, E. Mazzucato, M. P. McCarthy, D. C. McCune, K. McGuire, D. H. McNeill, D. M. Meade, S. S. Medley, D. R. Mikkelsen, R. Motley, D. Mueller, J. A. Murphy, Y. Nagayama, D. R. Nazakian, D. K. Owens, H. Park, A. T. Ramsey, M. H. Redi, A. L. Roquemore, P. H. Rutherford, G. Schilling, J. Schivell, G. L. Schmidt, J. Stevens, B. C. Stratton, W. Stodiek, E. J. Synakowski, W. M. Tang, G. Taylor, J. R. Timberlake, H. H. Towner, M. Ulrickson, S. von Goeler, R. Wieland, M. Williams, J. R. Wilson, K.-L. Wong, S. Yoshikawa, K. M. Young, M. C. Zarnstorff, and S. J. Zweben, "Correlations of Heat and Momentum Transport in the TFTR Tokamak," *Phys. Fluids B* **2** (6), 1300–1305 (1990)

K. C. Shaing, "Neoclassical Quasilinear Transport Theory of Fluctuations in Toroidal Plasmas: Further Considerations," *Phys. Fluids B* **2** (4), 764–72 (1990)

K. C. Shaing, "Poloidal and Parallel Plasma Viscosities in Tokamak Geometry," *Phys. Fluids B* **2** (11), 2847–49 (1990)

K. C. Shaing, "The Role of the Radial Electric Field in Enhanced Confinement Regimes in Stellarators," pp. 97–100 in *Stellarator Physics: Proceedings of the 7th International Workshop*, IAEA-TECDOC-558, ed. J. F. Lyon, IAEA, Vienna, 1990

K. C. Shaing, B. A. Carreras, E. C. Crume, N. Dominguez, S. P. Hirshman, V. E. Lynch, J. S. Tolliver, and W. I. van Rij, "Bootstrap Current Control and the Effects of the Radial Electric Field in Stellarators," pp. 611–20 in *Stellarator Physics: Proceedings of the 7th International Workshop*, IAEA-TECDOC-558, ed. J. F. Lyon, IAEA, Vienna, 1990

K. C. Shaing, E. C. Crume, and W. A. Houlberg, "Bifurcation of Poloidal Rotation and Suppression of Turbulent Fluctuations: A Model for the L-H Transition in Tokamaks," *Phys. Fluids B* **2** (6, Pt. 2), 1492–98 (1990)

K. C. Shaing and R. D. Hazeltine, "Enhanced Pinch Effect Due to Electrostatic Potential," *Phys. Fluids B* **2** (10), 2353–57 (1990)

K. C. Shaing and D. A. Spong, "Extending the Collisional Fluid Equations into the Long Mean-Free-Path Regime: I. Plasma Viscosity," *Phys. Fluids B* **2** (6), 1190–94 (1990)

J. Sheffield, "Scaling from JET to CIT and ITER-Like Devices Using Dimensionless Parameters," *Europhys. Conf. Abstr.* **14B**, 102–5 (1990)

E. R. Solano, G. H. Neilson, and L. L. Lao, "Equilibrium and Stability Studies for an Iron Core Tokamak with a Poloidal Divertor," *Nucl. Fusion* **30** (6), 1107 (1990)

D. A. Spong, J. A. Holmes, J.-N. Leboeuf, and P. J. Christenson, "Destabilization of Tokamak Pressure-Gradient-Driven Instabilities by Energetic Alpha Populations," *Fusion Technol.* **18**, 496–504 (1990)

R. D. Stambaugh, S. M. Wolfe, R. J. Hawryluk, J. H. Harris, H. Biglari, S. C. Prager, R. J. Goldston, R. J. Fonck, T. Ohkawa, B. G. Logan, and E. Oktay, "Enhanced Confinement in Tokamaks," *Phys. Fluids B* **2** (12), 2941–60 (1990)

J. Stevens, C. Bush, P. L. Colestock, G. L. Greene, K. W. Hill, J. C. Hosea, C. K. Phillips, B. Stratton, S. von Goeler, J. R. Wilson, W. Gardner, D. Hoffman, and A. Lysojvan, "The Effect of ICRF Antenna Phasing on Metal Impurities in TFTR," *Plasma Phys. Controlled Fusion* **32**, 196 (1990)

J. Stevens, P. Colestock, D. Hoffman, J. Hosea, C. K. Phillips, J. R. Wilson, M. Beer, M. Bell, M. Bitter, R. Boivin, N. Bretz, C. Bush, A. Cavallo, E. Fredrickson, G. Greene, G. Hammett, K. Hill, A. Janos, D. Jassby, F. Jobes, D. Johnson, R. Kaita, S. J. Kilpatrick, B. LeBlanc, K. McGuire, S. Medley,

Y. Nagayama, D. Mueller, D. Mansfield, D. Owens, H. Park, A. Ramsey, J. Schivell, G. L. Schmidt, B. Stratton, G. Taylor, S. von Goeler, K.-L. Wong, S. J. Zweben, and the TFTR Group, "ICRF Heating up to the 4.5 MW Level on TFTR," *Europhys. Conf. Abstr.* **14B**, 1048 (1990)

W. L. Stirling, W. R. Becraft, J. H. Whealton, and H. H. Haselton, "A Neutral Particle Beam System for ITER with RF Acceleration," pp. 1448–54 in *Proceedings of the IEEE Thirteenth Symposium on Fusion Engineering*, Vol. 2, ed. M. S. Lubell, M. B. Nestor, and S. F. Vaughan, IEEE, New York, 1990

M. Suzuki, A. Hishinuma, P. Maziasz, and T. Sawai, "Void Formation in 10Cr–2Mo Ferritic Steel Irradiated in HFIR," *J. Nucl. Mater.* **170**, 270–75 (1990)

Y. Takeiri, F. Sano, M. Sato, T. Mutoh, H. Okada, S. Sudo, H. Zushi, K. Kondo, H. Kaneko, T. Mizuuchi, N. Noda, K. Akaishi, K. Hanatani, M. Nakasuga, O. Motojima, T. Obiki, A. Iiyoshi, M. Murakami, and H. C. Howe, "Confinement Scaling Studies of Radiofrequency and Neutral Beam Heated Currentless Heliotron E Plasmas," *Nucl. Fusion* **30** (12), 2521–31 (1990)

C. E. Thomas, Jr., and R. F. Gandy, "Autocorrelation and Crossed-Sightline Correlation of ECE for Measurements of Electron Temperature and Density Fluctuations on ATF and TEXT," *Rev. Sci. Instrum.* **61**, 3570–80 (1990)

C. E. Thomas, J. T. Woo, E. Saravia, and D. P. Hutchinson, "Cross-Sightline Correlation of Faraday Rotation for Measurement of Perpendicular Magnetic Fluctuations," pp. 139–45 in *Stellarator Physics: Proceedings of the 7th International Workshop*, IAEA-TECDOC-558, ed. J. F. Lyon, IAEA, Vienna, 1990

S. L. Thomson, J. D. Blevins, and M. W. Delisle, "ITER Reactor Building Design Study," pp. 424–27 in *Proceedings of the IEEE Thirteenth Symposium on Fusion Engineering*, Vol. 1, ed. M. S. Lubell, M. B. Nestor, and S. F. Vaughan, IEEE, New York, 1990

C. C. Tsai, M. A. Akerman, W. R. Becraft, W. K. Dagenhart, H. H. Haselton, D. E. Schechter, W. L. Stirling, J. H. Whealton, and J. J. Donaghy, "Factors Affecting Emittance Measurements of Ion Beams," *Rev. Sci. Instrum.* **61**, 783–87 (1990)

C. C. Tsai, L. A. Berry, H. H. Haselton, D. E. Schechter, and W. L. Stirling, "Potential Applications of an Electron Cyclotron Resonance Multicusp Plasma Source," *J. Vac. Sci. Technol. A* **8** (3), 2900 (1990)

T. Uckan, C. Hidalgo, J. D. Bell, J. H. Harris, J. L. Dunlap, G. R. Dyer, P. K. Mioduszewski, and J. B. Wilgen, "ATF Edge Plasma Turbulence Studies Using a Fast Reciprocating Langmuir Probe," *J. Nucl. Mater.* **176 & 177**, 693–98 (1990)

A. Varias, C. Alejaldre, A. L. Fraguas, L. Garcia, B. A. Carreras, N. Dominguez, and V. E. Lynch, "Ideal Mercier Stability for the TJ-II Flexible Heliac," *Nucl. Fusion* **30** (12), 2597 (1990)

A. Varias, C. Alejaldre, A. López-Fraguas, B. A. Carreras, N. Dominguez, and V. E. Lynch, "Stability Studies for TJ-II," pp. 341–45 in *Stellarator Physics: Proceedings of the 7th International Workshop*, IAEA-TECDOC-558, ed. J. F. Lyon, IAEA, Vienna, 1990

M. R. Wade, R. J. Colchin, G. L. Bell, R. H. Fowler, J. M. Gossett, R. H. Goulding, L. D. Horton, R. C. Isler, M. Kwon, J. F. Lyon, M. M. Menon, R. N. Morris, D. A. Rasmussen, T. M. Rayburn, J. A. Rome, T. D. Shepard, and C. E. Thomas, "Measurements of the Fast Ion Distribution During Neutral Beam and Ion Cyclotron Resonance Heating in ATF," *Europhys. Conf. Abstr.* **14B**, 439 (1990)

M. R. Wade, R. J. Colchin, J. F. Lyon, R. N. Morris, C. E. Thomas, and A. L. Roquemore, "ATF Neutral Particle Analysis System," *Rev. Sci. Instrum.* **61** (10), 3202 (1990)

J. H. Whealton, P. S. Meszaros, K. E. Rothe, R. J. Raridon, and P. M. Ryan, "Extraction Induced Emittance Growth for Negative Ion Sources," *Rev. Sci. Instrum.* **61** (1), 568 (1990)

J. H. Whealton, P. M. Ryan, and R. J. Raridon, "ICRF Antenna Faraday Shield Plasma Sheath Model," *Fusion Eng. Des.* **12** (1 & 2), 121 (1990)

A. J. Wootton, B. A. Carreras, H. Matsumoto, K. McGuire, W. A. Peebles, C. P. Ritz, P. W. Terry, and S. J. Zweben, "Fluctuations and Anomalous Transport in Tokamaks," *Phys. Fluids B* **2** (12), 2879–2903 (1990)

J. J. Zielinski, S. C. Aceto, K. A. Connor, J. F. Lewis, J. C. Glowienka, G. H. Henkel, D. T. Fehling, W. R. DeVan, K. D. St. Onge, D. K. Lee, and A. Carnevali, "ATF Heavy Ion Beam Probe: Installation and Initial Operation," *Rev. Sci. Instrum.* **61** (10), 2961 (1990)

S. J. Zinkle and J. S. Huang, "Mechanical Properties of Carbon-Implanted Niobium," pp. 121–26 in *Proceedings of the Materials Research Society Spring Meeting,* Vol. 188, ed. M. F. Doerner, W. C. Oliver, G. M. Pharr, and F. R. Brotzen, Materials Research Society, Pittsburgh, 1990

1990 CONFERENCE PRESENTATIONS

January

ITER Workshop, Princeton, New Jersey, January 10, 1990

D. L. Hillis, R. C. Isler, C. C. Klepper, J. T. Hogan, P. K. Mioduszewski, L. D. Horton, R. Moyer, D. Gray, R. W. Conn, R. Doerner, A. Pospieszczyk, D. Rusbüldt, R. Schorn, K. H. Dippel, K. H. Finken, H. Euringer, A. Miyahara, K. Akaishi, R. Hulse, and R. Budny, "Initial Helium Removal Experiments with ALT-II Pumping on TEXTOR"

ITER Winter Work Session, Garching, Federal Republic of Germany, January 22–March 23, 1990

D. B. Batchelor, E. F. Jaeger, and M. D. Carter, "Fast Wave Current Drive for ITER Using the ORION Code"

CIT West Coast Physics Meeting, San Diego, California, January 29, 1990

E. A. Lazarus, "High Elongation Plasmas"

ICH Design Workshop, Boulder, Colorado, January 31–February 2, 1990

D. J. Hoffman, F. W. Baity, R. H. Goulding, P. M. Ryan, D. J. Taylor, and M. J. Mayberry, "Fast-Wave Current Drive Design Issues"

February

Topical Conference on Research Trends in Nonlinear and Relativistic Effects in Plasmas, San Diego, California, February 5–8, 1990

B. A. Carreras, J.-N. Leboeuf, D. K. Lee, J. A. Holmes, and V. E. Lynch, "Fluid Approach to Plasma Turbulence: Tokamak Edge Fluctuations"

Second TTF Transport Workshop, Hilton Head, South Carolina, February 19–23, 1990

N. Dominguez, B. A. Carreras, V. E. Lynch, J.-N. Leboeuf, L. Garcia, and P. H. Diamond, "Numerical Approach to Dissipative-Trapped-Electron-Mode Driven Drift Wave Turbulence"

C. L. Hedrick and J.-N. Leboeuf, "Effect of Tokamak Electrostatic Edge Fluctuations on Orbits and Transport"

C. Hidalgo, T. Uckan, J. D. Bell, J. H. Harris, J. L. Dunlap, G. R. Dyer, Ch. P. Ritz, K. Carter, T. L. Rhodes, and A. J. Wootton, "Turbulence Studies in ATF"

S. Hiroe, D. W. Johnson, and R. J. Goldston, "Difference in Electron Thermal Diffusivity and Profile Between Interior and Exterior of TFTR L-Mode Plasmas"

J.-N. Leboeuf, B. A. Carreras, J. A. Holmes, D. K. Lee, V. E. Lynch, Ch. P. Ritz, A. J. Wootton, P. H. Diamond, A. S. Ware, and D. R. Thayer, "Recent Progress in TEXT Edge Turbulence Modeling"

M. Murakami, G. L. Bell, T. S. Bigelow, B. A. Carreras, A. C. England, J. C. Glowienka, H. C. Howe, D. K. Lee, V. E. Lynch, J. S. Tolliver, D. A. Rasmussen, W. R. Wing, and the ATF Group, "Bootstrap Current and Energy Confinement Studies in the Advanced Toroidal Facility"

D. A. Spong and B. A. Carreras, "Stochastic Magnetic Fields and Electron Heat Transport Induced by Neoclassical MHD Instabilities"

D. R. Thayer, P. H. Diamond, A. S. Ware, B. A. Carreras, C. Hidalgo, J. A. Holmes, J. N. Leboeuf, P. W. Terry, Ch. P. Ritz, and A. J. Wootton, "Radiative Enhanced Fluctuation Induced Transport in Sheared Systems (Rippling and Drift Wave Turbulence)"

Waste Management '90: 16th Symposium on Waste Management, Tucson, Arizona, February 25–March 1, 1990

T. L. White, E. L. Youngblood, J. B. Berry, and A. J. Mattus, "Status of Microwave Process Development for RH-TRU Wastes at Oak Ridge National Laboratory"

U.S./Japan Workshop on Development of Plasma-Facing Components for Next Large Fusion Devices, La Jolla, California, February 28–March 2, 1990

T. D. Burchell, G. Hollenberg, and O. D. Slagle, "The Effects of Neutron Irradiation on the Structure and Properties of Graphite and Carbon-Carbon Composites"

March

ITER Specialists' Meeting on Beta Limits and Profiles, Garching, Federal Republic of Germany, March 5–6, 1990

B. A. Carreras, "Oak Ridge National Laboratory Research Highlights"

B. A. Carreras (with contributions from L. A. Charlton, J. A. Holmes, V. E. Lynch, K. C. Shaing, D. A. Spong, and the ATF Experimental Group), "Resistive Stability in the Region $2.1 < q_\psi < 3.1$ and Bootstrap Current Evaluation"

B. A. Carreras, J.-N. Leboeuf, D. K. Lee, J. A. Holmes, and V. E. Lynch, "Effect of the Equilibrium Magnetic Field on Plasma Edge Fluctuations"

B. A. Carreras, J.-N. Leboeuf, D. K. Lee, J. A. Holmes, V. E. Lynch, J. Harris, C. Hidalgo, R. Isler, T. Uckan, R. Bravenec, Ch. P. Ritz, W. Rowan, A. J. Wootton, P. H. Diamond, A. S. Ware, and D. R. Thayer, "Plasma Edge Fluctuations and Transport: TEXT and ATF Modeling"

M. Murakami, G. L. Bell, B. A. Carreras, A. C. England, J. C. Glowienka, H. C. Howe, D. K. Lee, V. E. Lynch, J. S. Tolliver, D. A. Rasmussen, W. R. Wing, and the ATF Group, "Energy Confinement and Bootstrap Current Studies in the Advanced Toroidal Facility"

First Los Alamos Symposium on Ultra-Wideband Radar, Los Alamos, New Mexico, March 5–8, 1990. Proceedings published by CRC Press

D. B. Batchelor and E. F. Jaeger, "Full-Wave Computation of Electromagnetic Wave Excitation, Propagation, and Absorption at the Ion Cyclotron Frequency in Fusion Experiments"

Applied Computational Electromagnetics Society 6th Annual Review of Progress in Applied Computational Electromagnetics, Monterey, California, March 19–22, 1990

D. B. Batchelor and E. F. Jaeger, "Full-Wave Computation of Electromagnetic Wave Excitation, Propagation, and Absorption at the Ion Cyclotron Frequency in Fusion Experiments"

Special Operations Expo '90, Idaho Falls, Idaho, March 20–22, 1990

S. K. Combs, H. H. Haselton, and S. L. Milora, "Simple Light Gas Guns for Hypervelocity Studies"

First Annual Cold Fusion Conference, Salt Lake City, Utah, March 27–30, 1992

D. P. Hutchinson, C. A. Bennett, R. K. Richards, J. Bullock IV, and G. L. Powell, "Initial Calorimetry Experiments in the Physics Division of ORNL," invited

April

Materials Research Society Spring Meeting, San Francisco, California, April 16–20, 1990. Proceedings published as *Proceedings of the Materials Research Society Spring Meeting*, ed. M. F. Doerner, W. C. Oliver, G. M. Pharr, and F. R. Brotzen, Materials Research Society, Pittsburgh, 1990

H. D. Kimrey, J. O. Kiggans, M. A. Janney, and R. L. Beatty, "Microwave Sintering of Zirconia-Toughened Alumina Composites"

T. L. White, E. L. Youngblood, J. B. Berry, and A. J. Mattus, "First Results of In-Can Microwave Processing Experiments for Radioactive Liquid Wastes at the Oak Ridge National Laboratory"

S. J. Zinkle and J. S. Huang, "Mechanical Properties of Carbon-Implanted Niobium," Vol. 188, pp. 121–26

Meeting of the Fusion Policy Advisory Committee, Oak Ridge, Tennessee, April 18, 1990

E. E. Bloom and A. F. Rowcliffe, "Development of Materials for Fusion Applications"

1990 Sherwood International Conference on Controlled Fusion Theory, Williamsburg, Virginia, April 23–25, 1990. Abstract booklet distributed to participants

B. A. Carreras, V. E. Lynch, and L. Garcia, "Turbulence Saturation and Poloidal Flow Velocity"

M. D. Carter, D. B. Batchelor, and E. F. Jaeger, "Effects of Non-Boltzmann Electrons on the Plasma Potential"

J. R. Cary and J. A. Rome, "Symplectic Integration of Guiding-Center Orbits"

L. A. Charlton, B. A. Carreras, J.-N. Leboeuf, and V. E. Lynch, "Stability Properties of the ATF Torsatron During Entry to the Second Stability Regime"

N. Dominguez, B. A. Carreras, V. E. Lynch, L. A. Charlton, L. Garcia, and P. H. Diamond, "Dissipative Trapped Electron Drift Wave Turbulence"

R. C. Goldfinger and D. B. Batchelor, "Fast Wave Current Drive Calculations Using the Geometrical Optics Code RAYS"

C. L. Hedrick and J.-N. Leboeuf, "Effect of Tokamak Electrostatic Edge Fluctuations on Orbits and Transport"

W. A. Houlberg and M. J. Gouge, "Particle Transport and Fueling Issues for DT Diverted Plasmas"

E. F. Jaeger, D. B. Batchelor, and M. D. Carter, "Fast Wave Current Drive Calculations for ITER Using the ORION Code"

J.-N. Leboeuf, B. A. Carreras, J. A. Holmes, D. K. Lee, V. E. Lynch, Ch. P. Ritz, A. J. Wootton, P. H. Diamond, A. S. Ware, and D. R. Thayer, "Modeling of Fluctuations at the Plasma Edge of the TEXT Tokamak"

V. E. Lynch, B. A. Carreras, J. B. Drake, and J.-N. Leboeuf, "Plasma Turbulence Calculations on the Intel RX Hypercube"

D. A. Spong and B. A. Carreras, "Stochastic Magnetic Fields and Electron Heat Transport Induced by Neoclassical MHD Instabilities"

K. C. Shaing and R. D. Hazeltine, "Poloidal Plasma Rotation in Tokamaks"

Post-Sherwood Meeting on Massively Parallel Computing, Williamsburg, Virginia, April 25, 1990

V. E. Lynch, B. A. Carreras, J. Drake, J.-N. Leboeuf, M. D. Carter, D. B. Batchelor, and E. F. Jaeger, "Parallel Computing at ORNL"

May

Eighth Topical Conference on High-Temperature Plasma Diagnostics, Hyannis, Massachusetts, May 6–10, 1990. Proceedings published in *Rev. Sci. Instrum.* **61**, No. 10, Pt. II (1990)

S. C. Aceto, K. A. Connor, P. E. McLaren, J. J. Zielinski, J. G. Schatz, and G. H. Henkel, "Energy Analyzer for the ATF Heavy Ion Beam Probe," p. 2958

C. E. Bush, J. Schivell, G. Taylor, N. Bretz, A. Cavallo, E. Fredrickson, A. Janos, D. K. Mansfield, K. McGuire, R. Nazikian, H. Park, A. T. Ramsey, B. Stratton, and E. J. Synakowski, "Application of TFTR Diagnostics to Study Limiter *H*-Modes," p. 3532

T. P. Crowley, S. C. Aceto, K. A. Connor, J. W. Heard, R. L. Hickok, J. W. Lewis, P. E. McLaren, A. Ouroua, J. G. Schatz, P. M. Schoch, J. Schwelberger, V. J. Simcic, and J. J. Zielinski, "Recent Advances in Heavy Ion Beam Probe Diagnostics," p. 2989

E. C. Crume, L. D. Horton, R. C. Isler, and S. Morita, "Ion Temperature Measurements in the ATF Torsatron Using Titanium Forbidden Lines," p. 3147 (abstract only)

G. R. Hanson, J. B. Wilgen, E. Anabitarte, J. D. Bell, J. H. Harris, J. L. Dunlap, and C. E. Thomas, "The ATF Two-Frequency Correlation Reflectometer," p. 3049

D. P. Hutchinson, R. K. Richards, H. T. Hunter, and C. A. Bennett, "A Proof-of-Principle Test of a Thomson Scattering Alpha Particle Diagnostic"

C. C. Klepper, J. E. Simpkins, D. L. Hillis, P. K. Mioduszewski, R. A. Moyer, D. Gray, K. H. Dippel, and A. Pospieszczyk, "Application of Modern Optical Fiber Technology to the Study of Plasmas of Closed Divertors and Pump Limiters in Reactor-Relevant Conditions," p. 2943

C. H. Ma, D. P. Hutchinson, and K. L. Vander Sluis, "A Difluoromethane Laser Interferometer System on ATF," p. 2891

M. R. Wade, R. J. Colchin, J. F. Lyon, R. N. Morris, C. E. Thomas, and A. L. Roquemore, "ATF Neutral Particle Analysis System," p. 3202

W. R. Wing, G. R. Dyer, J. C. Glowienka, J. H. Harris, J. W. Halliwell, and G. H. Neilson, "The ATF Diamagnetic Diagnostic: Status and Results," p. 2987 (abstract only)

J. J. Zielinski, S. C. Aceto, K. A. Connor, J. F. Lewis, J. C. Glowienka, G. H. Henkel, D. T. Fehling, W. R. DeVan, K. D. St. Onge, D. K. Lee, and A. Carnevali, "ATF Heavy Ion Beam Probe: Installation and Initial Operation," p. 2961

ICMC-90/Nonmetallic: Topical Conference on Nonmetallic Metals and Composites at Low Temperatures, Heidelberg, Federal Republic of Germany, May 17–18, 1990

T. J. McManamy, G. Kanemoto, and P. Snook, "The Insulation Irradiation Test Program for the Compact Ignition Tokamak"

9th International Conference on Plasma Surface Interactions in Controlled Fusion Devices, Bournemouth, England, May 20–25, 1990. Proceedings published in *J. Nucl. Mater.* **176 & 177** (1990)

C. E. Bush, E. Fredrickson, N. Bretz, A. Cavallo, A. Janos, Y. Nagayama, H. Park, J. Schivell, G. Taylor, R. Nazikian, and A. T. Ramsey, "ELM Activity During Limiter *H*-Modes on TFTR," p. 786

D. L. Hillis, J. T. Hogan, C. C. Klepper, P. K. Mioduszewski, R. C. Isler, L. D. Horton, A. Pospieszczyk, K. H. Finken, K. H. Dippel, D. Rusbüldt, H. Euringer, R. Schorn, R. Moyer, D. Gray, and R. A. Hulse, "Helium Exhaust Studies with the ALT-II Pump Limiter in TEXTOR"

J. T. Hogan and P. K. Mioduszewski, "Global Particle Balance Modeling for Open Divertors"

R. C. Isler, G. L. Bell, T. S. Bigelow, E. C. Crume, A. C. England, J. C. Glowienka, L. D. Horton, T. C. Jernigan, R. A. Langley, P. K. Mioduszewski, M. Murakami, D. A. Rasmussen, J. E. Simpkins, J. B. Wilgen, and W. R. Wing, "The Effects of Chromium and Titanium Gettering on the Operation of the Advanced Toroidal Facility," pp. 332–36

C. C. Klepper, P. Bonnel, J. L. Bruneau, M. Chatelier, C. Gil, C. Grisolia, G. R. Haste, L. D. Horton, T. Loarer, G. Martin, P. K. Mioduszewski, B. Pegourie, L. Rodriguez, T. Uckan, and J. G. Watkins, "Particle Exhaust Studies in Tore Supra with a Pump Limiter," pp. 798–802

M. M. Menon, P. K. Mioduszewski, and J. E. Simpkins, "Pumping Characteristics of Thick Titanium Films"

P. K. Mioduszewski, L. W. Owen, M. M. Menon, and J. T. Hogan, "Particle Exhaust Modeling for the Collaborative DIII-D Advanced Divertor Program," pp. 733–38

L. W. Owen, T. Uckan, P. K. Mioduszewski, and A. Pospieszczyk, "H_α Measurements and Modeling of Plasma Confinement in TEXTOR with the ALT-II Pump Limiter," pp. 803–9

T. Uckan, C. Hidalgo, J. D. Bell, J. H. Harris, J. L. Dunlap, G. R. Dyer, P. K. Mioduszewski, J. B. Wilgen, C. P. Ritz, A. J. Wootton, T. L. Rhodes, and K. Carter, "ATF Edge Plasma Turbulence Studies Using a Fast Reciprocating Langmuir Probe," pp. 693–98

Workshop on Ceramic Composite Materials for Structural Applications in Fusion Reactors, Santa Barbara, California, May 21, 1990

T. D. Burchell, "Radiation Damage in Carbon Fiber Composites"

F. W. Wiffen, "Ceramic Composite Materials for Structural Applications in Fusion Reactors—OFE Perspective and Expectations"

Annual Meeting of the American Physical Society Division of Atomic, Molecular, and Optical Physics, Monterey, California, May 21–23, 1990. Abstracts published in *Bull. Am. Phys. Soc.* **35** (1990)

F. W. Meyer, C. C. Havener, and P. A. Zeijlmans van Emmichoven, "Electron Spectroscopic Studies of the Neutralization of Slow Multicharged Ions Close to Metal Surfaces," p. 1200

M. S. Pindzola, G. J. Bottrell, and C. R. Bottcher, "Multiphoton Ionization of Atoms Using Time-Dependent Hartree-Fock Methods," p. 1151

17th IEEE International Conference on Plasma Science, Oakland, California, May 21–23, 1990. Abstracts published in conference record

J. C. Glowienka and the ATF Group, "Status of Studies in the ATF Torsatron"

M. Kwon, C. E. Thomas, D. J. Hoffman, and C. L. Rettig, "Measurement of the Effects of Faraday Shields on ICRH Antenna Coupling"

Satellite Workshop for the 9th International Conference on Plasma Surface Interactions in Controlled Fusion Devices, Cadarache, France, May 28–30, 1990

R. C. Isler, J. D. Bell, G. L. Bell, T. S. Bigelow, E. C. Crume, J. L. Dunlap, A. C. England, J. C. Glowienka, J. H. Harris, D. L. Hillis, S. Hiroe, C. Hidalgo, L. D. Horton, T. C. Jernigan, R. A. Langley, P. K. Mioduszewski, M. Murakami, D. A. Rasmussen, J. E. Simpkins, T. Uckan, J. B. Wilgen, and W. R. Wing, "Boundary Radiation and Plasma Stability in Currentless Confinement Devices"

June

U.S./Japan Symposium on Advances in Weldings Metallurgy, San Francisco, California, June 6–8, 1990, and Yokohama, Japan, June 12–13, 1990

G. M. Goodwin, "Test Methods for Evaluating Hot Cracking: Review and Perspective"

Spring Meeting of the American Nuclear Society, Nashville, Tennessee, June 10–14, 1990

M. L. Grossbeck and T. Sawai, "Properties of Austenitic Stainless Steels in a Simulated ITER Irradiation Environment"

B. E. Nelson, D. E. Williamson, D. C. Lousteau, C. J. Hammonds, P. L. Goranson, and R. O. Sayer, "The Effect of Electromagnetically Induced Eddy Currents on the Design of ITER In-Vessel Components"

17th European Physical Society Conference on Controlled Fusion and Plasma Heating, Amsterdam, The Netherlands, June 25–29, 1990. Contributed papers published in *Europhys. Conf. Abstr.* **14B**, Pts. I–IV (1990); invited papers published in *Plasma Phys. Controlled Fusion* **32**, No. 11 (1990)

C. Alejaldre, A. Varias, A. L. Fraguas, B. Carreras, N. Dominguez, and V. E. Lynch, "Self-Stabilization of Ideal Modes in a Heliac," *Europhys. Conf. Abstr.* **14B**, 497 (1990)

E. Anabitarte, G. R. Hanson, J. D. Bell, J. L. Dunlap, J. H. Harris, C. Hidalgo, C. E. Thomas, T. Uckan, and J. B. Wilgen, "Density Fluctuation Measurements on ATF Using a Two-Frequency Reflectometer," *Europhys. Conf. Abstr.* **14B**, 1492–5 (1990)

S. E. Attenberger, B. Balet, D. J. Campbell, J. P. Christiansen, G. A. Cottrell, A. Edwards, T. T. C. Jones, P. Kupschus, P. J. Lomas, P. Nielsen, J. O'Rourke, D. Pasini, R. Prentice, G. Sadler, G. Schmidt, P. Stubberfield, A. Tataroni, F. Tibone, and H. Weisen, "Peaked Profiles in Low q High Current Discharges in JET," *Europhys. Conf. Abstr.* **14B**, 5 (1990)

J. R. Ferron, M. S. Chu, F. J. Helton, W. Howl, A. G. Kellman, L. L. Lao, E. A. Lazarus, J. K. Lee, T. H. Osborne, R. D. Stambaugh, E. J. Strait, T. S. Taylor, and A. D. Turnbull, "The Beta Limit in the DIII-D Tokamak," *Europhys. Conf. Abstr.* **14B**, 371 (1990)

A. L. Fraguas, A. Varias, C. Alejaldre, B. Carreras, N. Dominguez, and V. E. Lynch, "Equilibrium and Stability of High q TJ-II Configurations," *Europhys. Conf. Abstr.* **14B**, 509 (1990)

R. J. Goldston, G. Bateman, M. G. Bell, R. Bickerton, E. A. Chaniotakis, D. R. Cohn, P. L. Colestock, D. N. Hill, W. A. Houlberg, S. C. Jardin, S. S. Medley, G. H. Neilson, W. A. Peebles, F. W. Perkins, N. Pomphrey, M. Porkolab, J. A. Schmidt, D. J. Sigmar, R. D. Stambaugh, D. P. Stotler, M. Ulrickson, R. E. Waltz, and K. G. Young, "A Physics Perspective on CIT," *Europhys. Conf. Abstr.* **14B**, 134–37 (1990)

R. H. Goulding, F. W. Baity, D. B. Batchelor, S. C. Chiu, D. J. Hoffman, E. F. Jaeger, M. J. Mayberry, and P. M. Ryan, "Development of Fast-Wave ICRF Current Drive Systems at ORNL," *Europhys. Conf. Abstr.* **14B**, 1311 (1990)

W. Hess, M. Druetta, T. Fall, D. Guilhem, C. C. Klepper, and M. Mattioli, "Fast Scanning Fiber-Multiplier Used for Plasma-Edge Visible Spectroscopy on Tore Supra," *Europhys. Conf. Abstr.* **14B**, 1580 (1990)

C. Hidalgo, T. Uckan, J. D. Bell, J. H. Harris, B. A. Carreras, J. L. Dunlap, G. R. Dyer, C. P. Ritz, K. Carter, T. L. Rhodes, and A. J. Wootton, "Edge Turbulence Studies in ATF," *Europhys. Conf. Abstr.* **14B**, 1353–56 (1990)

L. D. Horton, R. C. Isler, E. C. Crume, T. C. Jernigan, and S. Morita, "Impurity Transport in ATF and the Effect of Controlled Impurity Injection," *Europhys. Conf. Abstr.* **14B**, 447–50 (1990)

H. Iguchi, M. Hosokawa, H. C. Howe, K. Ida, H. Idei, O. Kaneko, S. Kubo, K. Masai, K. Matsuoka, S. Morita, K. Nishimura, N. Noda, S. Okamura, T. Ozaki, A. Sagara, H. Sanuki, T. Shoji, S. Sobhanian, C. Takahashi, Y. Takeiri, Y. Takita, K. Tsuzuki, H. Yamada, T. Amano, and M. Fujiwara, "Transport Study on ECH- and NBI-Heated Plasmas in the Low-Aspect-Ratio Helical System CHS," *Europhys. Conf. Abstr.* **14B**, 451–54 (1990)

R. C. Isler, G. L. Bell, T. S. Bigelow, E. C. Crume, A. C. England, J. C. Glowienka, L. D. Horton, T. C. Jernigan, R. A. Langley, J. F. Lyon, P. K. Mioduszewski, S. Morita, M. Murakami, D. A. Rasmussen, J. E. Simpkins, J. B. Wilgen, and W. R. Wing, "Cleanup and Improvement of Operational Performance of ATF by Chromium and Titanium Gettering," *Europhys. Conf. Abstr.* **14B**, 455–58 (1990)

T. T. C. Jones, P. J. Lomas, S. E. Attenberger, J. P. Christiansen, G. A. Cottrell, R. Gianelli, L. de Kock, P. Kupschus, A. McCracken, C. G. Lowry, P. Nielsen, D. Pasini, R. Prentice, G. Sadler, M. F. Stamp, D. D. R. Summers, M. von Hellerman, and H. Weisen, "Fusion Performance of JET Limiter Plasmas Using Be-Coated Graphite and Solid Be Surfaces," *Europhys. Conf. Abstr.* **14B**, 9 (1990)

E. A. Lazarus, A. D. Turnbull, A. G. Kellman, J. R. Ferron, F. J. Helton, L. L. Lao, J. A. Leuer, E. J. Strait, and T. S. Taylor, "Experiments at High Elongation in DIII-D," *Europhys. Conf. Abstr.* **14B**, 429 (1990)

J. F. Lyon, "Review of Recent Stellarator Results in the U.S.A., the U.S.S.R., and Japan," invited, *Plasma Phys. Controlled Fusion* **32** (11), 1041–59 (1990)

R. A. Moyer, K. H. Finken, D. Reiter, C. C. Klepper, R. W. Conn, K. H. Dippel, D. Gray, D. L. Hillis, A. Pospieszczyk, G. H. Wolf, the TEXTOR Team, and the NI Team, "Influence of Plasma-Neutral

Interactions on ALT-II Pump Limiter Performance During NI Heating of TEXTOR," *Europhys. Conf. Abstr.* **14B**, 1447 (1990)

M. Murakami, B. A. Carreras, G. L. Bell, T. S. Bigelow, G. R. Dyer, A. C. England, J. C. Glowienka, S. Hiroe, H. C. Howe, T. C. Jernigan, D. K. Lee, V. E. Lynch, S. Morita, D. A. Rasmussen, J. S. Tolliver, M. R. Wade, J. B. Wilgen, W. R. Wing, and the ATF Group, "Bootstrap Current Studies in the Advanced Toroidal Facility," *Europhys. Conf. Abstr.* **14B**, 443–46 (1990)

A. Nicolai, Y-K. M. Peng, and J. T. Hogan, "Implementation of Scaling Laws in the 1-1/2-D Transport Code and Applications to the Ignition Spherical Torus," *Europhys. Conf. Abstr.* **14B**, 825 (1990)

A. Rodriguez Yunta, W. I. van Rij, and S. P. Hirshman, "Bootstrap Currents in Heliac TJ-II Configurations," *Europhys. Conf. Abstr.* **14B**, 505 (1990)

G. Sadler, J. M. Adams, S. E. Attenberger, B. Balet, J. G. Cordey, O. N. Jarvis, T. T. C. Jones, P. Kupschus, B. Laundy, P. J. Lomas, M. J. Loughlin, F. B. Marcus, M. Olsson, P. Stubberfield, D. F. H. Start, A. Tanga, P. R. Thomas, B. Tubbing, and P. van Belle, "D-D Neutron Production from JET Plasmas," *Europhys. Conf. Abstr.* **14B**, 1 (1990)

J. Sheffield, "Scaling from JET to CIT and ITER-Like Devices Using Dimensionless Parameters," *Europhys. Conf. Abstr.* **14B**, 102–5 (1990)

J. Stevens, P. Colestock, D. Hoffman, J. Hosea, C. K. Phillips, J. R. Wilson, M. Beer, M. Bell, M. Bitter, R. Boivin, N. Bretz, C. Bush, A. Cavallo, E. Fredrickson, G. Greene, G. Hammett, K. Hill, A. Janos, D. Jassby, F. Jobes, D. Johnson, R. Kaita, S. J. Kilpatrick, B. LeBlanc, K. McGuire, S. Medley, Y. Nagayama, D. Mueller, D. Mansfield, D. Owens, H. Park, A. Ramsey, J. Schivell, G. L. Schmidt, B. Stratton, G. Taylor, S. von Goeler, K.-L. Wong, S. J. Zweben, and the TFTR Group, "ICRF Heating up to the 4.5 MW Level on TFTR," *Europhys. Conf. Abstr.* **14B**, 1048 (1990)

M. R. Wade, R. J. Colchin, G. L. Bell, R. H. Fowler, J. M. Gossett, R. H. Goulding, L. D. Horton, R. C. Isler, M. Kwon, J. F. Lyon, M. M. Menon, R. N. Morris, D. A. Rasmussen, T. M. Rayburn, J. A. Rome, T. D. Shepard, and C. E. Thomas, "Measurements of the Fast Ion Distribution During Neutral Beam and Ion Cyclotron Resonance Heating in ATF," *Europhys. Conf. Abstr.* **14B**, 439 (1990)

July

Workshop on Transport and Confinement in Toroidal Devices, Universidad Internacional Menendez Pelayo, Santander, Spain, July 2, 1990

B. A. Carreras, "Resistive MHD Turbulence"

B. A. Carreras and V. E. Lynch, "Effect of the Radial Electric Field on Turbulence"

IEA Workshop on Recent Results from Stellarators, Garching, Federal Republic of Germany, July 2–6, 1990

R. H. Goulding, "Recent Results of ICRF Heating Experiments on ATF"

R. C. Isler and the ATF Group, "Energy Confinement and Transport in ATF"

R. C. Isler and the ATF Group, "Plasma Collapses in ATF"

J. F. Lyon, "Status of the ATF Experiment"

J. F. Lyon, B. A. Carreras, and M. Murakami, "Bootstrap Current Studies in ATF"

J. F. Lyon and S. L. Painter, "Fast 1-D Code for Transport Scoping Studies"

15th International Conference on X-Ray and Inner-Shell Processes, Knoxville, Tennessee, July 9–13, 1990

J. K. Swenson, J. Burgdorfer, C. C. Havener, D. C. Gregory, N. Stolterfoht, and F. W. Meyer, "Coloumb Focussing and Interference of Autoionization Electrons Produced in Slow He^+ + He Collisions"

ITER Workshop on Fuelling and Plasma Operational Control, Garching, Federal Republic of Germany, July 9–13, 1990. Papers issued as internal reports by the ITER Conceptual Design Activity, Garching, Federal Republic of Germany

W. A. Houlberg, "Discussions and Conclusions on Density/Density Profile Control and DT Mix," ITER-IL-PH-9-0-U-13

W. A. Houlberg, "Pellet Ablation Results from JET," ITER-IL-PH-9-0-U-3

W. A. Houlberg and M. J. Gouge, "Pellet and Gas Puffing Scenarios for ITER," ITER-IL-PH-9-0-U-9

ARIES Project Meeting, Troy, New York, July 11, 1990

C. C. Baker, "Folded Waveguide Update"

August

DOE Workshop on Radiation Effects on Materials in High Radiation Environments, Salt Lake City, Utah, August 13–15, 1990

F. W. Wiffen, "Needed Radiation Effects Research for Fusion Reactors"

S. J. Zinkle, "Microstructure and Electrical Properties of Irradiated Ceramics"

Second Edward Bouchet International Conference on Physics and Technology, Accra, Ghana, August 14–17, 1990

C. E. Bush, "Circular Limiter H-Mode Plasmas on the Tokamak Fusion Test Reactor (TFTR)"

Workshop on Reviewing Energy Selective Neutron Irradiation Test Facility (ESNIT), Tokai-mura, Japan, August 26, 1991

F. W. Wiffen, "Materials Test Facilities for the Fusion Program—A U.S. Perspective on Neutron Sources"

International School of Plasma Physics "Piero Caldirola" 6: Theory of Fusion Plasmas, Varenna, Italy, August 27–31, 1990. Proceedings published as *Theory of Fusion Plasmas: ISPP-6 Piero Caldirola,* Societa Italiana di Fisica/Editrice Compositore, Bologna, Italy, 1990

Y. Nakamura, K. Ichiguchi, M. Wakatani, B. A. Carreras, N. Dominguez, J.-N. Leboeuf, V. E. Lynch, J. L. Johnson, and G. Rewoldt, "Beta-Limit Study of $\ell = 2$ Heliotron/Torsatron and a New Low-n Mode Stability Analysis"

1990 European Workshop on Lithium and Lead-Lithium Corrosion and Chemistry, Nottingham, England, August 30–September 1, 1990

P. F. Tortorelli, "Deposition in Pb–17 at. % Li"

September

16th Symposium on Fusion Technology, London, England, September 3–7, 1990. Proceedings published as *Fusion Technology 1990: Proceedings of the 16th Symposium on Fusion Technology, London, U.K., 3–7 September 1990,* ed. B. E. Keen, M. Huguet and R. Hemsworth, North-Holland, Amsterdam, 1991

F. W. Baity, R. H. Goulding, D. J. Hoffman, P. M. Ryan, D. J. Taylor, and M. J. Mayberry, "Fast-Wave Current Drive System for DIII-D," Vol. 2, p. 1035

R. Carrera, J. L. Anderson, R. Arslangoglu, T. Bauer, E. Becker, W. D. Booth, J. Borcherding, G. Brunson, R. Charbeneau, D. Coffin, P. Cooper, J. Q. Dong, M. D. Driga, R. Durrer, T. Elevant, S. E. Eways, S. Fetter, G. Y. Fu, J. Gilligan, J. H. Gully, Z. Guo, G. A. Hallock, F. J. Helton, N. E. Hertel, L. M. Hively, H. C. Howe, J. Howell, K. T. Hsieh, Y. L. Hwang, E. F. Jaeger, M. J. Johnson, R. Khayrutdinov, D. Klein, J. Q. Ling, M. Manavazhi, H. Marcus, S. S. Medley, G. Miley, R. Mohanti, E. Montalvo, M. E. Oakes, C. A. Ordonez, D. E. Palmrose, T. A. Parish, J. Quinones, G. Roden, M. N. Rosenbluth, G. Shlapper, B. R. Shi, B. Shofolu, R. L. Sledge, S. Tamor, K. Tani, D. Tesar, J. W. Van Dam, P. Varghese, W. A. Walls,

Y. Watanabe, B. W. Wehring, D. Wehrlen, W. F. Weldon, M. D. Werst, H. H. Woodson, and H. Xiao, "Design and Analysis of the IGNITEX Approach for a Laboratory Fusion Experiment," Vol. 1, p. 528

R. J. Dowling, R. E. Price, F. W. Wiffen, and S. A. Eckstrand, "Overview of the U.S. Magnetic Fusion Energy Program," Vol. 1, p. 199

M. J. Gouge, B. E. Argo, L. R. Baylor, S. K. Combs, D. T. Fehling, P. W. Fisher, C. A. Foster, C. R. Foust, S. L. Milora, A. L. Qualls, D. E. Schechter, D. W. Simmons, D. O. Sparks, and C. C. Tsai, "Pellet Injector Development at ORNL," Vol. 1, p. 675

A. G. Kellman, J. R. Ferron, T. H. Jensen, L. L. Lao, E. A. Lazarus, J. B. Lister, J. L. Luxon, D. G. Skinner, E. J. Strait, E. Reis, T. S. Taylor, and A. D. Turnbull, "Vertical Stability, High Elongation and the Consequences of Loss of Vertical Control on DIII-D," Vol. 2, p. 1045

F. Najmabadi, R. W. Conn, C. G. Bathke, L. Bromberg, E. T. Cheng, D. R. Cohn, P. I. H. Cooke, R. L. Creedon, D. A. Ehst, K. Evans, Jr., N. M. Ghoniem, S. P. Grotz, M. Z. Hasan, J. T. Hogan, J. S. Herring, A. W. Hyatt, E. Ibrahim, S. A. Hardin, C. Kessel, M. Klasky, R. A. Krakowski, T. Kunugi, J. A. Leuer, J. Mandrekas, R. C. Martin, T.-K. Mau, R. L. Miller, Y-K. M. Peng, R. L. Reid, J. F. Santarius, M. J. Schaffer, J. Schultz, K. R. Schultz, J. Swartz, S. Sharafat, C. E. Singer, L. Snead, D. Steiner, D. J. Strickler, D.-K. Sze, M. Valenti, D. J. Ward, J. E. C. Williams, L. J. Wittenberg, and C. P. C. Wong, "The ARIES-1 Tokamak Reactor Study," Vol. 1, p. 253

K. A. Niemer, J. C. Gilligan, C. D. Croessman, and A. C. England, "Theoretical Analysis of a Runaway Electron Suppression Device," Vol. 1, p. 346

Y-K. M. Peng and J. B. Hicks, "Engineering Feasibility of Tight Aspect Ratio Tokamak (Spherical Torus) Reactors," Vol. 2, p. 1287

Fifth International Conference on the Physics of Highly Charged Ions, Giessen, Federal Republic of Germany, September 10–14, 1990

C. C. Havener and R. A. Phaneuf, "Electron Capture in Slow Collisions of Multicharged Ions with Hydrogen Atoms Using Merged Beams," invited

E. K. Wahlin, J. S. Thompson, G. H. Dunn, R. A. Phaneuf, D. C. Gregory, and A. C. H. Smith, "Electron Impact Excitation, $e + Si^3 + (2S^{1/2}) \bullet e + Si^3 + (2P^{1/2,3/2})$, Using Electron Energy Loss in Merged Beams"

11th Executive Committee Meeting, IEA: Research and Development on Fusion Materials, Karlsruhe, Germany, September 11, 1990

F. W. Wiffen, "Review of the United States Fusion Reactor Materials Program"

International Conference on Radiation Materials Science, Leningrad, U.S.S.R., September 18–20, 1990

R. L. Klueh, "Helium Effects on the Mechanical Properties of Neutron-Irradiated Cr–Mo Ferritic Steels"

A. F. Rowcliffe, M. L. Grossbeck, P. J. Maziasz, A. Hishinuma, and S. Jitsukawa, "Property Changes in Austenitic Stainless Steels Irradiated in a Spectrally Tailored Reactor Experiment"

Meeting of the IAEA Coordinated Research Programme on "Atomic and Molecular Data for Fusion Edge Plasmas," Vienna, Austria, September 24–26, 1990

R. A. Phaneuf, "Assessment of Ion-Atom Collision Data for Magnetic Fusion Plasma Edge Modelling," invited

U.S./U.S.S.R. Exchange 1.5: Conference on Fusion Materials, Moscow, U.S.S.R., September 24–26, 1990

R. L. Klueh, P. J. Maziasz, and E. A. Kenik, "High-Manganese Austenitic Stainless Steels"

A. F. Rowcliffe, "Summary of ORNL Fusion Program on Neutron Interactive Materials"

F. W. Wiffen, "Review of the United States Fusion Reactor Materials Program"

Applied Superconductivity Conference, Aspen, Colorado, September 24–28, 1990. Proceedings published in *IEEE Trans. Magn.* **MAG-27** (1991)

L. Dresner, "Thermal-Hydraulic Quenchback in Cable-in-Conduit Superconductors"

R. A. Hawsey, W. K. Kahl, S. W. Schwenterly, J. M. Bailey, J. N. Luton, B. W. McConnell, and V. W. Campbell, "Analysis and Performance of an Axial-Gap Superconducting Motor," pp. 2252–55

J. W. Lue, S. W. Schwenterly, L. Dresner, and M. S. Lubell, "Quench Propagation in a Cable-in-Conduit Force-Cooled Superconductor—Preliminary Results," pp. 2072–75

S. W. Schwenterly, J. N. Luton, J. W. Lue, W. J. Kenney, M. S. Lubell, and B. W. McConnell, "Design and Testing of a Four-Pole Superconducting Motor Stator"

Informed Plasma Modeling Workshop, Yorktown Heights, New York, September 25, 1990

D. B. Batchelor and M. D. Carter, "Modeling of Radio Frequency Driven Plasma Devices"

D. B. Batchelor, M. D. Carter, E. F. Jaeger, R. C. Goldfinger, and J. S. Tolliver, "Theoretical Plasma Research for Fusion—Applications to Plasma Processing"

M. D. Carter, "Plasma Production by Non-Resonant RF in the Uragan-3 Torsatron"

U.S./Japan Workshop on Advances in Simulation Techniques Applied to Plasmas and Fusion, Los Angeles, California, September 26–28, 1990

J.-N. Leboeuf, C. L. Hedrick, L. Garcia, and B. A. Carreras, "Fluid Approach to Kinetic Phenomena or How to Include Landau Damping in Fluid Models of Plasma Turbulence"

October

U.S./Japan Workshop on Low-Temperature Structural Materials, Vail, Colorado, October 1–2, 1990

D. J. Alexander and G. M. Goodwin, "Evaluation of Weldments in Type 21-6-9 Stainless Steel"

Thirteenth International Conference on Plasma Physics and Controlled Nuclear Fusion, Washington, D.C., October 1–6, 1990. Proceedings published by the International Atomic Energy Agency, Vienna, 1991

D. B. Batchelor, R. C. Goldfinger, E. F. Jaeger, M. D. Carter, D. W. Swain, D. Ehst, and C. F. F. Karney, "Fast-Wave Current Drive Modelling for ITER," Vol. 1, p. 817

C. D. Beidler, N. T. Besedin, V. E. Bykov, B. A. Carreras, N. Dominguez, D. L. Grekov, J. Kisslinger, A. V. Khodyachikh, Yu. K. Kuznetsov, G. G. Lesnyakov, V. E. Lynch, I. M. Pankratov, O. S. Pavlichenko, V. G. Peletminskaya, V. D. Pustovitov, F. Rau, A. A. Shishkin, I. N. Sidorenko, M. S. Smirnova, J. S. Tolliver, and A. V. Zolotukhim, "Physics Studies for Uragan-2M," Vol. 2, p. 663

H. Biglari, P. H. Diamond, Y. B. Kim, B. A. Carreras, V. E. Lynch, F. L. Hinton, G. M. Staebler, R. W. Waltz, Ch. P. Ritz, H. Lin, T. L. Rhodes, A. J. Wootton, P. W. Terry, and L. Garcia, "Influence of Sheared Poloidal Rotation on Edge Turbulence Dynamics and Access to Enhanced Confinement Regimes," Vol. 2, p. 191

K. Borrass, S. A. Cohen, R. B. Campbell, F. Engelmann, N. Fujisawa, A. Fukuyama, S. Haney, S. K. Ho, W. A. Houlberg, H. Kimura, V. Lukash, J. Mandrekas, V. Mukhovatov, W. M. Nevins, H. Pacher, V. Parail, L. J. Perkins, A. Polevoy, D. Post, S. Putvinskij, D. Swain, T. Tsuda, T. Tsunematsu, N. A. Uckan, J. G. Wegrowe, R. Yoshino, and ITER Conceptual Design Activities Participants, "Plasma Operation Control in ITER," Vol. 3, pp. 343–49

C. E. Bush et al., "Limiter H-Mode Experiments on TFTR," Vol. 1, p. 309

M. S. Chance, S. C. Jardin, C. E. Kessel, J. Manickam, D. A. Monticello, Y-K. M. Peng, J. A. Holmes, D. J. Strickler, J. C. Whitson, A. H. Glasser, A. Sykes, and J. J. Ramos, "Ideal MHD Stability of Very High Beta Tokamaks," Vol. 2, p. 87

P. H. Diamond, H. Biglari, F.-X. Gang, Y-B. Kim, M. N. Rosenbluth, X-H. Wang, X-Q. Xu, N. Dominguez, B. A. Carreras, J.-N. Leboeuf, V. E. Lynch, L. A. Charlton, P. W. Terry, D. E. Newman, A. E. Koniges, J. Crotinger, W. Dannevik, and B. D. Scott, "Developments in the Theory of Trapped Particle Pressure Gradient-Driven Turbulence in Tokamaks and Stellarators," Vol. 2, p. 9

F. Engelmann, N. Fujisawa, J. Luxon, V. Mukhovatov, H. D. Pacher, D. Post, M. Sugihara, D. Swain, T. Tsunematsu, K. Young, and ITER Conceptual Design Activities Participants, "ITER Physics R and D Programme," Vol. 3, p. 435

C. A. Flanagan for the ITER CDA, "ITER: Plant Systems and Site Requirements," Vol. 3, p. 405

J. H. Harris, L. A. Charlton, G. L. Bell, J. D. Bell, T. S. Bigelow, B. A. Carreras, R. J. Colchin, N. A. Crocker, E. C. Crume, N. Dominguez, J. L. Dunlap, G. R. Dyer, A. C. England, J. C. Glowienka, G. R. Hanson, D. L. Hillis, S. Hiroe, L. D. Horton, H. C. Howe, R. C. Isler, T. C. Jernigan, J.-N. Leboeuf, D. K. Lee, V. E. Lynch, J. F. Lyon, M. M. Menon, M. Murakami, D. A. Rasmussen, C. P. Ritz, C. E. Thomas, T. Uckan, M. R. Wade, J. B. Wilgen, W. R. Wing, E. Anabitarte, B. Brañas, C. Hidalgo, and J. Sanchez, "Fluctuations and Stability in the ATF Torsatron," Vol. 2, p. 677

A. B. Hassam, T. M. Antonsen, Jr., A. M. Dimits, J. F. Drake, P. N. Guzdar, Y. T. Lau, C. S. Liu, K. C. Shaing, P. J. Christenson, W. A. Houlberg, and R. D. Hazeltine, "Spontaneous Poloidal Spin-Up of Tokamaks and the Transition to H-Mode," Vol. 2, pp. 311–20

D. L. Hillis, J. T. Hogan, L. D. Horton, R. C. Isler, C. C. Klepper, P. K. Mioduszewski, K. H. Finken, K. H. Dippel, A. Pospieszczyk, D. Rusbüldt, H. Euringer, G. H. Wolf, R. A. Moyer, R. W. Conn, D. S. Gray, K. Akaishi, A. Miyahara, R. V. Budny, and R. A. Hulse, "Helium Removal and Transport Studies in TEXTOR," Vol. 3, p. 597

J. Hosea, M. Beer, M. G. Bell, M. Bitter, R. Boivin, N. L. Bretz, C. E. Bush, A. Cavallo, T. K. Chu, S. A. Cohen, P. L. Colestock, H. F. Dylla, P. C. Efthimion, E. D. Fredrickson, R. J. Goldston, G. J. Greene, B. Grek, L. R. Grisham, G. W. Hammett, R. J. Hawryluk, K. W. Hill, D. J. Hoffman, H. Hsuan, M. H. Hughes, R. A. Hulse, A. C. Janos, D. L. Jassby, F. C. Jobes, D. W. Johnson, R. Kaita, C. Kieras-Phillips, S. J. Kilpatrick, P. H. LaMarche, B. Leblanc, D. M. Manos, D. K. Mansfield, E. Mazzucato, K. M. McGuire, D. M. Meade, S. S. Medley, D. R. Mikkelsen, R. W. Motley, D. Mueller, Y. Nagayama, M. Ono, D. K. Owens, H. K. Park, M. W. Phillips, A. T. Ramsey, M. H. Redi, A. L. Roquemore, G. Schilling, J. Schivell, G. L. Schmidt, S. D. Scott, J. E. Stevens, J. D. Strachan, B. C. Stratton, E. J. Synakowski, G. Taylor, J. R. Timberlake, H. H. Towner, M. Ulrickson, S. von Goeler, J. R. Wilson, K. L. Wong, M. C. Zarnstorff, and S. J. Zweben, "ICRF Heating in Several Regimes of TFTR," Vol. 1, p. 669

R. C. Isler, L. D. Horton, E. C. Crume, M. Murakami, G. L. Bell, T. S. Bigelow, A. C. England, J. C. Glowienka, S. Hiroe, T. C. Jernigan, R. A. Langley, J. F. Lyon, P. K. Mioduszewski, S. Morita, D. A. Rasmussen, J. E. Simpkins, J. B. Wilgen, and W. R. Wing, "Impurity Effects and Impurity Transport in ATF," Vol. 2, p. 685

JET Team (Fusion Program staff members: S. E. Attenberger, L. R. Baylor, and S. L. Milora), "Comparison of Beryllium and Graphite First-Walls in JET," Vol. 1, p. 375

JET Team (Fusion Program staff members: S. E. Attenberger, L. R. Baylor, and S. L. Milora), "High Density Regimes and Beta Limits in JET," Vol. 1, p. 219

JET Team (Fusion Program staff members: S. E. Attenberger, L. R. Baylor, and S. L. Milora), "High Performance H-Modes in JET," Vol. 1, p. 261

JET Team (Fusion Program staff members: S. E. Attenberger, L. R. Baylor, and S. L. Milora), "ICRF Heating in Reactor Grade Plasmas," Vol. 1, p. 679

JET Team (Fusion Program staff members: S. E. Attenberger, L. R. Baylor, and S. L. Milora), "ICRF Heating in Reactor Grade Plasmas," Vol. 1, p. 679

JET Team (Fusion Program staff members: S. E. Attenberger, L. R. Baylor, and S. L. Milora), "Optimisation of Performance in JET Results Limiter Plasmas," Vol. 1, p. 425

JET Team (Fusion Program staff members: S. E. Attenberger, L. R. Baylor, and S. L. Milora), "Sawteeth and Their Stabilization in JET," Vol. 1, p. 437

Y. B. Kim, H. Biglari, B. A. Carreras, P. H. Diamond, R. J. Groebner, O. J. Kwon, D. A. Spong, J. D. Callen, Z. Chang, J. B. Hollenberg, A. K. Sundaram, P. W. Terry, and J. P. Wang, "Tokamak Fluidlike Equations, with Applications to Turbulence and Transport in H-Mode Discharges," Vol. 2, p. 327

W. Lindquist, F. Casci, N. Fujisawa, H. Hofmann, H. Kimura, W. Nevins, V. Parail, L. Rebuffi, M. Sironi, D. Swain, J. G. Wegrowe, and ITER Conceptual Design Activities Participants, "ITER Current Drive and Heating Systems," Vol. 3, p. 337

M. A. Mahdavi, M. J. Schaeffer, P. Anderson, C. Baxi, J. N. Brooks, D. Buchenauer, R. Doerner, A. Futch, G. Haas, D. N. Hill, J. T. Hogan, W. L. Hsu, G. L. Jackson, T. Jarboe, A. G. Kellman, C. C. Klepper, E. A. Lazarus, B. Leitkind, S. Lippman, J. Luxon, G. F. Matthews, M. M. Menon, P. K. Mioduszewski, B. Mills, R. A. Moyer, T. H. Osborne, L. Owen, P. Peterson, G. D Porter, E. Reis, M. E. Rensink, L. Schmitz, J. T. Scoville, J. Smith, G. M. Staebler, R. D. Stambaugh, P. Taylor, J. Watkins, and C. Wong, "Divertor Baffling and Biasing Experiments on DIII-D," Vol. 1, p. 335

M. Murakami, S. C. Aceto, E. Anabitarte, D. T. Anderson, F. S. B. Anderson, D. B. Batchelor, B. Brañas, L. R. Baylor, G. L. Bell, J. D. Bell, T. S. Bigelow, B. A. Carreras, R. J. Colchin, E. C. Crume, N. Dominguez, R. A. Dory, J. L. Dunlap, G. R. Dyer, A. C. England, O. I. Fedyanin, R. H. Fowler, R. F. Gandy, J. C. Glowienka, R. C. Goldfinger, R. H. Goulding, G. R. Hanson, J. H. Harris, C. L. Hedrick, C. Hidalgo, D. L. Hillis, S. Hiroe, S. P. Hirshman, L. D. Horton, H. C. Howe, D. P. Hutchinson, R. C. Isler, T. C. Jernigan, H. Kaneko, M. Kwon, R. A. Langley, J.-N. Leboeuf, D. K. Lee, V. E. Lynch, J. F. Lyon, C. H. Ma, M. A. Meier, M. M. Menon, P. K. Mioduszewski, S. Morita, R. N. Morris, M. Murakami, G. H. Neilson, M. A. Ochando, S. Okamura, S. Paul, A. L. Qualls, D. A. Rasmussen, R. Richards, C. P. Ritz, J. A. Rome, J. Sanchez, F. Sano, K. C. Shaing, T. D. Shepard, A. A. Shishkin, J. E. Simpkins, S. Sudo, Y. Takeiri, C. E. Thomas, J. S. Tolliver, T. Uckan, K. L. Vander Sluis, M. R. Wade, J. B. Wilgen, W. R. Wing, H. Yamada, and J. J. Zielinski, "Energy Confinement and Bootstrap Current in the Advanced Toroidal Facility," Vol. 2, pp. 455–70

M. Wakatani, H. Zushi, F. Sano, S. Sudo, M. Harada, T. Mizuuchi, K. Kondo, M. Sato, S. Besshou, H. Okada, Y. Nakamura, K. Ichiguchi, H. Sugama, T. Obiki, B. A. Carreras, N. Dominguez, J.-N. Leboeuf, V. E. Lynch, J. L. Johnson, and G. Rewoldt, "Stabilization of the Interchange Modes by a Magnetic Axis Shift and a Toroidal Field in Heliotron E, and a New Low-*n* Mode Stability Analysis," Vol. 2, p. 567

L. J. Perkins, D.T. Blackfield, S. J. Brereton, S. A. Cohen, G. A. Emmert, F. Engelmann, C. A. Flanagan, J. D. Galambos, G. Harris, M. F. A. Harrison, H. Iida, A. Kostenko, J. R. Miller, T. Mizoguchi, G. W. Pacher, H. D. Pacher, D. E. Post, S. Putvinskii, Y. Shimomura, W. R. Spears, N. A. Uckan, J. Wesley, and ITER Conceptual Design Activities Participants, "ITER System Studies and Design Space Analysis," Vol. 3, p. 413

ITER Physics Team (Fusion Program staff member: N. A. Uckan), "ITER Physics Basis," Vol. 3, p. 239

Ch. P. Ritz, T. L. Rhodes, H. Lin, R. D. Bengtson, W. L. Rowan, H. Tsuji, M. Meier, A. J. Wootton, B. A. Carreras, J.-N. Leboeuf, D. K. Lee, J. H. Harris, C. Hidalgo, J. D. Bell, J. A. Holmes, R. C. Isler, V. E. Lynch, T. Uckan, P. H. Diamond, A. S. Ware, and D. R. Thayer, "Comparative Studies of Edge Turbulence in the TEXT Tokamak and the ATF Stellarator," Vol. 2, p. 589

S. D. Scott, C. W. Barnes, L. R. Grisham, G. W. Hammett, W. W. Heidbrink, D. W. Johnson, Y. Kusama, M. C. Zarnstorff, S. J. Zweben, M. G. Bell, M. Bitter, R. Boivin, R. Budny, C. E. Bush, A. Cavallo, C. Z. Cheng, V. Decaux, P. C. Efthimion, R. J. Fonck, E. D. Fredrickson, R. J. Goldston, B. Grek, R. J. Hawryluk, K. W. Hill, H. Hsuan, A. C. Janos, D. L. Jassby, F. C. Jobes, L. C. Johnson, R. Kaita, S. M. Kaye, P. H. LaMarche, B. Leblanc, D. K. Mansfield, J. McCauley, D. C. McCune, K. M. McGuire, S. S. Medley, D. Mueller, J. Murphy, H. Mynick, Y. Nagayama, D. K. Owens, H. K. Park, R. Perkins, S. Pitcher, A. T. Ramsey, A. L. Roquemore, J. Schivell, G. L. Schmidt, W. Stodiek, B. C. Stratton, E. J. Synakowski, W. M. Tang, G. Taylor, H. H. Towner, S. von Goeler, R. E. Waltz, R. M. Wieland, M. Williams, and K. M. Young, "Local Transport Measurements During Auxiliary Heating in TFTR," Vol. 1, p. 235

D. J. Sigmar, D. B. Batchelor, G. Bateman, M. G. Bell, B. J. Braams, J. N. Brooks, C. Z. Cheng, D. R. Cohn, R. J. Goldston, J. Haines, D. N. Hill, W. A. Houlberg, C. T. Hsu, S. C. Jardin, S. S. Medley, G. H. Neilson, W. A. Peebles, F. W. Perkins, N. Pomphrey, M. Porkolab, W. T. Reiersen, R. O. Sayer, J. A. Schmidt, C. E. Singer, R. D. Stambaugh, D. P. Stotler, D. J. Strickler, M. Ulrickson, R. E. Waltz, R. White, and K. M. Young, "Physics Objectives and Design of CIT," Vol. 3, pp. 455–71

T. Tsunematsu, K. Borrass, S. Cohen, F. Engelmann, J. Hogan, A. Krasheninnikov, T. Mizoguchi, V. Mukhovatov, G. W. Pacher, H. D. Pacher, V. Parail, D. Post, N. A. Uckan, J. Wesley, R. Yoshino, and ITER Conceptual Design Activities Participants, "Operational Limits and Disruptions in ITER," Vol. 3, p. 315

N. A. Uckan, P. Yushmanov, T. Takizuka, K. Borrass, J. D. Callen, J. G. Cordey, S. A. Cohen, F. Engelmann, O. Kardaun, S. V. Kaye, K. Lackner, V. Mukhovatov, A. Nocentini, V. V. Parail, D. E. Post, S. Putvinskii, K. Riedel, T. Tsunematsu, R. Yoshino, and ITER Conceptual Design Activities Participants, "Energy and Particle Confinement in ITER," Vol. 3, p. 307

J. Wesley, V. Beljakov, R. Bulmer, J. Hogan, T. Kaiser, A. Kavin, K. Kurihara, V. Korshakov, A. Kostenko, J. R. Miller, N. Mitchell, G. W. Pacher, H. D. Pacher, L. D. Pearlstein, D. Robinson, A. Roshal, Y. Shimomura, K. Shinya, M. Sugihara, R. Yoshino, L. Zakharov, and ITER Conceptual Design Activities Participants, "The ITER Poloidal Field System," Vol. 3, p. 421

M. C. Zarnstorff, C. W. Barnes, P. C. Efthimion, G. W. Hammett, W. Horton, R. A. Hulse, D. K. Mansfield, S. Marmar, K. M. McGuire, G. Rewoldt, B. C. Stratton, E. J. Synakowski, W. M. Tang, J. L. Terry, X. Q. Xu, M. G. Bell, M. Bitter, N. L. Bretz, R. Budny, C. E. Bush, P. H. Diamond, R. J. Fonck, E. D. Fredrickson, H. P. Furth, R. J. Goldston, B. Grek, R. J. Hawryluk, K. W. Hill, H. Hsuan, D. W. Johnson, D. C. McCune, D. M. Meade, D. Mueller, D. K. Owens, H. K. Park, A. T. Ramsey, M. N. Rosenbluth, J. Schivell, G. L. Schmidt, S. D. Scott, G. Taylor, and R. M. Wieland, "Advances in Transport Understanding Using Perturbative Techniques in TFTR," Vol. 1, p. 109

Seventh American Physical Society Topical Conference on Atomic Processes in Plasmas, Gaithersburg, Maryland, October 2, 1990

J. T. Hogan and A. Pospieszczyk, "Modelling of Hydrocarbon Fueling"

9th Topical Meeting on the Technology of Fusion Energy, Oak Brook, Illinois, October 7–11, 1990. Proceedings published in *Fusion Technol.* **19** (1991)

C. C. Baker, "ITER Long-Term Research and Development (R&D) Requirements" (not published)

S. Brereton, S. Piet, D. Holland, M. J. Gouge, and W. A. Houlberg, "Fueling Source Considerations for Optimization of Operational and Safety Constraints," p. 1375

J. D. Galambos, Y-K. M. Peng, and L. J. Perkins, "Comparison of ITER Single-Null and Double-Null Operation," p. 1463

I. C. Gomes and P. N. Stevens, "Generalized Albedo Option in the MORSE Monte Carlo Code," p. 2001

L. M. Gomes and P. N. Stevens, "First and Second Collision Source for Mitigating Ray Effects in Discrete Ordinates Coordinates," p. 1996

J. T. Hogan, D. L. Hillis, J. D. Galambos, N. A. Uckan, K. H. Dippel, K. H. Finken, R. A. Hulse, and R. V. Budny, "ITER Helium Ash Accumulation," p. 1509

J. T. Hogan and N. A. Uckan, "ITER Global Stability Limits," p. 1504

R. Maingi, J. Gilligan, O. Hankins, L. Owen, P. Mioduszewski, and T. Uckan, "Comparison Between Pump Limiter Performance and Modeling Predictions on Tore Sup[illegible]," p. 1788

T. K. Mau, D. A. Ehst, D. J. Hoffman, and the ARIES Team, "Current Drive Using Fast Waves and Folded-Waveguide Launchers for the ARIES-I Tokamak Reactor," p. 882

P. J. Maziasz, A. F. Rowcliffe, M. L. Grossbeck, E. E. Bloom, D. C. Lousteau, A. Hishinuma, T. Kondo, R. F. Mattas, and D. L. Smith, "Some Implications of Radiation-Induced Property Changes in Austenitic Stainless Steels on ITER First-Wall Design and Performance," p. 1571

G. H. Neilson, D. B. Batchelor, G. Bateman, M. G. Bell, J. Bialek, B. J. Braams, J. N. Brooks, R. J. Goldston, J. R. Haines, D. N. Hill, W. A. Houlberg, S. C. Jardin, C. E. Kessel, S. S. Medley, F. W. Perkins, R. D. Pillsbury, N. Pomphrey, M. Porkolab, W. T. Reiersen, R. O. Sayer, J. E. Scharer, J. A. Schmidt, D. J. Sigmar, J. C. Sinnis, R. D. Stambaugh, D. P. Stotler, D. J. Strickler, M. Ulrickson, R. W. Waltz, K. M. Young, and J. J. Yugo, "Overview of the CIT Physics Design," p. 1109

K. A. Niemer, J. C. Gilligan, C. D. Croessman, A. C. England, and D. L. Hillis, "Studies of Runaway Electron Damage on Plasma Facing Components," p. 1717

D. J. Strickler, Y-K. M. Peng, S. C. Jardin, and N. Pomphrey, "Dependence of CIT PF Coil Currents on Profile and Shape Parameters Using the Control Matrix," p. 1452

N. A. Uckan and the ITER Physics Group, "ITER Physics Design Guidelines," p. 1493

N. A. Uckan and D. E. Post, "ITER Physics Basis," p. 1411

N. A. Uckan and J. T. Hogan, "ITER Confinement Capability," p. 1499

IEA Stellarator Workshop on Future Large Devices, Oak Ridge, Tennessee, October 8–10, 1990

J. H. Harris for the ATF Group, "Recent ATF Results"

J. F. Lyon, "Review of Stellarator Reactor Studies"

J. F. Lyon and S. L. Painter, "Transport Analysis of Stellarator Reactors"

American Vacuum Society 37th Annual Symposium and Topical Conferences, Toronto, Ontario, Canada, October 12–16, 1990. Proceedings published in *J. Vac. Sci. Technol. A* **9** (1991)

W. L. Gardner, "Scaling PACVD Diamond Film Growth to Large Areas"

R. A. Langley, E. C. Crume, Jr., J. C. Glowienka, L. D. Horton, R. C. Isler, M. Murakami, and J. E. Simpkins, "Effects of Wall Conditioning on Plasma Performance in the Advanced Toroidal Facility Stellarator," pp. 848–51

R. A. Langley, A. L. Qualls, and J. B. Wilgen, "Absolute Calibration of a Frozen Hydrogen Pellet Mass Detector," pp. 737–41

M. M. Menon, L. W. Owen, J. E. Simpkins, T. Uckan, and P. K. Mioduszewski, "Energetic Particle-Induced Desorption of Water Vapor Cryo-Condensates"

J. E. Simpkins, P. K. Mioduszewski, T. S. Bigelow, J. C. Glowienka, L. D. Horton, R. C. Isler, R. A. Langley, M. Murakami, and T. Uckan, "Gettering in ATF"

C. C. Tsai, L. A. Berry, H. H. Haselton, and D. E. Schechter, "Discharge Mechanism of an Electron Cyclotron Resonance Multicusp Plasma Source"

CIT ICRH Meeting, Princeton, New Jersey, October 12, 1990

D. B. Batchelor, "ICRF Scenarios and Miscellaneous Physics Issues"

Symposium on Detector Research and Development for the Superconducting Supercollider, Fort Worth, Texas, October 15–18, 1990

J. N. Luton, Jr., "The Feasibility of Low-Mass Conductors for Toroidal Superconducting Magnets for SSC Detectors"

43rd Annual Gaseous Electronics Conference, Urbana-Champaign, Illinois, October 16–19, 1990

F. W. Meyer, "The Use of Electron Cyclotron Resonance Ion Sources for Multicharged Ion Collision Studies," invited

R. A. Phaneuf, "Future Opportunities in Research, " invited

U.S.–U.S.S.R. Exchange on Stellarator Physics, Kharkov, U.S.S.R., October 26–November 3, 1990

B. A. Carreras, "Radial Electric Field and Turbulence"

B. A. Carreras for the ATF Group, "Recent ATF Experimental Results"

N. Dominguez, B. A. Carreras, and P. H. Diamond, "Trapped Electron Modes in Stellarators"

N. Dominguez, B. A. Carreras, V. E. Lynch, V. E. Bykov, D. L. Grekov, and A. A. Shishkin, "Uragan-2M Stability Studies"

M. Murakami, B. A. Carreras, G. L. Bell, T. S. Bigelow, G. R. Dyer, A. C. England, J. C. Glowienka, S. Hiroe, H. C. Howe, T. C. Jernigan, D. K. Lee, V. E. Lynch, S. Morita, D. A. Rasmussen, J. S. Tolliver, M. R. Wade, J. B. Wilgen, W. R. Wing, and the ATF Group, "Bootstrap Current Studies in the Advanced Toroidal Facility"

Steady-State Tokamak Workshop, San Diego, California, October 30–November 1, 1990

S. L. Milora, "Pellet Fueling and ICRF Issues and Technology for Steady State"

November

10th International Workshop on ECR Ion Sources, Knoxville, Tennessee, November 1–2, 1990. Proceedings published as CONF-90-11-136, ed. F. W. Meyer and M. I. Kirkpatrick, January 1991

C. C. Tsai, "Characteristics and Potential Applications of an ORNL Microwave ECR Multicusp Plasma Ion Source"

11th International Conference on the Application of Accelerators in Research and Industry, Denton, Texas, November 5–8, 1990. Abstracts published in *Bull. Am. Phys. Soc.* **35** (1990)

L. A. Berry, "Characteristics of ECR Plasmas for Advanced Deposition and Etch Technology"

C. C. Havener, "Electron Capture by Multicharged Ions from Hydrogen Atoms at eV Energies," invited, p. 1779

R. A. Phaneuf, "Atomic Physics Experiments at the ORNL-ECR Multicharged Ion Research Facility," invited, p. 1754

J. K. Swenson, J. Burgdorfer, F. W. Meyer, C. C. Havener, D. C. Gregory, and N. Stolterfoht, "Coulomb 'Path' Interference in Low Energy He^+ + He Collisions," invited, p. 1768

C. C. Tsai, "Potential Applications of a New Microwave ECR Multicusp Plasma Ion Source"

J. H. Whealton and R. J. Raridon, "Aberration Production in Liquid Metal Ion Sources"

P. A. Zeijlmans van Emmichoven, "Electron Emission During Multicharged Ion–Surface Interactions," invited, p. 1777

CIT PF Working Group, Princeton, New Jersey, November 8, 1990

D. J. Strickler, "Equilibrium Modeling"

Symposium on Ceramic, Polymer, and Metal Matrix Composites, Orlando, Florida, November 12, 1990

L. L. Snead, S. J. Zinkle, and D. Steiner, "Interfacial Push-Out Measurements of Fully Bonded SiC/SiC Composites"

Thirty-Second Annual Meeting of the American Physical Society Division of Plasma Physics, Cincinnati, Ohio, November 12–16, 1990. Abstracts published in *Bull. Am. Phys. Soc.* **35** (1990)

S. C. Aceto, K. A. Connor, J. G. Schwelberger, J. J. Zielinski, J. C. Glowienka, A. Carnevali, S. P. Reedy, and G. E. Drohman, "Preliminary Fluctuation Measurements on ATF Using the Heavy Ion Beam Probe"

D. T. Anderson, F. S. B. Anderson, D. L. Hillis, T. Uckan, R. H. Fowler, and J. A. Rome, "Particle Flux Studies of the ATF Divertor Stripes"

F. W. Baity, D. B. Batchelor, M. D. Carter, R. H. Goulding, D. J. Hoffman, and P. M. Ryan, "Measurements of Folded Waveguide Performance During Plasma Operation on RFTF and Comparison to a Loop Antenna"

L. R. Baylor, H. C. Howe, M. Murakami, A. C. England, D. P. Hutchinson, C. H. Ma, A. L. Qualls, D. A. Rasmussen, K. L. Vander Sluis, and J. B. Wilgen, "Particle and Thermal Transport Analysis in ATF"

G. L. Bell, J. B. Wilgen, T. S. Bigelow, and R. F. Gandy, "Third-Harmonic ECE Polarization Measurements on the Advanced Toroidal Facility"

J. D. Bell, J. H. Harris, J. L. Dunlap, N. A. Crocker, and G. R. Hanson, "Magnetic Fluctuations in ATF"

T. S. Bigelow, R. A. Lindley, D. B. Batchelor, R. C. Goldfinger, C. R. Schaich, J. B. Wilgen, and G. L. Bell, "ECH Analysis, Experimental Results, and Plans for ATF"

R. Budny, M. G. Bell, C. Bush, D. McCune, H. Park, E. Synakowski, G. Taylor, R. M. Wieland, S. A. Sabbagh, M. Mauel, and S. Hirshman, "Transport Analysis of Discharges with High Poloidal β in TFTR"

C. E. Bush, G. Taylor, N. Bretz, J. Schivell, K. McGuire, E. Fredrickson, R. Nazikian, R. Budny, A. Cavallo, P. Efthimion, A. Janos, D. K. Mansfield, H. K. Park, S. Paul, A. T. Ramsey, S. D. Scott, H. H. Towner, R. M. Wieland, and J. R. Wilson, "H-Mode Studies on TFTR"

B. A. Carreras, V. E. Lynch, and L. Garcia, "Sheared Electric Field Effects on the Resistive Pressure-Gradient-Driven Turbulence"

M. D. Carter, E. F. Jaeger, D. B. Batchelor, and F. W. Baity, "ORION 1-D Analysis of ICRF Performance for a Folded Waveguide"

L. A. Charlton, B. A. Carreras, N. Dominguez, and V. E. Lynch, "Compressibility and Diamagnetic Drift Effects in Resistive ATF High β Plasmas"

P. J. Christenson, D. A. Spong, N. Dominguez, J.-N. Leboeuf, B. A. Carreras, and T. A. Kammash, "Hybrid Fluid-Kinetic Models of the Alpha Destabilized TAE Gap Mode for Low Poloidal Mode Numbers"

R. J. Colchin, M. R. Wade, G. L. Bell, E. C. Crume, A. C. England, R. H. Fowler, R. H. Goulding, L. D. Horton, R. C. Isler, M. Kwon, J. F. Lyon, R. N. Morris, M. Murakami, D. A. Rasmussen, T. D. Shepard, and C. E. Thomas, "Ion Confinement in ATF"

K. A. Connor, S. C. Aceto, J. G. Schwelberger, J. J. Zielinski, J. C. Glowienka, A. Carnevali, S. P. Reedy, and G. E. Drohman, "Initial Measurements of the Plasma Potential on ATF Using the Heavy Ion Beam Probe"

N. A. Crocker, J. H. Harris, J. D. Bell, J. L. Dunlap, and G. R. Hanson, "Relational Database Analysis of Fluctuations in ATF"

E. C. Crume, Jr., L. D. Horton, R. C. Isler, and S. Morita, "Ion Temperature Measurements in the ATF Torsatron Using Titanium Forbidden Lines"

N. Dominguez, B. A. Carreras, V. E. Lynch, L. A. Charlton, J.-N. Leboeuf, L. Garcia, and P. H. Diamond, "Numerical Approach to Dissipative Trapped Electron Drift Wave Turbulence"

R. A. Dory, M. Murakami, and the ATF Experimental Team, "Energy Confinement Scaling in the ATF Torsatron"

A. C. England, D. A. Rasmussen, L. R. Baylor, T. L. Clark, J. M. Gossett, H. C. Howe, D. P. Hutchinson, G. T. King, K. C. Klos, C. H. Ma, M. Murakami, T. M. Rayburn, P. S. Rogers, P. L. Shaw, K. A. Stewart, C. E.

Thomas, and K. L. Vander Sluis, "Equilibrium Studies Using Two Dimensional Electron Temperature and Density Thomson Scattering Measurements in ATF"

J. R. Ferron, M. S. Chu, F. J. Helton, L. L. Lao, E. A. Lazarus, H. Matsumoto, R. Snider, E. J. Strait, T. S. Taylor, and A. D. Turnbull, "Discharges near an Ideal Beta Limit in the DIII-D Tokamak"

C. A. Foster, W. L. Stirling, L. Horton, G. Haste, A. Geraud, E. Agostini, J. L. Bruneau, M. Chatelier, H. W. Drawin, T. Fall, C. Gil, W. Hess, T. Hutter, C. Laviron, P. Millot, P. Monier-Garbet, F. Mourques, A. L. Pecquet, L. Rodriguez, M. Talvard, and D. Van Houtte, "First Pellet Injection Experiments on the Tore Supra Tokamak"

R. H. Fowler, R. N. Morris, M. Murakami, S. Okamura, and J. A. Rome, "Studies of Neutral Beam Injection for ATF and CHS"

L. Garcia, N. Dominguez, B. A. Carreras, K. Sidikman, and P. H. Diamond, "Dissipative Trapped Electron Drift Wave Turbulence"

J. C. Glowienka, T. S. Bigelow, G. R. Dyer, R. A. Langley, M. Murakami, J. E. Simpkins, and W. R. Wing, "Operational Improvements in the ATF Torsatron"

R. C. Goldfinger, D. B. Batchelor, E. F. Jaeger, D. Ehst, D. W. Swain, and J. S. Tolliver, "Fast Wave Current Drive Calculations Using the Geometrical Optics Code RAYS"

R. J. Goldston, G. Bateman, M. G. Bell, R. Bickerton, E. A. Chaniotakis, D. R. Cohn, D. N. Hill, W. A. Houlberg, S. C. Jardin, S. S. Medley, G. H. Neilson, W. A. Peebles, F. W. Perkins, N. Pomphrey, M. Porkolab, J. A. Schmidt, D. J. Sigmar, R. D. Stambaugh, D. P. Stotler, M. Ulrickson, R. W. Waltz, and K. A. Young, "Performance Projections for CIT," p. 1920

R. H. Goulding, D. J. Hoffman, F. W. Baity, E. F. Jaeger, and P. M. Ryan, "Development of a Fast Wave Current Drive Array for DIII-D"

D. Gray, R. A. Moyer, R. W. Conn, K. H. Dippel, K. H. Finken, W. Baek, Y. T. Lie, A. Pospieszczyk, D. Reiter, B. Schweer, G. H. Wolf, NI Team, M. Ciotti, D. L. Hillis, J. T. Hogan, L. W. Owen, T. Uckan, and P. K. Mioduszewski, "Influence of SOL Response During NBI on Particle Exhaust in TEXTOR"

D. Guilhem, M. Chatelier, T. Evans, Ph. Ghendrih, W. Hess, L. D. Horton, T. Loarer, P. K. Mioduszewski, F. Nguyen, and A. Samain, "Ergodic Divertor Effect on Heat and Particle Flux in Tore Supra"

G. R. Hanson, J. H. Harris, J. D. Bell, J. B. Wilgen, E. Anabitarte, B. Brañas, J. L. Dunlap, C. Hidalgo, J. Sanchez, C. E. Thomas, and T. Uckan, "Correlation Reflectometry on ATF"

J. H. Harris, J. D. Bell, N. A. Crocker, J. L. Dunlap, G. R. Hanson, C. Hidalgo, Ch. P. Ritz, T. Uckan, and J. B. Wilgen, "Fluctuation Studies in ATF"

C. L. Hedrick and J.-N. Leboeuf, "*N*-Pole Approximate Fluid Treatments of Landau and Cyclotron Damping"

C. Hidalgo, T. Uckan, J. D. Bell, G. R. Dyer, J. H. Harris, M. Meier, Ch. P. Ritz, T. L. Rhodes, and A. J. Wootton, "Fluctuation Measurements in the ATF Torsatron Edge"

D. L. Hillis (with K. H. Finken, J. T. Hogan, K. H. Dippel, R. Moyer, A. Pospieszczyk, D. Rusbüldt, D. Reiter, K. Akaishi, R. W. Conn, H. Euringer, D. S. Gray, L. D. Horton, R. A. Hulse, R. C. Isler, C. C. Klepper, P. K. Mioduszewski, A. Miyahara, and G. H. Wolf), "Helium Exhaust and Transport Studies with the ALT-II Pump Limiter in TEXTOR," invited

S. Hiroe, S. Paul, and C. E. Bush, "Radiated Power Profile in ATF"

S. P. Hirshman, R. P. Gormley, and J. A. Rome, "Self-Consistent Effects of Finite-Beta on Ripple and Transport in ITER"

D. J. Hoffman, F. W. Baity, D. B. Batchelor, R. H. Goulding, E. F. Jaeger, P. M. Ryan, J. S. Tolliver, J. C. Hosea, J. E. Stevens, and J. R. Wilson, "Loading Analyses on the Bay L and Bay M Antennas"

J. A. Holmes, Y-K. M. Peng, and D. J. Strickler, "MHD Stability of Free Boundary Equilibria with Separatrices"

W. A. Houlberg and M. J. Gouge, "Influence of Fueling on Density Profiles and Confinement in DT Plasmas," p. 1922

H. Hsuan, M. Bitter, C. E. Bush, A. Cavallo, V. Decaux, K. W. Hill, H. K. Park, and S. von Goeler, "Poloidal Rotation of the Central TFTR Plasmas During Operatings of Supershots and Limiter H-Mode"

D. P. Hutchinson, R. K. Richards, C. A. Bennett, and H. T. Hunter, "Results from an Alpha Particle Diagnostic Proof-of-Principle Test"

R. C. Isler, L. D. Horton, E. C. Crume, and M. Murakami, "Effects of Gettering on Plasma Performance in ATF"

E. F. Jaeger, L. A. Berry, and D. B. Batchelor, "Characteristics of a Cylindrical Langmuir Probe of Finite Length"

T. C. Jernigan, W. R. Wing, D. T. Anderson, F. S. B. Anderson, T. S. Bigelow, D. L. Hillis, S. Hiroe, R. C. Isler, M. Murakami, and T. Uckan, "Long Pulse Operation of ATF (at 3rd and 4th Harmonic ECH)"

C. C. Klepper, L. W. Owen, M. M. Menon, P. K. Mioduszewski, G. L. Jackson, D. N. Hill, and G. Haas, "Pressure Measurements Inside the Closed Divertor Region of DIII-D"

M. Kwon, T. D. Shepard, R. H. Goulding, M. D. Carter, R. J. Colchin, D. J. Hoffman, C. E. Thomas, and M. R. Wade, "ICRF Fast Wave Minority-Regime Experiments on the ATF Torsatron"

L. L. Lao, E. A. Lazarus, M. S. Chu, J. R. Ferron, F. J. Helton, W. Howl, A. G. Kellman, T. Osborne, R. D. Stambaugh, E. J. Strait, T. S. Taylor, and A. D. Turnbull, "Equilibrium and Stability of Highly Elongated DIII-D Divertor Discharges"

E. A. Lazarus, "Higher Beta at Higher Elongation in DIII-D," invited

J.-N. Leboeuf, "TEXT Edge Turbulence Modeling"

J.-N. Leboeuf, B. A. Carreras, N. Dominguez, D. K. Lee, A. S. Ware, P. H. Diamond, Ch. P. Ritz, A. J. Wootton, and D. R. Thayer, "Impurity Radiation and Ionization Driven Drift Waves as Models of TEXT Edge Fluctuations"

D. K. Lee and S. P. Hirshman, "Rapid Determination of a Straight Magnetic Field Coordinate System for Stellarators"

V. E. Lynch, B. A. Carreras, J. B. Drake, and J.-N. Leboeuf, "Plasma Turbulence Calculations on a Massively Parallel Computer"

J. F. Lyon and T. C. Jernigan, "ATF Steady-State Program"

C. H. Ma, L. R. Baylor, M. J. Crouse, D. P. Hutchinson, M. Murakami, K. L. Vander Sluis, and J. B. Wilgen, "Density Profile Measurement Using a Difluoromethane Laser Interferometer System on ATF"

R. Maingi, L. Owen, T. Uckan, J. G. Gilligan, and P. K. Mioduszewski, "Comparison Between Measured Parameters and Modelling Predictions on Pump-Limiter Tokamaks"

R. Maingi, J. G. Gilligan, O. Hankins, L. Owen, T. Uckan, and P. K. Mioduszewski, "Comparison Between Pump Limiter Performance and Modelling Predictions on Tore Supra"

P. K. Mioduszewski, P. Bonnel, J. L. Bruneau, M. Chatelier, C. Gil, C. Grisolia, G. R. Haste, J. T. Hogan, L. D. Horton, C. C. Klepper, T. Loarer, B. Pegourie, and T. Uckan, "Pump Limiter Studies in Tore Supra"

R. A. Moyer, D. Gray, R. W. Conn, K. H. Finken, D. Reiter, K. H. Dippel, A. Pospieszczyk, G. H. Wolf, TEXTOR Team, NI Team, C. C. Klepper, and D. L. Hillis, "Influence of Plasma-Neutral Interactions on ALT-II Pump Limiter Performance During NI Heating at TEXTOR"

M. Murakami (with the ATF Group), "Recent Results from the ATF Torsatron," invited

M. Murakami, L. R. Baylor, G. L. Bell, T. S. Bigelow, B. A. Carreras, R. J. Colchin, A. C. England, J. C. Glowienka, H. C. Howe, D. K. Lee, V. E. Lynch, C. H. Ma, G. H. Neilson, D. A. Rasmussen, J. S. Tolliver, M. R. Wade, J. B. Wilgen, and W. R. Wing, "Configuration Effects on Bootstrap Current and Energy Transport in the Advanced Toroidal Facility"

R. Nazikian, N. Bretz, C. E. Bush, E. Fredrickson, K. McGuire, and A. T. Ramsey, "Microwave Scattering from Transient Broad-Band Density Fluctuations in Ohmic and H-Mode Plasmas in TFTR"

G. H. Neilson, "Physics Design of the Compact Ignition Tokamak," invited

L. W. Owen, T. Uckan, P. K. Mioduszewski, A. Pospieszczyk, and R. A. Moyer, "Neutral Transport Modeling of H_α Measurements in TEXTOR with the ALT-II Pump Limiter"

S. L. Painter and J. F. Lyon, "1-D Transport Analysis of Stellarator Reactors"

N. Pomphrey, D. J. Strickler, and S. C. Jardin, "Elements of Shape Control for CIT"

A. L. Qualls, J. B. Wilgen, P. N. Stevens, C. H. Ma, D. A. Rasmussen, T. M. Rayburn, J. M. Gossett, G. T. King, L. R. Baylor, A. C. England, and W. R. Wing, "Modification of Density Profiles in ATF Plasmas Using Pellet Injection"

D. A. Rasmussen, D. B. Batchelor, L. R. Baylor, G. L. Bell, J. D. Bell, T. S. Bigelow, B. A. Carreras, A. C. England, R. F. Gandy, R. C. Goldfinger, J. M. Gossett, H. C. Howe, D. P. Hutchinson, G. T. King, K. C. Klos, C. H. Ma, M. Murakami, T. M. Rayburn, K. A. Stewart, C. E. Thomas, K. L. Vander Sluis, J. B. Wilgen, and W. R. Wing, "Electron Confinement Studies in ATF"

Ch. P. Ritz, H. Lin, R. D. Bengtson, M. Meier, T. L. Rhodes, H. Y. W. Tsui, A. J. Wootton, C. Hidalgo, T. Uckan, J. D. Bell, J. L. Dunlap, and J. H. Harris, "Velocity Shear Effects on Turbulence in Different Devices"

J. A. Rome, J. W. Schumer, R. J. Colchin, and M. R. Wade, "High Energy Loss Cones in ATF"

P. M. Ryan, K. E. Roth, F. W. Baity, R. H. Goulding, and D. J. Hoffman, "Calculation of Slot Transparency in ICRH Antenna Walls and Septa"

R. O. Sayer, Y-K. M. Peng, and S. C. Jardin, "TSC Halo Disruption-Induced Forces on the CIT Vacuum Vessel"

J. Schivell and C. E. Bush, "Use of Marfes to Disperse Plasma Power Outflow"

J. G. Schwelberger, S. C. Aceto, J. J. Zielinski, K. A. Connor, and A. Carnevali, "Attenuation Calculations for the ATF Heavy Ion Beam Probe"

S. D. Scott, Cris W. Barnes, R. Budny, C. E. Bush, B. Grek, L. R. Grisham, D. W. Johnson, D. K. Mansfield, H. K. Park, A. T. Ramsey, J. Schivell, B. C. Stratton, E. J. Synakowski, G. Taylor, and M. C. Zarnstorff, "Steady-State Transport Measurements in TFTR Supershots"

K. C. Shaing and R. D. Hazeltine, "Shock Formation in a Poloidally Rotating Plasma"

K. L. Sidikman, S. D. Schultz, P. W. Terry, and G. C. Craddock, "Numerical Study of the Saturation of Coupled g-Mode/Resistivity-Gradient-Driven Turbulence in the RFP Edge"

D. J. Sigmar, C. T. Hsu, and K. C. Shaing, "Transport Theory of Alpha Particles in ITER"

R. Snider, T. N. Carlstrom, R. J. Groebner, E. A. Lazarus, W. Meyer, and G. D. Porter, "Soft X-Ray Emissivity 'Hole' in High-Performance Plasmas in DIII-D"

D. A. Spong and B. A. Carreras, "Nonlinear Studies of Neoclassical MHD Instabilities"

W. L. Stirling, L. R. Baylor, C. A. Foster, W. A. Houlberg, S. L. Milora, H. W. Drawin, B. Pegourie, M. Chatelier, and A. Geraud, "Pellet Ablation and Transport Modeling in Tore Supra," p. 1998

D. W. Swain, D. B. Batchelor, E. F. Jaeger, J. Jacquinot, and V. Bhatnagar, "Fast Ion Cyclotron Wave Heating and Current Drive System for ITER"

G. Taylor, C. E. Bush, A. Cavallo, E. Fredrickson, D. K. Mansfield, K. McGuire, H. K. Park, and A. T. Ramsey, "Phenomenology of Edge Localized Modes During TFTR Limiter H-Mode Plasmas"

J. S. Toiliver and D. B. Batchelor, "A 2D Model for Recessed Phase Antenna Arrays"

C. C. Tsai, C. A Foster, S. L. Milora, D. E. Schechter, B. E. Argo, G. C. Barber, D. T. Fehling, D. W. Simmons, and R. W. Kincaid, "Performance of a Proof-of-Principle Electron-Beam-Rocket Pellet Injector"

T. Uckan, P. K. Mioduszewski, T. S. Bigelow, J. C. Glowienka, S. Hiroe, M. Murakami, J. B. Wilgen, and W. R. Wing, "Power and Particle Balance Studies Using an Instrumented Limiter System on ATF"

S. von Goeler, C. W. Barnes, M. Bitter, C. E. Bush, H. F. Dylla, K. W. Hill, H. Hsuan, P. LaMarche, A. T. Ramsey, J. Schivell, and S. D. Scott, "Recycling of Neon Gas in TFTR"

M. R. Wade, R. J. Colchin, A. C. England, R. H. Fowler, R. H. Goulding, M. Kwon, R. N. Morris, D. A. Rasmussen, J. A. Rome, T. D. Shepard, and C. E. Thomas, "Fast Ion Behavior in ATF"

J. H. Whealton and R. J. Raridon, "The Electrohydrodynamical Ion Source: A Case Study of Self-Consistent Multiple Spatial Scale Plasmas"

R. M. Wieland, D. C. McCune, and S. P Hirshman, "The Use of the VMEC Equilibrium Code in the Analysis of TFTR and PBX-M Plasmas"

J. B. Wilgen, M. G. Shats, J. H. Harris, K. M. Likin, A. V. Saphozhnikov, K. A. Sarksyan, G. R. Hanson, and N. Dominguez, "Microwave Scattering in the ATF Torsatron"

W. R. Wing, J. C. Glowienka, C. H. Ma, M. Murakami, D. A. Rasmussen, and J. B. Wilgen, "Energy Confinement Scaling in ATF"

J. J. Zielinski, S. C. Aceto, J. G. Schwelberger, and G. A. Hallock. "Particle Trajectories and Magnetic Field Effects in the Energy Analyzer of the ATF Heavy Ion Beam Probe"

Symposium on Superconductor Stability, Yokohama, Japan, November 13–15, 1990. Proceedings published in *Cryogenics* (1991)

L. Dresner, "Superconductor Stability '90: A Review"

L. Dresner, "Theory of Thermal Hydraulic Quenchback in Cable-in-Conduit Superconductors"

IAEA Technical Committee Meeting on Time Resolved Two- and Three-Dimensional Plasma Diagnostics, Nagoya, Japan, November 19–22, 1990. Proceedings to be published by the International Atomic Energy Agency, Vienna

D. A. Rasmussen, S. C. Aceto, L. R. Baylor, G. L. Bell, J. D. Bell, R. J. Colchin, M. J. Crouse, J. L. Dunlap, A. C. England, R. F. Gandy, J. C. Glowienka, S. Hiroe, J. H. Harris, H. C. Howe, D. P. Hutchinson, R. C. Isler, H. Kaneko, K. C. Klos, C. H. Ma, M. Murakami, S. Okamura, S. Paul, V. K. Paré, R. K. Richards, J. G. Schwelberger, C. E. Thomas, K. L.Vander Sluis, M. R. Wade, J. B. Wilgen, H. Yamada, and J. J. Zielinski, "Time Resolved Multidimensional Plasma Diagnostics for ATF"

Second International Toki Conference on Nonlinear Phenomena in Fusion Plasmas, Toki, Japan, November 27, 1990

B. A. Carreras, V. E. Lynch, and L. Garcia, "Sheared Electric Field Effects on the Resistive Pressure-Gradient-Driven Turbulence"

Neutron Source Workshop, Oak Brook, Illinois, November 27–28, 1990

D. Macdonald and R. W. Mouring (presented by C. C. Baker), "Comments on Facility Considerations for a Fusion Neutron Source"

F. W. Wiffen, "Japan's ESNIT Program"

CIT Physics Workshop, Oak Ridge, Tennessee, November 28, 1990

D. B. Batchelor, "ICRF Physics"

W. A. Houlberg, "CIT Fueling"

December

U.S./Japan Workshop on Critical Topics of Plasma-Facing Materials/ Plasma-Facing Components Data for the Next Step Fusion Devices, Nagoya, Japan, December 3–7, 1990

T. D. Burchell, "Neutron Damage Effects on Carbon-Based Plasma Facing Materials"

International Workshop on ECH Transmission Systems, Cocoa Beach, Florida, December 5–8, 1990

T. S. Bigelow and C. R. Schaich, "ATF ECH System Performance Measurements and Recent Upgrades"

15th International Conference on Infrared and Millimeter Waves, Lake Buena Vista, Florida, December 10–14, 1990

C. H. Ma, L. R. Baylor, D. P. Hutchinson, M. Murakami, K. L. Vander Sluis, J. B. Wilgen, and M. G. Crouse, "Density Profile Measurements Using a Multichannel Difluoromethane Laser Interferometer System on ATF"

Energy Research Systems User Group Meeting, Oak Ridge, Tennessee, December 11–12, 1990

V. E. Lynch, B. A. Carreras, J. Drake, J.-N. Leboeuf, and J. R. Ruiter, "Parallel Computing at ORNL"

1990 SEMINARS

J. C. Glowienka, "Current Status of the ATF Magnetic Confinement Experiment at ORNL," Department of Electrical and Computer Engineering, University of Tennessee, Knoxville, February 16, 1990

J. H. Harris, "Plasma Physics in Stellarators," College of William and Mary, Williamsburg, Virginia, December 7, 1990

J. H. Harris, "Recent Results from ATF," Institute of General Physics, Moscow, U.S.S.R., March 12, 1990; Kharkov Physical-Technical Institute, Kharkov, U.S.S.R., March 19, 1990; and University of Wisconsin, Madison, May 7, 1990

J. H. Harris, E. Anabitarte, J. D. Bell, J. L. Dunlap, and G. R. Hanson, "Edge Fluctuations in Neutral Beam Heated Discharges in ATF," Institute of General Physics, Moscow, U.S.S.R., March 12, 1990, and Kharkov Physical-Technical Institute, Kharkov, U.S.S.R., March 19, 1990

R. L. Klueh, "Tensile and Microstructural Behavior of Solute-Modified Manganese-Stabilized Austenitic Steels," Oak Ridge National Laboratory, Oak Ridge, Tennessee, June 25, 1990

P. J. Maziasz, "Swelling and Microstructural Examination of EP-838 Austenitic Stainless Steel Irradiated in HFIR and FFTF," Oak Ridge National Laboratory, Oak Ridge, Tennessee, June 25, 1990

A. L. Qualls, P. W. Fisher, M. J. Cole, A. C. England, D. T. Fehling, M. J. Gouge, W. A. Houlberg, T. C. Jernigan, S. L. Milora, and J. B. Wilgen, "Pellet Ablation Studies on ATF," Institute of General Physics, Moscow, U.S.S.R., March 12, 1990

J. A. Rome, "The Status and Future of Fusion Energy," Western Kentucky University, Bowling Green, Kentucky, January 22, 1990

J. Sheffield, "Status of Magnetic Fusion," College of Nuclear Engineering and Health Physics, Georgia Institute of Technology, Atlanta, March 15, 1990

J. B. Wilgen, J. D. Bell, A. C. England, P. W. Fisher, H. C. Howe, M. Murakami, D. A. Rasmussen, R. K. Richards, T. Uckan, W. R. Wing, G. L. Bell, A. L. Qualls, and S. Sudo, "Pellet Injection into ATF Plasmas," Institute of General Physics, Moscow, U.S.S.R., March 12, 1990, and Kharkov Physical-Technical Institute, Kharkov, U.S.S.R., March 19, 1990

S. J. Zinkle, "Neutron Irradiation Effects on the Structure and Physical Properties of Ceramics," Westinghouse–Bettis Atomic Power Laboratory, West Mifflin, Pennsylvania, April 27, 1990

1990 REPORTS

ORNL Technical Memoranda

L. R. Baylor, *Particle Transport in Pellet Fueled JET Plasmas,* ORNL/TM-11420, Martin Marietta Energy Systems, Inc., Oak Ridge National Laboratory, January 1990

L. Dresner, *Asymptotic Behavior of Solutions of Diffusion-Like Partial Differential Equations Invariant to a Family of Affine Groups,* ORNL/TM-11559, Martin Marietta Energy Systems, Inc., Oak Ridge National Laboratory, July 1990

L. Dresner, *The Superfluid Diffusion Equation* $S(T)\frac{\partial T}{\partial t} = \nabla \cdot [K(T)(\nabla T^{1/3}]$, ORNL/TM-11480, Martin Marietta Energy Systems, Inc., Oak Ridge National Laboratory, June 1990

J. T. Hogan, *Model for Particle Balance in Pumped Divertors (pre-VORTEX),* ORNL/TM-11562, Martin Marietta Energy Systems, Inc., Oak Ridge National Laboratory, August 1990

J. T. Hogan and A. Pospieszczyk, *Modeling of Hydrocarbon Fueling,* ORNL/TM-11542, Martin Marietta Energy Systems, Inc., Oak Ridge National Laboratory, July 1990

H. C. Howe, *Physics Models in the Toroidal Transport Code PROCTR,* ORNL/TM-11521, Martin Marietta Energy Systems, Inc., Oak Ridge National Laboratory, August 1990

D. K. Lee, J. H. Harris, and G. S. Lee, *Formation of Magnetic Islands due to Field Perturbations in Toroidal Stellarator Configurations,* ORNL/TM-11523, Martin Marietta Energy Systems, Inc., Oak Ridge National Laboratory, June 1990

J. F. Lyon, *Review of Recent Stellarator Results in the U.S.A., the U.S.S.R., and Japan,* ORNL/TM-11620, Martin Marietta Energy Systems, Inc., Oak Ridge National Laboratory, November 1990

J. F. Lyon, G. Grieger, F. Rau, A. Iiyoshi, A. P. Navarro, L. M. Kovrizhnykh, O. S. Pavlichenko, and S. M. Hamberger, *Stellarator Status—1989,* ORNL/TM-11558, Martin Marietta Energy Systems, Inc., Oak Ridge National Laboratory, May 1990

S. L. Milora, S. K. Combs, M. J. Gouge, and R. W. Kincaid, *QUICKGUN: An Algorithm for Estimating the Performance of Two-Stage Light Gas Guns,* ORNL/TM-11561, Martin Marietta Energy Systems, Inc., Oak Ridge National Laboratory, September 1990

M. Murakami, E. Anabitarte, F. S. B. Anderson, G. L. Bell, J. D. Bell, T. S. Bigelow, B. A. Carreras, L. A. Charlton, T. L. Clark, R. J. Colchin, E. C. Crume, N. Dominguez, J. L. Dunlap, G. R. Dyer, A. C. England, P. W. Fisther, R. F. Gandy, J. C. Glowienka, R. H. Goulding, G. R. Hanson, J. H. Harris, G. R. Haste, C. Hidalgo-Vera, D. L. Hillis, S. Hiroe, L. D. Horton, H. C. Howe, D. E. Hutchinson, R. C. Isler, T. C. Jernigan, K. L. Kannan, H. Kaneko, M. Kwon, R. A. Langley, J.-N. Leboeuf, D. K. Lee, J. W. Lue, V. E. Lynch, J. F. Lyon, C. H. Ma, M. M. Menon, P. K. Mioduszewski, R. N. Morris, G. H. Neilson, A. L. Qualls, D. A. Rasmussen, C. P. Ritz, P. S. Rogers, S. W. Schwenterly, K. C. Shaing, P. L. Shaw, T. D. Shepard, J. E. Simpkins, K. A. Stewart, S. Sudo, C. E. Thomas, J. S. Tolliver, T. Uckan, M. R. Wade, J. B. Wilgen, W. R. Wing, H. Yamada, and J. J. Zielinski, *Overview of Recent Results from the Advanced Toroidal Facility,* ORNL/TM-11453, Martin Marietta Energy Systems, Inc., Oak Ridge National Laboratory, February 1990

C. C. Tsai, L. A. Berry, S. M. Gorbatkin, H. H. Haselton, J. B. Roberto, D. E. Schechter, and W. L. Stirling, *Potential Applications of an Electron Cyclotron Resonance Multicusp Plasma Source,* ORNL/TM-11442, Martin Marietta Energy Systems, Inc., Oak Ridge National Laboratory, March 1990

ORNL Fusion Engineering Design Center Reports

J. D. Galambos and Y-K. M. Peng, *International Thermonuclear Engineering Reactor: Bimodal Device and Design Sensitivities to Energy Confinement H-Factors,* ORNL/FEDC-89/1, Martin Marietta Energy Systems, Inc., Oak Ridge National Laboratory, January 1990

D. L. Henderson, and I. C. Gomes, *NUFACE: An Interface Code for the Calculation of Nuclear Responses*, ORNL/FEDC-90/2, Martin Marietta Energy Systems, Inc., Oak Ridge National Laboratory, January 1990

R. O. Sayer, Y-K. M. Peng, D. J. Strickler, and S. C. Jardin, *TSC Disruption Scenarios and CIT Vacuum Vessel Force Evolution*, ORNL/FEDC-89/3, Martin Marietta Energy Systems, Inc., Oak Ridge National Laboratory, January 1990

D. J. Strickler, Y-K. M. Peng, N. Pomphrey, and S. C. Jardin, *Equilibrium Calculations for Plasma Control in CIT*, ORNL/FEDC-89/4, Martin Marietta Energy Systems, Inc., Oak Ridge National Laboratory, January 1990

Reports Published by Other Institutions

J. R. Ferron, M. S. Chu, F. J. Helton, W. Howl, A. G. Kellman, L. L. Lao, E. A. Lazarus, J. K. Lee, T. H. Osborne, R. D. Stambaugh, E. J. Strait, T. S. Taylor, and A. D. Turnbull, *The Beta Limit in the DIII-D Tokamak*, GA-A20063, General Atomics, San Diego, California, April 1990

S. M. Kaye, C. W. Barnes, M. G. Bell, J. C. Deboo, M. Greenwald, K. Riedel, D. J. Sigmar, N. A. Uckan, and R. Waltz, *Status of Global Energy Confinement Studies*, PPPL-2670, Princeton Plasma Physics Laboratory, Princeton, New Jersey, 1990

J. B. Lister, E. A. Lazarus, A. G. Kellman, J. M. Moret, J. R. Ferron, F. J. Helton, L. L. Lao, J. A. Leuer, E. J. Strait, T. S. Taylor, and A. D. Turnbull, *Experimental Study of the Vertical Stability of High Decay Index Plasmas in the DIII-D Tokamak*, GA-A19843, General Atomics, San Diego, California, February 1990

J. F. Lyon, ed., *Stellarator Physics: Proceedings of the 7th International Workshop*, IAEA-TECDOC-558, IAEA, Vienna, 1990

K. C. Shaing and R. D. Hazeltine, *Enhanced Pinch Effect due to the Electrostatic Potential*, IFSR-415 (DOE/ET-53088-415), Institute for Fusion Studies, January 1990

C. E. Thomas and R. F. Gandy, *Autocorrelation and Crossed-Sightline Correlation of ECE for Measurements of Electron Temperature and Density Fluctuations on ATF and TEXT*, GTFR-94, Georgia Institute of Technology, May 1990

N. A. Uckan and ITER Physics Group, *ITER (International Thermonuclear Engineering Reactor) Physics Design Guidelines: 1989*, ITER-DS-10, International Atomic Energy Agency, Vienna, Austria, February 1990

1990 THESES AND DISSERTATIONS

G. L. Bell, "Third-Harmonic Electron Cyclotron Emission Studies on the Advanced Toroidal Facility," Ph.D. dissertation, Auburn University, Auburn, Alabama, 1990

T. S. Bigelow, "A High-Power Microwave Transmission and Launching System for Plasma Heating on the ORNL ATF Experiment," Ph.D. dissertation, University of Tennessee, Knoxville, 1990

J. H. Han, "Particle Simulation of Finite Beta Interchange Modes in a Sheared Magnetic Field," Ph.D. dissertation, University of Texas, Austin, 1990

M. Kwon, "Fast Wave Ion Cyclotron Resonance Heating Experiments on the Advanced Toroidal Facility," Ph.D. dissertation, Georgia Institute of Technology, Atlanta, 1990

S. L. Painter, "Performance Analysis and Parametric Optimization Study of Torsatron Fusion Reactors," Ph.D. dissertation, University of Tennessee, Knoxville, 1990

1991 BOOKS AND JOURNAL ARTICLES

S. C. Aceto, J. G. Schwelberger, J. J. Zielinski, K. A. Connor, T. P. Crowley, J. W. Heard, R. L. Hickok, P. E. McLaren, A. Ouroua, P. M. Schoch, V. J. Simic, R. C. Isler, J. H. Harris, M. Murakami, J. C. Glowienka, T. Uckan, and H. Okada, "Heavy Ion Beam Probe Measurements of ECH Heated Plasma in the Advanced Toroidal Facility," *Europhys. Conf. Abstr.* **15C**, Pt. II, 161–64 (1991)

F. W. Baity, R. H. Goulding, D. J. Hoffman, P. M. Ryan, D. J. Taylor, and M. J. Mayberry, "Fast-Wave Current Drive System for DIII-D," p. 1035 in *Fusion Technology 1990: Proceedings of the 16th Symposium on Fusion Technology, London, U.K., 3–7 September 1990*, Vol. 2, ed. B. E. Keen, M. Huguet, and R. Hemsworth, North-Holland, Amsterdam, 1991

C. C. Baker, "Magnetic Fusion Energy Development Beyond 2000," *J. Fusion Energy* **10** (4), 357–58 (1991)

D. B. Batchelor, M. D. Carter, R. H. Goulding, D. J. Hoffman, E. F. Jaeger, P. M. Ryan, D. W. Swain, J. S. Tolliver, J. J. Yugo, R. J. Goldston, J. C. Hosea, S. M. Kaye, C. K. Phillips, J. R. Wilson, J. E. Scharer, and T. K. Mau, "ICRF Heating on the Burning Plasma Experiment (BPX)," p. 113 in *Controlled Fusion and Plasma Physics: Proceedings of the 18th European Conference, Berlin, 3–7 June 1991*, Pt. I, ed. P. Bachmann and D. C. Robinson, European Physical Society, Petit-Lancy, Switzerland, 1991 [*Europhys. Conf. Abstr.* **15C**, Pt. I, 113 (1991)]

D. B. Batchelor, E. F. Jaeger, M. D. Carter, D. W. Swain, D. Ehst, and C. F. F. Karney, "Fast-Wave Current Drive Modelling for ITER," pp. 817–22 in *Proceedings of the Thirteenth International Conference on Plasma Physics and Controlled Nuclear Fusion*, Vol. 1, International Atomic Energy Agency, Vienna, 1991

L. R. Baylor, W. A. Houlberg, S. L. Milora, and G. L. Schmidt, "Particle Transport in Pellet Fueled JET Plasmas," *Nucl. Fusion* **31** (7), 1249–59 (1991)

L. A. Berry and S. M. Gorbatkin, "Electron Cyclotron Resonance Microwave Ion Sources for Thin Film Processing," *Nucl. Instrum. Methods Phys. Res.* **B 56/57**, 1133 (1991)

R. Carrera, J. L. Anderson, R. Arslanoglu, T. Bauer, E. Becker, W. D. Booth, J. Borcherding, G. Brunson, R. Charbeneau, D. Coffin, P. Cooper, J. Q. Dong, M. D. Driga, R. Durrer, T. Elevant, S. E. Eways, S. Fetter, G. Y. Fu, J. Gilligan, J. H. Gully, Z. Guo, G. A. Hallock, F. J. Helton, N. E. Hertel, L. M. Hively, H. C. Howe, J. Howell, K. T. Hsieh, Y. L. Hwang, E. F. Jaeger, M. J. Johnson, R. Khayrutdinov, D. Klein, J. Q. Ling, M. Manavazhi, H. Marcus, S. S. Medley, G. H. Miley, R. Mohanti, E. Montalvo, M. E. Oakes, C. A. Ordoñez, D. E. Palmrose, T. A. Parish, J. Quiñones, G. Rodin, M. N. Rosenbluth, G. Schlapper, B. R. Shi, B. Shofolu, R. L. Sledge, S. Tamor, K. Tani, D. Tesar, J. W. Van Dam, P. Varghese, W. A. Walls, Y. Watanabe, B. W. Wehring, D. Wehrlen, W. F. Weldon, M. D. Werst, H. H. Woodson, and H. Xiao, "Description of the Fusion Experiment IGNITEX," p. 567 in *Proceedings of the Thirteenth International Conference on Plasma Physics and Controlled Nuclear Fusion*, Vol. 2, International Atomic Energy Agency, Vienna, 1991

R. Carrera, J. L. Anderson, R. Arslanoglu, T. Bauer, E. Becker, W. D. Booth, J. Borcherding, G. Brunson, R. Charbeneau, D. Coffin, P. Cooper, J. Q. Dong, M. D. Driga, R. Durrer, T. Elevant, S. E. Eways, S. Fetter, G. Y. Fu, J. Gilligan, J. H. Gully, Z. Guo, G. A. Hallock, F. J. Helton, N. E. Hertel, L. M. Hively, H. C. Howe, J. Howell, K. T. Hsieh, Y. L. Hwang, E. F. Jaeger, M. J. Johnson, R. Khayrutdinov, D. Klein, J. Q. Ling, M. Manavazhi, H. Marcus, S. S. Medley, G. Miley, R. Mohanti, E. Montalvo, M. E. Oakes, C. A. Ordoñez, D. E. Palmrose, T. A. Parish, J. Quiñones, G. Rodin, M. N. Rosenbluth, G. Schlapper, B. R. Shi, B. Shofolu, R. L. Sledge, S. Tamor, K. Tani, D. Tesar, J. W. Van Dam, P. Varghese, W. A. Walls, Y. Watanabe, B. W. Wehring, D. Wehrlen, W. F. Weldon, M. D. Werst, H. H. Woodson, and H. Xiao, "Design and Analysis of the IGNITEX Approach for a Laboratory Fusion Experiment," p. 528 in *Fusion Technology 1990: Proceedings of the 16th Symposium on Fusion Technology, London, U.K., 3–7 September 1990*, Vol. 1, ed. B. E. Keen, M. Huguet, and R. Hemsworth, North-Holland, Amsterdam, 1991

B. A. Carreras, "ITER: The Next Step in the Development of Fusion as an Energy Source," *Politica Cientifica* **26**, 46 (1991)

B. A. Carreras, N. Dominguez, V. E. Lynch, C. D. Beidler, J. Kisslinger, F. Rau, H. Wobig, D. L. Grekov, A. V. Zolotukhin, and O. S. Pavlichenko, "Plasma Stability, Equilibrium, and Transport in URAGAN-2M Torsatron," p. 149 in *Controlled Fusion and Plasma Physics: Proceedings of the 18th European Physical Society Conference, Berlin, 3–7 June 1991*, Pt. II, ed. P. Bachmann and D. C. Robinson, European Physical Society, Petit-Lancy, Switzerland, 1991 [*Europhys. Conf. Abstr.* **15C**, Pt. II, 149 (1991)]

B. A. Carreras, V. E. Lynch, and L. Garcia, "Electron Diamagnetic Effects on the Resistive Pressure-Gradient-Driven Turbulence and Poloidal Flow Generation," *Phys. Fluids B* **3** (6), 1434–38 (1991)

L. A. Charlton, L. R. Baylor, A. W. Edwards, G. W. Hammett, W. A. Houlberg, P. Kupschus, V. E. Lynch, S. L. Milora, J. O'Rourke, and G. L. Schmidt, "Theoretical Analysis of the Role of the Infernal Mode in the Stability of Peaked Pressure Profiles in Pellet Fuelled JET Discharges," *Nucl. Fusion* **31** (10), 1835–42 (1991)

L. A. Charlton, J.-N. Leboeuf, and V. E. Lynch, "Resistive Magnetohydrodynamic Stability of Stellarators with Increasing Plasma Pressure," *Phys. Fluids B* **3** (8), 2028–37 (1991)

S. K. Combs, C. R. Foust, D. T. Fehling, M. J. Gouge, and S. L. Milora, "Repetitive Two-Stage Light Gas Gun for High-Speed Pellet Injection," *Rev. Sci. Instrum.* **61** (8), 1978–89 (1991)

S. O. Dean, C. C. Baker, D. R. Cohn, and S. D. Kinkead, "An Accelerated Fusion Power Development Plan," *J. Fusion Energy* **10** (2), 197 (1991)

R. A. Dory, "Contour Plots for Spreadsheets," *Comput. Phys.* **5** (5), 529–32 (1991)

R. A. Dory, M. Murakami, W. R. Wing, and the ATF Team, "Energy Confinement Scaling in the ATF Stellarator," *Comments Plasma Phys. Controlled Fusion* **14** (4), 237–48 (1991)

R. J. Dowling, R. E. Price, F. W. Wiffen, and S. A. Eckstrand, "Overview of the U.S. Magnetic Fusion Energy Program," p. 199 in *Fusion Technology 1990: Proceedings of the 16th Symposium on Fusion Technology, London, U.K., 3–7 September 1990*, Vol. 1, ed. B. E. Keen, M. Huguet, and R. Hemsworth, North-Holland, Amsterdam, 1991

L. Dresner, "Excess Heat Production in Composite Superconductors During Current Redistribution," in *Advances in Cryogenic Engineering*, Vol. 37, Plenum Publishing Corporation, New York, 1991

L. Dresner, "Rational Design of High-Current Cable-in-Conduit Superconductors," pp. 149–63 in IAEA-TECDOC-594, International Atomic Energy Agency, Vienna, 1991

L. Dresner, "Superconductor Stability '90: A Review," *Cryogenics* **31** (7), 489 (1991)

L. Dresner, "Theory of Thermal Hydraulic Quenchback in Cable-in-Conduit Superconductors," *Cryogenics* **31** (7), 557–61 (1991)

A. C. England, G. L. Bell, R. H. Fowler, J. C. Glowienka, J. H. Harris, M. Murakami, G. H. Neilson, D. A. Rasmussen, J. A. Rome, M. J. Saltmarsh, and J. B. Wilgen, "Runaway Electron Studies in the ATF Torsatron," *Phys. Fluids B* **3**, 1671–86 (1991)

R. H. Fowler, R. N. Morris, and J. A. Rome, "A Study of Neutral Beam Injection for the Advanced Toroidal Facility," *Fusion Technol.* **20** (2), 200–207 (1991)

J. Galambos and Y-K. M. Peng, "Ignition and Burn Criteria for D-^{3}He Tokamak and Spherical Torus Reactors," *Fusion Technol.* **19** (1), 31 (1991)

J. D. Galambos and Y-K. M. Peng, "Comparison of ITER Single-Null and Double-Null Operations," *Fusion Technol.* **19**, 1463 (1991).

L. Garcia, B. A. Carreras, and V. E. Lynch, "Electric Field Effects on the Resistive Pressure-Gradient-Driven Turbulence," p. 13 in *Controlled Fusion and Plasma Physics: Proceedings of the 18th European Conference, Berlin, 3–7 June 1991*, Pt. IV, ed. P. Bachmann and D. C. Robinson, European Physical Society, Petit-Lancy, Switzerland, 1991 [*Europhys. Conf. Abstr.* **15C**, Pt. IV, 13 (1991)]

R. C. Goldfinger, D. K. Lee, K. M. Likin, and B. D. Ochirov, "Ray Tracing and Absorption of Electron Cyclotron Waves in the L-2 Stellarator," *Nucl. Fusion* **31** (12), 2305 (1991)

R. J. Goldston, G. Bateman, W. A. Houlberg, S. M. Kaye, G. H. Neilson, F. W. Perkins, N. Pomphrey, M. Porkolab, K. S. Riedel, R. D. Stambaugh, D. P. Stotler, R. E. Waltz, and M. C. Zarnstorff, "Confinement Projections for the Burning Plasma Experiment (BPX)," pp. 93–96 in *Controlled Fusion and Plasma Physics: Proceedings of the 18th European Conference, Berlin, 3–7 June 1991*, Pt. I, ed. P. Bachmann and D. C. Robinson, European Physical Society, Petit-Lancy, Switzerland, 1991 [*Europhys. Conf. Abstr.* **15C**, Pt. I, 93–96 (1991)]

M. J. Gouge, B. E. Argo, L. R. Baylor, S. K. Combs, D. T. Fehling, P. W. Fisher, C. A. Foster, C. R. Foust, S. L. Milora, A. L. Qualls, D. E. Schechter, D. W. Simmons, D. O. Sparks, and C. C. Tsai, "Pellet Injector Development at ORNL," p. 675 in *Fusion Technology 1990: Proceedings of the 16th Symposium on Fusion Technology, London, U.K., 3–7 September 1990*, Vol. 1, ed. B. E. Keen, M. Huguet, and R. Hemsworth, North-Holland, Amsterdam, 1991

M. J. Gouge, W. A. Houlberg, and S. L. Milora, "A Comparison of Hydrogenic Pellet Ablation Models with Experiment," *Fusion Technol.* **19**, 95–101 (1991)

M. J. Gouge, "HTGR Gas Turbine Power Plant for Submarine Propulsion in the 21st Century," *Submarine Review*, July 86 (1991)

L. R. Grisham, S. D. Scott, R. J. Goldston, M. G. Bell, R. Bell, N. L. Bretz, C. E. Bush, B. Grek, G. W. Hammett, K. Hill, F. Jobes, D. Johnson, S. Kaye, D. Mansfield, D. Mueller, H. K. Park, A. Ramsey, J. Schivell, B. Stratton, E. J. Synakowski, G. Taylor, and H. H. Towner, "Scaling of Confinement with Major and Minor Radius in the Tokamak Fusion Test Reactor," *Phys. Rev. Lett.* **67**, 66 (1991)

M. L. Grossbeck and L. K. Mansur, "Low-Temperature Creep Properties of Fusion Reactor Structural Materials," *J. Nucl. Mater.* **179–81**, 130–34 (1991)

J. H. Harris, J. D. Bell, J. L. Dunlap, V. K. Paré, G. L. Bell, T. S. Bigelow, A. C. England, J. C. Glowienka, L. D. Horton, H. C. Howe, R. C. Isler, M. M. Menon, M. Murakami, R. N. Morris, G. H. Neilson, D. A. Rasmussen, J. B. Wilgen, and W. R. Wing, "Magnetic Fluctuations in Currentless Plasmas in the ATF Torsatron," *Nucl. Fusion* **31** (6), 1099–1106 (1991)

J. H. Harris, L. A. Charlton, G. L. Bell, J. D. Bell, T. S. Bigelow, B. A. Carreras, R. J. Colchin, N. A. Crocker, E. C. Crume, N. Dominguez, J. L. Dunlap, G. R. Dyer, A. C. England, J. C. Glowienka, G. R. Hanson, D. L. Hillis, S. Hiroe, L. D. Horton, H. C. Howe, R. C. Isler, T. C. Jernigan, J.-N. Leboeuf, D. K. Lee, V. E. Lynch, J. F. Lyon, M. M. Menon, M. Murakami, D. A. Rasmussen, C. P. Ritz, C. E. Thomas, T. Uckan, M. R. Wade, J. B. Wilgen, W. R. Wing, E. Anabitarte, B. Brañas, C. Hidalgo, and J. Sanchez, "Fluctuations and Stability in the ATF Torsatron," pp. 677–84 in *Proceedings of the Thirteenth International Conference on Plasma Physics and Controlled Nuclear Fusion*, Vol. 2, International Atomic Energy Agency, Vienna, 1991

J. H. Harris, M. Murakami, S. Aceto, B. Brañas, L. R. Baylor, B. A. Carreras, et al., "Configuration Control, Fluctuations, and Transport in Low-Collisionality Plasmas in the ATF Torsatron," p. 169 in *Controlled Fusion and Plasma Physics: Proceedings of the 18th European Conference, Berlin, 3–7 June 1991*, Pt. I, ed. P. Bachmann and D. C. Robinson, European Physical Society, Petit-Lancy, Switzerland, 1991 [*Europhys. Conf. Abstr.* **15C**, Pt. I, 169 (1991)]

R. J. Hawryluk, V. Arunasalam, C. W. Barnes, M. Beer, M. Bell, R. Bell, H. Biglari, M. Bitter, R. Boivin, N. L. Bretz, R. V. Budny, C. E. Bush, C. Z. Cheng, T. K. Chu, S. A. Cohen, S. Cowley, P. C. Efthimion, R. J. Fonck, E. Fredrickson, H. P. Furth, R. J. Goldston, G. Greene, B. Grek, L. R. Grisham, G. Hammett, W. Heidbrink, K. W. Hill, J. Hosea, R. A. Hulse, H. Hsuan, A. Janos, D. Jassby, F. C. Jobes, D. W.

Johnson, L. C. Johnson, J. Kesner, C. Kieras-Phillips, S. J. Kilpatrick, H. Kugel, P. H. LaMarche, B. LeBlanc, D. M. Manos, D. K. Mansfield, E. S. Marmar, E. Mazzucato, M. P. McCarthy, M. Mauel, D. C. McCune, K. M. McGuire, D. M. Meade, S. S. Medley, D. R. Mikkelsen, D. Monticello, R. Motley, D. Mueller, Y. Nagayama, G. A. Navratil, R. Nazikian, D. K. Owens, H. Park, W. Park, S. Paul, F. Perkins, S. Pitcher, A. T. Ramsey, M. H. Redi, G. Rewoldt, D. Roberts, A. L. Roquemore, P. H. Rutherford, S. Sabbagh, G. Schilling, J. Schivell, G. L. Schmidt, S. D. Scott, J. Snipes, J. Stevens, B. C. Stratton, W. Stodiek, E. Synakowski, Y. Takase, W. Tang, G. Taylor, J. Terry, J. R. Timberlake, H. H. Towner, M. Ulrickson, S. von Goeler, R. Wieland, M. Williams, J. R. Wilson, K.-L. Wong, M. Yamada, S. Yoshikawa, K. M. Young, M. C. Zarnstorff, and S. J. Zweben, "Overview of TFTR Transport Studies," *Plasma Phys. Controlled Fusion* **33** (13), 1509–36 (1991)

R. A. Hawsey, W. K. Kahl, S. W. Schwenterly, J. M. Bailey, J. N. Luton, B. W. McConnell, and V. W. Campbell, "Analysis and Performance of an Axial-Gap Superconducting Motor," *IEEE Trans. Magn.* **MAG-27** (2), 2252–55 (1991)

C. Hidalgo, J. H. Harris, T. Uckan, J. D. Bell, B. A. Carreras, J. L. Dunlap, G. R. Dyer, C. P. Ritz, A. J. Wootton, M. A. Meier, T. L. Rhodes, and K. Carter, "Plasma Fluctuations near the Shear Layer in the ATF Torsatron," *Nucl. Fusion* **31** (8), 1471–78 (1991)

D. N. Hill, T. W. Petrie, J. N. Brooks, D. Buchenauer, A. Futch, G. Haas, J. T. Hogan, W. L. Hsu, G. L. Jackson, C. C. Klepper, R. J. La Haye, B. Leikind, S. Lippmann, M. A. Mahdavi, G. F. Matthews, M. M. Menon, B. Mills, P. K. Mioduszewski, G. D. Porter, M. E. Rensink, T. D. Rognlien, M. Schaffer, L. Schmitz, G. M. Staebler, J. Watkins, J. Winter, and J. Wood, "Divertor-Plasma Studies on DIII-D," p. 487 in *Proceedings of the Thirteenth International Conference on Plasma Physics and Controlled Nuclear Fusion*, Vol. 2, International Atomic Energy Agency, Vienna, 1991

S. P. Hirshman and O. Betancourt, "Preconditioned Descent Algorithm for Rapid Calculation of Magnetohydrodynamic Equilibria," *J. Comput. Phys.* **96** (1), 99–109 (1991)

A. L. Hoffman, R. K. Linford, D. Overskei, R. R. Parker, D. M. Meade, and J. Sheffield, "Progress and Plans for Magnetic Fusion," *J. Fusion Energy* **10**, 71 (1991)

D. J. Hoffman, R. H. Goulding, P. M. Ryan, D. B. Batchelor, E. F. Jaeger, F. W. Baity, M. J. Mayberry, R. I. Pinsker, and C. C. Petty, "Design and Matching Problems Associated with Fast-Wave Current Drive Antennas," invited, p. 456 in *Proceedings of the IAEA Technical Committee Meeting on Fast Wave Current Drive in Reactor Scale Tokamaks, Arles (France), September 23–25, 1991*, ed. D. Moreau, A. Bécoulet, and Y. Peysson, Association EURATOM-CEA sur la Fusion, 1991

J. T. Hogan, D. L. Hillis, J. D. Galambos, N. A. Uckan, K. H. Dippel, K. H. Finken, R. A. Hulse, and R. V. Budny, "ITER Helium Ash Accumulation," *Fusion Technol.* **19** (3), 1509 (1991)

J. T. Hogan and N. A. Uckan, "ITER Global Stability Limits," *Fusion Technol.* **19** (3), 1504 (1991)

J. A. Holmes, "Nonlinear Evolution of Resistive Modes for $q < 1$ in Tokamaks," *Phys. Fluids B* **3** (3), 594 (1991)

R. C. Isler, E. C. Crume, L. D. Horton, M. Murakami, L. R. Baylor, G. L. Bell, T. S. Bigelow, A. C. England, J. C. Glowienka, T. C. Jernigan, R. A. Langley, P. K. Mioduszewski, D. A. Rasmussen, J. E. Simpkins, J. B. Wilgen, and W. R. Wing, "Radiative Losses and Improvement of Plasma Parameters Following Gettering in the Advanced Toroidal Facility," *Nucl. Fusion* **31** (2), 245–59 (1991)

R. C. Isler, L. D. Horton, E. C. Crume, M. Murakami, G. L. Bell, T. S. Bigelow, A. C. England, J. C. Glowienka, S. Hiroe, T. C. Jernigan, R. A. Langley, J. F. Lyon, P. K. Mioduszewski, S. Morita, D. A. Rasmussen, J. E. Simpkins, J. B. Wilgen, and W. R. Wing, "Impurity Effects and Impurity Transport in ATF," pp. 685–92 in *Proceedings of the Thirteenth International Conference on Plasma Physics and Controlled Nuclear Fusion*, Vol. 2, International Atomic Energy Agency, Vienna, 1991

T. Inazumi, G. E. C. Bell, E. A. Kenik, and K. Kiuchi, "Evaluation of Radiation-Induced Sensitization of Austenitic Stainless Steels Using Electrochemical Potentiokinetic Reactivation Techniques," *Corrosion* **46** (10), 786–92 (1991)

G. L. Jackson, J. Winter, T. S. Taylor, K. H. Burrell, J. C. DeBoos, E. A. Lazarus, et al., "Regime of Very High Confinement in the Boronized DIII-D Tokamak," *Phys. Rev. Lett.* **67**, 3098 (1991)

E. F. Jaeger and D. B. Batchelor, "Full-Wave Calculation of Fast-Wave Current Drive in Tokamaks Including $k_{||}$ Variations," p. 86 in *Proceedings of the IAEA Technical Committee Meeting on Fast Wave Current Drive in Reactor Scale Tokamaks, Arles (France), September 23–25, 1991*, ed. D. Moreau, A. Bécoulet, and Y. Peysson, Association EURATOM-CEA sur la Fusion, 1991

E. F. Jaeger, L. A. Berry, and D. B. Batchelor, "Characteristics of a Cylindrical Langmuir Probe of Finite Length," *J. Appl. Phys.* **69** (10), 6918–22 (1991)

D. L. Jassby, C. W. Barnes, M. G. Bell, M. Bitter, R. Boivin, N. L. Bretz, R. V. Budny, C. E. Bush, H. F. Dylla, P. C. Efthimion, E. D. Fredrickson, R. J. Hawryluk, K. W. Hill, J. Josea, H. Hsuan, A. C. Janos, F. C. Jobes, D. W. Johnson, L. C. Johnson, J. Kamperschroer, C. Kieras-Phillips, S. J. Kilpatrick, P. H. LaMarche, B. LeBlanc, D. K. Mansfield, E. S. Marmar, D. C. McCune, K. M. McGuire, D. M. Meade, S. S. Medley, D. R. Mikkelsen, D. Mueller, D. K. Owens, H. K. Park, S. F. Paul, S. Pitcher, A. T. Ramsey, M. H. Redi, S. A. Sabbagh, S. D. Scott, J. Snipes, J. Stevens, J. D. Strachan, B. C. Stratton, E. J. Synakowski, G. Taylor, J. L. Terry, J. R. Timberlake, H. H. Towner, M. Ulrickson, S. von Goeler, R. M. Wieland, M. Williams, J. R. Wilson, K.-L. Wong, K. M. Young, M. C. Zarnstorff, and S. J. Zweben, "High-Q Plasmas in the TFTR Tokamak," *Phys. Fluids B* **3** (8, Pt. 2), 2308 (1991)

A. G. Kellman, J. R. Ferron, T. H. Jensen, L. L. Lao, E. A. Lazarus, J. B. Lister, J. L. Luxon, D. G. Skinner, E. J. Strait, E. Reis, T. S. Taylor, and A. D. Turnbull, "Vertical Stability, High Elongation and the Consequences of Loss of Vertical Cotnrol on DIII-D," p. 1045 in *Fusion Technology 1990: Proceedings of the 16th Symposium on Fusion Technology, London, U.K., 3–7 September 1990*, Vol. 2, ed. B. E. Keen, M. Huguet, and R. Hemsworth, North-Holland, Amsterdam, 1991

E. A. Kenik, J. Bentley, and N. D. Evans, "Application of Electron Energy Loss Spectroscopy to Microanalysis of Irradiated Stainless Steels," pp. 732–33 in *Proceedings of the 49th Annual Meeting of the Electron Microscopy Society of America, San Jose, California, August 4–9, 1991*, ed. G. W. Bailey, Electron Microscopy Society of America, San Francisco, 1991

H. E. Kim, S. J. Zinkle, and W. R. Allen, "Preparation of $MgAl_2O_4$ Spinel Containing Controlled Amounts of ^{17}O Isotope," *J. Am. Ceram. Soc.* **74** (6), 1442–44 (1991)

R. L. Klueh and J. M. Vitek, "Tensile Properties of 9Cr–1MoVNb Steels Irradiated to 23 dpa at 390 to 550°C," *J. Nucl. Mater.* **182**, 230–39 (1991)

R. A. Langley, E. C. Crume, Jr., J. C. Glowienka, L. D. Horton, R. C. Isler, M. Murakami, and J. E. Simpkins, "Effects of Wall Conditioning on Plasma Performance in the Advanced Toroidal Facility Stellarator," *J. Vac. Sci. Technol. A* **9** (3), 848–51 (1991)

R. A. Langley, A. L. Qualls, and J. B. Wilgen, "Absolute Calibration of a Frozen Hydrogen Pellet Mass Detector," *J. Vac. Sci. Technol. A* **9** (3), 737–41 (1991)

E. A. Lazarus, M. S. Chu, J. R. Ferron, F. J. Helton, J. T. Hogan, A. G. Kellman, L. L. Lao, J. B. Lister, T. H. Osborne, R. Snider, E. J. Strait, T. S. Taylor, and A. D. Turnbull, "Higher Beta at Higher Elongation in DIII-D," *Phys. Fluids B* **3** (8, Pt. 2), 2220 (1991)

J.-N. Leboeuf, D. K. Lee, B. A. Carreras, N. Dominguez, J. H. Harris, C. L. Hedrick, C. Hidalgo, J. A. Holmes, J. Ruiter, P. H. Diamond, A. S. Ware, C. P. Ritz, A. J. Wootton, W. L. Rowan, and R. V. Bravenec, "TEXT Tokamak Edge Turbulence Modeling," *Phys. Fluids B* **3** (8, Pt. 2), 2291–99 (1991)

B. Lembege, J.-N. Leboeuf, P. Liewer, and M. Ashour-Abdalla, eds., *From Fusion to Light Surfing: Lectures on Plasma Physics Honoring John Dawson*, Addison-Wesley, New York, 1991

B. Lloyd, G. L. Jackson, T. S. Taylor, E. A. Lazarus, T. C. Luce, and R. Prater, "Low Voltage Ohmic and ECH-Assisted Startup in DIII-D," *Nucl. Fusion* **31**, 2031 (1991)

J. W. Lue, S. W. Schwenterly, L. Dresner, and M. S. Lubell, "Quench Propagation in a Cable-in-Conduit Force-Cooled Superconductor—Preliminary Results," *IEEE Trans. Magn.* **MAG-27** (2), 2072–75 (1991)

V. E. Lynch, B. A. Carreras, J. B. Drake, J.-N. Leboeuf, and J. R. Ruiter, "Plasma Turbulence Calculations on the INTEL IPSC/860 (RX) Hypercube," *Int. J. Comput. Sys. Eng.* **2**, 299 (1991)

R. Maingi, J. Gilligan, O. Hankins, L. Owen, P. Mioduszewski, and T. Uckan, "Comparison Between Pump Limiter Performance and Modelling Predictions on Tore Supra," *Fusion Technol.* **19**, 1778 (1991)

P. J. Maziasz, A. F. Rowcliffe, M. L. Grossbeck, G. E. C. Bell, E. E. Bloom, D. C. Lousteau, A. Hishinuma, T. Kondo, R. F. Mattas, and D. L. Smith, "Some Implications of Radiation-Induced Property Changes in Austenitic Stainless Steels on ITER First-Wall Design and Performance," *Fusion Technol.* **19** (3), 1571–79 (1991)

D. Moreau, Tore Supra Team (ORNL members: C. A. Foster, L. Horton, P. Mioduszewski, T. Shepard, W. Stirling, and T. Uckan), and C. Gormezano, "Lower Hybrid Current Drive in Tore Supra and JET," *Plasma Phys. Controlled Fusion* **33** (13), 1621–38 (1991)

D. Mueller, P. H. LaMarche, M. G. Bell, W. Blanchard, C. E. Bush, H. F. Dylla, C. Gentile, R. J. Hawryluk, K. W. Hill, A. C. Janos, F. C. Jobes, D. K. Owens, G. Pearson, J. Schivell, M. A. Ulrickson, C. Vannoy, and K.-L. Wong, "Discharge Cleaning on Tokamak Fusion Test Reactor After Boronization," *J. Vac. Sci. Technol. A* **9**, 2713 (1991)

M. Murakami, S. C. Aceto, E. Anabitarte, D. T. Anderson, F. S. B. Anderson, D. B. Batchelor, B. Brañas, L. R. Baylor, G. L. Bell, J. D. Bell, T. S. Bigelow, B. A. Carreras, R. J. Colchin, E. C. Crume, N. Dominguez, R. A. Dory, J. L. Dunlap, G. R. Dyer, A. C. England, O. I. Fedyanin, R. H. Fowler, R. F. Gandy, J. C. Glowienka, R. C. Goldfinger, R. H. Goulding, G. R. Hanson, J. H. Harris, C. L. Hedrick, C. Hidalgo, D. L. Hillis, S. Hiroe, S. P. Hirshman, L. D. Horton, H. C. Howe, D. P. Hutchinson, R. C. Isler, T. C. Jernigan, H. Kaneko, M. Kwon, R. A. Langley, J.-N. Leboeuf, D. K. Lee, V. E. Lynch, J. F. Lyon, C. H. Ma, M. A. Meier, M. M. Menon, P. K. Mioduszewski, S. Morita, R. N. Morris, G. H. Neilson, M. A. Ochando, S. Okamura, S. Paul, A. L. Qualls, D. A. Rasmussen, R. K. Richards, Ch. P. Ritz, J. A. Rome, J. Sanchez, F. Sano, K. C. Shaing, T. D. Shepard, A. A. Shishkin, J. E. Simpkins, S. Sudo, Y. Takeiri, C. E. Thomas, J. S. Tolliver, T. Uckan, K. L. Vander Sluis, M. R. Wade, J. B. Wilgen, W. R. Wing, H. Yamada, and J. J. Zielinski, "Energy Confinement and Bootstrap Current in the Advanced Toroidal Facility," pp. 455–70 in *Proceedings of the Thirteenth International Conference on Plasma Physics and Controlled Nuclear Fusion*, Vol. 2, International Atomic Energy Agency, Vienna, 1991

M. Murakami, S. C. Aceto, E. Anabitarte, D. T. Anderson, F. S. B. Anderson, D. B. Batchelor, B. Brañas, L. R. Baylor, G. L. Bell, J. D. Bell, T. S. Bigelow, B. A. Carreras, R. J. Colchin, E. C. Crume, N. Dominguez, R. A. Dory, J. L. Dunlap, G. R. Dyer, A. C. England, O. I. Fedyanin, R. H. Fowler, R. F. Gandy, J. C. Glowienka, R. C. Goldfinger, R. H. Goulding, G. R. Hanson, J. H. Harris, C. L. Hedrick, C. Hidalgo, D. L. Hillis, S. Hiroe, S. P. Hirshman, L. D. Horton, H. C. Howe, D. P. Hutchinson, R. C. Isler, T. C. Jernigan, H. Kaneko, M. Kwon, R. A. Langley, J.-N. Leboeuf, D. K. Lee, V. E. Lynch, J. F. Lyon, C. H. Ma, M. A. Meier, M. M. Menon, P. K. Mioduszewski, S. Morita, R. N. Morris, G. H. Neilson, M. A. Ochando, S. Okamura, S. Paul, A. L. Qualls, D. A. Rasmussen, R. K. Richards, Ch. P. Ritz, J. A. Rome, J. Sanchez, F. Sano, K. C. Shaing, T. D. Shepard, A. A. Shishkin, J. E. Simpkins, S. Sudo, Y. Takeiri, C. E. Thomas, J. S. Tolliver, T. Uckan, K. L. Vander Sluis, M. R. Wade, J. B. Wilgen, W. R. Wing, H. Yamada, and J. J. Zielinski, "Recent Results from the ATF Torsatron," *Phys. Fluids B* **3** (8, Pt. 2), 2261–69 (1991)

M. Murakami, B. A. Carreras, L. R. Baylor, G. L. Bell, T. S. Bigelow, A. C. England, J. C. Glowienka, H. C. Howe, T. C. Jernigan, D. K. Lee, V. E. Lynch, C. H. Ma, D. A. Rasmussen, J. S. Tolliver, M. R. Wade, J. B. Wilgen, and W. R. Wing, "Bootstrap-Current Experiments in a Toroidal Plasma-Confinement Device," *Phys. Rev. Lett.* **66** (6), 707–10 (1991)

F. Najmabadi, R. W. Conn, C. G. Bathke, L. Bromberg, E. T. Cheng, D. R. Cohn, P. I. H. Cooke, R. L. Creedon, D. A. Ehst, K. Evans, Jr., N. M. Ghoniem, S. P. Grotz, M. Z. Hasan, J. T. Hogan, J. S. Herring, A. W. Hyatt, E. Ibrahim, S. A. Hardin, C. Kessel, M. Klasky, R. A. Krakowski, T. Kunugi, J. A. Leuer, J. Mandrekas, R. C. Martin, T.-K. Mau, R. L. Miller, Y-K. M. Peng, R. L. Reid, J. F. Santarius, M. J. Schaffer, J. Schultz, K. R. Schultz, J. Swartz, S. Sharafat, C. E. Singer, L. Snead, D. Steiner, D. J. Strickler, D.-K. Sze, M. Valenti, D. J. Ward, J. E. C. Williams, L. J. Wittenberg, and C. P. C. Wong, "The ARIES-1 Tokamak Reactor Study," p. 253 in *Fusion Technology 1990: Proceedings of the 16th Symposium on*

Fusion Technology, London, U.K., 3–7 September 1990, Vol. 1, ed. B. E. Keen, M. Huguet, and R. Hemsworth, North-Holland, Amsterdam, 1991

Y. Nakamura, N. Wakatani, J.-N. Leboeuf, B. A. Carreras, N. Dominguez, J. A. Holmes, V. E. Lynch, S. L. Painter, and L. Garcia, "Equilibrium, Stability, and Deeply Trapped Energetic Particle Confinement Calculations for $l = 2$ Torsatron/Heliotron Configurations," *Fusion Technol.* **19** (2), 217–33 (1991)

G. H. Neilson, D. B. Batchelor, G. Bateman, M. G. Bell, J. Bialek, B. J. Braams, J. N. Brooks, R. J. Goldston, J. R. Haines, D. N. Hill, W. A. Houlberg, S. C. Jardin, C. E. Kessel, S. S. Medley, F. W. Perkins, R. D. Pillsbury, N. Pomphrey, M. Porkolab, W. T. Reiersen, R. O. Sayer, J. E. Scharer, J. A. Schmidt, D. J. Sigmar, J. C. Sinnis, R. D. Stambaugh, D. P. Stotler, D. J. Strickler, M. Ulrickson, R. W. Waltz, K. M. Young, and J. J. Yugo, "Overview of the CIT Physics Design," *Fusion Technol.* **19** (3), 1109 (1991)

K. A. Niemer, J. C. Gilligan, C. D. Croessman, and A. C. England, "Theoretical Analysis of a Runaway Electron Suppression Device," p. 346 in *Fusion Technology 1990: Proceedings of the 16th Symposium on Fusion Technology, London, U.K., 3–7 September 1990*, Vol. 1, ed. B. E. Keen, M. Huguet, and R. Hemsworth, North-Holland, Amsterdam, 1991

K. A. Niemer, J. C. Gilligan, C. D. Croessman, A. C. England, and D. L. Hillis, "Studies of Runaway Electron Damage on Plasma Facing Components," *Fusion Technol.* **19**, 1717 (1991)

S. L. Painter and J. F. Lyon, "Transport Analysis of Stellarator Reactors," *Nucl. Fusion* **31** (12), 2271 (1991)

Y-K. M. Peng and J. B. Hicks, "Engineering Feasibility of Tight Aspect Ratio Tokamak (Spherical Torus) Reactors," p. 1287 in *Fusion Technology 1990: Proceedings of the 16th Symposium on Fusion Technology, London, U.K., 3–7 September 1990*, Vol. 2, ed. B. E. Keen, M. Huguet, and R. Hemsworth, North-Holland, Amsterdam, 1991

R. Prater, M. J. Mayberry, C. C. Petty, R. I. Pinsker, M. Porkolab, S. C. Chiu, R. W. Harvey, T. C. Luce, P. Bonoli, F. W. Baity, R. H. Goulding, D. J. Hoffman, R. A. James, H. Kawashima, A. Bécoulet, D. Moreau, and V. Trukhin, "Initial Fast Wave Heating and Current Drive Experiments on DIII-D Tokamak," invited, p. 308 in *Proceedings of the IAEA Technical Committee Meeting on Fast Wave Current Drive in Reactor Scale Tokamaks, Arles (France), September 23–25, 1991*, ed. D. Moreau, A. Bécoulet, and Y. Peysson, Association EURATOM-CEA sur la Fusion, 1991

A. T. Ramsey, C. E. Bush, H. F. Dylla, D. K. Owens, C. S. Pitcher, and M. Ulrickson, "Enhanced Carbon Influx into TFTR Supershots," *Nucl. Fusion* **31**, 1811 (1991)

P. M. Ryan, F. W. Baity, D. B. Batchelor, R. H. Goulding, D. J. Hoffman, and J. S. Tolliver, "The Effect of Realistic Antenna Geometry on Plasma Loading Predictions," p. 307 in *Controlled Fusion and Plasma Physics: Proceedings of the 18th European Conference, Berlin, 3–7 June 1991*, Pt. III, ed. P. Bachmann and D. C. Robinson, European Physical Society, Petit-Lancy, Switzerland, 1991 [*Europhys. Conf. Abstr.* **15C**, Pt. III, 307 (1991)]

S. A. Sabbagh, R. A. Gross, M. E. Mauel, G. A. Navratil, M. G. Bell, R. Bell, M. Bitter, N. L. Bretz, R. V. Budny, C. E. Bush, M. S. Chance, P. C. Efthimion, E. D. Fredrickson, R. Hatcher, R. J. Hawryluk, S. P. Hirshman, A. C. Janos, S. C. Jardin, D. L. Jassby, J. Manickam, D. C. McCune, K. M. McGuire, S. S. Medley, D. Mueller, Y. Nagayama, D. K. Owens, M. Okabayashi, H. K. Park, M. C. Zarnstorff, J. Kesner, E. S. Marmar, and J. L. Terry, "High Poloidal Beta Equilibria in the Tokamak Fusion Test Reactor Limited by a Natural Inboard Poloidal Field Null," *Phys. Fluids B* **3** (8, Pt. 2), 2277 (1991)

R. T. Santoro, R. G. Alsmiller, Jr., and J. M. Barnes, "Reaction Rate Distributions and Related Data in the Fusion Neutron Source Phase II Experiments: Comparison of Measured and Calculated Data," *Fusion Technol.* **19**, 449 (1991)

K. C. Shaing, "Suppression of Turbulent Fluctuations by Radial Electric Fields and Confinement Enhancement in Toroidal Plasmas," *Comments Plasma Phys. Controlled Fusion* **14** (1), 41–47 (1991)

K. C. Shaing, E. C. Crume, Jr., and W. A. Houlberg, "Erratum: 'Bifurcation of Poloidal Rotation and Suppression of Turbulent Fluctuations: A Model for the L-H Transition in Tokamaks' [*Phys. Fluids B* **2**, 1492 (1990)]," *Phys. Fluids B* **3** (12), 3542 (1991)

D. J. Sigmar, D. B. Batchelor, G. Bateman, M. G. Bell, B. J. Braams, J. N. Brooks, C. Z. Cheng, D. R. Cohn, R. J. Goldston, J. Haines, D. N. Hill, W. A. Houlberg, C. T. Hsu, S. C. Jardin, S. S. Medley, G. H. Neilson, W. A. Peebles, F. W. Perkins, N. Pomphrey, M. Porkolab, W. T. Reiersen, R. O. Sayer, J. A. Schmidt, C. E. Singer, R. D. Stambaugh, D. P. Stotler, D. J. Strickler, M. Ulrickson, R. E. Waltz, R. White, and K. M. Young, "Physics Objectives and Design of CIT," pp. 455–71 in *Plasma Physics and Controlled Nuclear Fusion Research: Proceedings of the 13th International Conference, Washington, D.C., 1990*, Vol. 3, International Atomic Energy Agency, Vienna, 1991

P. F. Tortorelli, "Deposition Behavior of Ferrous Alloys in Molten Lead-Lithium," *Fusion Eng. Des.* **14**, 335–45 (1991)

C. C. Tsai, "Potential Applications of New Microwave FCR Multicusp Plasma Ion Source," *Nucl. Instrum. Methods, Phys. Res. B* **56**, 1166 (1991)

N. A. Uckan and J. T. Hogan, "ITER Confinement Capability," *Fusion Technol.* **19** (3), 1499 (1991)

N. A. Uckan and D. E. Post, "ITER Physics Basis," *Fusion Technol.* **19** (3), 1411 (1991)

N. A. Uckan and D. E. Post, "ITER Physics Design Guidelines," *Fusion Technol.* **19** (3), 1493 (1991)

T. Uckan, C. Hidalgo, J. D. Bell, J. H. Harris, J. L. Dunlap, J. B. Wilgen, C. P. Ritz, T. L. Rhodes, and A. J. Wootton, "Characteristics of Edge Plasma Turbulence on the ATF Torsatron," *Phys. Fluids B* **3** (4), 1000–1005 (1991)

T. Uckan, P. K. Mioduszewski, T. S. Bigelow, J. C. Glowienka, S. Hiroe, M. Murakami, J. B. Wilgen, and W. R. Wing, "Power and Particle Balance Studies Using an Instrumented Limiter System on ATF," *Plasma Phys. Controlled Fusion* **33** (6), 703–12 (1991)

A. Varias, A. Alvarez, A. L. Fraguas, C. Alejaldre, N. Dominguez, B. A. Carreras, and V. E. Lynch, "Effect of the Aspect Ratio on the Stability Limits of TJ-II-Like Stellarators," p. 125 in *Controlled Fusion and Plasma Physics: Proceedings of the 18th European Conference, Berlin, 3–7 June 1991*, Pt. II, ed. P. Bachmann and D. C. Robinson, European Physical Society, Petit-Lancy, Switzerland, 1991 [*Europhys. Conf. Abstr.* **15C**, Pt. II, 125 (1991)]

J. R. Wilson, J. C. Hosea, M. G. Bell, M. Bitter, R. Boivin, E. D. Fredrickson, G. J. Greene, G. W. Hammett, K. W. Hill, D. J. Hoffman, H. Hsuan, M. Hughes, A. C. Janos, D. L. Jassby, F. C. Jobes, D. W. Johnson, C. K. Phillips, D. K. Mansfield, K. M. McGuire, S. S. Medley, D. Mueller, Y. Nagayama, M. Ono, D. K. Owens, H. K. Park, M. Phillips, A. T. Ramsey, G. L. Schmidt, S. D. Scott, J. E. Sievens, B. C. Stratton, E. J. Synakowski, G. Taylor, M. Ulrickson, K. L. Wong, M. C. Zarnstorff, and S. J. Zweben, "Experiments Utilizing Ion Cyclotron Resonant Frequency Heating on the TFTR Tokamak," *Phys. Fluids B* **3** (8, Pt. 2), 2270 (1991)

1991 CONFERENCE PRESENTATIONS

January

International Panel on 14 MeV Intense Neutron Source Based on Accelerators for Fusion Materials Studies, Tokyo, Japan, January 14–16, 1991

F. W. Wiffen and A. F. Rowcliffe, "User-Developed Criteria for a Neutron Source"

Workshop on Edge Plasma Physics for BPX and ITER, Princeton, New Jersey, January 15–17, 1991

C. E. Bush, G. Taylor, R. Nazikian, N. Bretz, R. Budny, E. Fredrickson, K. Hill, A. Janos, S. Kilpatrick, D. Manos, D. Mansfield, K. McGuire, H. Park, S. Paul, S. Sabbagh, and J. Schivell, "ELM Behavior in TFTR H-Modes"

SPIE Symposium on Intense Microwave and Particle Beams II, Los Angeles, California, January 20, 1991

J. H. Whealton, P. S. Meszaros, R. J. Raridon, and K. E. Rothe, "Extraction Induced Emittance Growth for Negative Ion Sources"

Workshop on Plasma Modeling as a Grand Challenge for Computing, Los Angeles, California, January 22–23, 1991

J.-N. Leboeuf, "The Numerical Tokamak: Possible ORNL Contributions"

February

Symposium on Parallel Methods for Large-Scale Structural Analysis and Physics Applications, NASA Langley Research Center, February 5–6, 1991. Proceedings published in *Int. J. Comput. Sys. Eng.* **2** (1991)

V. E. Lynch, B. A. Carreras, J. B. Drake, J.-N. Leboeuf, and J. R. Ruiter, "Plasma Turbulence Calculations on the INTEL IPSC/860 (RX) Hypercube," p. 299

BPX PF Working Group Meeting, Princeton, New Jersey, February 7, 1991

D. J. Strickler, "Equilibrium Modeling"

U.S. Technical Review of the ITER Conceptual Design Activity, February 7, 1991

J. T. Hogan, "ITER Operational Limits"

W. A. Houlberg, "ITER Fueling"

N. A. Uckan, "ITER Confinement Capability"

TMS/AIME Annual Meeting, New Orleans, Louisiana, February 17–21, 1991

E. A. Kenik and J. Bentley, "Application of Electron Energy Loss Spectroscopy to Microanalysis of Irradiated Stainless Steel"

S. J. Zinkle, "Ion Beam Irradiation of Ceramics at Fusion-Relevant Conditions"

WATTec, Knoxville, Tennessee, February 22, 1991

C. T. Wilson, "Process Display Technologies—Virtual Instruments"

Fourth Topical Conference on Robotics and Remote Systems, Albuquerque, New Mexico, February 27–March 1, 1991

D. Macdonald, D. P. Kuban, D. C. Watkin, M. J. Hollis, and R. E. DePew, "Remote Replacement of TF and PF Coils for the Compact Ignition Tokamak"

U.S.–Japan RF Workshop, Mito, Japan, February 27–March 1, 1991

D. J. Hoffman, "Fast Wave Current Drive Antenna Technology for DIII-D and Other Advanced Tokamaks"

Washington Materials Forum, Washington, D.C., February 28–March 1, 1991

L. A. Berry, "Introduction to Electron Cyclotron Resonance Microwave Plasmas and Their Use for Materials Processing"

March

Saturday Academy of Computing and Mathematics, Oak Ridge, Tennessee, March 9, 1991

R. A. Dory, D. B. Batchelor, and S. P. Hirshman, "Physics Analysis, Mathematics, and Computing"

Workshop on ICRF Physics and Design, Boulder, Colorado, March 11–13, 1991

D. B. Batchelor, "Antenna Design Issues for BPX"

M. D. Carter, D. B. Batchelor, and E. F. Jaeger, "The Folded Waveguide as an ICRF Launcher"

Third U.S.–Mexico Cooperative Joint Symposium on Atomic and Molecular Physics, Mexico City, Mexico, March 13–16, 1991

R. A. Phaneuf, F. W. Meyer, D. C. Gregory, C. C. Havener, P. A. Zeijlmans van Emmichoven, S. H. Overbury, D. M. Zehner, G. H. Dunn, J. S. Thompson, E. K. Wahlin, and A. C. H. Smith, "Low-Energy Collisions of Multiply Charged Ions with Electrons, Atoms and Surfaces," invited

Ninth Topical Conference on High-Temperature Plasma Diagnostics, Santa Fe, New Mexico, March 15–19, 1991

D. P. Hutchinson, R. K. Richards, C. A. Bennett, and C. H. Ma, "Proof-of-Principle of a Diagnostic for D-T Fusion-Produced Alpha Particles"

C. H. Ma, L. R. Baylor, D. P. Hutchinson, M. Murakami, and J. B. Wilgen, "Density Profile Measurement Using a Multichannel Difluoromethane Laser Interferometer System on ATF"

Fourth TTF Workshop on Plasma Turbulence and Transport, Austin, Texas, March 18–21, 1991

C. E. Bush, R. Nazikian, N. Bretz, G. Taylor, J. Schivell, S. D. Scott, R. Budny, E. D. Fredrickson, S. Kilpatrick, B. LeBlanc, D. M. Manos, K. M. McGuire, S. S. Medley, H. Park, S. Paul, A. T. Ramsey, S. Sabbagh, and R. M. Wieland, "Characteristics of the Transition and ELMs During H-Modes in TFTR"

N. Dominguez, B. A. Carreras, V. E. Lynch, and P. H. Diamond, "Linear Study of High-n Dissipative Trapped Electron Modes in $\ell = 2$ Torsatrons"

J. H. Harris, "Fluctuations and Transport in Low Collisionality Plasmas in the ATF Torsatron"

J.-N. Leboeuf, B. A. Carreras, L. A. Charlton, P. H. Diamond, A. S. Ware, C. P. Ritz, and A. J. Wootton, "Fluid Models of the Turbulence at the Edge of the TEXT Tokamak"

K. L. Sidikman, B. A. Carreras, N. Dominguez, L. Garcia, and P. H. Diamond, "Relating Turbulent Fluctuations and Radial Electric Fields: A Drift Wave Turbulence Model"

BPX Conceptual Design Review, Princeton, New Jersey, March 25–27, 1991

D. B. Batchelor, M. D. Carter, R. H. Goulding, D. J. Hoffman, J. C. Hosea, E. F. Jaeger, S. M. Kaye, T. K. Mau, C. K. Phillips, P. M. Ryan, J. E. Scharer, D. W. Swain, J. S. Tolliver, J. R. Wilson, J. J. Yugo, J. Jacquinot, M. J. Mayberry, F. W. Perkins, and D. Van Eester, "ICRF Physics"

First Workshop on Alpha Physics in TFTR, Princeton, New Jersey, March 28–29, 1991

D. A. Spong, "TAE Gap Mode in TFTR Using MHD Fluid Models"

April

IEA Workshop on Low Activation Materials for Fusion Reactor Components, Culham, England, April 3–12, 1991

E. E. Bloom, D. S. Gelles, and R. L. Klueh, "Development of Ferritic/Martensitic Steels as Low Activation Fusion Reactor Structural Materials"

F. A. Garner and R. L. Klueh, "U.S. Research Activities on Reduced Activation Austenitic Stainless Steels"

F. W. Wiffen, "Ceramic Matrix Composite Materials for First Wall/Blanket Structures in Fusion Reactors"

F. W. Wiffen, "The United States Program on Low Activation Materials for Fusion Energy Applications"

72nd Annual American Welding Society Convention, Detroit, Michigan, April 14–19, 1991

D. J. Alexander and G. M. Goodwin, "An Assessment of High-Strength Stainless Steel Weldments for Fusion Energy Applications"

International Workshop on Helium Transport and Exhaust, Gatlinburg, Tennessee, April 16–18, 1991

M. M. Menon, L. W. Owen, et al., "Techniques for Injection and Exhaust of He for Transport Studies in DIII-D"

Sherwood International Fusion Theory Conference, Seattle, Washington, April 22–24, 1991

D. B. Batchelor, M. D. Carter, E. F. Jaeger, J. S. Tolliver, and R. C. Goldfinger, "Two-Dimensional Modeling of Loop and Folded Waveguide ICRF Antennas"

L. A. Charlton, J.-N. Leboeuf, B. A. Carreras, P. H. Diamond, A. S. Ware, Ch. P. Ritz, and A. J. Wootton, "Fluid Model Description of Tokamak Edge Turbulence"

N. Dominguez, B. A. Carreras, V. E. Lynch, and P. H. Diamond, "Linear Stability Study of High-n Trapped Electron Modes for the ATF Torsatron"

F. Y. Gang, D. J. Sigmar, and J.-N. Leboeuf, "Study of Alfvén Wave Instabilities Using a Hybrid Particle–Fluid Code"

C. L. Hedrick, "Landau Fluid Equations for Finite Beta Three Species Alfvén Waves"

J. L. Johnson, D. A. Monticello, A. H. Reiman, A. Salas, and S. P. Hirshman, "Comparison of ATF and TJ-II Stellarator Equilibria as Computed by the 3-D VMEC and PIES Codes"

V. E. Lynch, B. A. Carreras, J. B. Drake, and J.-N. Leboeuf, "Comparison of the Performance of a Fluid Code on Different Machines"

K. C. Shaing and R. D. Hazeltine, "Reduction of Tokamak Ion Transport in the Banana Regime by Orbit Squeezing"

K. L. Sidikman, B. A. Carreras, N. Dominguez, L. Garcia, and P. H. Diamond, "Relating Turbulent Fluctuations and Radial Electric Fields: A Drift Wave Turbulence Model"

D. A. Spong, B. A. Carreras, C. L. Hedrick, N. Dominguez, L. A. Charlton, and J.-N. Leboeuf, "Destabilization of the Toroidicity-Induced Shear Alfvén Eigenmode by Alpha Populations Using Fluid Moment Descriptions"

Spring Meeting of the American Physical Society, Washington, D.C., April 22–25, 1991. Abstracts published in *Bull. Am. Phys. Soc.* **36**, No. 4 (1991)

C. C. Havener, "Merged-Beams Measurements of Total Electron Capture by Multicharged Ions Colliding with Hydrogen at Energies below 1 eV/u," invited, p. 1326

F. W. Meyer, S. H. Overbury, C. C. Havener, P. A. Zeijlmans van Emmichoven, and D. M. Zehner, "Evidence for Above-Surface Neutralization During Interactions of Highly Charged Ions with a Metal Surface," p. 1371

P. A. Zeijlmans van Emmichoven, C. C. Havener, F. W. Meyer, and D. M. Zehner, "Computer Simulations of the Neutralization of Multicharged Ions Close to Metal Surfaces," p. 1371

Spring Meeting of the Materials Research Society, Anaheim, California, April 29–May 3, 1991

L. A. Berry, "ECR Plasma Sources for Film Deposition"

May

Innovative Technologies for Processing and Characterization: 11th Annual TVC-AVS Symposium and Equipment Exhibit, Oak Ridge, Tennessee, May 15–16, 1991

P. W. Fisher, "Tritium Pellet Development for Fusion Reactors"

C. A. Foster, "Surface Impact Cleaning by High Speed Cryogenic Pellets"

B. E. Nelson, "Vacuum Pumping System for the Burning Plasma Experiment"

Energy Research Power Supercomputer Users Symposium, Gaithersburg, Maryland, May 21–22, 1991

B. A. Carreras, L. A. Charlton, N. Dominguez, J. B. Drake, L. Garcia, J.-N. Leboeuf, D. K. Lee, V. E. Lynch, K. Sidikman, and D. A. Spong, "Plasma Turbulence Calculations on Supercomputers," invited

8th International Stellarator Workshop, Kharkov, U.S.S.R., May 27–31, 1991. Proceedings published by the International Atomic Energy Agency, Vienna, 1991

S. C. Aceto, D. T. Anderson, F. S. B. Anderson, B. Brañas, L. R. Baylor, G. L. Bell, J. D. Bell, T. S. Bigelow, B. A. Carreras, R. J. Colchin, N. A. Crocker, E. C. Crume, Jr., N. Dominguez, R. A. Dory, J. L. Dunlap, G. R. Dyer, A. C. England, R. H. Fowler, R. F. Gandy, J. C. Glowienka, R. C. Goldfinger, R. H. Goulding, G. R. Hanson, J. H. Harris, C. Hidalgo, D. L. Hillis, S. Hiroe, S. P. Hirshman, L. D. Horton, H. C. Howe, D. P. Hutchinson, R. C. Isler, T. C. Jernigan, H. Kaneko, S. Kubo, M. Kwon, R. A. Langley, J.-N. Leboeuf, D. K. Lee, K. M. Likin, D. H. C. Lo, V. E. Lynch, J. F. Lyon, C. H. Ma, M. A. Meier, M. M. Menon, P. K. Mioduszewski, S. Morimoto, S. Morita, O. Motojima, M. Murakami, M. A. Ochando, S. Okamura, H. Okada, S. F. Paul, A. L. Qualls, D. A. Rasmussen, R. K. Richards, Ch. P. Ritz, J. A. Rome, J. Sanchez, A. V. Sapozhnikov, K. A. Sarksyan, M. Sato, J. G. Schwelberger, K. C. Shaing, M. G. Shats, T. D. Shepard, J. E. Simpkins, C. E. Thomas, J. S. Tolliver, T. Uckan, K. L. Vander Sluis, M. R. Wade, J. B. Wilgen, W. R. Wing, H. Yamada, and J. J. Zielinski, "Overview of Recent Results from the Advanced Toroidal Facility"

C. D. Beidler, N. T. Besedin, B. A. Carreras, N. Dominguez, V. E. Dyakov, D. L. Grekov, J. Kisslinger, G. B. Lesnyakov, V. E. Lynch, H. Maassberg, I. M. Pankratov, O. S. Pavlichenko, V. D. Pustovitov, T. Rau, S. G. Shasharino, A. A. Shishkin, In. N. Sidorenko, M. S. Smirnova, J. S. Tolliver, Y. A. Volkov, H. Wobig, and A. V. Zolatukhin, "Physics Studies for URAGAN-2M," pp. 519–24

R. J. Colchin, M. R. Wade, R. H. Fowler, R. C. Isler, J. F. Lyon, J. A. Rome, and C. E. Thomas, "Ion Confinement in the Advanced Toroidal Facility"

K. A. Connor, S. C. Aceto, J. G. Schwelberger, J. J. Zielinski, J. C. Glowienka, A. Carnevali, and H. Okada, "First Results from the ATF Heavy Ion Beam Probe"

J. H. Harris, M. Murakami, B. A. Carreras, S. C. Aceto, B. Brañas, L. R. Baylor, J. D. Bell, T. S. Bigelow, R. A. Dory, J. L. Dunlap, N. Dominguez, G. R. Dyer, A. C. England, J. C. Glowienka, G. R. Hanson, C. Hidalgo, R. C. Isler, T. C. Jernigan, J. N. Leboeuf, D. K. Lee, K. M. Likin, J. F. Lyon, C. H. Ma, M. A. Meier, M. A. Ochando, S. F. Paul, D. A. Rasmussen, Ch. P. Ritz, J. Sanchez, A. V. Sapozhnikov, K. A. Sarksyan, M. G. Shats, C. E. Thomas, J. B. Wilgen, W. R. Wing, A. J. Wootton, and J. J. Zielinski, "Fluctuations and Transport in Low-Collisionality Plasmas in the ATF Torsatron"

R. C. Isler, S. C. Aceto, R. J. Colchin, J. G. Schwelberger, T. Uckan, and J. J. Zielinski, "Plasma Potential and Electric Field Investigations in ATF"

J. F. Lyon, "Overview of the ATF Program"

J. F. Lyon and S. L. Painter, "Stellarator Reactor Optimization"

W. R. Wing, L. R. Baylor, T. S. Bigelow, R. J. Colchin, T. C. Jernigan, M. Murakami, J. B. Wilgen, S. C. Aceto, J. D. Bell, B. A. Carreras, E. C. Crume, R. A. Dory, J. L. Dunlap, G. R. Dyer, A. C. England, J. C. Glowienka, G. R. Hanson, R. C. Isler, J. H. Harris, D. L. Hillis, S. Hiroe, H. C. Howe, D. P. Hutchinson, R. A. Langley, D. K. Lee, J. F. Lyon, C. H. Ma, M. A. Ochando, S. Morimoto, O. Motojima, S. Paul, D. A. Rasmussen, J. E. Simpkins, C. E. Thomas, T. Uckan, K. L. Vander Sluis, M. R. Wade, and J. J. Zielinski, "Configuration Control and Modulation Experiments Using Long-Pulse ECH Discharges in the ATF Torsatron"

J. Sanchez, B. Brañas, T. Estrada, E. De La Luna, A. Navarro, G. R. Hanson, J. H. Harris, J. D. Bell, J. B. Wilgen, and H. J. Hartfuss, "Application of Microwave Reflectometry to Stability and Turbulence Studies in Stellarators," pp. 503–6

Workshop on Electrical Breakdown of Ceramics in a High Radiation Field, Vail, Colorado, May 28–June 1, 1991

R. E. Stoller, R. H. Goulding, and S. J. Zinkle, "Measurement of Dielectric Properties in Alumina under Ionizing and Displacive Irradiation Conditions"

June

18th IEEE International Conference on Plasma Science, Williamsburg, Virginia, June 3–6, 1991

G. Bateman, R. J. Goldston, W. A. Houlberg, S. C. Jardin, S. M. Kaye, N. Pomphrey, C. E. Singer, D. P. Stotler, R. E. Waltz, D. B. Batchelor, M. G. Bell, D. Hill, R. A. Langley, S. S. Medley, G. H. Neilson, W. A. Peebles, M. Porkolab, D. J. Sigmar, R. D. Stambaugh, and M. Ulrickson, "Confinement Projections for the Burning Plasma Experiment (BPX) Design"

J. J. Zielinski, S. C. Aceto, A. Carnevali, K. A. Connor, W. R. DeVan, G. E. Drohman, D. T. Fehling, J. C. Glowienka, G. H. Henkel, D. K. Lee, J. F. Lewis, H. Okada, S. D. Reedy, J. G. Schwelberger, and K. D. St. Onge, "An Overview of the First Year of Operation of the Heavy Ion Beam Probe on the Advanced Toroidal Facility (ATF)"

18th European Physical Society Conference on Controlled Fusion and Plasma Physics, Berlin, Germany, June 3–7, 1991. Contributed papers published in *Controlled Fusion and Plasma Physics: Proceedings of the 18th European Conference, Berlin, 3–7 June 1991*, Pts. I–IV, ed. P. Bachmann and D. C. Robinson, European Physical Society, Petit-Lancy, Switzerland, 1991 [*Europhys. Conf. Abstr.* **15C** (1991)]; invited papers published in *Plasma Phys. Controlled Fusion* **33**, No. 13 (1991)

S. C. Aceto, J. G. Schwelberger, J. J. Zielinski, K. A. Connor, T. P. Crowley, J. W. Heard, R. L. Hickok, P. E. McLaren, A. Ouroua, P. M. Schoch, V. J. Simic, R. C. Isler, J. H. Harris, M. Murakami, J. C. Glowienka, T. Uckan, and H. Okada, "Heavy Ion Beam Probe Measurements of ECH Heated Plasma in the Advanced Toroidal Facility," *Europhys. Conf. Abstr.* **15C**, Pt. II, 161–64 (1991)

D. B. Batchelor, M. D. Carter, R. H. Goulding, D. J. Hoffman, E. F. Jaeger, P. M. Ryan, D. W. Swain, J. S. Tolliver, J. J. Yugo, R. J. Goldston, J. C. Hosea, S. M. Kaye, C. K. Phillips, J. R. Wilson, J. E. Scharer, and T. K. Mau, "ICRF Heating on the Burning Plasma Experiment (BPX)," *Europhys. Conf. Abstr.* **15C**, Pt. I, 113 (1991)

B. A. Carreras, N. Dominguez, V. E. Lynch, C. D. Beidler, J. Kisslinger, F. Rau, H. Wobig, D. L. Grekov, A. V. Zolotukhin, and O. S. Pavlichenko, "Plasma Stability, Equilibrium, and Transport in URAGAN-2M Torsatron," *Europhys. Conf. Abstr.* **15C**, Pt. II, 149 (1991)

L. Garcia, B. A. Carreras, and V. E. Lynch, "Electric Field Effects on the Resistive Pressure-Gradient-Driven Turbulence," *Europhys. Conf. Abstr.* **15C**, Pt. IV, 13 (1991)

R. J. Goldston, G. Bateman, W. A. Houlberg, S. M. Kaye, G. H. Neilson, F. W. Perkins, N. Pomphrey, M. Porkolab, K. S. Riedel, R. D. Stambaugh, D. P. Stotler, R. E. Waltz, and M. C. Zarnstorff,

"Confinement Projections for the Burning Plasma Experiment (BPX)," *Europhys. Conf. Abstr.* **15C**, Pt. I, 93–96 (1991)

J. H. Harris, M. Murakami, S. Aceto, B. Brañas, L. R. Baylor, J. D. Bell, T. S. Bigelow, B. A. Carreras, R. J. Colchin, E. C. Crume, Jr., N. Dominguez, R. A. Dory, J. L. Dunlap, G. R. Dyer, A. C. England, J. C. Glowienka, G. R. Hanson, C. Hidalgo, D. L. Hillis, S. Hiroe, H. C. Howe, D. P. Hutchinson, R. C. Isler, T. C. Jernigan, R. A. Langley, J. N. Leboeuf, D. K. Lee, K. M. Likin, J. F. Lyon, C. H. Ma, M. A. Meier, S. Morimoto, O. Motojima, M. A. Ochando, S. F. Paul, D. A. Rasmussen, J. E. Simpkins, Ch. P. Ritz, J. Sanchez, A. V. Sapozhnikov, K. A. Sarksyan, M. G. Shats, C. E. Thomas, T. Uckan, K. L.Vander Sluis, M. R. Wade, J. B. Wilgen, W. R. Wing, and J. J. Zielinski, "Fluctuations and Transport in Low-Collisionality Plasmas in the ATF Torsatron," *Europhys. Conf. Abstr.* **15C**, Pt. I, 169 (1991)

C. Hidalgo, M. A. Meier, T. Uckan, Ch. P. Ritz, J. H. Harris, A. J. Wootton, and T. L. Rhodes, "Scaling Properties for the Edge Turbulence in the ATF Torsatron," *Europhys. Conf. Abstr.* **15C**, Pt. III, 61 (1991)

R. C. Isler, R. J. Colchin, M. R. Wade, J. F. Lyon, R. H. Fowler, J. A. Rome, S. Hiroe, L. R. Baylor, M. Ochando, S. Paul, A. England, C. H. Ma, and D. A. Rasmussen, "Ion Confinement and Radiation Losses in the Advanced Toroidal Facility," *Europhys. Conf. Abstr.* **15C**, Pt. II, 157 (1991)

T. S. Petrie, D. N. Hill, D. Buchenauer, A. Futch, C. Klepper, S. Lippman, and M. A. Mahdavi, "Divertor Experiments in DIII-D," *Europhys. Conf. Abstr.* **15C**, Pt. III, 237 (1991)

C. K. Phillips, G. Hammett, J. Hosea, E. Marmar, M. Phillips, J. Snipes, J. Stevens, J. Terry, J. R. Wilson, M. Bell, M. Bitter, C. E. Bush, E. Fredrickson, K. Hill, D. J. Hoffman, H. Hsuan, M. Hughes, A. Janos, D. Jassby, K. McGuire, Y. Nagayama, K. Owens, H. Park, A. Ramsey, J. Schivell, E. Synakowski, B. Stratton, G. Taylor, and the TFTR Group, "Sawtooth Stabilization Studies on TFTR," *Europhys. Conf. Abstr.* **15C**, Pt. II, 9 (1991)

C. S. Pitcher, P. C. Stangeby, R. V. Budny, C. E. Bush, J. D. Elder, K. W. Hill, S. J. Kilpatrick, D. M. Manos, S. S. Medley, A. T. Ramsey, J. F. Schivell, and M. Ulrickson, "The Effect of Density on Boundary Plasma Behavior in TFTR," *Europhys. Conf. Abstr.* **15C**, Pt. III, 145 (1991)

P. M. Ryan, F. W. Baity, D. B. Batchelor, R. H. Goulding, D. J. Hoffman, and J. S. Tolliver, "The Effect of Realistic Antenna Geometry on Plasma Loading Predictions," *Europhys. Conf. Abstr.* **15C**, Pt. III, 307 (1991)

T. Uckan, S. C. Aceto, L. R. Baylor, J. D. Bell, T. Bigelow, A. C. England, J. H. Harris, R. C. Isler, T. C. Jernigan, J. F. Lyon, P. K. Mioduszewski, M. Murakami, D. A. Rasmussen, J. B. Wilgen, W. R. Wing, and J. J. Zielinski, "Biasing Experiments on the ATF Torsatron," *Europhys. Conf. Abstr.* **15C**, Pt. II, 165 (1991)

A. Varias, A. Alvarez, A. L. Fraguas, C. Alejaldre, N. Dominguez, B. A. Carreras, and V. E. Lynch, "Effect of the Aspect Ratio on the Stability Limits of TJ-II-Like Stellarators," *Europhys. Conf. Abstr.* **15C**, Pt. II, 125 (1991)

H-Mode Workshop, Abingdon, England, June 10, 1991

K. C. Shaing, "A Theory of the H-Mode Bifurcation"

U.S./Japan Workshop on Structural Materials, Huntsville, Alabama, June 10, 1991

D. J. Alexander and G. M. Goodwin, "Thick-Section Weldments in 21-6-9 and 316LN Stainless Steel for Fusion Energy Applications"

IAEA Technical Committee Meeting on Alpha Particles in Fusion Research, Goteborg, Sweden, June 10–14, 1991

D. A. Spong, "Destabilization of the Toroidicity-Induced Shear Alfvén Eigenmode by Alpha Populations Using Fluid Moment Descriptions"

International Cryogenic Materials Conference, Huntsville, Alabama, June 11–14, 1991. Proceedings published in *Adv. Cryog. Mater.* **37**, 1992

S. W. Schwenterly, J. N. Luton, J. W. Lue, W. J. Kenney, and M. S. Lubell, "Design and Testing of a Four-Pole Superconducting Motor Stator," p. 473

20th Biennial Conference on Carbon, Santa Barbara, California, June 23–28, 1991

T. D. Burchell, W. P. Eatherly, G. W. Hollenberg, O. D. Slagle, and R. D. Watson, "The Effects of Neutron Irradiation on the Structure of Carbon-Carbon Composites"

Fusion Facilities Planning for the 1990s, Princeton, New Jersey, June 25–26, 1991. Proceedings published in *J. Fusion Energy* **10**, No. 4 (1991)

C. C. Baker, "Magnetic Fusion Energy Development Beyond 2000," pp. 357–58

July

XVII International Conference on the Physics of Electronic and Atomic Collisions, Brisbane, Australia, July 10–14, 1991

J. Burgdorfer, P. Lerner, and F. Meyer, "Formation of 'Hollow' Atoms near Surfaces: The Classical 'Over-the-Barrier' Model"

C. C. Havener, F. W. Meyer, and R. A. Phaneuf, "Electron Capture in Very Low Energy Collisions of Multicharged Ions with H and D in Merged Beams," invited

F. W. Meyer, S. H. Overbury, C. C. Havener, P. A. Zeijlmans van Emmichoven, and D. M. Zehner, "Above- and Below-Surface Auger Electron Emission During Interactions of Highly Charged Ions with Metal Surfaces"

M. S. Pindzola, D. C. Griffin, and N. R. Badnell, "Angular Differential Cross Sections for the Electron-Impact Excitation of Ar^{7+}"

P. A. Zeijlmans van Emmichoven, C. C. Havener, F. W. Meyer, and D. M. Zehner, "Measurements and Simulations of the Neutralization of Multicharged Ions Close to Metal Surfaces"

ITER Work Session on Physics and Design Options, San Diego, California, July 10–18, 1991

W. A. Houlberg and N. A. Uckan, "ITER 1-1/2-D Time-Dependent Performance Analysis Using WHIST"

High-Beta Tokamak Workshop, San Diego, California, July 13–18, 1991

J. H. Harris, "Interchange Instabilities in Stellarators"

August

49th Annual Meeting of the Electron Microscopy Society of America, San Jose, California, August 4–9, 1991. Proceedings published as *Proceedings of the 49th Annual Meeting of the Electron Microscopy Society of America, San Jose, California, August 4–9, 1991*, ed. G. W. Bailey, Electron Microscopy Society of America, San Francisco, 1991

E. A. Kenik, J. Bentley, and N. D. Evans, "Application of Electron Energy Loss Spectroscopy to Microanalysis of Irradiated Stainless Steels," pp. 732–33

E. A. Kenik and K. Hojou, "Radiation-Induced Segregation in Austenitic Stainless Steels"

Ninth Topical Conference on Radio Frequency Power in Plasmas, Charleston, South Carolina, August 19–21, 1991. Proceedings published as *Radio Frequency Power in Plasmas*, ed. D. B. Batchelor, American Institute of Physics, New York, 1992 [*AIP Conf. Proc.* **244** (1992)]

F. W. Baity, T. S. Bigelow, M. D. Carter, W. L. Gardner, R. H. Goulding, G. R. Haste, D. J. Hoffman, and D. O. Sparks, "Results of Folded Waveguide Tests on RFTF," p. 298

T. D. Shepard, G. R. Haste, F. W. Baity, G. Agarici, B. Beaumont, A. Bécoulet, H. Kuus, B. Saoutic, G. Martin, and T. E. Evans, "Fast-Wave ICRF Minority-Regime Heating Experiments on the Tore Supra Tokamak," p. 142

D. W. Swain, "Tuning and Matching of the BPX ICH System," p. 306

8th Topical Conference on Atomic Processes in Plasmas, Portland, Maine, August 25–29, 1991

A. Muller, A. Frank, J. Haselbauer, G. Hofmann, J. Neumann, U. Pracht, E. Salzborn, S. Schennach, W. Spies, M. Stenke, O. Uwira, R. Vogel, M. Wagner, R. Becker, E. Jennewein, M. Kleinod, U. Probstel, R. A. Phaneuf, G. H. Dunn, E. M. Bernstein, N. Angert, and P. H. Mokler, "Recombination of Highly Charged Ions with Free Electrons"

R. A. Phaneuf, "Progress in Collisions of Multiply Charged Ions," invited

U.S.–Japan Workshop on Edge Turbulence and the Physics of the H-Mode, Madison, Wisconsin, August 26–30, 1991

C. E. Bush, N. Bretz, R. Nazikian, B. C. Stratton, E. Synakowski, S. D. Scott, H. Biglari, R. Budny, E. Fredrickson, K. M. McGuire, D. Manos, Y. Nagayama, H. Park, S. Paul, A. T. Ramsey, S. Sabbagh, J. Schivell, G. Taylor, R. M. Wieland, and M. C. Zarnstorff, "The Transitions, ELMs, and Fluctuations During Limiter H-Modes on TFTR"

Second Joint Seminar (U.S.–Japan) on Basic Mechanisms of Helium Heat Transfer and Related Influence of Superconducting Magnets, August 26–30, 1991. Proceedings published in *Cryogenics* **32**, No. 5 (1992)

L. Dresner, "Gorter-Mellink Pulsed-Source Problem in Cylindrical and Spherical Coordinates," pp. 450–54

International School of Plasma Physics "Piero Caldirola," Varenna, Italy, August 27–September 6, 1991. Proceedings to be published in *Nuovo Cimento*

R. C. Isler, "Charge-Exchange Spectroscopy for Plasma Diagnostics"

September

Workshop on Fusion Pilot Plants, Oak Ridge, Tennessee, September 2–13, 1991

E. E. Bloom, "Materials Issues for a Fusion Pilot Plant"

IAEA Specialists' Meeting on Status of Graphite Development for Gas-Cooled Reactors, Tokai, Japan, September 9–12, 1991

T. D. Burchell, "Graphite Development for Gas-Cooled Reactors in the USA"

IAEA Technical Committee Meeting on Fast Wave Current Drive in Reactor Scale Tokamaks, Arles, France, September 23–35, 1991. Proceedings published by Association EURATOM-CEA sur la Fusion, 1991

D. J. Hoffman, R. H. Goulding, P. M. Ryan, D. B. Batchelor, E. F. Jaeger, F. W. Baity, M. J. Mayberry, R. I. Pinsker, and C. C. Petty, "Design and Matching Problems Associated with Fast-Wave Current Drive Antennas," invited, p. 456

E. F. Jaeger and D. B. Batchelor, "Full-Wave Calculation of Fast-Wave Current Drive in Tokamaks Including $k_{||}$ Variations," p. 86

R. Prater, M. J. Mayberry, C. C. Petty, R. I. Pinsker, M. Porkolab, S. C. Chiu, R. W. Harvey, T. C. Luce, P. Bonoli, F. W. Baity, R. H. Goulding, D. J. Hoffman, R. A. James, H. Kawashima, A. Bécoulet, D. Moreau, and V. Trukhin, "Initial Fast Wave Heating and Current Drive Experiments on DIII-D Tokamak," invited, p. 308

14th IEEE/NPSS Symposium on Fusion Engineering, San Diego, California, September 30–October 3, 1991. Proceedings published by IEEE, New York, 1991

C. B. Baxi et al., "Verification of the Advanced Divertor Pump Cryogenic System for DIII-D"

T. W. Burgess and F. C. Davis, "BPX Committed to Total Remote Maintenance"

T. W. Burgess and F. C. Davis, "Remote Maintenance Development Plans for the Burning Plasma Experiment"

D. C. Lousteau, F. C. Davis, and B. E. Nelson, "ITER Remote Maintenance"

R. Maingi, M. A. Rensink, J. G. Gilligan, O. E. Hankins, C. C. Klepper, P. K. Mioduszewski, D. A. Hill, R. D. Stambaugh, and D. B. Buchenauer, "Coupled Two-Dimensional Edge Plasmas and Neutral Gas Modelling of the DIII-D Scrape-Off Layer"

T. J. McManamy, G. Kanemoto, and P. Snook, "BPX Insulation Irradiation Program Results"

K. Schaubel et al., "Design of the Advanced Divertor Pump Cryogenic System for DIII-D"

J. P. Smith et al., "The Design and Fabrication of a Toroidally Continuous Cryocondensation Pump for DIII-D Advanced Divertor"

C. C. Tsai, C. A. Foster, S. L. Milora, and D. E. Schechter, "Characteristics of an Electron-Beam Rocket Pellet Accelerator"

Fourth ANS Topical Meeting on Tritium Technology in Fission, Fusion, and Isotopic Applications, Albuquerque, New Mexico, September 30–October 4, 1991. Proceedings published in *Fusion Technol.* **21**, No. 2, Pt. 2 (1992)

P. W. Fisher, "Properties of Tritium Inferred from Pellet Injector Experiments," pp. 794–99

October

L-H Transition Working Group Meeting, San Diego, California, October 10–11, 1991

C. E. Bush, "Supershot to H-Mode Transitions on TFTR"

44th Annual Gaseous Electronics Conference, Albuquerque, New Mexico, October 22–25, 1991

F. W. Meyer, S. H. Overbury, C. C. Havener, P. A. Zeijlmans van Emmichoven, and D. M. Zehner, "Evidence for Above- and Sub-Surface Neutralization During Interactions of Highly Charged Ions with a Metal Plate"

November

33rd Annual Meeting of the Division of Plasma Physics, American Physical Society, Tampa, Florida, November 5–8, 1991. Abstracts published in *Bull. Am. Phys. Soc.* **36** (1991)

S. C. Aceto, K. A. Connor, J. G. Schwelberger, J. J. Zielinski, A. C. England, J. C. Glowienka, and D. A. Rasmussen, "Measurements of the Plasma Potential Profile in the ATF Torsatron Using a Heavy Ion Beam Probe," p. 2292

C. Alejaldre, L. Garcia, J. A. Jimenez, A. Lopez-Fraguas, A. Salas, A. Varias, B. Carreras, N. Dominguez, and V. E. Lynch, "Ballooning Calculations in a Helical Axis Stellarator," p. 2294

S. E. Attenberger, C. A. Foster, W. A. Houlberg, C. C. Klepper, S. L. Milora, P. K. Mioduszewski, L. W. Owen, T. Uckan, H. Capes, M. Chatelier, A. Geraud, and T. Loarer, "Edge Particle Transport Modeling in Tore Supra," p. 2368

L. R. Baylor, G. L. Schmidt, W. A. Houlberg, S. L. Milora, P. Kupschus, and C. Gowers, "Pellet Deposition and Penetration in JET and TFTR," p. 2366

J. D. Bell, J. H. Harris, J. L. Dunlap, G. R. Hanson, D. A. Rasmussen, A. C. England, L. R. Baylor, and M. Murakami, "Pressure Effects on Magnetic Fluctuations in ATF," p. 2291

L. I. Krupnik, A. V. Mel'nikov, I. S. Nedzelskij, M. V. Samochvalov, J. G. Schwelberger, S. C. Aceto, K. A. Connor, J. J. Zielinski, D. K. Lee, and V. E. Lynch, "A Comparison of the Proposed Uragan-2M HIBP System with the ATF HIBP," p. 2292

L. L. Lao, J. R. Ferron, T. S. Taylor, E. J. Strait, V. S. Chan, M. S. Chu, E. A. Lazarus, K. Matsuda, H. St. John, and A. D. Turnbull, "Dependence of Plasma Stability and Confinement on the Current Density Profile," p. 2477

E. A. Lazarus, L. L. Lao, T. H. Osborne, M. S. Chu, A. D. Turnbull, E. J. Strait, and T. S. Taylor, "Second Stable Core Plasma in DIII-D," p. 2324

J.-N. Leboeuf, C. L. Hedrick, D. A. Spong, M. J. Lebrun, and T. Tajima, "Particle/Fluid Hybrid, Landau Fluid, and Fluid Models for Alpha Particle Instabilities," p. 2392

D. K. Lee, D. A. Rasmussen, L. R. Baylor, A. C. England, J. M. Gossett, S. Hiroe, S. P. Hirshman, H. C. Howe, G. T. King, K. C. Klos, M. Murakami, and C. E. Thomas, "Magnetic Configuration Studies Using Two-Dimensional Profile Measurements in ATF," p. 2291

R. L. Lee, K. Holtrop, A. Kellman, M. Menon, P. Petersen, J. T. Scoville, E. J. Strait, and P. Taylor, "An Operations and Disruption Database for DIII-D," p. 2478

V. E. Lynch, B. A. Carreras, J. B. Drake, J.-N. Leboeuf, and D. W. Walker, "The Performance of a Fluid Code on the Connection Machine 2," p. 2433

J. F. Lyon, "Stellarator Reactor Optimization Studies," p. 2273

C. H. Ma, L. R. Baylor, M. J. Crouse, D. P. Hutchinson, M. Murakami, and J. B. Wilgen, "FIR Density Profile Measurement on ATF," p. 2291

R. Maingi, M. Rensink, J. Gilligan, O. Hankins, and P. Mioduszewski, "Use of Non-Orthogonal Grids in Edge Plasma Transport Calculations," p. 2489

D. R. Mikkelsen, C. E. Bush, B. Grek, K. W. Hill, D. W. Johnson, D. K. Mansfield, H. K. Park, A. T. Ramsey, G. Schilling, J. Schivell, S. D. Scott, B. C. Stratton, E. J. Synakowski, G. Taylor, H. H. Towner, and M. C. Zarnstorff, "Tests of the Rebut-Lallia Transport Model in TFTR," p. 2448

M. Murakami, T. S. Bigelow, L. R. Baylor, G. R. Dyer, A. C. England, T. C. Jernigan, D. K. Lee, C. H. Ma, D. A. Rasmussen, J. A. White, J. B. Wilgen, and W. R. Wing, "Dynamic Configuration Control Experiments in ATF," p. 2429

R. M. Nazikian, N. Bretz, R. J. Fonck, E. D. Fredrickson, K. McGuire, S. Paul, C. E. Bush, A. Cavallo, Y. Nagayama, H. K. Park, A. T. Ramsey, G. Taylor, M. C. Zarnstorff, M. Diesso, and J. Felt, "Modulational Processes in Broadband Turbulence on TFTR," p. 2444

G. H. Neilson, D. J. Strickler, T. G. Brown, R. J. Goldston, J. R. Haines, C. E. Kessel, and N. Pomphrey, "Optimization of the BPX Divertor Geometry," p. 2369

L. W. Owen, C. C. Klepper, J. T. Hogan, and P. K. Mioduszewski, "Transport Modeling of Baffle Pressure in the Collaborative DIII-D Advanced Divertor Experiment," p. 2471

L. J. Perkins and J. D. Galambos, "The Reasons Why the International Thermonuclear Experimental Reactor (ITER) Should Be a High Aspect Ratio Tokamak," p. 2275

T. W. Petrie, D. N. Hill, D. Buchenauer, A. Futch, K. Holtrop, C. Klepper, A. Leonard, S. Lippmann, M. A. Mahdavi, and W. P. West, "Radiative Experiments in ELMing H-Mode Plasmas in DIII-D," p. 2471

C. C. Petty, R. I. Pinsker, M. J. Mayberry, S. C. Chiu, T. C. Luce, T. Osborne, R. Prater, R. James, M. Porkolab, F. W. Baity, R. H. Goulding, and D. J. Hoffman, "Direct Electron Absorption of 60 MHz Fast Waves on DIII-D," p. 2470

R. I. Pinsker, C. C. Petty, M. J. Mayberry, S. C. Chiu, R. Harvey, T. C. Luce, T. Osborne, M. Porkolab, R. Prater, T. Taylor, R. A. James, F. W. Baity, R. H. Goulding, D. J. Hoffman, and the DIII-D Group, "Initial Results from the DIII-D Fast Wave Current Drive Experiment," p. 2470

D. Post, S. Cohen, J. Hogan, W. Nevins, P. Rutherford, D. Sigmar, N. Uckan, and J. Wesley, "Critical Physics Issues for ITER," p. 2273

A. L. Qualls, P. N. Stevens, J. B. Wilgen, N. Dominguez, C. H. Ma, A. C. England, D. A. Rasmussen, L. R. Baylor, and J. D. Bell, "Fluctuation Studies in Pellet Fueled ATF Plasmas," p. 2430

D. A. Rasmussen, L. R. Baylor, J. D. Bell, A. C. England, J. M. Gossett, S. Hiroe, H. C. Howe, D. P. Hutchinson, G. T. King, K. C. Klos, D. K. Lee, C. H. Ma, M. Murakami, and C. E. Thomas, "Thomson Scattering Electron Density and Temperature Profile Measurements in ATF," p. 2291

M. E. Rensink, J. L. Milovich, T. D. Rognlien, A. H. Futch, R. A. Jong, G. D. Porter, D. N. Hill, T. W. Petrie, D. Buchenauer, C. Klepper, A. W. Leonard, R. Moyer, J. Watkins, and M. A. Mahdavi, "Modeling of DIII-D Divertor Plasmas at ITER-Like Power Levels," p. 2472

R. K. Richards, D. P. Hutchinson, and C. A. Bennett, "Recent Results from an Alpha Particle Diagnostic Proof-of-Principle," p. 2492

C. Ronchi, A. Bhattacharjee, and J. Leboeuf, "Numerical Simulation of Collisionless Tearing Instabilities," p. 2360

M. J. Schaffer, D. N. Hill, N. Brooks, A. Hyatt, C. Klepper, L. L. Lao, S. Lippmann, M. A. Mahdavi, T. Osborne, T. Petrie, G. Porter, J. Smith, R. Stambaugh, and G. Staebler, "Biased Divertor Experiment in DIII-D," p. 2325

J. G. Schwelberger, S. C. Aceto, K. A. Connor, J. J. Zielinski, A. C. England, J. C. Glowienka, C. H. Ma, D. A. Rasmussen, and J. B. Wilgen, "Electron Density Profile Measurement of ECH Heated ATF Plasmas Using a Heavy Ion Beam Probe," p. 2292

K. C. Shaing, P. J. Christenson, and W. A. Houlberg, "Ion Orbit Loss and Radial Electric Field Profile in the L-H Transition in Tokamaks," p. 2395

M. G. Shats, K. M. Likin, K. A. Sarksyan, J. H. Harris, J. B. Wilgen, L. R. Baylor, and J. D. Bell, "Microwave Scattering Diagnostic for ATF," p. 2291

K. L. Sidikman, B. A. Carreras, N. Dominguez, L. Garcia, and P. H. Diamond, "Numerical Study of Radial Electric Field Effects on Multiple-Helicity Drift Wave Turbulence," p. 2345

D. A. Spong, B. A. Carreras, C. L. Hedrick, P. J. Christenson, L. Charlton, N. Dominguez, and J.-N. Leboeuf, "Fluid/Kinetic Models for Shear Alfvén TAE Modes in TFTR," p. 2394

P. N. Stevens, A. L. Qualls, J. B. Wilgen, L. R. Baylor, C. H. Ma, and R. A. Langley, "Particle Deposition Due to Pellet Fueling on ATF," p. 2292

D. P. Stotler, D. J. Sigmar, G. Bateman, R. J. Goldston, and G. H. Neilson, "Survey of Operating Modes for BPX and ITER," p. 2369

N. A. Uckan and U.S. ITER Home Team, "ITER Physics R&D Assessment for Confinement and Plasma Performance Projections," p. 2274

T. Uckan, L. R. Baylor, J. D. Bell, T. Bigelow, A. C. England, J. H. Harris, R. C. Isler, T. C. Jernigan, J. F. Lyon, P. K. Mioduszewski, M. Murakami, D. A. Rasmussen, J. B. Wilgen, W. R. Wing, S. C. Aceto, and J. J. Zielinski, "Biased Limiter Experiments on ATF," p. 2292

M. Ulrickson, H. F. Dylla, R. Goldston, J. N. Brooks, J. Haines, D. N. Hill, K. L. Wilson, R. A. Langley, and G. H. Neilson, "Impurity Control and Materials Physics in BPX," p. 2370

A. Varias, J. A. Jimenez, N. Dominguez, and B. A. Carreras, "Stability Criterion for Localized Perturbations for Torsatrons and Heliacs," p. 2310

M. R. Wade, R. J. Colchin, R. H. Fowler, L. D. Horton, R. C. Isler, J. A. Rome, and C. E. Thomas, "Effect of Fast-Ion Confinement on the Global Power Balance During Neutral Beam Injection in ATF," p. 2430

W. P. West, N. H. Brooks, S. Lippmann, C. C. Klepper, G. L. Jackson, J. M. McChesney, and J. Winter, "Impurities in DIII-D After Boronization and During VH-Mode," p. 2476

J. H. Whealton, R. J. Raridon, M. W. Childs, H. T. Elliott, and D. A. Harris, "Ion Thruster Modeling," p. 2424

R. M. Wieland, M. G. Bell, D. C. McCune, H. Takahashi, M. C. Zarnstorff, and S. P. Hirshman, "Multi-Code MHD Equilibrium Analysis of TFTR Plasmas," p. 2450

J. B. Wilgen, L. R. Baylor, T. S. Bigelow, A. C. England, R. C. Goldfinger, H. C. Howe, S. Kubo, M. Murakami, D. A. Rasmussen, and W. R. Wing, "Modulation Studies of Transport and Power Deposition in ATF," p. 2429

J. R. Wilson, J. Hosea, F. Jobes, C. K. Phillips, G. Schilling, J. Stevens, R. Goulding, and D. Hoffman, "Loading and Heating Characterization of the Modified TFTR Antenna," p. 2449

J. J. Zielinski, S. C. Aceto, A. Carnevali, K. A. Connor, J. C. Glowienka, C. Hidalgo, R. C. Isler, J. F. Lewis, M. Murakami, H. Okada, J. G. Schwelberger, and T. Uckan, "Electric Field Studies on the ATF Torsatron," p. 2430

American Vacuum Society 38th Annual Symposium and Topical Conference, Seattle, Washington, November 11–15, 1991. Proceedings to be published in *J. Vac. Sci. Technol.* **10** (1992)

C. A. Foster, P. W. Fisher, and D. W. Simmons, "Surface Impact Cleaning by High-Speed Pellets"

R. A. Langley, "A Simple Aluminum Gasket for Use with Both Stainless Steel and Aluminum Flanges"

M. Menon, J. F. Smith, K. M. Schaubel, L. W. Owen, M. A. Mahdavi, C. B. Baxi, J. Luxon, and M. J. Schaffer, "A Cryocondensation Pump for Particle Exhaust in the DIII-D Tokamak"

J. E. Simpkins, P. K. Mioduszewski, and T. F. Rayburn, "Impurity and Recycling Control with Gettering in ATF"

M. Ulrickson, R. Goldston, G. H. Neilson, B. Nelson, W. Fragetta, R. Rocco, J. Warren, J. Haines, and H. Mantz, "The Design of the BPX Vacuum Vessel"

Fifth International Conference on Fusion Reactor Materials, Clearwater, Florida, November 17–22, 1991

D. J. Alexander, G. M. Goodwin, and E. E. Bloom, "Thick-Section Weldments in 21-6-9 and 316LN Stainless Steel for Fusion Energy Applications"

G. E. C. Bell, "Lithium Purification at Temperatures Below 500°"

G. E. C. Bell, E. A. Kenik, and L. Heatherly, "Characterization of Radiation-Induced Segregation in Austenitic Stainless Steels Using Analytical Electron Microscopy and Scanning Auger Microprobe Techniques"

G. E. C. Bell, E. A. Kenik, and T. Inazumi, "Electrochemical and Microstructural Properties of Austenitic Stainless Steels Irradiation by Heavy Ions Above 600°"

G. E. Bell and T. Inazumi, "Radiation Induced Sensitization to Corrosion in Fusion Reactor Materials"

F. W. Clinard, E. H. Farnum, D. L. Griscom, F. R. Mattas, S. S. Medley, F. W. Wiffen, S. S. Wojtowicz, K. M. Young, and S. J. Zinkle, "Materials Issues in Diagnostic Systems for BPX and ITER"

M. L. Grossbeck, P. J. Maziasz, and A. F. Rowcliffe, "Modeling of Strengthening Mechanisms in Irradiated Fusion Reactor First Wall Materials"

T. Inazumi, G. E. Bell, P. J. Maziasz, and T. Kondo, "Radiation-Induced Sensitization of Ti-Modified Austenitic Stainless Steel Irradiated in Spectrally Tailored Experiments at 60 to 400°C"

S. Jitsukawa, M. L. Grossbeck, and A. Hishinuma, "Stress-Strain Relations of Irradiated Stainless Steels Below 473 K"

S. Jitsukawa, K. Hojou, M. Suzuki, A. Hishinuma, and E. A. Kenik, "Segregation at Radiation-Induced Defects and at Grain Boundaries in Austenitic Stainless Steels"

S. Jitsukawa, P. J. Maziasz, T. Ishiyama, and L. T. Gibson, "Tensile Properties of Austenitic Stainless Steel Base-Metal and Weld-Joint Specimens Irradiated in ORR Spectrally Tailored Experiments"

R. L. Klueh, "Effect of Irradiation in HFIR on Tensile Properties of Cr–Mo Steels"

R. L. Klueh and D. J. Alexander, "Heat Treatment Effects on Toughness of Irradiated 9Cr–1MoVNb and 12Cr–1MoVW Steels"

R. L. Klueh and K. Ehrlich, "Ferritic/Martensitic Steels for Fusion Reactor Applications"

A. Kohyama, M. L. Grossbeck, and G. Piatti, "The Application of Austenitic Stainless Steels in Advanced Fusion Systems: Current Limitations and Future Prospects"

T. Kondo, D. G. Doran, K. Ehrlich, and F. W. Wiffen, "The Status and Prospects of High-Energy Neutron Test Facilities for Fusion Materials Development"

P. J. Maziasz, "Temperature Dependence of the Dislocation Microstructure of PCA Austenitic Stainless Steel Irradiated in ORR Spectrally Tailored Experiments"

P. J. Maziasz, "Void Swelling Resistance of Phosphorus-Modified Austenitic Stainless Steels During HFIR Irradiation to 57 dpa at 300 to 500°C"

T. Sawai, P. J. Maziasz, H. Kanazawa, and A. Hishinuma, "Microstructural Evolution of Austenitic Stainless Steels Irradiated in Spectrally Tailored Experiments in ORR at 400°C"

L. L. Snead, D. Steiner, and S. J. Zinkle, "Measurement of the Effect of Radiation Damage on Ceramic Composite Interfacial Strength"

L. L. Snead and S. J. Zinkle, "Radiation-Induced Microstructure and Mechanical Property Evolution of SiC/C/SiC Composites"

M. Suzuki, A. Hishinuma, N. Yamanouchi, T. Tamura, and A. F. Rowcliffe, "Alloy Preparation for Studying the Effects of Hydrogen Production During Neutron Irradiation Using an ^{54}Fe Isotope"

M. Suzuki, P. J. Maziasz, S. Jitsukawa, S. Hamada, and A. Hishinuma, "Chemical Compositional Change in Precipitates During HFIR Irradiation in Austenitic and Ferritic Steels"

P. F. Tortorelli, "Dissolution Kinetics of Steels Exposed in Lead-Lithium and Lithium Environments"

P. F. Tortorelli, G. E. C. Bell, and E. A. Kenik, "Effects of Compositional Modifications on the Sensitization Behavior of Fe-Cr-Mn Austenitic Stabilized Steels"

R. Yamada, S. J. Zinkle, and G. P. Pells, "Radiation Damage in Al_2O_3 and $MgAl_2O_4$ Preimplanted with H, He, C, and Irradiated with Ar^+ Ions"

C. A. Wang, H. T. Lin, M. L. Grossbeck, and B. A. Chin, "Suppression of HAZ Cracking During Welding of Helium-Containing Materials"

S. J. Zinkle, "Anisotropic Dislocation Loop Nucleation in Ion-Irradiated $MgAl_2O_4$"

S. J. Zinkle, "Anomalous Microstructural Effects Associated with Light Ion Irradiation of Ceramics"

S. J. Zinkle and E. R. Hodgson, "Radiation-Induced Changes in the Physical Properties of Ceramic Materials"

U.S./Japan Workshop on High-Heat-Flux Components, Santa Fe, New Mexico, November 25–28, 1991

T. D. Burchell, "Irradiation-Induced Dimensional and Property Changes in 2D and 3D Carbon-Carbon Composite Materials"

1991 CONGRESSIONAL TESTIMONY

J. Sheffield, Statement to the House Science and Technology Committee, Washington, D.C., March 13, 1991

1991 SEMINARS

G. E. C. Bell, "Current Research Activities on IASCC at Oak Ridge National Laboratory," NKK Corporation Steel Research Center, Kawasaki, Japan, June 17, 1991

G. E. C. Bell, T. Tsukuda, and H. Nakajima, "ORNL/JAERI Collaboration for Fusion Reactor Materials: Slow Strain Rate Tensile Testing of Spectrally Tailored Type 316 Stainless Steel in High-Purity Water," Japan Atomic Energy Research Institute, Ibaraki-ken, Tokai, Japan, July 10, 1991

R. C. Isler, "Spectroscopy of Fusion Plasmas," University of Lund, Lund, Sweden, September 12, 1991

P. J. Maziasz, "Analytical Electron Microscopy: Microstructural Design of New Steels and Iron-Based Alloys for Advanced Energy Systems," Argonne National Laboratory, Argonne, Illinois, July 29, 1991

M. Murakami, "Overview of ATF Experimental Results," Columbia University, New York, January 18, 1991

S. J. Zinkle, "Radiation Effects in Ceramics for Fusion Diagnostic Systems," Princeton Plasma Physics Laboratory, Princeton, New Jersey, March 19, 1991

S. J. Zinkle, "Microstructural Changes in Irradiated Copper," Risø National Laboratory, Roskilde, Denmark, June 4, 1991

S. J. Zinkle, "Effect of Irradiation on the Microstructure and Electrical Properties of Ceramics," Risø National Laboratory, Roskilde, Denmark, June 28, 1991

1991 REPORTS

ORNL Reports

J. Sheffield, C. C. Baker, M. J. Saltmarsh, and Fusion Energy Division Staff, *Fusion Energy Division Annual Progress Report for the Period Ending December 31, 1989*, ORNL-6624, July 1991

ORNL Technical Memoranda

D. J. Alexander, G. M. Goodwin, and E. E. Bloom, *Evaluation of Weldments in Type 21-6-9 Stainless Steel for Compact Ignition Tokamak Structural Applications, Phase I*, ORNL/TM-11739, June 1991

L. R. Baylor, C. H. Ma, and S. Hiroe, *Inversion of Chordal Data from the ATF Torsatron*, ORNL/TM-11758, February 1991

N. Dominguez, B. A. Carreras, V. E. Lynch, J. S. Tolliver, V. E. Bykov, D. L. Grekov, and A. A. Shishkin, *Mercier Stability and Transport Properties of the URAGAN-2M and ATF Torsatrons*, ORNL/TM-11701, February 1991

L. Dresner, *Excess Heat Production in Composite Superconductors During Current Redistribution*, ORNL/TM-11827, May 1991

P. W. Fisher, *Tritium Proof-of-Principle Pellet Injector*, ORNL/TM-11781, July 1991

S. Morita, R. K. Richards, L. D. Horton, R. C. Isler, E. C. Crume, Jr., and M. Murakami, Z_{eff} *Measurements in ATF Using Visible Bremsstrahlung*, ORNL/TM-11737, April 1991

S. L. Painter and J. F. Lyon, *Transport Analysis of Stellarator Reactors*, ORNL/TM-11756, February 1991

T. Uckan, C. Hidalgo, J. D. Bell, J. H. Harris, J. L. Dunlap, G. R. Dyer, P. K. Mioduszewski, J. B. Wilgen, C. P. Ritz, A. J. Wootton, T. L. Rhodes, and K. Carter, *ATF Edge Plasma Turbulence Studies Using a Fast Reciprocating Langmuir Probe*, ORNL/TM-11545, January 1991

T. Uckan, C. Hidalgo, J. D. Bell, J. H. Harris, J. L. Dunlap, J. B. Wilgen, C. P. Ritz, T. L. Rhodes, and A. J. Wootton, *Characteristics of Edge Plasma Turbulence on the ATF Torsatron*, ORNL/TM-11623, March 1991

T. Uckan, P. K. Mioduszewski, T. S. Bigelow, J. C. Glowienka, S. Hiroe, M. Murakami, J. B. Wilgen, and W. R. Wing, *Power and Particle Balance Studies Using an Instrumented Limiter System on ATF*, ORNL/TM-11520, June 1991

ORNL Fusion Engineering Design Center Reports

J. D. Galambos, Y.-K. M. Peng, and L. J. Perkins, *Methodology for the ITER Technology Phase Operational Scenario Analysis*, ORNL/FEDC-90/1, January 1991

Reports Published by Other Institutions

F. Y. Gang, D. J. Sigmar, and J. N. Leboeuf, *Saturation of Energetic Particle Driven Alfvén Wave Instability through Velocity Space Diffusion*, MIT/PFC/JA-91-24, Massachusetts Institute of Technology, 1991

R. Budny, M. G. Bell, H. Biglari, M. Bitter, C. E. Bush, C. Z. Cheng, E. D. Fredrickson, B. Grek, K. W. Hill, H. Hsuan, A. Janos, D. L. Jassby, D. W. Johnson, L. C. Johnson, B. LeBlanc, D. C. McCune, D. R. Mikkelsen, H. Park, A. T. Ramsey, S. A. Sabbagh, S. D. Scott, J. Schivell, J. D. Strachan, B. C. Stratton, E. Synakowski, G. Taylor, M. C. Zarnstorff, and S. J. Zweben, *Simulations of DT Experiments in TFTR*, PPPL-2808, Princeton Plasma Physics Laboratory, Princeton, New Jersey, December 1991

C. E. Bush, N. Bretz, E. D. Fredrickson, K. M. McGuire, R. Nazikian, H. K. Park, J. Schivell, G. Taylor, C. W. Barnes, M. Bitter, R. Budny, S. A. Cohen, R. J. Fonck, S. J. Kilpatrick, D. M. Manos, D. Meade, S. F. Paul, S. D. Scott, B. C. Stratton, E. J. Synakowski, H. H. Towner, R. M. Wieland, V. Arunasalam, G. Bateman, M. G. Bell, R. Bell, R. Boivin, A. Cavallo, C. Z. Cheng, T. Z. Chu, S. Cowley, S. L. Davis, V. Decaux, D. L. Dimock, J. Dooling, H. F. Dylla, P. C. Efthimion, A. B. Ehrhardt, H. P. Furth, R. J. Goldston, G. Greene,

B. Grek, L. R. Grisham, G. Hammett, R. J. Hawryluk, K. W. Hill, J. Hosea, R. B. Howell, R. A. Hulse, H. Hsuan, A. Janos, D. L. Jassby, F. C. Jobes, D. W. Johnson, L. C. Johnson, R. Kaita, J. H. Kamperschroer, S. Kaye, J. Kesner, C. Kieras-Phillips, H. Kugel, Y. Kusama, P. H. LaMarche, D. K. Mansfield, E. Mazzucato, M. P. McCarthy, M. Mauel, D. C. McCune, S. S. Medley, D. R. Mikkelsen, D. Monticello, R. W. Motley, D. Mueller, J. Murphy, Y. Nagayama, G. A. Navratil, D. K. Owens, W. Park, R. Perkins, S. Pitcher, A. T. Ramsey, M. H. Redi, G. Rewoldt, D. Roberts, A. L. Roquemore, P. H. Rutherford, S. Sabbagh, G. Schilling, G. L. Schmidt, J. Snipes, J. Stevens, W. Stodiek, W. Tang, R. J. Taylor, J. Terry, J. R. Timberlake, M. Ulrickson, S. von Goeler, M. Williams, J. R. Wilson, K. L. Wong, M. Yamada, S. Yoshikawa, K. M. Young, M. C. Zarnstorff, and S. J. Zweben, *Limiter H-Mode Experiments on TFTR*, PPPL-2743, Princeton Plasma Physics Laboratory, Princeton, New Jersey, May 1991

D. L. Jassby, C. W. Barnes, M. G. Bell, M. Bitter, R. Boivin, N. Bretz, R. V. Budny, C. E. Bush, H. F. Dylla, P. C. Efthimion, E. D. Fredrickson, R. J. Hawryluk, K. W. Hill, J. Hosea, H. Hsuan, A. Janos, F. C. Jobes, D. W. Johnson, L. C. Johnson, J. H. Kamperschroer, C. Kieras-Phillips, S. J. Kilpatrick, P. H. LaMarche, B. LeBlanc, D. K. Mansfield, E. S. Marmar, D. C. McCune, K. M. McGuire, D. M. Meade, S. S. Medley, D. R. Mikkelsen, D. Mueller, D. K. Owens, H. K. Park, S. F. Paul, S. Pitcher, A. T. Ramsey, M. H. Redi, S. A. Sabbagh, S. D. Scott, J. Snipes, J. Stevens, J. D. Strachan, B. C. Stratton, E. J. Synakowski, G. Taylor, J. L. Terry, J. R. Timberlake, H. H. Towner, M. Ulrickson, S. von Goeler, M. Williams, J. R. Wilson, K. L. Wong, K. M. Young, M. C. Zarnstorff, and S. J. Zweben, *High-Q Plasmas in the TFTR Tokamak*, PPPL-2756, Princeton Plasma Physics Laboratory, Princeton, New Jersey, May 1991

D. W. Meade, V. Arunasalam, C. W. Barnes, M. G. Bell, R. Bell, M. Bitter, R. Boivin, N. Bretz, R. V. Budny, C. E. Bush, A. Cavallo, C. Z. Cheng, T. Z. Chu, S. A. Cohen, S. Cowley, S. L. Davis, D. L. Dimock, J. Dooling, H. F. Dylla, P. C. Efthimion, A. B. Ehrhardt, R. J. Fonck, E. D. Fredrickson, H. P. Furth, R. J. Goldston, G. Greene, B. Grek, L. R. Grisham, G. Hammett, R. J. Hawryluk, K. W. Hill, J. Hosea, R. B. Howell, R. A. Hulse, H. Hsuan, A. Janos, D. L. Jassby, F. C. Jobes, D. W. Johnson, L. C. Johnson, R. Kaita, S. Kaye, J. Kesner, B. LeBlanc, D. M. Manos, D. K. Mansfield, E. S. Marmar, E. Mazzucato, M. P. McCarthy, M. Mauel, D. C. McCune, K. M. McGuire, S. S. Medley, D. R. Mikkelsen, D. Monticello, R. W. Motley, D. Mueller, J. Murphy, Y. Nagayama, G. A. Navratil, R. Nazikian, D. K. Owens, H. Park, W. Park, S. F. Paul, R. Perkins, S. Pitcher, A. T. Ramsey, M. H. Redi, G. Rewoldt, D. Roberts, A. L. Roquemore, P. H. Rutherford, S. Sabbagh, G. Schilling, J. Schivell, G. L. Schmidt, S. D. Scott, J. Snipes, J. Stevens, W. Stodiek, B. C. Stratton, E. J. Synakowski, W. Tang, R. J. Taylor, J. R. Terry, J. R. Timberlake, H. H. Towner, M. Ulrickson, S. von Goeler, R. M. Wieland, M. Williams, J. R. Wilson, K. L. Wong, M. Yamada, S. Yoshikawa, K. M. Young, M. C. Zarnstorff, and S. J. Zweben, *Recent TFTR Results*, PPPL-2769, Princeton Plasma Physics Laboratory, Princeton, New Jersey, July 1991

D. Mueller, H. F. Dylla, P. H. LaMarche, M. G. Bell, W. Blanchard, C. E. Bush, C. Gentile, R. J. Hawryluk, K. W. Hill, A. Janos, F. C. Jobes, D. K. Owens, G. Pearson, J. Schivell, M. A. Ulrickson, C. Vannoy, and K.-L. Wong, *Discharge Cleaning in TFTR after Boronization*, PPPL-2758, Princeton Plasma Physics Laboratory, Princeton, New Jersey, May 1991

M. H. Redi, J. C. Cummings, C. Bush, E. Fredrickson, B. Grek, T. S. Hahm, K. W. Hill, D. W. Johnson, D. K. Mansfield, H. Park, S. D. Scott, B. C. Stratton, E. Synakowski, W. M. Tang, and G. Taylor, *Transport Simulations of TFTR: Theoretically-Based Transport Models and Current Scaling*, PPPL-2784, Princeton Plasma Physics Laboratory, Princeton, New Jersey, December 1991

1991 THESES AND DISSERTATIONS

G. R. Hanson, "Microwave Reflectometry on the Advanced Toroidal Facility to Measure Density Fluctuations and Their Radial Correlation Lengths," Ph.D. dissertation, Georgia Institute of Technology, Atlanta, August 1991

M. R. Wade, "An Experimental Study of Ion Behavior in the Advanced Toroidal Facility," Ph.D. dissertation, Georgia Institute of Technology, Atlanta, September 1991

Appendix 2

ABBREVIATIONS AND ACRONYMS

ABBREVIATIONS AND ACRONYMS

ADP	Advanced Divertor Program
AEM	analytical electron microscopy
ALT-II	Advanced Limiter Test II
amu	atomic mass unit
appm	atomic parts per million
ARIES	Advanced Reactor Innovation and Evaluation Studies
ATD	Applied Technology Division
ATF	Advanced Toroidal Facility
bcc	body-centered cubic
BPX	Burning Plasma Experiment
C/C	carbon-carbon
CCD	charge-coupled device
CEA	Commissariat à l'Energie Atomique
CFADC	Controlled Fusion Atomic Data Center
CHS	Compact Helical System
CIEMAT	Centro de Investigaciones Energéticas, Medioambientales, y Tecnológicas
CIT	Compact Ignition Tokamak
CPU	central processing unit
CRADA	cooperative research and development agreement
CVD	chemical vapor deposition
CW	cold-worked
cw	continuous wave
CXE	charge-exchange excitation
DBTT	ductile-to-brittle transition temperature
D-D	deuterium-deuterium
DOE	U.S. Department of Energy
dpa	displacements per atom
DPI	deuterium pellet injector
D-T	deuterium-tritium
DTE	dissipative trapped-electron
DIII-D	tokamak experiment at General Atomics
e-beam	electron beam
EBR-II	Experimental Breeder Reactor-II
ECE	electron cyclotron emission
ECH	electron cyclotron heating
ECR	electron cyclotron resonance
ECRH	electron cyclotron resonance heating
EHD	electrohydrodynamic
EPPC	Edge Physics and Particle Control

EPR	electrochemical potentiokinetic reactivation
ES&H	environmental, safety, and health
ETD	Engineering Technology Division
Euratom	European Atomic Energy Community
FED	Fusion Energy Division
FEDC	Fusion Engineering Design Center
FENDL	Fusion Evaluated Nuclear Data Library
FFTF	Fast Flux Test Facility
FIR	far-infrared
FRLP	fast reciprocating Langmuir probe
FTU	Frascati Tokamak Upgrade
FWB	first wall and blanket
FWCD	fast-wave current drive
FWHM	full width at half-maximum
FWG	folded waveguide
FY	fiscal year
GA	General Atomics
GDC	glow discharge cleaning
GIF	Gamma Irradiation Facility
GPP	General Plant Project
HF	helical field
HFIR	High-Flux Isotope Reactor
HHF	high heat flux
HIBP	heavy-ion beam probe
IAEA	International Atomic Energy Agency
IASCC	irradiation-assisted stress-corrosion cracking
IBW	ion Bernstein wave
ICRF	ion cyclotron range of frequencies
ICRH	ion cyclotron resonance heating
IFSMTF	International Fusion Superconducting Magnet Test Facility
IGSSC	intergranular stress-corrosion cracking
IPP Garching	Max Planck Institut für Plasmaphysik, Garching, Federal Republic of Germany
ISX-B	Impurity Study Experiment
ITER	International Thermonuclear Experimental Reactor
JAERI	Japan Atomic Energy Research Institute
JET	Joint European Torus
JILA	Joint Institute for Laboratory Astrophysics
KFA	Kernforschungsanlage
KfK	Kernforschungszentrum Karlsruhe

LANL	Los Alamos National Laboratory
LBL	Lawrence Berkeley Laboratory
LCFS	last closed flux surface
LCT	Large Coil Task
LED	light-emitting diode
LHCD	lower hybrid current drive
LHD	Large Helical Device
LHe	liquid helium
LHH	lower hybrid heating
LIDT	laser-induced damage threshold
LLNL	Lawrence Livermore National Laboratory
M&S	Magnetics and Superconductivity
MFTF	Mirror Fusion Test Facility
MHD	magnetohydrodynamic
MSG	Management Services Group
MTX	Microwave Tokamak Experiment
NBI	neutral beam injection
NGS	neutral gas shielding
NMFECC	National Magnetic Fusion Energy Computer Center
NPA	neutral particle analyzer
NPDES	National Pollutant Discharge Elimination System
ODIS	Optics Damage and Radiation Studies
OFHC	oxygen-free, high-conductivity
ORNL	Oak Ridge National Laboratory
ORR	Oak Ridge Research Reactor
PBX	Princeton Beta Experiment
PC	personal computer
PCA	prime candidate alloy
PCI	postcollision interaction
PEP	pellet-enhanced performance
PF	poloidal field
PI	plasma-interactive
PIE	postirradiation examination
PLC	programmable logic controller
PLT	Princeton Large Torus
POP	proof-of-principle
PPPL	Princeton Plasma Physics Laboratory
QA	quality assurance
QMS	quadrupole mass spectrometer

R&D	research and development
rf	radio frequency
RFQ	radio-frequency quadrupole
RFTF	Radio-Frequency Test Facility
RH-TRU	remote-handled transuranic
RISC	reduced instruction set computer
RPI	Rensselaer Polytechnic Institute
RSIC	Radiation Shielding Information Center
RTD	resistance temperature detector
SA	solution-annealed
SMRF	Superconducting Motor Research Facility
SSC	Superconducting Super Collider
SMES	superconducting magnetic energy storage
TEM	transmission electron microscopy
TEXT	Texas Experimental Tokamak
TEXTOR	Torus Experiment for Technology Oriented Research
TF	toroidal field
TFTR	Tokamak Fusion Test Reactor
THQ	thermal hydraulic quenchback
TPI	tritium pellet injector
TPX	Tokamak Physics Experiment
TPOP	tritium proof-of-principle
TSC	Tokamak Simulation Code
TSCA	Toxic Substances Control Act
TST	"Triple-S Tokamk," for small Steady-State Tokamak
TSTA	Tritium Systems Test Assembly
TTF	Transport Task Force
TTI	Tokamak Transport Initiative
TTMP	transit-time magnetic pumping
USASDC	U.S. Army Strategic Defense Command
USC	User Service Center
VF	vertical field
VV	vacuum vessel
WHPP	Waste Handling and Packaging Plant
XPS	x-ray photoelectron spectroscopy
XVRM	ex-vessel remote maintenance
1-D	one-dimensional
2-D	two-dimensional
3-D	three-dimensional

Appendix 3

FUSION ENERGY DIVISION

ORGANIZATION CHART

FUSION ENERGY DIVISION

SEPTEMBER 1991

ORNL-DWG 91M-3423 FED

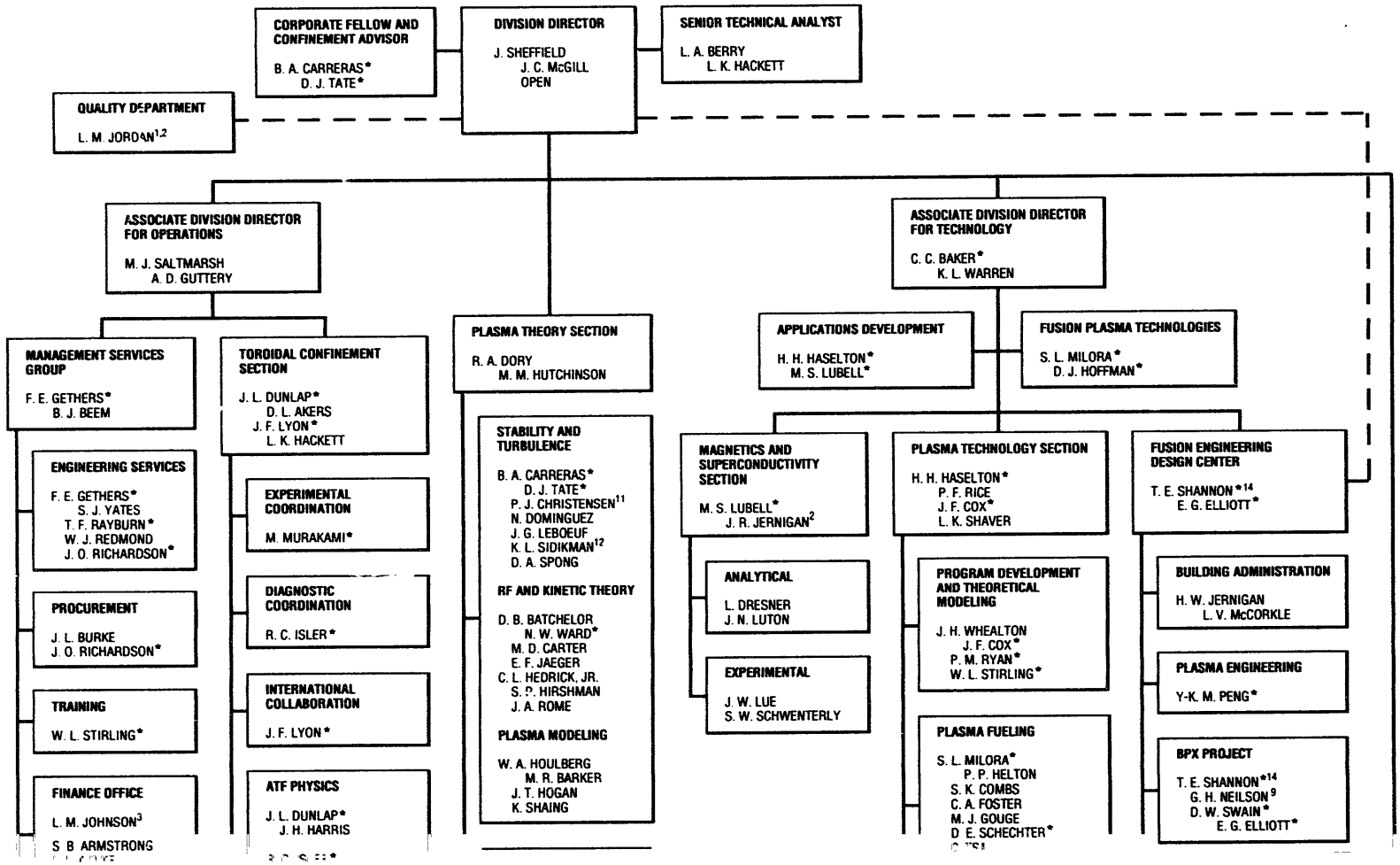

E. M. RUCKART

LIBRARY

J. B. BOOTH[4]

ASSIGNED TO ET/FE DIVISION PUBLICATIONS OFFICE

E. W. WHITFIELD[5]

M. B. NESTOR

S. C. ACETO[6]
J. G. SCHWELBERGER[6]
J. J. ZIELINSKI[6]

J. F. LYON*
R. J. COLCHIN
M. J. CROUSE[7]
M. R. WADE[8]
A. C. ENGLAND
S. HIROE
D. A. RASMUSSEN
J. B. WILGEN
I. COLLAZO
G. R. HANSON[8]
A. L. QUALLS[7]

M. MURAKAMI*

C. E. BUSH[9]
E. A. LAZARUS[10]

ATF OPERATIONS

T. C. JERNIGAN*
G. H. HENKEL
R. A. LANGLEY
C. R. SCHAICH
J. L. YARBER

ATF PROJECTS

T. C. JERNIGAN*
G. R. DYER

EDGE PHYSICS AND PARTICLE CONTROL

P. K. MIODUSZEWSKI
R. W. JONES
D. L. HILLIS[10]
C. C. KLEPPER[10]
M. M. MENON[10]
J. E. SIMPKINS
T. UCKAN
T. F. RAYBURN*

D. R. OVERBEY
N. W. WARD*
D. T. FEHLING
C. E. GIBSON
T. C. PATRICK

* DUAL CAPACITY
[1] QUALITY DEPARTMENT
[2] PART-TIME
[3] FINANCE AND MATERIALS DIVISION
[4] INFORMATION SERVICES DIVISION
[5] PUBLICATIONS DIVISION
[6] RENSSELAER POLYTECHNIC INSTITUTE
[7] UNIVERSITY OF TENNESSEE
[8] GEORGIA INSTITUTE OF TECHNOLOGY
[9] ASSIGNMENT, PRINCETON PLASMA PHYSICS LABORATORY
[10] ASSIGNMENT, GENERAL ATOMICS
[11] UNIVERSITY OF MICHIGAN
[12] OAK RIDGE ASSOCIATED UNIVERSITIES
[13] Y-12 DEVELOPMENT
[14] ENGINEERING

SPECIAL ASSIGNMENTS

ES&H UPGRADE – F. E. GETHERS
SAFETY OFFICER – F. E. GETHERS
ENVIRONMENTAL PROTECTION OFFICER – OPEN
RADIATION CONTROL OFFICER – A. C. ENGLAND
COMPUTER SECURITY OFFICER – D. R. OVERBEY
AFFIRMATIVE ACTION – K. L. WARREN

C. R. FOUST

RF PLASMA HEATING

D. J. HOFFMAN*
OPEN
G. A. WHITE
F. W. BAITY
G. C. BARBER*
T. S. BIGELOW
W. L. GARDNER
R. H. GOULDING
G. R. HASTE
P. M. RYAN*
D. E. SCHECHTER*
T. L. WHITE*
B. E. ARGO*
A. FADNEK
R. L. LIVESEY
D. O. SPARKS*

CERAMIC PROCESSING

H. D. KIMREY
C. CALHOUN[13]
S. C. FORRESTER

ELECTRICAL ENGINEERING

G. C. BARBER*
J. F. COX*
B. E. ARGO*
D. O. SPARKS*

WASTE PROCESSING

T. L. WHITE*

ARIES PROJECT

Y-K. M. PENG*

SPHERICAL TORUS PROGRAM

Y-K. M. PENG*

ITER PROJECT

N. A. UCKAN

ITER ENGINEERING

C. A. FLANAGAN[14]
D. C. LOUSTEAU[14]

ORNL-6714
Dist. Category UC-420

INTERNAL DISTRIBUTION

1–5. R. G. Alsmiller
6. F. W. Baity
7–11. C. C. Baker
12. L. R. Baylor
13. J. D. Bell
15. L. A. Berry
17–21. E. E. Bloom
16. J. L. Burke
22. B. A. Carreras
23. L. A. Charlton
24. R. E. Clausing
25–26. R. J. Colchin
27. S. K. Combs
28. E. C. Crume, Jr.
29. N. Dominguez
30–31. R. A. Dory
32. L. Dresner
33. J. L. Dunlap
34. G. R. Dyer
35. P. W. Fisher
36. S. C. Forrester
37. R. H. Fowler
38. W. Fulkerson
39. W. L. Gardner
40–44. F. E. Gethers
45. R. W. Glass
46. J. C. Glowienka
47. R. C. Goldfinger
48. R. H. Goulding
49. D. C. Gregory
50. G. R. Hanson
51. H. H. Haselton
52. G. R. Haste
53. G. H. Henkel
55. D. J. Hoffman
56. J. A. Holmes
58. W. A. Houlberg
59. D. W. Jared
60. T. C. Jernigan
61. P. W. King, ORNL Honors and Awards Office
62. C. C. Klepper
63. J-N. Leboeuf
64. D. K. Lee
65. R. P. Leinius
66. M. S. Lubell
67. J. N. Luton, Jr.
68. J. F. Lyon
69–75. J. C. McGill
76. M. M. Menon
77. F. W. Meyer
78. S. L. Milora
79. P. K. Mioduszewski
80. C. I. Moser
81. M. Murakami
82. G. H. Neilson
83. M. B. Nestor, Office of Planning and Management, Bldg. 4500N, MS 6251
84. D. R. Overbey
85. V. K. Paré
86–87. J. C. Parrott
88. Y-K. M. Peng
89. D. A. Rasmussen
90. R. K. Richards
91. J. A. Rome
92. M. W. Rosenthal
93. R. W. Roussin
94. P. M. Ryan
95. M. J. Saltmarsh
96. C. R. Schaich
97. D. E. Schechter
98. S. W. Schwenterly
99. T. E. Shannon
100. J. Sheffield
101. W. L. Stirling
102. D. J. Strickler
103. D. W. Swain
104. D. J. Taylor
105. A. Trivelpiece
106. C. C. Tsai
107. N. A. Uckan

108. T. Uckan
109. W. I. van Rij
110. J. H. Whealton
111. J. A. White
112. T. L. White
113. F. W. Wiffen
114. J. B. Wilgen
115. W. R. Wing
116. R. A. Zuhr
117–118. Laboratory Records Department
119. Laboratory Records, ORNL-RC
120. Central Research Library
121. Document Reference Section
122. Fusion Energy Division Library
123–124. Engineering Technology/Fusion Energy Division Publications Office
125. ORNL Patent Office

EXTERNAL DISTRIBUTION

Office of Fusion Energy, Office of Energy Research, Germantown, U.S. Department of Energy, Washington, DC 20545

126. S. E. Berk
127. R. A. Blanken
128. C. Bolton
129. M. Cohen
130. D. H. Crandall
131. R. Dagazian
132. N. A. Davies
133. V. Der
134. W. F. Dove
135. S. A. Eckstrand
136. T. V. George
137. J. Hoy
138. T. R. James
139. A. Katz
140. D. Markevich
141. W. Marton
142. R. H. McKnight
143. G. R. Nardella
144. D. B. Nelson
145. E. Oktay
146. A. Opdenaker
147. R. E. Price
148. T. C. Reuther
149. W. Sadowski
150. C. Sege
151. H. S. Staten
152. J. W. Willis

Lawrence Livermore National Laboratory, P.O. Box 5511, Livermore, CA 94550

153. D. E. Baldwin
154. J. Denavit, L-18
155. F. Coensgen
156. C. D. Henning, L-644
157. B. G. Logan
158. L. D. Pearlstein, L-630
159. R. F. Post
160. K. I. Thomassen, L-637

Los Alamos National Laboratory, P.O. Box 1663, Los Alamos, NM 87545

161. J. L. Anderson
162. H. Dreicer, MS-F640
163. R. A. Krakowski
164. R. K. Linford, MS-F646
165. J. D. Rogers

National Institute of Standards and Technology, University of Colorado, Campus Box 440, Boulder, CO 80309

166. V. D. Arp
167. A. Clark
168. G. H. Dunn
169. A. V. Phelps
170. F. R. Fickett

Naval Research Laboratory, Washington, DC 20375

171. W. R. Ellis
172. B. Hui
173. B. H. Ripin
174. A. Robson, Code 4760

Oak Ridge Institute for Science and Education, DOE/Oak Ridge Associated Universities, P.O. Box 117, Oak Ridge, TN 37831-0117

175. A. M. Weinberg, IEA
176. University Programs Department
177. Institute for Energy Analysis
178. Information Center/EES (attention H. T. Burn)

Pacific Northwest Laboratories, Battelle Boulevard, P.O. Box 999, Richland, WA 99352

179. D. A. Dingee
180. B. F. Gore
181. L. L. Schmid

Princeton Plasma Physics Laboratory, P.O. Box 451, Princeton, NJ 08543

182. T. K. Chu
183. R. C. Davidson
184. J. File
185. R. B. Fleming
186. J. W. French
187. R. J. Goldston
188. K. W. Hill
189. J. C. Hosea
190. S. M. Kaye
191. D. M. Meade
192. R. G. Mills
193. P. H. Rutherford
194. J. A. Schmidt
195. T. H. Stix
196. S. Yoshikawa

Sandia National Laboratories, P.O. Box 5800, Albuquerque, NM 87185

197. W. B. Gauster, Div. 1837
198. F. L. Vook, Org. 1100
199. J. B. Whitley, Div. 6248

Bechtel National, Inc., P.O. Box 3965, San Francisco, CA 94119

200. E. von Fischer
201. H. K. Forsen, Advanced Technology Division

EG&G ORTEC, 100 Midland Road, Oak Ridge, TN 37830

202. J. Ayers
203. D. A. Gedcke

General Atomics, P.O. Box 85608, San Diego, CA 92186-9784

204. R. L. Freeman
205. R. Harder
206. C. Moeller
207. D. O. Overskei

208. T. Ohkawa
209. J. M. Rawls
210. T. Simonen
211. R. D. Stambaugh
212. T. Tamano
213. M. R. Wade

General Dynamics-Convair Division, P.O. Box 85377, San Diego, CA 92138

214. R. F. Beuligmann
215. D. S. Hackley
216. R. A. Johnson, MZ 16-1070

Grumman Corporation, Bethpage, NY 11714

217. R. Botwin
218. A. Favale

TRW, Inc., 1 Space Park, Redondo Beach, CA 92078

219. J. Gordon
220. N. H. Lazar
221. J. A. Maniscalco

Westinghouse Electric Corporation, Advanced Reactors Division, P.O. Box 158, Madison, PA 15663

222. A. Anderson
223. G. G. Gibson

Atlanta University, Atlanta, GA 30314

224. C. R. Handy
225. R. E. Mickens

Auburn University, Auburn, AL 36849-3511

226. M. S. Pindzola, Physics Department
227. D. G. Swanson
228. R. F. Gandy, Physics Department

Denison University, Granville, OH 43032

229. W. A. Hoffman
230. R. R. Winters

University of California at Los Angeles, Los Angeles, CA 90024

231. M. Abdou
232. R. W. Conn, Mechanical, Aerospace, and Nuclear Engineering Department

University of California at San Diego, La Jolla, CA 92093

233. M. N. Rosenbluth
234. P. H. Diamond

Georgia Institute of Technology, Atlanta, GA 30332

235. J. N. Davidson
236. R. K. Feeney, School of Electrical Engineering
237. W. M. Stacey, School of Nuclear Engineering
238. C. E. Thomas, School of Nuclear Engineering
239. E. W. Thomas, School of Physics

University of Illinois, Urbana, IL 61801

240. K. K. Kim, Department of Electrical Engineering
241. W. Sutton, Department of Nuclear Engineering

University of Maryland, College Park, MD 20742

242. V. L. Granatstein, Electrical Engineering Department
243. H. R. Griem, Laboratory for Plasma and Fusion Studies
244. C. S. Liu, Department of Physics and Astronomy

Massachusetts Institute of Technology, 77 Massachusetts Ave., Cambridge, MA 02139

245. G. Bekefi, 36-213
246. D. R. Cohn
247. B. Coppi, 26-217
248. J. P. Freidberg, NW16-240
249. K. Molvig, NW16-240
250. D. B. Montgomery, NW17-288
251. R. R. Parker, NW16-288
252. J. Schultz
253. R. J. Thome, NW17-223

Rensselaer Polytechnic Institute, P.O. Box 2000, Troy, NY 12181

254. R. L. Hickok
255. W. C. Jennings
256. D. Steiner

The University of Tennessee, Knoxville, TN 37996

257. I. Alexeff, Dept. of Electrical Engineering
258. E. G. Harris, Dept. of Physics
259. J. R. Roth, Dept. of Electrical Engineering
260. P. N. Stevens, Dept. of Nuclear Engineering

University of Texas, Austin, TX 78712

261. H. L. Berk, Institute for Fusion Studies
262. K. W. Gentle, Dept. of Physics
263. D. W. Ross, Dept. of Physics
264. H. H. Woodson, Dept. of Electrical Engineering
265. A. J. Wootton, Fusion Research Center

University of Wisconsin, Madison, WI 53706

266. J. D. Callen, Nuclear Engineering Department
267. J. R. Conrad, Nuclear Engineering Department
268. D. W. Kerst
269. G. Kulcinski
270. D. C. Larbalestier
271. J. L. Shohet, Torsatron/Stellarator Laboratory
272. J. C. Sprott, Department of Physics

Research School of Physical Sciences, Australian National University, P.O. Box 4, Canberra, A.C.T. 2601, Australia

273. S. M. Hamberger, Plasma Research Laboratory
274. Plasma Research Laboratory

Plasma Research Section, Physics Division, Forskningscenter, Risø, P.O. Box 49, DK-4000 Roskilde, Denmark

275. C. T. Chang
276. V. O. Jensen
277. O. Kofoed-Hansen

JET Joint Undertaking, Abingdon, Oxon OX14 3EA, United Kingdom

278. J. G. Cordey
279. K. J. Dietz
280. D. Düchs
281. A. Gibson
282. L. D. Horton
283. M. Keilhacker

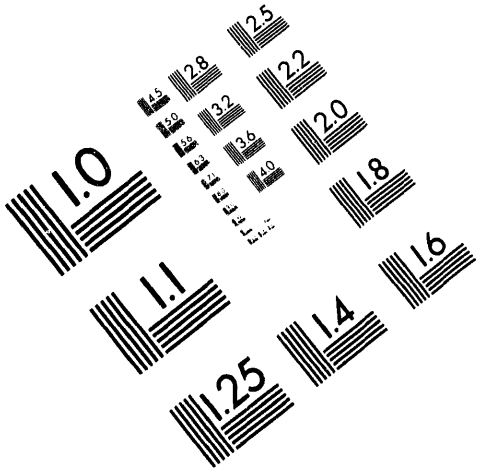

Association for Information and Image Management
1100 Wayne Avenue, Suite 1100
Silver Spring, Maryland 20910
301/587-8202

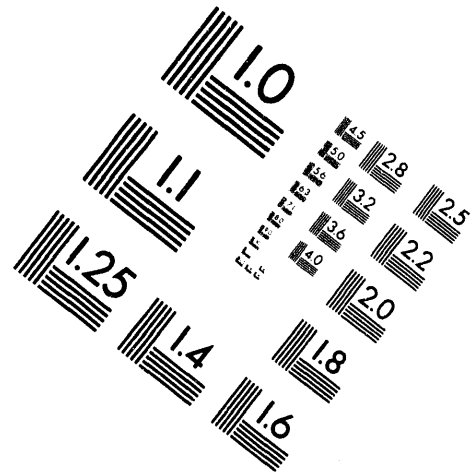

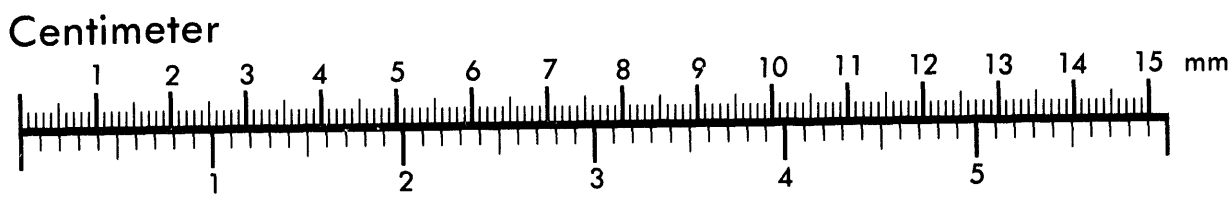

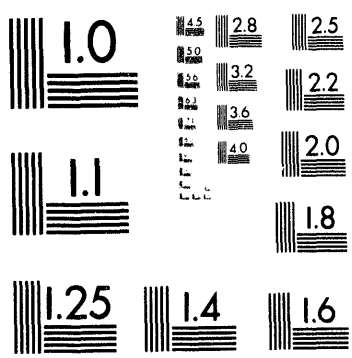

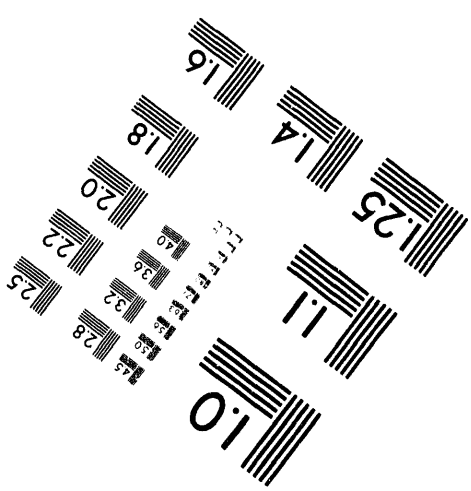

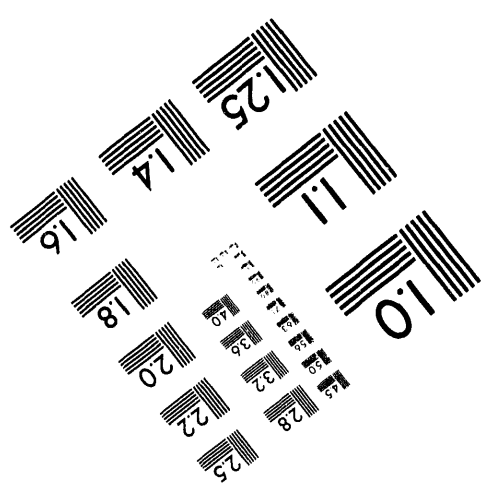

4 of 4

284. P. H. Rebut
285. P. E. Stott
286. E. Thompson
287. Library

UKAEA, Culham Laboratory, Abingdon, Oxon OX14 3DB, United Kingdom

288. R. Hancox
289. T. C. Hender
290. Library
291. M. W. Lomer
292. D. C. Robinson
293. D. R. Sweetman
294. J. B. Taylor

CEN/Cadarache, B.P. 1, F-13108 Saint-Paul-lez-Durance, France

295. C. Mercier
296. J. Tachon
297. Bibliothèque

CEN/Saclay, B.P. No. 2, F-91191 Gif-sur-Yvette, France

298. H. Desportes, STIPE
299. J. C. Lottin

IPP/KFA Jülich, Postfach 1913, D-5170 Jülich 1, Federal Republic of Germany

300. Bibliothek
301. H. Conrads
302. K.-H. Dippel
303. E. Hintz
304. H. Euringer
305. K.-H. Finken
306. A. Rogister
307. G. Wolf

Kernforschungszentrum Karlsruhe GmbH, Postfach 3640, D-7500 Karlsruhe 1, Federal Republic of Germany

308. O. Hagena, Nuclear Engineering Institute
309. W. Klose, Division of New Technology and Basic Research
310. P. Komarek, Institute for Technical Physics
311. A. Ulbricht, Institute for Technical Physics
312. J. E. Vetter, Nuclear Fusion Project
313. Bibliothek

Max-Planck Institut für Plasmaphysik, D-8046 Garching, Federal Republic of Germany

314. Bibliothek
315. G. von Gierke
316. G. Grieger
317. J. Junker
318. M. Kaufman
319. M. Keilhacker
320. A. Knobloch
321. K. Lackner
322. L. L. Lengyel
323. D. Pfirsch
324. K. Pinkau
325. H. Renner
326. A. Schlüter
327. R. Toschi
328. F. Wagner

ENEA Centro di Frascati, C.P. 65, I-00044 Frascati (Roma), Italy

329. A. Bracci, Fusion Department
330. H. E. Knoepfel
331. Biblioteca
332. N. Sacchetti, Technology Division
333. G. Sacerdoti
334. M. Spadoni, Fusion Reactor Engineering Project

International Centre for Theoretical Physics, P.O. Box 586, I-34100 Trieste, Italy

335. A. M. Hamende
336. Library

National Institute for Fusion Science, Chikusa-ku, Nagoya 464-01, Japan

337. T. Amano
338. M. Fujiwara
339. K. Husimi
340. A. Iiyoshi
341. H. Ikegami
342. S. Okamura
343. Research Information Center
344. T. Uchida
345. Library

Japan Atomic Energy Research Institute, Naka Fusion Research Establishment, Naka-machi, Naka-gun, Ibaraki-ken 311-01, Japan

346. S. Shimamoto
347. K. Tomabechi
348. M. Yoshikawa
349. Library

Plasma Physics Laboratory, Kyoto University, Gokasho, Uji, Kyoto 531, Japan

350. Library
351. K. Uo
352. M. Wakatani
353. T. Obiki

Plasma Research Center, University of Tsukuba, Sakura-mura, Niihari-gun, Ibaraki Japan

354. Y. Kiwamoto
355. S. Miyoshi

FOM-Instituut voor Plasmafysica, Rijnhuizen, Postbus 1207, NL-3430 BE Nieuwegein, The Netherlands

356. M. J. van der Wiel
357. Library

Division de Fusion Termonuclear, EURATOM/CIEMAT, Avenida Complutense 22, 28040 Madrid, Spain

358. J. Alvarez-Rivas
359. A. Perez Navarro
360. M. Soler
361. B. Zurro

Centre de Récherches en Physique des Plasmas, Ecole Polytechnique Fédérale de Lausanne, 21 Avenue des B ıs, CH-1007 Lausanne, Switzerland

362. Bibliothèque
363. F. Troyon

Paul Scherrer Institute, CH-5234 Villigen, Switzerland

364. Library
365. G. Vécsey

I. V. Kurchatov Institute of Atomic Energy, P.O. Box 3402, 123182 Moscow, Russia

366. G. A. Eliseev
367. V. D. Shafranov

Institute of General Physics, Russian Academy of Sciences, Ulitsa Vavilova 38, 1779246 Moscow, Russia

368. I. S. Danilkin
369. L. M. Kovrizhnykh
370. I. Shpigel

Kharkov Physico-Technical Institute, Ukranian Academy of Sciences, 310108 Kharkov, Ukraine

371. A. Y. Omelchenko
372. O. S. Pavlichenko

373. R. E. Aamodt, Lodestar Research Corporation, 2400 Central Ave., Boulder, CO 80301
374. E. Anabitarte, Avenida de los Castros s/n, Dpt. Fisica Aplicada, Universidad de Cantabria, 39005 Santander, Spain
375. W. D. Ard, McDonnell Douglas Astronautics Company, P.O. Box 516, St. Louis, MO 63166
376. M. P. G. Avanzini, NIRA S.p.A., C.P. 1166, 16100 Genova, Italy
377. W. Bauer, Dept. 8340, Sandia National Laboratories, P.O. Box 969, Livermore, CA 94550
378. P. R. Bell, 132 Westlook Circle, Oak Ridge, TN 37830
379. K. H. Berkner, B50 Rm 150, Lawrence Berkeley Laboratory, Cyclotron Road, Berkeley, CA 94720
380. R. A. Berry, Varian Associates, Inc., 611 Hansen Way, Palo Alto, CA 94303
381. G. Bohner, Forschungslaboratorien, Siemens AG, Postfach 325, D-8520 Erlangen 2, Federal Republic of Germany
382. R. A. E. Bolton, IREQ Hydro-Quebec Research Institute, 1800 Montée Ste.-Julie, Varennes, P.Q. JOL 2PO Canada
383. M. H. Brennan, Australian Atomic Energy Commission, Lucas Heights Research Laboratories, New Illawara Road, Lucas Heights, Private Mail Bag, Sutherland, N.S.W., Australia 2232
384. G. Briffod, CEN/Grenoble, B.P. 85X, F-38041 Grenoble, France
385. P. Catto, Lodestar Research Corporation, P.O. 2400 Central Ave., Boulder, CO 80301
386. R. N. Cherdack, Burns & Roe, Inc., 700 Kinder Kamack Road, Oradell, NJ 07649
387. E. W. Collings, Battelle Memorial Institute, 505 King Ave., Columbus, OH 43201
388. J. G. Crocker, EG&G Idaho, Inc., Idaho National Engineering Laboratory, Idaho Falls, ID 83401
389. F. L. Culler, Electric Power Research Institute, P.O. Box 10412, Palo Alto, CA 94303
390. R. A. Dandl, Applied Microwave Plasma Concepts, Inc., 2075 N. Portico de Nogal, Carlsbad, CA 92009

391. S. O. Dean, Fusion Power Associates, Inc., 2 Professional Drive, Suite 248, Gaithersburg, MD 20879
392. H. W. Deckman, Advanced Energy Systems Laboratory, Exxon Research and Engineering Company, P.O. Box 8, Linden, NJ 07306
393. Department of Nuclear Engineering Sciences, 202 Nuclear Science Center, University of Florida, Gainesville, FL 32611
394. Director, Technical Library, Defense Atomic Support Agency, Sandia Base, Albuquerque, NM 87185
395. T. J. Dolan, Department of Nuclear Engineering, University of Missouri, Rolla, MO 65401
396. G. W. Donaldson, School of Electrical Engineering, University of New South Wales, P.O. Box 1, Kensington, N.S.W., Australia
397. D. A. Dreyfus, Gas Research Institute, 1331 Pennsylvania Ave., N.W., Suite 730N, Washington, DC 20004-1703
398. E. Dullni, NB-05/639, Experimentalphysik, Ruhr-Universität Bochum, D-4630 Bochum, Federal Republic of Germany
399. W. G. Ellis, DP-20, U.S. Department of Energy, Washington, DC 20545
400. T. K. Fowler, University of California at Berkeley, Berkeley, CA 92740
401. H. B. Gilbody, Department of Pure and Applied Physics, Queens University, Belfast BT7 1NN, Northern Ireland, United Kingdom
402. R. W. Gould, California Institute of Technology, Building 116-81, Pasadena, CA 91125
403. D. C. Griffin, Rollins College, Winter Park, FL 32789
404. R. A. Gross, Department of Applied Physics & Nuclear Engineering, Columbia University, New York, NY 10027
405. T. G. Heil, Department of Physics and Astronomy, University of Georgia, Athens, GA 30602
406. J. P. Holdren, Energy and Resources Group, Building T-4, Room 100, University of California, Berkeley, Berkeley, CA 94720
407. W. R. Husinsky, Technical University of Vienna, Karlsplatz 13, A-1040 Vienna, Austria
408. S. Ihara, Central Research Laboratory, 8th Department, Hitachi Ltd., Kokubunji, Tokyo 185, Japan
409. M. Iwamoto, Central Research Laboratory, Mitsubishi Electric Corporation, 80 Nakano, Minamishimizu, Amagasaki, Hyogo 661, Japan
410. Japan Atomic Energy Research Institute, 1825 K Street, Washington, DC 20006
411. C. K. Jones, Cryogenic Research Laboratory, Westinghouse Electric Corporation, Research and Development Center, 1310 Beulah Road, Pittsburgh, PA 15235
412. R. W. Jones, Physics Department, Emporia State University, 1200 Commercial, Emporia, KS 66801
413. R. Jones, Department of Physics, National University of Singapore, Bukit Timah Road, Singapore 10.25
414. D. Klein, Westinghouse Electric Corporation, Strategic Operations Division, P.O. Box 598, Pittsburgh, PA 15230
415. A. C. Kolb, Maxwell Laboratories, Inc., 9244 Balboa Avenue, San Diego, CA 92123
416. K. Koyama, Electrotechnical Laboratory, 1-1-4 Umezono, Sakura-mura, Niihari-gun, Ibaraki-ken 305, Japan

417. N. A. Krall, Krall Associates, 1070 America Way, Del Mar, CA 92014
418. A. H. Kritz, 69 Lillie Street, Princeton Junction, NJ 08550
419. K. Kuroda, Central Research Laboratory, 1-280, Higa Shiko Igakubo, Kokubumji, Tokyo 185, Japan
420. Laboratorio Associado de Plasma, Instituto Nacional de Pesquisas Espaciais, Caixa Postal 515, 122201, Sao Jose dos Campos, SP, Brazil
421. Laboratory for Plasma and Fusion Studies, Department of Nuclear Engineering, Seoul National University, Shinrim-dong, Gwanak-ku, Seoul 151, Korea
422. Laser Fusion Group, Department of Mechanical and Aerospace Science, River Campus Station, University of Rochester, Rochester, NY 14627
423. B. Lehnert, Department of Plasma Physics and Fusion Research, Royal Institute of Technology, S-10044 Stockholm 70, Sweden
424. P. C. Liewer, MS 198-231, Jet Propulsion Laboratory, 4800 Oak Grove Dr., Pasadena, CA 91109
425. C. M. Loring, EIMAC Division of Varian, 301 Industrial Way, San Carlos, CA 94070-2682
426. V. A. Maroni, CEN 205, Argonne National Laboratory, Argonne, IL 60439
427. A. Maschio, Istituto Gas Ionizzati, Corso Statti Uniti 4, I-35020 Padova, Italy
428. E. A. Mason, Brown University, Providence, RI 02912
429. D. G. McAlees, Advanced Nuclear Fuels Corporation, 600 108th Ave., NE, Bellevue, WA 98009
430. R. L. McCrory, Jr., Laboratory for Laser Energetics, University of Rochester, 250 East River Road, Rochester, NY 14623-1299
431. O. Mitarai, Department of Electrical Engineering, Kumamoto Institute of Technology, Ikeda 4-22-1, Kumamoto 860, Japan
432. F. Moon, Department of Theoretical and Applied Mechanics, Cornell University, Ithaca, NY 14850
433. T. J. Morgan, Physics Department, Wesleyan University, Middletown, CT 06457
434. K. G. Moses, JAYCOR, 2811 Wilshire Boulevard, Suite 690, Santa Monica, CA 90403
435. N. F. Ness, Bartol Research Institute, University of Delaware, Newark, DE 19716
436. C. Oberly, Aero Propulsion Laboratory, Power Distribution Branch, Wright-Patterson Air Force Base, OH 45433
437. T. Ogasawara, Department of Physics, College of Science and Technology, Nihon University, Kanda-Surugadai, Chiyoda-ku, Tokyo 101, Japan
438. H. Ogiwara, Toshiba Research and Development Center, 1 Komukai Tsohiba-cho, Saiwai, Kawasaki, Kanagawa 210, Japan
439. R. J. Onega, Nuclear Engineering Group, College of Engineering, Virginia Polytechnic Institute and State University, Blacksburg, VA 24061
440. B. Outten, Jr., Western Metal Products Company, 1300 Weber Stree , Orlando, FL 32803
441. D. Palumbo, via Gabriele d'Annunzio 52, Palermo I-90144, Italy
442. K. Prelec, Brookhaven National Laboratory, Upton, NY 11973
443. F. C. Rock, Plasma Physics Laboratory, Department of Physics and Astronomy, Brigham Young University, Provo, UT 84602
444. R. H. Rohrer, Department of Physics, Emory University, Atlanta, GA 30322

445. M. Rosenbaum, Director, Nuclear Science Institute, Universidad Nacional Autonoma de Mexico, Circuito Exterior, Ciudad Universitaria, Delegación Coyoacán, Apartado Postal 70-360, 04510 Mexico D.F.
446. P. A. Sanger, Airco, 600 Milik St., Carteret, NJ 07008
447. S. St. Lorant, Stanford Linear Accelerator Center, P.O. Box 4349, Stanford, CA 94305
448. M. M. Satterfield, The Nucleus, 761 Emory Valley Road, Oak Ridge, TN 37830
449. Y. Sawada, Heavy Apparatus Engineering Laboratory, Toshiba Corp., 2-4 Suehirocho, Tsurumi-ki, Yokohama 230, Japan
450. J. H. Schneider, Joint Research Centre, Ispra Establishment, I-21020 Ispra (Varese), Italy
451. G. R. Siegel, Tennessee Valley Authority, 25 33A Missionary Ridge Place, Chattanooga, TN 37402
452. P. Staudhammer, Vice President and Director, Center for Automative Technology, TRW, Inc., Bldg. E1, Room 2091, One Space Park, Redondo Beach, CA 90278
453. Z. J. J. Stekly, Magnetics Corporation of America, 47 Hartz St., No. 2, Gloucester, MA 01930
454. U. Stiefel, Eidg. Institut für Reaktorforschung, CH-5301 Wurenlingen, Switzerland
455. K. Tachikawa, Chief, Electric Materials Laboratory, National Research Institute for Metals, 3-12, 2-Chome, Nakameguro, Meguru, Tokyo, Japan
456. R. J. Taylor, Center for Plasma Physics and Fusion Engineering, University of California, Los Angeles, CA 90024
457. D. P. Tewari, Department of Physics, Indian Institute of Technology, New Delhi 110016, India
458. M. Thumm, Institut fur Plasmaforschung, Pfaffenwaldring 31, D-7000 Stuttgart 80, Federal Republic of Gerrnany
459. J. F. Traexler, Westinghouse Electric Corp., Quadrangle 2WII-203, Orlando, FL 32817
460. G. Vahala, Department of Physics, College of William and Mary, Williamsburg, VA 23185
461. T. C. Varljen, Westinghouse Hanford, P.O. Box 1970, Richland, WA 99352
462. R. Varma, Physical Research Laboratory, Navrangpura, Ahmedabad 380009, India
463. C. Walters, Technology Division, Building R25, Rutherford Laboratory, Chilton, Didcot, Oxon OX11 OQX, United Kingdom
464. C. N. Watson-Munro, University of Sydney, Wills Plasma Project, Sydney, N.S.W., Australia
465. H. Weitzner, Courant Institute for Mathematical Sciences, New York University, 251 Mercer St., New York, NY 10012
466. S. B. Woo, Department of Physics, University of Delaware, Newark, DE 19711
467. H. Yoshikawa, Manager, Materials Engineering, Hanford Engineering Development Laboratory, P.O. Box 1970, Richland, WA 99352
468. V. A. Glukhikh, Scientific-Research Institute of Electro-Physical Apparatus, 188631 St. Petersburg, Russia
469. D. D. Ryutov, Institute of Nuclear Physics, Siberian Branch of the Academy of Sciences, Sovetskaya St. 5, 630090 Novosibirsk, Russia
470. Deputy Director, Southwestern Institute of Physics, P.O. Box 15, Leshan, Sichuan, China (PRC)

471. Library, The Institute of Plasma Physics, Academia Sinica, P.O. Box 1126, Hefei, Anhui, China (PRC)
472. M-L. Xue, Institute of Mechanics, Academia Sinica, Beijing, China (PRC)
473. Office of Assistant Manager for Energy Research and Development, U.S. Department of Energy, Oak Ridge Operations Office, P.O. Box 2001, Oak Ridge, TN 37831-8705

474–513. Given distribution as shown in DOE/OSTI-4500/R75, Energy Research (Category UC-420, Magnetic Fusion Energy) (40 copies)

☆U.S. GOVERNMENT PRINTING OFFICE: 1994-550-165-80021

DATE
FILMED
8/26/94
END